Alkylation of 1-Butene with Isobutane using EMT and Y Zeolites

by

Gail Robertson Walker

A thesis
presented to the University of Waterloo
in fulfillment of the
thesis requirement for the degree of
Doctor of Philosophy
in
Chemical Engineering

Waterloo, Ontario, Canada, 2000

The University of Waterloo requires the signatures of all persons using or photocopying this thesis. Please sign below, and give address and date.

Acknowledgements

After being an at-home-mother for six years, enrolling in a PhD program presented a formidable challenge. Accomplishing this goal was not an autonomous effort but rather the culmination of hard work and invaluable support from many special people (see page v). First and foremost, I would like to acknowledge my family, Larry, Kelsey and Ben, for their unconditional love and encouragement along this journey and for providing ballast during the challenging periods of my research. A warm thank you must be extended to the Papps and the Cooks, for participating in the milestone celebrations and keeping me focussed on my goals. My Sunshine Montessori School family deserves special mention for supplying a rich and nurturing educational environment for my children, as well as their continued interest in the progress of my academic studies.

I am indebted to Prof. J. Martens and Ann Gossens (K.U. Leuven, Belgium) for generously providing the elusive EMT catalyst recipe. Equipment challenges are inherent in any research, and this project was no exception. Invaluable technical support was provided by Frank Wassmer, Burt Habicher, Neil McManus, Ralph Dickhout as well as John Kindland (Autoclave Engineers), for which I am eternally grateful.

I would be remiss if I didn't acknowledge Prof. Rempel for bringing me back to the university environment through sessional lecturing and for the use of the Parr batch autoclave. I would like to thank my supervisor, Prof. Ng, for encouraging me to enroll in the PhD program, as well as her input in my research. The "bulk" of this thesis demands a special thank you to my PhD Thesis Examination Committee, Prof. Scharer, Prof. Pritzker, Prof. Tchir and Prof. Kaliaguine (Université Laval, Québec), for review of this thesis as well as their insightful comments.

Financial support is always appreciated in any scholarly work. I would like to thank the Ontario Graduate Scholarship fund for their financial assistance in this endeavour as well as the National Sciences and Engineering Research Council for equipment (BTRS-Jr) and project grants.

Research friends are the core support community for any graduate work. I would like to acknowledge my Grad House friends, Jun Gao, Loui Polic and Luigi D'Agnillo for sharing a glass of wine and lively conversation. I am indebted to Prof. Soares and especially Prof. Penlidis and Prof. Duever for their commitment during the trying phases of my research. My final thanks are directed to my colleagues, Kira Onysko, Dave Strutt, Asif Rashid and Lora Celebre for friendship, and particularly Chuncheng Huang and Mure Te for unfailing support.

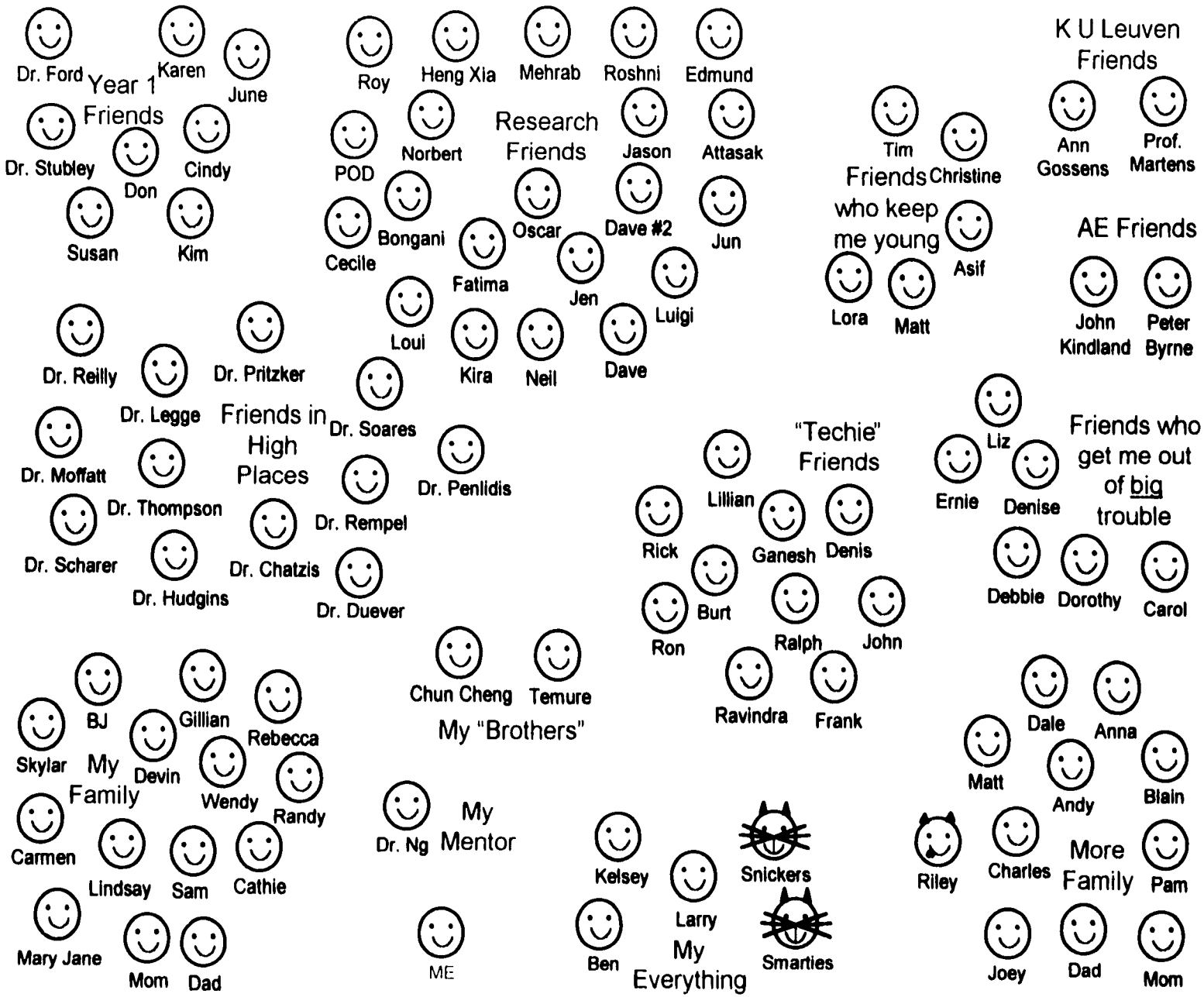
Dr. Ford
Karen
June
Year 1 Friends
Dr. Stubley
Don
Cindy
Susan
Kim
Roy
Heng Xia
Mehrab
Roshni
Edmund
POD
Norbert
Research Friends
Jason
Attasak
Cecile
Bongani
Oscar
Dave #2
Jun
Fatima
Jen
Luigi
Loui
Kira
Neil
Dave
Tim
Christine
Friends who keep me young
Asif
Lora
Matt
K U Leuven Friends
Ann Gossens
Prof. Martens
AE Friends
John Kindland
Peter Byrne
Dr. Reilly
Dr. Pritzker
Dr. Legge
Dr. Soares
Friends in High Places
Dr. Moffatt
Dr. Thompson
Dr. Penlidis
Dr. Rempel
Dr. Scharer
Dr. Chatzis
Dr. Hudgins
Dr. Duever
"Techie" Friends
Lillian
Rick
Ganesh
Denis
Burt
Ralph
John
Ron
Ravindra
Frank
Liz
Ernie
Denise
Friends who get me out of big trouble
Debbie
Dorothy
Carol
Chun Cheng
Temure
My "Brothers"
Skylar
BJ
Gillian
Rebecca
My Family
Devin
Wendy
Randy
Carmen
Lindsay
Sam
Cathie
Mary Jane
Mom
Dad
Dr. Ng
My Mentor
ME
Kelsey
Snickers
Larry
Ben
Smarties
My Everything
Dale
Anna
Matt
Andy
Blain
Riley
Charles
More Family
Pam
Joey
Dad
Mom

Dedication

I dedicate this thesis to working mothers.

Abstract

Alkylation of 1-Butene with Isobutane using EMT and Y Zeolites

Alkylate is the preferred blending stock of reformulated gasoline as it is clean burning, producing less emissions, and possesses high energy and octane. Commercial liquid catalysts employed for the alkylation of butene with isobutane pose significant environmental hazards. Many solid acids have been investigated towards this reaction, but none have reached commercial success. Although high initial activity is demonstrated, rapid deactivation ensues, primarily due to a loss in hydride transfer functioning.

The preferential adsorption of the olefin relative to the isoparaffin makes deactivation an inevitable outcome. The catalyst surface selectively adsorbs butene from the feed, regardless of the feed composition. Eventually the surface acid sites become saturated with oligomers of butene. Pulse feed delivery, with interim isobutane flush periods, can restore deactivated catalysts to fresh state levels. It is possible that catalytic distillation may hold some promise for this challenging reaction, if a suitable solid acid catalyst can be found.

The zeolite, EMT, is a hexagonal phase faujasite synthesized in the presence of a crown-ether template. Literature measurements for pyridine desorption conclude that this zeolite possesses primarily Bronsted acidity, with significant amounts of strong acid sites. These properties are ideally suited to promote efficient hydride transfer in the alkylation of butene with isobutane.

The catalyst, EMT, demonstrated superior performance relative to Y zeolite, improving the Useful Catalyst Lifetime period (butene conversion maintained above 80%) by 41%. Approximately half of the alkyate produced was composed of C_8 compounds, of which roughly 60 to 80 % were trimethylpentanes (TMPs). The most valuable octane isomer, 2,2,4-TMP, was present in the largest quantities in the

alkylate, accounting for 30 to 60 % of the TMP fraction. It is believed that the uneven distribution of acid sites on EMT discourages deactivation processes. Alternatively, it is also possible that isobutane adsorption capacity on EMT is improved relative to Y.

The impregnation of 0.5 % Pt onto EMT (0.5%Pt/EMT) produced a minor improvement in the Useful Catalyst Lifetime period and alkylate quality (as measured by TMP content). The levels of TMP were notably higher on 0.5%Pt/EMT, accounting for 80% of the C_8 fraction. These improvements are attributed to an increase in the concentration of reactive hydrogen, possibly hydrogen spillover, in the vicinity of the acid site, which enhances the desorption rate of TMP isomers.

The same loading of Pt impregnated on Y zeolite (0.5%Pt/Y) did not exhibit a notable change on catalyst performance. It is suggested that the reactive hydrogen population was overdeveloped, causing the *tert*-C_4^+ carbenium ion population to diminish. This behaviour promoted DMH formation and expedited the onset of deactivation. A fine balance between reactive hydrogen participation and active hydride transfer from isobutane is necessary to favour TMP formation and prolong catalyst lifetime.

The efficacy of regeneration was improved on EMT in the presence of Pt. A significant loss in catalyst activity was noted for regenerated EMT whereas recovery of catalyst activity was almost complete on Pt/EMT systems. The same benefits were not observed on 0.5%Pt/Y. Although alkylate quality was similar for fresh and regenerated Pt/Y systems, the amount of liquid produced per gram of catalyst was reduced. It is possible that excessive involvement of reactive oxygen during recalcination caused the noble metal to sinter on the catalyst surface, reducing Pt dispersion. Regenerated Pt/Y behaved in a similar manner to regenerated Y, with no beneficial effect being demonstrated by Pt.

Table of Contents

CHAPTER 1: INTRODUCTION 1

1.1 MERIT OF ALKYLATION RESEARCH 1

1.2 BUTENE/ISOBUTANE ALKYLATION WITH LIQUID ACIDS 3
- 1.2.1 Commercial Liquid Acid Catalysts 3
- 1.2.2 Product Distribution from Liquid Acid Catalysed Butene/Isobutane Alkylation 4

1.3 MAJOR PROCESS LICENSORS ENGAGED IN SOLID ACID CATALYSED BUTENE/ISOBUTANE ALKYLATION RESEARCH 7

1.4 PROPOSED BUTENE/ISOBUTANE ALKYLATION REACTION MECHANISM ON SOLID ACIDS 9
- 1.4.1 Traditional Mechanism via Carbenium Ions 9
  - *1.4.1.1 Protonation of the Olefin to form sec-C_4^+ ion* 10
  - *1.4.1.2 Formation of tert-C_4^+ ion* 10
  - *1.4.1.3 Addition of tert-C_4^+ ion to Second Olefin* 11
  - *1.4.1.4 Isomerizaiton of C_8^+ ion to more Stable Forms* 12
  - *1.4.1.5 Hydride Transfer to C_8^+ ion* 13
- 1.4.2 Mechanism via Covalent Surface Esters 13

1.5 SIDE REACTIONS OF BUTENE/ISOBUTANE ALKYATION 15
- 1.5.1 Oligomerization 16
- 1.5.2 Polymerization 17
- 1.5.3 Disproportionation 17
- 1.5.4 Cracking 17
- 1.5.5 Self-Alkylation 18

1.6 MEASURES OF CATALYST PERFORMANCE 19
- 1.6.1 Butene Conversion (Butene Disappearance) 19
- 1.6.2 Alkylate Yield 20
- 1.6.3 Classification of C_5+ Product Distribution 20
- 1.6.4 Classification of C_8 Fraction 20
- 1.6.5 Measures of Selectivity in C_8 Fraction 22
- 1.6.6 Indicator of Steric Effects on Reaction 22
- 1.6.7 Indicator of Effective Hydride Transfer 23

1.7 COMPARISON OF BUTENE/ISOBUTANE ALKYLATE COMPOSITION WITH THERMAL EQUILIBRIUM MEASUREMENTS 23

1.8 RESEARCH METHODOLOGY 24
1.8.1 Problem Statement and Objectives 24
1.8.2 Catalyst Requirements 25
1.8.2.1 Chemical Properties 26
1.8.2.2 Physical Properties 27
1.8.3 Approach to Evaluating Catalyst Performance 28
1.8.4 Chronological Phases of Research Plan 28
1.8.4.1 Phase I: Catalyst Development 28
1.8.4.2 Phase II: Equipment Set-up for Flow Experiments 28
1.8.4.3 Phase III: Preparation and Characterization of Catalyst Systems 29
1.8.4.4 Phase IV: Effect of Operating Conditions 29
1.8.4.5 Phase V: Effect of Pt on Catalyst Performance 29

CHAPTER 2: CATALYST DESIGN 30

2.1 REVIEW OF LARGE PORE ZEOLITES FOR BUTENE/ISOBUTANE ALKYLATION 31
2.1.1 Properties of Zeolites 31
2.1.1.1 Nature of Acidity in Zeolites 31
2.1.1.2 Hydrocarbon Adsorption on Zeolites 33
2.1.2 Cubic Phase Faujasites Prepared from Na-rich Hydrogels - Y and USY (Dealuminated Y) 34
2.1.3 Faujasites Prepared in the Presence of Crown Ether Templates - EMT (Hexagonal Phase) and FAU (Cubic Phase) 40

2.2 IDENTIFICATION OF PREFERRED ACIDIC SUPPORT 50

2.3 REVIEW OF HYDROGEN SPILLOVER 52
2.3.1 Definition of Hydrogen Spillover 52
2.3.2 Nature of Spillover Species 54

2.4 INCORPORATION OF HYDRIDE TRANSFER PROMOTER INTO SOLID ACID ALKYLATION CATALYST DESIGN 56
2.4.1 Proposed Alkylation Mechanism Involving Spillover 56
2.4.2 Mode of Incorporation of Spillover Activator into Catalyst Design 58

CHAPTER 3: CATALYST PREPARATION 59

3.1 METHOD OF PREPARATION OF Na-EMT 61
3.1.1 Chemical Sources and their Functions 61
3.1.2 List of Materials 64
3.1.3 Preparation of the Hydrogel 64
3.1.4 The Aging Period 65
3.1.5 The Crystallization Step 66
3.1.6 Template Removal 67
3.1.7 Phase Identification 69

3.2 BATCH TO BATCH VARIATION OF EMT SYNTHESIS 70

3.3 AMMONIUM ION EXCHANGE OF Na-EMT TO H-EMT 71

3.4 CHARACTERIZATION OF EMT AND Y 72

3.5 PREPARATION OF Pt SUPPORTED ZEOLITES 73
3.5.1 Method of Preparation 73
3.5.2 Calcination and Reduction 74

3.6 CHARACTERIZATION OF Pt/EMT AND Pt/Y 74

CHAPTER 4: SET-UP OF MICROFLOW REACTOR 76

4.1 AE/BTRS-Jr/PC MICROFLOW REACTOR DESCRIPTION 77
4.1.1 Overview of System 77
4.1.2 Software Capabilities 81

4.2 INTERFACING THE BTRS REACTOR SYSTEM WITH THE ON-LINE GC 81
4.2.1 Electronic Communication between PLC, GC and Integrator 83
4.2.2 Flow Connection between Heated Enclosure and GC 84
4.2.3 Design of the Split Injector 86
4.2.4 Development of GC Temperature Program 87

4.3 MAJOR HARDWARE CHALLENGES 90
4.3.1 Inlet Check Valves for HPL Pumps 90
4.3.2 Seat Material for AE Brand Manual Operated Valves 91
4.3.3 Seat Materials for Multiposition Valves: Valcon T vs. Valcon E 91
4.3.4 Manual Control of Liquid Feed Flow 93
4.3.5 Heated Enclosure Design 94

4.4 SOFTWARE ISSUES 96
4.4.1 Software "Bugs" 96
4.4.2 Faulty PLC Module 96

CHAPTER 5: PRELIMINARY BATCH REACTOR STUDIES USING Y ZEOLITE 98

5.1 CATALYST PRE-TREATMENT AND STORAGE 98

5.2 BATCH REACTOR DESCRIPTION AND EXPERIMENTAL PROCEDURE 99

5.3 PRODUCT COLLECTION AND ANALYSIS 100

5.4 EFFECT OF STORING CATALYST IN HEPTANE 101

5.5 EFFECT OF PRE-SOAKING CATALYST WITH ISOBUTANE 102

5.6 EFFECT OF REACTION TEMPERATURE 104

5.7 EFFECT OF REACTION DURATION 106

CHAPTER 6: EFFECT OF PROCESS PARAMETERS ON ALKYLATION YIELD AND SELECTIVITY FOR EMT AND Y ZEOLITES IN A FLOW REACTOR 108

6.1 EXPERIMENTAL PROCEDURE 109

6.2 STAGES OF CATALYST ACTIVITY AND SELECTIVITY ON EMT AND Y ZEOLITES 110

6.3 SENSITIVITY ANALYSIS ON EMT AND Y ZEOLITES 116

6.4 EFFECT OF CALCINATION TEMPERATURE ON EMT AND Y ZEOLITES 117
6.4.1 Effect of Calcination Temperature on Butene Disappearance 118
6.4.2 Effect of Calcination Temperature on C_5+ Product Distribution 120
6.4.3 Effect of Calcination Temperature on C_8 Selectivity 124
6.4.4 Effect of Calcination Temperature on 2,2,4-TMP Level in TMP Fraction 128
6.4.5 Synopsis of Effect of Calcination Temperature 131

6.5 EFFECT OF REACTION TEMPERATURE ON EMT AND Y ZEOLITES 135
6.5.1 Effect of Reaction Temperature on Butene Disappearance 136
6.5.2 Effect of Reaction Temperature on C_5+ Product Distribution 137
6.5.3 Effect of Reaction Temperature on C_8 Selectivity 141
6.5.4 Effect of Reaction Temperature on TMP Selectivity 144
6.5.5 Synopsis of Effect of Reaction Temperature 147

6.6 EFFECT OF 1-BUTENE WHSV ON Y ZEOLITE 150
6.6.1 Effect of 1-$C_4^=$ WHSV on Butene Disappearance 151
6.6.2 Effect of 1-$C_4^=$ WHSV on C_5+ Product Distribution 152
6.6.3 Effect of 1-$C_4^=$ WHSV on C_8 Selectivity 154
6.6.4 Effect of 1-$C_4^=$ WHSV on TMP Selectivity 156
6.6.5 Synopsis of Effect of 1-$C_4^=$ WHSV 158

6.7 EFFECT OF CYCLICAL FEED OPERATION USING Y ZEOLITE 161

6.8 EFFECT OF CATALYST 164
6.8.1 Comparison of Calcination Temperature Effects on EMT and Y Zeolites 165
6.8.2 Comparison of Reaction Temperature Effects on EMT and Y Zeolites 166
6.8.3 Comparison of EMT and Y Control Experiments for Pt Study 167
6.8.1.1 Comparison of Control Experiments (for Pt Study) with respect to Butene Disappearance 168
6.8.1.2 Comparison of Control Experiments (for Pt Study) with respect to C_5+ Product Distribution 169
6.8.1.3 Comparison of Control Experiments (for Pt Study) with respect to C_8 Selectivity 169
6.8.1.4 Comparison of Control Experiments (for Pt Study) with respect to TMP Selectivity 172
6.8.1.4 Synopsis of Control Experiments (for Pt Study) Comparison 174

6.9 COMPARISON OF EMT AND Y ZEOLITES TO LITERATURE RESULTS 176

CHAPTER 7: PRELIMINARY STUDIES ON THE EFFECT OF Pt THE PERFORMANCE OF EMT AND Y ZEOLITES 181

7.1 EFFECT OF Pt ON FRESH CATALYST PERFORMANCE OF EMT AND Y ZEOLITES 182
7.1.1 Effect of Pt on Butene Disappearance for Fresh Catalysts 183
7.1.2 Effect of Pt on C_5+ Product Distribution for Fresh Catalysts 184

7.1.3 Effect of Pt on C_8 Selectivity for Fresh Catalysts 187
7.1.4 Effect of Pt on TMP Selectivity for Fresh Catalysts 187
7.1.5 Synopsis of Pt Effects for Fresh Catalysts 191

7.2 EFFECT OF Pt ON THE EFFICACY OF REGENERATION 202
7.2.1 Effect of Pt on Butene Disappearance for Regenerated Catalysts 202
7.2.2 Effect of Pt on C_5+ Product Distribution for Regenerated Catalysts 203
7.2.3 Effect of Pt on C_8 Selectivity for Regenerated Catalysts 210
7.2.4 Effect of Pt on TMP Selectivity for Regenerated Catalysts 217
7.2.5 Synopsis of Pt Effects for Regenerated Catalysts 217

CONCLUSIONS **222**

RECOMMENDATIONS **227**

REFERENCES **231**

APPENDIX 1: CATALYST PREPARATION AND CHARACTERIZATION **240**

A1.1 EMT SYNTHESIS 240

A1.2 PHASE IDENTIFICATION 242

A1.3 AMMONIUM ION EXCHANGE OF Na-EMT 243

A1.4 Na CONTENT 245
A1.4.1 Experimental 245
A1.4.2 Sample Calculation 247

A1.5 ^{29}Si AND ^{27}Al MAS NMR 248
A1.5.1 Experimental 248
A1.5.2 Sample Calculation for Si/Al Ratio 249

A1.6 TGA/DTA 254
A1.6.1 Experimental 254
A1.6.2 Sample Calculation 255

A1.7 BET SURFACE AREA ANALYSIS 256
A1.7.1 Experimental 256
A1.7.2 Sample Calculation 258

A1.8 MEASUREMENT OF Pt DISPERSION 259
A1.8.1 Experimental 259
A1.8.2 Sample Calculation 261

A1.9 MEASUREMENT OF PORE VOLUME 262
A1.9.1 Experimental 262
A1.9.2 Sample Calculation 263

APPENDIX 2: BTRS SYSTEM DIARY 265

APPENDIX 3: FLOW REACTOR OPERATION AND SAMPLE CALCULATIONS 275

A3.1 OPERATION OF FLOW REACTOR 275
A3.1.1 Overview of Wonderware Software 275
A3.1.2 Catalyst Addition 277
A3.1.3 Calcination/Reduction Procedure 279
A3.1.4 Feed Sampling 281
A3.1.5 Reaction and Product Analysis 283

A3.2 SAMPLE CALCULATIONS 286
A3.2.1 Butene WHSV 286
A3.2.2 Butene Conversion 287
A3.2.3 Mass Balance in Flow Reactor 288
A3.2.4 Number of Successful Catalyst Cycles 289
A3.2.5 Lennard Jones Diameter 289

APPENDIX 4: RAW DATA 291

A4.1 EXPERIMENTAL SUMMARY FOR PROCESS AND CATALYST EFFECTS 291

A4.2 RAW DATA 293

A4.3 SENSITIVITY ANALYSIS 354

Table of Figures

Figure		Page
1.1	Isomerization of 2,2,3-TMP$^+$ via Methyl and Hydride Shifts	12
1.2	Proposed States of Butene Adsorption on Heterogeneous Acid Sites, based on Quantum Mechanical Calculations	14
1.3	Routes for DMH Formation	21
2.1	Interconversion of Bronsted and Lewis Acidity on Zeolites	32
2.2	Schematic of Donor and Acceptor Phases for Spillover Species	53
2.3	Energetics for Spillover of Gaseous Diatomic Molecule from the Gas Phase to the Accepting Surface	54
2.4	Proposed Mechanism for Hydrogen Spillover Participation in Butene/Isobutane Alkylation	57
3.1	Polyhedral Cages occurring in cubic (Y, FAU) and hexagonal (EMT) phase Faujasites	60
3.2	Assembly of Faujasite Sheets to yield FAU and EMT Phases	62
3.3	Structure of 18-crown-6 Ether Template	63
3.4	Evolution of pH during the Aging and Crystallization Periods	66
3.5	Thermal Decomposition Patterns for Template Removal from EMT	68
3.6	Published Powder X-ray Diffraction Pattern for cubic (FAU) and hexagonal (EMT) phase Faujasites	69
3.7	Powder X-ray Diffraction Pattern of Synthesized EMT (Batch G5019)	70
4.1	Flow Schematic of BTRS Reactor System	78
4.2	Flow Schematic of BTRS Sampling System	80
4.3	Information Flow and Control Strategy of BTRS	82

Figure		Page
4.4	Interface between PLC, GC and Integrator	84
4.5	Sample Chromatogram of Alkylate Product	88
5.1	Timing of 1-$C_4^=$ Addition for Batch Reaction	103
6.1	Stages of Catalyst Activity on EMT Zeolite with respect to C_5+ Product Distribution	112
6.2	Stages of Catalyst Activity on EMT Zeolite with respect to C_8 Fraction Distribution	113
6.3	Stages of Catalyst Activity on Y Zeolite with respect to C_5+ Product Distribution	114
6.4	Stages of Catalyst Activity on Y Zeolite with respect to C_8 Fraction Distribution	115
6.5	Effect of EMT Calcination Temperature on C_5+ Product Distribution at a Reaction Temperature of 55°C	121
6.6	Effect of EMT Calcination Temperature on C_5+ Product Distribution for Reaction Temperatures between 77 and 100°C	122
6.7	Effect of Y Calcination Temperature on C_5+ Product Distribution for Reaction Temperatures between 70 and 100°C	123
6.8	Effect of EMT Calcination Temperature on C_8 Selectivity at a Reaction Temperature of 55°C	125
6.9	Effect of EMT Calcination Temperature on C_8 Selectivity for Reaction Temperatures between 77 and 100°C	126
6.10	Effect of Y Calcination Temperature on C_8 Selectivity for Reaction Temperatures between 70 and 100°C	127
6.11	Effect of EMT Calcination Temperature on 2,2,4-TMP Content in TMP Fraction for Reaction Temperatures between 55 and 100°C	129
6.12	Effect of EMT Calcination Temperature on 2,2,4-TMP Content in TMP Fraction for Reaction Temperatures between 55 and 100°C	130
6.13	Effect of Reaction Temperature on Useful Catalyst Lifetime for EMT and Y Zeolites	136

Figure		Page
6.14	Effect of Reaction Temperature on C_5+ Product Distribution on EMT Zeolite	138
6.15	Effect of Reaction Temperature on C_5+ Product Distribution on Y Zeolite	139
6.16	Effect of Reaction Temperature on C_8 Selectivity on EMT Zeolite	142
6.17	Effect of Reaction Temperature on C_8 Selectivity on Y Zeolite	143
6.18	Effect of Temperature on Thermal Equilibrium Composition of TMPs	146
6.19	Effe6t of Reaction Temperature on Surface Area of Spent Catalyst	148
6.20	Effect of Butene WHSV on C_5+ Product Distribution on Y Zeolite	153
6.21	Effect of Butene WHSV on C_8 Selectivity on Y Zeolite	155
6.22	Effect of Butene WHSV on 2,2,4-TMP Level in TMP Fraction on Y Zeolite	156
6.23	Effect of Butene Exposure on Surface Area of Spent Catalyst	159
6.24	Effect of Cyclical Feed Operation on Catalyst Activity and Selectivity using Y Zeolite	162
6.25	Effect of Catalyst Support on Butene Disappearance	168
6.26	Effect of Catalyst Support on C_5+ Product Distribution	170
6.27	Effect of Catalyst Support on C_8 Selectivity	171
6.28	Effect of Catalyst Support on 2,2,4-TMP Level in TMP Fraction	172
7.1	Effect of Pt on C_5+ Product Distribution of Fresh EMT Systems	185
7.2	Effect of Pt on C_5+ Product Distribution of Fresh Y Systems	186
7.3	Effect Pt on C_8 Selectivity of Fresh EMT Systems	188
7.4	Effect Pt on C_8 Selectivity of Fresh Y Systems	189
7.5	Stages of Catalyst Activity on 0.1%Pt/EMT with respect to C_5+ Product Distribution	192

Figure		Page
7.6	Stages of Catalyst Activity on 0.1%Pt/EMT with respect to C_8 Fraction Distribution	193
7.7	Stages of Catalyst Activity on 0.5%Pt/EMT with respect to C_5+ Product Distribution	194
7.8	Stages of Catalyst Activity on 0.5%Pt/EMT with respect to C_8 Fraction Distribution	195
7.9	Stages of Catalyst Activity on 0.5%Pt/Y with respect to C_5+ Product Distribution	196
7.10	Stages of Catalyst Activity on 0.5%Pt/Y with respect to C_8 Fraction Distribution	197
7.11	Proposed Effect of Excessive Hydrogen Spillover Participation	200
7.12	Effect of Regeneration on C_5+ Product Distribution of EMT	204
7.13	Effect of Regeneration on C_5+ Product Distribution of Y	205
7.14	Effect of 0.1%Pt Loading on Regeneration of EMT with respect to C_5+ Product Distribution	207
7.15	Effect of 0.5%Pt Loading on Regeneration of EMT with respect to C_5+ Product Distribution	208
7.16	Effect of 0.5%Pt Loading on Regeneration of Y with respect to C_5+ Product Distribution	209
7.17	Effect of Regeneration on C_8 Selectivity of EMT	211
7.18	Effect of Regeneration on C_8 Selectivity of Y	212
7.19	Effect of 0.1%Pt Loading on Regeneration of EMT with respect to C_8 Selectivity	214
7.20	Effect of 0.5%Pt Loading on Regeneration of EMT with respect to C_8 Selectivity	215
7.21	Effect of 0.5%Pt Loading on Regeneration of Y with respect to C_8 Selectivity	216
A1.1	Methodology for Ammonium Ion Exchange of Na-EMT	244

Figure		Page
A1.2	Solutions for Method of Additions	246
A1.3	Absorbance Spectra for Digested EMT	247
A1.4	^{29}Si MAS NMR for EMT Zeolite	250
A1.5	^{29}Si MAS NMR for Y Zeolite	251
A1.6	^{27}Al MAS NMR for EMT Zeolite	252
A1.7	^{27}Al MAS NMR for Y Zeolite	253
A1.8	TGA/DTA Data for Run F29Y	255
A1.9	Multipoint BET Plot for F29Y	258
A1.10	H_2 Chemisorption Data for 0.5%Pt/EMT	262
A1.11	N_2 Isotherm for Y Zeolite	264
A3.1	Catalyst Bed in Flow Reactor	278
A3.2	Gas Supplies for MFC Inlets	279

Table of Tables

Table		Page
1.1	CAA Formulation Requirements for RFG	2
1.2	Pure Component Octane Numbers	6
1.3	Typical Product Distribution from *n*-Butene/Isobutane Alkylation using H_2SO_4 Catalyst	7
1.4	Comparison of 1-Butene Isomerizaiton on REHY with Thermal Equilibrium Composition	9
1.5	Comparison of TMP and DMH Selectivity on Liquid and Solid Acid Catalysts, with Thermal Equilibrium Composition	24
2.1	Structural Properties of Y and USY	34
2.2	Acidity of USY Samples, on the Basis of IR Pyridine Adsorption as a Function of DesorptionTemperature	35
2.3	Alkylate Product Distribution on USY, as a Function of UCS	37
2.4	Structural Properties of EMT and FAU	40
2.5	Acidity of EMT, La-exchanged EMT, FAU and USY, on the Basis of IR Pyridine Adsorption as a Function of DesorptionTemperature	41
2.6	Analysis of Acid Site Distribution with respect to Site Type and Strength, for EMT, La-exchanged EMT, FAU and USY	42
2.7	Alkylate Product Distribution on Ce-Y, H-FAU and H-EMT	44
2.8	Alkylate Product Distribution on Parent and Dealuminated FAU and EMT	46
2.9	Alkylate Product Distribution on EMT and La-Exchanged EMT	49
3.1	Chemical Sources and their Function in EMT Synthesis	62
3.2	List of Materials for EMT Synthesis	64

Table		Page
3.3	ANOVA Analysis on Batch Surface Area Measurement for Na-EMT	71
3.4	Summary of Catalyst Properties for EMT and Y	72
3.5	Quantities used in the Preparation of Pt/EMT and Pt/Y Systems	73
3.6	Summary of Catalyst Properties for Pt/EMT and Pt/Y Systems	75
4.1	Operating Conditions of GC and Integrator for Alkylate Analysis	89
5.1	Effect of Catalyst Storage Method on Batch Reactor Alkylate Composition	102
5.2	Effect of Pre-Soaking Catalyst (stored in heptane) with Isobutane on Batch Rector Alkylate Composition	104
5.3	Effect of Reaction Temperature on Batch Reactor Alkylate Composition	105
5.4	Effect of Reaction Duration on Batch Reactor Alkylate Composition	106
6.1	Sensitivity Analysis for Measures of Catalyst Performance of Flow Runs using EMT and Y Zeolites	117
6.2	Effect of Calcination Temperature on Useful Catalyst Lifetime period of EMT and Y Zeolites	119
6.3	Effect of Calcination Temperature on Catalyst Performance and Average Alkylate Quality using EMT and Y Zeolites	132
6.4	Effect of Calcination Temperature on Surface Area of Spent Catlayst	134
6.5	TGA/DTA of Spent EMT as a Function of Calcination Temperatures	135
6.6	Effect of Reaction Temperature on Average Alkylate Quality using EMT and Y Zeolites	145
6.7	Effect of Reaction Temperature on Catalyst Properties	149
6.8	Effect of Butene WHSV on the Number of Successful Catalyst Cycles Achieved during the Useful Catalyst Lifetime period on Y Zeolite	151
6.9	Effect of Butene WHSV on Catalyst Performance of Y Zeolite	157

Table		Page
6.10	Comparison of TMP Selectivity, using Different Catalyst Systems, with Thermal Equilibrium Values	158
6.11	Effect of Butene WHSV on Properties of Spent Catalyst	160
6.12	Comparison of Average Catalyst Performance on EMT and Y Zeolites	173
6.13	Comparison of EMT and Y Spent Catalyst Properties	176
6.9	Comparison of Experimental EMT and Y Alkylation Data with Literature Results	178
7.1	Effect of Pt on Useful Catalyst Lifetime period of Fresh EMT and Y Systems	184
7.2	Comparison of Average Catalyst Activity during first 5 min of Useful Catalyst Lifetime Period for Fresh Parent and Pt Supported Catalysts	190
7.3	Effect of Pt Presence on TGA/DTA Measurements of Spent Catalysts	201
7.4	Effect of Pt on Useful Catalyst Lifetime of Fresh and Regenerated EMT and Y Systems	203
7.5	Comparison of Average Catalyst Activity during first 5 min of Useful Catalyst Lifetime Period for Regenerated Parent and Supported Catalysts	218
7.6	Effect of Pt on TGA/DTA Measurements of Regenerated Catalysts	220
A1.1	Description of Reagents Employed for EMT Synthesis	240
A1.2	Reagents in EMT Synthesis	242
A1.3	Sample Calculation of Si/Al Ratio for EMT using ^{29}Si MAS NMR Data	249
A1.4	T_d vs. Weight % from TGA/DTA Data for F29Y	256
A3.1	Automatic Cycle Recipe for Calcination Cycle	280
A3.2	Sample Control Recipe for Calcination Cycle	281
A3.3	Automatic Cycle Recipe for Feed Sampling Program	282
A3.4	Sample Control Recipe for Feed Analysis	283

Table		Page
A3.5	Automatic Cycle Recipe for Reaction	284
A3.6	Sample Control Recipe for Reaction - Sample Collection	285
A3.7	Sample Control Recipe for Reaction - Product Analysis	286
A3.8	Calculation of Butene Mass Flow Rate for Run F66EMT	287
A3.9	Calculation of Lennard-Jones Diameter for TMP Isomers	290
A4.1	Experimental Summary for Effect of Calcination Temperature	291
A4.2	Experimental Summary for Effect of Reaction Temperature	291
A4.3	Experimental Summary for Effect of Butene WHSV	292
A4.4	Experimental Summary for Effect of Pt Supported on Acidic Carrier	292
A4.5	Complete Experimental Summary	293
A4.6	Experimental Summary for Replicated Experiments	354

Nomenclature

AA	atomic absorption
AE	Autoclave Engineers
A/H	acid to hydrocarbon ratio
ANOVA	analysis of variance method
alkylate	C_5^+ liquid produced from butene/isobutane alkylation
BET	Brunauer-Emmett-Teller method
BPR	back pressure regulator
CAA	Clean Air Act
Ce-Y	Cerium exchanged Y zeolite
CE	18-crown-6 ether template used in EMT synthesis
DMH	dimethylhexanes
DTA/TGA	differential temperature analysis used in conjunction with thermogravimetric analysis
EFAL	extraframework aluminum in zeolite structure
EMT	acidic form of hexagonal phase faujasite prepared using 18-crown-6 ether template
ESR	electron spin resonance
FAU	acidic form of cubic phase faujasite prepared using a 15-crown-5 ether template
FCC	fluid catalytic cracking
FID	flame ionization detector
FTIR	Fourier Transform Infrared Spectroscopy
GC	gas chromatography
GC-MS	gas chromatography used in conjunction with mass spectroscopy

H_o	Hammett acidity
H_{so}	spillover hydrogen
H-EMT	acidic form of EMT zeolite
HPLC	high pressure liquid pump
HTL	heated transfer line
H-Y	acidic form of Y zeolite
ID	inner diameter
i-NNN	i next-nearest alumina neighbours in a zeolite framework where i = 0 to 4
I/O	isoparaffin (isobutane) to olefin (butene) molar ratio in feed stream
IR	Infrared spectroscopy
LaxEMT	x % of Na are exchanged for La in EMT
MFC	mass flow controller
MON	motor octane number
MSA	mesoporous silica alumina
MTBE	methyl tertiary butyl ether
Na-EMT	sodium form of EMT zeolite
Na-Y	sodium form of Y zeolite
NMR	nuclear magnetic reasonance
NMRPG	nuclear magnetic reasonance pulse field gradient method
PC	personal computer
PE	Perkin Elmer
PLC	programmable logic controller
RE	rare earth metal
RE-Y	rare earth metal exchanged Y zeolite
RE-USY	rare earth metal exchanged Ultra Stable Y zeolite
RFG	reformulated gasoline to meet CAA requirements
RON	research octane number
RVP	Reid vapour pressure
SA	surface area

Si/Al	Silicon to aluminum mole ratio
surf	surface
TEOS	tetraethylortho silicate
TGA	thermogravimetric analysis
TMOS	tetramethylortho silicate
TMP	trimethylpentane
TMP/DMH	trimethylpentane to dimethylhexane mole ratio
TOS	time on stream
TPD	temperature programmed desorption
UCS	unit cell size
UHP	ultra high purity
USHY	ultrastable HY
WHSV	weight hourly space velocity
XRD	powder X-ray diffraction
Y	acidic form of Y
C_5+	hydrocarbons with greater than or equal to 5 carbons in their structure
C_5-C_7	hydrocarbons with between 5 to 7 carbons in their structure
$C_8^=$	olefins containing 8 carbons in the structure
C_8	hydrocarbon with 8 carbons in the structure
C_9+	hydrocarbons with greater than or equal to 9 carbons in their structure
0.1 % Pt/EMT	0.1 % Pt impregnated on H-EMT
0.5 % Pt/EMT	0.5 % Pt impregnated on H-EMT
0.5 % Pt/Y	0.5 % Pt impregnated on H-Y

Letters of Permission for use of Published Figures

Dear Ms Walker

MICROPOROUS & MESOPOROUS MATERIALS,(Formerely known as Zeolites)Vol 10, pp 546-552, "Synthesis of new silica..."Figures 4 and 5 only, Vol 9, pp 423-427, "Investigation of the pore..."Figure 1 only.

As per your letter, we hereby grant you permission to reprint the aforementioned material at no charge in your thesis subject to the following conditions:

1. If any part of the material to be used (for example, figures) has appeared in our publication with credit or acknowledgement to another source, permission must also be sought from that source. If such permission is not obtained then that material may not be included in your publication/copies.

2. Suitable acknowledgment to the source must be made as follows:

"Reprinted from Journal title, Volume number, Author(s), Title of article, Pages No., Copyright (Year), with permission from Elsevier Science".

3. Reproduction of this material is confined to the purpose for which permission is hereby given.

4. This permission is granted for non-exclusive world English rights only. For other languages please reapply separately for each one required. Permission excludes use in an electronic form. Should you have a specific electronic project in mind please reapply for permission.

5. This includes permission for the National Library of Canada to supply single copies, on demand, of the complete thesis. Should your thesis be published commercially, please reapply for permission.

Yours sincerely

Frances Rothwell (Mrs)
Subsidiary Rights Manager

The processing of permission requests for all Elsevier Science (including Pergamon imprint) journals has been centralised in Oxford, UK. Your future requests will be handled more quickly if you write directly to: Subsidiary Rights Department, Elsevier Science, PO Box 800, Oxford OX5 1DX, UK. Fax: 44-1865 853333; e-mail: permissions@elsevier.co.uk

Permission Request Form

ACS PUBLICATIONS DIVISION
JAN 2 4 2000
COPYRIGHT OFFICE

PERMISSION REQUEST FORM

Date: Jan. 17/00

To: Copyright Office
Publications Division
American Chemical Society
1155 Sixteenth Street, N.W.
Washington, DC 20036

FAX: 202-776-8112

From: Gail Walker, PhD candidate
Dept. of Chem. Eng.,
University of Waterloo
Waterloo, Ontario, Canada
N2L 3G1
Your Phone No. (519) 886-5684
Your Fax No. c.o. Larry Rodricks
(519) 579-8986

PhD thesis

I am preparing a paper entitled:
"the elucidation of 1-Butene with isobutane using EMT and Y zeolites"
to appear in a (circle one) book, magazine, journal, proceedings, other (thesis)
at
entitled: Dept. of Chem. Eng., University of Waterloo
~~to be published by:~~ Waterloo, Ontario, Canada

I would appreciate your permission to use the following ACS material in print and other formats with the understanding that the required ACS copyright credit line will appear with each item and that this permission is for only the requested work listed above:

From ACS journals or magazines (for ACS magazines, also include issue no.):
ACS Publication Title Issue Date Vol. No. Page(s) Material to be used*
Journal of the American Chemical Society
Volume: 116 Issue: 7 Year: 1994
Figure 1 on page 2951
from article "Role of 18-crown-6 and 15-crown-5 ethers in the Crystallization of Polytype Faujasite Zeolites"

From ACS books: include ACS book title, series name and number, year, page(s), book editor's name(s), chapter author's name(s), and material to be used, such as Figs. 2 & 3, full text, etc.*

* If you use more than three figures/tables from any article and/or chapter, the author's permission will also be required.
Questions? Please call Arleen Courtney at (202) 872-4368.

This space is reserved for
ACS Copyright Office Use

PERMISSION GRANTED BY THE AMERICAN CHEMICAL SOCIETY
ACS COPYRIGHT CREDIT LINE REQUIRED. Please follow this Sample: Reprinted with permission from [reference citation]. Copyright [year] American Chemical Society.
PUBLICATIONS Division
ACS
1155 - 16th St., N.W.
Washington, DC 20036
APPROVED BY C. Arleen Courtney
ACS Copyright Office
1-27-00
☐ If this box is checked, author permission is also required. See original article for address.

12/3/99

1/17/00 1:31 PM

Chapter 1

Introduction

1.1 MERIT OF ALKYLATION RESEARCH

Ground-level ozone, formed by photochemical reactions involving nitrogen oxides and hydrocarbons, is a serious air pollution problem. Automobiles contribute roughly one-third of the total hydrocarbon emissions feeding this problem. The U.S. Clean Air Act (CAA) of 1990, has favoured strict upper limits on the Reid vapour pressure (RVP), as well as the oxygenate, benzene, aromatic and olefin content in

the gasoline pool (Gonzalez, 1992; Rhodes, 1994; Khan & Reynolds, 1996). This has directed a dramatic review of current gasoline composition, in an effort to combat this problem (see Table 1.1). Refineries are being forced to reformulate gasoline composition, to satisfy environmental regulations while still maintaining high efficiency and performance.

Table 1.1: CAA Formulation Requirements for RFG

Gasoline Property	RFG Specification
RVP	7.2 psi max.
Oxygen	2 wt. % min.
Benzene	1 vol. % max.
Aromatics	25 vol. % max.
Olefins	9.9 vol. % max.
Sulfur	500 ppm max.
Metals	none

Aromatics represent a high energy, high octane value fraction of gasoline. Therefore, restrictions in the amounts of aromatics, implies an overall reduction in the octane rating and energy content of the gasoline pool. Oxygenates are a viable blending stock to elevate octane rating; however, they possess the lowest energy content of all components in gasoline (Rhodes, 1994a). In addition, they have not demonstrated a positive effect on ozone formation (Bell et al, 1995). Clearly, they are not the sole answer.

Alkylate, the product of alkylation reactions, is an ideal candidate to resolve this issue. The term "alkylation", encompasses any reaction involving the addition of alkyl groups to an organic molecule, to yield a branched organic product. Highly branched alkanes possess both a high Motor Octane Number (MON) and Research Octane Number (RON). For this reason, alkylate has become the preferred blending stock in reformulated gasoline. Aside from enhancing octane levels, it is clean burning producing less emissions, possesses low volatility and density and contains

no sulfur or aromatics. There are projections that alkylate will eventually comprise 36 % of the reformulated gasoline in the U.S to meet the stringent criteria (Corma & Martinez, 1993). This would require between 10 to 35 % expansion of existing capacity to meet this demand.

Alkylation of butene with isobutane, offers several advantages over other alkylation reactions. Firstly, isooctane, the product of this reaction, has a very high octane rating. Another advantage of alkylation of butene with isobutane, is that the C_4 reactants necessary for this reaction, are readily available as a low value Raffinate I (by-product of fluid catalytic cracking (FCC) and steam cracking units) as well as Raffinate II (raffinate from MTBE process).

1.2 BUTENE/ISOBUTANE ALKYLATION WITH LIQUID ACIDS

1.2.1 Commercial Liquid Acid Catalysts

The two catalysts, which are used commercially for the alkylation of isobutane with C_3 to C_5 olefins, are sulfuric acid and hydrofluoric acid. In 1994, approximately 212,000 m^3/d of alkylate were produced worldwide from these feedstocks, with roughly 60 % made from HF alkylation units (Sheckler et al, 1994; Rao & Vatcha, 1996).

The mechanisms using each liquid acid are different, with HF demonstrating superior activity for the production of high octane alkylate. Although Hammett acidity measurements indicate that H_2SO_4 possesses a higher acid strength than HF (Misono & Okuhara, 1993), the solubility of isobutane in HF is superior. Hydrofluoric acid is better able to facilitate hydride transfer reactions between dissolved isobutane and octyl carbenium ions, resulting in superior alkylate quality. Overall, HF demonstrates higher activity for isoparaffin/olefin alkylation relative to H_2SO_4 and is the preferred liquid acid (Corma & Martinez, 1993). In addition, catalyst costs are much lower for

HF processes relative to those involving H_2SO_4.

Unfortunately, both catalyst systems pose significant corrosion hazards during transportation, storage and handling. The formation of acidic, sludge-containing spent acid and high molecular weight hydrocarbons, is an unavoidable by-product of the H_2SO_4 process. The sludge must be separated and regenerated off site to recycle the acid, incurring additional risk and expense. The residual acidic sludge must be disposed, presenting further environmental concern and cost to the operation.

The high volatility of HF makes it prone to forming mists upon release to the atmosphere, endangering public safety. The modification of HF through the use of less volatile pyridinium-polyhydrogen fluoride (PPHF) has repressed this tendency making HF operation somewhat safer.

Since 1990, there has been substantial pressure to develop a more environmentally friendly catalyst for alkylation of isobutane with normal C_3 to C_4 olefins. Economic advantages also exist in replacing liquid acid technology. Liquid acid costs account for approximately 30 % of the total catalyst cost in petroleum refining (Corma & Martinez, 1993). In addition, the rate of catalyst consumption for H_2SO_4 alkylation processing is two orders of magnitude (by weight) greater than that for catalytic cracking catalysed by zeolites (Corma & Martinez, 1993). Clearly, the potential for economic benefits in replacing liquid acid technology, and the more benign nature of solid acids, encourage further research in this area.

1.2.2 Product Distribution from Liquid Acid Catalysed Butene/Isobutane Alkylation

The reaction temperature for H_2SO_4 catalysed butene/isobutane alkylation is in the range of 0 to 10°C and employs an I/O ratio (molar ratio of isoparaffin/olefin in feed stream) between 5 to 8. Hydrofluoric acid systems can operate at higher temperatures, in the vicinity of 10 to 40°C, but require higher I/O ratios in the range of

10 to 15.

The principle of partial molal quantities can be used to estimate the octane values of the alkylate produced from both processes (Hutson & Logan, 1975) (see Equation 1-1):

$$\text{Octane Number}_{\text{Alkylate}} = \sum_{i=1}^{n} (\text{Octane Number}_{\text{Pure Cmpt } i}) (\text{Mole Fraction}_{\text{Cmpt } i}) \quad (1\text{-}1)$$

Using pure component octane numbers (see Table 1.2), the octane number of the alkylate can be calculated.

Octane values of alkylate from processes using H_2SO_4 or HF, range from 95 to 98 (Corma & Martinez, 1993). In general, butene/isobutane alkylate using H_2SO_4, is lower in octane value relative to the product from the HF process. A typical alkylate product distribution from butene/isobutane alkylation using H_2SO_4 is shown in Table 1.3.

Trimethylpentanes (TMPs) are the preferred products of alkylation, as they possess a RON $\geq$ 100 (see Table 1.2). The isomer, 2,2,4-TMP, is the preferred isomer since it has the highest MON with zero sensitivity (difference between MON and RON). Although other TMP isomers exhibit higher RON values, they also show significantly greater sensitivity levels. Dimethylhexanes (DMH) are secondary products and possess an octane number between 55 and 82. Clearly, maximizing the TMP/DMH ratio is the goal of any alkylation process.

Conjunct polymers are acid-soluble polymers, or red oil, with a molecular weight in the general range of 300 to 500. This high molecular weight material is formed as a minor by-product during the alkylation of isobutane with butene, particularly when H_2SO_4 is employed and less so with HF (Albright et al, 1988). Conjuct polymers contain C_5 and possibly C_6 ring groups and are highly unsaturated, with a hydrogen to carbon ratio of 1.52 to 1.75 (Albright et al, 1993). A small amount of conjunct polymers is desirable in liquid acid catalysed alkylation as they are excellent sources of hydride ions and improve alkylate quality. Excessive levels of

the polymers dilute the strength of the liquid acid reducing its effectiveness. Feed acids typically contain 98 to 99 % acid, with the balance being water. For H_2SO_4, spent acids consist of 90 to 92 % acid, 4 to 6 % conjunct polymers and the remainder is water (Albright et al, 1988).

Table 1.2: Pure Component Octane Numbers[1]

Component		RON[2]	MON[3]	Sensitivity = RON - MON[4]
C_4	*i*-C_4	102.1	97.0	5.1
	n-C_4	94.0	89.1	4.9
C_5	*i*-C_5	93.0	89.7	3.3
	n-C_5	61.8	63.2	-1.4
C_6	2,2-DMB	91.8	93.4	-1.6
	2,3-DMB	104.3	94.2	10.1
	2-MP	73.4	73.5	-0.1
	3-MP	74.5	73.3	1.2
	n-C_6	24.8	26.0	-1.2
C_7	2-MH	42.4	46.4	-4.0
	3-MH	52.0	55.0	-3.0
	2,2-DMP	92.8	95.6	-2.8
	2,3-DMP	91.1	88.5	2.6
	2,4-DMP	83.1	83.8	-0.7
	3,3-DMP	80.8	86.6	-5.8
	2,2,3-TMB	112.1	101.3	10.8
C_8	2-MHp	21.7	23.8	-2.1
	3-MHp	26.8	35.0	-8.2
	2,2-DMH	72.0	77.0	-5.0
	2,3-DMH	71.3	78.9	-7.6
	2,4-DMH	65.2	69.9	-4.7
	2,5-DMH	55.5	55.7	-0.2
	3,4-DMH	76.3	81.7	-5.4
	2,2,3-TMP	109.6	99.9	9.7
	2,2,4-TMP	100.0	100.0	0.0
	2,3,3-TMP	106.1	99.4	6.7
	2,3,4-TMP	102.7	95.9	6.8
C_9	2,2,5-TMH	91.0	88.0	3.0

1 Hutson & Logan, 1975; Chauvin et al, 1994; Olah et al, 1996
2 RON is a measure of highway performance of fuel
3 MON is a measure of city performance of fuel
4 Sensitivity is difference between highway and city performance of fuel

Table 1.3: Typical Product Distribution from *n*-Butene/Isobutane Alkylation using H_2SO_4 Catalyst[1]

C_5^+ Liquid (mol %)	
C_5 - C_7	7.5
C_8	88.1
C_9^+	4.4
C_8 Fraction (mol %)	
TMP	90.8
DMH	9.2
Indicators	
TMP / DMH	9.9
RON	97.8
MON	93.9
(RON + MON) / 2	95.9

1 Albright et al, 1992; Corma & Martinez, 1993

1.3 MAJOR PROCESS LICENSORS ENGAGED IN SOLID ACID CATALYSED BUTENE/ISOBUTANE ALKYLATION RESEARCH

Many companies are actively engaged in the development of an alternative catalyst for alkylation of isobutane with butene. The success of zeolites in catalytic cracking, created interest in applying them for isoparaffin-olefin alkylation reactions. Zeolites display high initial activity but deactivate rapidly. To date, no technology has reached commercial success (Rotman, 1996).

The Exxon / Haldor Topsoe A/S /Kellog process uses fixed-bed technology (Rhodes, 1994b), and a catalyst consisting of liquid trifluoromethane sulfonic acid supported on a solid silica medium (Crossland, 1993). The paraffin-olefin mixture is passed through the catalyst bed and the flow reversed when acid is detected in the product stream. The process has been tested at a 0.5 b/d pilot plant starting in 1991 (Rhodes, 1994a; Rotman, 1996). Existing reactor systems would have to be replaced

to employ this technology.

The catalyst technology used in the Kerr-McGee (HAT Process) system is a very low concentration of hydrocarbon-soluble alkylaluminum chloride (Crossland, 1993; Rhodes, 1994b). The catalyst is first mixed with the isobutane and then mixed with the olefin stream. As the reaction nears completion, the catalyst degrades to a less active form and precipitates out of solution. The spent catalyst is gravity-separated and regenerated. The HAT process has lower operating costs than those using H_2SO_4 and offers the advantage of retrofit capabilities with existing HF units.

The catalyst technology for the Catalytica / Neste / Conoco process involves a solid and inexpensive catalyst incorporating BF_3 on an ETA/Gamma alumina or zirconium carrier (Crossland, 1993; Rhodes, 1994b). The 7 b/d pilot plant unit has experienced difficulties in keeping the acid on the carrier. Although a slight financial advantage over H_2SO_4 technology has been demonstrated, the margin is not sufficient to justify implementation of the new technology. This group is currently looking for additional partners to continue the program (Rotman, 1996).

Chemical Research & Licensing Co. (CR & L) / Chevron / Sheridan have developed technology which uses a slurry catalyst, involving an organometallic "salt" of SbF_5 supported on a SiO_2 carrier (Rhodes, 1994a; Rotman, 1996). A refinery pilot plant running at 10 b/d, has been in operation since 1993, using temperatures in the range of H_2SO_4 systems.

Several other groups are pursuing research in alkylation, but details are not as readily available (Crossland, 1993). Mobil Oil is exploring catalysts of the type $BF_3 \cdot H_3PO_4$, $BF_3 \cdot SiO_2$ or BF_3 supported on β-zeolite. Institute Français du Pétrole (IFP) is applying fluorine modified zeolite. UOP is examining carbon supported HF and several zeolites.

1.4 PROPOSED BUTENE/ISOBUTANE ALKYLATION REACTION MECHANISM ON SOLID ACIDS

1.4.1. Traditional Mechanism via Carbenium Ions

It is generally accepted that isoparaffin-olefin alkylation proceeds via a carbenium ion mechanism, in the presence of a liquid acid catalyst. Although it is assumed that the same type of mechanism proceeds on a heterogeneous catalyst, no direct evidence has been show to support this theory.

The mechanism for the alkylation of 1-$C_4^=$ with *i*-C_4 will be described (Corma et al, 1993). Isomerization of 1-$C_4^=$ is rapidly facilitated on fresh and aged Y zeolites (see Table 1.4), with 2-$C_4^=$ being the preferred isomer (Chu & Chester, 1986).

Table 1.4: Comparison of 1-Butene Isomerization on REHY[1] with Thermal Equilibrium Composition
(semi-batch reactor; T_{calc}=538°C; T_{rxn}=91°C; P=320psig; $C_4^=$ WHSV=7.2h^{-1}; I/O=9)

Butene Isomer	REHY @ 90°C (Experimentally Determined)		Thermal Equilibrium @ 90°C
	Fresh	Aged	
1-$C_4^=$	22	15	1.9
trans-2-$C_4^=$	48	58	10.7
cis-2-$C_4^=$	30	27	10.3
i-$C_4^=$	N.D.	N.D.	77.1

1 Chu & Chester, 1986
N.D. = not detected

Although the formation of *i*-$C_4^=$ is highly favoured thermodynamically, based on calculations using $\Delta H_f°$ and $\Delta S_f°$ data (Reid, Prausnitz & Sherwood, 1977), it is rarely detected in alkylation reactor effluents. This is believed to be a consequence of its highly reactive nature.

1.4.1.1 Protonation of the olefin to form sec-C_4^+ ion

The first step of the mechanism is the protonation of the olefin (C_nH_{2n}), by a Bronsted acid site ($H^+_{(surf)}$), to form a secondary butyl carbenium ion (note that *sec*-$C_nH_{(2n+1)}{}^+_{(surf)}$ = *sec*-$C_4{}^+_{(surf)}$) (see Equation 1-2).

$$C{=}C-C-C \quad + \quad H^+_{(surf)} \longrightarrow \quad C-C^+-C-C_{(surf)} \qquad (1\text{-}2)$$

This initiation step is highly important in the early stages of the reaction, in order to generate high surface concentration of ions.

1.4.1.2 Formation of tert-C_4^+ ion

Isomerization of primary and secondary-butyl carbenium ions, via hydride and methyl shifts, are not highly favoured, as they are short chain carbocations. Rather, a more likely event is hydride transfer from an adsorbed molecule of isobutane, to form a more stable, tertiary butyl carbenium ion (*tert*-C_4^+) and *n*-butane (see Equation 1-3).

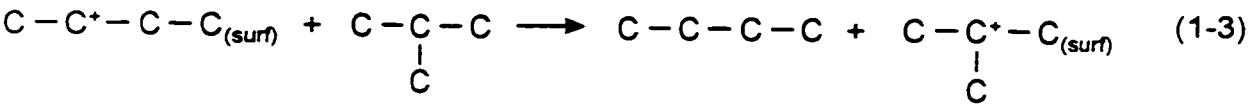

$$C-C^+-C-C_{(surf)} + C-\underset{\displaystyle C}{\underset{|}{C}}-C \longrightarrow C-C-C-C + C-\underset{\displaystyle C}{\underset{|}{C^+}}-C_{(surf)} \qquad (1\text{-}3)$$

Hydride transfer to secondary carbenium ions (*sec*-R^+) is very slow and therefore, an induction period is often observed until a high concentration of *tert*-C_4^+ has been generated (Corma & Martinez, 1993). At longer reaction times, regeneration of the *tert*-C_4^+ is facilitated in the last stage of the chain sequence.

Another possible route of *tert*-C_4^+ formation, involves hydride transfer from isobutane to an adsorbed tertiary carbenium ion (*tert*-R^+) since hydride transfer to *tert*-R^+ is faster than to *sec*-R^+ (Cardona et al, 1995) (see Equation 1-4):

$$tert\text{-}R^+_{(surf)} + i\text{-}C_4 \longrightarrow R + tert\text{-}C_4^+{}_{(surf)} \qquad (1\text{-}4)$$

1.4.1.3 Addition of tert-C_4^+ ion to second olefin

The *tert*-C_4^+ combines with a second butene molecule to form the corresponding C_8 carbenium ion (see Equation 1-5).

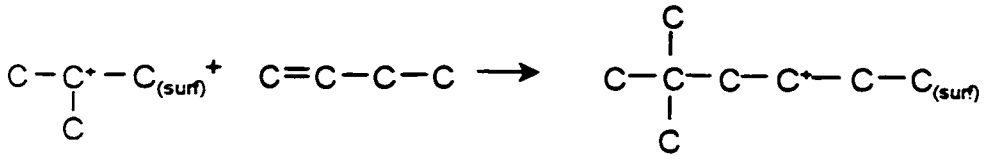

2,2-DMH$^+$ (1-5)

The addition of *tert*-C_4^+ to other isomers of butene (see Equations 1-6 and 1-7) are also illustrated, as they will be present due to the rapid isomerization of 1-$C_4^=$ to 2-$C_4^=$ and *i*-$C_4^=$ on solid acid catalysts (Chu & Chester, 1986).

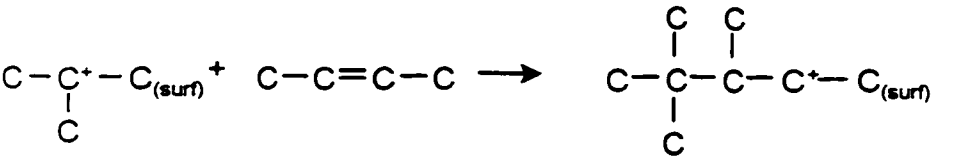

2,2,3-TMP$^+$ (1-6)

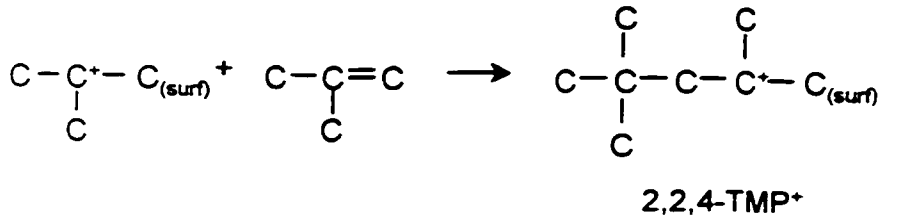

(1-7)

1.4.1.4 Isomerization of C_8^+ ion to more stable forms

The octyl carbenium ion may undergo rapid isomerization, via hydride and methyl shifts, to form more stable carbenium ions (note that hydride shifts are much faster than methyl shifts). The rearrangements, which are possible for 2,2,3-TMP$^+$, are illustrated in Figure 1.1.

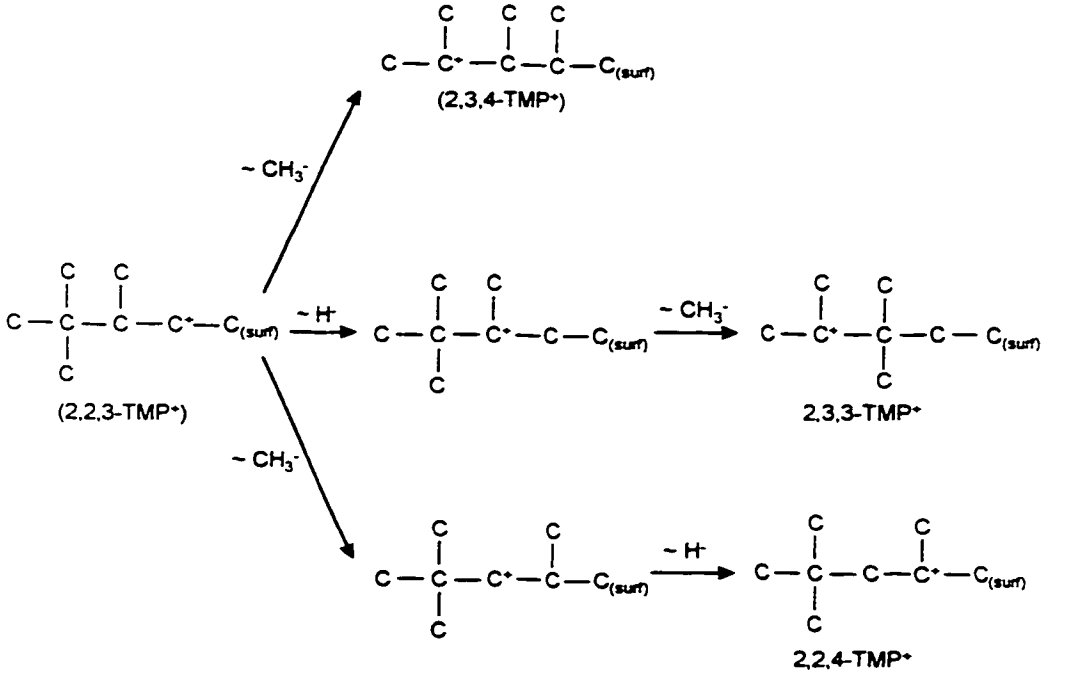

Figure 1.1: Isomerization of 2,2,3-TMP$^+$ via Methyl and Hydride Shifts

1.4.1.5 Hydride transfer to C_8^+ ion

The octyl carbenium ion can undergo hydride transfer from isobutane, yielding the corresponding isoparaffin. In addition, the *tert*-butyl cation is regenerated in this last step thus perpetuating the chain sequence. The reaction involving 2,2,4-TMP$^+$ is shown in Equation 1-8. Relative amounts of *n*-butane and TMPs in the product distribution during the initial stages of the reaction, suggest that the formation of *tert*-butyl cation, via Equation 1-3, is approximately 15 times slower than that produced via Equation 1-8, on Ultrastable HY (USY) (Cardona et al, 1995).

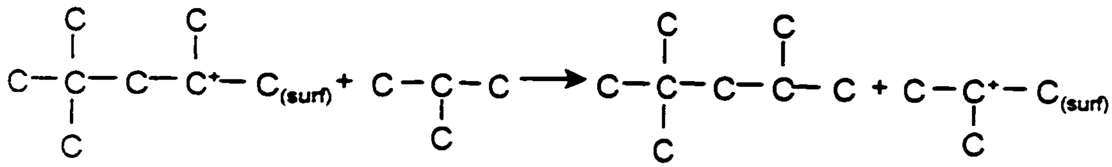

(1-8)

2,2,4-TMP

It is also possible for hydride transfer to be facilitated by a molecule other than isobutane (see Equation 1-9):

$$C_8^+{}_{(surf)} + R \longrightarrow C_8 + R^+{}_{(surf)} \qquad (1\text{-}9)$$

1.4.2 Mechanism via Covalent Surface Esters

Recently, it has been suggested that acidic heterogeneous conversion of hydrocarbons is facilitated by the bifunctional character of zeolite catalysts of high Si content, complementing the traditional carbenium ion mechanism. It is proposed that

a Bronsted site transfers a proton to the adsorbed molecule, while simultaneously, a proton is abstracted from the "protonated" species by a surface basic site (Pine et al, 1984; van Santen, 1991).

The driving force of this concerted mechanism is the compensation effect of energy gained from broken bonds, with energy required for those which are newly formed, thus eliminating excessive activation barriers. The adsorbed species can be regarded as a covalently bonded surface ester rather than a carbenium ion (see Figure 1.2). These results were substantiated using quantum mechanical calculations, to determine the geometry and electronic structure of the surface alkoxides in their ground state (Kazansky & Senchenya, 1989).

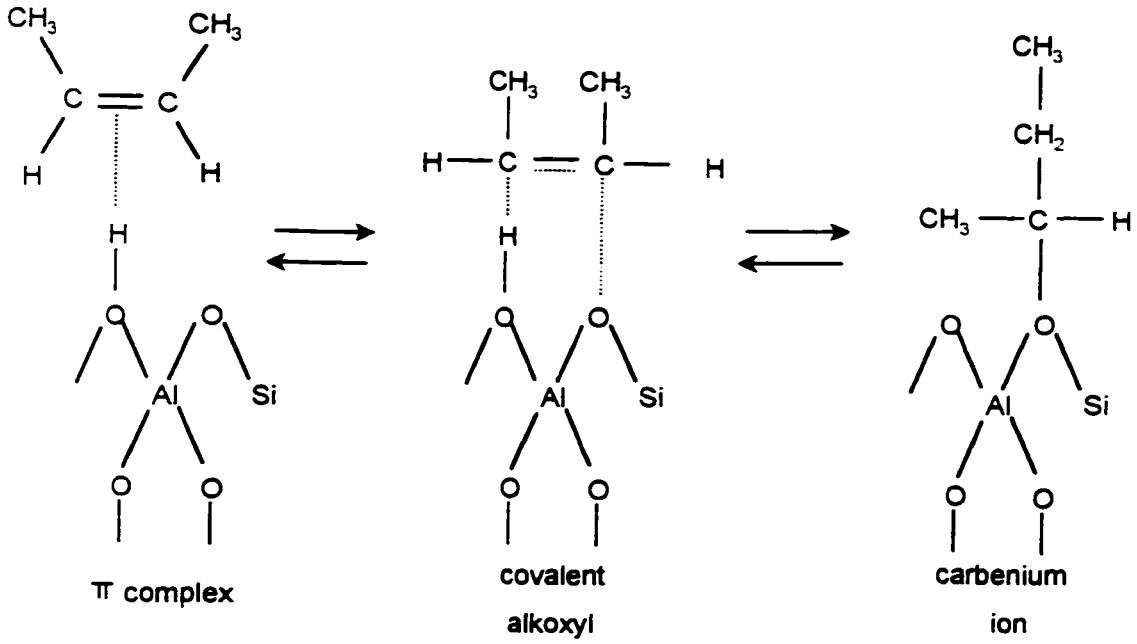

Figure 1.2: Proposed States of Butene Adsorption on Heterogeneous Acid Sites, based on Quantum Mechanical Calculations (van Santen, 1991)

Vibrational excitation of the covalent ester causes the C-O bond to stretch. As this bond elongates, the surface alkoxyl groups become structurally more like a carbenium ion (see Figure 1.2). Predicted activation energies for lengthening of the C-O bond, are relatively low. In this way, the covalent alkoxides can behave as a transition state to the formation of a carbenium ion, through elongation of the C-O bond.

In addition to these two adsorption modes, π complexes of the olefin to surface OH groups can also result in the formation of a carbenium ion (see Figure 1.2). In this sense, equilibria should exist between the three complex forms, during catalytic reactions of olefins.

The π complexes are less stable than covalent alkoxyls (Kazansky & Senchenya, 1989). In contrast, low activation energies are required for proton transfer to an olefin. Hence, chemisorption is highly favourable at low temperatures and acts as the principal source of carbenium ion formation.

At higher temperatures, the π complexes decompose more rapidly than surface esters, and therefore, act as the major source for carbenium ion formation. In this fashion, quasicarbenium ion transition states result from two different rate-limiting steps:

- protonation of π-bonded olefins which dominates at low temperatures
- vibrational excitation of covalent surface esters which becomes the main route of carbenium ion formation at high temperatures

1.5 SIDE REACTIONS OF BUTENE/ISOBUTANE ALKYLATION

Unfortunately, alkylation of butene with isobutane is not the only reaction, which occurs under alkylation conditions. Side reactions occur simultaneously, including:

- oligomerization
- polymerization
- disproportionation
- cracking
- self-alkylation

1.5.1 Oligomerization

Oligomerization results from desorption of the octyl carbenium ion to form the corresponding C_8 olefin, and regenerating the surface acid site (see Equation 1-10).

$$C_8^{+}{}_{(surf)} \longrightarrow C_8^{=} + H^{+}{}_{(surf)} \qquad (1\text{-}10)$$

The preferential adsorption of olefins over paraffins in zeolites with low Si/Al ratio (Corma, Faraldos, et al., 1990), as well as the concentration effect in the small zeolite cavity, favours oligomerization over alkylation for catalysts with high Bronsted acidity.

Oligomerization is also promoted by nickel compounds (sulfates and chlorides are best) supported on oxides (silica, alumina, silica-alumina or zeolites) (Chauvin et al., 1988, Chauvin et al, 1997). In this case, the active site is generally assumed to be a hydride complex of Ni^{+}. This reaction, as well as polymerization of butene, are the major side reactions, which proceed under alkylation conditions.

1.5.2 Polymerization

Polymerization reactions result from the addition of a second olefin to the octyl carbenium ion (see Equation 1-11).

$$C_8^{+}{}_{(surf)} + C_4^{=} \longrightarrow C_{12}^{+}{}_{(surf)} \xrightarrow{R} C_{12} + R^{+}{}_{(surf)} \qquad (1\text{-}11)$$

Polymerization reactions are promoted by sites of medium acidity which are not sufficiently strong to facilitate the hydride transfer step from an isobutane molecule. Similar to the case of oligomerization, the preferential adsorption of olefins over paraffins, in conjunction with the concentration effect inherent in zeolites, favour polymerization reactions.

1.5.3 Disproportionation

Disproportionation is the combination of two molecules of the same type to form two molecules of differing type, one of higher molar mass and the other of lower molar mass (see Equation 1-12).

$$2\ C_8H_{18} \longrightarrow C_7H_{16} + C_9H_{20} \qquad (1\text{-}12)$$

1.5.4 Cracking

Larger isoalkyl cations can undergo cracking, yielding smaller isoalkyl cations and olefins (see Equations 1-13 and 1-14)).

$$C_{12}^{+}{}_{(surf)} \longrightarrow C_5, C_6, C_7 \text{ compounds} \qquad (1\text{-}13)$$

$$C_{16}^{+}{}_{(surf)} \longrightarrow C_8 \text{ isomers} \qquad (1\text{-}14)$$

This can lead to the formation of the desired product, isooctane, and is claimed to occur extensively on zeolites (Chu & Chester, 1986). Cracking reactions are favoured by strong acid catalysts and elevated temperatures (Corma et al, 1994b; Corma et Wojciechowski, 1982, Corma et al, 1994a, O'Young et al, 1994; Corma et al, 1996a).

1.5.5 Self-Alkylation

Self-alkylation of isobutane involves the alkylation of isobutane with isobutene, which is produced through hydride abstraction from another isobutane molecule. The primary product of the reaction is 2,2,4-TMP (see Equations 1-15, 1-16 and 1-7).

$$i\text{-}C_4 + R^{+}{}_{(surf)} \longrightarrow \text{tert-}C_4^{+}{}_{(surf)} \qquad (1\text{-}15)$$

$$\text{tert-}C_4^{+}{}_{(surf)} \longrightarrow i\text{-}C_4^{=} + H^{+}{}_{(surf)} \qquad (1\text{-}16)$$

$$\text{tert-}C_4^{+}{}_{(surf)} + i\text{-}C_4^{=} \longrightarrow \text{2,2,4-TMP}^{+}{}_{(surf)} \qquad (1\text{-}7)$$

Isobutane self-alkylation has been demonstrated to be of considerable importance in the formation of the preferred isomer 2,2,4 –TMP, using HF and zeolite catalysts (Corma & Martinez, 1993; Kazansky & Senchenya, 1989; Cardona et al, 1995).

1.6 MEASURES OF CATALYST PERFORMANCE

It is very difficult to assess catalyst performance when several competing side reactions are occurring simultaneously. A general guideline for comparing catalyst performance will be provided in this section.

1.6.1 Butene Conversion (Butene Disappearance)

An excess of isobutane is used in alkylation due to the preferential adsorption of olefins over paraffins in zeolites and other solid acids. For this reason, the progression of the reaction is monitored by the conversion of butene, as it is the limiting reactant.

It is important to realize that butene conversion is not a true indication of the amount of product formed. Accumulation of products in the catalyst pores occurs, even in the absence of catalyst deactivation, due to the strong adsorption of butene to the acid sites. It can be said that product retention will be small in the initial stages of the reaction, but will increase with longer time-on-stream (TOS), eventually reaching some asymptotic value.

In spite of this complication, butene disappearance is a reliable indicator of catalyst activity. An active catalyst will adsorb butene readily whereas a deactivated catalyst will demonstrate limited ability for this function.

1.6.2 Alkylate Yield

The alkylate yield can be expressed on several different bases. The expressions used in the literature are listed below:

$$\text{Alkylate Yield} = \frac{\text{g } C_5+}{\text{g } C_4^= \text{ fed}} \quad , \quad \frac{\text{g } C_5+}{\text{g } C_4^= \text{ fed} \cdot \text{g cat}}$$

Ideally, the alkylate yield should be 2 g C_5^+/g $C_4^=$ fed. This estimate is based on a 1:1 stoichiometric ratio of reaction between butene:isobutane and assumes that the molar mass of butene and isobutane are approximately the same.

1.6.3 Classification of C_5^+ Product Distribution

The product distribution is classified into three basic fractions, which are used to denote relative catalyst activity for those particular reactions. The fractions and their classifications are:

C_5 - C_7	Cracking
C_8	Alkylation, Oligomerization, Cracking
C_9^+	Polymerization

1.6.4 Classification of C_8 Fraction

The C_8 fraction is divided into three basic classes with each class used as a measure of a particular reaction:

TMP	Alkylate with High Octane Value
DMH	Alkylate with Low Octane Value
$C_8^=$	Oligomerization Products

The TMPs are the most desirable class, as they possess the highest octane value (see Table 1.2). The isomer, 2,2,3-TMP^+, is the primary product of the alkylation of 2-$C_4^=$ with *i*-C_4 (see Equation 1-6), whereas self-alkylation of *i*-C_4 results in the primary product 2,2,4-TMP^+ (see Equation 1-7). Other TMP isomers are formed through isomerization of these TMP^+ isomers through methyl and hydride shifts (see Figure 1.1).

The DMHs are less preferable than the TMPs, as their octane values are significantly less. They are believed to primarily result via two mechanisms (Simpson et al, 1996), which are shown in Figure 1.3. The group, $C_8^=$s, are the least desirable class in the C_8 fraction, as their amounts are limited in the gasoline pool according to CAA formulation requirements for RFG (see Table 1.1).

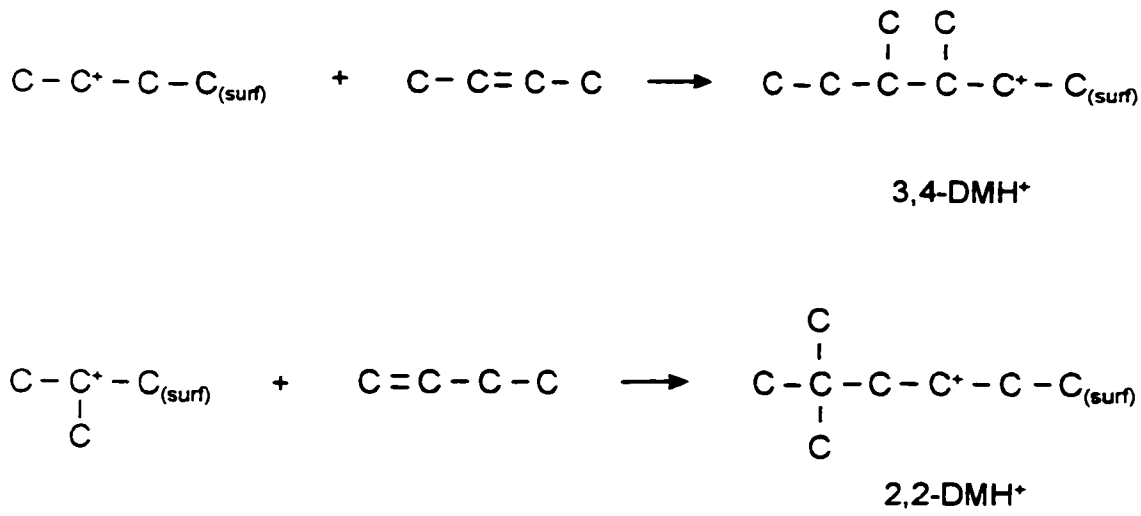

Figure 1.3: Routes for DMH Formation

1.6.5 Measures of Selectivity in C_8 Fraction

Several expressions (molar ratios) are used to measure the efficiency of the reaction to the most valued octane product. The objective is to maximize these measures of C_8 selectivity.

$$\frac{\text{TMP}}{\text{DMH}} = \frac{\text{High Octane Products}}{\text{Low Octane Products}}$$

$$\frac{\text{2,2,4-TMP}}{\text{TMP}} = \text{fraction of most valued (octane) TMP isomer}$$

1.6.6 Indicator of Steric Effects on Reaction

From a structural viewpoint, 2,3,4-TMP and 2,3,3-TMP have the least steric hindrance of the TMP isomers, on the basis of Lennard-Jones diameter calculations (see Appendix A3.2.5). In addition, these isomers possess the highest diffusivity values, relative to the other TMP isomers (Chu & Chester, 1986). From a structural point of view, 2,2,3-TMP and 2,2,4-TMP are the only TMP isomers which can be formed by C_4 fragments, and are also thermodynamically more favourable (see Section 1.7). Therefore, the ratio of thermodynamically favoured isomers divided by least sterically hindered isomers, provides a measure of the importance of steric factors on the reaction.

$$\frac{\text{2,2,4-TMP} + \text{2,2,3-TMP}}{\text{2,3,4-TMP} + \text{2,3,3-TMP}} = \frac{\text{thermodynamically favoured isomers}}{\text{isomers with least steric restrictions}}$$

1.6.7 Indicator of Effective Hydride Transfer

Effective hydride transfer results in saturated products such as TMPs and DMHs. Unsaturated and high molecular weight compounds are formed in an environment with poor hydride transfer functioning. The mass ratio of saturated to unsaturated products in the C_8 fraction, provides a measure of the effectiveness of the hydride transfer functioning.

$$\frac{\text{TMP} + \text{DMH}}{C_8^{=} + C_9^{+}} = \frac{\text{saturated products in } C_8 \text{ fraction}}{\text{oligomerization and polymerization products}}$$

1.7 COMPARISON OF BUTENE/ISOBUTANE ALKYLATE COMPOSITION WITH THERMAL EQUILIBRIUM MEASUREMENTS

Product distributions, obtained experimentally from liquid and solid acids, deviate considerably from those measured at thermal equilibrium (see Table 1.5). The deviation noted for liquid acid systems, is most likely a consequence of changes in solubility of reactants, particularly isobutane, in the acid. On solid acids, three factors can explain the departure from equilibrium predictions. Firstly, strong adsorption of hydrocarbons, particularly at low temperatures, creates a concentration effect such that the actual amounts of reactants in the vicinity of the acid site are quite high. This strongly favours consecutive bimolecular reactions. Secondly, olefins are preferentially adsorbed over paraffins onto solid acid sites, particularly on zeolites with low Si/Al ratio. This promotes oligomerization and polymerization reactions over alkylation reactions (see Chapter 2). Finally, the pore sizes of solid acids will introduce steric effects during product formation, as well as imposing

restrictions on the diffusional rates of products out of the pore network.

Table 1.5: Comparison of TMP and DMH Selectivity on Liquid and Solid Acid Catalysts, with Thermal Equilibrium Composition

Catalyst	HF[1]	H_2SO_4[1]	REHY[1]	Thermal Equilibrium Composition			
Temperature [°C]	n.a.	~10	90	~20[1]	50[2]	90[3]	127[1]
TMP Dist. [%]							
2,2,4-TMP	65.5	47.0	29.8	67.1	63.5	61.4	59.2
2,2,3-TMP	2.5	3.1	5.6	16.8	17.5	16.5	16.6
2,3,4-TMP	17.0	26.5	25.8	8.0	9.0	10.8	11.2
2,3,3-TMP	14.9	23.4	38.8	8.1	10.0	11.3	13.0
DMH Dist. [%]							
2,5-DMH	21.4	64.7	23.9		55.0		30.4
2,4-DMH	34.8		49.2		36.2		25.5
2,3-DMH	38.4	29.4	6.0		4.0		4.0
2,2-DMH		2.0					22.2
3,3-DMH							12.7
3,4-DMH	5.4	4.0	20.9		4.8		5.1

1 Chu & Chester, 1986
2 Cardona et al, 1995
3 Corma & Martinez, 1993

1.8 RESEARCH METHODOLOGY

1.8.1 Problem Statement and Objectives

A catalyst is a material which increases the rate of reaction towards equilibrium without being substantially consumed in the process (Gates, 1995). The **activity** of a catalyst is a measure of how quickly it catalyses a reaction. The effectiveness of the catalyst at promoting the reaction to the desired products is called the **selectivity**. The **stability** of the catalyst is an indication of how quickly it loses its activity or selectivity while in operation. The measure of how effectively a deactivated catalyst can be brought back to a state of high activity and selectivity is called the

regenerability of a catalyst.

No solid acid has achieved commercial success in the production of alkylate due to short catalyst lifetime. The failure of solid acids is primarily a loss in hydride transfer function after a short time on stream.

The present study examined the alkylation reaction in detail, to isolate the essential catalyst properties required to activate alkylation and identify weaknesses or limitations of solid acids. Particular attention was focused on the ability of the catalyst to promote hydride transfer, as the loss of this function expedites the onset of deactivation. This provided the foundation for the catalyst design. A reaction mechanism was proposed incorporating the routes where hydride transfer ability can be improved, using the newly designed catalyst system.

The catalyst should maintain high activity and stability for isobutane alkylation with 1-butene. The catalyst should also maximize the selectivity to the TMP isomers, particularly 2,2,4-TMP, as these possess the highest octane values of all C_8 products. The performance of the proposed catalyst was compared to that of Y zeolite, in a flow reactor. The catalyst design was critically evaluated to assess the effectiveness of hydride transfer ability in the new design.

Deactivation appears inevitable on any solid acid catalyst system. Therefore, the catalyst must be able to withstand the rigors of regeneration. The performance of the regenerated catalyst systems, was compared to their fresh catalyst performance levels.

1.8.2 Catalyst Requirements

The primary reason for rapid catalyst deactivation is the loss of the hydride transfer function, which ultimately favours oligomerization and polymerization reactions and leads to coke formation. For this reason, the main focus in the catalyst development was the promotion and maintenance of the hydride function, for extended reaction times.

Certain properties have been identified as necessary to achieve a high alkylation yield and selectivity. These can be categorized into two types: chemical properties and physical properties.

1.8.2.1 Chemical Properties

The catalytic properties should facilitate the desired alkylation reaction and promote the desorption of the isooctane product. Simultaneously, these chemical properties should minimize the occurrence of undesirable side reactions. The salient chemical properties are listed below:

1. Bronsted acid sites of medium to strong strength are preferred (Corma & Martinez, 1993).

2. An isomerization function, primarily for sec-C_4^+ to tert-C_4^+ and for C_8^+ to TMPs is required. This demands large catalyst pores to eliminate steric restrictions.

3. The catalyst must facilitate hydride transfer selectively from isobutane to ensure rapid desorption of the octyl carbenium ion. This is necessary to minimize consecutive reactions leading to high molecular weight products which ultimately result in coke formation.

4. The catalyst should not promote undesirable side reactions, such as oligomerization, polymerization or cracking of C_8 product. This may be difficult, as many of the catalyst requirements for alkylation are similar, to those required by oligomerization, polymerization and cracking reactions. Cracking reactions demand strong acid sites, whereas oligomerization and polymerization reactions require medium strength acid sites. This suggests that a narrow distribution of acid strength is best suited to alkylation, a requirement that is very difficult to achieve on solid acid

catalysts.

1.8.2.2 Physical Properties

Certain physical properties are necessary to facilitate the diffusion of the reactants to the active sites as well as effectively promote diffusion of the products out of the catalyst pores. In addition, certain physical properties are essential for application in an industrial setting, to ensure that the catalyst can withstand the rigours of transport and regeneration conditions. A list of the important attributes are:

1. Large internal pore sizes to facilitate the diffusion of reactants to the active site, isomerization of the octyl carbenium ion and, most importantly, diffusion of the desired TMP products out of the pore network.

2. A tri-directional pore network is essential to efficiently facilitate diffusion of reactants and products.

3. Good thermal and hydrothermal stability are critical to favour effective regenerability.

4. The catalyst must demonstrate robustness and be able to withstand handling stresses during transport.

5. The catalyst must possess sufficient crush strength to endure the weight of catalyst particles above them in the bed.

1.8.3 Approach to Evaluating Catalyst Performance

The performance of the newly designed catalyst was evaluated using a computer controlled flow reactor, equipped with on-line sampling and gas chromatographic (GC) analysis. The influence of reactor operating conditions, as well as catalyst pretreatment parameters, was evaluated and compared to a reference catalyst, Y zeolite.

1.8.4 Chronological Phases of Research Plan

The research plan can be divided into six chronological phases. A brief description is provided outlining the scope of each phase involved in the project.

1.8.4.1 Phase I: Catalyst Development

The literature was reviewed to identify potential candidates for catalytic components suited for alkylation. A methodical approach was taken to catalyst development, identifying the shortcomings of existing catalytic systems. With this knowledge, as well as theoretical considerations, a catalyst design was proposed.

1.8.4.2 Phase II: Equipment Set-up for Flow Experiments

The computer controlled flow reactor to be used for assessing catalyst performance, was installed, tested and brought to a fully operational state. On-line GC analysis was implemented, including establishing communication lines between the BTRS reactor software and GC software, as well as designing and installing a manual splitting valve to act as a GC split injector. Once complete functioning of the on-line GC component was established, chromatographic component identification was performed using injections of known standards as well as GC-MS.

1.8.4.3 *Phase III: Preparation and Characterization of Catalyst Systems*

The catalyst was synthesized using methods established in the literature. Phase identification was confirmed by comparison to published X-ray diffraction (XRD) spectra. The reproducibility of the synthesized material was carefully examined in this phase, as this has been reported to be a source of variability in catalyst performance.

1.8.4.4 *Phase IV: Effect of Operating Conditions*

Factors, which have been identified as influential on alkylation (i.e. reaction temperature, calcination temperature, olefin weight-hourly-space-velocity (WHSV) and cyclical feed addition, catalyst type), were examined. The effects of these variables on alkylate yield and selectivity were evaluated, and the preferred operating conditions identified.

1.8.4.5 *Phase V: Effect of Pt on Catalyst Performance*

The effect of catalyst properties, on alkylate yield and selectivity, was explored in Phase V. These include the nature of catalyst support and Pt loading. Spent catalysts from previous experiments, were regenerated *in situ*, and their performance was assessed in the reconditioned state. The influence of Pt, on the efficacy of regeneration, was a primary focus in this phase.

Chapter 2

Catalyst Design

The viability of solid acid catalysts employed for alkylation, has been studied intensively for the last three decades. Solid acid systems typically demonstrate a high initial activity but rapidly undergo deactivation with longer times on stream. A review of the solid acid systems investigated as potential alkylation catalysts, is provided in this section.

2.1 REVIEW OF LARGE PORE ZEOLITES FOR BUTENE / ISOBUTANE ALKYLATION

2.1.1 Properties of Zeolites

The successful application of Y zeolites as the active ingredient in cracking catalysts during the 1960's, prompted research into the usage of zeolites for alkylation reactions. The preferential adsorption of olefins over paraffins on zeolites, implies that the actual isoparaffin/olefin (I/O) ratio on the catalyst surface, is much less than the I/O ratio in the bulk liquid phase surrounding the catalyst (Corma et al, 1990). To enhance the adsorption of isobutane over butene, reactions are performed at bulk I/O ratios in excess of the stoichiometric amounts required.

It has been nearly a quarter of a century since zeolites were first demonstrated to catalyse isobutane/olefin alkylation (Garwood & Venuto, 1968). To date, zeolites have still not achieved commercial success in the production of alkylate, primarily due to rapid catalyst deactivation (Rotman, 1996). In spite of the lack of success, alkylation research involving zeolites continues.

2.1.1.1 Nature of Acidity in Zeolites

The zeolite lattice consists of a three dimensional network of cations with valences of 4 or 3 (usually Si^{4+} and Al^{3+} respectively) attached to four neighbouring oxygen atoms. The SiO_4 tetrahedra are neutral, whereas, a "-1" charge is associated with the AlO_4^- tetrahedra. Electrical neutrality of the AlO_4^- tetrahedra is achieved by the presence of cations located at various crystallographically defined positions, with a large proportion being in internal locations. When the cations are H^+, a Bronsted acid site is created, and the zeolite assumes an acidic form (see Figure 2.1). The "onium" type coordination of the oxygen atom is the basis of the high acidity of the

attached proton.

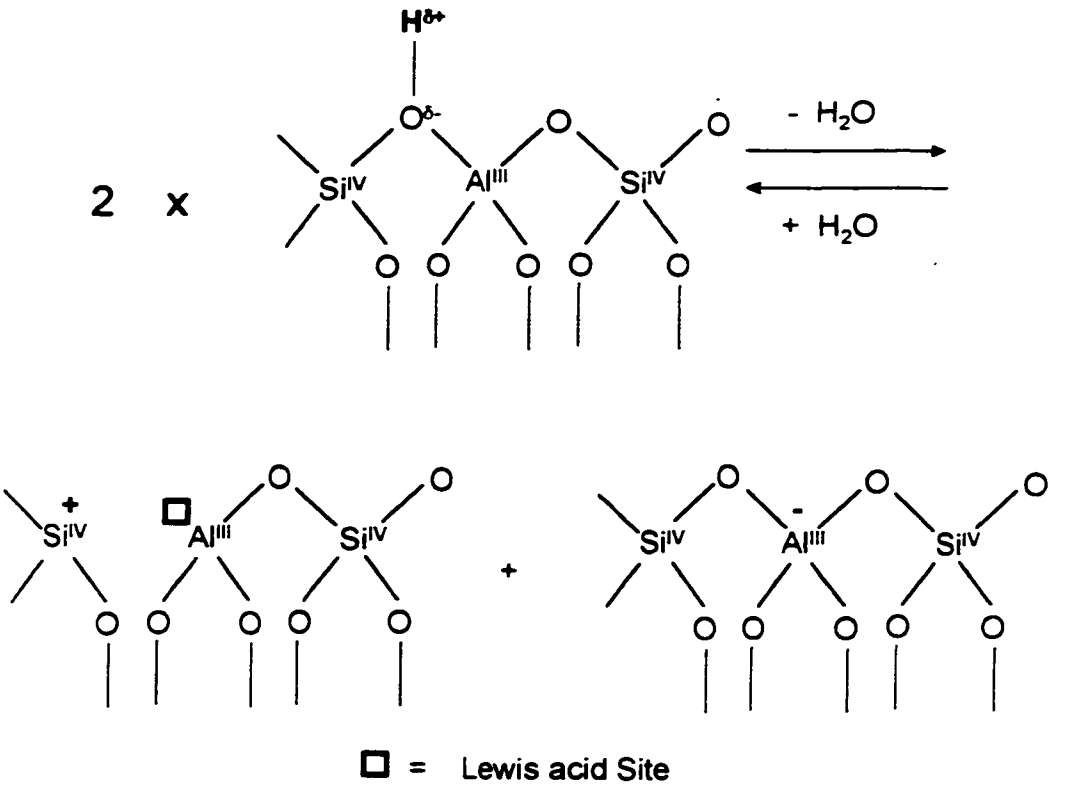

Figure 2.1: Interconversion of Bronsted and Lewis Acidity on Zeolites

Two Bronsted acid sites can be converted to one Lewis acid site, through the removal of a water molecule. A simplified, but not complete, depiction of the process is shown in Figure 2.1 (Gates, 1992). Note that Lewis acid sites can be converted back to a Bronsted sites through water addition, provided that the crystal phase has not been altered by severe thermal treatment. Calcination temperatures in excess of approximately 700°C, cause extensive dealumination to occur (Ward, 1967). Extra-framework Al species develop, bearing Lewis acid sites which do not convert to Bronsted acid sites upon water addition. Therefore, provided calcination temperature are sufficiently mild to ensure structure stability, high calcination temperatures support the formation of Lewis acid sites as more and more water is driven off. In

contrast, lower calcination temperatures favour the domination of Bronsted type acidity.

The unit cell size (UCS) is a function of the Si/Al ratio in the zeolite framework and also provides a measure of the total number of tetrahedrally coordinated Al atoms in the framework. Since aluminum atoms are responsible for acidity in zeolites, the UCS provides a direct measure of the number of potential acid sites. It is generally accepted that as the UCS decreases, the acid site density decreases. It is believed that the strength of an acid site is directly related to its degree of isolation from neighbouring acid sites. In this way, the most isolated acid sites, are those which have zero next-nearest alumina neighbours (0-NNN). These sites will exhibit the highest acid strength followed by 1-NNN and so on (Pine et al, 1984).

Adsorption of hydrocarbons onto the Bronsted acid site is dependent upon the stability of the carbenium ion/surface ester intermediates. This in turn, is a function of the deprotonation energy of the proton, as well as the stabilization of the protonated species by the negative charge generated on the lattice oxygen. This emphasizes the complexity of the dynamic behavior of acidity in a solid acid relative to a liquid acid.

2.1.1.2 Hydrocarbon Adsorption on Zeolites

The adsorption properties of zeolites arise from van der Waals and electrostatic forces, due to overlapping adsorption potentials within the small cavities of the pore network. The adsorption behaviour of paraffins and olefins differs, as a result of their interaction with the zeolite surface.

FTIR spectroscopy revealed only weak interaction, or physisorption, between isobutane and zeolitic acid sites, on La-Y zeolite at 25 and 80°C (Flego et al, 1995). The adsorption FTIR spectrum for 1-butene, indicated chemical interaction between zeolite hydroxyl groups and 1-butene molecules, as well as the formation of oligomers. Hydroxyl bands at 3558 (OH in sodalite), 3624 cm^{-1} (OH associated with Al defects) and 3668 cm^{-1} (OH in supercages) disappeared, and chain oligomer

formation was revealed at 1370 cm^{-1}. As the loading of 1-butene was increased, the concentration of adsorbed oligomers increased. Similarly, unreacted physisorbed 1-butene (1630 cm^{-1}) also increased with 1-butene loading (Flego et al, 1995).

The adsorption characteristics of isobutane/1-butene mixtures (I/O = 9) at 80°C were also examined with FTIR (Flego et al, 1995). The spectrum revealed that isobutane reduced the extent of chemisorbed 1-butene and also suppressed oligomerization activity. It appears that the isobutane exhibited a dilution effect, reducing the probability of oligomerization reactions from occurring.

The Si/Al ratio has a strong influence on the adsorption properties of Y zeolite. The higher the degree of dealumination, the lower the capacity of adsorption (Stach et al, 1986; Corma et al, 1990). Olefins adsorb preferentially over paraffins (Corma et al, 1990) and isoparaffins over straight chain paraffins (Santilli et al, 1993; Denayer et al, 1998), particularly at low Si/Al ratios. Dealumination of the zeolite, reduces the adsorption selectivity towards the olefin. For dealuminated Y zeolite with Si/Al=140, the extent of adsorption of butene and butane are approximately equal at 80°C (Corma et al, 1990).

2.1.2 Cubic Phase Faujasites Prepared from Na-rich Hydrogels - Y and USY (Dealuminated Y)

Table 2.1: Structural Properties of Y and USY

Nomenclature	Y	USY
Si/Al Ratio	1 - 3	> 3
Phase	Cubic	
Number of O Atoms in Aperture	12	
Network	3-dimensional	
Mean Pore Diameter	7.4 Å	

Higher Si/Al ratios in Y zeolites can be achieved through dealumination, using either steam treatment or chemical means. The dealuminated Y materials, which have Si/Al ratios greater than 3, are called Ultrastable Y (USY). Removal of aluminum from the unit cell causes an overall reduction in the UCS and total number of acid sites (total acidity). The reduced concentration of acid sites suppresses the probability of polymerization reactions from occurring, thus improving catalyst stability. The properties of both Y and USY zeolites are summarized in Table 2.1.

Initially, Y zeolites demonstrated very high activity at temperatures below 100°C yielding product distributions drastically different from thermodynamic predictions. Similar product arrays were achieved when alkylating either 1-butene or 2-butene with isobutane. This suggests that isomerization of 1-butene to 2-butene, the thermodynamically preferred isomer, is faster than alkylation of 1-butene with isobutane (Kirsch et al, 1972).

The influence of steam dealumination on catalyst acidity, as measured by infrared spectroscopy (IR) of adsorbed pyridine, is summarized in Table 2.2 (Corma et al, 1994b). The results indicate that dealumination of USY by steam treatment leads to a reduction in total acidity, particularly Bronsted type.

Table 2.2: Acidity of USY Samples, on the Basis of IR Pyridine Adsorption as a Function of Desorption Temperature (Corma et al, 1994b)

I.D.	Steam Deal. Temp [°C]	USC [nm]	Si/Al Ratio[1]	TGA ANALYSIS Acidity [μmole pyridine retained/g catalyst][2]					
				BRONSTED			LEWIS		
DTA Desorption Temp [°C]				250	350	400	250	350	400
USY-1	500	2.450	5.4	110	58	28	41	34	27
USY-2	712	2.435	13.6	80	32	13	29	14	14
USY-3	740	2.428	35.3	46	18	4	16	7	7
USY-4	760	2.426	62.2	39	15	2	20	13	13

1 framework Si/Al ratio reported

2 pyridine desorption temperature used as a measure of quality (i.e. strength) of acid site and amount of pyridine retained as a measure of quantity of acid sites

Comparison of alkylate yield and selectivity on USY zeolites (steam dealuminated at various temperatures) at short TOS, is maximized for the largest UCS (lowest Si/Al ratio) as shown in Table 2.3. These results suggest that alkylate production is favoured by a high density of strong acid sites having either 0 or 1 Al in the next nearest neighbour (0-NNN or 1-NNN respectively) position (Corma et al, 1994b). Alternatively, it is also possible that the cavity becomes too small as more Al is removed, preventing formation of the bulky TMP isomers.

The extraframework aluminum (EFAL) species generated during the dealumination process, have been found to interact with HF and LF hydroxyls, creating Bronsted sites of superacid strength (will not desorb pyridine at 400°C) (Corma, 1989). The presence of EFAL in mildly dealuminated catalysts has been demonstrated to exert a positive effect on extending catalyst lifetime and enhancing alkylation activity (Corma et al, 1996a).

It is possible that EFAL species are present in the sample dealuminated under mild steaming conditions (500°C). This would explain the large amounts of strong acid sites (as measured by the amount of pyridine retained by Bronsted acid sites after heating to 400°C during Fourier Transform infrared spectroscopy (FTIR) analysis) measured for this sample. This would enhance catalyst performance with respect to alkylation, as well as prolong the catalyst lifetime. Unfortunately, EFAL was not investigated by the authors (Corma et al, 1994b), and therefore, any conclusions are purely speculative.

A decrease in the UCS via dealumination compromises the quality of the alkylate, as indicated by the TMP/DMH ratio. This is most likely a consequence of steric factors, resulting from the reduction in space available, which favours the formation of DMHs over TMPs (see Table 2.3).

The primary product of alkylation of 2-butene with isobutane is 2,2,3-TMP. However, substantial levels of 2,2,4-TMP are observed for the Y-zeolites with UCS $\geq$ 2.435 nm (see Table 2.3). This suggests that either these catalysts have strong isomerization capabilities or they promote self-alkylation of isobutane, which has been reported elsewhere (Kirsch, et al, 1972).

Table 2.3: Alkylate Product Distribution on USY, as a Function of UCS (TOS=1min., T_{rxn}=50°C, I/O=15) (Corma et al, 1994b)

Steam Dealumination Temp. [°C]	500	712	740	760	• As UCS is reduced • Si/Al ratio increases • Strength of acid site increases • Density of acid site decreases
Si/Al Ratio	5.4	13.6	35.3	62.2	
USC [nm]	2.450	2.435	2.428	2.426	
2-$C_4^=$ Conv [%]	99.6	100.0	90.6	92.0	
Alkylate Yield [g C_5+/g $C_4^=$ fed]	0.84	0.49	0.19	0.20	• ideally should be: 2 g C_5^+/g $C_4^=$ fed
C_5+ Liquid [mass%]					
C_5-C_7	34	34	11	13	• cracking activity
C_8	49	42	49	40	
C_9+	17	24	40	47	• polymerization activity
C_8 Fraction [mass%]					
TMP	78	72	12	18	• high octane alkylate
DMH	20	28	55	55	• low octane alkylate
$C_8^=$	2	0.4	33	27	• oligomerization products
TMP Fraction [%]					
2,2,4-TMP	39	39	23	27	• highest octane value
2,2,3-TMP[1]	7	6	18	15	• direct product of rxn
2,3,4-TMP	23	27	37	36	• least sterically hindered
2,3,3-TMP	31	28	22	22	• least sterically hindered
Indicators [mass fr]					
$\frac{\text{TMP}}{\text{DMH}}$	3.8	2.6	0.2	0.3	• high/low octane alkyiate
$\frac{\text{2,2,3- + 2,2,4-TMP}}{\text{2,3,4- + 2,3,3-TMP}}$	0.88	0.82	0.69	0.71	• thermodynam. favoured /least sterically hindered
$\frac{\text{TMP+DMH}}{C_8^= + C_9^+}$	2.6	1.8	0.6	0.5	• effective/ineffective hydride transfer

1 separation of 2,2,3-TMP and 2,4-DMH not achieved; each component assumed to be half of total

The hydride transfer ability of the catalyst is critical to favour the formation of the *tert*-butyl carbenium ions as well as promoting desorption of the octyl carbenium ions. It is well established that reducing the UCS below 2.430 nm severely decreases the hydride transfer activity, resulting in a higher olefinic content in the alkylate (as

measured by alkylate MON) (Pine et al, 1984). Significant levels of isooctenes for Y-zeolites with UCS below 2.430 nm were observed, in agreement with this trend (see Table 2.3).

The levels of *n*-butane produced in the preliminary stages of the reaction in the absence of catalyst deactivation, provide another measure of the hydride transfer ability of the catalyst (Corma et al, 1994b). Successful hydride transfer from isobutane to a *sec*-butyl carbenium ion, yields *n*-butane and a *tert*-butyl carbenium ion (see Equation 1-3):

$$sec\text{-}C_4^{+}{}_{(surf)} + i\text{-}C_4 \longrightarrow n\text{-}C_4 + tert\text{-}C_4^{+}{}_{(surf)} \qquad (1\text{-}3)$$

As expected, low levels of *n*-butane are observed after 1 minute TOS for the catalysts with UCS below 2.430 nm. In contrast, Y-zeolite with UCS > 2.430 nm, produced elevated levels of *n*-butane for the same TOS.

These results, in conjunction with the distribution of the different acid sites on the catalyst, suggest that hydride transfer was best facilitated by a low Si/Al ratio (large UCS). Similarly, the steric requirements of alkylation, demand a catalyst with a large UCS.

As the catalyst ages, high molecular weight carbonaceous type species are retained on the active sites, preferentially the stronger Bronsted acid sites. This reduces the hydride transfer ability of the catalyst as well as inducing pore blockage. The decaying catalyst promotes oligomerization rather than alkylation. Desorption of the octyl and higher carbenium ions from the acid centers, occurs by loss of a proton by the cation, rather than uptake of a hydride ion from an isobutane molecule. This results in a higher olefinic content in the product distribution (Corma et al, 1994b). The behaviour of the deactivating catalyst suggests that the acid site strength needed to promote reactions under alkylation conditions can be ranked as follows: cracking > alkylation > dimerization (oligomerization) (Corma et al, 1994b; Corma &

Wojciechowski, 1982; Corma et al, 1994a; O'Young et al, 1994; Corma et al, 1996a).

Another approach to tempering catalyst acidity and extending catalyst lifetime, is to cation exchange the parent material (Y or USY) with a rare earth metal (RE). La and Ce have been exchanged in Y zeolite (RE-Y), to increase the density of acid sites with suitable strength for isobutane/butene alkylation, according to the Hirschler-Plank mechanism (see Equation 2-1).

$$RE(H_2O)^{3+} + \text{Zeol-}O^- \longrightarrow RE(OH)^{2+} + \text{Zeol-OH} \qquad (2\text{-}1)$$

Upon ion exchange, hydrated complexes of the RE ions occupy the supercages, but later migrate to sites in the sodalite cages during calcination. At higher RE exchange, the RE ions occupy additional sites in the supercages as well.

The performance of RE-Y applied to alkylation of butene with isobutane has been explored. The catalyst Ce-Y demonstrated improved catalyst performance over Y and RE-USY with respect to alkylate yield (g C_5^+/g 1-$C_4^=$ fed) (Chu & Chester, 1986). However, rapid catalyst deactivation still ensued, mainly due to the loss of hydride transfer function, resulting in oligomerization activity being facilitated rather than alkylation (Rorvik et al, 1996b).

2.1.3 Faujasites Prepared in the Presence of Crown Ether Templates - EMT (Hexagonal Phase) and FAU (Cubic Phase)

Table 2.4: Structural Properties of EMT and FAU

Nomenclature	FAU	EMT	
Phase	cubic	Hexagonal	
Si/Al Ratio	3-5	3-5	
Template	15-crown-5 ether	18-crown-6 ether	
# of O Atoms in smallest Aperture	12	12	
Network	3-dimensional	3-dimensional	
Cages	supercage	hypercage (50 %)	hypocage (50 %)
Void Volume [nm^3]	1.15	1.24	0.61
Accessibility to Cages	4 circular channels (0.74 nm)	2 circular channels (0.74 nm) 3 elliptical channels (0.69 x 0.74 nm)	3 elliptical channels (0.69 x 0.74 nm)

A method has been recently proposed for preparation of cubic (FAU) and hexagonal (EMT) faujasite-type zeolites with Si/Al ratios up to 5, by using crown-ether templates (Delprato, et al, 1990). The hexagonal phase can be synthesized from aluminosilicate hydrogels containing 18-crown-6 ether, whereas, the cubic phase is produced when 15-crown-5 is used as the template (see Table 2.4). Up to this time, high yields of well-defined faujasite-type zeolites with a framework Si/Al ratio greater than 3 could not be achieved, without post-synthesis treatment (i.e. chemical dealumination or steam dealumination).

FAU and EMT have similar structure types, and hence, geometrical pore sizes. Both are built from truncated octahedra, called "sodalite cages" or cubo-octehadra, which are linked together through hexagonal prisms to form faujasite sheets.

Different linking of the sodalite cages produces the different microporous structures of FAU and EMT (see Chapter 3).

Although the EMT, FAU and USY have similar physical structures, acidity measured by pyridine FTIR spectra reveal significant differences in the distribution and predominance of the type of acid sites (see Table 2.5). EMT and FAU were both calcined at 540°C for 5 h whereas the conditions for USY were 500°C for 3 h. At these calcination temperatures, all of the faujasites favour the formation of Bronsted acid sites over Lewis acid sites. Spectra of pyridine desorption reveal that Bronsted acid site concentrations are significantly greater those of Lewis acid sites, for all catalysts and all desorption temperatures. The relative ratio of pyridine adsorption at 400°C versus 250°C, used as a measure of strong to weak acid sites (Corma et al, 1994b), indicates that the EMT and FAU have a much greater proportion of strong to weak acid sites (see Table 2.6).

Table 2.5: Acidity of EMT, La-exchanged EMT, FAU and USY, on the Basis of IR Pyridine Adsorption as a Function of Desorption Temperature[1]

	BRONSTED Acidity [mmol pyridine retained/g cat.]			LEWIS Acidity [mmol pyridine retained/g cat.]		
DTA [°C]	250	350	400	250	350	400
EMT[2]	0.50	0.43	0.42	0.08	0.07	0.07
La40EMT[3]	0.40	0.34	0.32	0.18	0.14	0.14
La80EMT[3]	0.38	0.31	0.29	0.07	0.06	0.05
FAU[2]	0.51	0.45	0.39	0.12	0.12	0.12
USY[4]	0.20	0.11	0.05	0.07	0.04	0.04

1 pyridine desorption temperature used as a measure of quality (i.e. strength) of acid site and amount of pyridine retained as a measure of quantity (i.e. density) of acid sites

2 data from Stocker et al, 1996; Si/Al =3.5; Extinction coefficients: IMEC(B) = 1.67 cm/μmol, IMEC(L) = 2.22 cm/μmol

3 data from Mostad et al, 1997; LaxEMT represent x % La exchange of parent EMT (Si/Al =3.9); Extinction coefficients: IMEC(B) = 1.67 cm/μmol, IMEC(L) = 2.22 cm/μmol

4 data from Corma, Martinez & Martinez, 1994b; Si/Al = 2.6; re-calculated data such that the extinction coefficients applied by Stocker et al, 1996 were also applied

Table 2.6: Analysis of Acid Site Distribution with respect to Site Type and Strength, for EMT, La-exchanged EMT[1], FAU and USY

	Relative Strength of BRONSTED Acid Sites [400/250][2]	Relative Strength of LEWIS Acid Sites [400/250][2]
EMT	0.84	0.88
La40EMT	0.80	0.78
La80EMT	0.76	0.71
FAU	0.76	1.00
USY	0.25	0.57

1 LaxEMT where *x* indicates % exchange of La
2 Strong (400°C desorption temperature) / Weak (250°C desorption temperature) Acid Sites on the basis of pyridine desorption

A comprehensive review of the Bronsted acidity on USY and EMT, supports these observations (Su et al, 1993). The catalyst EMT demonstrated higher thermal stability of the hydroxyls and pore structure, a greater mean acid strength and larger proportion of very strong protonic sites relative to USY.

Recent efforts modelling the siting patterns of Si and Al in the framework for FAU and EMT synthesized in the presence of crown ethers, have concluded that the Al ordering is not random, as is the case in parent and dealuminated Y zeolites crystallized from a sodium aluminosilicate hydrogel. Rather, the models predict Al-enriched and Al-depleted regions for the crown ether prepared materials, in agreement with experimentally determined Si(nAl) populations (where n = 0, 1, 2, 3 or 4) based on Si NMR spectra (Feijen et al, 1996). It is proposed that the presence of one crown ether in each cage directs the aluminum placement on the basis of charge balance with the Na cation (Feijen et al, 1994b; Feijen et al, 1996). The effect of uneven Al distribution, on acidity, is not known, as it is unique to the crown ether synthesized faujasites. However, pyridine desorption IR spectra suggest that high concentrations of strong acid sites are formed. This type of acid site density may be well suited to alkylation.

Preliminary results confirmed this hypothesis using EMT for alkylation of 2-butene with isobutane (Stocker et al, 1994; Rorvik et al, 1996; Stocker et al, 1996). In

a 300 mL stirred semibatch autoclave, isobutane was added first under nitrogen pressure and heated to the reaction pressure. The reagent, 2-Butene, was charged at a constant WHSV for 2 h^{-1}, until an I/O ratio of 5, 10 or 20 is reached. A disadvantage of this approach is that a time-averaged picture of the catalytic events is depicted. Differential samples of gas-phase products were collected and analyzed on-line. Heavier liquid products were collected using an ice trap and evaluated off-line.

Very high I/O ratios were inherent during the initial stages of the reaction. This ratio gradually declined through further butene addition, until the final I/O ratio was reached at 2 h. After this time, butene addition was ceased. Under these circumstances, very high alkylation yields and reduced oligomerization are expected. In addition, self-alkylation is strongly favoured, a condition not mentioned by the authors. A separate study involving isobutane as the only reactant using EMT would reveal its ability for self-alkylation reactions.

Catalyst performance, with respect to alkylate yield, can be ranked as follows: EMT > FAU > Ce-Y (98 % Ce exchanged Y zeolite). The high densities of strong acid sites may explain the superior performance of FAU and EMT over the Y zeolite. Temperature demonstrated little effect on the yield of alkylate in the range of 80 to 100°C. The I/O ratio exerted considerable influence when increased from 5 to 20 (Rorvik et al, 1996).

The high levels of TMP production suggest that self-alkylation of isobutane may be important. This was also supported by the dependence of 2,2,4-TMP production on the stirring speed (Rorvik et al, 1996). At lower stirrer rpm, 2,2,4-TMP wafavoured. As the stirrer speed was increased, the quantity of 2,2,4-TMP formed declined to a steady value. These results suggest that a uniform dispersion of the olefin in the isoparaffin under high stirring speeds, reduced the probability of 2,2,4-TMP formation, through self-alkylation of the isoparaffin. Also, the semi-batch nature for reactant addition favours self-alkylation of the isoparaffin.

The catalyst, EMT, strongly favoured highly branched alkylate, as indicated by the TMP/DMH ratio (see Table 2.7). The least sterically hindered isomers (2,3,3- and

2,3,4-TMP) predominated in the TMP distribution, similar to fixed bed studies for long TOS involving other catalytic systems (Cardona et al, 1995).

Table 2.7: Alkylate Product Distribution on Ce-Y, H-FAU and H-EMT[1] (T = 80°C, semi-batch, I/O=20, t = 3h) (Rorvik et al, 1996)

Catalyst	Ce-Y	FAU	EMT	• FAU and EMT synthesized using crown ether templates
2-$C_4^=$ Conv [%]	34	70	89	
Alkylate Yield [g C_5+/g $C_4^=$ fed]	0.30	1.30	3.65	• ideally should be: 2 g C_5^+/g $C_4^=$ fed
C_5+ Liquid [mass%]				
C_5-C_7	12	13	8	• cracking activity
C_8	84	74	82	
C_9+	4	13	10	• polymerization activity
C_8 Fraction [mass%]				
TMP	43	56	86	• high octane alkylate
DMH	14	14	11	• low octane alkylate
$C_8^=$	43	30	3	• oligomerization products
TMP Fraction [%]				
2,2,4-TMP	18	20	17	• highest octane value
2,2,3-TMP	5	7	9	• direct product of reaction
2,3,4-TMP	38	36	34	• least sterically hindered
2,3,3-TMP	40	37	40	• least sterically hindered
Indicators [mass fr]				
TMP / DMH	3.2	3.9	4.1	• high/low octane alkylate
2,2,3- + 2,2,4-TMP / 2,3,4- + 2,3,3-TMP	0.29	0.37	0.35	• thermod. favoured /least sterically hindered isomers
(TMP+DMH) / ($C_8^=$ + C_9^+)	1.2	1.5	6.4	• effective/ineffective hydride transfer

1 Catalyst calcined externally at 540°C for 5 hours in air during catalyst preparation. Prior to reaction, catalyst calcined externally at 400°C for 2 h, then transferred to reactor and pre-treated at 200°C for 2 h.

The most encouraging aspect of EMT is the effectiveness at which it facilitated hydride transfer ((TMP + DMH)/($C_8^=$ + C_9^+)). The proportion of $C_8^=$ and C_9^+ in the product distribution in substantially less than the C_8 paraffin production (see Table

2.7). It appears that the slightly larger hypercage, improved accessibility through additional openings in the larger hypercage, as well as straight channel access to hypercage, strongly favour efficient hydride transfer for this reaction. This has long been a stumbling block in the application of heterogenous catalysts for alkylation, whereby, rapid catalyst deactivation ensues primarily as a consequence of loss of hydride transfer ability.

Similar to Y and USY, EMT and FAU possess a high density of acid sites. These sites promote alkylation; however, the close proximity of acid sites also encourages oligomerization activity. For this reason, dealumination of EMT and FAU zeolites, using either a chemical or physical (steam) method, have been explored to better tailor the acidity level to alkylation.

A recent investigation used $(NH_4)_2SiF_6$ to dealuminate FAU and EMT (Stocker et al, 1996). The performance of the parent and dealuminated materials, with respect to alkylation, were studied (see Table 2.8). The catalyst, EMT, demonstrated superior performance over FAU in all regards. This agrees with the findings of previous investigations for the parent materials (Stocker et al, 1994; Rorvik et al, 1996).

The effect of EFAL was not investigated by the authors. A recent investigation examining *n*-hexane cracking, concluded that dealumination in EMT, FAU and USY proceeded in a similar manner (Zholobenko et al, 1995), whereby, dealuminated catalysts were more active than the parent materials. Enhanced Bronsted acidity, due to the formation of tetrahedrally coordinated EFAL species, was concluded to be responsible for the improved performance. Another interesting finding of this study was that EMT exhibited shape selectivity effects and produced significantly higher yields of iso-products relative to FAU and USY.

Table 2.8: Alkylate Product Distribution on Parent and Dealuminated FAU and EMT[1] (t = 3h, T = 80°C, semi-batch reactor) (Stocker et al, 1996)

Catalyst	Par. EMT	Deal. EMT	Par. FAU	Deal. FAU	• FAU and EMT synthesized using crown ether templates
2-$C_4^=$ Conv [%]	88	98	66	67	
Alkylate Yield [g C_5+/g $C_4^=$ fed]	4.13	5.70	1.54	2.33	• Ideally should be: 2 g C_5^+/g $C_4^=$ fed
C_5+ Liquid [mass%]					
C_5-C_7	10	8	23	18	• Cracking activity
C_8	82	76	68	72	
C_9+	8	16	9	10	• Polymerization activity
C_8 Fraction [mass%]					
TMP	83	85	82	80	• high octane alkylate
DMH	16	15	14	16	• low octane alkylate
$C_8^=$	1	0	4	4	• oligomerization products
TMP Fraction [%]					
2,2,4-TMP	29	39	23	27	• highest octane value
2,2,3-TMP	9	6	18	15	• direct product of reaction
2,3,4-TMP	27	27	37	36	• least sterically hindered
2,3,3-TMP	35	28	22	22	• least sterically hindered
Indicators [mass fr]					
$\frac{\text{TMP}}{\text{DMH}}$	5.2	5.8	5.3	5.1	• high/low octane alkylate
$\frac{\text{2,2,3- + 2,2,4-TMP}}{\text{2,3,4- + 2,3,3-TMP}}$	0.62	0.36	0.57	0.49	• thermodyn. favoured/least sterically hindered isomers
$\frac{\text{TMP+DMH}}{C_8^= + C_9^+}$	9.8	4.8	5.2	5.5	• effective/ineffective hydride transfer

1 Catalyst calcined externally at 540°C for 5 hours in air during catalyst preparation. Prior to reaction, catalyst calcined externally at 400°C for 2 h, then transferred to reactor and pre-treated at 200°C for 2 h.

The ratio of pyridine adsorption at 400°C relative to that at 250°C (ratio of strong to weak acid sites) for the parent and dealuminated EMT, are 0.84 and 0.85 respectively (Stocker et al, 1996). For FAU, the respective ratios are 0.76 and 0.72. All samples retained some pyridine at 550°C, indicating the presence of very strong acid sites. These ratios emphasize the distinctive characters of EMT and FAU despite their similar structure, and may explain the differences observed in their

performance with respect to alkylation.

The EMT system favoured the formation of TMPs over DMHs, with 2,3,3-TMP and 2,3-DMH being the dominant isomers in each respective fraction. In contrast, FAU demonstrated a greater tendency to oligomerize, as reflected by the higher $C_8^=$ content in the product distribution. Polymerization proceeded to a greater extent on FAU relative to EMT, which is not surprising in view of its greater preponderance to oligomerize.

Dealumination of EMT enhanced alkylation yield, primarily in favour of greater C_9^+ formation at the expense of the preferred C_8 fraction. Although 2,3,3-TMP continued to be the dominant TMP isomer, dealumination of EMT resulted in a decline of 2,2,4-TMP formation. Under all conditions, 2,2,3-TMP, the primary product of 2-$C_4^=$ and *i*-C_4 alkylation, was the least favoured TMP isomer.

Recall that dealumination of Y zeolites results in the formation of EFAL species, which have been found to exert a pronounced effect on catalytic activity. It is of interest to examine whether FAU or EMT synthesized using crown-ether templates, display the same effect, particularly in view of the unique Al distribution in the catalyst.

A much higher C_9^+ content was observed in the product distribution for the dealuminated EMT suggesting enhanced polymerization. In addition, a drop in cracking activity was evidenced by the lower C_5 - C_7 levels. These results suggest that catalyst deactivation, as a result of coke deposition, proceeded at a more rapid rate on the dealuminated EMT catalyst. This restricted the formation of 2,2,4-TMP and favoured the formation of the least sterically hindered TMP isomers. This hypothesis is supported by the fact that hydride transfer declined as a consequence of dealumination.

Dealumination of FAU produced a similar increase in alkylation yield and selectivity. No significant change in the TMP/DMH ratio was noted, although dealumination of FAU appeared to discourage the formation of 2,2,4-TMP. This agrees with the trend observed for EMT and USY.

Similar to Y and USY zeolites, rare earth metal exchange (i.e. La) in EMT and FAU, have also been explored, to determine if the acidity can be tuned to fit alkylation demands. The exchange of 40 % and 80 % La in EMT (La40EMT and La80EMT respectively) caused an overall reduction Bronsted acidity (Mostad et al, 1997).

The catalyst, La40EMT, demonstrated superior performance over EMT, in terms of alkylate yield (g C_5-C_8 paraffins/g dry cat) and selectivity (g C_5-C_8 paraffins/g 2-$C_4^=$ conv.). It appears that the hydride transfer ability was improved with the introduction of La, as indicated by a suppression of oligomerization and polymerization activities and elevated cracking and alkylation activities (see Table 2.9).

Although similar TMP/DMH ratios were observed for both EMT and La40EMT, the latter catalyst improved 2,2,4-TMP selectivity significantly. In general, the introduction of La enhanced the production of the TMP isomers that are more sterically hindered and slower to diffuse out of the catalyst pores.

The effect of calcination temperature, on alkylate yield and selectivity, was also explored. At 45 % La exchange, the optimal calcination temperature was identified as 450°C. This calcination temperature possessed the highest proportion of strong Bronsted acid sites (see Table 2.6) of those exchanged with La, supporting the belief that very strong acid sites are necessary to promote hydride transfer and delay the onset of catalyst deactivation.

At higher exchange levels (80 % La exchange), a decrease in butene conversion, yield and selectivity resulted, with elevated amounts of C_9^+ produced. Studies at 51 % La exchange in EMT concluded that the optimum ion exchange level was below 51 % (Rorvik et al, 1997).

The catalyst, La40FAU (40 % La exchange in FAU), demonstrated inferior performance to EMT and La40EMT, and favoured higher levels of cracking, oligomerization and polymerization levels at the expense of alkylation (Mostad et al, 1997). Although La40FAU and La40EMT possess similar geometrical sizes and total acidities, structural differences exist. The catalyst, EMT, possesses larger hypercages and improved accessibility to these cages through five channels, as

opposed to four in FAU. It may be that these structure differences are responsible for the enhanced performance of La40EMT over La40FAU.

Table 2.9: Alkylate Product Distribution on EMT and La-Exchanged EMT[1] (t = 3h, T = 80°C, semi-batch reactor; I/O=10) (Rorvik et al, 1997)

Catalyst	EMT	La40 EMT	La80 EMT	• LaxEMT where x indicates degree of La exchange
2-$C_4^=$ Conv [%]	88	100	81	
Alkylate Yield [g C_5+/g $C_4^=$ fed]	1.7	2.2	1.2	• ideally should be: 2 g C_5^+/g $C_4^=$ fed
C_5+ Liquid [mass %]				
C_5-C_7	8	10	10	• cracking activity
C_8	82	85	78	• alkylation/oligomerization
C_9+	10	5	12	• polymerization activity
C_8 Fraction [mass%]				
TMP	82	84	84	• high octane alkylate
DMH	15	15	15	
$C_8^=$	3	1	1	• oligomerization products
TMP Fraction [%]				
2,2,4-TMP	18	38	20	• highest octane value
2,2,3-TMP	5	7	3	• direct product of reaction
2,3,4-TMP	36	23	41	• least sterically hindered
2,3,3-TMP	41	32	36	• least sterically hindered
Indicators [mass fr]				
$\frac{\text{TMP}}{\text{DMH}}$	5.6	5.6	5.7	• high/low octane alkylate
$\frac{\text{2,2,3- + 2,2,4-TMP}}{\text{2,3,4- + 2,3,3-TMP}}$	0.29	0.82	0.29	• thermodyn. favoured /least sterically hindered isomers
$\frac{\text{TMP+DMH}}{C_8^= + C_9^+}$	6.3	15.9	6.1	• effective/ineffective hydride transfer

1 Catalyst calcined externally at 540°C for 5 hours in air during catalyst preparation. Prior to reaction, catalyst calcined externally at 400°C for 2 h, then transferred to reactor and pre-treated at 200°C for 2 h.

2.2 IDENTIFICATION OF PREFERRED ACIDIC SUPPORT

Many solid acids have been explored for application to butene isobutane. These include β-zeolite (Corma et al, 1994a; Corma et al, 1994b; Corma et al. 1994c; Corma et al, 1994d; Nivarthy et al, 1998; Loenders et al, 1998), MCM-22 (Corma et al, 1994a), ZSM-5 (Chu & Chester, 1986; Weitkamp & Jacobs, 1993), SAPO-37 (Mostad et al, 1996), SO_4^{2-}/ZrO_2 (Cormaet al, 1994c; Corma et al, 1994d; Corma et al. 1994e; Xiao et al, 1998) and heteropoly acids and their salts (Corma et al, 1996d; Blasco et al, 1998). The catalyst Nafion-H, a solid superacid polymer, has also been applied to butene/isobutane alkylation (Rorvik et al, 1995). Although high activity is frequently demonstrated by several solid acid systems, rapid deactivation ultimately ensues, primarily due to loss of hydride transfer functioning.

The success of any solid acid, lies in its ability to maintain strong hydride transfer. A high density of strong Bronsted acid sites is necessary to facilitate alkylation of butene with isobutane. Unfortunately this arrangement also promotes oligomerization of butene, a more facile reaction. Literature studies on Y, FAU and EMT zeolites, conclude that catalyst performance improves by tempering catalyst acidity through partial dealumination or rare earth metal exchange. It appears that a compromise between enhancing hydride transfer and suppressing oligomerization tendencies is necessary.

This lays the foundation for the catalyst design requirements. The catalyst EMT, was chosen as the acidic support in the present research, for the following reasons. Firstly, EMT has a slightly higher Si/Al ratio (typically between 3 and 5) relative to that of Y zeolite (between 1 and 3), representing a slightly lower acid site density.

Secondly, EMT possesses a high density of strong Bronsted acid sites, which are isolated from other groups of strong sites by dense siliceous regions. The ratio of strong to weak acid sites is very high for EMT relative to USY. This type of acid strength distribution is ideally suited for alkylation, as it offers a high concentration of strong Bronsted acid sites to facilitate hydride transfer. These pockets of acid sites

are surrounded by inert siliceous regions, which may suppress oligomerization tendencies.

Thirdly, pyridine IR spectra suggest that EMT possesses predominantly Bronsted type acidity over the entire acid strength distribution. This is unique to this type of material. This is ideally suited for alkylation, as the carbenium mechanism is facilitated by strong Bronsted acid sites. Also, the low concentrations of Lewis acid sites, imply that undesirable side reactions promoted by Lewis acidity will be minimized.

Fourthly, the hypercages of EMT are slightly larger and have improved accessibility through five channels, relative to the smaller supercages of H-USY providing access through four channels. This is beneficial to the formation of isomerized products, based on alkylation and cracking studies, as well as favouring efficient diffusion of the products out of the catalyst network. Finally, the thermal and hydrothermal stability of EMT, are found to be very high. This is particularly important when considering the severe conditions employed during regeneration processes.

Research on EMT is relatively new. The material was first synthesized in 1990 and has not been studied extensively with respect to alkylation. Preliminary results on cracking and alkylation reactions, conclude that EMT is capable of maintaining high catalytic activity and postponing the onset of catalyst deactivation. For these reasons, EMT was chosen as the acidic component in the catalyst design of the present investigation.

2.3 REVIEW OF HYDROGEN SPILLOVER

2.3.1 Definition of Hydrogen Spillover

The loss of hydride transfer has been associated with catalyst deactivation in solid acid catalysed reactions. For this reason, a primary consideration in the catalyst design will be the enhancement of the hydride transfer ability of the catalyst, to delay the onset of deactivation. Spillover is a phenomenon, which offers potential to address this issue.

Spillover involves the transport of an active species, formed or sorbed on a surface, onto a second surface, that does not sorb or form active species under the same conditions. The spillover species can either react with other sorbing species on the second surface and/or it can serve to activate the second phase.

The surface, which adsorbs and forms the active species, is called the *donor surface* or *activator*. The surface that gains access to the activated species, by being in contact with the donor surface, is called the *accepting surface*. The donor surface can be mounted on an inert support and physically mixed with the acceptor phase or it can be mounted directly on the acceptor phase (see Figure 2.2).

Movement of the spillover species is achieved by the formation of equivalent bonds with similar neighbouring surface atoms. In essence, it is an effective exchange of bonds between the adsorbed species and the surface, which facilitates movement. Surface diffusion of the spillover species is generally agreed to be the rate limiting step in the overall process of spillover (Conner et al, 1986; Conner et al, 1995). The energetics of hydrogen spillover (H_{so}) is illustrated in Figure 2.3.

Reverse spillover occurs when the spillover species diffuses back to the activating center, where it can recombine (if dissociated), react or desorb. At steady state, spillover involves a competitive formation of spillover species and their demise through reverse spillover (Conner et al, 1995).

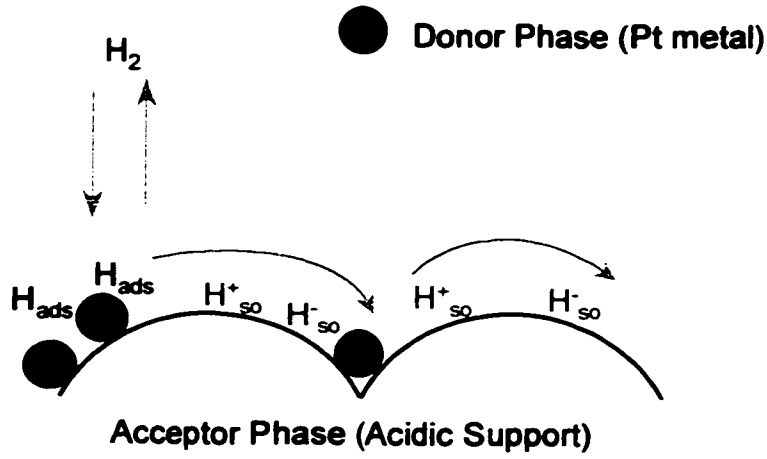

Figure 2.2: Schematic of Donor and Acceptor Phases for Spillover Species

The existence of spillover is a highly controversial subject, although recent evidence using electron spin resonance (ESR) in conjunction with a spin trap, provides convincing evidence of the existence of spillover (Spencer, 1994). Three conferences have been devoted entirely to the subject of spillover (Lyon, France (1983), Leipzig, Germany (1989) and Kyoto, Japan (1993)) echoing the support for this subject in the research community.

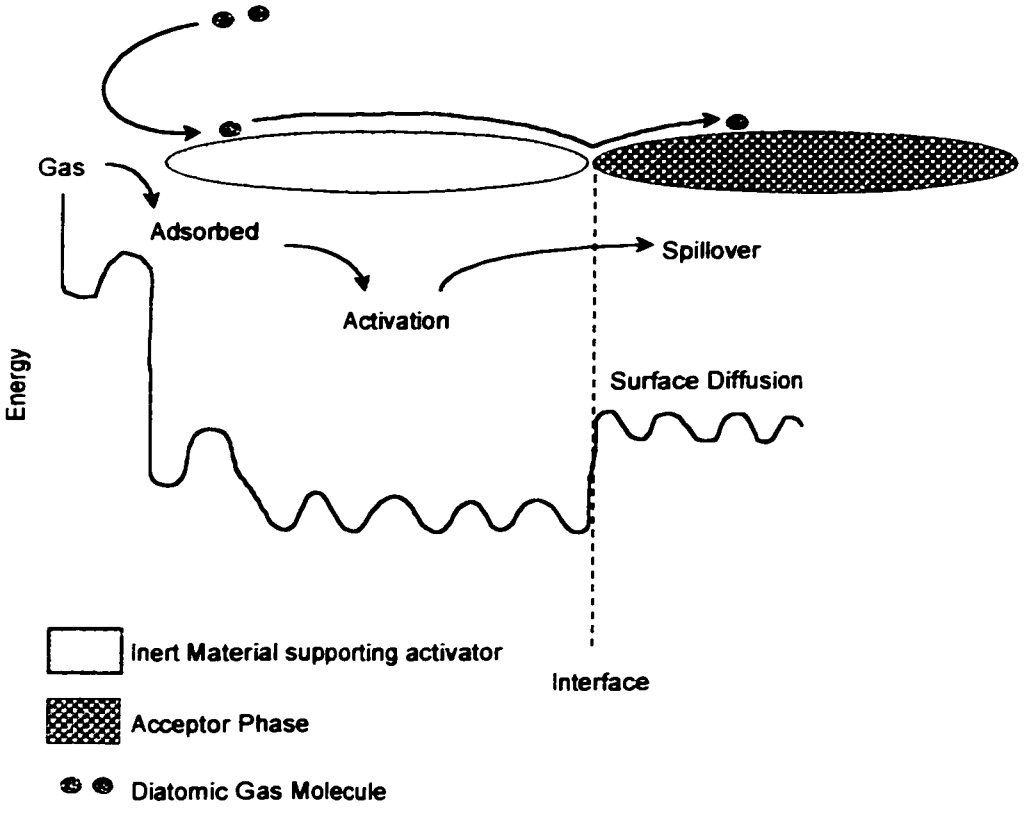

Figure 2.3: Energetics for Spillover of Gaseous Diatomic Molecule from the Gas Phase to the Accepting Surface (Conner et al, 1986)

2.3.2 Nature of Spillover Species

The most important spillover species are H_2 and O_2, although others such as CO (Teichner, 1993), N_2 (Conner & Falconer, 1995), isocyanate, methoxy (CH_3O), formate (CHOO) species as well as hydrocarbons, have been reported. Hydrogen is the fastest spillover process in terms of development of a spillover population, and is believed to be facilitated by surface hydroxyls (Ohgoshi et al, 1993; Dmitriev et al,

1983). A relationship between surface basicity and diffusion of O_{so} (spillover oxygen) has been suggested (Martin & Duprez, 1993).

A noble metal (Group VIII transition metal such as Pt, Pd or Ni, listed in order of preference) supported on an oxide (carbon, Al_2O_3, SiO_2 but zeolite also possible) is used to generate spillover hydrogen (Bond, 1983). The nature of the hydrogen spillover species is a subject of debate. Some groups claim that molecular hydrogen forms two protonic hydrogen species (H^+_{so}), with the electrons reducing the metal of the metal oxide surface (see Equation 2-2):

$$H_2 \longrightarrow 2\ H^+_{so} + 2\ e^-_{so} \qquad (2\text{-}2)$$

There is evidence of this form of spillover species, when the metal is supported on a reducible oxide. However, this mechanism is difficult to envision on non-reducible metal oxides where spillover is active.

Others claim that diatomic spillover hydrogen species are formed which become bound to the surface (H_{so}-) (see Equation 2-3):

$$H_2 \longrightarrow 2\ H_{so}- \qquad (2\text{-}3)$$

Still, others suggest the formation of ionic species (H^+_{so} or H^-_{so}) upon H_2 dissociation (see Equation 2-4):

$$H_2 \longrightarrow H^+_{so} + H^-_{so} \qquad (2\text{-}4)$$

although a H^-_{so} has never been detected.

Finally, a free radical species is proposed by some groups ($H\bullet_{so}$) (see Equation 2-5):

$$H_2 \longrightarrow 2\ H_{so}\bullet \qquad (2\text{-}5)$$

Irrespective of the nature of the spillover species, profound effects on the reaction rate are claimed. It is believed that spillover can proceed by a variety of mechanisms, and may involve any one of the proposed species under certain circumstances. It is generally believed that the nature of the acceptor is influential in determining the form of the spillover species.

2.4 INCORPORATION OF HYDRIDE TRANSFER PROMOTER INTO SOLID ACID ALKYLATION CATALYST DESIGN

Solid acid catalysed reactions suffer from the tendency for the acid sites to become deactivated due to coke deposition. It is proposed that the onset of catalyst deactivation can be delayed by incorporating a noble metal into the catalyst design to activate hydrogen spillover.

2.4.1 Proposed Alkylation Mechanism Involving Spillover

It is proposed that spillover hydrogen can diffuse to coke retained on the acid sites of the metal oxide surface, and hydrogenate it to form smaller hydrocarbons which can diffuse out of the pore network. The acid site will thus be regenerated and

the accumulation of polymerized materials will be minimized (Conner & Falconer, 1995). Catalyst lifetime will be extended and steric restrictions of transitional species minimized. Hopefully this will exert a positive effect on the production of the bulky isomer 2,2,4-TMP.

It is also possible for spillover hydrogen to enhance the hydride transfer ability of the catalyst (see Figure 2.4). As previously mentioned, the nature of the acceptor phase is influential in determining the form of the spillover species. For zeolites, it is generally believed that spillover species assume the form of H^+_{so} and H^-_{so}. The noble metal (Pt shown) will promote the adsorption of molecular hydrogen and form the spillover species (H^+_{so} and H^-_{so}) according to Equation 2-4. It has been well documented that exchange with surface -OH groups is promoted by noble metals, with Pt demonstrating superiority over all others (Dmitriev et al, 1983).

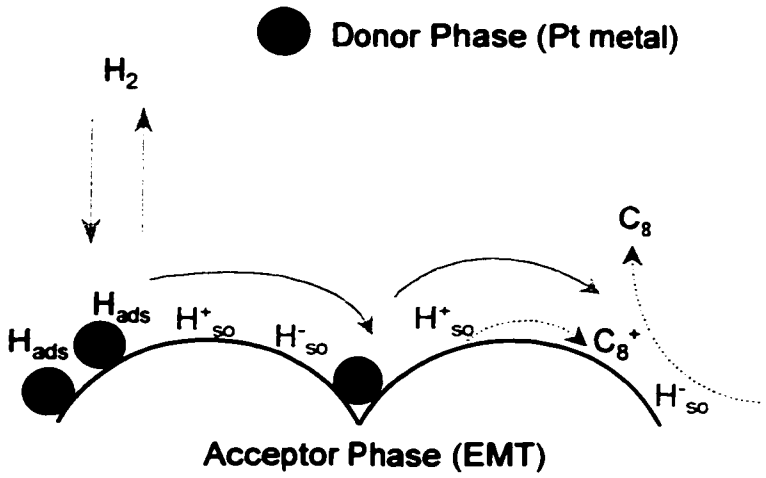

Figure 2.4: Proposed Mechanism for Hydrogen Spillover Participation in Butene/Isobutane Alkylation

It is proposed that an adsorbed octyl carbenium ion could accept a spillover hydride ion (H^-_{so}) and desorb as an octane product. The spillover hydrogen proton (H^+_{so}) could regenerate the acid site on the catalyst surface, thus completing the cycle

according to Equation 2-6 (see Figure 2.4).

$$i\text{-}C_8^{+}{}_{(surf)} + H^{+}{}_{so} + H^{-}{}_{so} \longrightarrow i\text{-}C_8 + H^{+}{}_{(surf)} \qquad (2\text{-}6)$$

This mode of hydride transfer could supplement that provided by the isobutane.

Spillover could provide additional benefits towards alkylation. During oxidative regeneration, the noble metal could facilitate oxygen spillover, such that lower temperatures could be employed to achieve the efficient removal of retained hydrocarbons. Incorporation of a metal into the catalyst design thus serves a multi-purpose.

2.4.2 Mode of Incorporation of Spillover Activator into Catalyst Design

There is considerable evidence that the rate-determining step of spillover is the diffusion of the spillover species from the donor phase to the acceptor (Conner & Falconer, 1995). For example, isomerization of *n*-C_5 demands intimate contact of the noble metal with the acidic support (Fujimoto, 1993; Aimoto et al, 1993). However, other reactions appear to be less sensitive to the span of separation (Conner & Falconer, 1995).

The noble metal, Pt, will be impregnated directly onto EMT and Y zeolites, to provide the minimum possible separation distance for spillover movement. The performance of the Pt impregnated materials will be compared to the parent materials, where no noble metal is present. Although hydrogen spillover can not be conclusively proven using this approach, it is expected that Pt will increase the amount of reactive hydrogen in the vicinity of the acid sites. Therefore, the benefit of Pt incorporation into the catalyst design with respect to reactive hydrogen concentration, can be assessed.

Chapter 3

Catalyst Preparation

Pure cubic polymorph of faujasite (FAU) can be synthesized from aluminosilicate hydrogels containing high concentrations of sodium (Na_2O/ Al_2O_3 = 3.1). The framework Si/Al ratio of the faujasite product ranges from 1.5 to 3 (Delprato et al, 1990), but impurity phases such as gismondine or gmelinite-type zeolites are often present in the crystalline product at the upper Si/Al limit.

The amount of aluminum incorporation into the matrix can be suppressed through the addition of an organic template to the hydrogel. Thus, the Si/Al ratio of the zeolite product can be increased without any need for post-synthesis treatment (i.e. chemical dealumination or steam dealumination). Recently, crown-ether templates have been applied successfully in this capacity, with both cubic (FAU) and hexagonal (EMT) phase polymorphs of faujasite being synthesized, with Si/Al ratio approaching 5 (Delprato et al, 1990). It is believed that the reduction of Al in the zeolite framework, is a consequence of the reaction mixture pH decreasing during aging and crystallization, in contradiction to what transpires during cubic phase synthesis from Na-rich hydrogels (Y zeolite).

FAU and EMT have similar structure types and hence, geometrical pore sizes and cages (see Figure 3.1). In FAU, the largest voids formed are called "supercages", with a diameter of 1.3 nm and a void volume of 1.15 nm^3 (van Santen, 1991). Accessibility to the supercage occurs through four circular 12-membered oxygen windows, each with a free dimension of 0.74 nm.

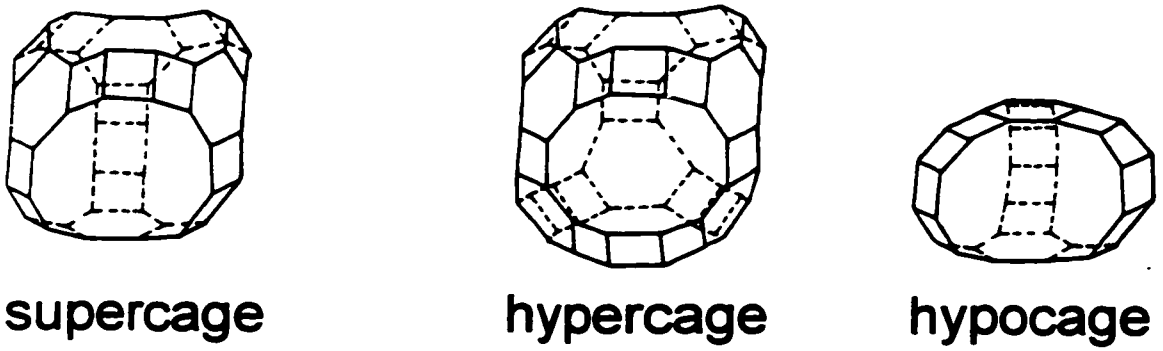

Figure 3.1: Polyhedral Cages occurring in cubic (Y, FAU) and hexagonal (EMT) phase Faujasites (*reprinted from Zeolites 9, Martens et al, "Investigation of the Pore Architecture of CSZ-1 Zeolites with the Decane Test Reaction", 423-427 (1989), Figure 1 only, with permission from Elsevier Science)*

EMT has an equal number of two types of large cages (Martens et al, 1989). The largest of the void spaces, called "hypercages", has a void volume of 1.24 nm^3, slightly greater than that of the supercages found in FAU. The "hypercages" have a free dimension of 1.3 x 1.3 x 1.4 nm and can be entered through a total of five channels: two circular channels similar to the entrances of the supercages in FAU and three elliptically shaped apertures with free diameters of 0.69 nm x 0.74 nm (Thomas et al, 1982). More importantly, the entrance to the "hypercage" is via straight channels. The smaller of the void spaces in EMT, called the "hypocages", have a void volume of 0.61 nm^3 which is significantly smaller than the "supercages" of FAU (van Santen, 1991). The "hypocages" have free dimensions of 0.69 x 1.3 x 1.3 nm and can be accessed through three elliptic windows (Thomas et al, 1982).

3.1 METHOD OF PREPARATION OF Na-EMT

The synthesis of Na-EMT appears to be more of an art than a science. Although recipes available in the literature are followed exactly, successful EMT synthesis is often elusive.

3.1.1 Chemical Sources and their Functions

The chemical species required for EMT synthesis and their functions, are summarized in Table 3.1 (Jansen, 1991; Feijen et al, 1994a). The choice of Al- and Si-sources does not appear to be critical for successful synthesis. Typical Si-sources include silicon alkoxides (TMAS, TEOS), water glass, colloidal silica (Ludox HS-40, Ludox AS-40) and fumed silica. Common Al-sources are gibbsite, sodium aluminate, metallic aluminum powder and pseudo-boehmite. Sodium is added in the form of sodium hydroxide with some potentially provided by the Si- and Al-sources.

Hydrated Na^+ cations (primary cation) direct the formation of the faujasite sheets, consisting of cubo-octahedra interconnected through hexagonal prisms. Cationic Na-18-crown-6 ether complexes act as secondary cations and facilitate the linking of the faujasite sheets into the hexagonal structure (see Figure 3.2).

Table 3.1: Chemical Sources and their Function in EMT Synthesis

SOURCE	FUNCTION(S)
SiO_2	• Primary building unit(s) of framework
AlO_2^-	• Origin of framework charge
OH^-	• Mineralizer, guest molecule
Na^+	• charge balancing cation for framework charge • primary directing cation
18-crown-6 ether (see Figure 3.3)	• secondary directing cation (complexes with Na^+ cation)
Water	• solvent, guest molecule

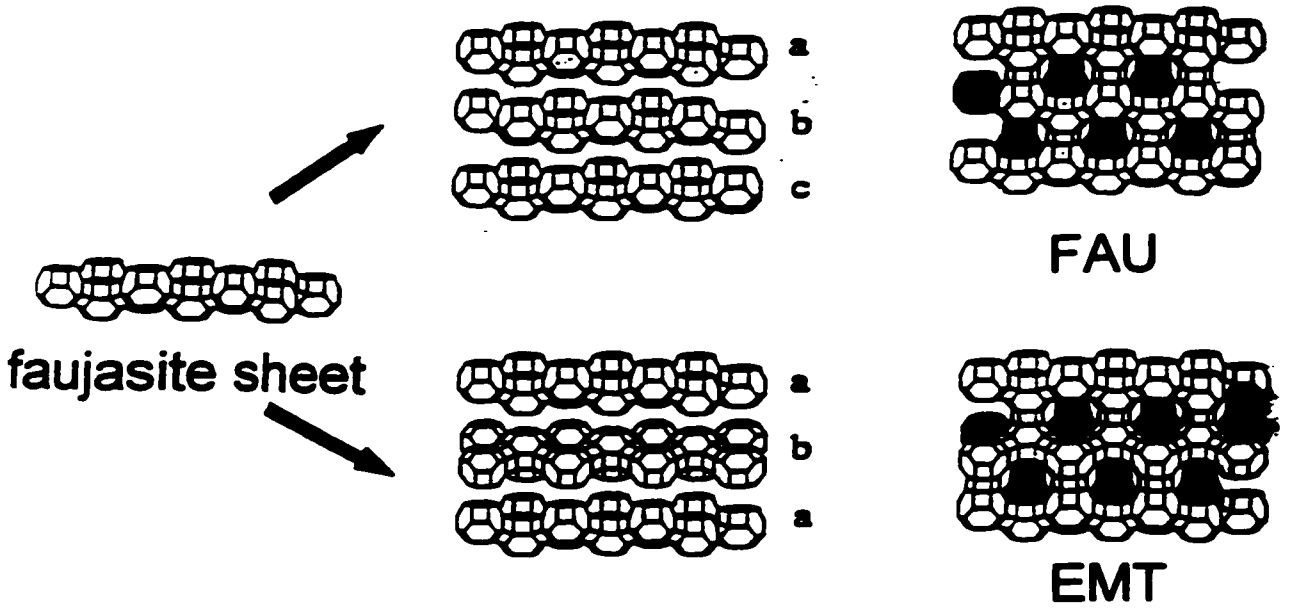

Figure 3.2: Assembly of Faujasite Sheets to yield FAU and EMT Phases (reprinted from J. Am. Chem. Soc. 116(7), Feijen et al, "Role of 18-Crown-6 and 15-Crown-5 Ethers in the Crystallization of Polytype Faujasite Zeolites", 2950-2957 (1994), with permission from ACS, Publications Division)

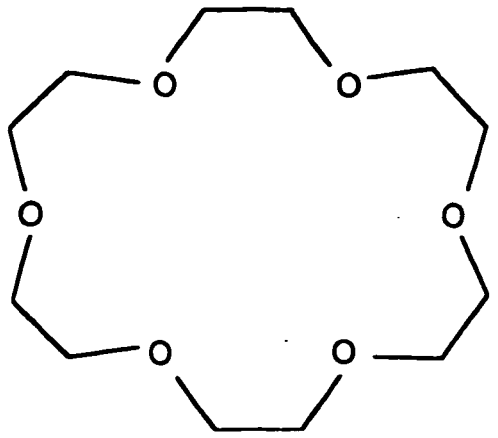

Figure 3.3: Structure of 18-crown-6 ether Template

Under conditions of high Na^+ content, the structure directing role of the crown ether is masked by the influence of the Na cation, favouring the formation of FAU (Burkett & Davis, 1993). This emphasizes the importance of the Na_2O/18-crown-6 ether ratio in the gel, and its crucial role in determining the outcome of the crystallization process.

The Na_2O/Al_2O_3 ratio is another important gel property, which is influential in determining the properties of the crystallized product. With a Na_2O/Al_2O_3 ratio of 2 and sufficient 18-crown-6 ether available, no crystallization occurs. At higher Na_2O/Al_2O_3 levels in the range of 2.4 to 3, the cubic polytype (FAU) is favoured, even in the presence of adequate 18-crown-6 ether. Pure hexagonal polytype (EMT) is produced from hydrogels containing sufficient 18-crown-6 ether and a Na_2O/Al_2O_3 ratio ranging from 2.0 to 2.4 (Delprato, 1990). Ideally, the Na_2O/Al_2O_3 level should be 2.4, to maximize the purity and crystallinity of EMT (Jansen, 1991).

3.1.2 List of Materials

The reagents employed in the present research are summarized in Table 3.2. Impurities such as Fe^{3+} and K^{+} exert minor influences compared to the effects of Al^{3+} and Na^{+}, respectively, during the synthesis.

Table 3.2: List of Materials for EMT Synthesis

Reagent	Source	Description
Ludox HS-40	Aldrich	• 40 wt. % colloidal SiO_2 in H_2O • Impurity: Al < 500 ppm
Gibbsite, $Al(OH)_3$	Fluka	• 64-66 % Al_2O_3 • Impurity: Fe < 3 ppm
NaOH Pellets, Technical grade	BDH	• 97 % purity • Impurities: K < 20,000 ppm, Fe < 1000 ppm, Ni < 1000 ppm
18-crown-6 ether	Acros Chemicals	• 99 % purity
Double de-ionized water		

3.1.3 Preparation of the Hydrogel

Synthesis of EMT is difficult. Nine months worth of catalyst preparation efforts, employing six different published methods, did not produce any batches of EMT with a high degree of purity. Prof. J. A. Martens (Centre for Surface Science and Catalysis, K. U. Leuven, Belgium) is an expert in the area of catalyst synthesis, characterizaiton and catalysis. He has experience in the synthesis of EMT and has co-authored several papers on the role of the crown-ether template during the crystallization step. Prof. Martens (Gossens, 1998) provided a detailed description for EMT synthesis (modified method of Feijen et al, 1994b). Fourteen successful batches of EMT have been prepared in this laboratory, using this approach (see Appendix A1.1).

The synthesis began with the preparation of a sodium aluminate solution (Gossens, 1998; Feijen et al, 1994b). The mixture was heated, as Al_2O_3 is not easily dissolved. Once Al_2O_3 dissolution was complete, the solution was cooled to room temperature. Some of the Al may precipitate but this does not appear to affect the synthesis. Upon reaching room temperature, the amount of water that had evaporated during the heating step, was determined, and added back to the solution.

The silica sol was diluted with water and then the crown ether was added. This is necessary to ensure adequate dissolution of the crown ether in the silica sol. This mixture was added to the sodium aluminate solution and then further diluted with water. The overall composition of the hydrogel was:

$$10\ SiO_2 : 1.00\ Al_2O_3 : 2.40\ Na_2O : 0.97\ \text{18-crown-6 ether} : 140.25\ H_2O$$

3.1.4 The Aging Period

The resulting gel was transferred into a teflon bottle and aged at room temperature for 3 days in the absence of agitation. Maintaining the gel at a temperature below the crystallization temperature is crucial, in order to achieve the desired product within an acceptable period of time. It is possible to shorten the aging period to 1 day, as suggested by Delprato et al (1990), but a longer aging period enhances uniformity in crystal size and composition.

One important step during the aging period is the depolymerization of the silica sol, increasing the concentration of dissolved silicate species. Monomeric silicate anions condense and polymerize to produce oligomeric species in solution, which in turn react with monomeric aluminate anions to produce aluminosilicate structures. These aluminosilicate species concomitantly undergo re-dissolution and re-condensation during the aging period (Feijen et al, 1994a).

The pH of the hydrogel was found to decrease significantly during the aging period (see Figure 3.4). This behavior is not reported by Delprato et al (1990), as the

aging period of one day was used in that particular study. However, a notable drop in the pH during the crystallization period is reported by the Delprato study.

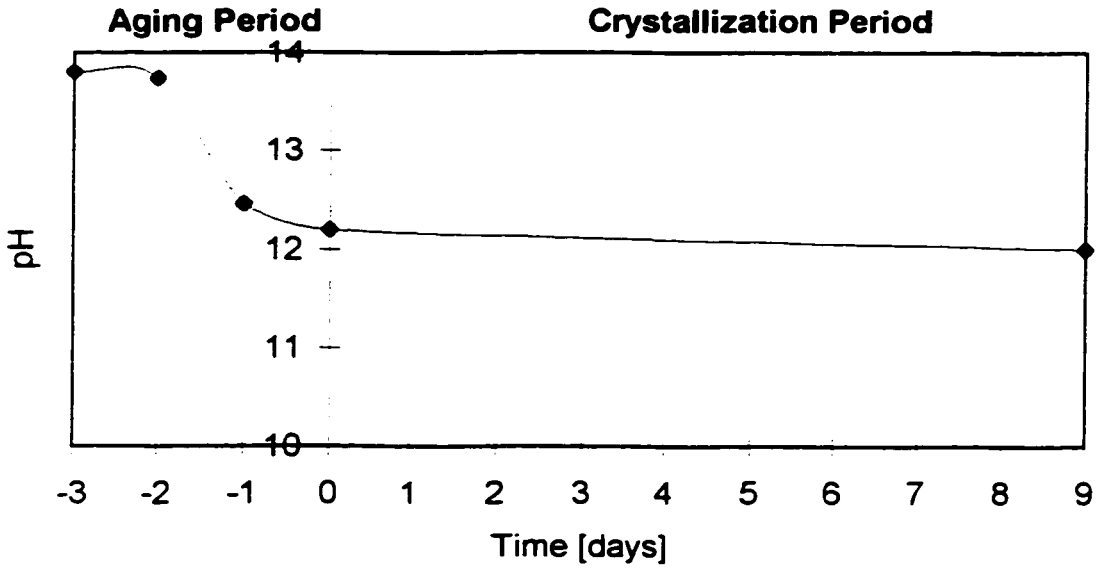

Figure 3.4: Evolution of pH during the Aging and Crystallization Periods

3.1.5 The Crystallization Step

Once the aging period had elapsed, the bottle was placed in an oven maintained at 100°C for a period of 9 days. The elevated temperature favours the formation of aluminosilicate structures, thus increasing their concentration in the solution. Eventually the solution becomes supersaturated with precursor species. Chemical aggregation of these precursors results in the formation of germ-nuclei, which can re-dissolve upon depolymerization. The germ-nuclei continue to grow over time until some nuclei achieve a critical dimension necessary to become viable and spontaneously spawn crystal growth.

Both nucleation and crystallization proceed simultaneously with both processes consuming the same precursors. Eventually, the source of precursor

species becomes depleted causing the nucleation and crystallization rates to decline.

The crystallization process follows Ostwald's rule, by which the thermodynamically least favourable phase forms first, followed by successively more stable phases. The sequence of phases which are formed during the synthesis are: amorphous $\Rightarrow$ EMT $\Rightarrow$ Na-P (Gismondine type) (Feijen et al, 1994a). Higher temperatures favour dense phase development (Na-P), as the amount of water in the liquid phase decreases.

Contrary to what takes place during Y zeolite synthesis from inorganic hydrogels, pH drops during the crystallization phase in hydrogels containing crown ethers. When a three day aging period was employed, the pH dropped slightly by 0.2 units during the crystallization phase (see Figure 3.4). With a shorter aging period, the drop in pH during the crystallization phase is more substantial. Over the course of an eight day crystallization period, the pH decreases by approximately 1.5 units (Delprato et al, 1990). This results in a Si/Al gradient in the crystals ranging from 3.5 at the center to greater than 5 at the edges. By extending the aging period to 3 days, the majority of the pH reduction occurred prior to the crystallization step, favouring a uniform Si/Al composition and size amongst the crystal population. Also, the lower pH reduces the extent of Al incorporation into the hexagonal lattice, resulting in a higher Si/Al ratio in the EMT crystals (Delprato et al, 1990; Feijen et al, 1994a).

3.1.6 Template Removal

After the crystallization period had elapsed, the teflon bottle was removed from the oven and cooled to room temperature. The product was recovered by filtration, washed with double de-ionized water until the pH of the filtrate was neutral, and dried overnight at 80°C.

The dried product was calcined in flowing air by increasing the temperature at a rate of 1°C/min, from room temperature to 200°C and sustained at this temperature

for 2 h. This removes the physisorbed water prior to the template combustion. The temperature was then ramped at a rate of 1°C/min to 425°C, where it was held constant for 5 h. Mass losses due to template combustion represent approximately 30 % of the calcined product mass. The average calcined product yield from a single batch is 10.50 g EMT (Na-form).

Figure 3.5 illustrates the thermogravimetric analysis/differential temperature analysis (TGA/DTA) employing 10 % O_2 in He gas mixture (details in Appendix A1.6). Two distinct stages of weight loss were apparent during template removal. The first mass loss is associated with an endothermic process occurring between 25 to 150°C, and represents the removal of physically adsorbed water. The second weight loss begins at approximately 325°C, and is accompanied by a steep exotherm accounting for combustion of the template. These results are similar to those reported for EMT in the literature (Feijen et al, 1994a; Annen et al, 1991).

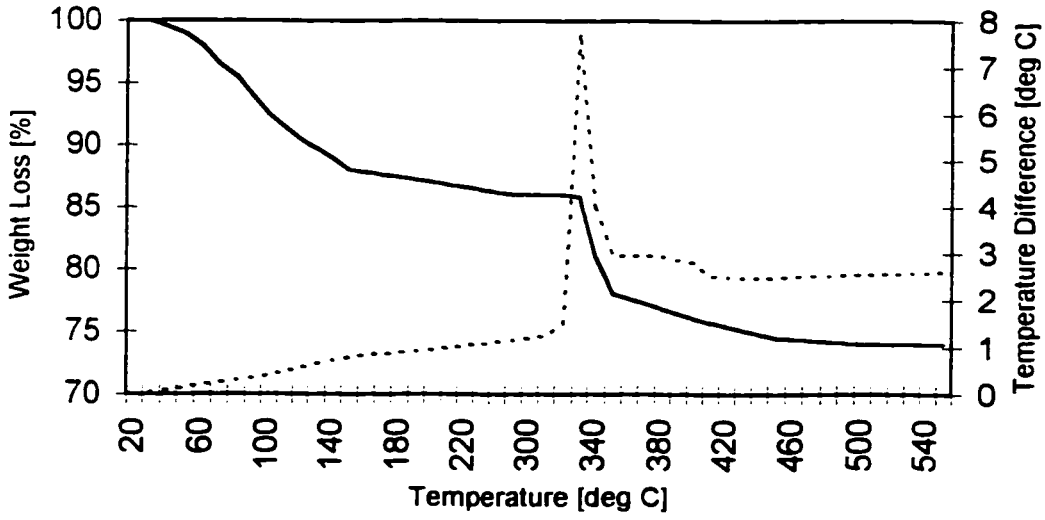

Figure 3.5: Thermal Decomposition Patterns for Template Removal from EMT (Batch G5019)

3.1.7 Phase Identification

The identification of a zeolite was made by comparing the sample powder X-ray diffraction (XRD) pattern (see Appendix A1.2 for details), with those of known standards or published patterns in the literature. The existence of EMT is validated using the diffractogram of Delprato et al (1990) as a reference. The presence of impurities or intergrowths of cubic polymorph (FAU) are indicated by the presence of major peaks of both EMT and FAU X-ray diffractograms in the sample pattern (see Figure 3.6). The XRD pattern of the final product matched that of Delprato et al (1990), confirming the identify of EMT and verifying a successful synthesis (see Figure 3.7).

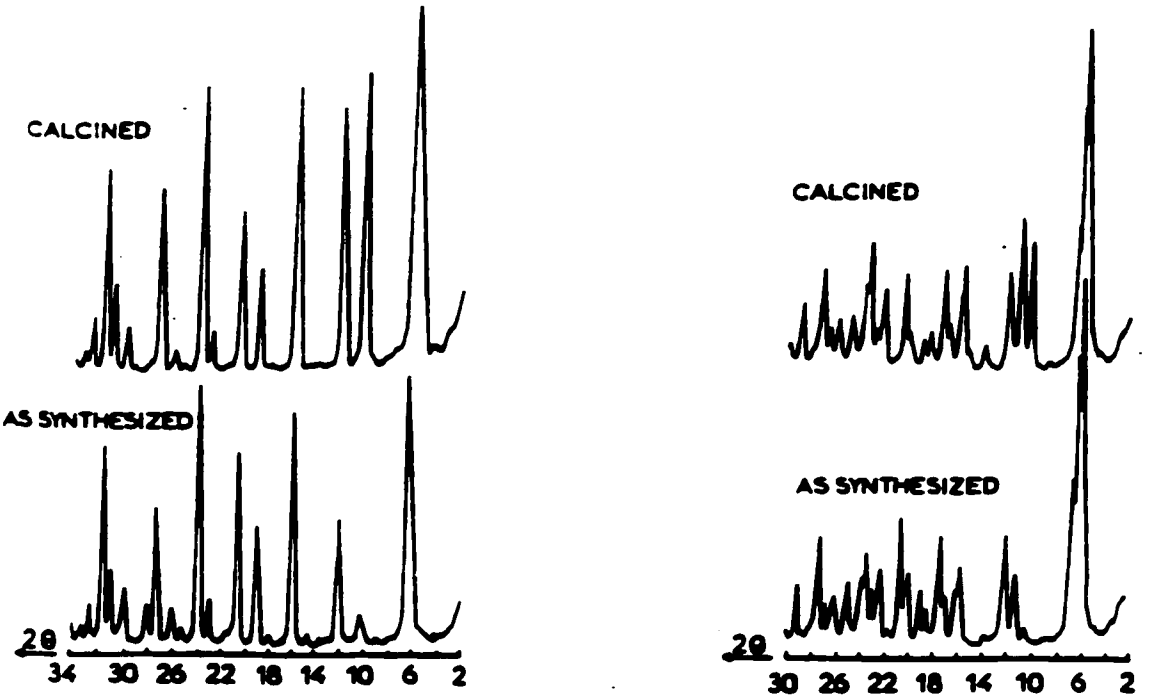

Figure 3.6: Published Powder X-ray Diffraction Pattern for cubic (FAU) and hexagonal (EMT) phase Faujasites (*reprinted from Zeolites 10, Delprato et al, "Synthesis of new silica-rich cubic and hexagonal faujasites using crown-ether-based supramolecules as templates", 546-552 (1990), Figures 4 & 5 only, with permission from Elsevier Science)*

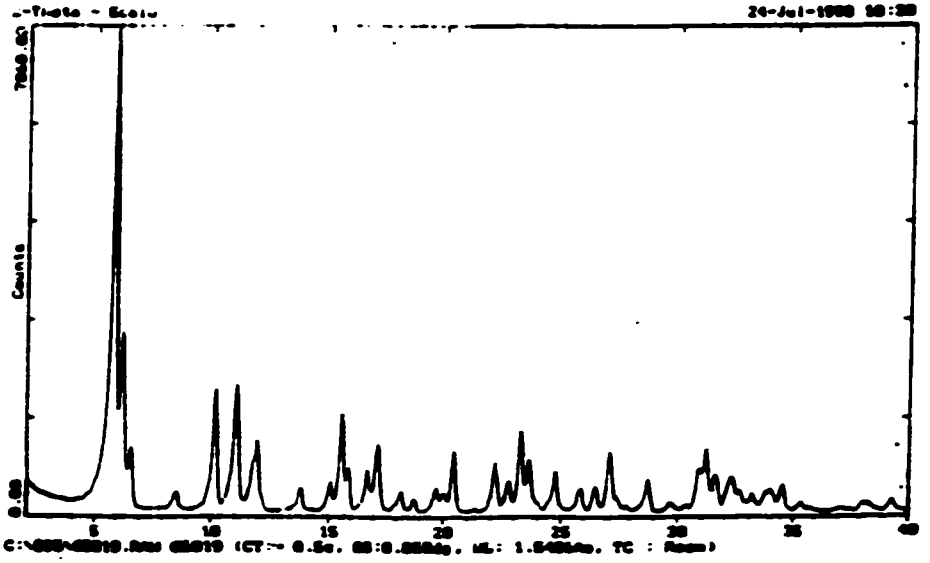

Figure 3.7: Powder X-ray Diffraction Pattern of Synthesized EMT (Batch G5019)

3.2 BATCH TO BATCH VARIATION OF EMT SYNTHESIS

The XRD patterns of all batches corresponded closely to that of Delprato et al, 1990 (Figure 3.6), confirming the existence of a hexagonal structure. No evidence of FAU impurities or intergrowths were detected in the synthesized products.

Surface area measurements confirmed the existence of a highly crystalline product (see Table 3.3). However, ANOVA analysis detected significant batch to batch variation. This conclusion was supported by a 12 % variation in XRD peak intensity for the strongest peak in the EMT diffraction pattern ($2\theta \sim 5.9°$). This emphasizes the importance of developing a strategy to minimize/eliminate the effects of batch to batch variation for the purposes of catalyst testing. This approach will be discussed in greater detail in Section 3.3.

Table 3.3: ANOVA Analysis on Batch Surface Area Measurements for Na-EMT

	ANOVA Results [m^2/g]
Grand Average	906
Between Batch Standard Deviation	25
Within Batch Standard Deviation	14
Equipment Standard Deviation	2

3.3 AMMONIUM ION EXCHANGE OF Na-EMT TO H-EMT

The H-form of EMT (H-EMT) was obtained by ion exchange of the parent material (Na-EMT) with an NH_4NO_3 solution, followed by calcination to drive off NH_3 (see Appendix A1.3 for details). In total, three exchange cycles are employed, with each exchange cycle followed by a calcination step. This is critical, as it redistributes the residual Na to new locations that are more accessible for removal during the subsequent exchange step. Literature measurements predict 71 % Na removal in the first exchange cycle, 85 % Na removal in the second exchange cycle and approximately 93 % overall Na removal is expected in the third exchange cycle (Dougnier et al, 1992).

The surface area of EMT was reduced by 17 % (from 906 m^2/g for Na-EMT to 755 m^2/g for H-EMT) as a result of the exchange process. The XRD measurements of H-EMT suggest that the crystallinity of the exchanged EMT improves, as indicated by an increase in the overall peak intensity on the X-ray diffractograms. This suggests that the removal of Na^+ does have a disruptive effect on the crystalline structure but rather causes the structure to contract with Na^+ removal. The material retains its structural integrity throughout the exchange process.

3.4 CHARACTERIZATION OF EMT AND Y

The H-EMT powder was pelletized, crushed and sieved to a particle size range of 0.25 to 0.50 mm diameter (60 US mesh and 35 US mesh respectively). Similarly, the commerical Y zeolite extrudate, was crushed and sieved to the same particle size range. A summary of the catalyst properties for both zeolites is provided in Table 3.4. Details of the analytical techniques used to characterize the catalysts, are provided in Appendix 1.

A slightly higher surface area and lower sodium content were measured for H-EMT relative to H-Y. Similar Si/Al ratios were estimated for both materials, although differences in aluminum environment were detected. A greater proportion of aluminum with one aluminum in the next-nearest neighbour position (Si(1Al)), were found to exist on H-EMT relative to H-Y. Tetrahedral and octehedral aluminum coordination were identified on both materials; however, evidence of hybrid structures were also found to exist on H-EMT.

Table 3.4: Summary of Catalyst Properties for EMT and Y (T_{calc}=425°C)

Property	H-EMT	H-Y	Method	Appendix Reference
Surface Area [m^2/g]	755	620	5-point BET (N_2 adsorption)	A1.7
Na Content [ppm]	255	930	Atomic Absorption	A1.4
Si/Al Ratio	6.94	6.26	^{29}Si MAS NMR	A1.5
Si(0Al) [%]	46.5	46.9		
Si(1Al) [%]	49.7	42.9		
Si(2Al) [%]	3.5	9.6		
Si(3Al) [%]	0.3	0.6		
Si(3Al) [%]	0.0	0.0		
Al Coordination	4, 6, hybrid	4, 6	^{27}Al MAS NMR	A1.5

3.5 PREPARATION OF Pt SUPPORTED ZEOLITES

The platinum was introduced into the zeolite by contact of the support, with an aqueous solution containing hexachloroplatinate (Aldrich). The method employed for impregnation was the incipient wetness technique, whereby, just enough solution is provided to completely fill the pores of the freshly calcined solid.

3.5.1 Method of Preparation

The zeolite was freshly calcined, weighed and stored in a dessicator. The amount of $H_2PtCl_6 \cdot xH_2O$ (38.7 wt. % Pt) (Aldrich) needed to achieve the desired Pt loading was calculated. Similarly, the amount of water which was required to exactly fill the pores of the zeolite, was determined, using pore volume measurements from nitrogen adsorption studies (see Appendix A1.9 for details).

The water was added to $H_2PtCl_6 \cdot xH_2O$ solid and mixed thoroughly (see Table 3.5). Next, the zeolite was added to the solution and stirred. The wetted solids were left at room temperature for 24 h, with periodic stirring. The dried solids were placed in an oven at 80°C overnight, to remove as much water as possible prior to the calcination and reduction steps.

Table 3.5: Quantities used in the Preparation of Pt/EMT and Pt/Y Systems

Catalyst System	Mass Calcined Zeolite	Mass Double De-ionized water [g]	Mass $H_2PtCl_6.xH_2O$[1] [g]
0.1%Pt/EMT	12.413 g EMT	6.62	0.03044
0.5%Pt/EMT	12.244 g EMT	6.75	0.16293
0.5%Pt/Y	25.000 g Y	12.598	0.32301

1 Aldrich, 38.7 wt% Pt

3.5.2 Calcination and Reduction

The excess material from the impregnating solution must be removed by calcination, and the metal reduced to its active form. Conditions for these steps are crucial, in order to minimize the extent of metal agglomeration (sintering), which can lead to partial collapse of the zeolite structure (Feijen et al, 1994a)

Activation in flowing air prior to reduction is recommended, to yield a highly dispersed platinum cluster in the zeolite. A low calcination temperature is critical, with suggested temperatures ranging from 300 to 350°C. An intermediate calcination temperature in the recommended range was selected for the present research. The calcination procedure applied for catalyst activation, increased the temperature at 5°C/min to 325°C in flowing air. The temperature was maintained at this temperature for a period of 3 h.

Immediately following the calcination step, the catalyst was reduced. The recommended temperature for the reduction step ranges from 350 to 500°C (Gates, 1995). Similar to calcination conditions, an intermediate temperature in the recommended range was chosen. The temperature was increased from 325°C to 425°C at a rate of 5°C/min in a flowing 10.1 % H_2/Ar gas mixture, and maintained at 425°C for 3 h. Both the calcination and reduction steps were performed externally prior to catalyst use in the reactor. When the catalyst was to be used for an experiment, the calcination and reduction were repeated *in situ*.

3.6 CHARACTERIZATION OF Pt/EMT AND Pt/Y

Hydrogen chemisorption measurements were performed on all Pt loaded catalysts, repeating the calcination and reduction cycles *in situ*, prior to chemisorption measurements. This data was used to determine the fraction of active Pt atoms exposed on the surface (see Appendix AI.8). This property is important as atoms

located within the metal particles are not active for surface reactions, and are inert with respect to catalytic processes.

The metal dispersion is defined as the percentage of metal atoms exposed on the surface of active metal particles, relative to all the metal atoms present in the sample (denoted by Pt loading). Calculated values for Pt dispersion ranged from 74 to 91 %. Note that the Pt loading is estimated from amount of Pt provided in the impregnating solution per gram of calcined solid.

Incorporation of Pt into the pore network reduces the available surface area for reaction. The loss incurred by Pt presence is more noticeable on EMT relative to Y zeolite, at the same Pt loading. This may be a result of the improved Pt dispersion achieved on Y zeolite. A summary of the relevant properties measured for Pt impregnated catalysts is provided in Table 3.6.

Table 3.6: Summary of Catalyst Properties for Pt/EMT and Pt/Y Systems (T_{calc}=325°C; T_{red}=425°C)

Property	EMT	0.1%Pt/ EMT	0.5%Pt/ EMT	Y	0.5%Pt/ Y	Appendix Reference
Pt Loading [%]	n.a.	0.1	0.5	n.a.	0.5	
Surface Area [m^2/g]	755	616	589	620	581	A1.7
Pt Dispersion [%]	n.a.	74	76	n.a.	91	A1.8

Chapter 4

Set-up of Microflow Reactor

The BTRS-Jr/PC reactor system is a new product line offered by Autoclave Engineers (AE), a Division of Snap-Tite. A basic form of the software control package, had been successfully demonstrated on other AE reactor systems, and was modified to meet the unique demands of our catalysis research. A complex sampling system was designed collaboratively with AE, permitting 15 samples to be collected with a minimum sampling frequency of 1 minute. This allows detailed evaluation of catalyst activity for the purpose of kinetic studies as well as monitoring the course of events leading to deactivation processes.

This chapter will provide a brief description of the capabilities of the equipment and the hardware and software challenges encountered during the design, installation and operational phases. The strategy for interfacing the reactor with the on-line GC will also be outlined, as well as the design of a split injector. A chronological log documenting the milestones and set-backs encountered from the design phase through the installation stage and concluding with the last experiment, is provided in Appendix 2.

4.1 AE BTRS-Jr/PC MICROFLOW REACTOR DESCRIPTION

4.1.1 Overview of System

The BTRS-Jr/PC reactor system is a bench-top reactor constructed entirely of 316 stainless steel (SS). It employs two mass flow controllers (MFC) and two high pressure liquid (HPL) pumps, for independent regulation of two gas and two liquid streams respectively (see Figure 4.1). The separate streams are pre-heated in the oven cabinet prior to mixing. The Reactor Status Valve, a 2-position 8-port valve located in the oven cabinet, facilitates the option of either diverting the pre-mixed feed stream off-line for feed analysis, or directing it to the reactor system for reaction.

The 0.413 in I.D. tubular style reactor is 12 in. in length, and is situated in the oven cabinet. A single thermowell runs down the center of the reactor with three separate thermocouples inserted at varying depths to measure the upper, middle and lower sections of the reactor bed. The total volume of void space in the reactor (excluding space occupied by thermowell) is 23 cm^3.

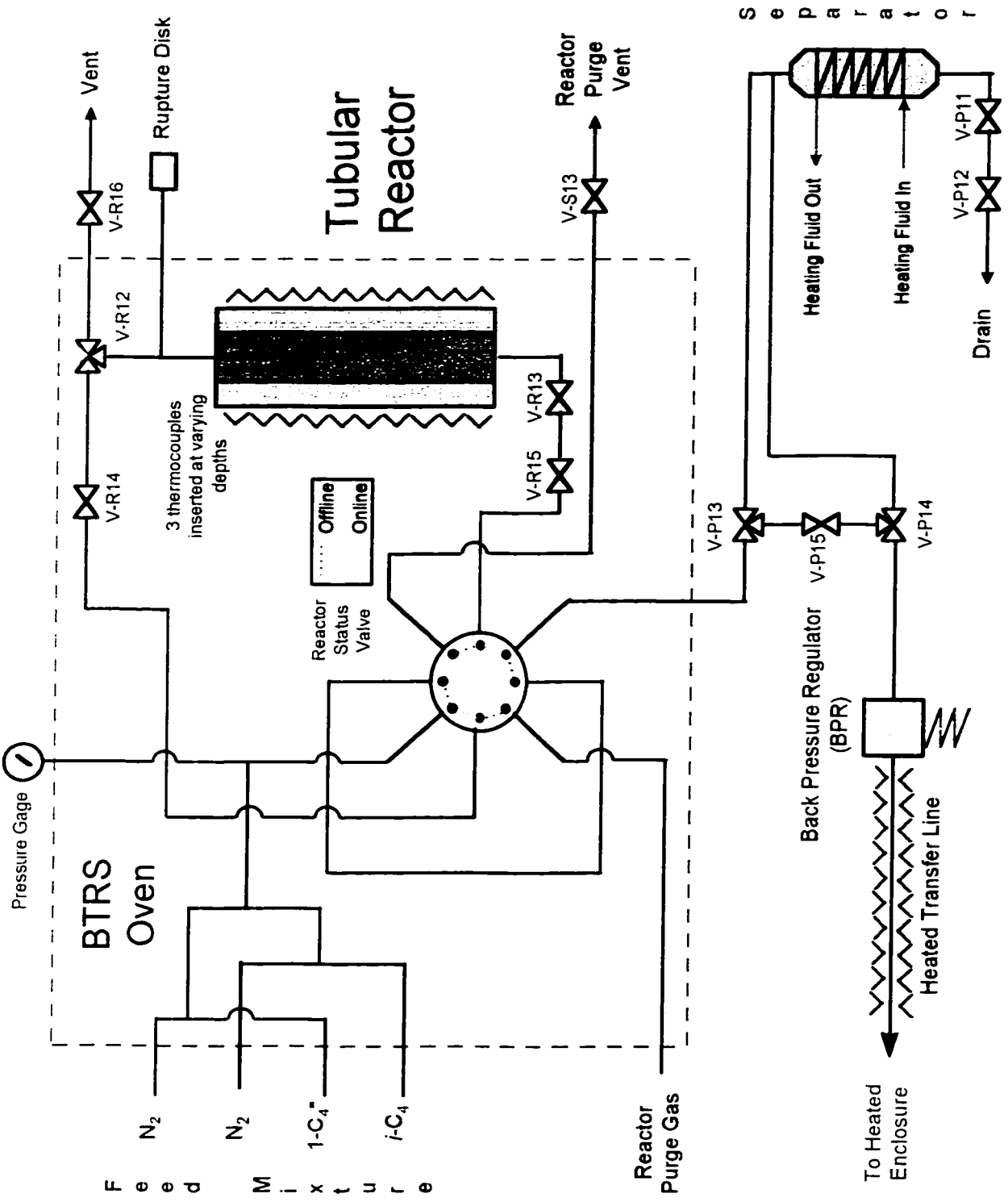

Figure 4.1: Flow Schematic of BTRS Reactor System

A single-zone clam-style furnace (T_{max} = 650°C) jackets the reactor, permitting high temperature operation. Reactor pressure is regulated through a manually controlled back pressure regulator (BPR), mounted on the inside of the reactor oven. The system is rated for a maximum operating pressure of 2500 psig at 650°C.

Effluent from the reactor passes through the BPR and out the oven cabinet (see Figure 4.1). The de-pressurized gas travels through a heated transfer line (HTL) into a Heated Sample Enclosure (see Figure 4.2), which contains a Sample Valve (2-position, 6-port valve) and a Multiposition Trapping Valve (16-loops, each of 0.25 mL volume).

If the Sample Valve is in the *Collect* position, the sample gases flush through the loop of the Multiposition Trapping Valve, and exit through the Vent line. Simultaneously, helium flows through a HTL connected to the on-line GC, providing carrier gas flow for the installed capillary column. Alternatively, when the Sample Valve is in the *Transfer* position, helium flow flushes out the loop of the Multiposition Trapping valve and transports the sample to the on-line GC for analysis. Concurrently, sample gases from the reactor system are directly vented from the system.

Efforts were made to collect a bulk liquid sample from the reaction, to provide an estimate of catalyst yield. The Vent line from the Sample valve was coiled and immersed in an acetone/ice water bath, with the end of the tubing placed in a partially submerged Erlenmeyer flask. The liquid product condensed and collected in the flask over the duration of the reaction period. At the conclusion of the experiment, the flask was removed from the acetone/ice water bath and weighed. Some samples were analyzed using PE Trio-1 GC-MS system equipped with VG Lab-Base software, for the purpose of component identification (see Section 4.2.4).

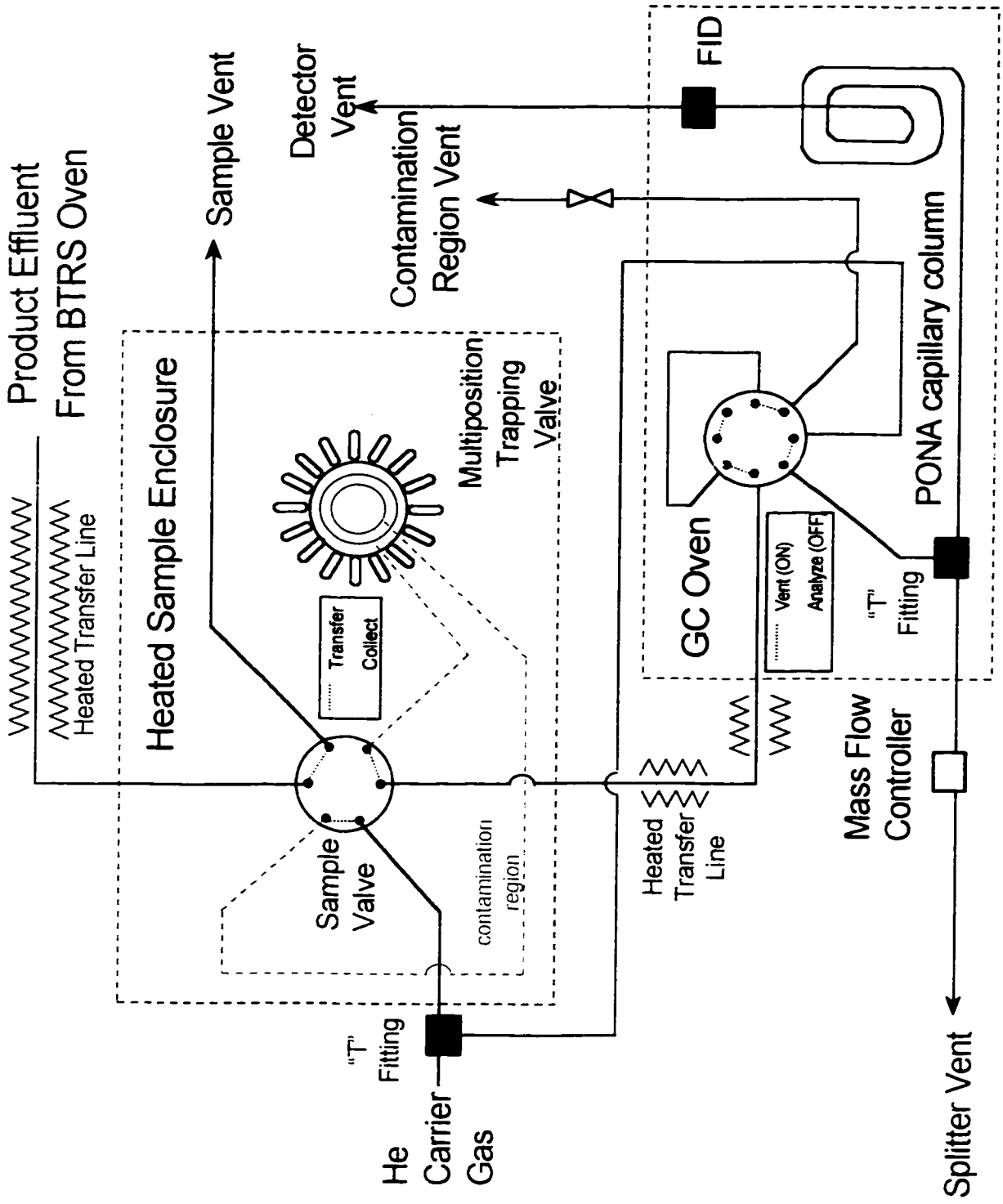

Figure 4.2: Flow Schematic of BTRS Sampling System

4.1.2 Software Capabilities

The reactor and sampling systems, with the exception of system pressure and GC programming, are computer controlled using a dual computing architecture strategy (see Figure 4.3). The Programmable Logic Controller (PLC) is dedicated to controlling the process, including implementing set point changes, switching valve positions, activating alarms and shutting down the equipment in the event of a dangerous operating condition. The (PC) workstation (using Wonderware software) acts as an interface between the operator and the equipment, facilitating manual entry of set point changes as well as activating programmed recipes for unattended operation. Details of the software capabilities are outlined in Appendix A3.1.1.

4.2 INTERFACING THE BTRS REACTOR SYSTEM WITH THE ON-LINE GC

The reactants and products from the BTRS system were analyzed on-line, using a Perkin Elmer (PE) Autosystem GC equipped with a PE NELSON 1020 GC Integrator. However, interfacing the GC with the reactor system was not included in the AE BTRS equipment purchase. The BTRS software could receive a READY (5 V) signal from the GC and send a START (24 V) signal to the GC, provided a GC READY signal was detected. These signals were to be received/sent from a module in the PLC. The procedure for wiring the connections to the GC were not provided in the purchasing contract with AE, and were part of the current research.

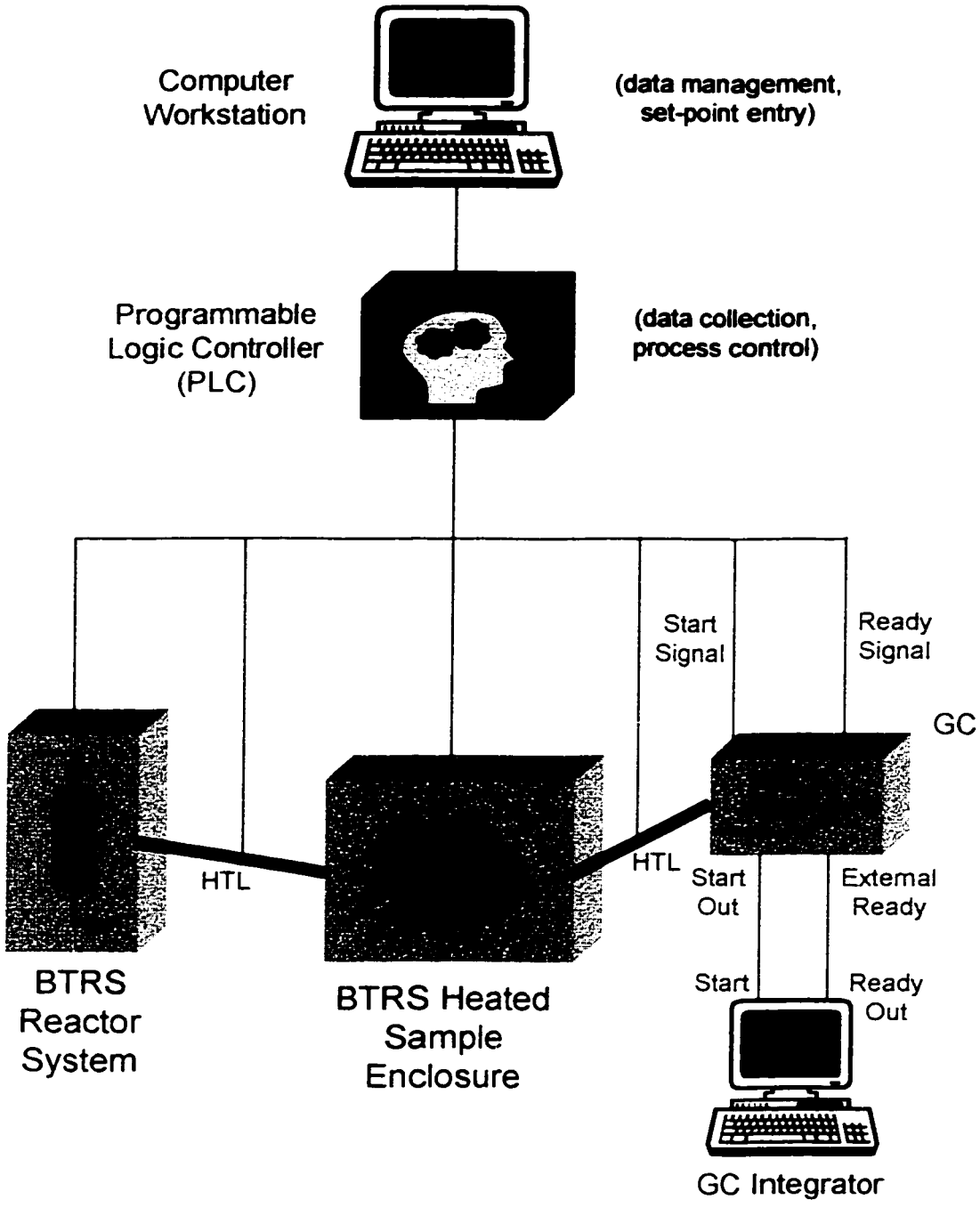

Figure 4.3: Information Flow and Control Strategy of BTRS

4.2.1 Electronic Communication between PLC, GC and Integrator

The Integrator and the GC have terminal strips with the following contact functions:

READY OUT	signals an external device that the instrument is READY
START OUT	used to start an external device
EXT. READY	prevents the instrument from becoming READY until the external device is READY
EXT. START	provides a means to start the instrument from an external device (equivalent to pressing the RUN key)

The terminal strips for the BTRS, GC and Integrator use the "NO" policy for contact closure, which means that the contact is normally open, but closed when READY.

Consultation with PE, resulted in a strategy to interface the Integrator to the GC and the GC to the PLC (see Figure 4.4). In this arrangement, the PLC displays the READY/NOT READY status of the GC. The GC does not achieve READY status until the integrator is READY. Therefore, a READY status at the PLC is only displayed when both the GC and Integrator are ready.

The PLC issues a START signal through the ENABLE command for GC Status. Note that a START signal for GC analysis cannot be sent unless a READY signal is detected by the PLC. If a READY signal is detected, the START signal from the PLC will initiate the active program loaded on the GC. Similarly, activation of the START signal at the GC automatically relays a START signal to the Integrator. This activates data collection and processing of peaks, according to the active program loaded on the Integrator.

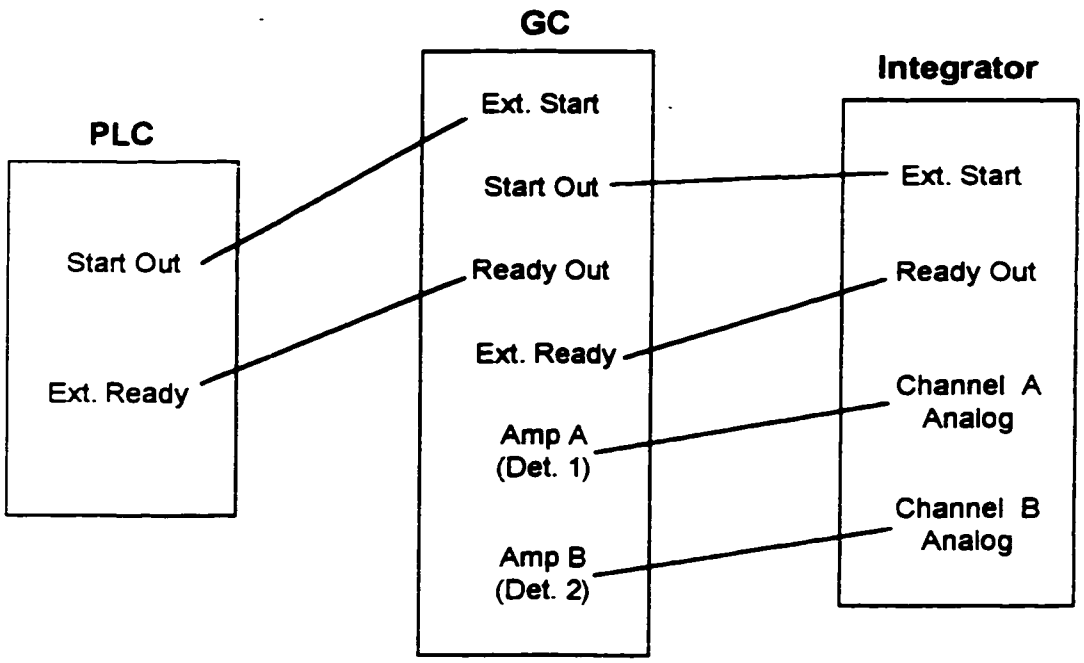

Figure 4.4: Interface between PLC, GC and Integrator

4.2.2 Flow Connection between Heated Enclosure and GC

The Autosorb GC system, equipped with one splitless injector, was installed adjacent to the BTRS equipment. A flow path between the Heated Enclosure and the GC was established, using a HTL provided by AE for this purpose. A hole (diameter slightly larger than the HTL) was drilled through the cap, covering the vacant injector port of the GC, to provide access for the HTL to the GC injector (see Section 4.2.3).

One end of the HTL was connected to the Sample Valve in the Heated Enclosure. The other free end was passed through the hole drilled in the GC injector

cap, and connected to an 8-port, 2 position valve (GC Valve) located in the GC oven (see Figure 4.2). Actuation of this valve is facilitated through a touch pad, located on the top panel of the GC instrument.

When the GC Valve is in the OFF position, flow follows the solid line path. Alternatively, the ON position chooses the dotted flow path. This valve serves an important role to flush the "contamination region" (dashed line flow path in Figure 4.2), between the Sample Valve and the Multiposition Valve, prior to sample injection. Before this function can be considered, provisions for carrier flow for both valve positions must be designed.

The carrier flow line was split using a "Tee" fitting after the MFC in the GC, to ensure uniform head pressure (see Figure 4.2). One branch from the "Tee" directed carrier flow to the Sample Valve in the Heated Enclosure. The second carrier branch was connected to the GC Valve in the GC oven. If the GC Valve was in the OFF position, carrier flow to the column was provided by the helium flow passing through the HTL to the GC. Simultaneously, the second carrier branch connected directly to the GC was directed to vent.

A needle valve with fine flow control was essential to create resistance to flow on the Vent line. Otherwise, the carrier flow would choose the path of least resistance and flow solely through the second branch (Vent). This would result in no flow passing through the column.

If the GC Valve is in the ON position, carrier gas from the Heated Enclosure is directed to Vent, and the second carrier branch supplies flow to the column. To collect a sample, the GC Valve is kept in the OFF position and the Sample Valve assumes the COLLECT position. Flow from the BTRS reactor flushes through a loop (for example, loop 1) in the Multiposition Trapping Valve, and exits to vent. After a minimum of one minute, the Multiposition Trapping Valve is actuated to a new loop position (for example, loop 2), trapping the sample in the previous active loop (loop 1). The GC Valve is then switched to the ON position sending the carrier flow from the Heated Enclosure to vent. The Sample Valve is switched to the INJECT position which flushes the contamination region and loop 2 contents out to vent, via the GC

valve. Once this task has been accomplished, the GC Valve is switched back to the OFF position. The "contamination" region is now filled with carrier gas and is sample free. The Sample Valve is switched to the INJECT position and simultaneously the Multiposition Valve is actuated back to loop 1. The sample is flushed out of loop 1 and sent via the HTL to the GC for sample analysis.

Adjustment of the needle valve position, used to create back pressure on the Vent line from the GC Valve, was a delicate process. Sufficient resistance must be created such that optimal carrier flow for sample analysis is established through the column, when the GC Valve is in the OFF position. However, this resistance must not be so great that it restricts flushing of the "contamination" region. Achieving a balance between these opposing needs, involved a tedious trial-and-error process. The final needle valve position achieved a carrier flow of 1 to 2 mL/min through the column, when the GC valve was in the OFF position. When the GC valve was in the ON position, the same needle valve position successfully flushed the entire "contamination" region to Vent, in a period of 5 minutes.

4.2.3 Design of the Split Injector

The GC did not possess a split injector, which is a requirement for capillary column applications to avoid sample overloading. Three different splitter designs were developed and tested for the current research.

The first two strategies located the splitter in the Heated Enclosure, between the Sample Valve and the HTL carrying flow to the GC. A "Tee" fitting served as the splitter, with the GC column attached to one branch and the Splitter Vent attached to the other. The difference between the two strategies was the method of imposing a resistance on the Splitter Vent line, to ensure adequate flow to the capillary column.

The first design utilized a fine-control needle valve to regulate Splitter Vent flow. The resulting split ratio was too small, resulting in sample overloading on the column. The second design used a capillary column, whose length was adjusted to

achieve the desired split ratio. It was found that Splitter Vent flow control was sporadic and reproducible GC results for standard injections were impossible. A large part of the failure of both of these designs, was the misleading temperature measurement in the Heated Enclosure (see Section 4.3.6).

The final design accommodated the splitter in the GC oven, between the GC Valve and the capillary column. Control of the Splitter Vent flow was achieved using a MFC, which was provided as a component of the Heated Enclosure. A split ratio of 100:1 was established and reliably sustained using this design.

4.2.4 Development of GC Temperature Program

A flame ionization detector (FID) was used for product analysis. Pre-purified helium, supplied by Praxair, was used as the carrier gas. Praxair zero hydrogen and compressed bench air (University of Waterloo) were used as combustion gases for the FID. A J & W Scientific PONA column (100 m x 0.25 mm ID x 0.5 μm film thickness) performed the sample separation. This column elutes compounds in the order of paraffins, olefins, naphthalenes and aromatics, with a minor degree of overlap. This is helpful in the present reaction, as several C_8 products are formed. The elution order assists in the separation and identification of olefins from paraffins. Component identification was accomplished through retention time matching of pure components (2-methylhexane, 2,2,4-TMP, 2,5-DMH, 2,3,4-TMP – all supplied from Aldrich) and GC-MS of bulk liquid samples. A sample chromatogram is illustrated in Figure 4.5.

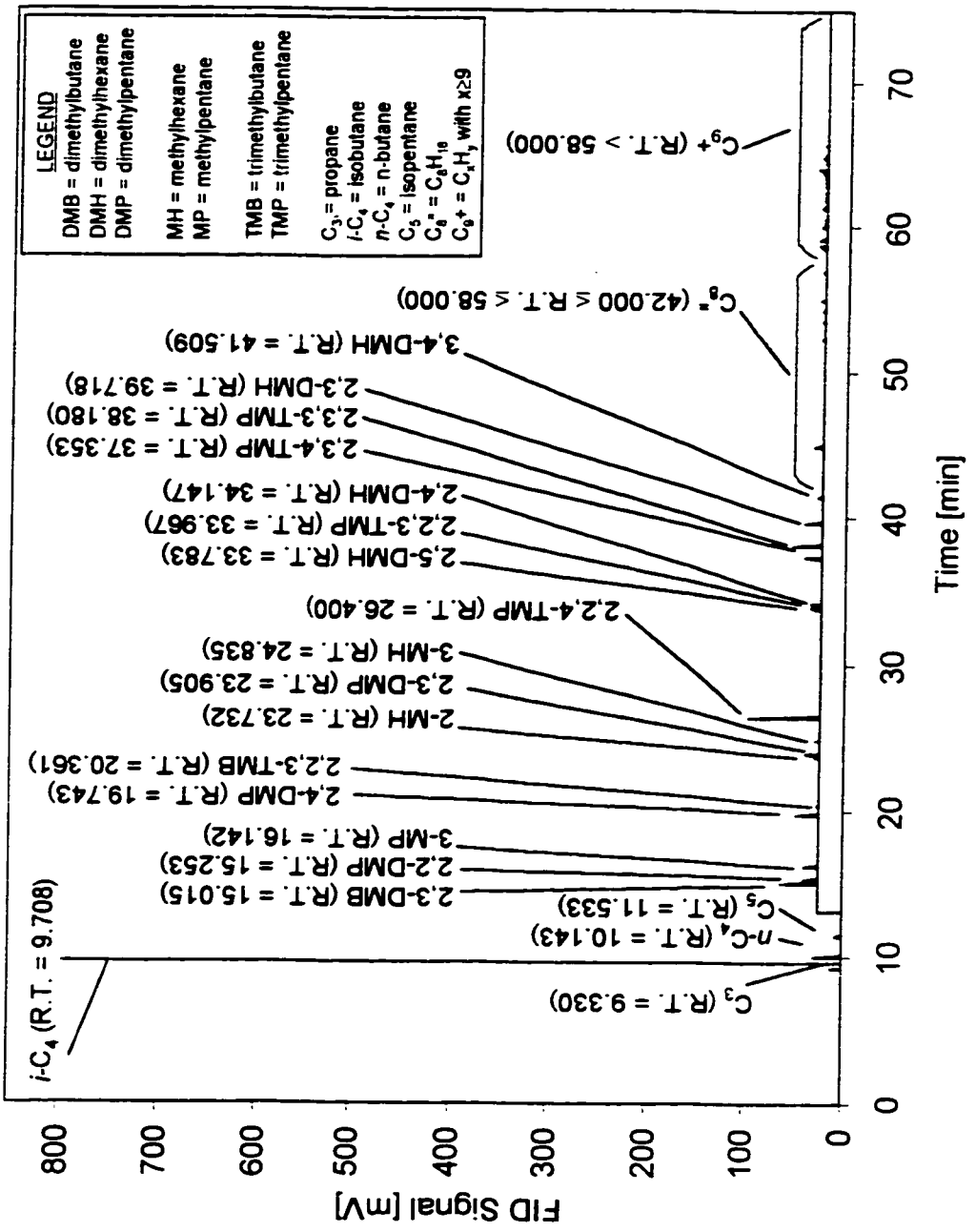

Figure 4.5: Sample Chromatogram of Alkylate Product
(F31EMT; T_{rxn}=77°C; T_{calc}=425°C; P=382psig; I/O=11; t=1h; $C_4^=$ WHSV=2.7h^{-1}; m_{cat}=2.78g)

The procedure used for separation of the alkylate is a multi-staged temperature program. It was derived from the ASTM D-2699 standard method for alkylate analysis. The program maintains an initial temperature of 35°C for 10 min, and then ramps the temperature at a rate of 1°C/min to 45°C. This temperature is maintained for 15 min. The oven is ramped a second time at 1°C/min to 60°C, where it is maintained isothermally for 2 min. The oven temperature is increased at a rate of 15°C/min to 250°C where it is held constant for 5 min.

The entire program requires 75 min. This excludes the cool down time, of approximately 20 minutes, which is necessary to bring the oven temperature back to 35°C. The operating conditions of the GC and Integrator are summarized in Table 4.1.

Table 4.1: Operating Conditions of GC and Integrator for Alkylate Analysis

	Setting
Inlet Pressure of Carrier Gas [psi]	30
Injector Temperature [°C]	280
Detector Temperature [°C]	280
Attenuation	4
FID Range Initial 13.0 min.	 20 (low) 1 (high)
Peak Width	Automatic
Area Sensitivity	50
Base Sensitivity	8

The detector is operated at low sensitivity for the initial 10 minutes of the program to allow the large excess of isobutane and unreacted butene to elute. After this time, the detector sensitivity is switched to high, in order to increase sensitivity to the smaller product peaks. Total peak areas for the sample are calculated by multiplying the peak areas at low sensitivity by 20, and adding them to the peak areas at high sensitivity.

4.3 MAJOR HARDWARE CHALLENGES

Numerous hardware challenges were faced during the installation and operation phases of the equipment. A chronological history of events is provided in Appendix 2.

4.3.1 Inlet Check Valves for HPL Pumps

Isobutane (T_{nb} = -11.85°C) and 1-butene (T_{nb} = -6.25°C) are gaseous at atmospheric conditions, but the liquid state can be maintained under a nitrogen blanket. The pumping of these pressurized liquids is made possible using feed tanks, equipped with dip tubes. The inlet check valve of the HPL pump presents a unique design challenge, as it must withstand pressure on the upstream side of the inlet check valve. The standard valve provided with the BTRS unit, is designed for atmospheric pressure operation on the upstream side. This valve was not suitable for the present application. A prototype, designed by Scientific Systems, Inc. (SSI), retrofitted the conventional inlet valve, with a metal ferrule, for a gas tight connection. SSI hypothesized that pump operation would not be jeopardized using an inlet pressure up to 125 psig, although no data were available to support this pressure limitation.

Preliminary testing on-site found that a 125 psig inlet pressure gave unreliable pump operation. Firstly, opening the prime/purge valve effectively caused a stream of gas to spew uncontrollably out the luer port in the stem assembly. In order to prime the pump, this flow must be regulated through the collection of the effluent in a liquid syringe, and manually controlling plunger withdrawal until the syringe is full. This proved to be quite a challenging task when working against a pressure of 125 psig! Secondly, employment of 125 psig inlet pressure, resulted in excessive pressure on the pump piston. This often forced the pump out of control and frequently resulted in motor stalling (i.e. pump losing prime). For this reason, the inlet

pressure (feed tank pressure) was reduced to 75 psig and more reliable operation achieved. Motor stalling continued to be problematic, but at a reduced incidence rate. A more important concern was unpredictable stroke or flow rate. Pump flow rate is based on the volume of a pressurized liquid passing through the pump. However, after the BPR, the feed is de-pressurized to atmospheric conditions, making verification of flow measurement next to impossible.

4.3.2 Seat Material for AE Brand Manual Operated Valves

After three months of operation, pressure tests failed, due to severe leakage from the manual operating valves (AE) isolating the reactor (V-R12, V-R13, V-R14, V-R15) and those closing the Reactor Line Vent (V-R16) and the Reactor Purge Vent (V-S13). The manufacturer expected that the thermal mass of the tubing and valve bodies would sufficiently cool the gases to warrant the use of a lower temperature seat design. This hypothesis proved incorrect and severe leakage occurred. The valves were replaced with high temperature valves with teflon packing producing satisfactory results.

4.3.3 Seat Materials for Multiposition Valves: Valcon T vs. Valcon E

The reactor system was originally delivered with Valcon T (polyimide / PTFE / carbon composite) seats installed in all Valco multiposition valves:

- Reactor Status Valve (BTRS Oven)
- Sample Valve (Heated Enclosure)
- Multiposition Trapping Valve (Heated Enclosure)

Valcon T permitted a maximum operating temperature of 280°C at 2500 psig. During preliminary testing, it was found that the Reactor Status Valve leaked at temperatures less than ~150°C with reliable sealing only evident at higher temperatures. After approximately one month of operation, complete seat failure

resulted with no sealing provided at any temperature. Consultation with Valco, the valve manufacturer, indicated that Valcon T is best suited for temperatures above 200°C. A plastic transition temperature occurs at ~150°C, above which the material softens and swells. Below this temperature, the material is brittle and tends to stick to the valve body making it difficult to turn. Although Valcon T is functional at lower temperatures, seat lifetime is severely reduced.

Valcon E (polyaryletherketone/PTFE composite) is a similar material to Valcon T providing reliable sealing from room temperature to 220°C at 2500 psig. Although the upper temperature limit is lower than that of Valcon T, reliable operation is provided throughout the temperature range. A new Valcon T seat had been installed in the Reactor Status Valve and operated reliably for 14 months. After this time period, leakage from the Reactor Status Valve was detected again. The Valcon T seat was removed from the Reactor Status Valve, and replaced with a Valcon E seat. The BTRS oven high temperature and alarm limits were adjusted to reflect the tolerance of the new seat material. After alignment, the valve has provided reliable sealing and actuation.

As mentioned previously, Valcon T was also installed in the Multiposition Trapping Valve. After a few months of operation, actuation of this valve became difficult due to sticking of the seat. This problem arised as a result of actuating the valves at temperatures below 150°C (see faulty Heated Enclosure Design in section 4.3.5). Valco recommended re-conditioning the valve at a high temperature, causing some of the Teflon to extrude to the surface and re-lubricate the valve. A modification to the Wonderware software was supplied by AE, to permit operation of the equipment at the elevated temperatures demanded by the re-conditioning step. The re-conditioning procedure was successful on two separate occasions, but a third sticking incidence ultimately caused the Valcon T seat to seize completely. The Multiposition valve was removed from the Heated Enclosure and sent to Valco for servicing. The Valcon T seat was replaced with a Valcon E type, thus compromising the upper temperature limit slightly. However, the new seat material is designed to provide reliable operation from 25 to 200°C. The Heated Enclosure high temperature

and alarm limits of the software were modified, to reflect the reduced temperature ceiling of the new seat material.

4.3.4 Manual Control of Liquid Feed Flow

Manual control of the liquid feed flow is regulated by a metering valve (V-F31 for Feed 3 and V-F41 for Feed 4), a 3-way ball (V-F32 for Feed 3 and V-F42 for Feed 4) and a check valve (CV-F31 for Feed 3 and CV-F41 for Feed 4). These valves are labelled on the AE BTRS Reactor Flow blueprint. The 3-way ball valves are an important component in the liquid feed system, as they are essential for isolation of the liquid pumps during priming. In addition, they provide a quick means for venting liquid feed in an emergency situation. The metering valve serves to manually regulate the fluid flow. The check valves are also an essential element as they ensure safe and accurate delivery of the liquid feed. They are also vital to prevent back flow of fluid, guaranteeing reliable fluid flow and preventing contamination in the feed cylinders.

Severe leakage resulted from the stems of both needle valves during the priming of one of the liquid pumps (note that all valves were supposedly in the closed position). This not only revealed leaking in the 3-way valves and catastrophic failure of the needle valves, but also exposed malfunctioning of the check-valves.

The 3-way valves in the original design employed a TFE packing, which offered an operational temperature range of 10 to 65°C. It is believed that the vapourization of the pressurized liquid feed may have lowered the temperature below the lower limit. This would induce the development of burrs on the Teflon seat, if the valve was switched under these conditions. Continual erosion of the seat would cause an overall deterioration in the quality of the sealing surface and eventually result in valve failure.

The reason for check valve failure is not completely clear. The failed "O" ring appeared slightly brittle and revealed definite evidence of wear. The original check

valves employed a Kalrez "O" ring, which easily accommodates the expected operating conditions of the liquid feed system. Review of the chemical incompatibilities for Kalrez, suggest that chemical attack is also unlikely. The most probable explanation for check valve failure is that incorrect "O" rings were assembled in the check valve by the equipment manufacturer, as the colour of the failed "O" rings differed from that of a fresh Kalrez "O" ring.

The failure of all valves prompted the re-design of the liquid delivery system. It was concluded that manual regulation of liquid flow rate was redundant, as operation of the equipment (i.e. mass flow controllers, liquid pumps, multiposition valve actuation, temperature controllers, etc.) is only possible using the computer software. For this reason, the failed needle valves regulating liquid flow rate, were not replaced.

The original 3-way ball valves were substituted with a spring-loaded version (Whitey), which minimizes the contacting area of the system fluid with the valve sealing materials. It utilizes a PFA packing, extending the lower temperature limit to -54°C, without compromising the upper temperature ceiling. The "O" ring of the check valves was replaced with a Teflon TFE type ,which is more chemically inert than the Viton "O" ring employed in the original design. A slightly higher cracking pressure is required to activate fluid flow through the valve, but this did not appear to affect operation. Reliable functioning of the liquid delivery system was confirmed and no subsequent leakage problems have been encountered.

4.3.5 Heated Enclosure Design

The Heated enclosure is an insulated box in which the Sample Valve and the Multiposition Trapping Valve are mounted. This unit is designed for sample collection, storage and injection at elevated temperatures. The orignial design is a standard Valco product, which utilizes a heater block equipped with a heater cartridge for thermal output. A hole is drilled in the side of the block and a thermocouple installed. Temperature measurements serve to regulate heater output and

maintaining temperature control. The Heated Enclosure was rated for 125 W/350°C service.

Persistent difficulties in sample injection quality to the on-line GC, prompted investigation into the reliability of the sample collection system. It was identified that a maximum temperature of 210°C could be reached at the maximum heater output, which was well below the upper temperature limit of 280°C specified by the AE BTRS blueprint. A higher wattage cartridge was supplied by AE and installed into the heater block. Sample injection problems persisted. The heater block temperature signal was verified using independent thermocouple measurements, to eliminate faulty heater operation as a possible explanation. A review of the Heated Enclosure blueprint revealed a definite weakness in the design. No mechanism for heat circulation (i.e. fan) is provided, implying that energy transfer from the heater block must be facilitated by conduction only. Independent temperature measurements revealed a significant temperature gradient from the heater block to the surrounding air space in the box. At a heater block temperature of 250°C, independent thermocouple measurements sense a temperature of less than 150°C in the surrounding air space. This would explain the sample injection problems.

The Heated Enclosure was returned to AE, as the unit failed to meet the maximum temperature specifications. A new unit was provided utilizing the same motor and blower assembly as well as insulation (1 inch thick), as the design of the BTRS oven. The temperature of the newly designed Heated Enclosure was confirmed with independent thermocouple measurements.

4.4 SOFTWARE ISSUES

4.4.1 Software "Bugs"

The addition of software control to a highly complex system greatly increases the level of difficulty in troubleshooting problems. Several bugs in the software were identified during the installation phase (see Appendix 2). Program seizures, at certain steps in the recipes of both the Automatic Control and Sample Control windows, were encountered. In addition, it was found that some set points were not adjustable under automatic control. "Ghost" commands were being issued by the software, without any prompt from the operator. A dangerous response in furnace output was diagnosed as a result of skin temperature thermocouple failure. All of these problems were isolated and demanded rectification before proper use of the equipment could be achieved.

Corrections to Wonderware software require the use of a proprietary design key, which is accessible to AE personnel only. When a software bug was identified, AE personnel were contacted and the corrections were coded at their facility. The revised software was sent and installed onto the PC. Testing of the re-coded software was required to confirm safe and proper operation of the equipment.

4.4.2 Faulty PLC Module

The thermocouple, which detects Reactor Skin Temperature, periodically failed with no signal being sent to the PLC. It is expected that this condition would DISABLE the system. However, the opposite action occurred. A failed furnace thermocouple was registered by the PLC, as a temperature below the set point temperature, triggering 100 % output from the furnace. Once the reactor temperature exceeded the High Limit of the equipment, the system was DISABLED.

Simultaneous to the skin temperature problem, the MFCs experienced similar behaviour. One MFC would suddenly shut off for no explainable reason. Complicating the issue further, were a malfunctioning BPR, sticking Multiposition valve and chronic pump problems. Several problems were happening simultaneously, making the diagnostic process highly complicated.

The skin temperature problem was attacked first. A new reactor skin thermocouple was installed to see if this corrected the problem. Thermocouple failure recurred, suggesting the source of the problem was either a software bug or a failed module in the PLC. The final diagnosis was a faulty PLC module. A replacement part was sent by AE and installed in the PLC and no subsequent problems were encountered with either the skin temperature or MFC operation. The problems with the pumps, BPR and Multiposition valves were unrelated software issues and were resolved sequentially as discussed in the Section 4.3.

Chapter 5

Preliminary Batch Reactor Studies using Y Zeolite

5.1. CATALYST PRE-TREATMENT AND STORAGE

The catalyst Y Zeolite (Si/Al ratio of 6.26; S.A. = 620 m^2/g) was generously donated by UOP (Y-84, Lot 966094061003~S). This material has been extruded into 1/8" pellets and was ion-exchanged by the manufacturer. Atomic absorption measurements estimate Na levels to be 930 ppm (see Appendix A1.4). The catalyst was crushed and sieved to a particle diameter range of 250 to 500 μm, and calcined in flowing air at 500°C for 5 h prior to use. Upon completion of the calcination program, the catalyst was cooled in flowing ultra-high purity (UHP) N_2 and

immediately transferred into a glove bag. Samples were measured into 3 g allotments and stored in sample vials.

5.2 BATCH REACTOR DESCRIPTION AND EXPERIMENTAL PROCEDURE

The batch alkylation experiments were performed in a 316 SS 300 mL Parr reactor equipped with a magnetic stirrer, internal water cooling coil and a dual action temperature controller. The reactor was loosely sealed and purged several times with UHP N_2 to remove air from the reactor. If heptane was used for catalyst storage (see Section 5.4), the excess heptane was decanted into a beaker. The reactor sealing clamps were loosened, the reactor top lifted slightly and the catalyst was quickly added to the reactor. The reactor top was replaced immediately, tightened and then the reactor was purged several times with nitrogen to remove residual air.

The reactants, *i*-C_4 (CP grade, Linde) and 1-$C_4^=$ (CP grade, Linde), were pre-weighed into separate sample bombs and pressurized to 800 psig with UHP N_2 at room temperature. The *i*-C_4 sample cylinder was connected to the reactor system, and the contents introduced into the reactor. Next, 1-$C_4^=$ was added in the same manner. The system was heated from ambient conditions to the reaction temperature, increasing the temperature at a rate of 5°C/min.

No duplicates were performed on batch experiments. The data presented depicts the results from a single run.

5.3 PRODUCT COLLECTION AND ANALYSIS

Reaction time zero was defined as the time at which the reaction temperature reached the set-point value. At the conclusion of the reaction, the furnace was lowered and the reactor submerged in an acetone-ice water bath. Cooling water flow was activated through the internal cooling coil to accelerate the cooling process.

Once the internal reactor temperature reached approximately 6°C, the pressure was slowly vented to ambient conditions. The autoclave was quickly opened and the product collected and weighed. Mass balance was poor, averaging at approximately 68 %. This is primarily a consequence of the excess isobutane employed in the feed, which vapourized when the reactor was opened at the conclusion of the experiment, incurring alkylate product losses.

The liquid product was separated from the spent catalyst and stored in a sample bottle, immersed in an acetone/ice water bath. The cap was loosely attached to the bottle, allowing excess isobutane to slowly evaporate over a period of 4 h. This step is necessary to successfully inject samples into the GC. Excessive amounts of isobutane in the product, result in complete evaporation of the sample from the syringe prior to injection. However, product analysis is sensitive to the duration of the evaporation step, with longer times favouring higher C_9^+ levels. This emphasizes the importance of employing consistent evaporation periods to permit comparison between experiments.

Once the evaporation time had expired, a 1.0 μL sample of residual liquid was aspirated using a chilled syringe. The sample was injected into a Perkin Elmer (PE) Autosystem GC equipped with a PE Nelson 1020 GC Plus Integrator. Pre-purified helium (Praxair) was used as the carrier gas in the separation, and Zero grade hydrogen (Praxair) and compressed bench air (University of Waterloo) were employed for the combustion gases of the FID detector. Separation was achieved using a DB-1 (J&W Scientific) capillary column (60 m x 0.325 mm OD x 1.0 μM film), using the temperature program described in Section 4.2.4.

5.4 EFFECT OF STORING CATALYST IN HEPTANE

Zeolites are known to be very hygroscopic, and hence, negligible conversion of butene was obtained when the catalyst was exposed to ambient air prior to reaction. For this reason, two methods of catalyst storage were explored. The first method employed a glove box for catalyst addition and reactor sealing, in order to avoid exposure to moisture in ambient air. The desired mass of catalyst was measured, added to the reactor and the autoclave sealed.

The second approach, stored the catalyst in pre-treated heptane (stored in a bottle containing freshly calcined 3A zeolite to remove any dissolved moisture). A mass of 3 g of catalyst was measured into a vial, and heptane added to completely submerge the catalyst. These steps were performed in a glove bag. The vial was capped, the stopper secured with electrical tape and the sample stored no longer than 48 hours prior to use.

The influence of storage methods on catalyst performance is summarized in Table 5.1. Pre-filling the catalyst pores with heptane, favoured the formation of C_8 products at the expense of C_9^+ products. The TMP/DMH ratio improved slightly in the presence of heptane, indicating that hydride transfer was enhanced under these conditions. It is possible that heptane is acting as a source of hydride transfer, thus suppressing deactivation processes. Alternatively, heptane may serve to dilute the concentration of the olefin in the pores. This reduces the probability of oligomers forming, thereby enhancing the opportunity for isobutane participation.

A higher surface area of the spent catalyst would be expected if polymerization reactions are reduced through enhanced hydride transfer. The experimental data support this hypothesis in that the catalyst surface area was better preserved employing heptane for storage, relative to the catalyst stored under a nitrogen blanket. No discernible change in yield was observed using either catalyst storage method. All subsequent batch experiment employed heptane for catalyst storage.

Table 5.1: Effect of Catalyst Storage Method on Batch Reactor Alkylate Composition (Y zeolite; T_{rxn}=80°C; P=450psig; I/O=10; t=30 min; m_{cat}=3.00 g)

Catalyst Storage Method	N_2 blanket	Heptane
Yield [g C_5^+/g $C_4^=$ fed]	0.254	0.267
C_5^+ Liquid [mass%]		
C_5 - C_7	5	9
C_8	42	47
C_9^+	53	44
C_8 Fraction [mass%]		
TMP	26	38
DMH	16	17
Other C_8 Saturates	4	2
$C_8^=$	54	43
TMP Fraction [%]		
2,2,4-TMP	29	34
2,2,3-TMP	9	9
2,3,4-TMP	32	28
2,3,3-TMP	30	29
Indicator [mass fraction] TMP / DMH	1.6	2.2
S.A. Spent Catalyst[1] [m^2/g]	304	359

1 SA fresh = 620 m^2/g

5.5 EFFECT OF PRE-SOAKING CATALYST WITH ISOBUTANE

The olefin preferentially adsorbs onto solid acids, favouring oligomerization and polymerization reactions rather than alkylation with the paraffin. For this reason, two different approaches were evaluated for 1-$C_4^=$ addition. The first method added 1-$C_4^=$ immediately after *i*-C_4 addition, at ambient temperature (see Figure 5.1). In the second technique, 1-$C_4^=$ addition was delayed until the reaction temperature was reached. In this manner, the catalyst was pre-soaked with *i*-C_4 (in the absence of 1-$C_4^=$) thus allowing it to adsorb alone onto the catalyst surface.

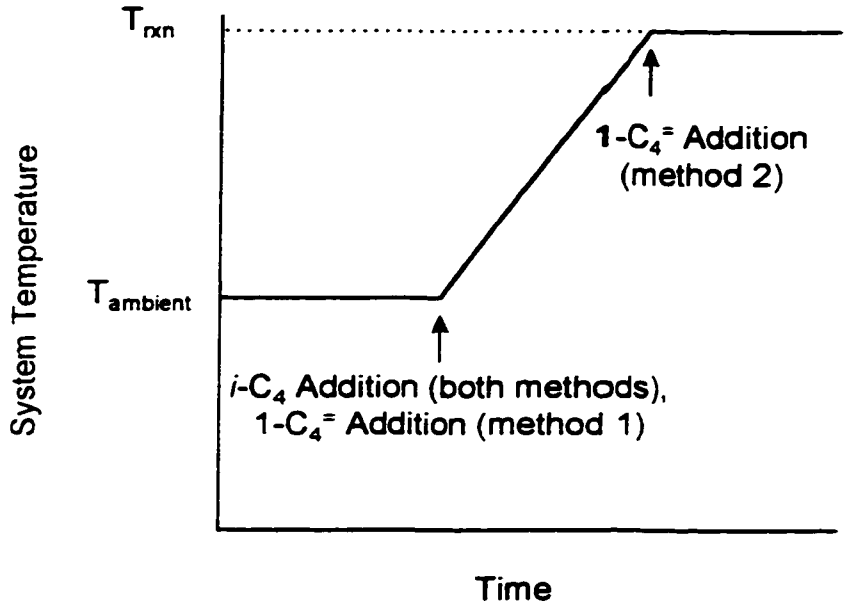

Figure 5.1: Timing of 1-$C_4^=$ Addition for Batch Reaction

Delaying the addition of 1-$C_4^=$ protected the strong acid sites responsible for cracking and alkylation reactions, and enhanced the selectivity to 2,2,4-TMP (see Table 5.2). Pre-soaking the catalyst in *i*-C_4, favours a high I/O ratio in the vicinity of the acid sites. This promoted the alkylation of **1**-$C_4^=$ with *i*-C_4 rather than oligomerization of the olefin, during the initial stages of the reaction. This environment would also favour self-alkylation of isobutane. This offers a possible explanation for the elevated levels of 2,2,4-TMP, as this TMP isomer is the primary product of self-alkylation of *i*-C_4.

The content of $C_8^=$ and C_9^+ levels, suggest that oligomerization and polymerization reactions were favoured with earlier butene addition. This is not surprising in view of the adsorption preference of olefins over paraffins on solid acid sites. This observation is supported by the larger surface area measurement, when 1-$C_4^=$ addition was delayed (see Table 5.2). Reduced polymerization activity would suggest a slower rate of catalyst deactivation and higher product yield, which is supported by the data.

Table 5.2: Effect of Pre-soaking Catalyst (stored in heptane) with Isobutane on Batch Reactor Alkylate Composition
(Y zeolite; P=450psig; I/O=10; t=30 min; m_{cat}=3.00 g)

Timing of 1-$C_4^=$ Addition	immediately after *i*-C_4	once T_{rxn} reached
Yield [g C_5^+/g $C_4^=$ fed]	0.239	0.267
C_5^+ Liquid [mass%]		
C_5 - C_7	2	9
C_8	43	47
C_9^+	55	44
C_8 Fraction [mass%]		
TMP	19	38
DMH	15	17
Other C_8 Saturates	3	2
$C_8^=$	63	43
TMP Fraction [%]		
2,2,4-TMP	13	34
2,2,3-TMP	7	9
2,3,4-TMP	40	28
2,3,3-TMP	40	29
Indicator [mass fraction] TMP / DMH	1.3	2.2
S.A. Spent Catalyst[1] [m^2/g]	111	359

1 SA fresh = 620 m^2/g

5.6 EFFECT OF REACTION TEMPERATURE

The effect of temperature was evaluated at 80 and 100°C, maintaining the I/O ratio constant at 10 for both experiments (see Table 5.3). Reaction temperatures in excess of 100°C, encourage excessive gas production and were therefore, not explored. Catalysts were stored in heptane for all experiments. In addition, butene addition was delayed until the reaction temperature was reached.

Table 5.3: Effect of Reaction Temperature on Batch Reactor Alkylate Composition (Y zeolite; T_{rxn}=80°C; P=450psig; I/O=10; t=30min; m_{cat}=3.00g, catalyst stored in heptane, catalyst pre-soaked with isobutane)

Temperature [°C]	80	100
Yield [g C_5^+/g $C_4^=$ fed]	0.267	0.276
C_5^+ Liquid [mass%]		
C_5 - C_7	9	12
C_8	47	47
C_9^+	44	41
C_8 Fraction [mass%]		
TMP	38	35
DMH	17	19
Other C_8 Saturates	2	1
$C_8^=$	43	44
TMP Fraction [%]		
2,2,4-TMP	34	34
2,2,3-TMP	9	13
2,3,4-TMP	28	27
2,3,3-TMP	29	26
Indicator [mass fraction] TMP/DMH	2.2	1.9
SA Spent Catalyst[1] [m^2/g]	359	265

1 SA fresh = 620 m^2/g

A higher reaction temperature produced an increase in C_5-C_7 levels and a decrease in C_9^+ levels, suggesting that heavier products were cracked to form smaller fragments. Deterioration in alkylate quality (TMP/DMH ratio) was also observed at the higher reaction temperature. It appears that the stability of alkylate precursors was jeopardized under these conditions. Surface area loss of the spent catalyst was more pronounced at the elevated reaction temperature. However, no significant effect on product yield was detected.

5.7 EFFECT OF REACTION DURATION

The commercial success of solid acids for alkylation of butene with isobutane is elusive, due to rapid catalyst deactivation. It was of interest to explore the effect of reaction duration on the product distribution and selectivity of the reaction. Two separate experiments were performed at 80°C and I/O of 10, varying the duration of the experiment from 15 to 30 minutes (see Table 5.4). Heptane was employed for catalyst storage in both experiments. Similarly, the catalysts were pre-soaked in isobutane for both runs.

Table 5.4: Effect of Reaction Duration on Batch Reactor Alkylate Composition (Y zeolite; T_{rxn}=80°C; P=450psig; I/O=10; t=30min; m_{cat}=3.00g, catalyst stored in heptane, catalyst pre-soaked in isobutane)

Run Number	B6	B4
Duration [min.]	15	30
Yield [g C_5^+/g $C_4^=$ fed]	0.214	0.267
C_5^+ Liquid [mass%]		
C_5 - C_7	10	9
C_8	47	47
C_9^+	43	44
C_8 Fraction [mass%]		
TMP	42	38
DMH	17	17
Other C_8 Saturates	1	2
$C_8^=$	39	43
TMP Fraction [%]		
2,2,4-TMP	33	34
2,2,3-TMP	9	9
2,3,4-TMP	28	28
2,3,3-TMP	29	29
Indicator [mass fraction] TMP / DMH	2.4	2.2
SA Spent Catalyst[1] [m^2/g]	344	359

1 SA fresh = 620 m^2/g

A 44 % loss in catalyst surface area occurred during the first 15 minutes of the reaction period. Extending the reaction duration to longer times does not reduce the surface area further. A slight increase in product yield was observed with longer reaction times, but the latter 15 minutes of the reaction favoured oligomerization activity rather than TMP production. This suggests that the ability to facilitate hydride transfer to the octyl carbenium ion was hindered as the reaction progressed. Instead of promoting hydride transfer from isobutane for desorption of a saturated C_8 product, a proton was returned to the surface, with an olefin desorbing as the final product.

Chapter 6

Effect of Process Parameters on Alkylation Yield and Selectivity for EMT and Y Zeolites in a Flow Reactor

This chapter investigates the effect of calcination temperature, reaction temperature, olefin WHSV, cyclical feed addition and catalyst type (EMT or Y) in a flow reactor. The influence of these operating conditions on the Useful Catalyst Lifetime period and alkylate quality will be investigated. The preferred operating conditions (of the levels tested), will be identified for EMT and Y zeolites.

6.1 EXPERIMENTAL PROCEDURE

The micro-reactor employed for the flow reaction studies is described in Chapter 4. A detailed description of the experimental procedure for its use is reviewed in Appendix 3.1. Sample calculations are outlined in Appendix A3.2. Raw data for all flow experiments are presented in Appendix 4.

The catalyst was pelletized, crushed and sieved to a particle diameter range of 0.25 (60 US mesh) to 0.50 (35 US mesh) mm. Due to the exothermicity of the reaction, 2.78 g of zeolite were diluted with inert 1 mm borosilicate glass beads (50/50 by weight). The pre-heat and cool down zones of the reactor bed were also filled with glass beads.

The reactor was re-attached to the BTRS system and the catalyst was calcined *in situ*. The reactor was heated to the calcination temperature and maintained isothermally for 5 h in a 50 sccm stream of nitrogen. After the calcination step, the catalyst bed was switched to the off-line position, and cooled under a nitrogen blanket to the reaction temperature level.

Prior to initiating the reaction, the feed mixture was sent off-line for analysis. Once constant feed composition was achieved, the mixture was directed on-line to the reactor to initiate the experiment. All runs employed a nitrogen flow rate of 35 sccm and a reaction pressure of 382 psig. The flow through the Vent line from the Sample Valve was measured using a bubble flow meter, after the Reactor Valve was switched to the on-line position. A dramatic increase in flow rate occurred once the liquid front reached the Heated Enclosure, indicating the break-through of the reaction front. This point defined the start of the reaction, or 0 min time-on-stream (0 min TOS). At this time, the sample program was activated and collection of the first sample was initiated.

6.2 STAGES OF CATALYST ACTIVITY AND SELECTIVITY ON EMT AND Y ZEOLITES

The reaction of isobutane with 1-butene in a flow reactor exhibits four distinct stages of catalyst activity and selectivity (Taylor & Sherwood, 1997). These four stages were distinguishable in the catalytic profiles of EMT and Y zeolites. The C_5+ product distributions are illustrated in Figures 6.1 and 6.3 for EMT and Y zeolites respectively. Selectivities within the C_8 fraction are shown in Figure 6.2 for EMT zeolite and Figure 6.4 for Y zeolite.

The first stage, termed "Initial Activity", is very short and is characterized by the highest catalyst activity. This stage is often not observed due to the brevity of the phase, as well as, restrictions on sample collection frequency of the reactor system (Taylor & Sherwood, 1997). This activity period was assumed to occur between 0 and 1 min TOS for the present study.

The second stage of catalyst activity represents the "Useful Catalyst Lifetime", and features butene conversion greater than 80 % (Taylor & Sherwood, 1997). Figures 6.1 and 6.3 demonstrate that the C_5+ liquid produced from EMT and Y zeolites, consisted of predominantly C_8 compounds, which in turn, are composed of primarily TMPs (see Figures 6.2 and 6.4). Typically, the alkylate (C_5+ liquid) consisted of 40 to 60 % C_8 compounds, with 60 to 80 % of the C_8 fraction being TMPs. Actual product levels depend upon the operating conditions (i.e. reaction temperature, olefin WHSV, etc.) employed. The C_5-C_7 fraction was also significant in this phase, suggesting that cracking of alkylation, oligomerization and polymerization products to smaller components, was occurring extensively. Levels of C_5-C_7 fraction, ranged between 20 to 50 % of the C_5+ liquid, with higher amounts observed at operating temperatures approaching 100°C. The TMP fraction was composed of primarily 2,2,4-TMP, with typical levels ranging from 40 to 60 %. The primary product of 1-butene/isobutane alkylation is 2,2,3-TMP. However, this product represented approximately 10 % of the TMP fraction and was consistently the least preferred of all

TMP isomers, for all operating conditions tested. Under similar operating conditions, EMT zeolite typically produced lower C_5-C_7 levels and higher C_8 and C_9+ amounts in the alkylate, relative to Y zeolite. Comparable C_8 and TMP selectivities were observed on both catalyst systems.

As the catalyst deactivated with longer TOS, butene conversion decreased and selectivity towards C_8 products in the C_5+ product declined. This was accompanied by a corresponding increase in C_5-C_7 levels as well as amounts of C_9+ products. Saturated C_8 compounds still remained the dominant fraction during this period; however, the selectivity within the C_8 fraction was increasingly favoured towards DMHs.

During the third stage of catalyst activity, termed "Rapid Deactivation", butene conversion dropped rapidly as the catalyst lost activity, but was sustained above 40 % (Taylor & Sherwood, 1997). Production of saturated C_8 products (TMP and DMH) declined sharply, due to a rapid decrease in TMP levels. This was particularly true on Y zeolite (see Figure 6.4), where the deactivation process appeared to proceed a faster rate relative to EMT (see Figure 6.2). The content of DMH in the C_8 fraction remained relatively unchanged from the levels observed during the Useful Catalyst Lifetime period. Levels of C_9+ products in the alkylate were high during this period, representing between 50 to 60 % of the alkylate composition. A dramatic increase in C_8 olefin production occurred during this phase, with levels reaching 60 to 70 % of the C_8 fraction. Cracking activity was lost completely during this phase. This suggests that deactivation occurred on the strongest acid sites first, resulting in a loss in cracking and alkylation activities. The rate of this process appeared to be suppressed on EMT relative to Y, resulting in a longer deactivation period observed on EMT.

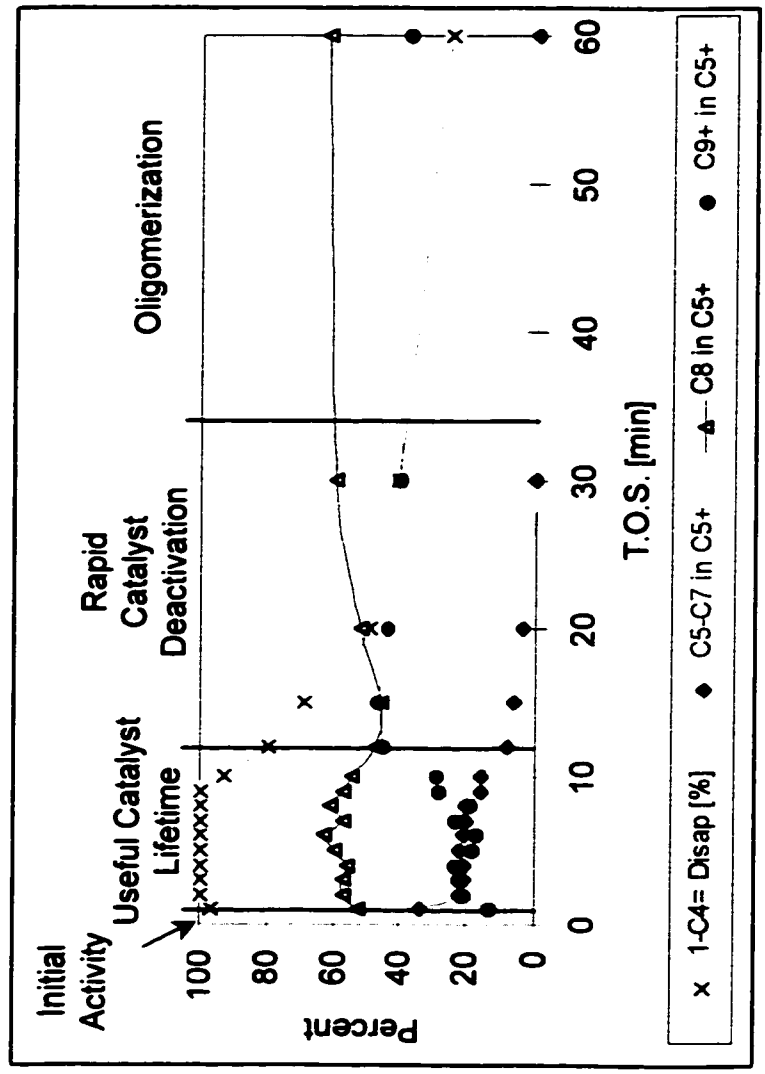

Figure 6.1: Stages of Catalyst Activity on EMT Zeolite with respect to C_5+ Product Distribution (F66EMT; T_{rxn}=50°C; T_{calc}=425°C; P=382psig; I/O=15; t=1h; $C_4^=$ WHSV=2.0h^{-1}; m_{cat}=2.78g)

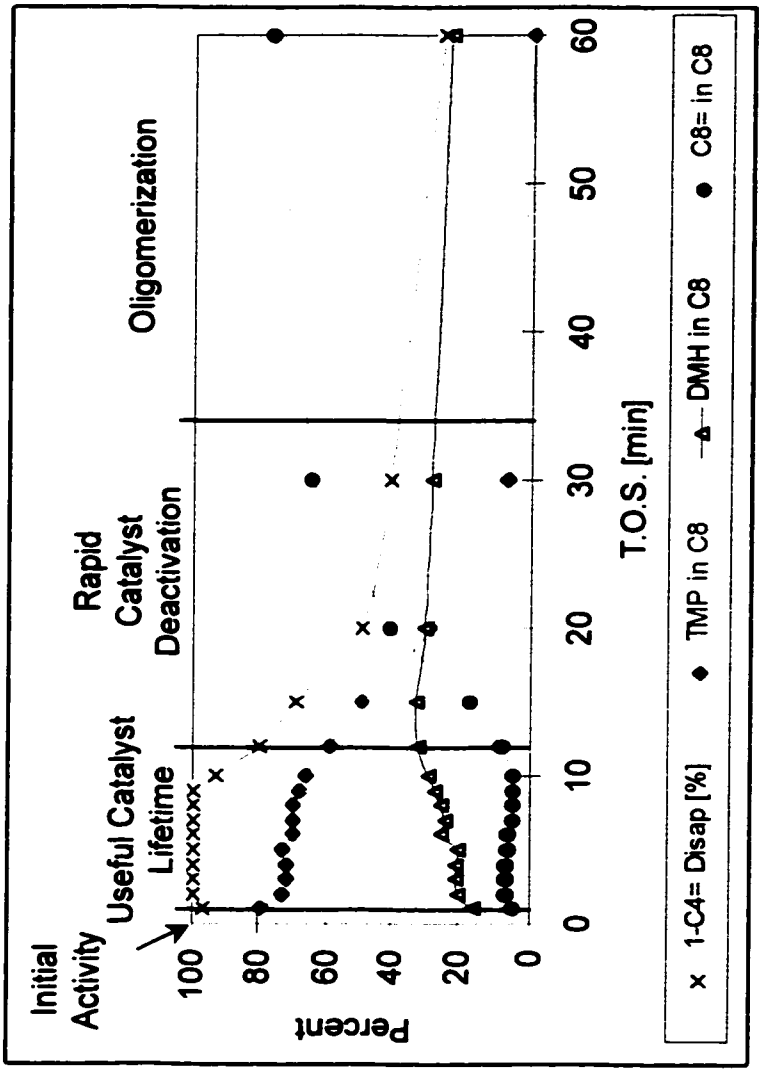

Figure 6.2: Stages of Catalyst Activity on EMT Zeolite with respect to C_8 Fraction Distribution (F66EMT; T_{rxn}=50°C; T_{calc}=425°C; P=382psig; I/O=15; t=1h; $C_4^=$ WHSV=2.0h^{-1}; m_{cat}=2.78g)

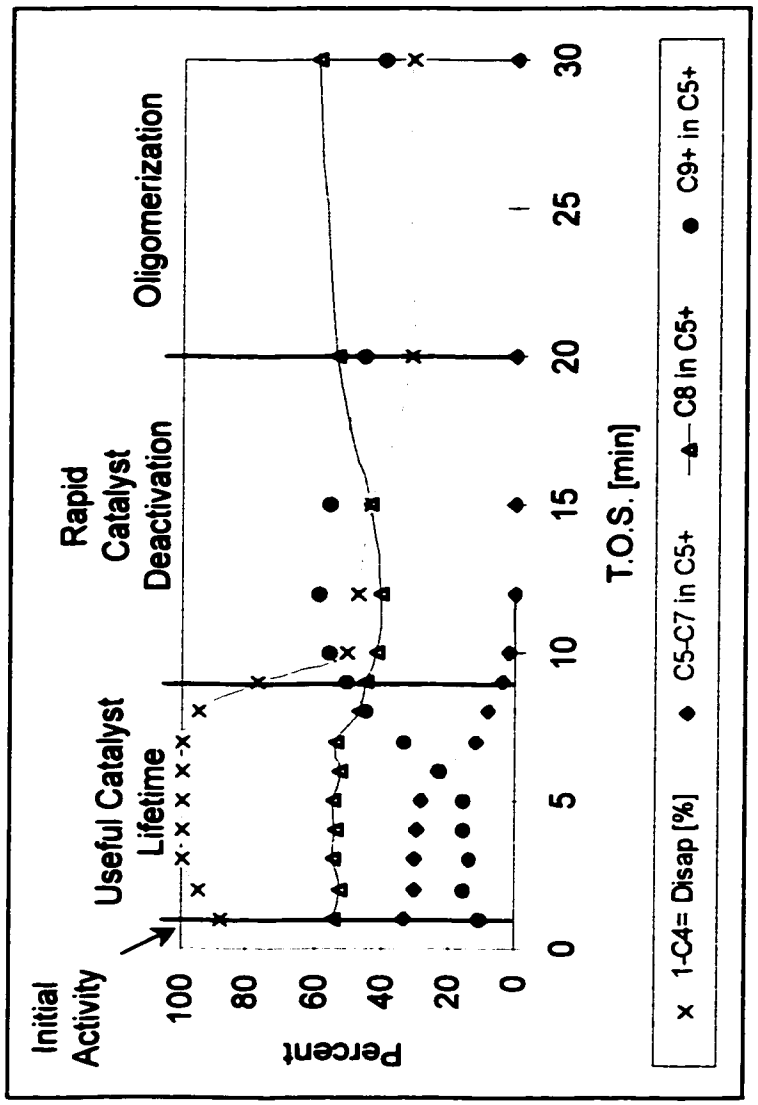

Figure 6.3: Stages of Catalyst Activity on Y Zeolite with respect to C_5+ Product Distribution (F54Y; T_{rxn}=50°C; T_{calc}=425°C; P=382psig; I/O=15; t=1h; $C_4^=$ WHSV=2.0h^{-1}; m_{cat}=2.78g)

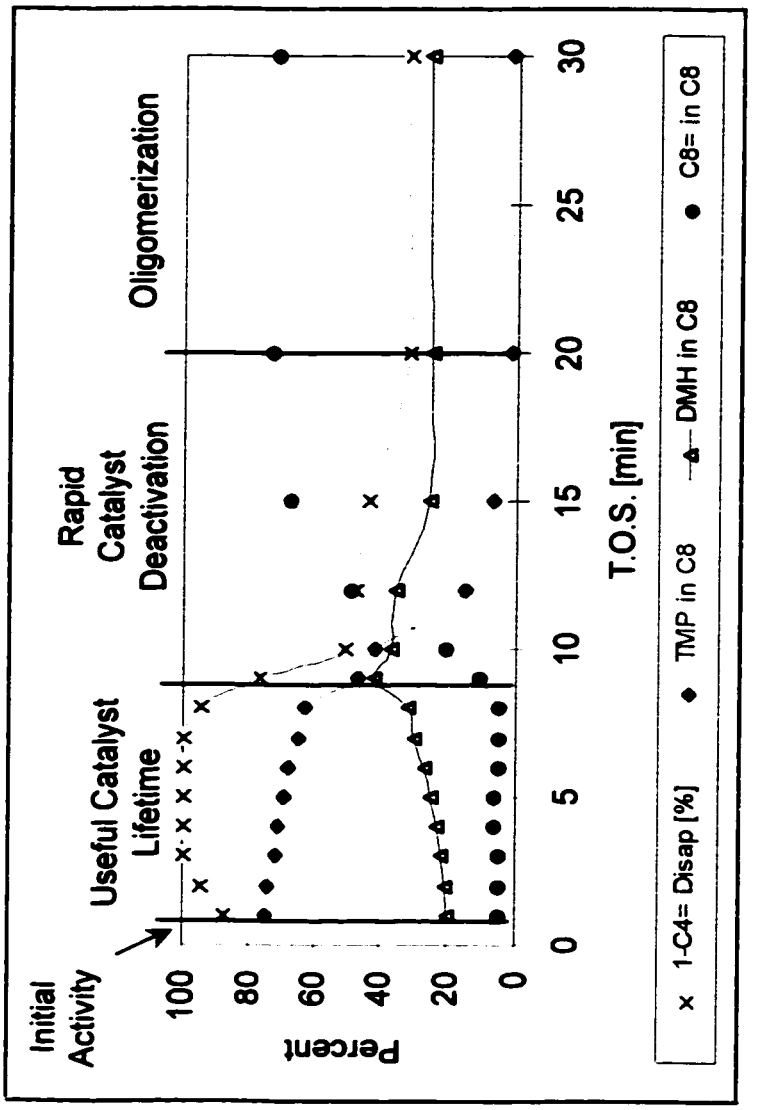

Figure 6.4: Stages of Catalyst Activity on Y Zeolite with respect to C_8 Fraction Distribution (F54Y; T_{rxn}=50°C; T_{calc}=425°C; P=382psig; I/O=15; t=1h; $C_4^=$ WHSV=2.0h^{-1}; m_{cat}=2.78g)

The fourth and final stage of catalyst activity is termed the "Oligomerization" phase. This period was characterized by a low but measurable amount of butene conversion (Taylor & Sherwood, 1997). The C_5+ liquid consisted of mainly C_8 olefins with some C_9+ products observed. Saturated C_8 production was low, and restricted to DMHs only. A typical alkylate composition from this phase was composed of 60 % C_8 products, of which 80 % were C_8 olefins. Similar behaviour was shown by EMT and Y zeolites during this final phase of catalyst activity.

6.3 SENSITIVITY ANALYSIS FOR EMT AND Y ZEOLITES

Sensitivity analysis is based on 3 sets of duplicated experiments and 1 set of triplicated results (see Appendix A4.3). These replicates involved catalyst systems of EMT, fresh 0.5%Pt/Y, regenerated 0.1%Pt/EMT and regenerated 0.5%Pt/EMT. Standard deviations were calculated during the initial 7 min of the Useful Catalyst Lifetime period. An overall average of the standard deviations was determined for all measures of catalyst performance (see Table 6.1). These values were used to assess the significance of experimental differences.

Table 6.1: Sensitivity Analysis for Measures of Catalyst Performance of Flow Runs using EMT and Y Zeolites

Measure of Catalyst Performance	Standard Deviation
Useful Catalyst Lifetime [min]	± 0.7
Yield [g C_5+/gcat/min]	± 0.016
C_5+ Product Distribution [mass %]	
C_5 - C_7	± 2.3
C_8	± 2.5
C_9^+	± 3.7
C_8 Fraction Distribution [mass %]	
TMP	± 3.3
DMH	± 2.7
$C_8^=$	± 0.8
TMP Isomer Distribution [mass %]	
2,2,4-TMP	± 2.5
2,2,3-TMP	± 2.1
2,3,3-TMP	± 2.4
2,3,4-TMP	± 2.1
Indicators [mass fraction]	
$\frac{\text{TMP}}{\text{DMH}}$	± 0.57
$\frac{\text{TMP + DMH}}{C_8^= + C_9^+}$	± 0.63
$\frac{\text{2,2,3-TMP + 2,2,4-TMP}}{\text{2,3,3-TMP + 2,3,4-TMP}}$	± 0.20
S.A. Spent Catalyst [m^2/g]	± 28.3

6.4 EFFECT OF CALCINATION TEMPERATURE ON EMT AND Y ZEOLITES

The calcination temperature has an effect on the relative amounts of Bronsted and Lewis acid sites in zeolites, as described in Section 2.1.1.1. Maximum Bronsted acidity is achieved at a calcination temperature of approximately 425°C for Y zeolite (Ward, 1967). Above this temperature, Bronsted acidity declines and Lewis acid sites increase in concentration. Once a calcination temperature of approximately

725°C is reached, Lewis and Bronsted acidity are approximately equal. As the calcination temperature is increased above 725°C, partial collapse of the zeolite structure occurs and the total number of acid sites decreases with only Lewis acid sites prevailing. No published information on the influence of EMT calcination temperature, with respect to Lewis and Bronsted acidity, is available. However, analogous behavior is expected, as both EMT and Y belong to the same faujasite family (see Chapter 3).

Calcination conditions for EMT and Y zeolites were tested at two levels: 425 and 540°C. The effect of calcination temperature was examined within the reaction temperature range of 55 to 100°C, at a reaction pressure of 382 psig and employing an I/O ratio of 11. Raw data for all experiments are found in Appendix 4.

6.4.1 Effect of Calcination Temperature on Butene Disappearance

The Useful Catalyst Lifetime of EMT was reduced by 40 % when the calcination temperature was increased from 425 to 540°C at a reaction temperature of 55°C (see Table 6.2). Calcination temperature effects were significantly diminished at higher reaction temperatures, on both EMT and Y zeolites. The Useful Catalyst Lifetime appeared to be compromised at higher temperatures; however, additional data are required to substantiate this claim.

These observations suggest that a calcination temperature of 540°C, which favours a higher concentration of Lewis acid sites and lower Bronsted acidity, expedited the onset of catalyst deactivation. This validates the approach to catalyst design, in which a primary screening criteria for potential candidates is maximizing Bronsted acidity and minimizing Lewis acidity. The data suggest that catalyst lifetime would be enhanced by employing a calcination temperature of 425°C, particularly when a low reaction temperature of 55°C is employed in the experiment.

Table 6.2: Effect of Calcination Temperature on Useful Catalyst Lifetime period of EMT and Y Zeolites (P=382psig, I/O=11; $C_4^=$ WHSV=2.6h^{-1}; m_{cat}=2.78g)

Catalyst	T_{rxn} [°C]	Useful Catalyst Lifetime period [min]	
		T_{calc}=425°C	T_{calc}=540°C
EMT	55	10.6	6.5
	77	7.6	n.a.
	88	n.a.	6.9
	100	6.8	n.a.
Y	70	8.4	n.a.
	86	n.a.	4.5
	100	4.5	n.a.

It is interesting that the effect of calcination temperature was more apparent at a lower reaction temperature, and became less significant as the temperature was elevated. It is possible that the hydrophilicity of the catalyst surface was influenced by calcination temperature (Kaliguine, 2000), with lower calcination temperatures favouring reduced desorption rates of *i*-C_4. As reaction temperature was increased, the desorption rate of *i*-C_4 increased, making the effect of calcination temperature less distinguishable. The reaction became less selective towards alkylation and therefore, the effect of acid site type was less significant.

Alternatively, pore volume may also be modified by calcination temperature affecting the concentration of reactants in the catalyst pores or rate of adsorption of *i*-C_4. These modifications to the local environment, may be more significant at lower reaction temperatures. These aspects were not considered in the present work and could be explored in future investigations.

6.4.2 Effect of Calcination Temperature on C_5+ Product Distribution

Calcination temperature demonstrated a measurable effect on alkylate composition during the Useful Catalyst Lifetime period. The fraction of C_5-C_7 components in the alkylate was reduced and polymerization levels were elevated, for the catalyst calcined at 540°C. This behaviour was found to be more significant on EMT at a reaction temperature of 55°C (see Figure 6.5) and Y zeolite between 70 and 100°C (see Figure 6.7). The effects were less notable on EMT between 77 to 100°C (see Figure 6.6).

The content of C_8 compounds in the alkylate, was not significantly altered by the calcination temperature. EMT achieved comparable C_8 levels at 55°C for both calcination temperatures (see Figure 6.5). However, these levels were sustained for a longer duration under the milder calcination conditions (i.e. T_{calc}=425°C). The content of C_8 compounds in the alkylate was reduced slightly at higher reaction temperatures on both EMT (see Figure 6.6) and Y (see Figure 6.7) zeolites, when the severity of the calcination step was increased to 540°C.

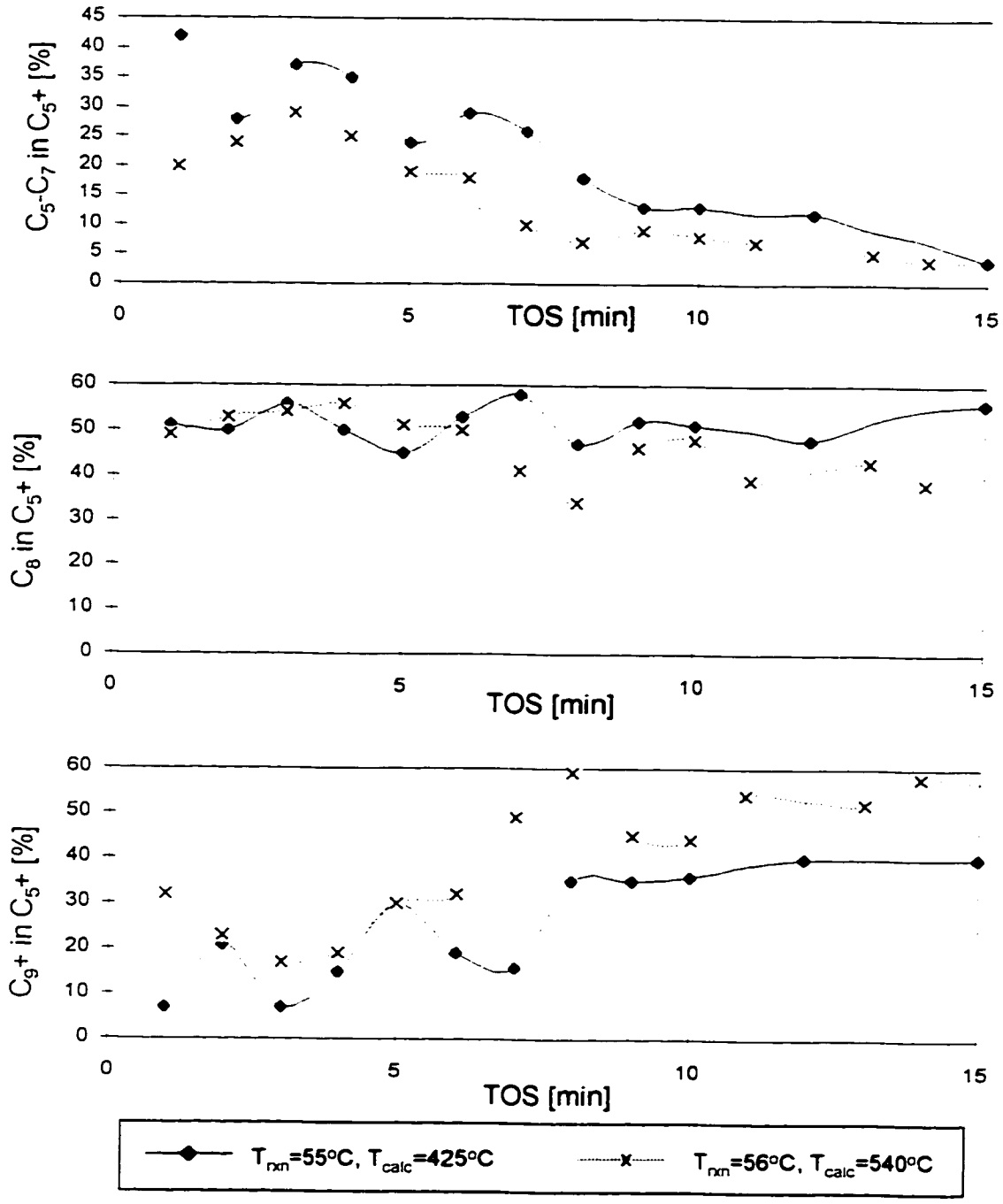

Figure 6.5: Effect of EMT Calcination Temperature on C_5+ Product Distribution at a Reaction Temperature of 55°C (P=382psig; I/O=11; $C_4^=$WHSV=2.60h^{-1}; m_{cat}=2.78g)

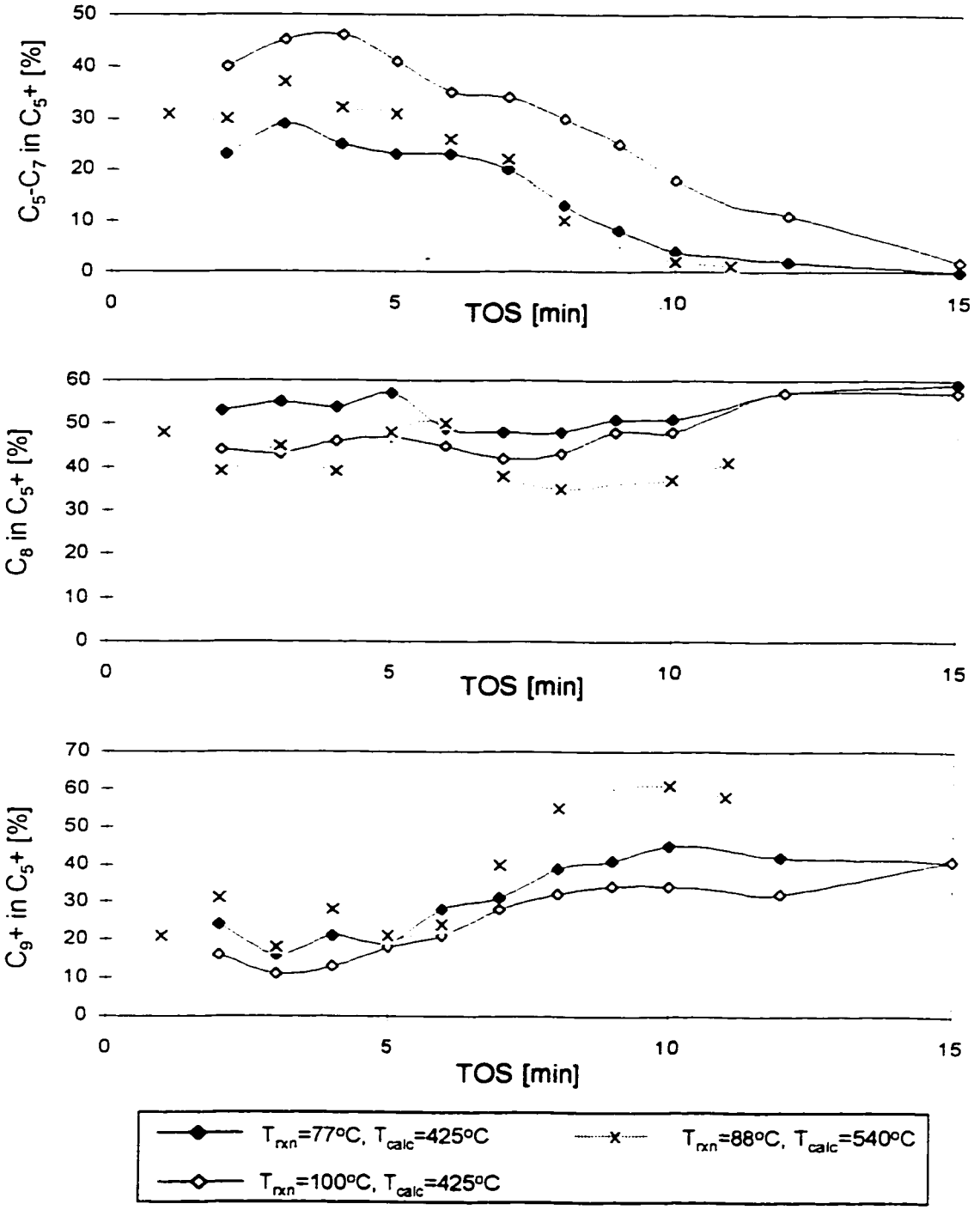

Figure 6.6: Effect of EMT Calcination Temperature on C_5+ Product Distribution for Reaction Temperatures between 77 and 100°C

(P=382psig; I/O=11; $C_4^=$WHSV=2.60h^{-1}; m_{cat}=2.78g)

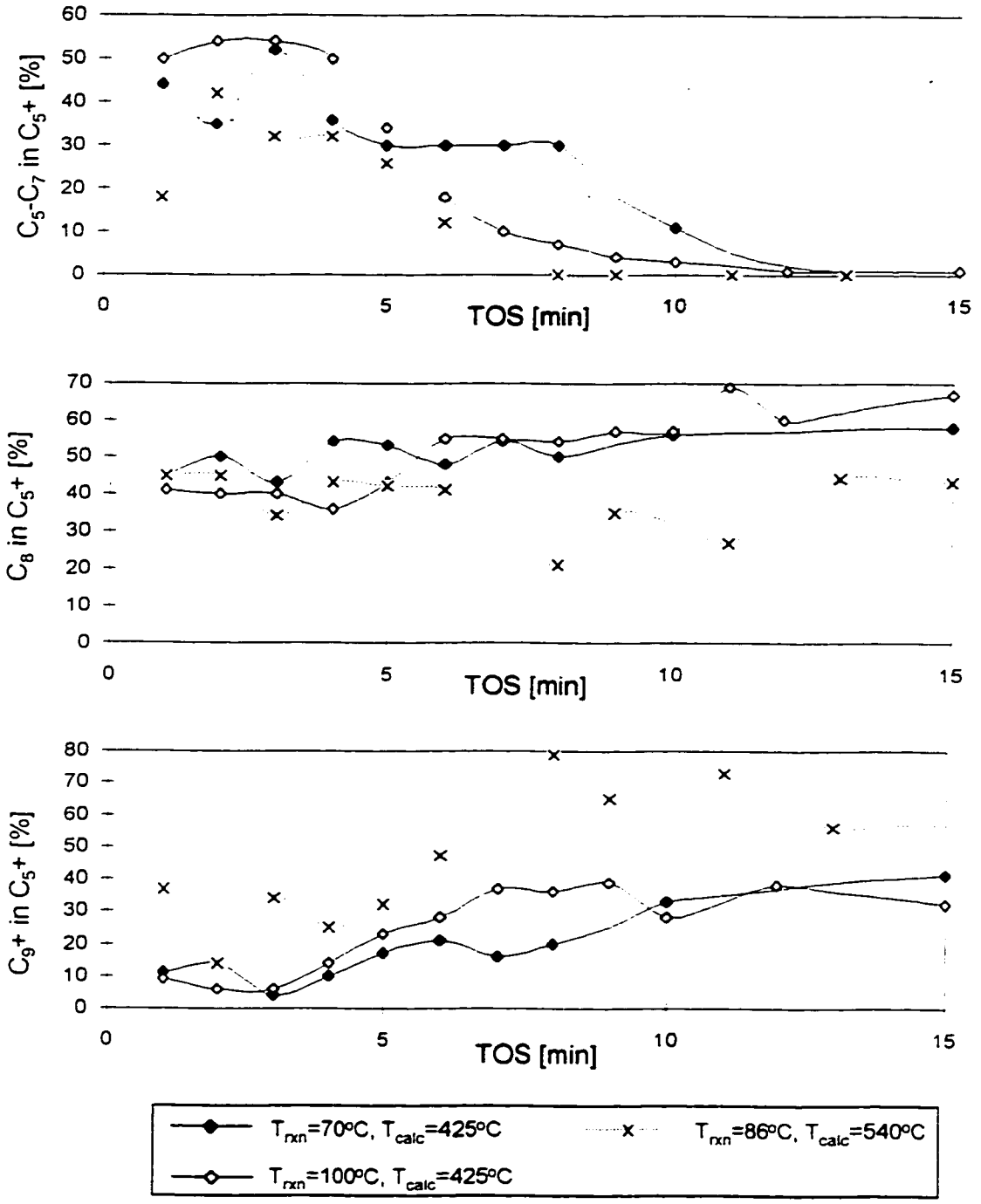

Figure 6.7: Effect of Y Calcination Temperature on C_5+ Product Distribution for Reaction Temperatures between 70 and 100°C (P=382psig; I/O=11; $C_4^=$WHSV=2.60h^{-1}; m_{cat}=2.78g)

6.4.3 Effect of Calcination Temperature on C_8 Selectivity

No significant change in TMP levels was noted during the Useful Catalyst Lifetime period on EMT, when the calcination temperature was increased from 425 to 540°C. However, TMP levels were sustained for a longer duration at 55°C, when the milder calcination temperature was employed (see Figure 6.8). The lower calcination temperature favoured increased DMH production, as compensated by suppressed oligomerization formation. Overall, more saturated C_8 products (TMPs and DMHs) were detected from EMT with higher Bronsted acidity, at a reaction temperature of 55°C. An increase in calcination temperature enhances Lewis acidity on EMT, which favoured oligomerization products over DMHs. Elevated levels of olefins are expected to enhance polymerization activity, which was observed for EMT calcined at 540°C.

The effects of calcination temperature were greatly diminished at elevated reaction temperatures on EMT (see Figure 6.9). A calcination temperature of 425°C produced slightly lower amounts of TMPs with increased levels of DMHs, for reaction temperatures of 77 and 100°C. This differs slightly from the behaviour at 55°C, where TMP levels were independent of calcination conditions.

Y zeolite behaved in a manner similar to EMT at higher reaction temperatures (see Figure 6.10). The catalyst calcined at 425°C produced less TMPs and more DMHs during the Useful Catalyst Lifetime period. Although the TMP content was improved by calcining at 540°C, the total amount of saturated C_8 products (TMPs and DMHs) was greatly reduced.

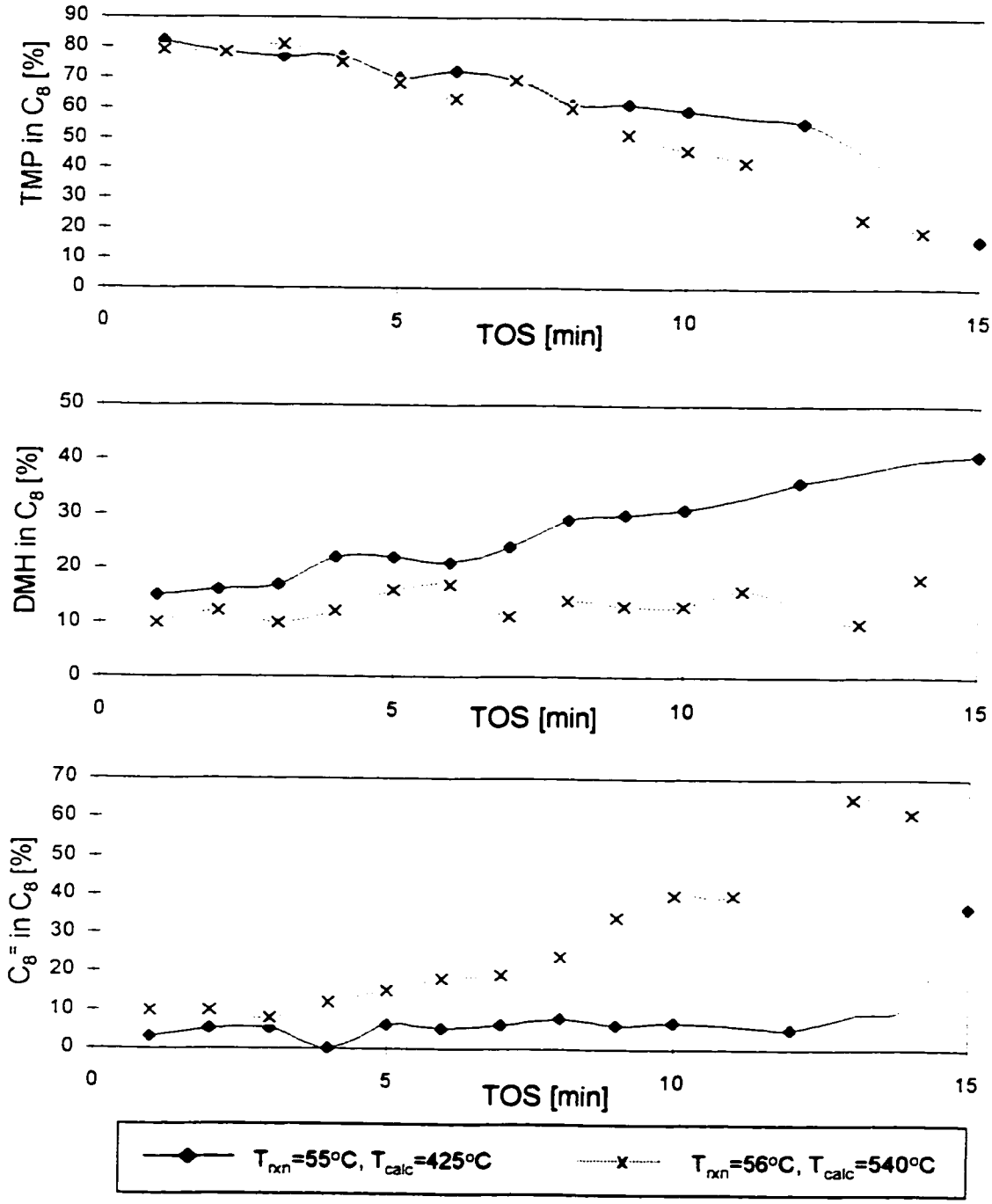

Figure 6.8: Effect of EMT Calcination Temperature on C_8 Selectivity at a Reaction Temperature of 55°C
(P=382psig; I/O=11; $C_4^=$WHSV=2.60h^{-1}; m_{cat}=2.78g)

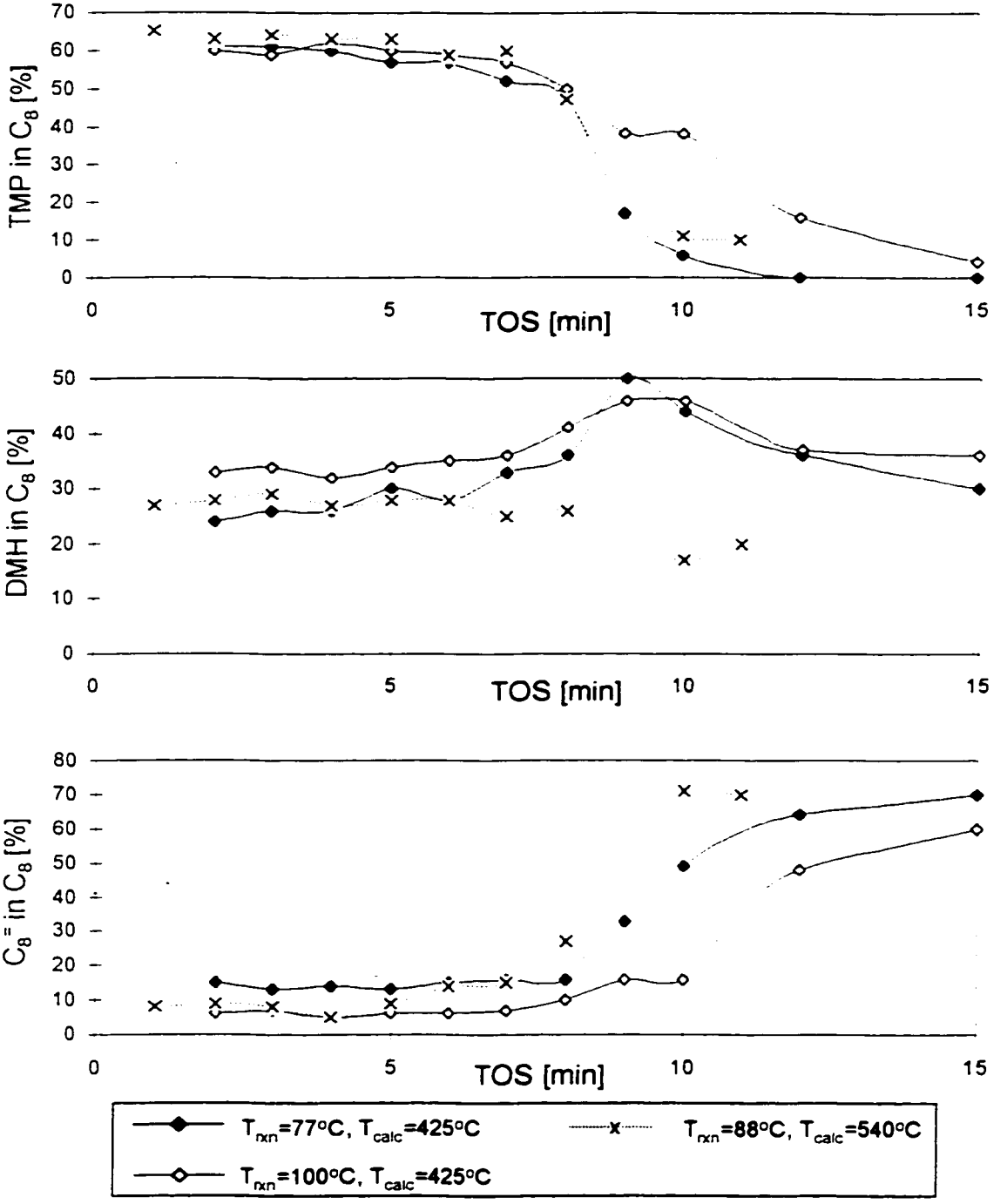

Figure 6.9: Effect of EMT Calcination Temperature on C_8 Selectivity For Reaction Temperatures between 77 and 100°C (P=382psig; I/O=11; $C_4^=$WHSV=2.60h^{-1}; m_{cat}=2.78g)

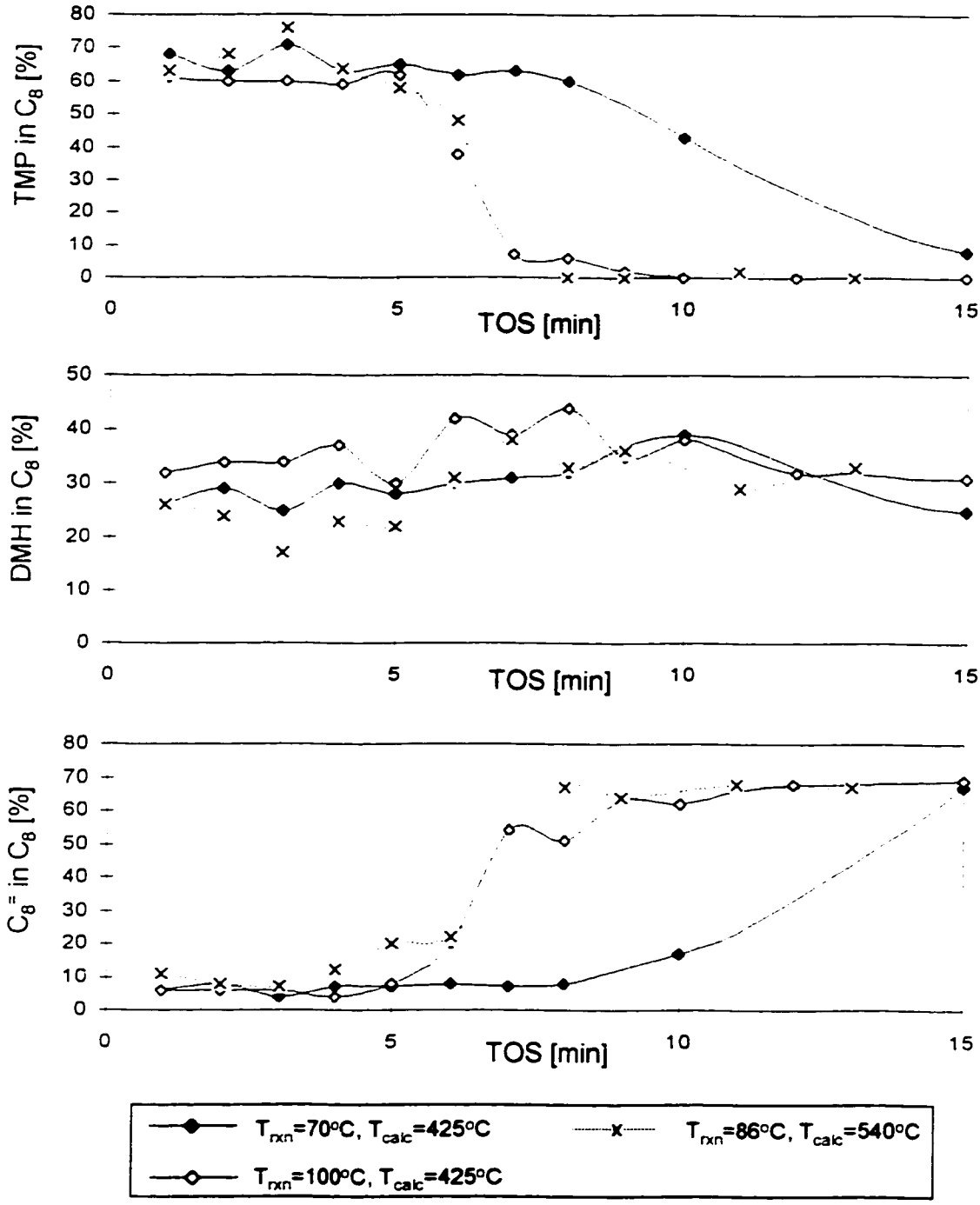

Figure 6.10: Effect of Y Calcination Temperature on C_8 Selectivity for Reaction Temperatures between 70 and 100°C (P=382psig; I/O=11; $C_4^=$WHSV=2.60h^{-1}; m_{cat}=2.78g)

Comparable behaviour between EMT and Y zeolites was observed during the other phases of catalyst activity (see Figures 6.8 to 6.10). The production of TMP was sustained more effectively during the Deactivation period on the catalysts calcined at 425°C. Elevated levels of DMH formation were noted during the Useful Catalyst Lifetime, for catalysts subjected to milder calcination treatment. This behaviour continued during the Deactivation phase, except on Y zeolite at reaction temperatures above 70°C. This catalyst favoured TMPs during the Deactivation phase when calcined at 425°C. The levels of $C_8^=$ were comparable during the Useful Catalyst Lifetime period, for all calcination conditions. However, content of $C_8^=$ was notably less during the Deactivation Period, for catalysts calcined at 425°C.

These results support the notion that the nature of the acid sites resulting from a calcination temperature of 425°C were better equipped to maintain a strong hydride transfer function, particularly at a reaction temperature of 55°C. Predominantly saturated products were detected in the C_8 fraction, which were less reactive towards undesirable side reactions. This delayed the onset of catalyst deactivation, allowing alkylation activity to be sustained for longer duration and favouring an extended Useful Catalyst Lifetime.

6.4.4 Effect of Calcination Temperature on 2,2,4-TMP Level in the TMP Fraction

The most valuable octane product, 2,2,4-TMP, can result from self-alkylation of *i*-C_4, isomerization of TMP^+ isomers formed or cracking of C_{12}^+ products. If cracking of C_{12}^+ components is the primary route of 2,2,4-TMP formation, it is expected that higher levels of 2,2,4-TMP would result at a higher reaction temperature and lower calcination temperature, as these conditions favour high cracking activity. This is contrary to what was observed experimentally (see Figure 6.11). This suggests that other routes of 2,2,4-TMP formation, such as self-alkylation of *i*-C_4, were being promoted on EMT.

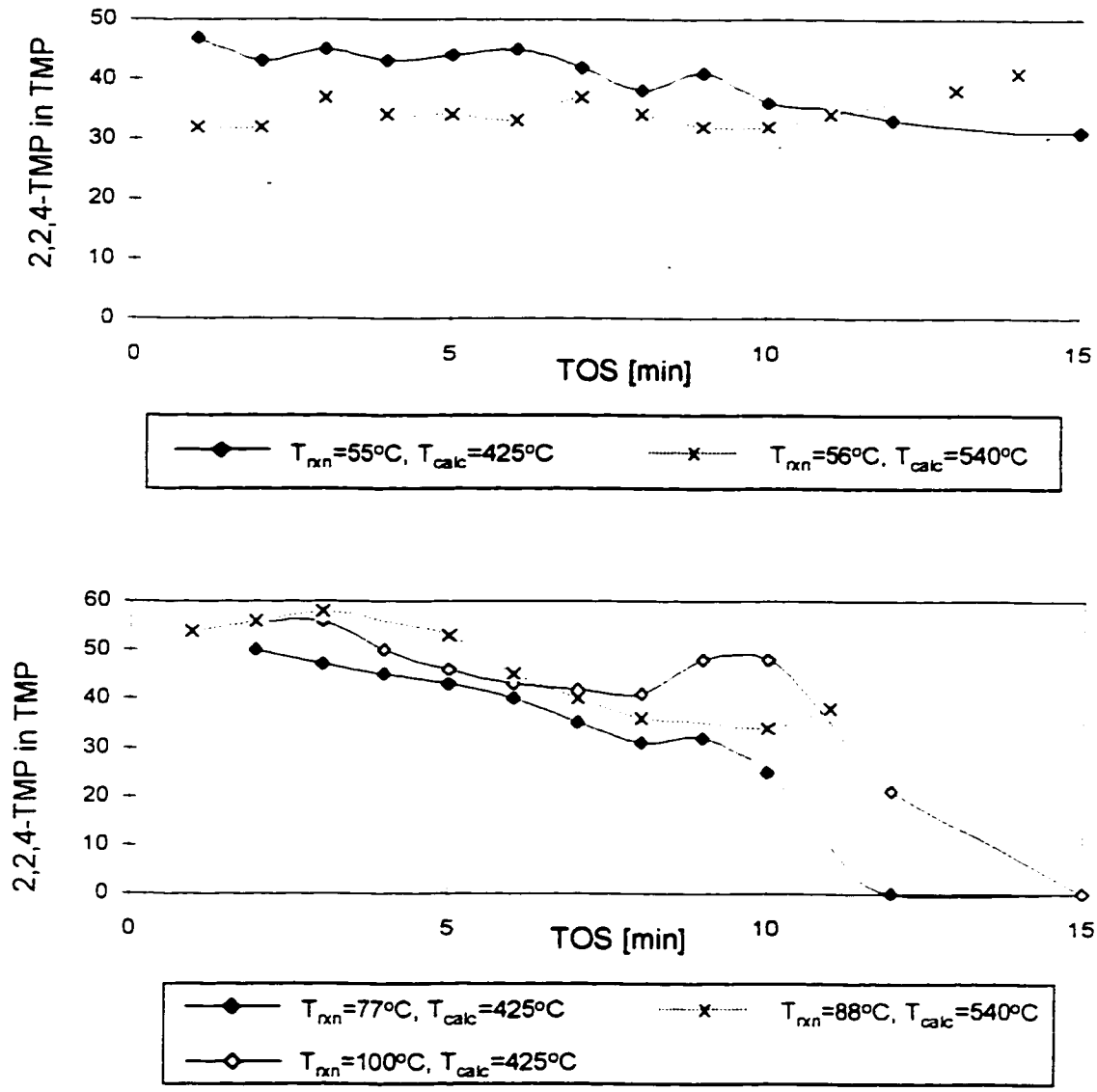

Figure 6.11: Effect of EMT Calcination Temperature on 2,2,4-TMP Content in TMP Fraction for Reaction Temperatures between 55 and 100°C (P=382psig; I/O=11; $C_4^=$WHSV=2.60h^{-1}; m_{cat}=2.78g)

Results on Y zeolite contrasted with those obtained on EMT, at higher reaction temperatures. A lower calcination temperature of 425°C favoured higher levels of 2,2,4-TMP in the TMP fraction, relative to those obtained on Y zeolite calcined at 540°C (see Figure 6.12). It may be that the primary route of 2,2,4-TMP formation on Y zeolite occurred through cracking of C_{12}^{+} compounds. Since the lower calcination temperature enhanced cracking activity, it is expected that 2,2,4-TMP levels would be greatest under these conditions. It is also possible that acid sites which could potentially facilitate other routes of 2,2,4-TMP production (i.e. self alkylation of isobutane), were converted to Lewis acid sites during the more severe calcination treatment at 540°C. These possibilities were not pursued in the present work, and could be considered in subsequent investigations.

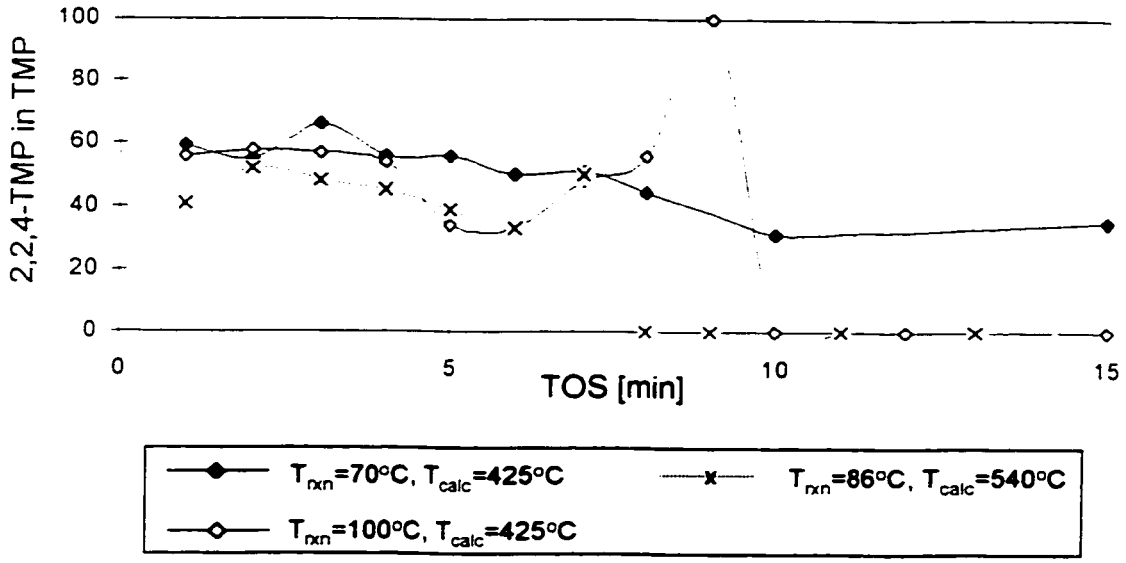

Figure 6.12: Effect of Y Calcination Temperature on 2,2,4-TMP Content in TMP Fraction for Reaction Temperatures between 70 and 100°C (P=382psig; I/O=11; $C_4^{=}$WHSV=2.60h^{-1}; m_{cat}=2.78g)

6.4.5 Synopsis of Effect of Calcination Temperature

The effect of calcination temperature is consistent with the hypothesis that the alkylation mechanism is facilitated by a Bronsted acid site. A calcination temperature of 425°C, which favours the maximum density of Bronsted acid sites, sustained catalyst activity for a longer duration on EMT and Y zeolites. This result is supported by other work in the literature. Simpson et al (1996) observed a striking correspondence between the relative number of Bronsted acid sites on Y zeolite and time-zero butene conversion, providing corroborating evidence of the nature of the acid site activating this reaction using solid acids.

Catalyst performance varied with changes in calcination temperature on both EMT and Y zeolites. Table 6.3 summarizes average alkylate quality during the first 5 min of the Useful Catalyst Lifetime period. A lower calcination temperature of 425°C promoted cracking activity whereas, a catalyst calcined at 540°C favoured polymerization reactions on both EMT and Y zeolites.

Although the TMP/DMH ratio was augmented by a calcination temperature of 540°C on EMT at a reaction temperature 55°C, the selectivity to saturated C_8 products was very poor ((TMP + DMH)/($C_8^=$ + C_9+)) (see Table 6.3). Similar behavior appeared to be demonstrated by Y zeolite at higher operating temperatures, between 70 and 100°C. However, this behaviour was not conclusively observed on EMT between 77 and 100°C. Additional experiments are required to definitively assess the influence of calcination treatment on catalyst performance at higher reaction temperatures.

All of the effects discussed above were more significant at a reaction temperature of 55°C when employing EMT. As the reaction temperature was increased, the effects of calcination temperature were found to be less important, with respect to maximizing saturated C_8 production levels and suppressing oligomerization activity. However, the lower calcination temperature still demonstrated superior catalyst performance in terms of maximizing the Useful Catalyst Lifetime period.

Table 6.3: Effect of Calcination Temperature on Catalyst Performance and Average Alkyate Quality (first 5 min of Useful Catalyst Lifetime period) using EMT and Y Zeolites (P=382psig, I/O=11; $C_4^=$ WHSV=2.6h^{-1}; m_{cat}=2.78g)

Catalyst	EMT						Y			
T_{calc} [°C]	425			540			425			540
Run	F28EMT	F31EMT	F34EMT	F23EMT	F22EMT		F29Y	F33Y		F21Y
T_{rxn} [°C]	55	77	100	56	88		70	100		86
Useful Catalyst Lifetime [min]	10.6	7.6	6.8	6.5	6.9		8.1	4.5		4.5
C_5+ Liquid [mass %]										
C_5 - C_7	33	25	41	23	32		39	49		30
C_8	51	55	45	53	45		49	40		42
C_9+	16	20	14	24	23		12	11		28
C_8 Fraction [mass %]										
TMP	77	60	61	76	64		66	61		66
DMH	19	26	33	13	28		27	33		22
$C_8^=$	4	14	6	11	8		7	6		12
TMP Distribution [%]										
2,2,4-TMP	44	46	52	34	55		58	53		45
2,2,3-TMP	15	10	12	11	13		9	10		5
2,3,4-TMP	15	17	14	23	11		12	15		22
2,3,3-TMP	26	27	22	32	21		21	22		28
Indicators [mass %]										
$\frac{TMP}{DMH}$	4.13	2.29	1.81	6.10	2.29		2.42	1.82		3.03
$\frac{TMP+DMH}{C_8^= + C_9+}$	3.57	1.74	2.49	1.65	1.61		3.63	3.20		1.26
$\frac{2,2,4\text{-}TMP+2,2,3\text{-}TMP}{2,3,3\text{-}TMP+2,3,4\text{-}TMP}$	1.49	1.30	1.82	0.81	2.15		2.05	1.68		1.01

These results support the notion that the nature of the acid sites resulting from a calcination temperature of 425°C were better equipped to maintain a strong hydride transfer function. Predominantly saturated products were detected in the C_8 fraction which were less reactive towards undesirable side reactions. This delayed the onset of catalyst deactivation allowing alkylation activity to be sustained for a longer duration thus extending the Useful Catalyst Lifetime period.

The severity of the calcination treatment influenced the distribution of TMP isomers. More severe calcination temperatures favoured the least sterically hindered isomers, 2,3,3-TMP and 2,3,4-TMP, at 55°C on EMT and on Y between 70 and 100°C (see Table 6.3). No significant effect of calcination temperature on TMP distribution was noted on EMT at reaction temperatures above 77°C. The most valuable octane isomer, 2,2,4-TMP, predominated on both catalysts under all conditions tested, reaching levels between 34 and 58 % of the TMP fraction. Cracking of C_{12}+ compounds was identified as the most probable route for 2,2,4-TMP formation, with self-alkylation of *i*-C_4 being suggested as a possible alternative on EMT.

Note that the product distribution observed is a qualitative assessment, on the basis of instantaneous product effluent analysis. This approach does not consider catalyst yield (i.e. g C_5+ produced/g $C_4^=$ fed/h) with TOS, which provides a measure of the quantity of alkylate collected. Since liquid product was not collected for these experiments, the most reliable indication of yield is the duration of the Useful Catalyst Lifetime. That is, a catalyst facilitating effective hydride transfer will desorb products efficiently, operate for a longer TOS and favour alkylation products. In contrast, catalysts which are deficient in this ability, will retain products on the catalyst surface and deactivate in a shorter period of time. On this basis, a catalyst calcined at 425°C is expected to achieve a higher yield and EMT is expected to behave in a superior manner relative to Y zeolite.

The explanations provided to rationalize the experimental data are further validated by surface area (SA) measurements of the spent catalyst (see Table 6.4). Those calcined at 425°C were less susceptible to SA loss despite the fact that catalyst exposure to the feed was four times longer. It appears that calcination

conditions promoting Bronsted acidity, yielded a catalyst which demonstrated superior resistance to catalyst deactivation. In contrast, a calcination temperature of 540°C. favouring increased Lewis acidity, promoted olefin adsorption. This favoured oligomerization and polymerization activities, promoting rapid surface area loss upon exposure to the feed.

Table 6.4: Effect of Calcination Temperature on Surface Area of Spent Catalyst (P=382 psig; I/O=11, $C_4^=$ WHSV=2.6h^{-1}; m_{cat}=2.78g)

Catalyst	Calcination Temperature [°C]	Reaction Temperature [°C]	Experiment Duration [min.]	Surface Area of Spent Catalyst [m^2/g]
EMT	425	55	60	377
		77	60	348
		100	60	309
EMT	540	56	15	148
		88	15	121
Y	425	70	60	374
		100	60	329
Y	540	80	15	205

S.A. fresh EMT = 755 m^2/g; S.A. fresh Y = 620 m^2/g

TGA/DTA of the spent catalyst provided further evidence of increased susceptibility to deactivation on EMT, when pre-treatment promoted increased Lewis acidity (see Table 6.5). The loss in active surface area was more significant for EMT calcined at 540°C, despite the brief exposure to the butene feed mixture. It is possible that adsorbed species on this catalyst are active in facilitating hydride transfer during the reaction, leading to polyaromatic deposits plugging the catalyst pores. In contrast, EMT calcined at 425°C, favouring increased Bronsted acidity, was better equipped to facilitate hydride transfer. Consequently, adsorbed species were less reactive towards polymerization reactions. The content of adsorbed species was suppressed and active surface area was preserved in a superior manner.

Table 6.5: TGA/DTA Analysis of Spent EMT as a Function of Calcination Temperature (T_{rxn}=55°C; P=382psig; I/O=11; $C_4^=$ WHSV=2.6h^{-1}; m_{cat}=2.78g)

Run	T_{calc} [°C]	Duration [min]	TGA [mass %] Desorption Temperature [°C] $T_d \leq 200$	$200 < T_d < 300$	$T_d \geq 300$	Total	SA Spent Catalyst [m^2/g]
F28EMT	425	60	3.8	2.5	3.0	9.3	377
F23EMT	540	15	2.8	2.7	3.0	8.5	148

S.A. fresh EMT = 755 m^2/g

Overall, a calcination temperature of 425°C promoted hydride transfer for a longer period of time and deferred the onset of catalyst deactivation. This resulted in high butene conversion being maintained for a longer TOS. Additional experiments, with the objective to optimize the calcination temperature for EMT and Y zeolite, were not attempted. All subsequent experiments utilized a calcination temperature of 425°C, unless otherwise specified.

6.5 EFFECT OF REACTION TEMPERATURE ON EMT AND Y ZEOLITES

Reaction temperature was not found to exercise a significant effect on the product distribution between 80 and 100°C in batch experiments. It is of interest to determine whether similar behavior is observed in a continuous flow environment. Flow experiments were performed in the temperature range of 29 to 100°C at 382 psig, using EMT and Y zeolites calcined at 425°C, and employing an I/O ratio of 11 ($C_4^=$ WHSV = 2.6 h^{-1}).

6.5.1 Effect of Reaction Temperature on Butene Disappearance

Of the reaction temperatures considered, a preferred level of 55°C was identified for EMT, whereas 70°C was concluded best on Y zeolite (see Figures 6.13). The result on Y zeolite closely matches that found by other authors utilizing a continuous stirred reactor (Taylor & Sherwood, 1997). Butene conversion was sustained for a longer duration under these preferred conditions, maximizing the length of the Useful Catalyst Lifetime period. Clearly, the optimum reaction temperature is specific to the nature of the catalyst (i.e. catalyst type, T_{calc}) and operating conditions (i.e. I/O, olefin WHSV, reactor geometry) employed for the experiment. This suggestion has been emphasized by other authors (Corma & Martinez,1993).

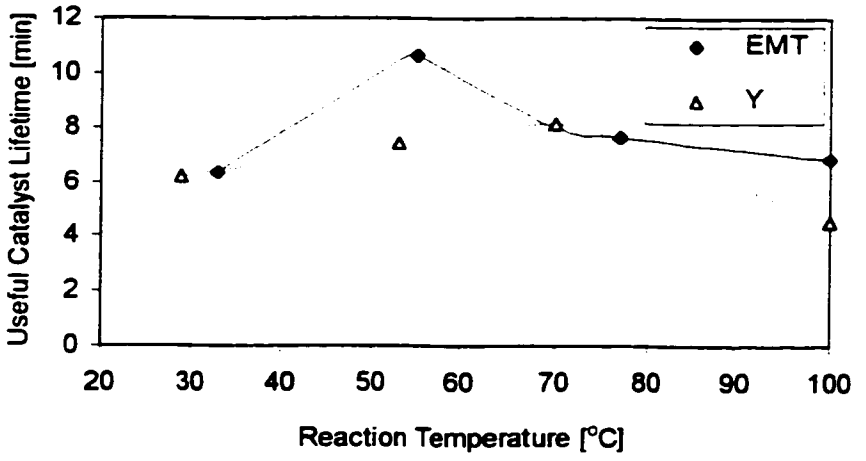

Figure 6.13: Effect of Reaction Temperature on Useful Catalyst Lifetime for EMT and Y Zeolites (T_{calc}=425°C; P=382psig; I/O=11; $C_4^=$WHSV=2.6h^{-1}; m_{cat}=2.78g)

EMT demonstrated superior ability over Y, and extended the Useful Catalyst Lifetime for a longer duration at their respective preferred temperature conditions. The Useful Catalyst Lifetime for EMT was more adversely affected at reaction temperatures below 55°C, relative to those above this preferred level. This trend was reversed when employing Y zeolite. The Useful Catalyst Lifetime was significantly reduced at temperatures above 70°C, and less sensitive to operating conditions below this preferred reaction temperature.

6.5.2 Effect of Reaction Temperature on C_5+ Product Distribution

At the preferred reaction temperature, cracking activity and alkylation activities were maximized and polymerization activity was suppressed for EMT and Y zeolites (see Figures 6.14 to 6.15). Since alkylation and cracking reactions demands similar acid site strength (Corma et al, 1994b; Corma & Wojciechowski, 1982; Corma et al, 1994a; O'Young et al, 1994; Corma et al, 1996a), it is difficult to promote one type of reaction without encouraging the other. Therefore, the optimum reaction temperature represents a compromise between two opposing forces. The reaction temperature must be sufficiently high to facilitate high olefin conversion for a long duration and crack bulky polymerization products. However, it cannot be excessively high, such that the stability of alkylate precursors is compromised. This complicated kinetic balance is a function of the process parameters employed, including catalyst type, calcination temperature and I/O ratio to name a few. Therefore, the preferred reaction temperature which has been identified, is specific to the process parameters which have been fixed in the experimental procedure.

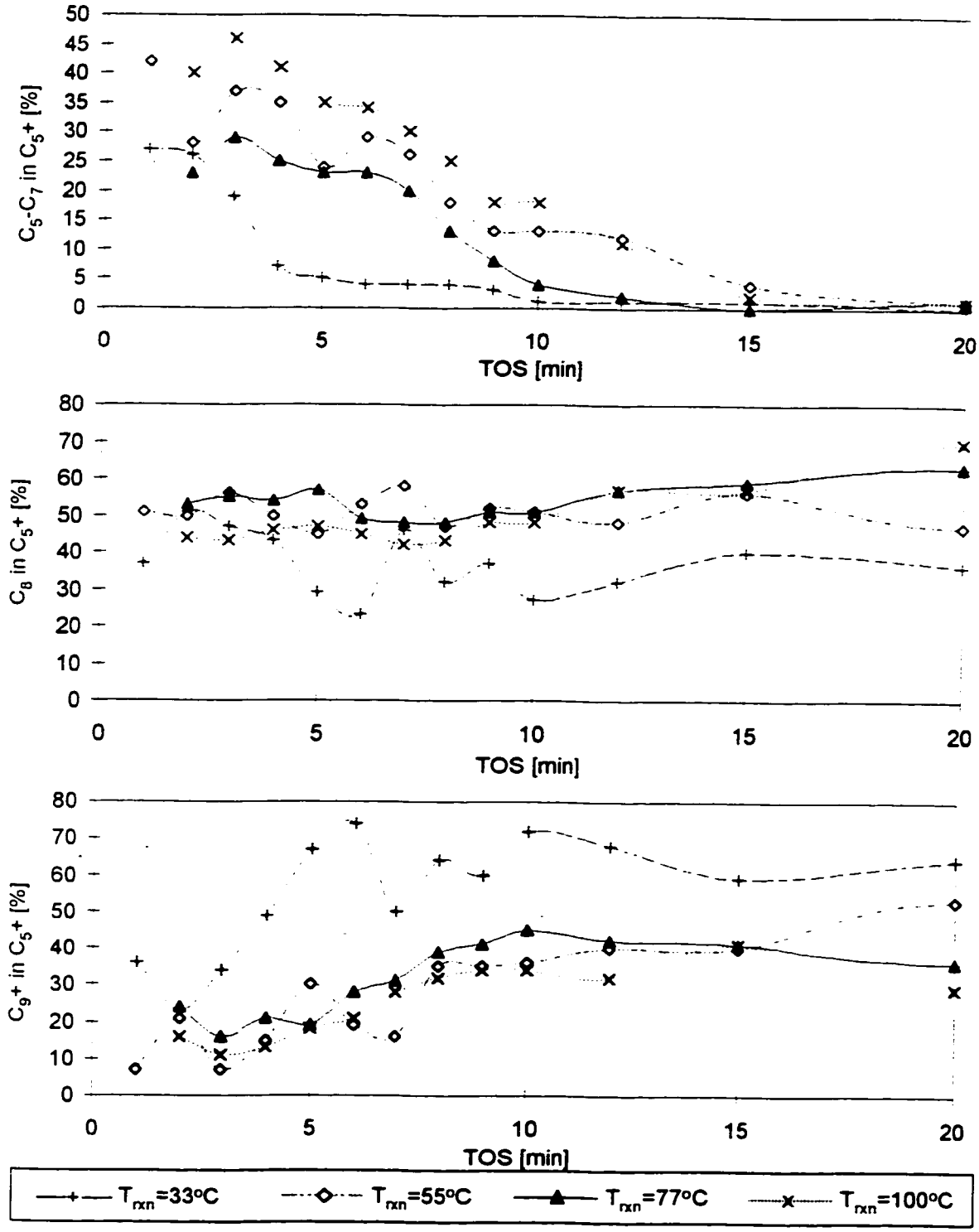

Figure 6.14: Effect of Reaction Temperature on C_5+ Product Distribution on EMT Zeolite (T_{calc}=425°C; P=382psig; I/O=11; $C_4^=$WHSV=2.6h^{-1}; m_{cat}=2.78g)

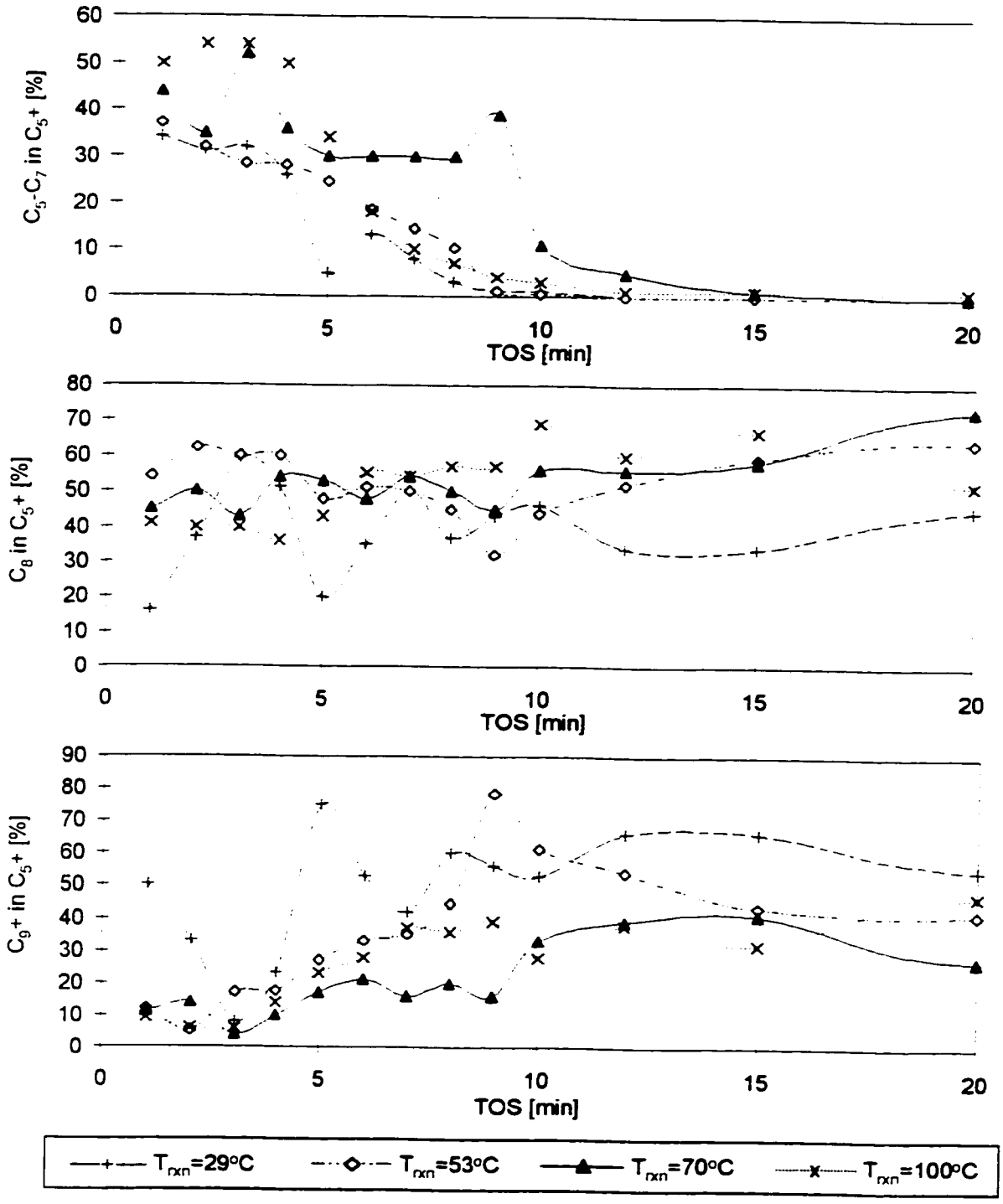

Figure 6.15: Effect of Reaction Temperature on C_5+ Product Distribution on Y Zeolite (T_{calc}=425°C; P=382psig; I/O=11; $C_4^=$WHSV=2.6h^{-1}; m_{cat}=2.78g)

Although the preferred reaction temperature was specific to the catalyst type, catalytic behavior was similar for EMT and Y zeolites as the reaction temperature was varied away from preferred levels. At temperatures lower than the preferred condition, cracking activity was diminished. Therefore, accumulation of polymerization was observed, agreeing with the results obtained by other authors (Taylor & Sherwood, 1997). It appears that the proportion of acid sites with sufficient strength for facilitating cracking reactions, is reduced at lower temperatures, resulting in more sites being active for less demanding activities such as polymerization reactions.

At reaction temperatures greater than the preferred level, cracking activity increased notably, on both EMT and Y zeolites. Polymerization activity was relatively unchanged from the levels obtained at the preferred reaction temperature, with the exception of experiments at approximately 30°C, where polymerization product levels were notably higher. Catalyst performance was unstable on both zeolites at approximately 30°C, as evidenced by irregular C_5+ liquid composition profiles. This is most likely a consequence of enhanced deactivation rates, favoured by elevated concentrations of polymerization products in the catalyst pores.

Batch reaction results were modestly affected by a change in reaction temperature from 80 to 100°C. Results from the flow reactor studies display similar behavior. Cracking activity was slightly elevated at the higher temperature in the flow experiments, agreeing with preliminary batch reactor data. A decrease in the polymerization activity was observed in the flow reactor results rather than the C_8 production levels, as was observed in batch experiments. This difference reflects the changes in residence time of the product on the catalyst surface, in a flow versus batch reactor geometry.

6.5.3 Effect of Reaction Temperature on C_8 Selectivity

The production of TMP was maximized at approximately 78 % of the saturated C_8 fraction (DMHs plus TMPs), using EMT at 55°C (see Figure 6.16). In contrast, only 69 % of the saturated C_8 fraction was TMP on Y zeolite at 29°C (see Figure 6.17). Both of these results differ considerably from the thermodynamic prediction of 10 to 12 % of C_8 paraffins in the C_8 fraction (Corma & Martinez, 1993). It is unknown what factors are controlling the reaction mechanism, preventing equilibrium from being attained. Important considerations include the strong adsorption capacity of zeolites, even at low temperatures, which equates to a high solubility of the reactants in a liquid acid. This factor, in conjunction with the concentration effect inherent in zeolite pores, as well as the preferential adsorption of olefins over paraffins, results in a product distribution significantly different from thermodynamic predictions.

Low reaction temperatures favoured elevated TMP levels, during the Useful Catalyst Lifetime on EMT (see Figure 6.16) and Y (see Figure 6.17) zeolites, agreeing with the results of other authors (Taylor & Sherwood, 1997). It was found that butene isomerization occurred rapidly on fresh and aged Y zeolite (Chu & Chester, 1986). Measured levels of butene isomers, found that 1-butene formation was suppressed at lower reaction temperatures on Y zeolite (Simpson et al, 1996). Reaction of 1-butene with *tert*-butyl carbenium ion leads to DMH^+ isomers, whereas combination of 2-butene with *tert*-butyl cation produces TMP^+ species. Therefore, increased isomerization of 1-butene to 2-butene is expected to enhance TMP formation at lower reaction temperatures. Alternatively, the improved stability of the *tert*-butyl cation relative to the *sec*-butyl cation, may exercise greater importance at low reaction temperatures, accounting for higher TMP levels.

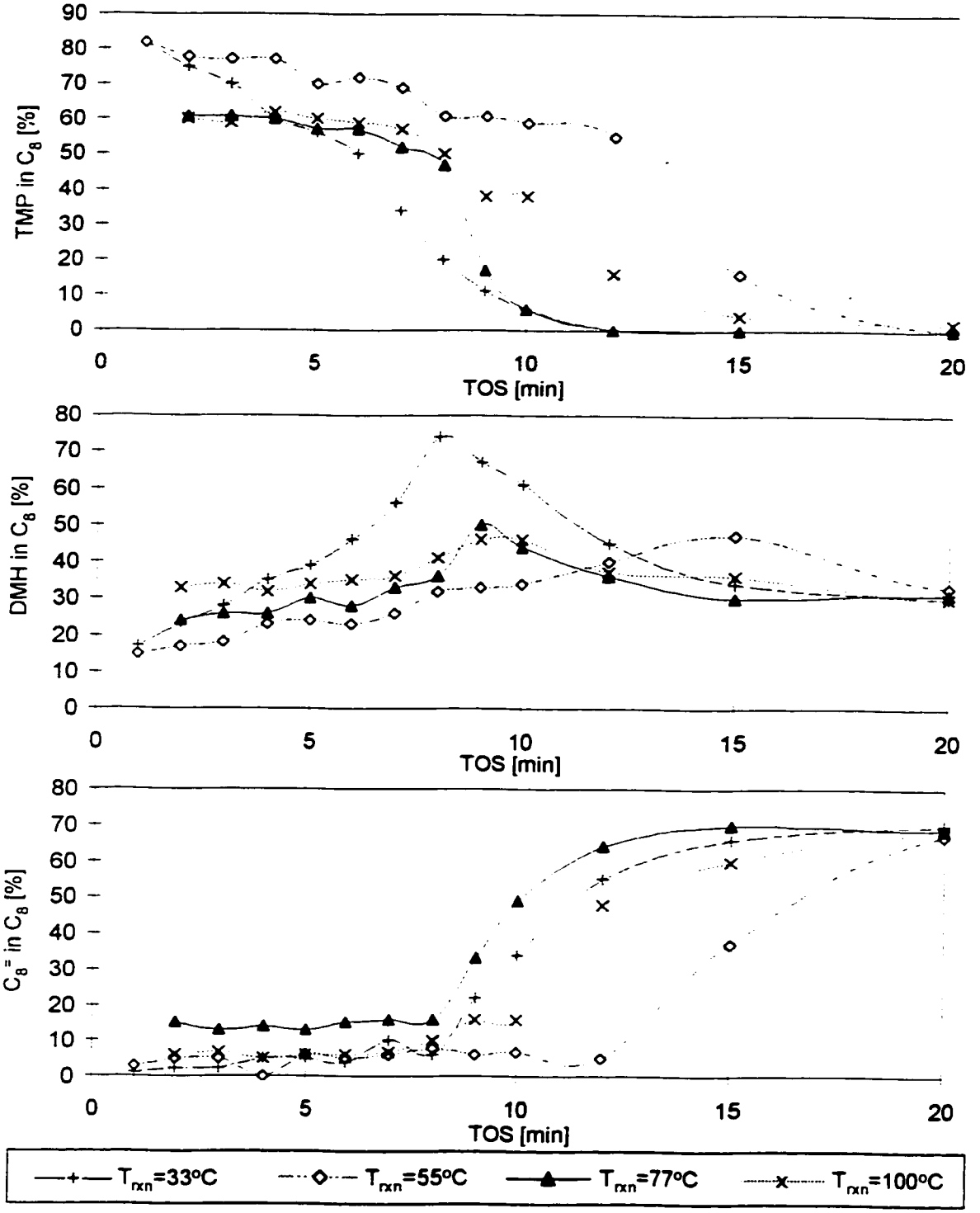

Figure 6.16: Effect of Reaction Temperature on C_8 Selectivity on EMT Zeolite (T_{calc}=425°C; P=382psig; I/O=11; $C_4^=$WHSV=2.6h^{-1}; m_{cat}=2.78g)

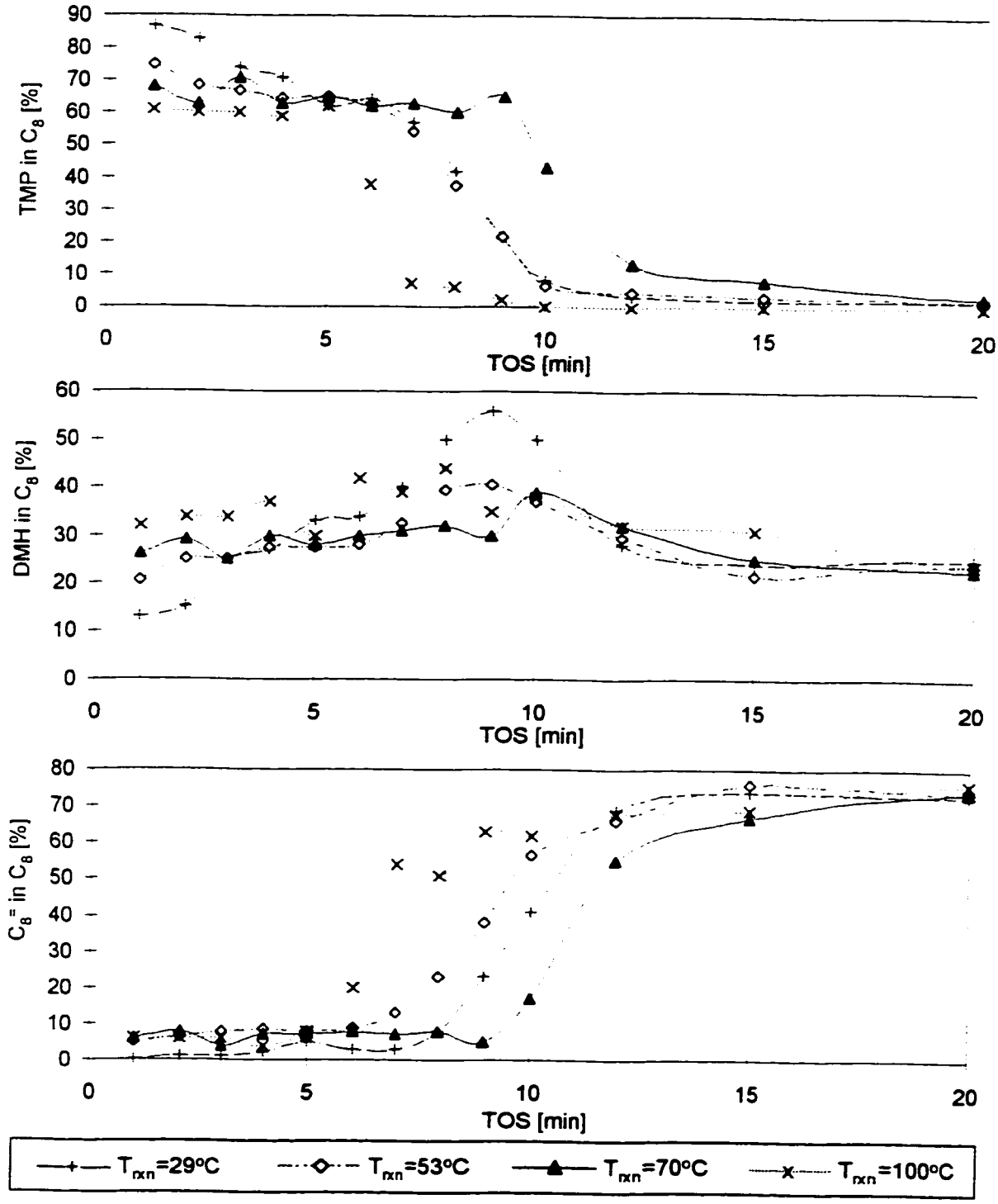

Figure 6.17: Effect of Reaction Temperature on C_8 Selectivity on Y Zeolite (T_{calc}=425°C; P=382psig; I/O=11; $C_4^=$WHSV=2.6h^{-1}; m_{cat}=2.78g)

Increasing the operating temperatures above 30°C, promoted cracking activity during the Useful Catalyst Lifetime period, jeopardizing the stability of TMP^+ species on both zeolites. Isomerization of *trans*-2-butene to 1-butene was found to be more favourable at higher reaction temperatures (Simpson et al, 1995), promoting the formation of DMH^+ isomers. In addition, polymerization of alkylate precursors (TMP^+ cations) at elevated temperatures, compromises catalyst selectivity to alkyate. Both of these factors likely contribute to lower TMP levels and higher DMH content, at higher reaction temperatures.

The production of TMP was sustained for the longest duration at the preferred reaction temperature of 55°C on EMT (see Figure 6.16). Similar behaviour was demonstrated by Y zeolite at 70°C (see Figure 6.17). As the reaction temperature deviated from the preferred level, DMH production increased at the expense of reduced TMP production, with little variation in oligomerization activity on both EMT (see Figure 6.16) and Y (see Figure 6.17).

Batch reactor results indicate a slight decrease in TMP levels as compensated by modest increase in DMH and $C_8^=$ levels when the reaction temperature is increased from 80 to 100°C. This agrees with results from the flow reactor in that TMP production is adversely affected by reaction temperatures in the vicinity of 100°C.

6.5.4 Effect of Reaction Temperature on TMP Selectivity

The content of 2,2,4-TMP in the TMP fraction increased as reaction temperature was elevated, following cracking activity trends (see Table 6.6). This behaviour supports literature claims that, 2,2,4-TMP is the predominant C_8 isomer produced from cracking of C_{12}+ species (Corma & Martinez, 1993). Levels of 2,3,3-TMP and 2,3,4-TMP decreased with increasing operating temperature, on both EMT and Y zeolites (see Table 6.6).

Table 6.6: Effect of Reaction Temperature on Average Alkylate Quality (first 5 min of Useful Catalyst Lifetime period) using EMT and Y Zeolites (T_{calc}=425°C; P=382psig; I/O=11; $C_4^=$WHSV=2.6h^{-1}; m_{cat}=2.78g)

Catalyst	EMT				Y			
Run	F25EMT	F28EMT	F31EMT	F34EMT	F27Y	F24Y F36Y	F29Y	F33Y
T_{rxn} [°C]	33	55	77	100	29	53	70	100
Useful Catalyst Lifetime [min]	6.3	10.6	7.6	6.8	6.2	7.4	8.1	4.5
C_5+ Liquid [mass %]								
C_5 - C_7	17	33	25	41	26	28	39	49
C_8	41	51	55	45	37	51	49	40
C_9+	42	16	20	14	37	21	12	11
C_8 Fraction [mass %]								
TMP	69	77	60	61	75	68	66	61
DMH	28	19	26	33	23	25	27	33
$C_8^=$	3	4	14	6	2	7	7	6
TMP Distribution [%]								
2,2,4-TMP	29	44	46	52	22	37	58	52
2,2,3-TMP	5	15	10	12	5	5	9	10
2,3,4-TMP	30	15	17	14	33	25	12	16
2,3,3-TMP	36	26	27	22	40	33	21	22
Indicators [mass %]								
$\frac{TMP}{DMH}$	2.77	4.13	2.29	1.81	3.91	2.76	2.42	1.82
$\frac{TMP+DMH}{C_8^= + C_9+}$	1.11	3.57	1.74	2.49	2.07	2.99	3.63	3.20
$\frac{2,2,4\text{-}TMP+2,2,3\text{-}TMP}{2,3,3\text{-}TMP+2,3,4\text{-}TMP}$	0.53	1.49	1.30	1.82	0.40	0.72	2.05	1.68

Temperature does not have a significant effect on thermodynamic predictions for the distribution of TMP isomers (see Figure 6.18). Thermodynamic estimates for 2,2,4-TMP levels, exceed 60 % of the TMP fraction, between 30 and 100°C. The response of the TMP distribution to reaction temperature is contrary to thermodynamic trends. Experiments employing lower temperatures favoured 2,3,3-TMP and 2,3,4-TMP, the least sterically hindered isomers (see Lennard Jones diameter calculations in Appendix A3.2.5). Higher operating conditions promoted 2,2,4-TMP production (see Table 6.6), in opposition to thermodynamic trends (see Figure 6.18).

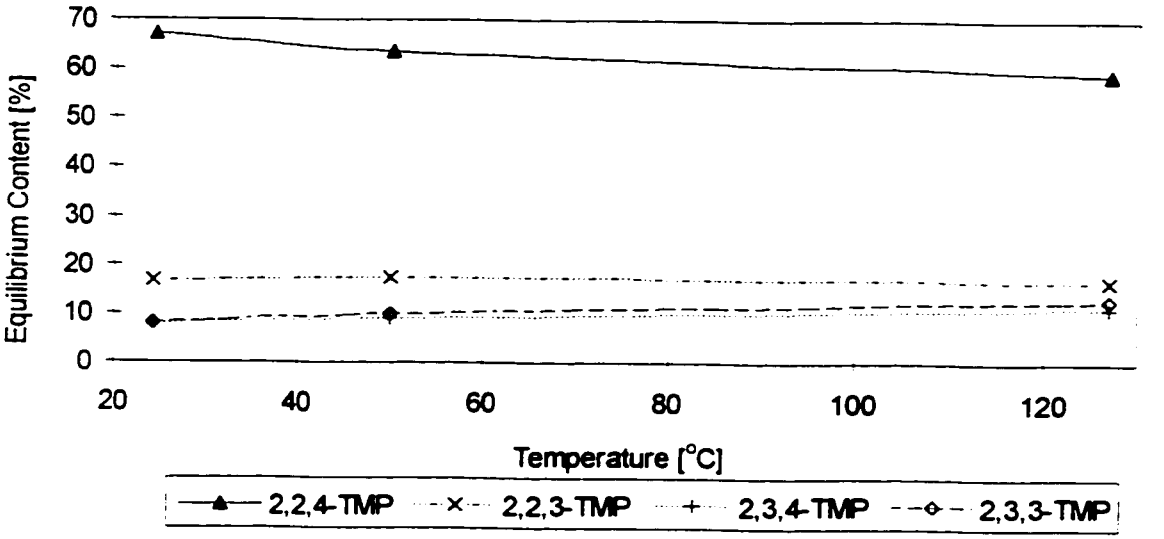

Figure 6.18: Effect of Temperature on Thermal Equilibrium Composition of TMPs (Cardona et al, 1995; Chu & Chester, 1986)

6.5.5 Synopsis of Effect of Reaction Temperature

Low reaction temperatures effected low butene conversion during the Useful Catalyst Lifetime period on EMT and Y zeolites (see Figures 6.14 and 6.15, Table 6.6). The rate of cracking reactions was reduced at lower operating temperatures, resulting in accumulation of polymerization products. This behaviour agrees with that observed by other authors (Taylor & Sherwood, 1997).

As the reaction temperature increased, olefin conversion was sustained for a longer duration. Cracking activity increased, exercising a negative effect on the stability of TMP precursors. Production of 2,2,4-TMP increased with reaction temperature, as this isomer appears to be correlated with cracking of C_{12}+ carbenium ions.

The preferred reaction temperature represents a balance between enhancing olefin conversion without degrading alkylate quality. The reaction temperature must be sufficiently high to suppress polymerization reactions, which are known to favour deactivation processes. However, excessive temperatures jeopardize the stability of alkylate precursors. At the preferred reaction temperature, the Useful Catalyst Lifetime period was maximized and TMP production levels were sustained for the longest duration. At an I/O ratio of 11, this temperature was concluded to be 55°C for EMT, whereas 70°C was identified for Y zeolite. These preferred temperatures are specific to the fixed operating conditions (i.e. I/O ratio of feed, T_{calc}, olefin WHSV, mass of catalyst, etc.) of the experiment.

The least sterically hindered TMP isomers, including 2,3,3-TMP and 2,3,4-TMP, were favoured at low reaction temperatures (see Table 6.6). These isomers offer the least resistance during formation of the activated complex, and diffuse most efficiently through the catalyst pores. At higher reaction temperatures, alternate reaction pathways become more facile. Cracking activity increased as the reaction temperature was elevated, favouring formation of 2,2,4-TMP via cracking of C_{12}^{+} carbocations (Corma & Martinez, 1993).

Temperature does not appear to exert a significant effect on alkylate yield (see Table 6.7). The Useful Catalyst Lifetime period represents approximately 15 % of the total time period for liquid collection, making sensitivity to operational changes poor. Secondly, the method of liquid collection is not responsive to small changes in liquid production levels. Although a distinctive temperature effect was not evident on either catalyst, significant differences between catalysts were found. For all reaction temperatures considered, EMT achieved a notably higher yield and longer Useful Catalyst Lifetime period, relative to those observed on Y zeolite.

Analysis of the catalyst performance and properties of the spent catalyst, reveal some interesting features. As the temperature was increased, the surface area of the spent catalyst decreased, with notable losses measured at low reaction temperatures (see Figure 6.19). Temperature does not appear to have a significant effect on preserving the active surface area of the catalyst.

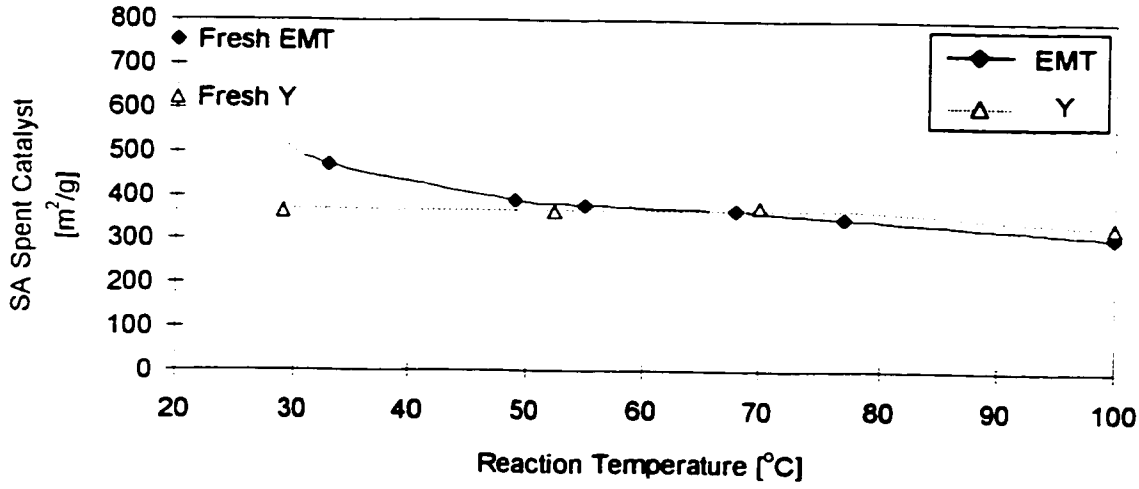

Figure 6.19: Effect of Reaction Temperature on Surface Area of Spent Catalyst (T_{calc} = 425°C, P=382psig; I/O = 11; $C_4^=$WHSV=2.6h^{-1}; m_{cat}=2.78g)

Carbonaceous deposits on the spent catalyst, measured between 9.1 and 10.2 % on EMT, whereas a lower range of 6.8 to 7.6 % was determined for Y zeolite (see Table 6.7). Comparable levels of retained hydrocarbons on spent catalysts (40 min. TOS) were reported by Querini & Roa (1997), where carbonaceous deposits varied between 5 to 13 % on Y and La-exchanged Y zeolites.

The amount of retained hydrocarbons on the spent catalyst was minimized at the preferred reaction temperature (see Table 6.7). This occurred at 55°C for EMT and 70°C on Y. Levels of hydrocarbons retention were significant on the spent catalyst from reactions undertaken at 30°C on both EMT and Y. This suggests that the adsorption of the olefin and oligomerization of the olefin, proceed much faster than hydride transfer and desorption of the product, under these conditions.

Table 6.7: Effect of Reaction Temperature on Catalyst Properties
(T_{calc} = 425°C; I/O = 11)

Catalyst @T_{rxn}[°C]	SA Spent Catalyst [m^2/g]	TGA of Spent Catalyst [mass %] Desorption Temperature [°C]				Yield* [gC_5^+/gcat/$gC_4^=$fed]
		< 200	200-300	>300	Total	
EMT						
33°C	470	3.9	3.0	3.3	10.2	n.a.
55°C	377	3.8	2.5	3.0	9.3	0.094
77°C	348	3.0	2.9	3.2	9.1	0.104
100°C	309	3.7	3.2	3.2	10.1	0.113
Y						
29°C	364	2.5	2.3	2.5	7.3	0.057
56°C	372	2.0	2.5	2.5	7.0	0.068
70°C	374	1.2	2.1	3.6	6.8	0.084
100°C	329	2.4	2.3	2.9	7.6	0.088

* liquid collected over a 1 hour reaction period

It is possible that high molecular weight hydrocarbons retained on the catalyst surface, act as hydride donors to other adsorbed species. The close proximity of the heavy compounds to the reactive carbocations in the zeolite cages, makes this form of hydride transfer favoured, over direct hydride transfer from isobutane (Cardona et al, 1995). Allylic carbenium ions are formed when high molecular weight hydrocarbons facilitate hydride transfer. These carbocations are more stable than the *tert*-butyl carbenium ion, which is formed upon hydride transfer from isobutane. However, the carbonaceous deposit becomes less saturated in nature and acts as a precursor to coke, favouring deactivation processes.

Weitkamp and Maixner (1987) characterized carbonaceous deposits on spent La-Y zeolite catalysts. The deposit from a catalyst operating at a reaction temperature of 80°C, appeared to be primarily paraffinic in nature, with a H/C ratio of 1.8. Higher reaction temperatures produced a carbonaceous deposit with a lower H/C ratio, indicative of an olefinic and aromatic nature. This suggests that adsorbed hydrocarbons become an important source of hydride transfer at higher reaction temperatures. The H/C ratio for the spent catalyst deposit was not analysed in the present investigation.

6.6 EFFECT OF 1-$C_4^=$ WHSV ON Y ZEOLITE

The preferential adsorption of olefins over paraffins in zeolites, favours oligomerization and polymerization reactions over alkylation. This phenomena, is exacerbated by the concentration effect and diffusional limitations, which are inherent in microporous solids. The I/O ratio and olefin WHSV are two process variables, which are used to circumvent these problems, and represent the most important parameters influencing alkylate quality and yield. A low concentration of the olefin (reflected by a high I/O ratio or a low 1-$C_4^=$ WHSV) increases the likelihood of alkylation reactions being facilitated. In contrast, oligomerization and polymerization

reactions are encouraged by higher concentrations of the olefin, conditions which are favoured by a low I/O ratio or a high olefin WHSV.

The importance of olefin WHSV was not studied extensively on EMT due to limited catalyst supply, but was explored on the commercially available product of Y zeolite. A calcination temperature of 540°C, a reaction temperature of 80°C and operating pressure of 382 psig, were employed for the olefin WHSV investigation. No reaction products were observed when pure isobutane was tested over a 1 hour reaction period. It appears that self-alkylation of isobutane cannot be initiated in the absence of an olefin, in agreement with other studies in the literature (Simpson et al, 1996).

6.6.1 Effect of 1-$C_4^=$ WHSV on Butene Disappearance

The Useful Catalyst Lifetime period was maintained for a longer duration on Y zeolite under conditions of low olefin WHSV (see Table 6.8). A reduction in the olefin WHSV from 2.57 (I/O=11) to 0.51 h^{-1} (I/O=58) extended the Useful Catalyst Lifetime from 4.5 minutes to 50 minutes, illustrating the positive influence of diluting the feed with excess isobutane.

Table 6.8: Effect of Butene WHSV on the Number of Successful Catalyst Cycles Achieved during Useful Catalyst Lifetime Period on Y Zeolite (T_{calc}=540°C; T_{rxn}=80°C; P=382psig; m_{cat}=2.78g)

Run	F11Y, F13Y, F15Y(first 40 min)	F21Y
$C_4^=$ WHSV [h^{-1}]	0.51	2.57
I/O	58	11
Useful Catalyst Lifetime [min]	~ 50	4.5
# Successful Cycles per Acid Site During Useful Catalyst Lifetime	55	22

The number of successful catalyst cycles (turn-over number) can be calculated by dividing the Useful Catalyst Lifetime period by the time required to adsorb one butene molecule on all active sites. Since acidity measurements are not available, published data for Y zeolite will be used. Pyridine desorption on Y zeolite with a Si/Al ratio of 5.4 detect 151 μmol acid sites/g catalyst (Corma et al, 1994b). The time required to provide sufficient butene to fully saturate all of the active acid sites can be approximated from the butene flow rate (see Appendix A3.2.4).

Decreasing the olefin WHSV from 2.57 to 0.51 h^{-1}, augmented the number of successful catalyst cycles achieved per acid site from 22 to 55, representing an increase of 150 % (see Table 6.8). The modest improvement in the turn-over number, emphasizes the strong control dictated by the preferential adsorption of the olefin over the paraffin. Deactivation appears inevitable regardless of the feed concentration in the olefin, but simply proceeds at a reduced rate under conditions of high I/O ratio.

6.6.2 Effect of 1-$C_4^=$ WHSV on C_5^+ Product Distribution

No significant change in cracking activity was observed with variation in the olefin WHSV, during the Useful Catalyst Lifetime (see Figure 6.20). However, high cracking was sustained for a longer duration under conditions of low olefin WHSV. Polymerization activity was greatly suppressed under conditions of low olefin WHSV (see Figure 6.20). This is expected, as a low concentration of butene (low olefin WHSV) diminishes the probability that two butene molecules will react with one another, enhancing the opportunity for isobutane participation in the reaction. As the olefin WHSV is increased, butene concentration is elevated, increasing the favourability of oligomerization and polymerization reactions.

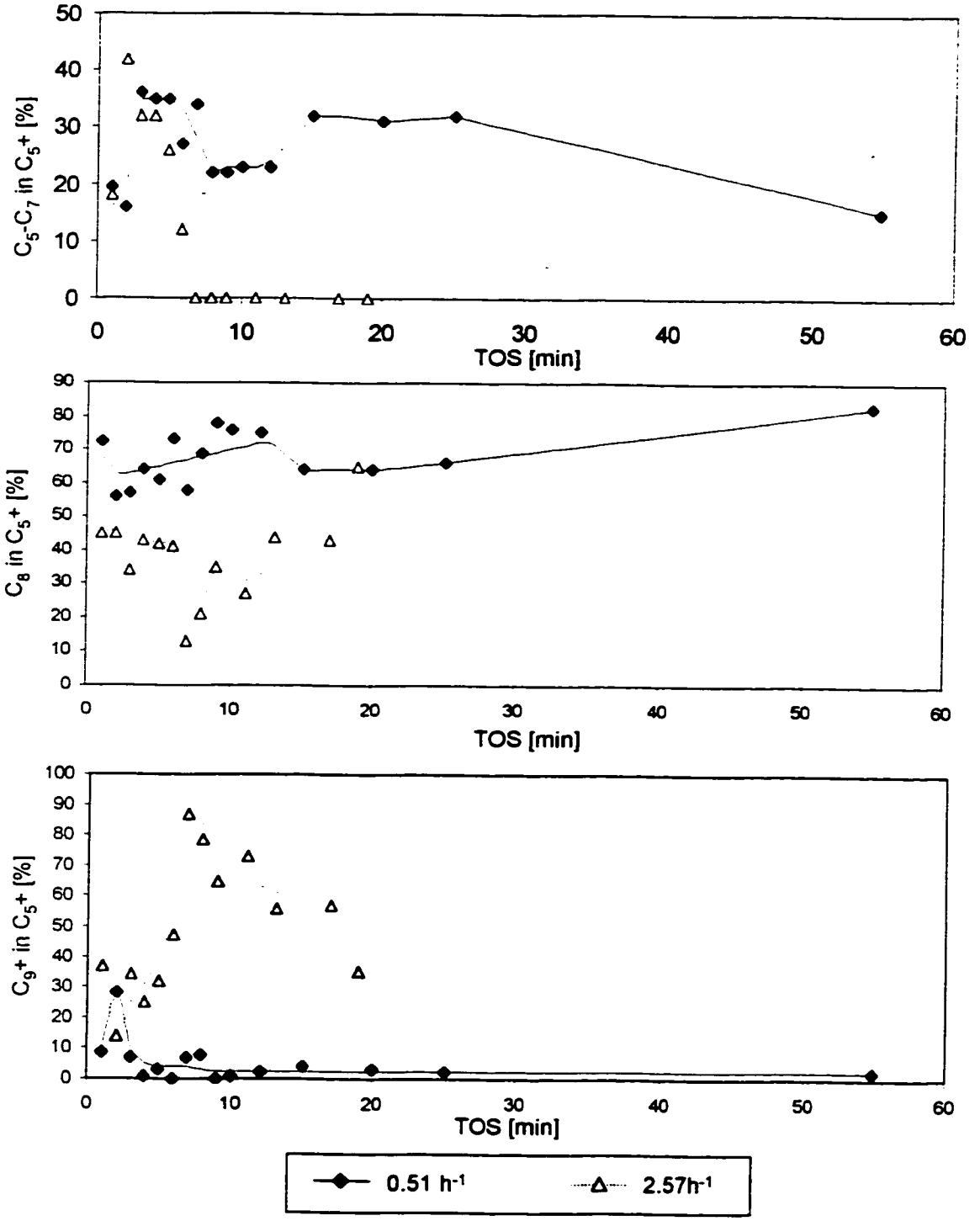

Figure 6.20: Effect of Butene WHSV on C_5+ Product Distribution on Y Zeolite (T_{rxn}=80°C; T_{calc}=540°C; P=382psig; m_{cat}=2.78g)

The content of C_8 in the C_5+ product increased as the olefin WHSV decreased (see Figure 6.20). It appears that a low concentration of butene enhanced the probability of alkylation reactions, leading to elevated levels of C_8 in the C_5^+ liquid. Although dimerization of the olefin will also increase the levels of C_8 in the C_5^+ liquid, adsorbed oligomers are more susceptible to secondary reactions (i.e. polymerize to higher molecular weight compounds). This explains the lower C_8 levels observed for higher olefin WHSV experiments.

6.6.3 Effect of 1-$C_4^=$ WHSV on C_8 Selectivity

The levels of TMP in the C_8 fraction decreased, with increasing olefin WHSV. In addition, high levels of TMP were sustained for longer TOS under conditions of low olefin WHSV (see Figure 6.21). It appears that the sites responsible for TMP production are deactivated rapidly, under conditions of high olefin concentration in the feed mixture. A low olefin WHSV suppresses the rate of this deactivation process, allowing these acid sites to remain active for TMP production for a longer duration.

The production of DMH and $C_8^=$ were enhanced by increasing the olefin WHSV (see Figure 6.21). It appears that the initial hydride transfer step to generate *tert*-C_4^+ is adversely affected by high concentrations of olefin in the feed mixture, leading to elevated DMH production levels. In addition, hydride transfer to adsorbed C_8^+ species is also hindered by high olefin levels in the feed, favouring desorption of an olefin product.

These results agree with those observed by Chu & Chester (1986) in which the concentration of TMPs decreased and DMHs increased, with increasing olefin WHSV. It is preferable to operate at a lower WHSV in order to maximize TMP production and maintain high catalyst activity.

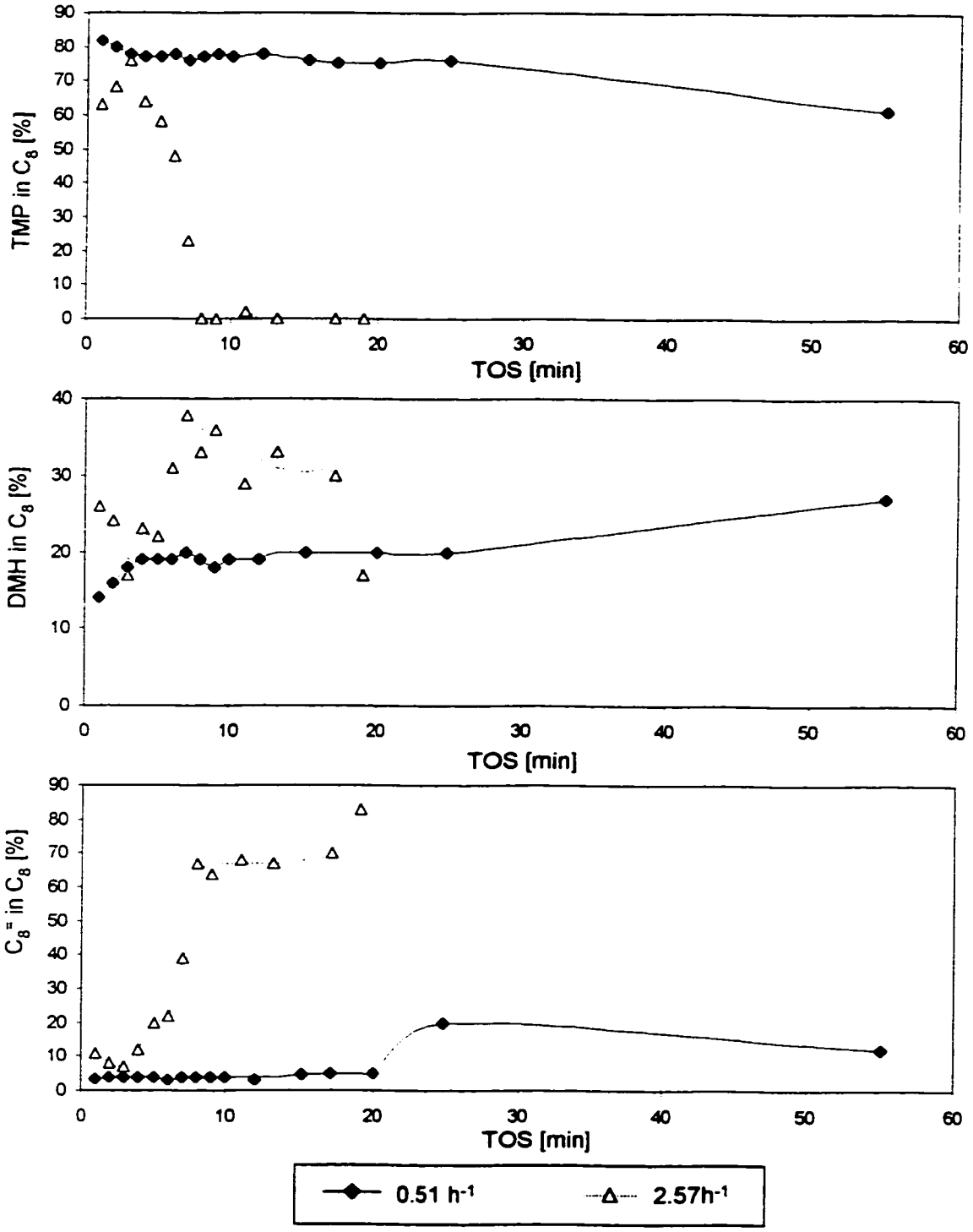

Figure 6.21: Effect of Butene WHSV on C_8 Selectivity on Y Zeolite (T_{rxn}=80°C; T_{calc}=540°C; P=382psig; m_{cat}=2.78g)

Catalyst activity was found to be relatively constant when operating at a low olefin WHSV, as indicated by stable product distributions. This contrasts with rapid catalyst deactivation at short TOS under conditions of high olefin WHSV. Clearly, a compromise must be made between extending catalyst lifetime through operation at low olefin WHSV, and maximizing alkylate production (g C_5^+ liquid collected per hour), which is compromised by utilization of a low olefin WHSV.

6.6.4 Effect of 1-$C_4^=$ WHSV on TMP Selectivity

The maximum 2,2,4-TMP levels achieved in the TMP fraction, were similar for both WHSV (see Figure 6.22). However, a high concentration of olefin in the feedstock accelerated the rate of deactivation, causing 2,2,4-TMP production to decline at earlier TOS. The selectivity of TMP isomers was not altered significantly by changes in olefin WHSV (see Table 6.9). Levels of 2,2,4-TMP and 2,2,3-TMP were enhanced slightly and amounts of 2,3,4-TMP were reduced, when operating at a low olefin WHSV.

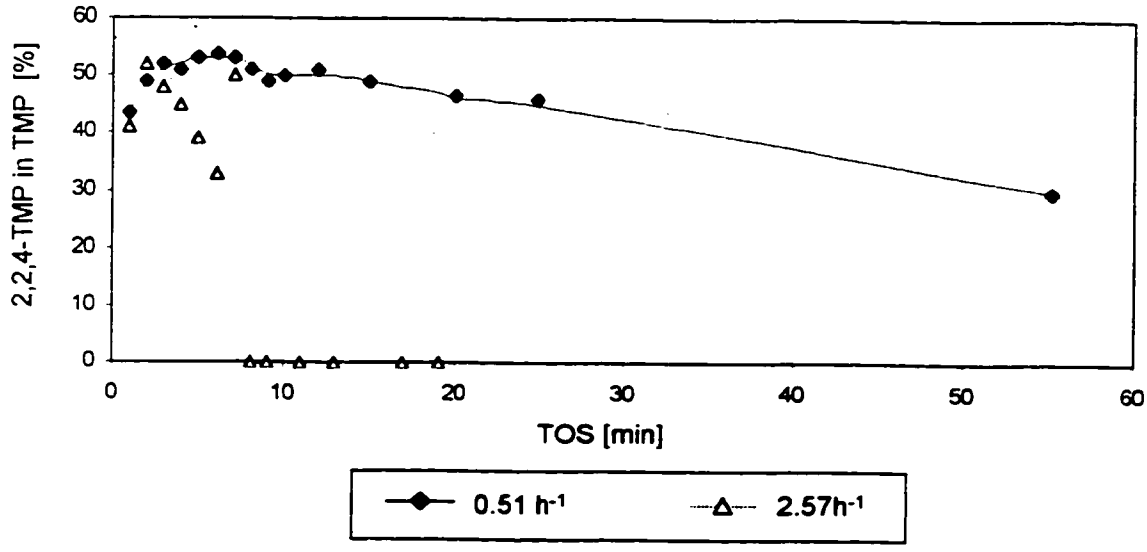

Figure 6.22: Effect of Butene WHSV on 2,2,4-TMP Level in TMP Fraction on Y Zeolite (T_{rxn}=80°C; T_{calc}=540°C; P=382psig; m_{cat}=2.78g)

Table 6.9: Effect of Butene WHSV on Catalyst Performance on Y Zeolite (T_{rxn}=80°C; T_{calc}=540°C; P=382psig; m_{cat}=2.78g)

Run	F11Y, F13Y, F15Y(first 40 min)	F21Y
$C_4^=$ WHSV [h^{-1}]	0.51	2.57
I/O	58	11
Useful Catalyst Lifetime [min]	~ 50	4.5
# Successful Cycles per Acid Site During Useful Catalyst Lifetime	55	22
Time Period Employed for Estimating Average C_5+ Analysis	Initial 25 min TOS	initial 5 min TOS
C_5^+ Liquid [mass %]		
C_5-C_7	28	30
C_8	67	42
C_9^+	5	28
C_8 Distribution [mass %]		
TMP	77	66
DMH	19	22
$C_8^=$	4	12
TMP Distribution [%]		
2,2,4-TMP	50	45
2,2,3-TMP	10	5
2,3,4-TMP	15	22
2,3,3-TMP	25	28
Indicators [mass fraction]		
$\frac{\text{TMP}}{\text{DMH}}$	4.10	3.03
$\frac{\text{TMP + DMH}}{C_8^= + C_9+}$	12.5	1.26
$\frac{\text{2,2,3-TMP + 2,2,4-TMP}}{\text{2,3,3-TMP + 2,3,4-TMP}}$	1.51	1.01

The isomer, 2,2,3-TMP, is a direct product of alkylation of 2-butene with isobutane, whereas, 2,2,4-TMP is the primary product of self-alkylation of isobutane. From a structural perspective, 2,3,4- and 2,3,3-TMP cannot be formed from C_4 fragments, and are presumably formed through isomerization of TMP^+ cations. Hydride transfer to a tertiary carbenium ion is notably faster that to a secondary one. Therefore, the TMP isomers, which are most favoured from a mechanistic standpoint,

are 2,3,4-TMP and 2,3,3-TMP. The former species involves hydride transfer to a tertiary carbenium ion, and the latter can be formed through a methyl shift (Cardona et al, 1995). Considering all of these factors, it appears that a low olefin WHSV promotes formation of the thermodynamically favoured isomers. In contrast, a high olefin WHSV encourages production of the kinetically preferred isomers.

The product selectivity achieved over Y zeolite at high olefin WHSV differed significantly from that catalysed by HF and H_2SO_4 (see Table 6.10). However, as the olefin WHSV is decreased, the TMP isomer distribution approached that obtained over H_2SO_4, but deviated considerably from equilibrium predictions. The concentration effect, inherent in zeolitic catalysts, in conjunction with the steric restrictions imposed by the microporous network, are most likely responsible for the differences observed.

Table 6.10: Comparison of TMP Selectivity using different Catalyst Systems with Thermal Equilibrium Values

Catalyst System	Y[1], WHSV= 0.51h^{-1}	Y[2], WHSV= 2.57h^{-1}	HF[3]	H_2SO_4[3]	Thermal Equilibrium		
Temperature [°C]	80	80	20	10	24[3]	50[4]	127[3]
2,3,4-TMP/2,3,3-TMP	0.6	0.8	1.2	0.6	1.0	0.9	0.8
2,2,3-TMP/2,2,4-TMP	0.2	0.1	<0.01	0.1	0.3	0.3	0.3
2,2,4-TMP + 2,2,3-TMP / 2,3,3-TMP + 2,3,4-TMP	1.6	1.0	1.7	1.4	5.2	4.3	3.1

1 average of 1-10 min T.O.S.
2 average of 1-5 min. T.O.S.
3 data from Chu & Chester, 1986
4 data from Cardona et al, 1995

6.6.5 Synopsis of Effect of 1-$C_4^=$ WHSV

Employing a lower olefin WHSV suppressed the rate of catalyst deactivation in a flow reactor. However, the loss in catalyst activity appears inevitable, due to

preferential adsorption of the olefin over the paraffin. This hypothesis can be tested, by examining the surface area measurements of the spent catalyst. A "Butene Exposure Index" can be calculated by multiplying the olefin WHSV by the duration of the experiment. In this manner, the magnitude of olefin WHSV and duration and be encompassed into a single dimensionless quantity, allowing experiments using different conditions to be compared. A distinctive trend in loss of SA is observed with increasing Butene Exposure Index, regardless of the operating conditions (see Figure 6.23). These results support the conjecture that deactivation is unavoidable, regardless of how dilute the feed is with the olefin. The same final outcome will result, but will simply require a longer time period to reach.

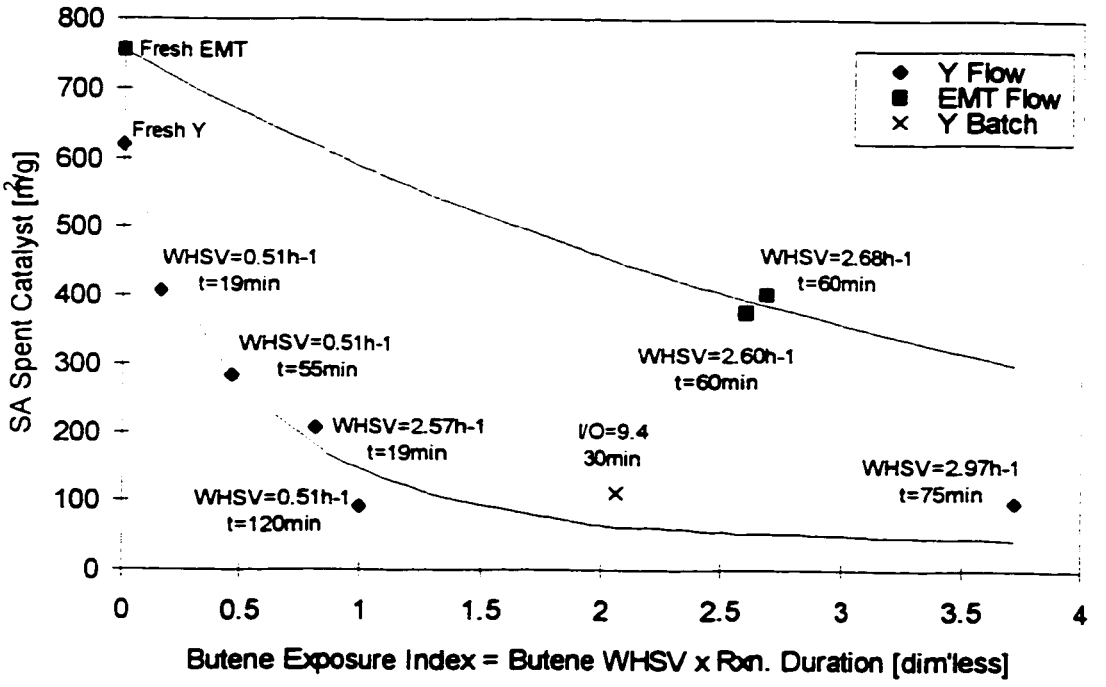

Figure 6.23: Effect of Butene Exposure on Surface Area of Spent Catalyst (T_{calc}=540°C, T_{rxn}=80°C; P=382psig, m_{cat}=2.78g)

This hypothesis is further validated by TGA/DTA measurements on the spent catalyst. Notable levels of adsorbed species were detected on the spent catalyst, which employed an olefin WHSV of 0.51 h^{-1} for a 20 min reaction period. A significant loss in active surface area was also measured for this experiment (see Table 6.11). Increasing the reaction duration to 60 min at the same olefin WHSV, resulted in additional deposition of higher molecular weight species (T_{desorp}>200°C), incurring a further loss in surface area. No change in the amounts of lighter compounds (T_{desorp}<200°C) was evidenced, after longer exposure to the feed mixture. Increasing the olefin WHSV to 2.57 h^{-1}, augmented the amounts of higher molecular weight compounds (T_{desorp}>200°C) retained on the catalyst causing a significant surface area loss after only 20 min of exposure to the feed stream.

This suggests that the rate of the reactions generating higher molecular weight species are greatly enhanced by elevated olefin WHSV conditions. Hence, the loss in surface area appears to be primarily a result of oligomerization and polymerization reactions, leading to elevated levels of high molecular weight compounds which are retained on the catalyst surface.

Table 6.11: Effect of Butene WHSV on Properties of Spent Catalyst (T_{calc}=540°C, T_{rxn}=80°C)

Butene WHSV [h^{-1}]	Run	Reaction Duration [min]	Exposure Index	TGA [mass %] Desorption Temperature [°C]				SA Spent Catalyst [m^2/g]
				< 200	200-300	> 300	Total	
0.51	F11Y	20	0.17	1.2	0.8	1.7	3.7	407
0.51	F13Y	60	0.51	1.2	1.2	2.2	4.6	284
2.57	F21Y	20	2.57	1.3	2.5	3.1	6.9	205

Although the effect of olefin WHSV was not investigated in detail on EMT, this catalyst appears to demonstrate superior ability in preserving active surface area upon exposure to butene, relative to the behaviour shown by Y zeolite. It is possible that EMT is more carbophylic than Y zeolite, enhancing isobutane adsorption

capabilities and improving resistance to deactivation. Alternatively, it is also possible that the unique arrangement of acid sites on EMT suppresses the extent undesirable side-reactions (i.e. oligomerization), which promote deactivation processes.

6.7 EFFECT OF CYCLICAL FEED OPERATION USING Y ZEOLITE

Hydride transfer can be improved by choosing calcination conditions which promote Bronsted acidity. Reaction temperature can be judiciously selected to enhance selectivity to alkylation. The feed mixture can be prepared with a high I/O, and flow rates operated to achieve a low olefin WHSV, to delay the onset of deactivation. However, optimization of all operating conditions cannot prevent deactivation from ensuing, due to the preferential adsorption of the olefin over the paraffin.

For this reason, cyclical feed operation was investigated as an alternative strategy to maintain high catalyst activity. The study evaluated Y zeolite calcined at 540°C, and employed operating conditions of 80°C and 382 psig. A feed mixture with an I/O ratio of 59 (1-$C_4^=$ WHSV = 0.51 h^{-1}) was delivered to the catalyst bed for a period of 40 minutes. This was followed by a 30 minute isobutane flush (I/O=3000 based on impurity butene in the isobutane cylinder), after which butene/isobutane feed (I/O=59) delivery to the catalyst was resumed for a period of 30 minutes. The experiment was concluded with a final 20 min isobutane flush.

Catalyst deactivation was apparent during the first mixture delivery period (see Figure 6.24). A loss in cracking activity was observed, and a significant elevation in polymerization products detected in the effluent at longer TOS.

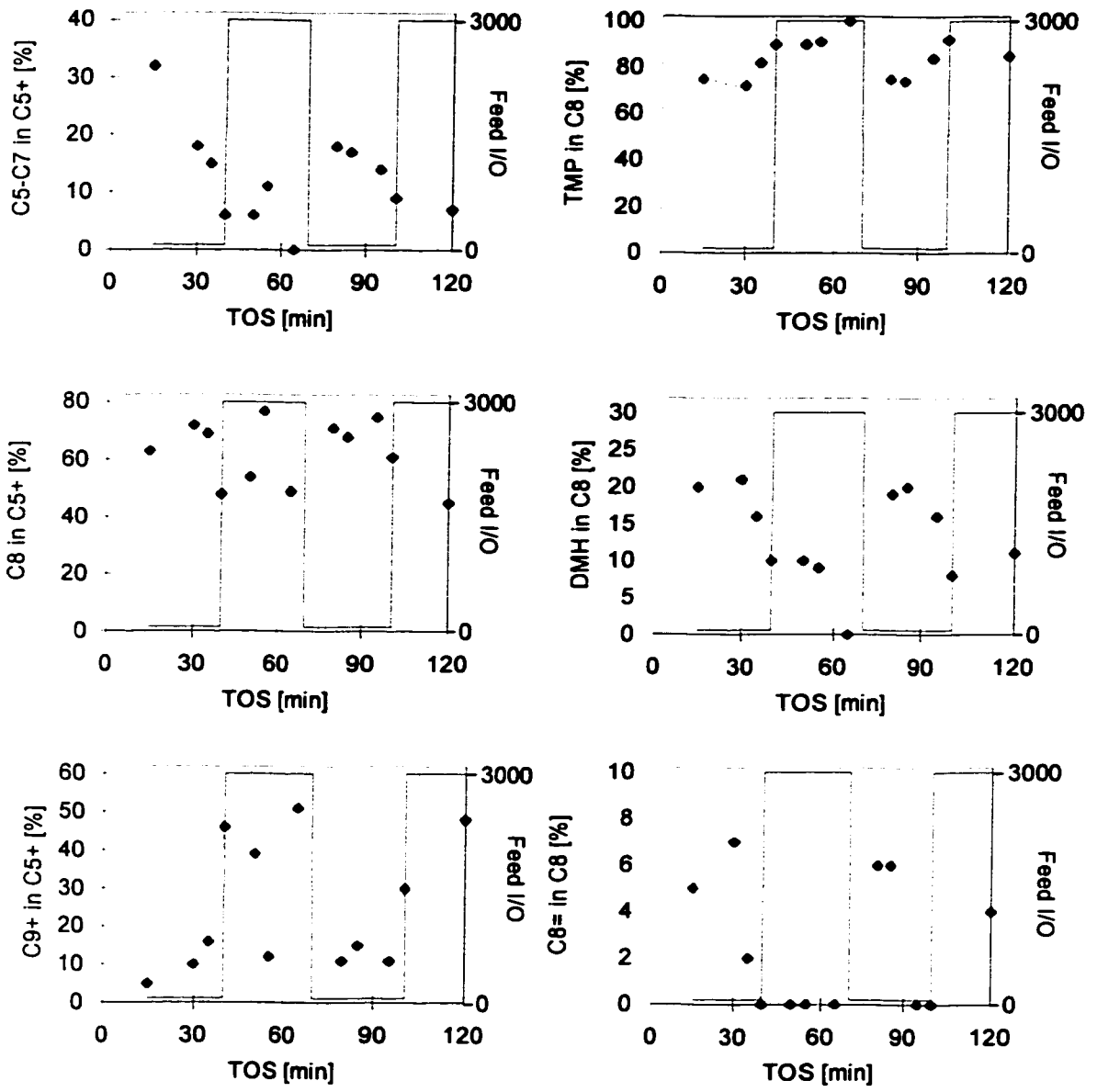

Figure 6.24: Effect of Cyclical Feed Operation on Catalyst Activity and Selectivity using Y Zeolite
(T_{calc}=540°; T_{rxn}=80°C; P=382psig; m_{cat}=2.78g; Feed: $C_4^=$WHSV=0.51h^{-1}(40min), pure *i*-C_4 (30min), $C_4^=$WHSV=0.51h^{-1}(40min), pure *i*-C_4 (30min))

During the isobutane flush period, notable levels of polymerization products, as well as C_8 compounds, were removed from the catalyst surface. Catalyst activity was restored upon resumption of the feed mixture to the catalyst bed. High cracking activity level was recovered and polymerization function suppressed, during the second feed delivery period. At longer TOS, a loss in catalyst activity recurred, mimicking the behaviour of the first feed delivery period.

Product selectivity can provide further insight into the events leading up to deactivation. During the first period of feed delivery, the content of TMP in the C_8 fraction increased with longer TOS. This is a reflection of the Induction Period, in which DMH formation and oligomerization products are favoured until a sufficient population of *tert*-$C_4^+{}_{(surf)}$ species has developed on the catalyst surface. Once this is established, alkylation activity is favoured, resulting in elevated amounts of TMP in the effluent.

During the isobutane flush, TMP content increased with further TOS. It may be that hydride transfer to TMP^+ cations by isobutane is facilitated in the early stages of the flush period. As spatial constraints are relieved with removal of C_8 product, it is possible that self-alkylation of isobutane is promoted, through hydride transfer to bulkier polymeric species retained on the catalyst surface. This produces elevated levels of C_9+ species, as well as increased amounts of TMP, in agreement with the experimental data.

The restoration of catalyst activity and selectivity after the isobutane flush period, is remarkable. These results suggest that the onset of deactivation is a consequence of the preferential adsorption of the olefin over the paraffin. The ability of isobutane to facilitate hydride tranfer to desorb product is limited, favouring oligomerization and polymerization reactions. Upon exposure to the feed mixture, the catalyst surface becomes saturated with oligomers of butene, stifling further activity. These oligomers can be removed in a non-competitive environment with pure isobutane, restoring catalyst activity to fresh performance levels.

Loss in active catalyst SA is suppressed in the cyclical operation. After 60 min of continuous exposure to the feed stream (1-$C_4^=$ WHSV = 0.51 h^{-1}), the surface area of the spent catalyst measured 284 m^2/g, representing 54% loss in active surface area. In contrast, the spent catalyst from the cyclical feed operation, with a cumulative feed exposure of 60 min, measured 396 m^2/g accounting for a 36 % reduction in active surface area. Clearly, benefits can be gained through cyclical operation where the isobutane serves to cleanse the catalyst surface of retained hydrocarbons and restore catalyst activity.

Catalytic distillation is a process, which combines reaction and distillation into one unit operation. This reactor geometry may offer some potential to this difficult reaction. By placing the catalyst bed near the top of the distillation tower, and operating under total reflux, isobutane will be continuously returned to the reaction section providing the positive cleansing benefits noted in the cyclical operation. The distillation action of the process will naturally remove product (i.e. TMP) from the reaction section on the basis of boiling point differences. In this manner, consecutive reactions are discouraged. The TMPs will concentrate in the reboiler and can be removed in the product stream. This mode of reactor geometry could be studied in subsequent investigations on this topic.

6.8 EFFECT OF CATALYST

The modest geometrical differences in the structural properties of EMT relative to Y, are hypothesized to produce positive benefits on alkylation. It is believed that the larger space available for reaction in the hypercages, will reduce steric restrictions during the formation of the bulky TMP isomers. The improvement in accessibility to the hypercages of EMT, via straight channels, is expected to reduce diffusional resistance during product transport.

Secondly, the nature, strength and distribution of acid sites on EMT and Y zeolite are subtly different. Although Bronsted acidity dominates on both catalyst systems, published acidity measurements suggest that Lewis acidity may be slightly greater on Y zeolite relative to EMT (see Table 2.5). The effect of calcination temperature (see Section 6.4) concluded that Lewis acidity favoured undesirable side reactions, compromising catalyst selectivity and accelerating deactivation. In addition, the data estimates a higher proportion of strong acid sites on EMT relative to Y zeolite (see Table 2.5). This is expected to exercise a favourable effect on the catalyst performance, as strong acid sites are believed to be necessary for facilitating alkylation.

Finally the distribution of acid sites on Y zeolite follows Lowenstein's rule, whereby no Al atoms are located in adjacent positions in the zeolite framework. The catalyst EMT, does not adhere to this rule, a contradiction that is not shared by any other zeolite. This is a direct consequence of the strong influences imposed by the crown ether during synthesis, which directs the Al arrangement in a unique pattern. This results in regions of high density of acid sites, separated by predominantly siliceous regions. The combined effects of these factors will be examined. The responses of EMT and Y zeolite to changes in pre-treatment and operating conditions will be compared.

6.8.1 Comparison of Calcination Temperature Effects on EMT and Y Zeolites

It was established that an increase in calcination temperature from 425 to 540°C, produced similar effects on alkylation activity on both EMT and Y zeolites, at an I/O ratio of 11 (see Section 6.4). A calcination temperature of 540°C suppressed cracking activity, causing polymerization products to accumulate in the effluent, thus abbreviating the Useful Catalyst Lifetime period (see Table 6.3). This behaviour was demonstrated on EMT between 55 and 100°C (see Figures 6.5 and 6.6), although the

effect was less significant above 77°C. Similar behaviour was also observed on Y zeolite between 70 and 100°C (see Figure 6.7).

The C_8 selectivity was modestly affected by calcination treatment on both zeolites, but the influence was dependent upon reaction temperature. Overall, catalysts calcined at 540°C produced less DMHs and favoured increased levels of $C_8^=$. This behaviour was demonstrated on EMT at 55°C (see Figure 6.8) and Y zeolite between 70 and 100°C (see Figure 6.10). However, the effect was not detected above 77°C on EMT (see Figure 6.9).

The calcination temperature exerted an influence on the distribution of the TMP isomers produced (see Table 6.3). A calcination temperature of 540°C favoured the least sterically hindered isomers, 2,3,3-TMP and 2,3,4-TMP, on EMT at 55°C and Y zeolite between 70 and 100°C. No significant effect of calcination temperature was noted on EMT above 77°C. The isomer 2,2,4-TMP predominated on all catalyst systems, regardless of the calcination temperature or reaction temperature. The levels of 2,2,4-TMP in the TMP fraction ranged from 34 % on EMT, calcined at 540°C using a reaction temperature of 56°C, to 58 % on Y, calcined at 425°C employing a reaction temperature of 70°C.

6.8.2 Comparison of Reaction Temperature Effects on EMT and Y Zeolites

Similar behaviour was demonstrated by both catalysts (calcined at 425°C) when reaction temperature was varied between 30 to 100°C, at an I/O ratio of 11 (see Section 6.5). The rate of cracking was reduced at 30°C, elevating polymerization product levels in the effluent on EMT (see Figure 6.14) and Y (see Figure 6.15). Production of TMPs was highest at the low reaction temperatures for both catalysts (see Figure 6.16 for EMT and Figure 6.17 for Y), which may be attributable to increased isomerization to 2-butene (Simpson et al, 1996). The Useful Catalyst Lifetimes of EMT and Y were brief, at a reaction temperature of 30°C (see Figure 6.13). This is primarily a consequence of the high polymerization rates (see Figures

6.14 and 6.15), which leads to notable amounts of hydrocarbon species retained on the catalyst surface (see Table 6.7).

A reaction temperature of 100°C promoted high cracking activity, reducing levels of C_8 and polymerization products in the effluent from both EMT (see Figure 6.14) and Y (see Figure 6.15). Levels of TMPs were lowered and DMHs elevated under this operating condition. This suggests that the stability of alkylate precursors was jeopardized by high reaction temperatures on both of these catalysts. The distribution of TMP isomers was also affected by reaction temperature on EMT and Y. The thermodynamically favoured isomers, 2,2,4-TMP and 2,2,3-TMP, predominated at high reaction temperatures, whereas the least sterically hindered isomers prevailed at low reaction temperatures (see Table 6.6). Overall, EMT demonstrated superior resistance to deactivation processes at 100°C relative to Y, achieving a longer Useful Catalyst Lifetime period (see Figure 6.13).

The optimal reaction temperature on both EMT and Y represents a compromise between achieving adequate cracking activity to suppress polymerization function, without encouraging excessive cracking activity leading to degradation of alkylate precursors. The former necessitates a high temperature and the latter demands a low temperature. The optimal temperature represents the balance between these opposing requirements. The best temperature was identified as 55°C for EMT and 70°C for Y, with respect to the temperature levels considered in the present investigation (see Figure 6.13).

6.8.3 Comparison of EMT and Y Control Experiments for Pt Study

The Pt study control experiments were investigated at 55°C and 382 psig employing an I/O ratio of 15 ($C_4^=$ WHSV=2.0 h^{-1}). Both EMT and Y were calcined *in situ* at 325°C for 3 h in flowing nitrogen, followed by 425°C in a flowing mixture of 10 % hydrogen in argon for 3 h (see Appendix A3.1.3). This pretreatment approach differs from that discussed previously in Chapter 6, as the Pt study control

experiments provide a baseline for Pt effects discussed in Chapter 7. The Pt supported catalysts require calcination and Pt reduction, and hence demand hydrogen in the pre-treatment stream for the reduction step. For this reason, the control experiments for this study involve pre-treating EMT and Y in a hydrogen mixture, to mimic the approach used for the Pt supported catalysts. The experiments were performed at approximately 53°C and 382 psig, employing an I/O ratio of 15 ($C_4^=$ WHSV = 2.0 h^{-1}) in a 12 sccm flowing stream of nitrogen.

6.8.3.1 Comparison of Control Experiments (for Pt Study) with respect to Butene Disappearance

Complete butene conversion was sustained for a longer duration on EMT relative to Y, translating into a 41 % increase in the Useful Catalyst (see Figure 6.25, Table 6.12). Another notable difference between the two solid acids, was the ability to suppress the decline in catalyst activity during the Rapid Deactivation Period. The rate of deactivation appears to proceed at a much slower rate on EMT, as indicated by the gentler slope on the butene conversion versus TOS curve.

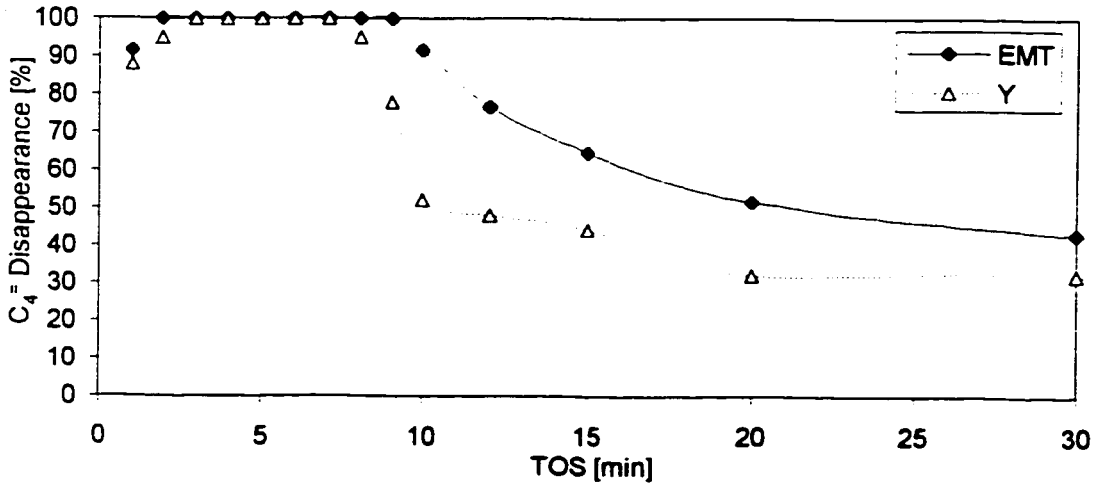

Figure 6.25: Effect of Catalyst Support on Butene Disappearance (T_{rxn}=53°C; P=382psig; T_{calc}=425°C, I/O=15; $C_4^=$WHSV=2.0h^{-1}; m_{cat}=2.78g)

Collectively, these observations suggest that the properties of EMT make it better suited to sustain high catalyst activity and maintain maximum butene conversion for a longer duration. It also implies that the structure of EMT is better equipped to combat the sequence of events responsible for deactivation.

6.8.3.2 Comparison of Control Experiments (for Pt Study) with respect to C_5^+ Product Distribution

The differences in physical structure and acidity between EMT and Y, did not effect a notable change on the C_5+ product distribution during the Useful Catalyst Lifetime period (see Figure 6.26). The cracking rate of EMT was slightly lower and C_8 production levels modestly increased, relative to those demonstrated by Y zeolite. It is interesting that the reduced cracking function of EMT did not appear to accelerate the onset of deactivation.

6.8.3.3 Comparison of Control Experiments (for Pt Study) with respect to C_8 Selectivity

No significant change in C_8 selectivity was observed between the two catalyst systems, during the Useful Catalyst Lifetime period (see Figure 6.27). However, EMT sustained TMP production for a longer duration and maintained higher levels during the deactivation period. Oligomerization function was notably suppressed during the deactivation period, suggesting that EMT was superior in sustaining hydride transfer. This ability is expected promote high butene conversion ability for a longer duration, as deactivation rates would be suppressed. This behaviour was observed on EMT (see Figure 6.25), providing further support for this hypothesis. Possible reasons for the improved hydride transfer ability of EMT, will be discussed in the Synopsis (Section 6.8.3.5).

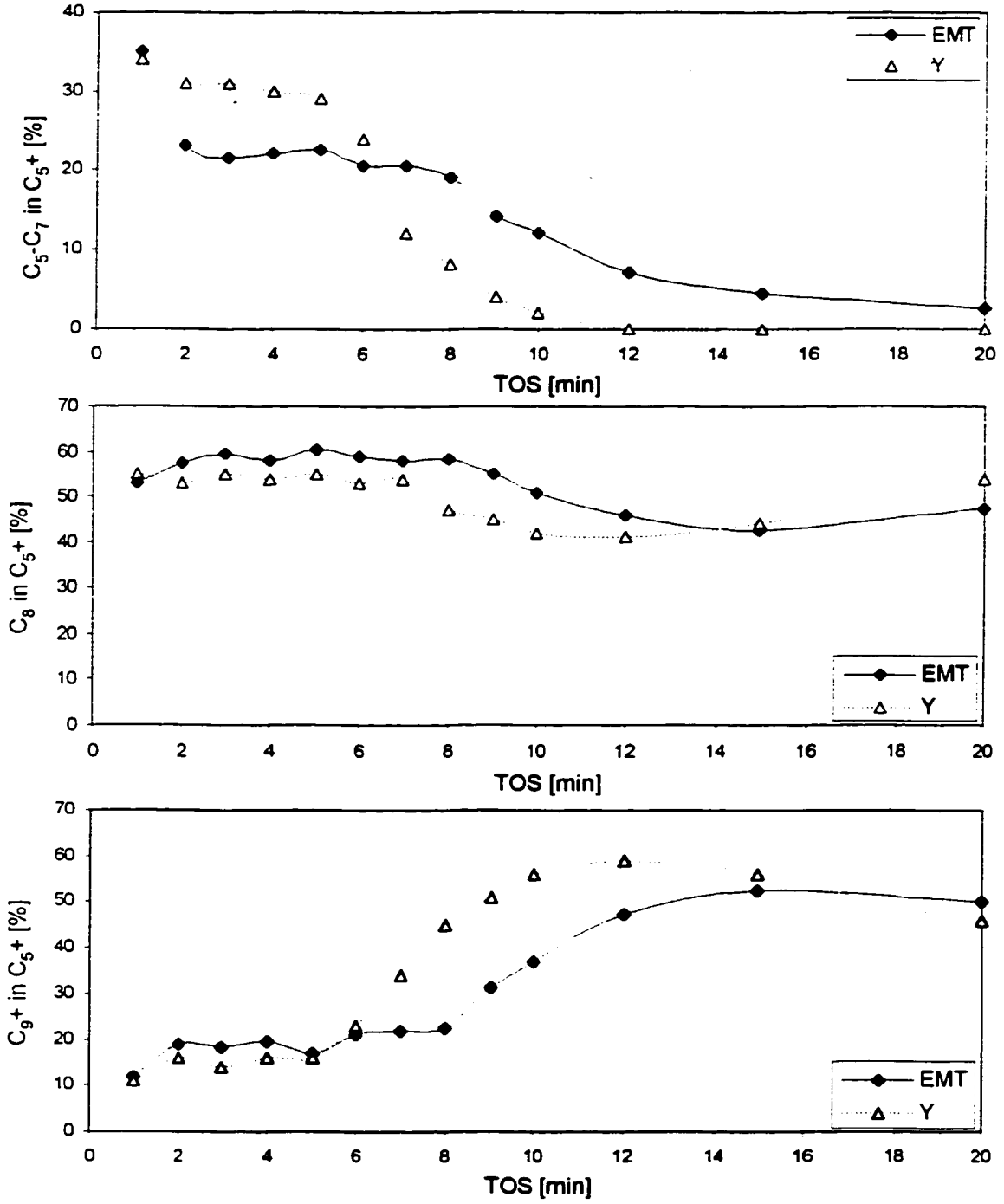

Figure 6.26: Effect of Catalyst Support on C_5^+ Product Distribution (T_{rxn}=53°C; P=382psig; T_{calc}=425°C, I/O=15; $C_4^=$WHSV=2.0h^{-1}; m_{cat}=2.78g)

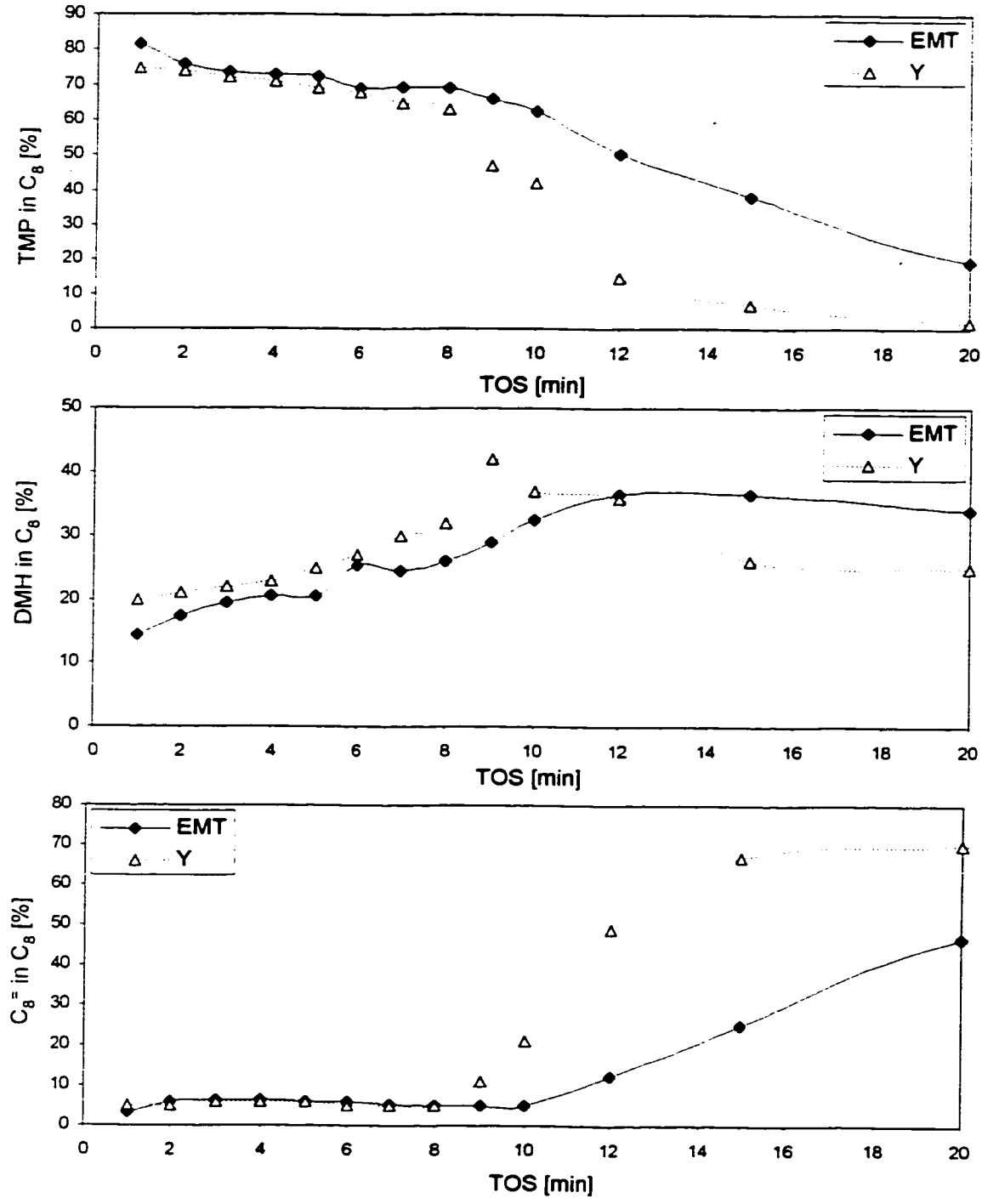

Figure 6.27: Effect of Catalyst Support on C_8 Selectivity
(T_{rxn}=53°C; P=382psig; T_{calc}=425°C, I/O=15; $C_4^=$WHSV=2.0h^{-1}; m_{cat}=2.78g)

6.8.3.4 *Comparison of Control Experiments (for Pt Study) with respect to TMP Selectivity*

Distinctive differences in the average composition of the TMP distribution produced during the Useful Catalyst Lifetime were detected (see Table 6.12). Both catalysts favoured the production of 2,2,4-TMP (see Figure 6.28). Although levels on Y were slightly higher during the Useful Catalyst Lifetime period, elevated 2.2,4-TMP levels were maintained on EMT during the Rapid Deactivation period. This is indicative of the superior ability of EMT to resist deactivation processes and sustain alkylation activity.

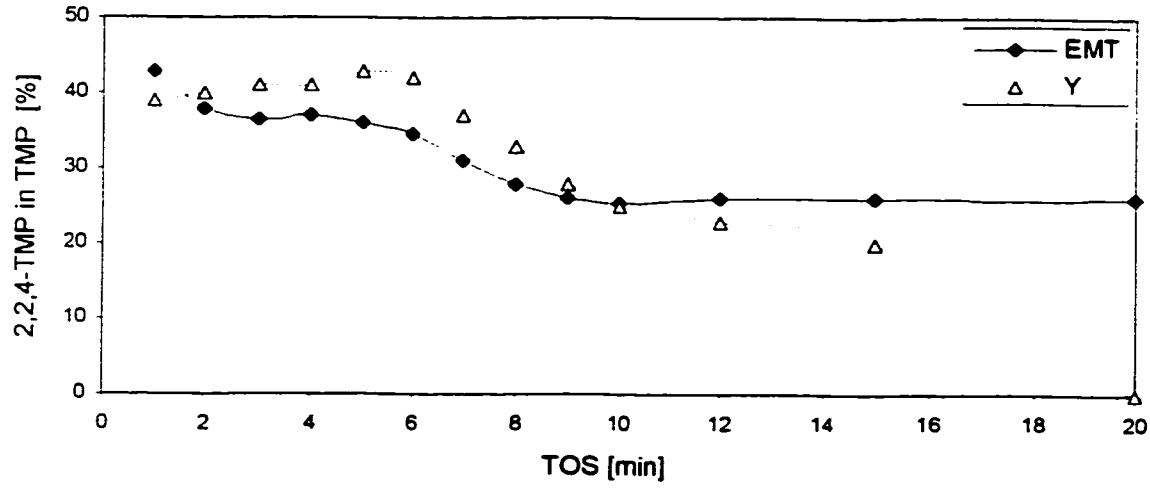

Figure 6.28: Effect of Catalyst Support on 2,2,4-TMP Level in TMP Fraction (T_{rxn}=53°C; P=382psig; T_{calc}=425°C, I/O=15; $C_4^=$WHSV=2.0h^{-1}; m_{cat}=2.78g)

Table 6.12: Comparison of Average Catalyst Performance (during first 5 min of Useful Catalyst Lifetime period) on EMT and Y Zeolites (T_{rxn}=53°C; P=382psig; T_{calc}=425°C, I/O=15; $C_4^=$WHSV=2.0h^{-1}; m_{cat}=2.78g)

Run(s)	F66EMT, F68EMT	F54Y
Catalyst	EMT	Y
Useful Catalyst Lifetime [min]	10.6	7.9
Yield [g C_5+/g cat/g 1-$C_4^=$ fed]	0.083	0.068
C_5^+ Liquid [mass %]		
C_5-C_7	25	31
C_8	58	55
C_9^+	17	14
C_8 Distribution [mass %]		
TMP	75	72
DMH	19	22
$C_8^=$	6	6
TMP Distribution [%]		
2,2,4-TMP	38	41
2,2,3-TMP	18	7
2,3,4-TMP	17	21
2,3,3-TMP	27	31
Indicators [mass fraction]		
$\frac{\text{TMP}}{\text{DMH}}$	4.2	3.3
$\frac{\text{TMP + DMH}}{C_8^= + C_9+}$	2.78	3.03
$\frac{\text{2,2,3-TMP + 2,2,4-TMP}}{\text{2,3,3-TMP + 2,3,4-TMP}}$	1.28	0.91

Recall that 2,2,4-TMP is claimed to be correlated to cracking activity (Corma & Martinez, 1993). Although comparable levels of 2,2,4-TMP were observed on both catalysts, cracking activity was higher on Y. It is possible that this isomer may be formed via alternative routes on EMT, such as self-alkylation of isobutane, for which 2,2,4-TMP is a direct product. This was suspected to be important in an investigation employing EMT applied to butene/isobutane alkylation (Rorvik, 1996) and will be discussed further in the Synopsis section. Evidence of self-alkylation of isobutane

on Y zeolite is difficult to ascertain, as no direct evidence can be provided by the current investigation.

The direct product of butene/isobutane alkylation isomer is 2,2,3-TMP. However, this isomer was found to be produced in the least amounts on both catalyst systems, suggesting that rapid isomerization of 2,2,3-TMP$^+$ was being facilitated under reaction conditions. It is interesting to note that EMT produced higher levels of 2,2,3-TMP, suggesting isomerization of 2,2,3-TMP$^+$ did not occur as extensively on this catalyst. Levels of the fastest diffusing isomers, 2,3,3-TMP and 2,3,4-TMP, were notably greater than thermodynamic predictions on both EMT and Y, suggesting that restrictions imposed by the pore cavities make the least sterically hindered isomers more favourable. The thermodynamically favourable isomers are bulkier and slower to diffuse, imposing an additional barrier to their formation in the zeolite cages. The catalyst EMT revealed superior ability in producing the thermodynamically favoured isomers relative to the fastest diffusing isomers ([2,2,3-TMP+2,2,4-TMP]/[2,3,3-TMP+2,3,4-TMP] ratio), which may be a direct consequence of the larger hypercages and improved accessibility to these cages.

6.8.3.5 Synopsis of Control Experiments (for Pt Study) Comparison

Similar product distributions were observed on EMT and Y for a reaction temperature of 53°C and an I/O ratio of 15 (see Table 6.12). Cracking activity was reduced on EMT and C_8 production levels were elevated. Although composition of the product was not significantly different, alkylation activity was sustained for a longer duration on EMT. A 40 % improvement in the Useful Catalyst Lifetime was observed on EMT relative to Y. In addition, yield was enhanced by 16 % on EMT. It was expected that a more active catalyst would increase the concentration of products in the catalyst pores, accelerating the onset of deactivation. However, EMT did not deactivate in a shorter period of time or at a faster rate.

These results lead to the hypothesis that perhaps adsorption/desorption phenomenon was exercising a significant influence on the product distribution, as was observed at higher olefin WHSV (see Section 6.6). It was found that the loss in surface area upon exposure to butene was more significant on Y, as compared to EMT. This suggests that the following are dictating catalyst activity:

- Y zeolite adsorbs butene more readily than EMT

  or

- The ability of EMT to involve isobutane, is superior to Y zeolite, enhancing hydride transfer to desorb C_8 product

The adsorption ability of EMT, with respect to butene, is not believed to be grossly inferior to that of Y zeolite. Complete butene disappearance was observed at similar TOS for both catalysts (see Figure 6.25). In addition, the product yield for EMT was superior to that obtained on Y zeolite (see Table 6.12). Therefore, it is suspected that EMT demonstrated superior ability in adsorbing isobutane and enhancing hydride transfer.

Published acidity measurements predict that EMT possesses a greater proportion of Bronsted acid sites relative to Y zeolite, particularly in the strong range (see Table 2.5). Spectroscopic studies on La-Y zeolite found only weak interaction, or physisorption, between isobutane and zeolite acid sites (Flego et al, 1995). It may be that the superior Bronsted acidity of EMT enhances the strength of this interaction.

The effects of WHSV (see Section 6.6) and cyclical feed delivery (see Section 6.7), suggest that many of the C_8^+ species adsorbed on Y zeolite grow in size, from subsequent reaction. It is possible that the close proximity of acid sites and higher content of Lewis acidity in Y favour these processes. This results in bulky oligomers populating the catalyst surface, restricting access to acid sites in the interior of the granule. Some of the larger C_8^+ adsorbed species on Y zeolite, will undergo cracking reactions, leading to elevated 2,2,4-TMP levels and an increase in the C_5-C_7 content in the C_5^+ liquid. Others will be retained on the catalyst surface blocking pores,

leading to significant surface area loss. This agrees with the experimental results reported.

TGA/DTA analysis of the spent catalyst detected a greater mass % of adsorbed species on EMT relative to Y zeolite (see Table 6.13). Although the amounts of adsorbed heavier compounds (T_{desorp}>300°C) is greater on EMT. it also revealed a significantly larger population of lighter adsorbed hydrocarbons (T_{desorp}>300°C). This suggests that EMT is able to adsorb more species without becoming deactivated. The improved accessibility to cages, nature of acid site and arrangement of acid sites potentially contribute to this behaviour.

The effect of granule size was not studied in detail in the flow reactor. However, a preliminary batch reactor experiment, employing Y catalyst pellets (1/8 " extrudate), revealed limited catalyst activity. The granule size employed for the flow reactor represents the smallest size that could safely be used, without concern for entrainment of catalyst particles in the reactor effluent.

Table 6.13: Effect of Catalyst Support (T_{rxn} = 50°C, I/O =15, T_{calc} = 425°C)

Catalyst	SA Spent Catalyst [m^2/g]	TGA of Spent Catalyst [mass%] Desorption Temperature [°C]				Yield
		<200	200-300	>300	Total	[$gC_5^+/gcat/g1\text{-}C_4^=fed$]
EMT	377	3.5	2.5	3.0	9.3	0.083
Y	372	2.0	2.5	2.5	7.0	0.068

6.9 COMPARISON OF EMT AND Y ZEOLITES TO LITERATURE RESULTS

Experimental results for EMT and Y zeolite are compared to those published in the literature (see Table 6.14). Note the difference in the reactor system applied in the literature study investigating EMT. Stocker et al (Stocker et al, 1996), employed a

semi-batch reactor, in which all of the isobutane was delivered to prior to reaction and then heated to 80°C. At this point, the butene was pumped to the reactor at a WHSV of 2 h^{-1} over a 2 h duration, resulting in an overall I/O ratio of 10. This mode of operation inherently provides a much higher local I/O ratio during the initial stages of the reaction.

Differences in reactor geometry and reaction temperature between the Stocker work and the present investigation, make direct comparisons impossible. It is difficult to predict the combined influence of all of these factors on the complex network of reactions that are being facilitated on these catalysts. However, knowledge of the effect of the I/O ratio and reaction temperature, can provide some insight into the estimated differences that may be imparted on product distributions.

It was found that a decrease in the olefin WHSV enhanced TMP formation and suppressed oligomerization and polymerization activities (see Section 6.6). Thermodynamic TMP isomers (2,2,3-TMP and 2,2,4-TMP) were favoured, over the least sterically hindered varieties (2,3,3-TMP and 2,3,4-TMP). An increase in reaction temperature favoured higher cracking activity, enhancing 2,2,4-TMP levels. An overall decrease in TMP production occurred at higher temperatures and a slight increase in DMH levels were noted.

Similar trends between the EMT experiments in the present work and the literature results are found. Both systems favoured high C_8 product levels to predominantly alkylation products. A higher TMP/DMH ratio is expected for the Stocker study, considering the mode of butene addition and lower olefin WHSV.

It is expected that the higher reaction temperature employed by the Stocker study would favour increased cracking activity, contrary to the results reported. It is possible that the method of sample collection used in the Stocker study does not provide a representative sample of the reaction products, due to dissolved (excess) isobutane. Evaporation of isobutane in the sample compromises the accuracy of the C_5 to C_7 fraction, as was found in batch experiments of the present study. The flow experiments of the present work are not vulnerable to this problem, due to the 16-loop Multiposition Trapping Valve in the on-line sampling system.

Table 6.14: Comparison of Experimental EMT and Y Alkylation Data with Literature Results

	EMT Stocker[1]	EMT[3]	Y-Corma[2]	Y[3]	Thermodynamic Equilibrium @50°C[4]
Run	parent H-EMT	F66EMT F68EMT	USY-1	F54Y	
Si/Al	3.5	6.9	5.4	6.3	
Calcination Temperature [°C]	540	425	500	425	
Reaction Temperature [°C]	80	50	50	50	
Pressure [psig]	n.a.	382	382	382	
I/O	10	15	15	15	
$C_4^=$ WHSV [h^{-1}]	1.2	2	1 - 2	2	
reactor	semi-batch	flow	flow	flow	
C_5^+ Dist. C_5-C_7	10	25	24	31	
C_8	82	58	59	55	
C_9^+	8	17	17	14	
C_8 Dist. TMP	83	75	70	72	
DMH	16	19	23	22	
$C_8^=$	1	6	7	6	
TMP Dist. 2,2,4-TMP	29	38	34	41	63.5
2,2,3-TMP	9	18	7	7	17.5
2,3,4-TMP	27	17	28	21	9.0
2,3,3-TMP	35	27	31	31	10.0
Indicator $\frac{TMP}{DMH}$	5.2	4.2	3.0	3.3	

1 bulk liquid sample after 3 h reaction, Stocker et al, 1996
2 instantaneous liquid sample (TOS=1min), Corma et al, 1994b
3 average alkylate quality during initial 5 min of Useful Catalyst Lifetime period
4 thermal equilibrium composition, Cardona et al, 1995

The high *local* I/O ratio inherent in the semi-batch reactor system, can explain the remainder of the differences noted between the Stocker study and the present work. A high *local* I/O ratio is expected to reduce polymerization content in the product and enhance TMP levels in the C_8 fraction. This agrees with the data presented in Table 6.14.

An increase in reaction temperature, combined with a high I/O, favour high 2,2,4-TMP levels. However, the work of Stocker et al (1996) detected significantly lower 2,2,4-TMP levels than those obtained in the present work. It was suggested that 2,2,4-TMP was formed via self-alkylation of isobutane on EMT (Stocker et al, 1996). It is possible that a flow reactor design, favours self-alkylation of isobutane to a more significant extent than the semi-batch reactor, where residence time of butene is significantly longer.

The literature results for Y zeolite (Corma et al, 1994b) employed a similar reactor system, method of product collection and analysis, as those applied in the present work. The Corma study revealed a lower cracking activity and higher C_8 production levels, as compared to those reported by the present study. This is a direct reflection of the method of reporting catalyst activity. The Corma study reported instantaneous catalyst activity in the absence of deactivation (TOS = 1 min), where maximum alkylation activity occurs. The present work reports an arithmetic average of catalyst activity, during the initial 5 min of the Useful Catalyst Lifetime period.

A higher calcination temperature has been found to suppress cracking activity and elevate polymerization function, with little significant effect on the distribution of components in the C_8 fraction. Comparison of the Corma study, which applied a higher calcination temperature than the present work, supports this behaviour. Cracking activity was reduced and polymerization product levels were slightly higher, in agreement with the predictions. The distribution of components in the C_8 in the Corma study, match closely with those obtained in the present work.

Slight differences in the TMP isomer distribution are observed with higher levels of 2,2,4-TMP reported for the present work. Lower 2,3,4-TMP levels were

found in the present study, with all other TMP isomer levels being comparable to Corma's work. This is consistent with the effect of calcination temperature previously established, in that more severe calcination conditions favour the least sterically hindered isomers of 2,3,3-TMP and 2,3,4-TMP.

Chapter 7

Preliminary Studies on the Effect of Pt on the Performance of EMT and Y Zeolites

It is hypothesized that the presence of Pt in the zeolite pores can activate spillover. Hydrogen spillover will increase the amount of available reactive hydrogen in the vicinity of the acid sites. Hydride transfer will be improved and the Useful Catalyst Lifetime period extended. The effect of Pt on fresh catalyst performance will be discussed in Section 7.1.

Pt can also activate oxygen during regeneration. This would enhance the removal of carbonaceous deposits on the spent catalyst, improving the efficacy of regeneration. The effect of Pt on regenerated catalyst performance will be discussed in Section 7.2.

7.1 EFFECT OF Pt ON FRESH CATALYST PERFORMANCE OF EMT AND Y ZEOLITES

The primary objective of this investigation was to examine the effect of Pt addition on catalyst activity and selectivity. Two levels of Pt (0.1% Pt and 0.5% Pt) were considered on EMT (denoted as 0.1%Pt/EMT and 0.5%Pt/EMT respectively) and a single fixed amount (0.5%Pt) on Y zeolite (denoted as 0.5%Pt/Y). These loadings represent typical amounts employed in hydrogen spillover research. Preparation details are described in Section 3.5.1. Catalyst properties for Pt/EMT and Pt/Y systems are summarized in Tables 3.4 and 3.6.

Results from the Pt/EMT and Pt/Y experiments were compared to those of parent materials, EMT and Y respectively, where no noble metal is present. In this manner it can be established whether positive benefits can be gained through Pt incorporation into the catalyst design.

Undoubtedly, a minimum amount of Pt is necessary to generate a sufficient population of spillover species to effect a significant change. However, it is expected that an excessive amount of Pt will impose steric restrictions in the catalyst pores, and the benefits of spillover will be lost to diffusional limitations. Therefore, it is reasonable to assume that a preferred Pt level exists. This provides the framework for the secondary objective of this study, which is to identify whether Pt loading is important. Results on EMT at 0.1% Pt and 0.5% Pt loadings were compared, to determine whether a preferable Pt level exists. The effect of Pt content was not investigated on Y zeolite.

All experiments were performed in a hydrogen atmosphere, at a reaction temperature of 53°C and an operating pressure of 382 psig employing an I/O ratio of 15 and a $C_4^=$ WHSV of 2.0 h^{-1}. Catalyst pre-treatment was performed *in situ* prior to initiation of the experiment. Calcination of Pt catalyst systems prior to the reduction step, has been reported to improve the dispersion of the noble metal. Milder calcination conditions are recommended as this reduces the risk of metal agglomeration (Gates, 1995). The Pt/zeolite systems were calcined at 325°C for 3 hours in a stream of nitrogen maintained at 50 sccm. The calcination treatment was immediately followed by the reduction step, performed at 425°C for 3 h in a flowing mixture of 10.1 wt% H_2 in Ar, at a combined flow rate of 2 sccm. Those catalyst systems, which do not incorporate a noble metal, were calcined in the same manner to permit comparison (see Section 6.8.3).

At the conclusion of the reduction cycle, the catalyst bed was flushed with nitrogen for 5 min and then cooled under a nitrogen blanket to the reaction temperature. Experiments for the Pt/EMT and Pt/Y catalysts were performed in a flowing stream of 1.4 wt% H_2 in an argon/nitrogen mixture using a combined flow rate of 12 sccm. Those reactions studying EMT and Y zeolites utilized a 12 sccm stream of nitrogen.

7.1.1 Effect of Pt on Butene Disappearance for Fresh Catalysts

A minor change in the Useful Catalyst Lifetime occurred with impregnation of Pt into the pore network of EMT. The lower loading of Pt (0.1%) on the EMT carrier, did not significantly affect the Useful Catalyst Lifetime period, whereas the higher Pt level (0.5%) improved the lifetime modestly by 11.3 % (see Table 7.1). It may be that the lower loading of Pt is inadequate to generate a sufficient population of reactive hydrogen to produce a positive effect on catalyst lifetime of EMT. Butene conversion was not significantly affected by impregnation of 0.5% Pt onto acidic Y zeolite (see Table 7.1).

Table 7.1: Effect of Pt on Useful Catalyst Lifetime of Fresh EMT and Y Systems (T_{calc}=325°C; T_{red}=425°C; T_{rxn}=53°C; P=382psig; I/O=15; $C_4^=$WHSV=2.0h^{-1}; m_{cat}=2.78g; 12 sccm H_2/Ar/N_2 mix with 1.4 wt%H_2 used for Pt runs)

Catalyst	Useful Catalyst Lifetime period [min][1]
EMT	10.6
0.1%Pt/EMT	9.5
0.5%Pt/EMT	11.8
Y	7.9
0.5%Pt/Y	8.0

Sensitivity limit = ± 0.7 min

7.1.2 Effect of Pt on C_5+ Product Distribution for Fresh Catalysts

The incorporation of 0.1% Pt impregnated in the EMT pore structure, did not significantly alter catalyst performance (see Figure 7.1). A loading of 0.1% Pt cannot develop the reactive hydrogen population necessary to enhance hydride transfer and improve catalyst performance relative to EMT. Increasing the Pt loading to 0.5 % on EMT, resulted in measurable benefits. Cracking activity and C_8 production levels were enhanced slightly, and polymerization function suppressed, on 0.5%Pt/EMT relative to parent EMT (see Figure 7.1). It appears that a minimum amount of Pt is necessary to establish a sufficient population of reactive hydrogen, possibly hydrogen spillover, to produce detectable differences in catalytic behaviour.

A similar loading of Pt on Y zeolite (0.5%Pt/Y) did not produce significant changes in the C_5+ liquid, during the Useful Catalyst Lifetime period. Cracking activity was lowered slightly, with very little differences in C_8 and C_9+ levels observed. This suggests that the reactive hydrogen generated by Pt on Y zeolite, does not exert a major effect on the alkylate composition from the catalyst.

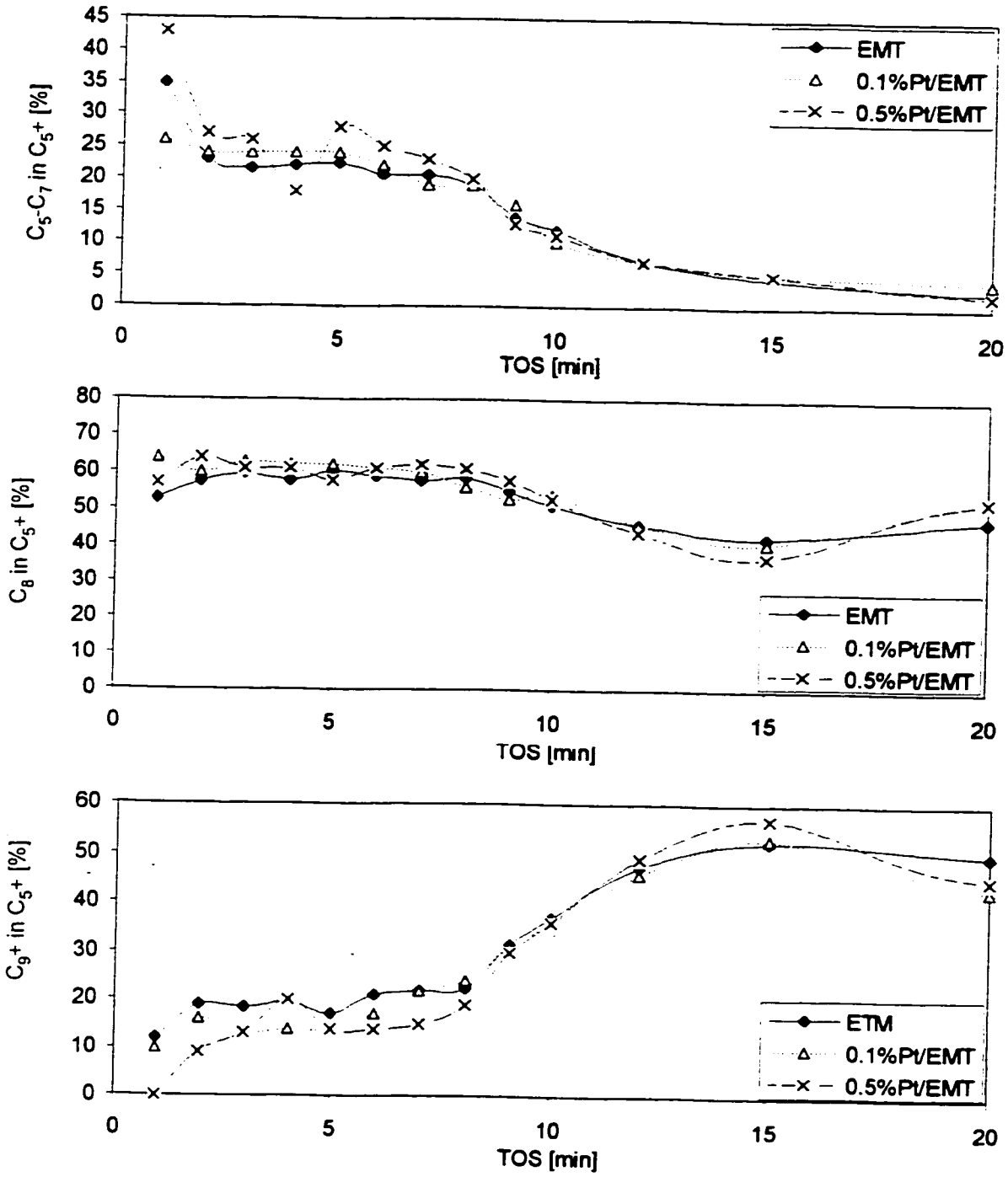

Figure 7.1: Effect of Pt on C_5+ Product Distribution of Fresh EMT Systems (T_{calc}=325°C; T_{red}=425°C; T_{rxn}=53°C; P=382psig; I/O=15; $C_4^=$WHSV=2.0h^{-1}; m_{cat}=2.78g; 12 sccm H_2/Ar,N_2 mix with 1.4 wt%H_2 used for Pt runs)

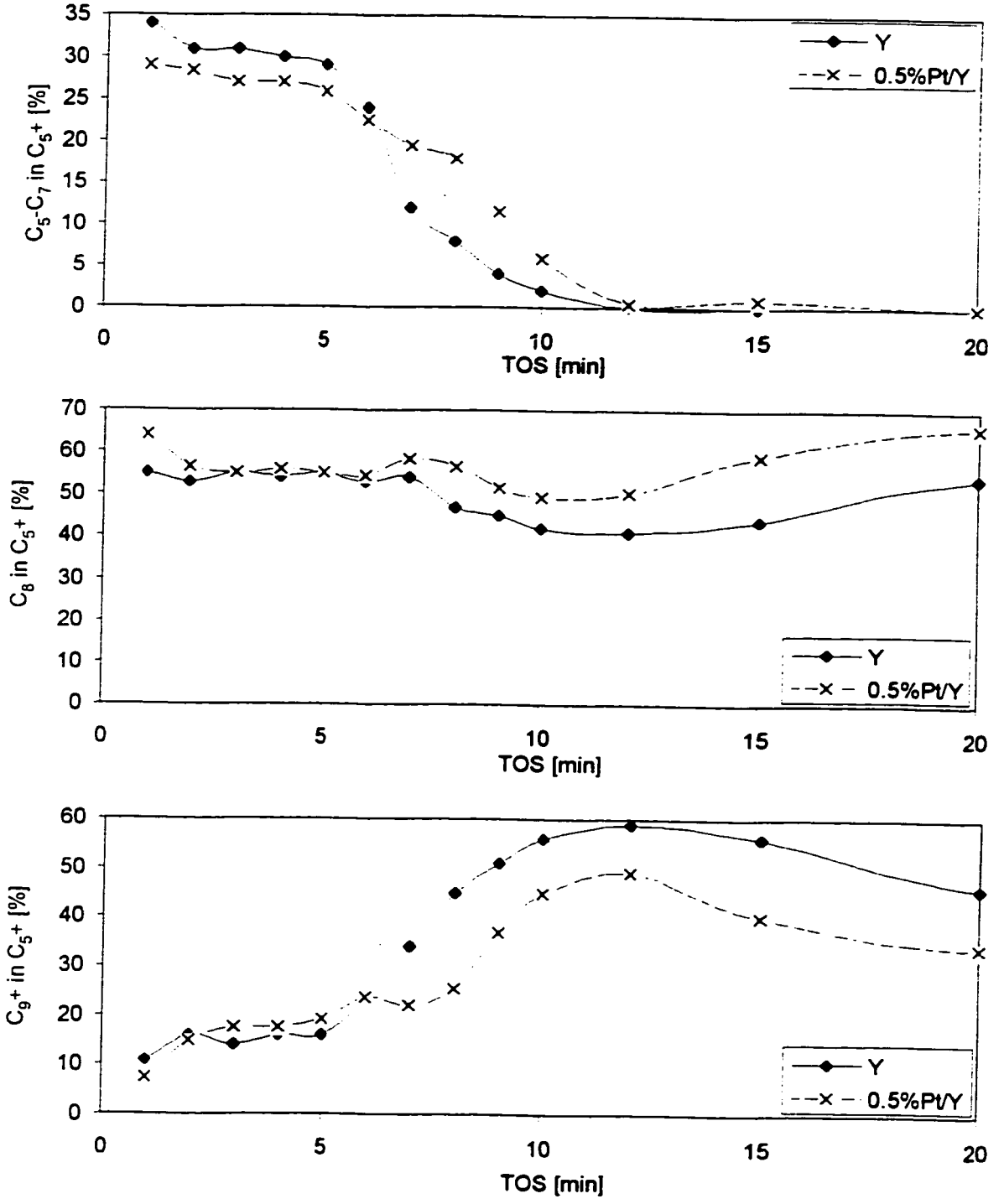

Figure 7.2: Effect of Pt on C_5+ Product Distribution of Fresh Y Systems (T_{calc}=325°C; T_{red}=425°C; T_{rxn}=53°C; P=382psig; I/O=15; $C_4^=$WHSV=2.0h^{-1}; m_{cat}=2.78g; 12 sccm H_2/Ar,N_2 mix with 1.4 wt%H_2 used for Pt runs)

7.1.3 Effect of Pt on C_8 Selectivity for Fresh Catalysts

No significant change in C_8 selectivity was observed for 0.1%Pt/EMT (see Figure 7.3). It appears that 0.1% Pt loading on EMT is inadequate to generate a sufficient reactive hydrogen population to exert a measurable effect on catalyst performance. Increasing the Pt loading to 0.5% on EMT caused slight changes in C_8 selectivity, during the Useful Catalyst Lifetime period (see Figure 7.3). Higher TMP levels were observed and reduced DMH formation noted. A modest increase in DMH levels was observed on Y zeolite using the same Pt loading of 0.5% (see Figure 7.4). The reactive hydrogen population developed by Pt on Y is not able to produce the same positive benefit of enhancing TMP levels, as noted for 0.5% Pt on EMT.

7.1.3 Effect of Pt on TMP Selectivity for Fresh Catalysts

TMP selectivity was not significantly altered by 0.1% Pt impregnated on EMT (see Table 7.2). This agrees with previous findings where no measurable change in the C_5+ product distribution and C_8 selectivity were observed on this catalyst.

Increasing the Pt loading to 0.5% produced a detectable change, favouring higher levels of the least sterically hindered isomers, 2,3,3-TMP and 2,3,4-TMP, and reduced amounts of 2,2,3-TMP and 2,2,4-TMP. Similar behaviour was observed for 0.5% Pt on Y zeolite, where levels of 2,3,3-TMP and 2,3,4-TMP were augmented in the presence of Pt.

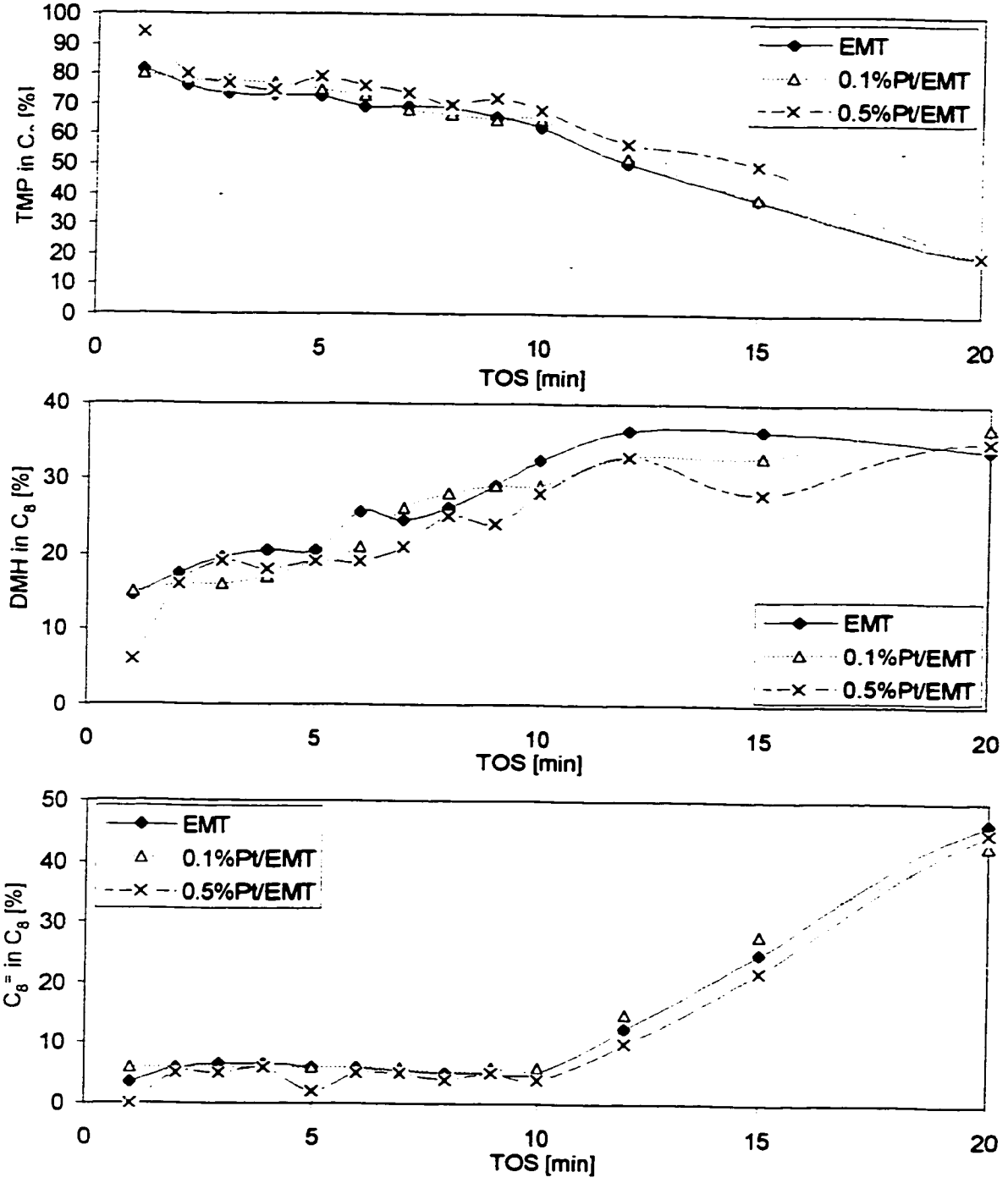

Figure 7.3: Effect of Pt on C_8 Selectivity of Fresh EMT Systems (T_{calc}=325°C; T_{red}=425°C; T_{rxn}=53°C; P=382psig; I/O=15; $C_4^=$WHSV=2.0h^{-1}; m_{cat}=2.78g; 12 sccm H_2/Ar,N_2 mix with 1.4 wt%H_2 used for Pt runs)

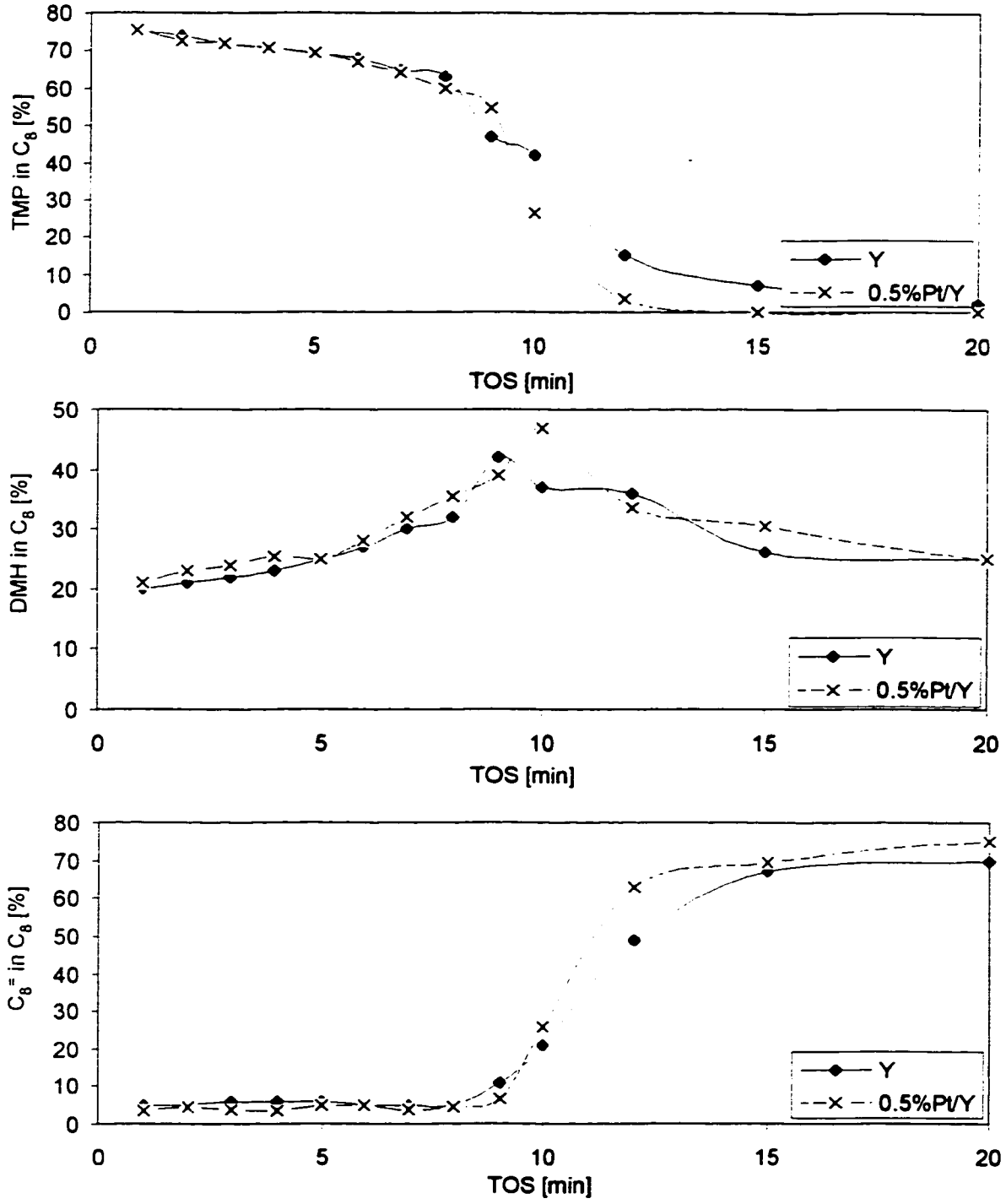

Figure 7.4: Effect of Pt on C_8 Selectivity of Fresh Y Systems (T_{calc}=325°C; T_{red}=425°C; T_{rxn}=53°C; P=382psig; I/O=15; $C_4^=$WHSV=2.0h^{-1}; m_{cat}=2.78g; 12 sccm H_2/Ar,N_2 mix with 1.4 wt%H_2 used for Pt runs)

Table 7.2: Comparison of Average Catalyst Activity during First 5 min of Useful Catalyst Lifetime Period for Fresh Parent and Pt Supported Catalysts (T_{calc}=325°C; T_{red}=425°C; T_{rxn}=53°C; P=382psig; I/O=15; $C_4^=$WHSV=2.0h^{-1}: m_{cat}=2.78g, 12 sccm H_2/Ar/N_2 mix with 1.4 wt%H_2 used for Pt runs)

Run	F66EMT F68EMT	F62Pt1EMT	F49Pt5EMT	Sensitivity	F54Y	F44Pt5Y F56Pt5Y
Catalyst	EMT	0.1% Pt/EMT	0.5% Pt/EMT		Y	0.5% Pt/Y
Pt Dispersion [%]	n.a.	74	76	n.a.	n.a.	91
Useful Catalyst Lifetime [min]	10.6	9.5	11.8	± 0.7	7.9	8.0
Time of Deactivation [min] (80% > $C_4^=$ Conversion > 50%)	10.4	12.5	12.6	± 1.6	1.9	3.2
Yield [g C_5^+/g cat/ g 1-$C_4^=$ fed]	0.083	0.078	0.095	± 0.016	0.068	0.063
C_5^+ Dist. [mass %]						
C_5-C_7	25	24	28	± 2.3	31	28
C_8	58	62	61	± 2.5	55	57
C_9^+	17	14	11	± 3.7	14	15
C_8 Dist. [mass %]						
TMP	75	77	81	± 3.3	72	71
DMH	19	17	15	± 2.7	22	25
$C_8^=$	6	6	4	± 0.8	6	4
TMP Dist. [%]						
2,2,4-TMP	38	36	33	± 2.5	41	35
2,2,3-TMP	18	18	14	± 2.1	7	4
2,3,4-TMP	17	18	20	± 2.1	21	28
2,3,3-TMP	27	28	33	± 2.4	31	33
Indicators [mass fraction]:						
$\frac{TMP}{DMH}$	4.2	4.7	6.6	± 0.57	3.3	2.9
$\frac{TMP + DMH}{C_8^= + C_9^+}$	2.78	3.47	3.73	± 0.63	3.03	3.35
$\frac{2,2,4\text{-}TMP + 2,2,3\text{-}TMP}{2,3,3\text{-}TMP + 2,3,4\text{-}TMP}$	1.28	1.17	0.90	± 0.20	0.91	0.63

7.1.5 Synopsis of Pt Effects for Fresh Catalysts

The stages of catalyst activity and selectivity that were observed for EMT and Y zeolites (see Section 6.2), are also demonstrated on Pt/EMT (see Figures 7.5 to 7.8) and Pt/Y (see Figures 7.9 to 7.10) systems. Supporting Pt on the zeolite support does not alter the Useful Catalyst Lifetime period, with the exception of 0.5%Pt/EMT where a modest improvement was noted.

No significant change in alkylate composition or yield, were observed on 0.1%Pt/EMT. This loading of Pt appeared to be insufficient to develop an adequate reactive hydrogen population to enhance hydride transfer. TGA/DTA data for 0.1%Pt/EMT was similar to EMT for all desorption temperatures, except T_d>300°C, where the mass retained was slightly higher on 0.1%Pt/EMT (see Table 7.2). It is possible that the Pt inside the catalyst pores of EMT, imposed steric constraints, increasing the likelihood of larger molecular weight species being retained on the surface. The formation of these polymeric species cannot be suppressed by reactive hydrogen, as the population is insufficiently developed at a Pt loading of 0.1%.

Increasing the Pt loading to 0.5 % on EMT, resulted in measurable benefits being demonstrated. It appears that this loading is equal to, or exceeds, the minimum amount of Pt necessary to establish a sufficient population of reactive hydrogen. Production of C_8 compounds was elevated on 0.5%Pt/EMT, relative to parent EMT (see Table 7.2), with TMP isomers favoured. Hence, a notable increase in the octane value of the alkylate, as measured by the TMP/DMH ratio, was observed on 0.5%Pt/EMT. Although alkylation activity was enhanced on 0.5%Pt/EMT, the distribution of TMP isomers was altered, favouring the less sterically hindered isomers of 2,3,3-TMP and 2,3,4-TMP. This is not unexpected, as these isomers will diffuse most efficiently out of the pore network, under conditions of increased TMP production.

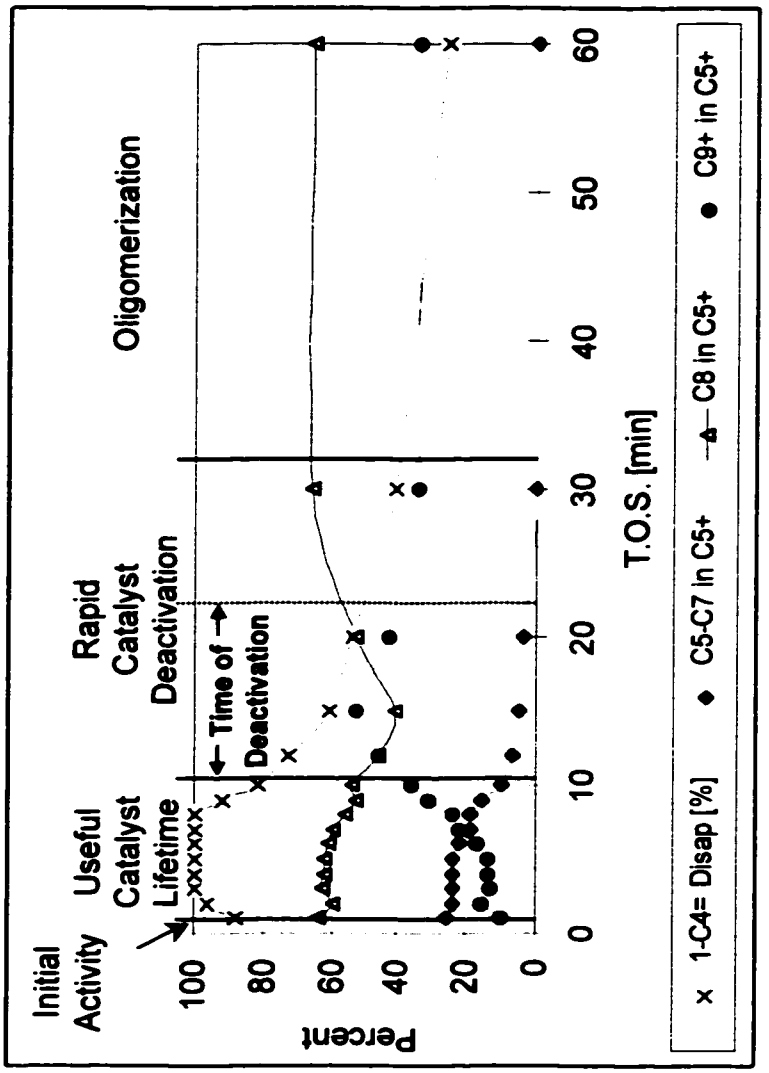

Figure 7.5: Stages of Catalyst Activity on 0.1%Pt/EMT with respect to C_5+ Product Distribution (F62Pt1EMT; T_{rxn}=53°C; T_{calc}=325°C; T_{red}=325°C; P=382psig; I/O=15; t=1h; $C_4^=$ WHSV=2.0h^{-1}; m_{cat}=2.78g; 12sccm H_2/Ar,N_2 with 1.4wt% H_2)

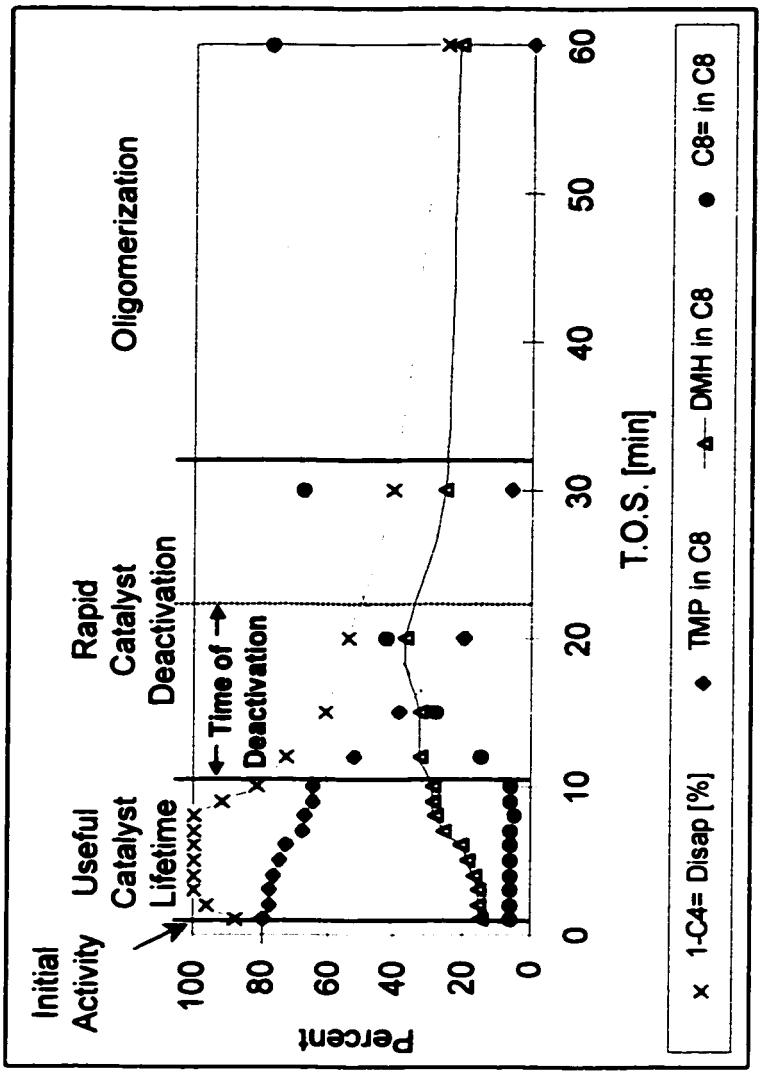

Figure 7.6: Stages of Catalyst Activity on 0.1%Pt/EMT with respect to C_8 Fraction Distribution (F62Pt1EMT; T_{rxn}=53°C; T_{calc}=325°C; T_{red}=325°C; P=382psig; I/O=15; t=1h; $C_4^=$ WHSV=2.0h^{-1}; m_{cat}=2.78g; 12sccm H_2/Ar,N_2 with 1.4wt% H_2)

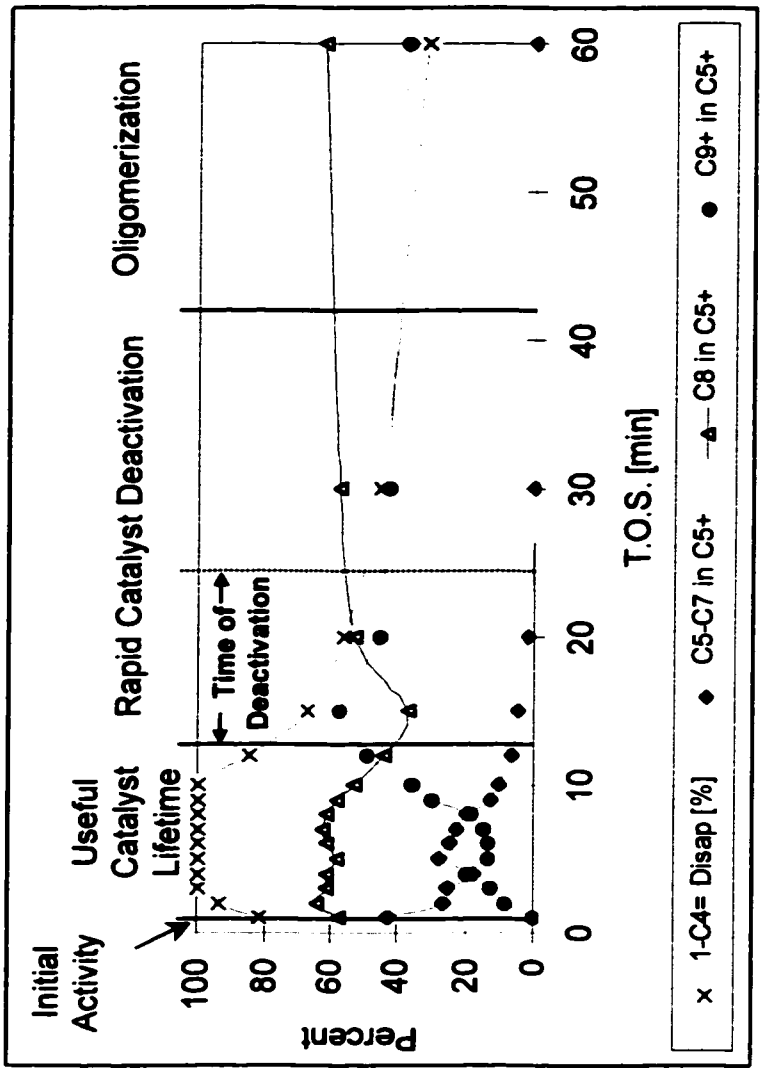

Figure 7.7: Stages of Catalyst Activity on 0.5%Pt/EMT with respect to C_5+ Product Distribution (F49Pt5EMT; T_{rxn}=53°C; T_{calc}=325°C; T_{red}=325°C; P=382psig; I/O=15; t=1h; $C_4^=$ WHSV=2.0h^{-1}; m_{cat}=2.78g; 12sccm H_2/Ar,N_2 with 1.4wt% H_2)

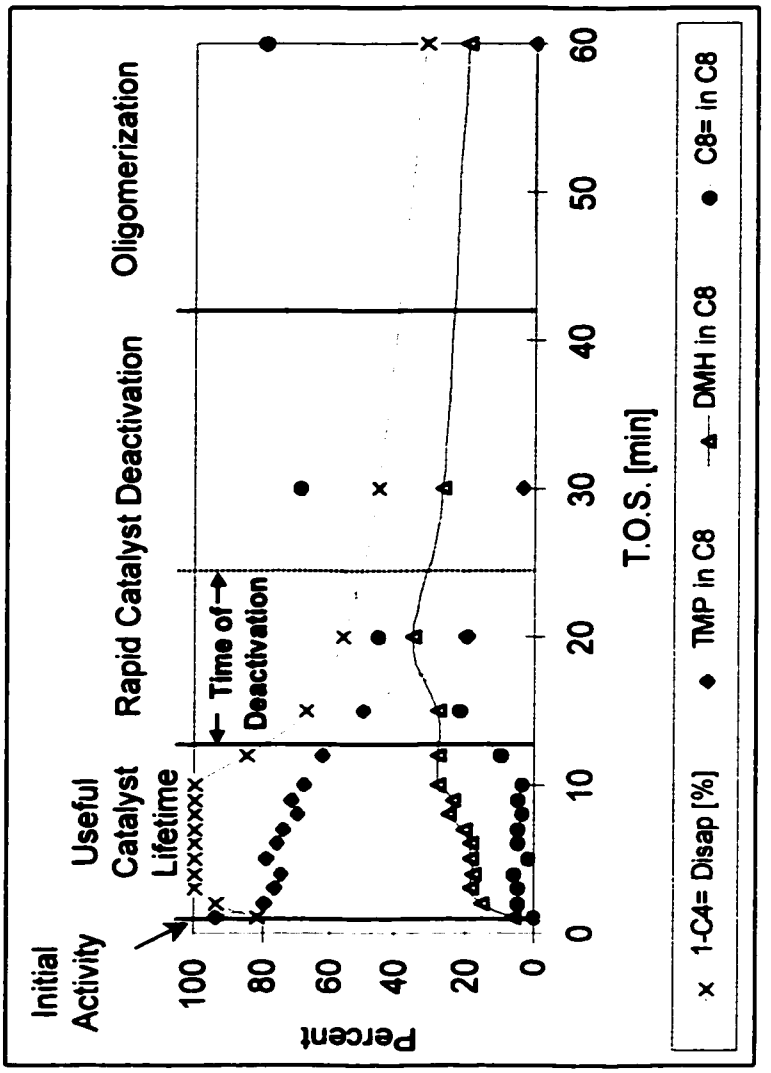

Figure 7.8: Stages of Catalyst Activity on 0.5%Pt/EMT with respect to C_8 Fraction Distribution (F49Pt5EMT; T_{rxn}=53°C; T_{calc}=325°C; T_{red}=325°C; P=382psig; I/O=15; t=1h; $C_4^=$ WHSV=2.0h^{-1}; m_{cat}=2.78g; 12sccm H_2/Ar,N_2 with 1.4wt% H_2)

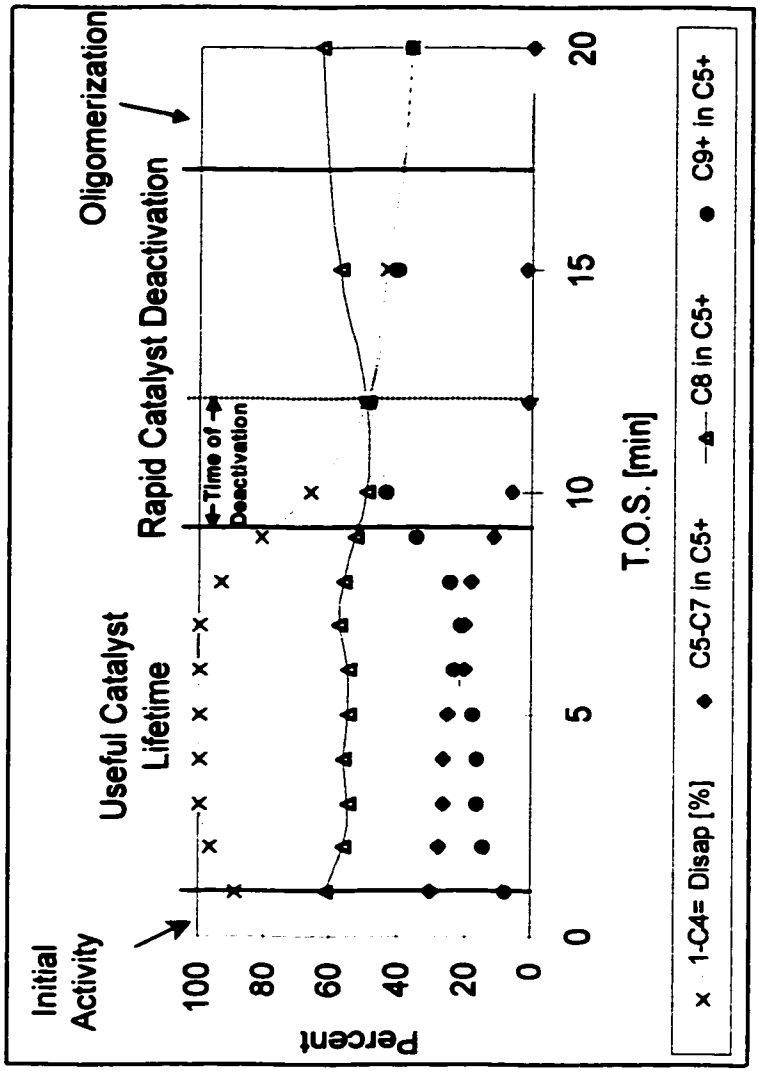

Figure 7.9: Stages of Catalyst Activity on 0.5%Pt/Y with respect to C_5+ Product Distribution (Average F44Pt5Y, F56Pt5Y; T_{rxn}=53°C; T_{calc}=325°C; T_{red}=325°C; P=382psig; I/O=15; t=1h; $C_4^=$ WHSV=2.0h^{-1}; m_{cat}=2.78g; 12sccm H_2/Ar,N_2 with 1.4wt% H_2)

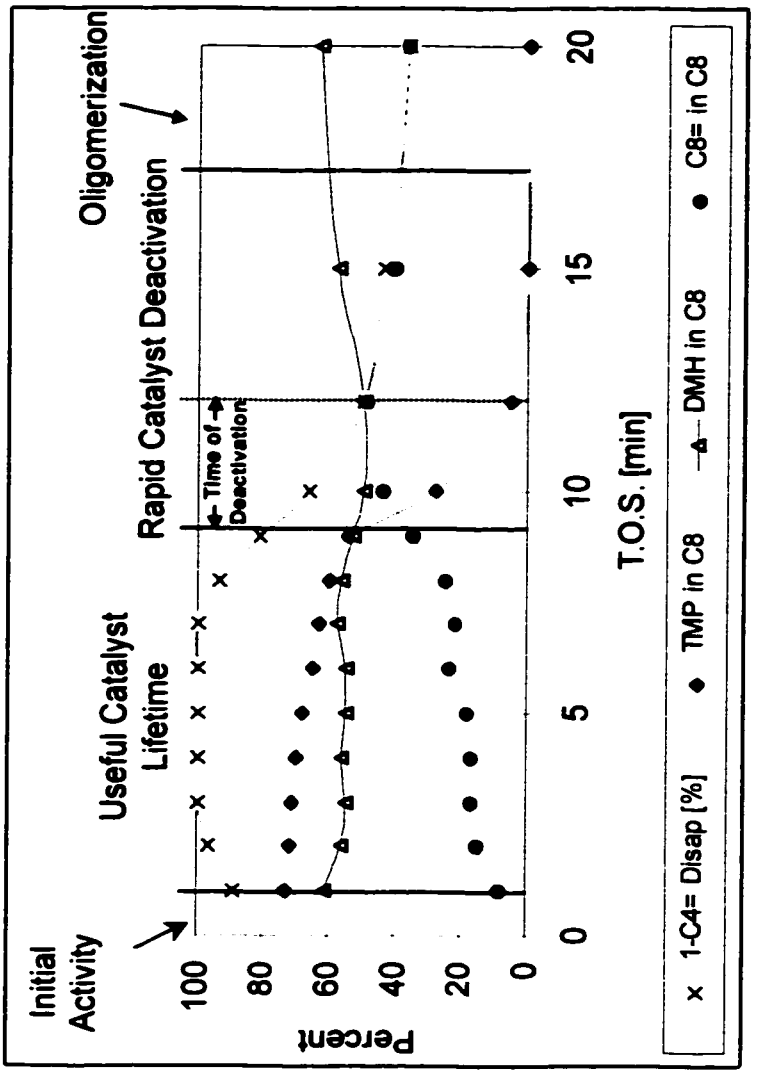

Figure 7.10: Stages of Catalyst Activity on 0.5%Pt/Y with respect to C_8 Fraction Distribution (Average F44Pt5Y, F56Pt5Y; T_{rxn}=53°C; T_{calc}=325°C; T_{red}=325°C; P=382psig; I/O=15; t=1h; $C_4^=$ WHSV=2.0h^{-1}; m_{cat}=2.78g; 12sccm H_2/Ar,N_2 with 1.4wt% H_2)

Evidence of hydride transfer is estimated by the proportion of branched saturated products in the alkylate. A loading of 0.5% Pt on EMT improved hydride transfer (see (TMP + DMH)/($C_8^=$ + C_9+) indicator of Table 7.2), producing higher levels of saturated, branched C_8 products and suppressing the formation of coke precursors ($C_8^=$ and C_9).

The increase in the concentration of reactive hydrogen in close proximity to the acid sites as a result of Pt presence, could enhance desorption of TMP products. This would suppress the opportunity for continued reaction of TMP^+ carbenium ions to higher molecular weight compounds, which are known to encourage deactivation. The rate of deactivation would be suppressed, allowing the acid sites to sustain activity for an extended duration.

The sampling frequency during the deactivation phase was inadequate to accurately estimate the duration of the Deactivation Period. Therefore, the "Time of Deactivation" was defined as the time period for butene conversion to decrease from 80% to 50% levels, where sufficient data was available. The presence of Pt on EMT, increased the Time of Deactivation, independent of the Pt loading (see Table 7.2, Figures 6.1, 6.2, 7.5 to 7.8). Active participation of reactive hydrogen could suppress the rate of deactivation by reducing hydride transfer contributions from adsorbed polymeric species, which lead to coke. Although 0.1% Pt/EMT did not develop an adequate reactive hydrogen population to effect a significant change during the Useful Catalyst Lifetime period, it appears that this loading was sufficient to suppress the rate of deactivation processes.

The positive benefits of Pt could also be related to butene hydrogenation, which would inflate the local I/O ratio in the vicinity of the acid site. It has been previously concluded (see Section 6.6) that a higher I/O ratio favoured increased C_8 production, particularly TMPs, and suppressed oligomerization and polymerization activity. These trends are consistent with the behaviour of 0.5%Pt/EMT. If butene hydrogenation was extensive, a significant increase in *n*-butane levels in the reactor effluent would be expected. In addition, a reduction in yield (g C_5+/g cat/g $C_4^=$ fed) is anticipated, as less butene is available for alkylation reaction. Levels of *n*-butane in

the product were not significantly higher for 0.5%Pt/EMT, although sensitivity to *n*-butane changes is poor in the experimental set-up. In addition, yield was not compromised on 0.5%Pt/EMT, relative to that achieved by EMT (see Table 7.2). Although butene hydrogenation cannot be excluded as a potential explanation for improved catalyst performance on 0.5%Pt/EMT, these contradictions suggest that other factors, such as hydrogen spillover, which may be responsible for the positive benefits observed.

The presence of Pt on Y zeolite did not produce the same benefits noted on EMT. No significant change in the Useful Catalyst Lifetime period or Time of Deactivation were noted (see Table 7.2, Figures 6.3, 6.4, 7.9, 7.10). The levels of DMH increased modestly on 0.5%Pt/Y, contradicting the trend of elevated TMP levels observed on EMT. A review of the alkylation mechanism presents a possible explanation for this behaviour. Under conditions of a well developed reactive hydrogen population, the TMP^+ cation can desorb via two mechanisms: hydride transfer from isobutane or reactive hydrogen, such as hydrogen spillover, which is facilitated by Pt (see Figure 7.11).

If hydride transfer is provided by isobutane, the *tert*-C_4^+ cation is regenerated eliminating the need for supplying this species via other reactions. However, if reactive hydrogen facilitates hydride transfer to desorb TMP, the *tert*-C_4^+ cation is not replenished, necessitating a re-establishment the *tert*-C_4^+ cation population through the "Induction Period" reactions. Under conditions of excessive involvement of reactive hydrogen, the *tert*-C_4^+ cation population becomes notably depleted. The population of *sec*-C_4^+ cation grows, favouring production of DMH through reaction with butene (see Figure 7.11), which was observed on 0.5%Pt/Y.

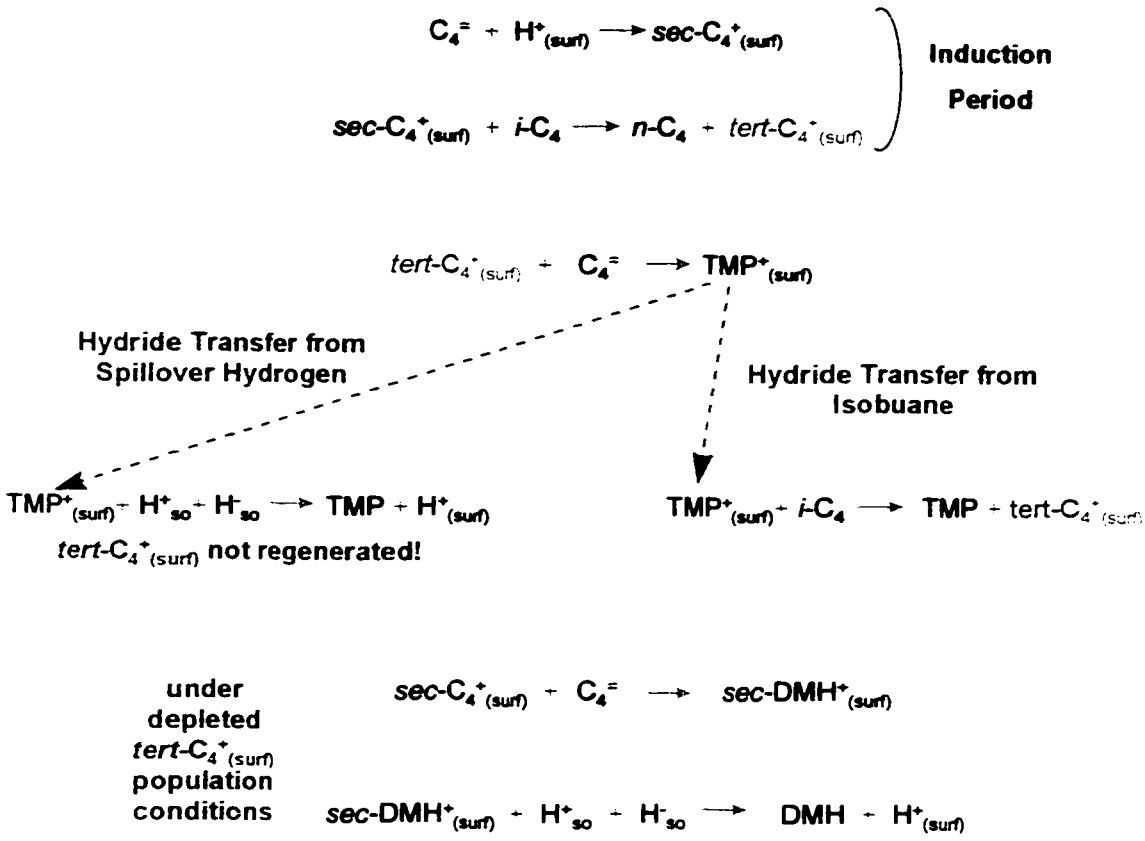

Figure 7.11: Proposed Effect of Excessive Hydrogen Spillover Participation

It is possible that reactive hydrogen population was developed too extensively on 0.5%Pt/Y, compromising the size of the *tert*-C_4^+ cation population and favouring DMH formation. Hydride transfer to a *sec*-C_8^+ cation is slower to than to a *tert*-C_8^+ cation (Cardona et al, 1995), increasing the lifetime of reactive oligomers on the catalyst surface under conditions of excessive reactive hydrogen involvement. This promotes the development of high molecular weight species on these catalysts, which is supported by TGA/DTA data for 0.5%Pt/Y relative to Y (see Table 7.3).

Table 7.3: Effect of Pt Presence on TGA/DTA Measurements of Spent Catalysts (T_{calc} = 425°C, T_{rxn} = 50°C, I/O =15, $C_4^=$ WHSV=2.0h^{-1}; 12 sccm H_2/Ar/N_2 mix with 1.4 wt%H_2 used for Pt runs)

Catalyst	TGA of Spent Catalyst [mass%] Desorption Temperature [°C]			
	<200	200-300	>300	Total
EMT	3.5	2.5	3.0	9.0
0.1%Pt/EMT	3.3	2.2	3.5	9.0
Y	2.0	2.5	2.5	7.0
0.5%Pt/Y	1.5	2.5	3.2	7.2

EMT and Y zeolites both possess a similar Si/Al ratio (see Tables 3.4 and 3.5) but differ slightly in the size of cages, accessibility to the cages and nature / distribution of acid sites. The dependency of the Pt effects on acidic support, emphasizes the sensitivity of catalyst activity to subtle changes in the local acidic environment. It is possible that Al-enriched and Al-depleted regions of EMT, relative to the random Al arrangement on Y zeolite, make EMT less effective at transporting reactive hydrogen.

Alternatively, the dispersion of Pt may be a contributing factor. Pt dispersion on Y zeolite was improved relative to the Pt/EMT systems (see Table 7.2). This could potentially explain why 0.5%Pt/Y would be more effective at facilitating the transport of hydrogen spillover, relative to 0.1%Pt/EMT and 0.5%Pt/EMT and could account for the negative effects imposed by Pt on Y zeolite.

These results suggest that the optimal extent of reactive hydrogen participation (possibly through spillover), represents a fine balance between promoting desorption of the product before consecutive reactions can occur. An adequate population of reactive hydrogen will increase the production of TMP improving alkylate quality. However, excessive amounts of reactive hydrogen, deplete the *tert*-C_4^+ poplulation, encouraging DMH formation and polymerization reactions. This compromises the octane value of the alkylate and expedites the onset of deactivation.

7.2 EFFECT OF Pt ON THE EFFICACY OF REGENERATION

Solid acid catalysts deactivate upon exposure to butene during butene/isobutane alkylation. Efficient regeneration is critical for a successful solid acid catalyst. Measures to improve the efficiency of regeneration are of paramount importance. As mentioned previously, Pt incorporation into the catalyst design could serve a dual purpose. Aside from promoting hydrogen spillover to enhance hydride transfer during butene/isobutane alkylation, Pt can also facilitate oxygen spillover and improve the efficacy of recalcination (Conner & Falconer, 1995). During the regeneration step, spillover oxygen can react with surface carbon, retained in the catalyst pores, and remove it as CH_4 or CO_2. An increase in the amount of reactive oxygen through the spillover, is expected to improve the efficacy of regeneration.

The spent catalysts from the fresh experiments were recalcined *in situ* for the regeneration runs. All spent catalysts (with or without Pt) were retreated in the same manner. Recalcination was performed *in situ* at 325°C for 3 h in 25 sccm of flowing air. This was immediately followed by a re-reduction cycle in which the catalyst bed was maintained at 425°C for 3 h in a flowing mixture of 10.1 % H_2 in Ar at a total flow rate of 2 sccm. Upon completion of the re-reduction step, the experimental procedure and reaction conditions outlined in Section 7.1 were followed.

All experiments employed a reaction temperature of 53°C and an operating pressure of 382 psig, with an I/O ratio of 15 and a $C_4^=$ WHSV of 2.0 h^{-1}. Experiments involving Pt catalysts employed a flowing stream of 1.4 wt% H_2 in an argon/nitrogen mixture, using a combined flow rate of 12 sccm. Those reactions investigating regenerated EMT and Y zeolites utilized a nitrogen stream maintained at 12 sccm.

7.2.1 Effect of Pt on Butene Disappearance for Regenerated Catalysts

The activity of EMT and Y zeolites was not fully recovered by the recalcination treatment. The Useful Catalyst Lifetime periods of regenerated EMT and Y were

notably reduced after retreatment (see Table 7.4). It is possible that residual material was not removed by the reconditioning step and is clogging the catalyst pores, preventing access to all catalytic sites in the subsequent experiment. No attempts were made to optimize the air flow rate or calcination conditions. Optimization of these parameters may improve the efficacy of the regeneration process.

The incorporation of Pt into the pore network improves the efficiency of the regeneration step. The Useful Catalyst Lifetime periods of regenerated 0.1%Pt/EMT and regenerated 0.5%Pt/EMT were comparable to their fresh performance levels (see Table 7.4). Although regenerated 0.5%Pt/Y did not demonstrate the same ability as Pt/EMT systems with respect to recovering the Useful Catalyst Lifetime period, it did exhibit superior regeneration efficacy over Y zeolite.

Table 7.4: Effect of Pt on Useful Catalyst Lifetime of Fresh and Regenerated EMT and Y Systems (T_{calc}=325°C; T_{red}=425°C; T_{rxn}=53°C; P=382psig; I/O=15; $C_4^=$WHSV=2.0h^{-1}; m_{cat}=2.78g; 12 sccm H_2/Ar/N_2 mix with 1.4 wt%H_2 used for Pt runs)

Catalyst	Useful Catalyst Lifetime Period [min]	
	Fresh	Regenerated
EMT	10.6	6.8
0.1%Pt/EMT	9.5	10.1
0.5%Pt/EMT	11.8	10.3
Y	7.9	5.5
0.5%Pt/Y	8.0	6.2

7.2.2 Effect of Pt on C_5+ Product Distribution of Regenerated Catalysts

Cracking activity of regenerated EMT was suppressed during the Useful Catalyst Lifetime period resulting in accumulation of polymerization products in the alkylate (see Figure 7.12). Similar behaviour was observed on Y zeolite, although regeneration appeared more efficient on Y, in terms of recovery of fresh catalyst activity (see Figure 7.13).

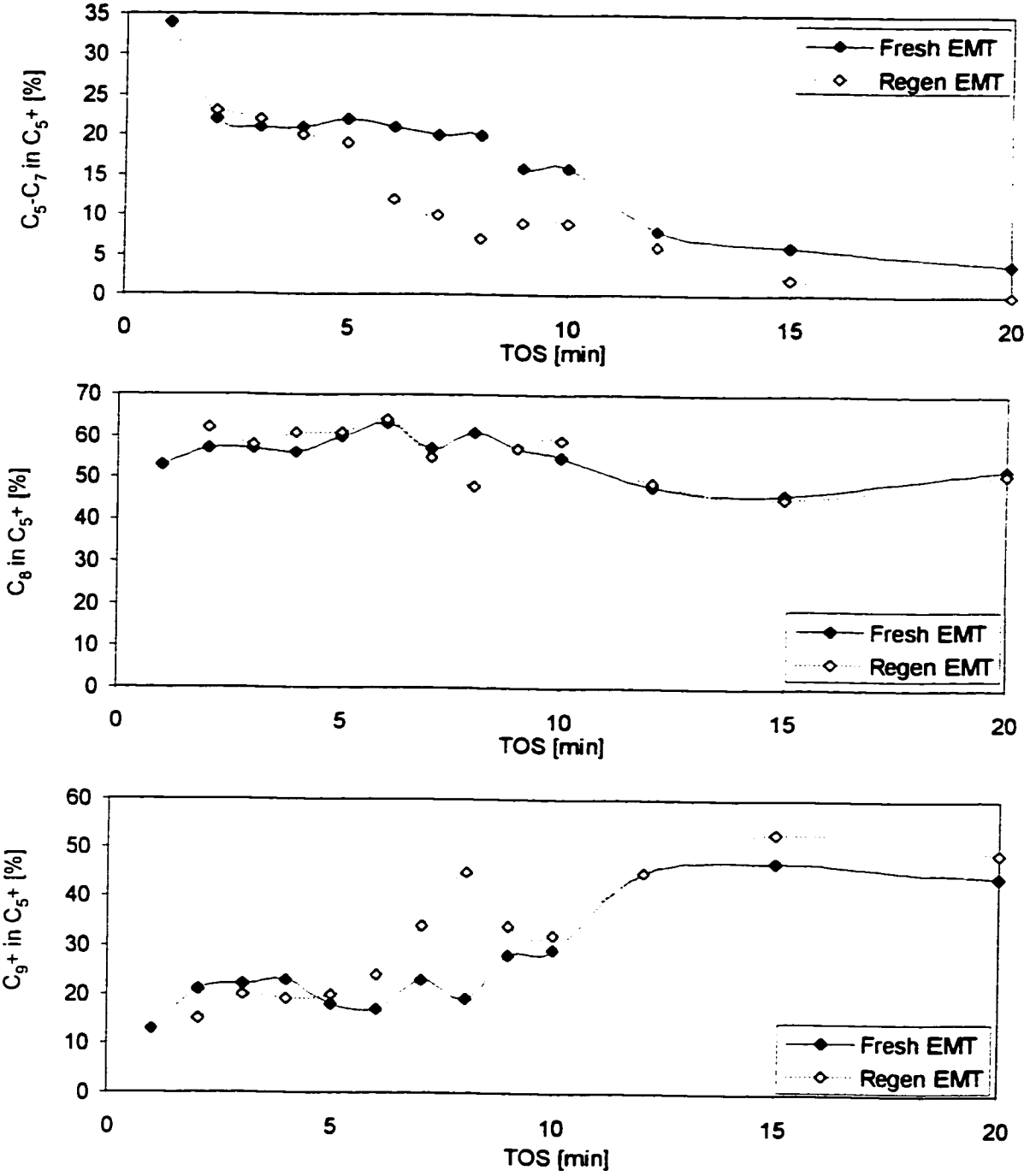

Figure 7.12: Effect of Regeneration on C_5+ Product Distribution of EMT (T_{calc}=425°C; T_{rxn}=53°C; P=382psig; I/O=15; $C_4^=$WHSV=2.0h^{-1}; m_{cat}=2.78g)

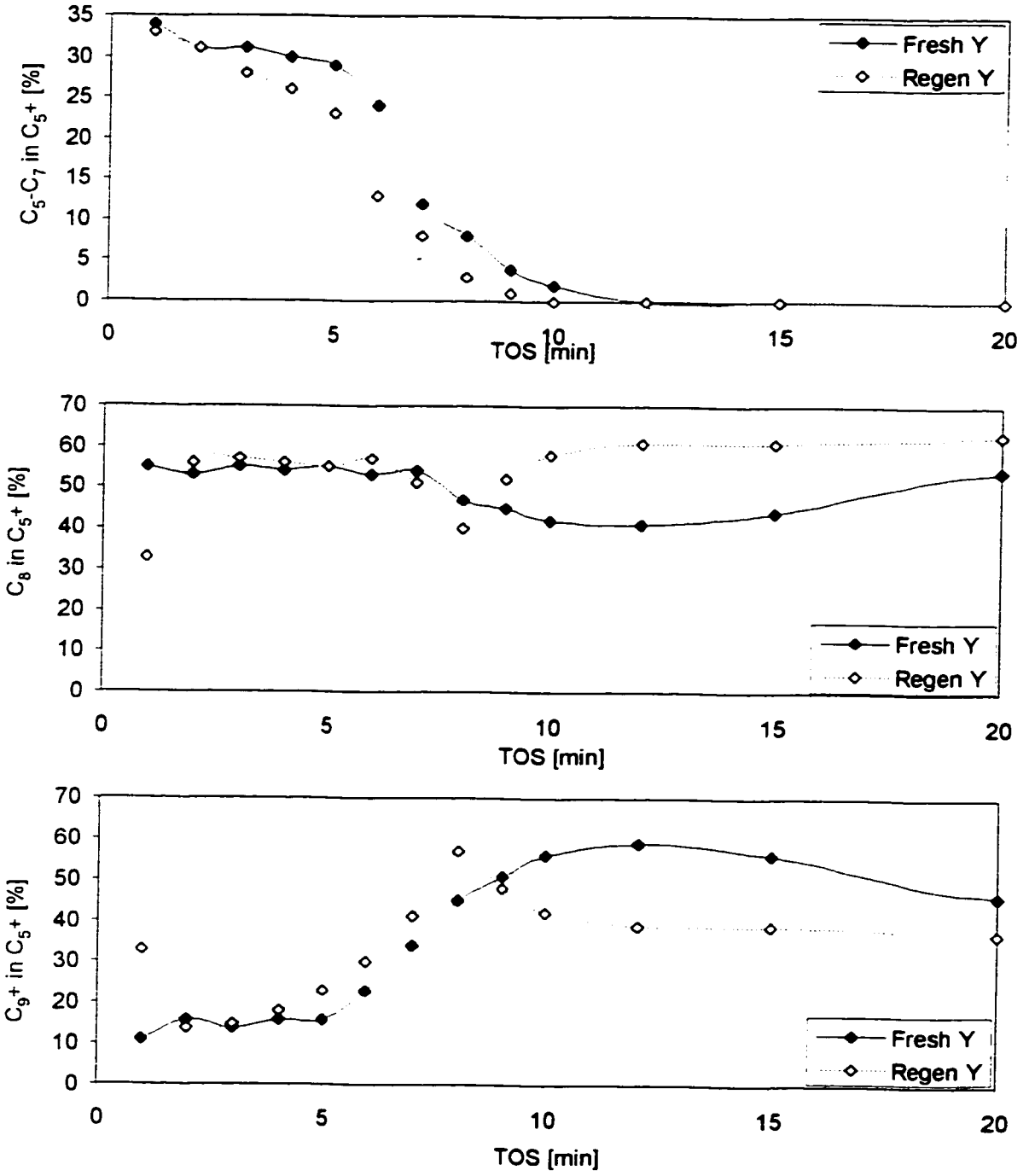

Figure 7.13: Effect of Regeneration on C_5+ Product Distribution of Y (T_{calc}=425°C; T_{rxn}=53°C; P=382psig; I/O=15; $C_4^=$WHSV=2.0h^{-1}; m_{cat}=2.78g)

Alkylation of butene with isobutane demands acid sites of similar strength to those required for cracking reactions (Corma et al, 1994b; Corma & Wojciechowski, 1982; Corma et al, 1994a; O'Young et al, 1994; Corma et al, 1996a). In contrast DMH production, oligomerization and polymerization reactions are facilitated by weaker acid sites. It appears that some strong acid sites are not reclaimed by the regeneration step, and rather promote less demanding reactions such as polymerization.

Impregnation of Pt into the pore network of EMT improved the efficacy of regeneration at both 0.1% (see Figure 7.14) and 0.5 % (see Figure 7.15) Pt loading. High cracking activity was recovered on regenerated Pt/EMT systems irrespective of the Pt loading, matching levels achieved by fresh catalysts. The levels of C_8 and polymerization product levels, were comparable to those obtained by fresh Pt/EMT catalyst systems. This behaviour contradicts regenerated EMT, where enhanced polymerization activity accelerated deactivation processes, abbreviating the Useful Catalyst Lifetime period. This suggests that Pt activates reactive oxygen on Pt/EMT systems during the reconditioning step, improving the extent of removal of retained hydrocarbons on the spent catalyst surface. The activity of strong acid sites on Pt/EMT is recovered more efficiently in the presence of Pt.

The benefits of Pt were not apparent on Y zeolite (see Figure 7.16). Cracking activity was lost at an earlier TOS on regenerated 0.5%Pt/Y relative to fresh performance levels, causing polymerization products to accumulate. The behaviour of Y and 0.5%Pt/Y, in terms of the efficacy of regeneration, is similar with no improvement in catalyst recovery demonstrated by Pt. This contradicts the behaviour of Pt on EMT systems where an improvement in regeneration efficiency was observed.

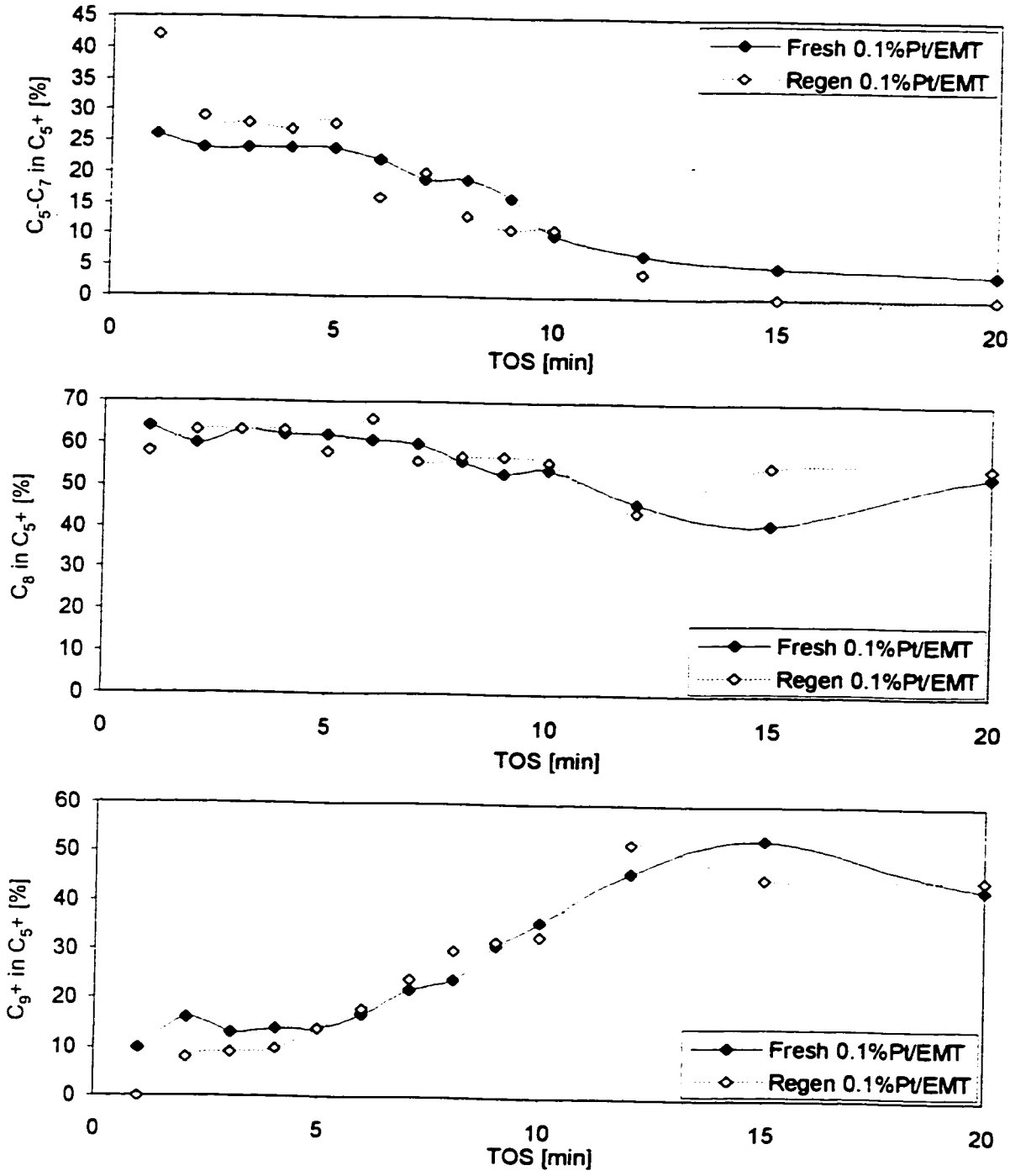

Figure 7.14: Effect of 0.1%Pt Loading on Regeneration of EMT with respect to C_5+ Product Distribution
(T_{calc}=325°C; T_{red}=425°C; T_{rxn}=53°C; P=382psig; I/O=15; $C_4^=$WHSV=2.0h^{-1}; m_{cat}=2.78g; 12 sccm H_2/Ar/N_2 mix with 1.4 wt%H_2 used for Pt runs)

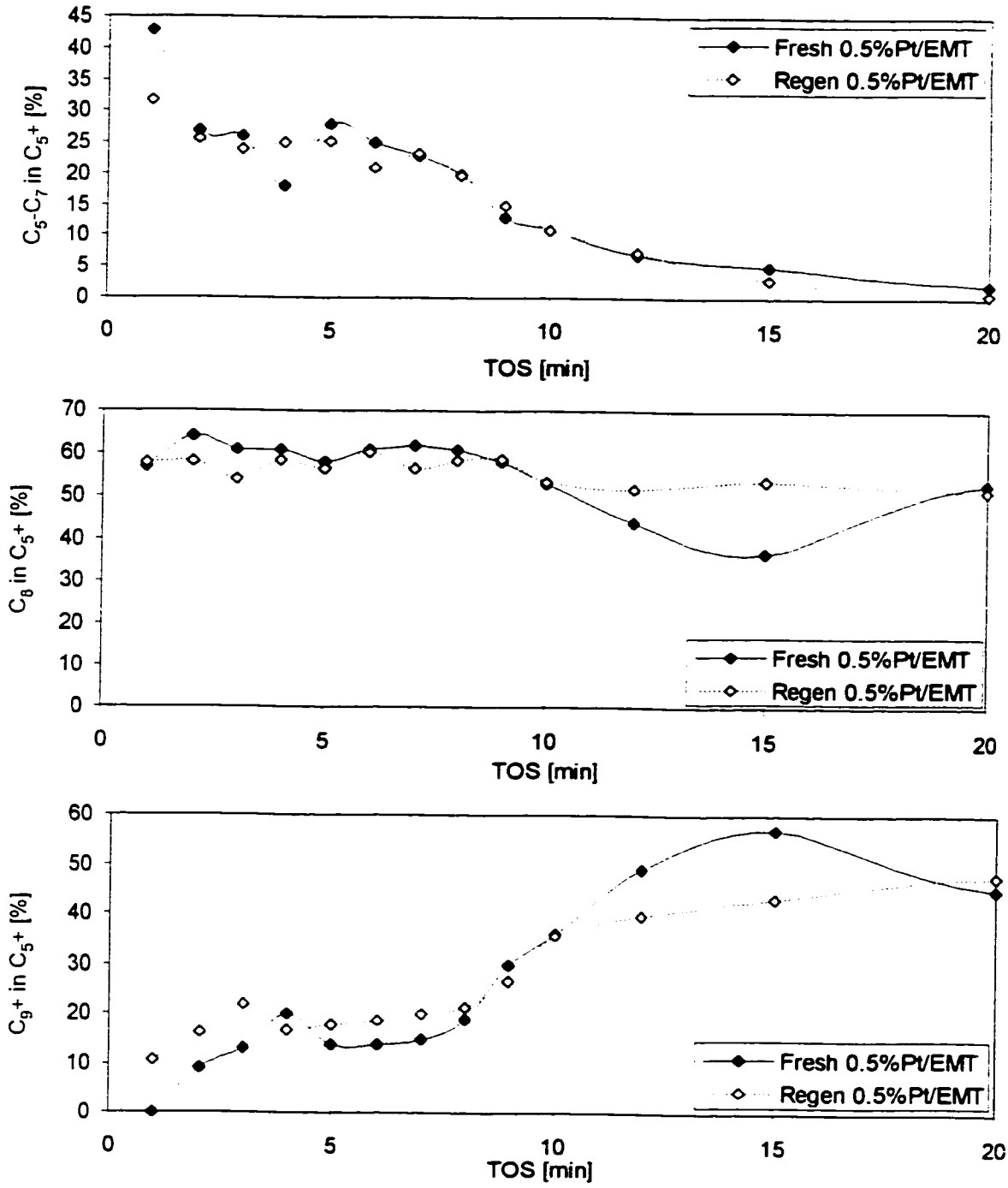

Figure 7.15: Effect of 0.5%Pt Loading on Regeneration of EMT with respect to C_5+ Product Distribution
(T_{calc}=325°C; T_{red}=425°C; T_{rxn}=53°C; P=382psig; I/O=15; $C_4^=$WHSV=2.0h^{-1}; m_{cat}=2.78g; 12 sccm H_2/Ar/N_2 mix with 1.4 wt%H_2 used for Pt runs)

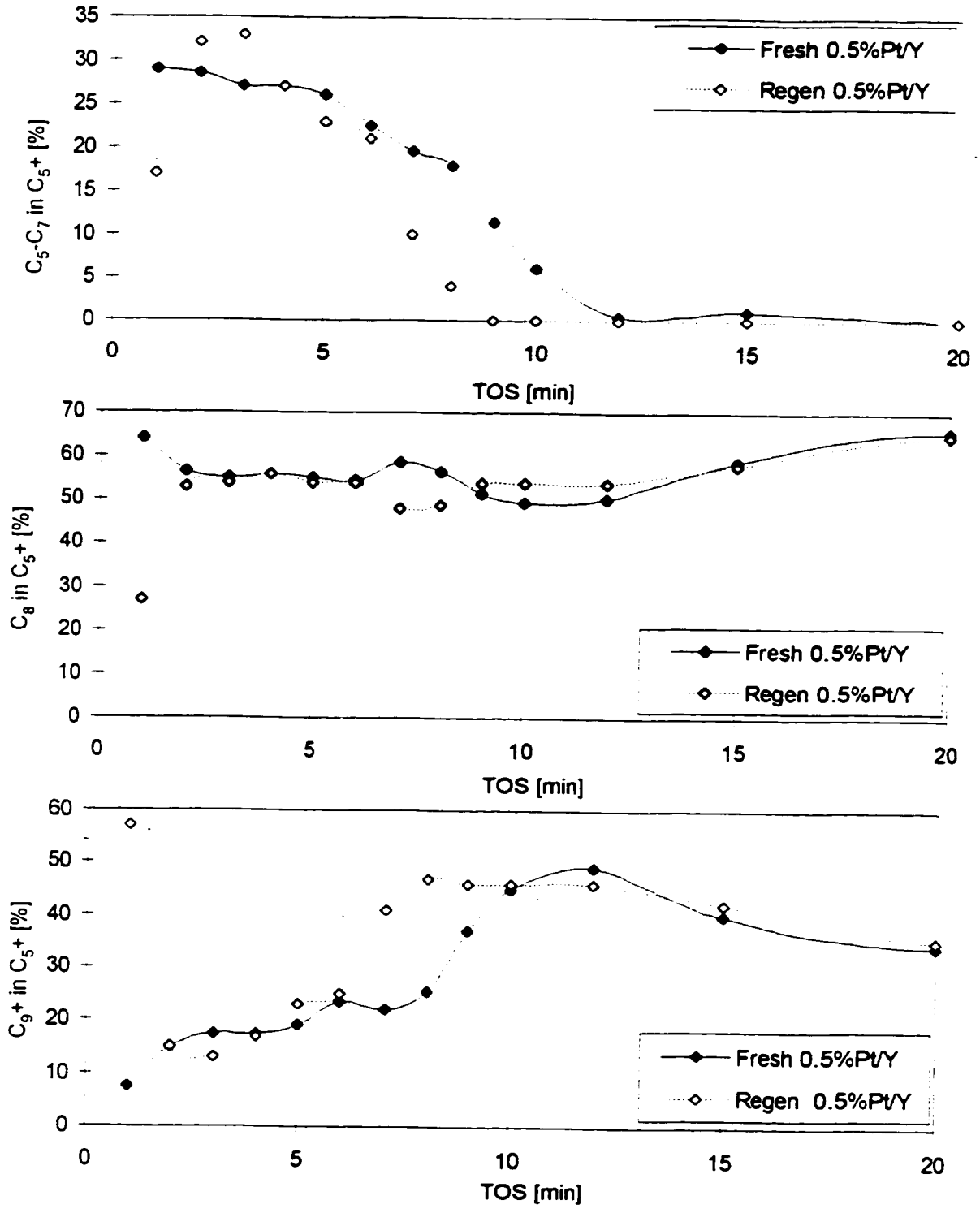

Figure 7.16: Effect of 0.5%Pt Loading on Regeneration of Y with respect to C_5+ Product Distribution
(T_{calc}=325°C; T_{red}=425°C; T_{rxn}=53°C; P=382psig; I/O=15; $C_4^=$WHSV=2.0h^{-1}; m_{cat}=2.78g; 12 sccm H_2/Ar/N_2 mix with 1.4 wt%H_2 used for Pt runs)

7.2.3 Effect of Pt on C_8 Selectivity for Regenerated Catalysts

The content of TMP declined at shorter TOS on regenerated EMT, relative to fresh performance levels (see Figure 7.17). The Useful Catalyst Lifetime period of the retreated catalyst was characterized by declining levels of TMP in the C_8 fraction, creating a larger disparity between fresh EMT and regenerated EMT activity. Initially, lost TMP ability was compensated by elevated DMH production, but as this capability was lost, oligomerization functions became increasingly important.

Note that regenerated EMT still sustained significant DMH production ability while undergoing rapid deactivation. It can be concluded that EMT, in both the fresh and regenerated state, is able to maintain a measurable degree of hydride transfer while deactivating. Unfortunately, it was not able to facilitate this hydride transfer to form TMP products, but rather favoured DMH formation. This is most likely a consequence of lost activity due to incomplete regeneration.

The catalyst Y zeolite revealed slightly different behavior. The regenerated catalyst rapidly lost the ability to produce TMPs from the onset of the reaction (see Figure 7.18). These results are consistent with the explanations discussed for the C_5^+ distribution on Y zeolite. The strong acid sites active for cracking reactions on fresh Y were not completely restored on regenerated Y. As alkylation and cracking reactions demand similar acid strength, it appears that some of the strong acid sites active for alkylation are not reconditioned as well. Instead, these sites become active for DMH production, a reaction that demands a lower acid strength. As this function becomes deactivated with additional exposure to butene, these sites become active for oligomerization activities. Recalcined Y zeolite was not able to sustain DMH production to the same extent observed on recalcined EMT, during the deactivation phase. Rather, retreated Y promoted higher oligomerization activity during this period.

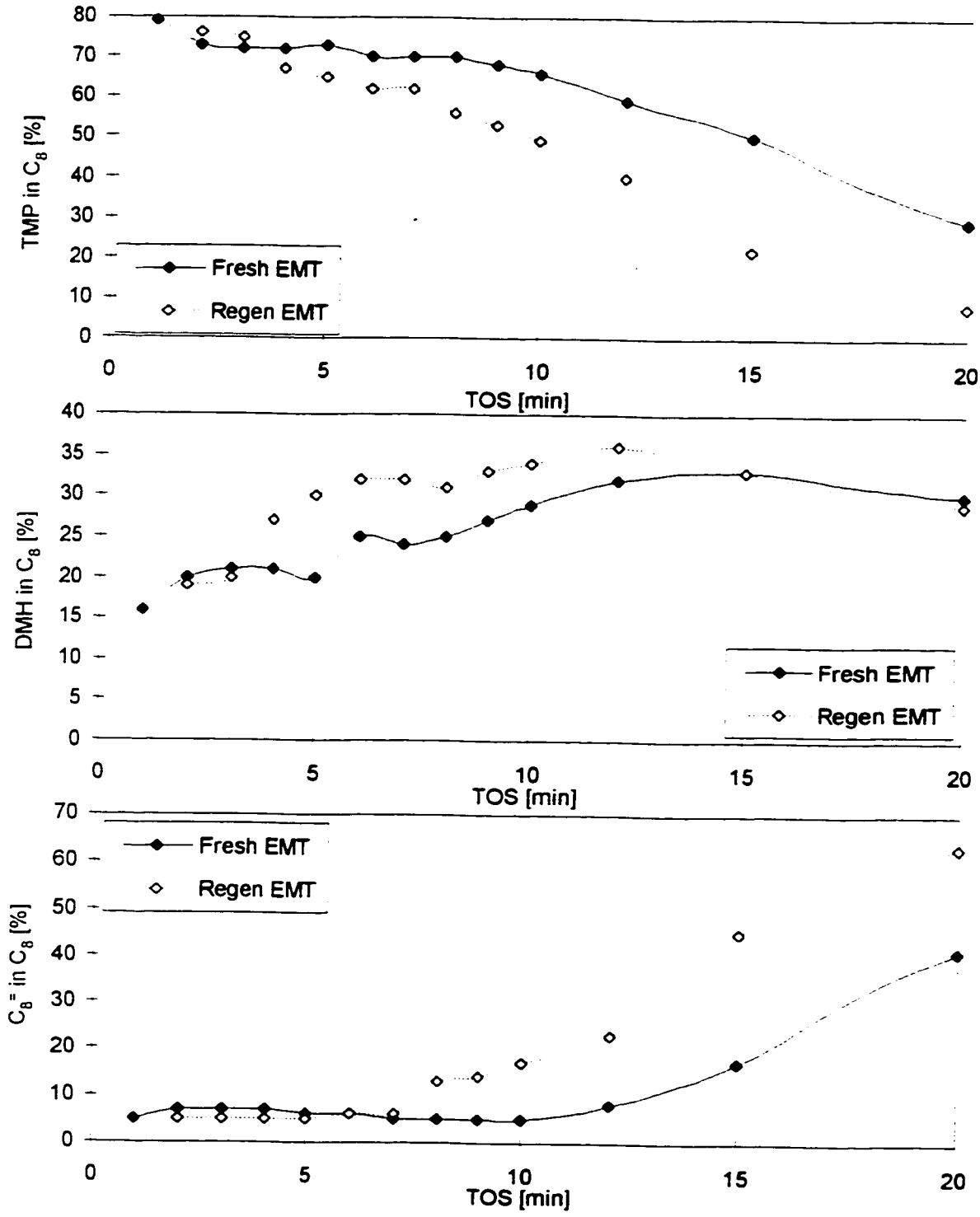

Figure 7.17: Effect of Regeneration on C_8 Selectivity of EMT
(T_{calc}=425°C; T_{rxn}=53°C; P=382psig; I/O=15; $C_4^=$WHSV=2.0h^{-1}; m_{cat}=2.78g)

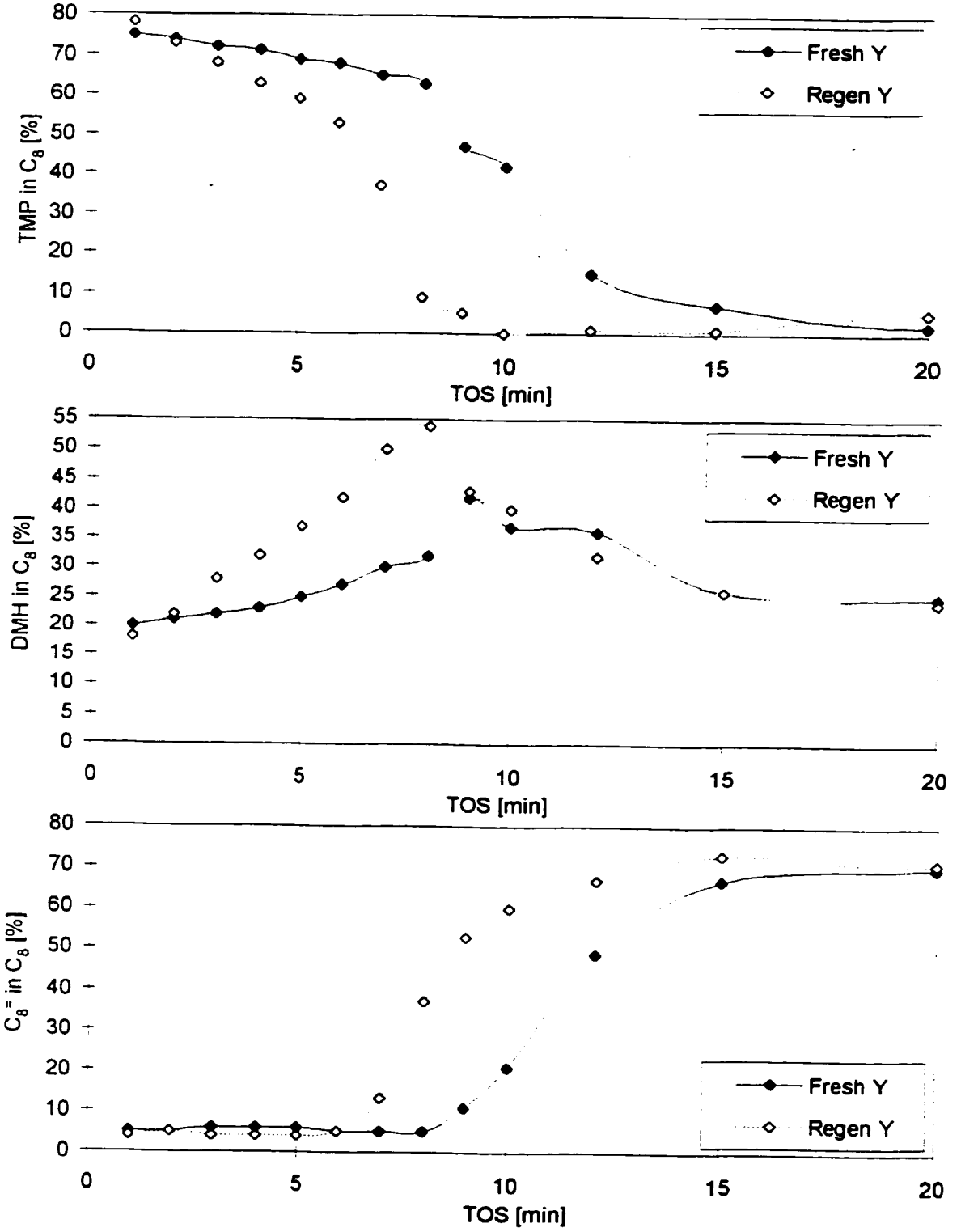

Figure 7.18: Effect of Regeneration on C_8 Selectivity of Y
(T_{calc}=425°C; T_{rxn}=53°C; P=382psig; I/O=15; $C_4^=$WHSV=2.0h^{-1}; m_{cat}=2.78g)

Plateaus regions in the product distributions established on fresh catalysts, were not observed on the regenerated materials when no noble metal was present (see Figures 7.17 and 7.18). The ability to sustain stable catalyst performance appears to be hampered after the regeneration treatment. This suggests that the distribution of acid strength had been altered from the original state in fresh materials.

Catalyst activity was completely restored on regenerated Pt/EMT systems, regardless of the Pt loading. Comparable levels of TMP, DMH and $C_8^=$ were observed on fresh and regenerated 0.1%Pt/EMT (see Figure 7.19) during the Useful Catalyst Lifetime period. Similarly, regenerated 0.5%Pt/EMT produced identical C_8 selectivity levels observed on fresh material (see Figure 7.20).

Although catalyst activity was restored during the Useful Catalyst Lifetime period on regenerated 0.1%Pt/EMT systems, hydride transfer ability was suppressed during the Deactivation period. This resulted in higher $C_8^=$ levels during this phase. This behaviour was not observed on regenerated 0.5%Pt/EMT, suggesting that the reactive hydrogen population was reduced on regenerated 0.1%Pt/EMT.

Regenerated 0.5%Pt/Y did not recover alkylation capacity, with TMP levels declining from the onset of the reaction in favour of increased DMH formation (see Figure 7.21). This imitates the behaviour of regenerated Y zeolite in the absence of the noble metal, suggesting that TMP activity is attributable to Y zeolite with no contribution made by Pt. The benefits of Pt are absent on Y zeolite in the regenerated state, similar to the behviour observed in the fresh state.

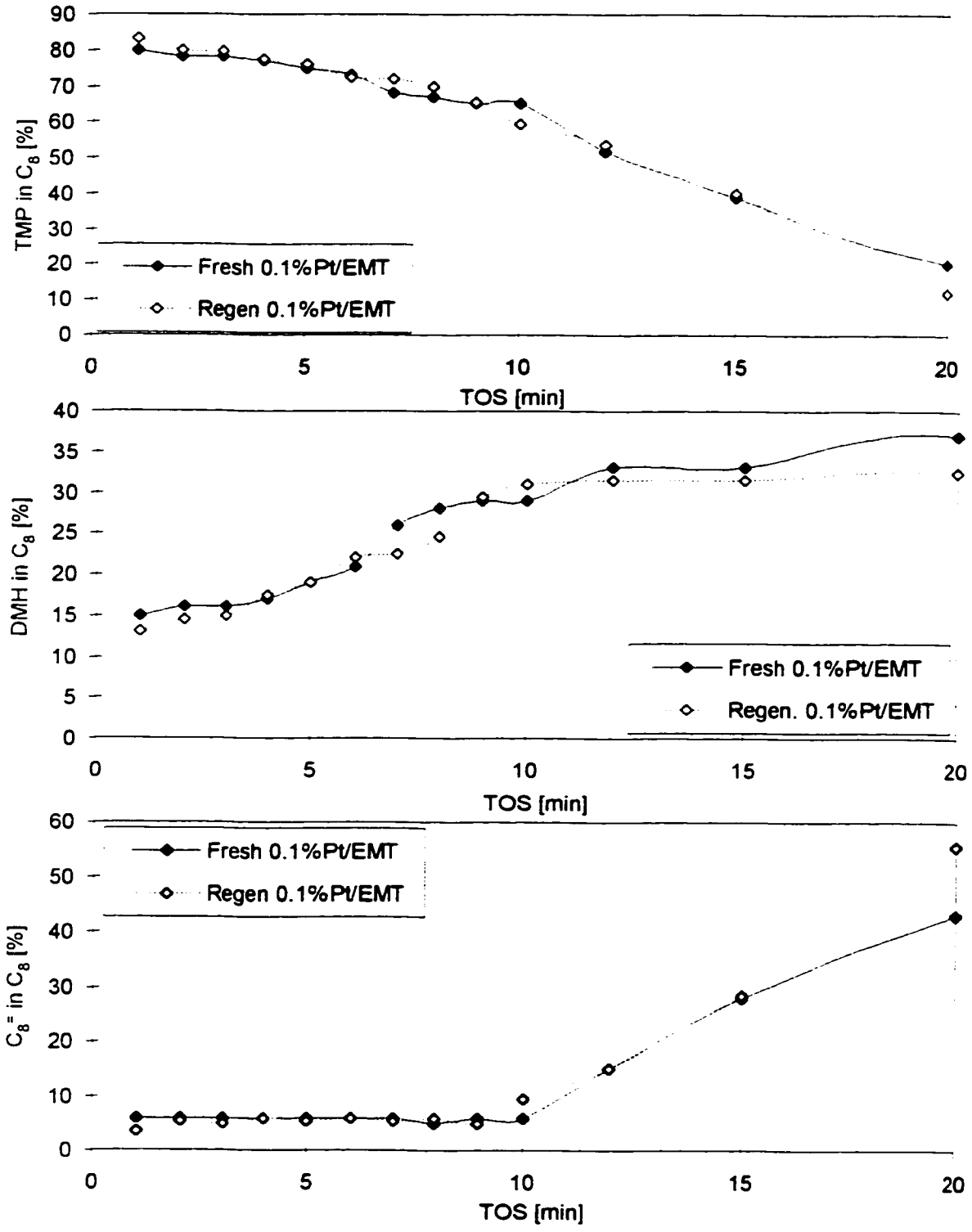

Figure 7.19: Effect of 0.1%Pt Loading on Regeneration of EMT with respect to C_8 Selectivity (T_{calc}=325°C; T_{red}=425°C; T_{rxn}=53°C; P=382psig; I/O=15; $C_4^=$WHSV=2.0h^{-1}; m_{cat}=2.78g; 12 sccm H_2/Ar/N_2 mix with 1.4 wt%H_2 used for Pt runs)

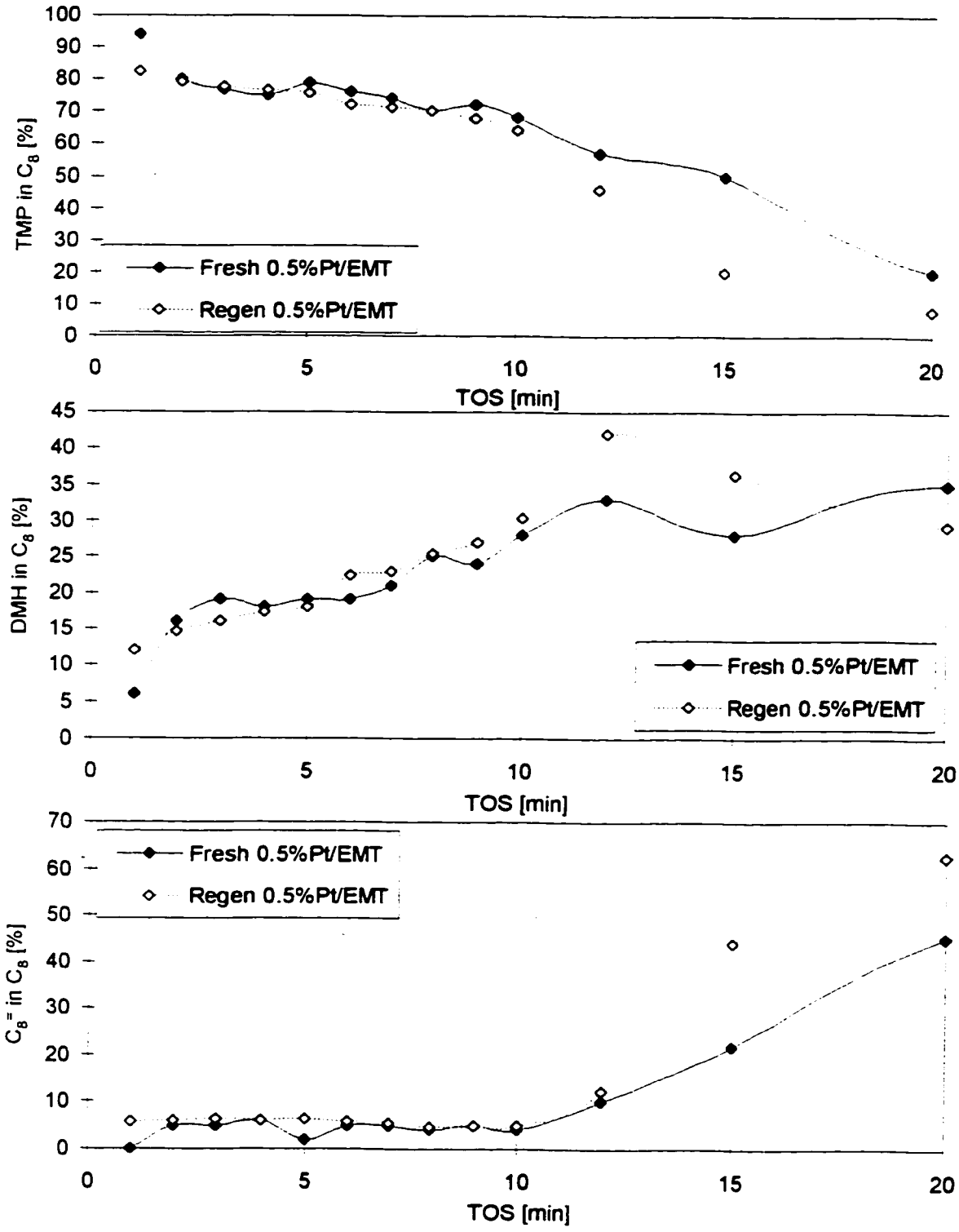

Figure 7.20: Effect of 0.5%Pt Loading on Regeneration of EMT with respect to C_8 Selectivity (T_{calc}=325°C; T_{red}=425°C; T_{rxn}=53°C; P=382psig; I/O=15; $C_4^=$WHSV=2.0h^{-1}; m_{cat}=2.78g; 12 sccm H_2/Ar/N_2 mix with 1.4 wt%H_2 used for Pt runs)

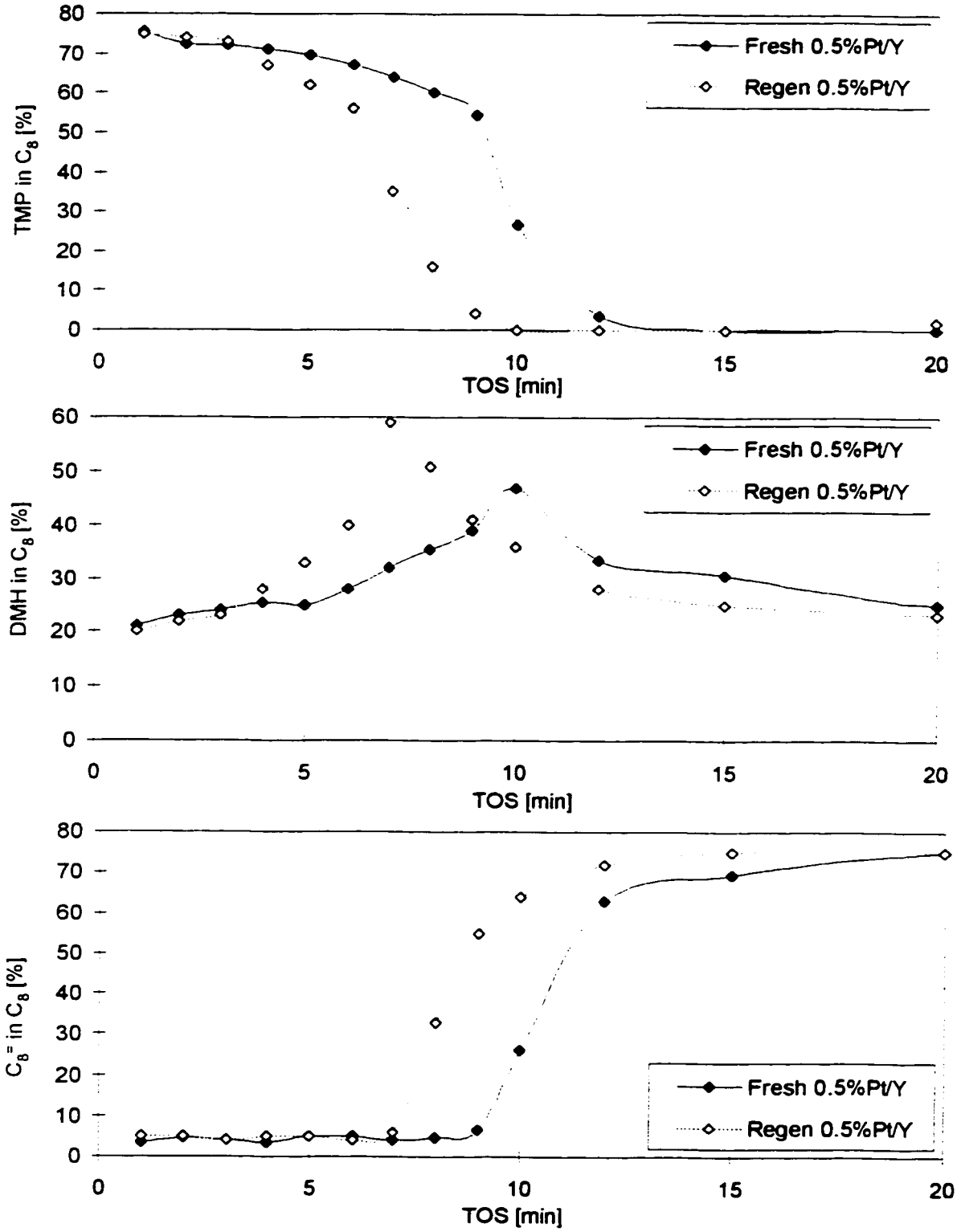

Figure 7.21: Effect of 0.5%Pt Loading on Regeneration of Y with respect to C_8 Selectivity (T_{calc}=325°C; T_{red}=425°C; T_{rxn}=53°C; P=382psig; I/O=15; $C_4^=$WHSV=2.0h^{-1}; m_{cat}=2.78g; 12 sccm H_2/Ar/N_2 mix with 1.4 wt%H_2 used for Pt runs)

7.2.5 Effect of Pt on TMP Selectivity for Regenerated Catalysts

The least sterically hindered isomers, 2,3,3-TMP and 2,3,4-TMP were favoured on recalcined EMT and Y zeolites, in comparison to fresh catalyst performance (see Table 7.5). These effects were not observed in the presence of Pt. Comparable TMP distributions were observed on regenerated and fresh Pt/EMT and Pt/Y systems. The benefits of Pt in improving the efficacy of regeneration hold true, in that the TMP selectivity is recovered more efficiently on regenerated catalysts that incorporate Pt into their design.

7.2.5 Synopsis of Pt Effects for Regenerated Catalysts

Regeneration of EMT and Y zeolites was incomplete in the absence of a noble metal. The Useful Catalyst Lifetime and yield were both reduced on recalcined EMT and Y (see Table 7.5). Some of the strong acid sites responsible for cracking activity and TMP formation in the fresh materials, were not reactivated by the reconditioning treatment. Instead, the regenerated zeolites favoured less demanding reactions, such as DMH production and polymerization activity. The distribution of TMP isomers was altered on recalcined materials relative to fresh material performance, favouring the less sterically hindered isomers, 2,3,4-TMP and 2,3,3-TMP.

Although the hydride transfer was not significantly different on regenerated materials (see (TMP + DMH)/($C_8^=$ + C_9+) ratio in Table 7.3), TGA/DTA data suggest that a greater proportion of hydride transfer was being provided by adsorbed species retained on the catalyst surface (see Table 7.6). High molecular weight, polymeric species, demanding high temperatures to desorb (T_d>300°C in TGA analysis) were detected. These are formed when extensive hydride transfer is provided by hydrocarbons trapped inside the catalyst pores.

Table 7.5: Comparison of Average Catalyst Activity during First 5 min of Useful Catalyst Lifetime Period for Regenerated Parent and Supported Catalysts (T_{calc}=325°C; T_{red}=425°C; T_{rxn}=53°C; P=382psig; I/O=15; $C_4^=$WHSV=2.0h^{-1}; m_{cat}=2.78g; 12 sccm H_2/Ar/N_2 mix with 1.4 wt%H_2 used for Pt runs)

Run	F66EMT F68EMT F67EMTr	F62Pt1EMT F45Pt1EMTr F63Pt1EMTr	F49Pt5EMT F48Pt5EMTr F60Pt5EMTr		F54Y F55Yr		F44Pt5Y F56Pt5Y F58Pt5Yr	
Catalyst System	EMT	0.1% Pt/EMT	0.5% Pt/EMT	Sensitivity	Y		0.5 % Pt/Y	
	Frsh. Reg.	Frsh. Reg.	Frsh. Reg.		Frsh. Reg.		Frsh. Reg.	
Pt Dispersion [%]	n.a.	74	76		n.a.		91	
Useful Catalyst Lifetime Period ($C_4^=$ Conv > 80%) [min]	10.6 6.8	9.5 10.1	11.8 10.3	± 0.7	7.9	5.5	8.0	6.2
Yield [gC_5^+/gcat/g$C_4^=$fed]	.083 .062	.078 .079	.095 .092	± 0.016	.068	.050	.063	.051
C_5^+ Dist. [mass %]								
C_5-C_7	25 21	24 25	28 24	± 2.3	31	28	28	26
C_8	58 61	62 62	61 57	± 2.5	55	52	57	49
C_9^+	17 18	14 13	11 19	± 3.7	14	20	15	25
C_8 Dist. [mass %]								
TMP	75 71	77 77	81 75	± 3.3	72	68	71	70
DMH	19 24	17 18	15 19	± 2.7	22	28	25	25
$C_8^=$	6 5	6 5	4 6	± 0.8	6	4	4	5
TMP Dist. [%]								
2,2,4-TMP	38 31	36 38	33 41	± 2.5	41	37	35	38
2,2,3-TMP	18 10	17 17	14 16	± 2.1	7	5	4	5
2,3,4-TMP	17 27	18 18	20 16	± 2.1	21	25	28	25
2,3,3-TMP	27 32	28 27	33 27	± 2.4	31	33	33	32
Indicators [mass fract.]								
TMP / DMH	4.2 3.08	4.7 4.5	6.6 4.1	± 0.57	3.3	2.7	2.9	2.9
TMP + DMH / $C_8^= + C_9^+$	2.78 2.68	3.47 4.74	3.73 2.87	± 0.63	3.03	2.43	3.35	2.29
2,2,4-TMP + 2,2,3-TMP / 2,3,3-TMP + 2,3,4-TMP	1.28 0.70	1.17 1.34	0.90 1.32	± 0.20	0.91	0.73	0.63	0.75

7.2.5 Effect of Pt on TMP Selectivity for Regenerated Catalysts

The least sterically hindered isomers, 2,3,3-TMP and 2,3,4-TMP were favoured on recalcined EMT and Y zeolites, in comparison to fresh catalyst performance (see Table 7.5). These effects were not observed in the presence of Pt. Comparable TMP distributions were observed on regenerated and fresh Pt/EMT and Pt/Y systems. The benefits of Pt in improving the efficacy of regeneration hold true, in that the TMP selectivity is recovered more efficiently on regenerated catalysts that incorporate Pt into their design.

7.2.5 Synopsis of Pt Effects for Regenerated Catalysts

Regeneration of EMT and Y zeolites was incomplete in the absence of a noble metal. The Useful Catalyst Lifetime and yield were both reduced on recalcined EMT and Y (see Table 7.5). Some of the strong acid sites responsible for cracking activity and TMP formation in the fresh materials, were not reactivated by the reconditioning treatment. Instead, the regenerated zeolites favoured less demanding reactions, such as DMH production and polymerization activity. The distribution of TMP isomers was altered on recalcined materials relative to fresh material performance, favouring the less sterically hindered isomers, 2,3,4-TMP and 2,3,3-TMP.

Although the hydride transfer was not significantly different on regenerated materials (see (TMP + DMH)/($C_8^=$ + C_9+) ratio in Table 7.3), TGA/DTA data suggest that a greater proportion of hydride transfer was being provided by adsorbed species retained on the catalyst surface (see Table 7.6). High molecular weight, polymeric species, demanding high temperatures to desorb (T_d>300°C in TGA analysis) were detected. These are formed when extensive hydride transfer is provided by hydrocarbons trapped inside the catalyst pores. The quantity of high molecular weight (T_d>300°C) material was augmented on the regenerated parent materials (see Table 7.6). These species act as coke precursors and are expected to abbreviate the

Useful Catalyst Lifetime and reduce the active surface area, in agreement with the experimental results for regenerated EMT and Y.

Pt, incorporated into the pore network of EMT, notably improved the efficacy of regeneration, independent of Pt loading. Similar Useful Catalyst Periods and yields were observed for all recalcined Pt/EMT systems, relative to their fresh performance levels (see Table 7.5). It is believed that the noble metal activates reactive oxygen, thus improving the removal of byproduct coke.

Table 7.6: Effect of Pt on TGA/DTA Measurements of Regenerated Catalysts (T_{calc}=325°C; T_{red}=425°C; T_{rxn}=53°C; P=382psig; I/O=15; $C_4^=$WHSV=2.0h^{-1}; m_{cat}=2.78g; 12 sccm H_2/Ar/N_2 mix with 1.4 wt%H_2 used for Pt runs)

Catalyst System	Catalyst State for Expt	SA of Spent Catalyst [m^2/g]	TGA of Spent Catalyst [mass%] Desorption Temperature [°C] <200	200-300	>300	Total
EMT	Fresh	377	3.5	2.5	3.0	9.0
	Regen	287	1.5	1.0	5.0	7.5
0.1%Pt/EMT	Fresh	263	3.3	2.2	3.5	9.0
	Regen	243	3.6	2.9	3.3	9.8
Y	Fresh	372	2.0	2.5	2.5	7.0
	Regen	n.a.	1.0	0.4	5.5	6.9
0.5%Pt/Y	Fresh	270	1.5	2.5	3.2	7.2
	Regen	280	1.9	2.3	3.0	7.2

The catalyst system employing a Pt loading of 0.1 % on EMT, displayed comparable results to fresh material performance. No significant differences were found in alkylate quantity or quality. TGA/DTA analysis of the spent recalcined catalyst, suggests that hydride transfer from adsorbed species in the pore network was not faciltated extensively (see Table 7.6). Similar spent surface areas were measured for fresh and regenerated 0.1%Pt/EMT, whereas a notable loss was observed between fresh and regenerated EMT.

The positive benefits of Pt on EMT were maintained at a higher Pt loading. Increasing the Pt loading to 0.5 % on EMT achieved similar results to those observed for regenerated 0.1%Pt/EMT, with respect to lifetime and yield.

The benefits of Pt, on the efficacy of EMT regeneration, were not apparent on recalcined 0.5%Pt/Y. The Useful Catalyst Lifetime period and yield were reduced on recalcined 0.5%Pt/Y relative to fresh performance levels (see Table 7.4). Polymerization levels are notably higher and C_8 production reduced on regenerated 0.5%Pt/Y. TGA/DTA measurements suggest that the diminished activity of the catalyst, was not a consequence of increased hydride transfer from adsorbed species, retained in the catalyst pores (see Table 7.6). Spent surface area provide additional support for this hypothesis, in that no significant difference was found between fresh versus regenerated surface area measurements for 0.5%Pt/Y experiments.

It was previously suggested that 0.5%Pt/Y may promote excessive reactive hydrogen involvement in the fresh state. Perhaps this same behaviour occurs with respect to reactive oxygen promotion. It is possible that 0.5%Pt/Y becomes sintered during regeneration, reducing Pt dispersion to low levels. This hypothesis is consistent with the behaviour of regenerated 0.5%Pt/Y, in that this catalyst appears to behave like Y zeolite in all respects. This re-emphasizes the sensitivity of the catalyst performance to Pt effects and the fine balance that must be achieved to produce beneficial results.

Chapter 8

Conclusions

Four distinct stages of catalyst activity and selectivity were observed for the alkylation of butene with isobutane in a flow reactor. The "Initial Activity" period was a brief phase of high catalyst activity of less than 1 min in duration. The "Useful Catalyst Lifetime" period represented the second stage of catalyst activity, and was characterized by butene conversion in excess of 80 %. Approximately half of the alkylate consisted of C_8 products, with TMPs accounting for approximately 60 to 80 % of the C_8 fraction. The isomer 2,2,4-TMP was the dominant product in the TMP

fraction. As butene conversion levels declined below 80%, the commencement of the "Rapid Deactivation" phase was marked. The loss in hydride transfer function favoured oligomerization and polymerization reactions. Cracking activity was completely lost during this phase. The final stage of catalyst activity was the "Oligomerization" phase, characterized by butene conversion levels below 40 %. The C_5+ liquid consisted of mainly $C_8^=$ and C_9+ products.

The effect of calcination temperature is consistent with the hypothesis that the alkylation mechanism is promoted by a Bronsted acid site. A calcination temperature of 425°C, which favours a higher density of Bronsted acid sites on both Y and EMT zeolites, effectively facilitated hydride transfer resulting in more saturated branched C_8 molecules being formed. Alkylation activity was sustained for a longer duration and the onset of deactivation was delayed, when a calcination temperature of 425°C was employed on both EMT and Y zeolites.

In contrast, a calcination temperature of 540°C, which increases Lewis acidity at the expense of reduced Bronsted acidity, had a detrimental effect on hydride transfer and favoured oligomerization and polymerization reactions over production of saturated compounds. High molecular weight species were retained on the acid sites, leading to rapid loss in catalyst surface area, accelerating the onset of deactivation. As a result, a shorter Useful Catalyst Lifetime was observed for catalysts calcined at 540°C.

Low reaction temperatures in the vicinity of 30°C, resulted in low butene conversion and favoured predominantly polymerization products. Reaction temperatures approaching 100°C promoted cracking activity, jeopardizing the stability of alkylate precursors. The optimal reaction temperature represents a compromise between cracking polymerization products without degrading alkylate quality.

No alkylate was produced when using pure isobutane as the feed, suggesting that the presence of small amounts of olefin are necessary to initiate the mechanism. A low olefin WHSV favoured alkyation reactions, and discouraged oligomerization and polymerization activities. The estimated number of successful catalyst cycles per active site was improved when the feed was less concentrated in the olefin.

Unfortunately, the preferential adsorption of the olefin over the isoparaffin made deactivation an inevitable outcome, regardless of the feed composition.

A definite trend in surface area loss with increasing Butene Exposure Index was observed. It appears that the catalyst acts as a sponge adsorbing butene from the feed, saturating the surface with oligomers. The isoparaffin acts as a diluent, rather than as a competitive reactant. Hence feed, which is more dilute in the olefin, simply takes longer to saturate all of the acid sites with oligomers of butene. This emphasizes the poor suitability of the fixed bed reactor for this reaction.

This hypothesis is consistent with the modest improvement in the number of successful catalyst cycles which was calculated for a significant decrease in the butene WHSV. Further evidence was provided by a cyclical feed study. Restoration in catalyst activity for a deactivating catalyst was remarkable after an isobutane flush period. In addition, the loss in active surface area of the catalyst was suppressed with cyclical feed operation relative to uninterrupted delivery.

The cleansing benefits of washing the catalyst with isobutane could be explored in catalytic distillation, which combines reaction and distillation in one process. Situating the reaction section near the top of the column and operating under total reflux, will increase the local I/O ratio. The distillation process will naturally remove the product from the reaction section, discouraging continued reaction of the product. This mode of reactor geometry may offer some promise for this challenging reaction, if a suitable solid acid catalyst is found.

The composition of the alkylate produced from EMT and Y zeolite was similar. However, EMT revealed superior resistance to deactivation relative to Y zeolite, in terms of extending the Useful Catalyst Lifetime by 41 % and increasing the yield by 16%. This behavior may be a consequence of the unique distribution of acid sites on EMT, which discourages deactivation processes. Alternatively, EMT may possess improved ability to adsorb isobutane relative to Y. An increase in the local I/O ratio is expected to improve catalyst lifetime as demonstrated by olefin WHSV studies.

TGA/DTA analysis revealed that the distribution of material retained on the spent EMT, was more heavily weighted toward low desorption temperatures relative to that measured on spent Y. It is speculated that the greater preference for olefin adsorption demonstrated by Y zeolite enhanced polymerization reactions, blocking access to acid sites deeper in the catalyst granule. In contrast, the uneven arrangement of acid sites in EMT may suppress the extent of this process.

A loading of 0.1 % Pt/EMT did not produce a significant effect on the Useful Catalyst Lifetime period or alkylate quality of the fresh catalyst, in the presence of hydrogen. A marginal improvement in the fraction of C_8 produced in C_5+ liquid was observed. It may be that a loading of 0.1 % Pt on EMT, was inadequate to generate a sufficient population of reactive hydrogen to produced a notable effect.

An improvement in fresh catalyst performance was achieved using a higher loading of Pt on EMT. Impregnation of 0.5 % Pt/EMT modestly extended the Useful Catalyst Lifetime period in a hydrogen containing environment, over fresh EMT. Although the product yield was not significantly altered by the presence of Pt, alkylate quality was notably enhanced. Polymerization activity and DMH production were suppressed and TMP formation promoted on 0.5 % Pt/EMT relative to EMT.

A similar loading of Pt on Y zeolite did not produce positive benefits in a hydrogen atmosphere. No significant change in the Useful Catalyst Lifetime period was detected. Although alkylate quality was not notably altered by Pt presence, a slight increase in DMH levels was observed.

The enhanced catalyst performance on Pt catalyst systems in the presence of hydrogen, does not appear to be a result of butene hydrogenation. Elevated *n*-butane levels were not detected in the effluent and catalyst yield was not compromised by Pt incorporation.

It was proposed that reactive hydrogen, such as hydrogen spillover, was responsible for the positive benefits in catalyst performance. A minimum amount of Pt was necessary, to generate an adequate population of reactive hydrogen species to effect a measurable change. A Pt loading of 0.1 % on EMT in the presence of hydrogen, was insufficient to meet the activity demands of alkylation. In contrast,

increasing the loading to 0.5 % Pt on EMT in the presence of hydrogen, developed an adequate population of reactive hydrogen species, improving the ability of the catalyst to desorb TMP product.

It is suggested that Y zeolite was more effective at transporting reactive hydrogen species than EMT. Hence, the population of reactive hydrogen species was overdeveloped for 0.5 % PT/Y. Excessive involvement of reactive hydrogen occurred, compromising the stability of the *tert*-C_4^+ cation population. This favoured DMH formation and accelerated deactivation. A balance between active participation of isobutane and reactive hydrogen is essential to improve alkylate quality and extend the Useful Catalyst Lifetime.

The benefits of Pt are reiterated in regenerated catalyst performance. Both EMT and Y revealed a notable loss in catalyst activity with respect to yield and alkylate quality after regeneration. Impregnation of Pt onto the catalyst surface of EMT, resulted in almost complete restoration of catalyst activity and recovery of the Useful Catalyst Lifetime period. The presence of Pt on Y zeolite, did not produce the same benefits as were observed on EMT. The yield and Useful Catalyst Lifetime period were reduced on regenerated 0.5%Pt/Y relative to those observed in the fresh state, but resembled those achieved on regenerated Y. This behaviour was attributed to excessive involvement of reactive oxygen during regeneration, which may sinter the catalyst and reduce Pt dispersion significantly.

It is concluded that Pt can serve a dual purpose in catalyst design. Firstly, regulated participation of hydrogen spillover can improve catalyst lifetime and alkylate quality. Secondly, incorporation of Pt into the catalyst system will promote oxygen spillover during the recalcination step, improving the efficacy of the regeneration treatment. The challenge for the catalyst design, is to promote reactive hydrogen involvement to improve desorption of TMP, but not encourage excessive involvement as this favours DMH formation.

Chapter 9

Recommendations

EMT reveals interesting behavior in terms of its ability to promote hydride transfer and suppress deactivation. An adsorption study employing FTIR measurements could compare the adsorption abilities of *i*-C_4 relative to $C_4^=$ on EMT and Y zeolites. These measurements would be useful in explaining catalytic behaviour towards alkylation.

Acidity estimates are largely dependent upon the method of measurement and constants (i.e. extinction coefficients of adsorbate when using TPD/FTIR technique) applied in the calculations. Comparison of acidity estimations is most reliable when the same method is applied for all materials and identical operating conditions employed for the analysis. The literature acidity measurements for EMT and Y, do not utilize the same extinction coefficients for TPD/FTIR pyridine desorption correlations. Results were re-calculated using a single set of extinction coefficients. However, this introduces a degree of uncertainty when attempting to qualify catalytic behavior in terms of differences in acidities.

A significant contribution to this study would be acidity measurements using FTIR/TPD with pyridine as the adsorbate. This will provide important information regarding the nature and strength of acid sites on EMT relative to Y zeolite. The effect of calcination temperature on Lewis and Bronsted acidity, could also be acertained using TPD/FTIR pyridine desorption measurements. This is particularly important to rationalize the catalytic differences observed with respect to product selectivity, alkylate yield and duration of Useful Catalyst Lifetime.

The hydride transfer ability of EMT and Y zeolite could be compared through characterization of the carbonaceous deposits on the spent catalysts. UV-VIS spectra of spent catalysts would provide information of the chain length of adorbed species, offering insight into the mechanism responsible for deactivation. The carbon bonding environment of adsorbed species could be investigated through ^{13}C CP/MAS NMR measurements to assess the degree of unsaturation of the adsorbed species. The effect of I/O ratio on the quality and quantity of the deposit could also be examined in this study, as this process variable is known to exert a positive influence on suppressing the rate of deactivation.

The positive benefits of Pt in terms of promoting hydrogen spillover, needs to be substantiated through replicated experiments. Catalyst preparation for this study should employ the exchange method for Pt incorporation, as this technique yields a more uniform distribution of Pt, relative to that achieved with the incipient wetness approach.

Performance of the exchanged materials could be assessed to confirm the distinctive differences noted with Pt incorporation into the catalyst design. The effect of hydrogen flow rate during the reduction step, as well as during the reaction, could be explored. Variation in air flow rate during recalcination could also be studied, to determine whether a preferred rate exists in terms of restoring catalyst activity on regenerated catalysts.

The equipment employed for hydrogen chemisorption measurements, reveals high variability in Pt dispersion estimations for the Pt standard sample. Undoubtedly, uncertainty in Pt dispersion measurements for prepared catalyst systems could significantly affect interpretation of results. Reliable estimates are necessary to accurately characterize the catalysts systems so that these properties can be related to catalyst activity with confidence.

Evidence of hydrogen spillover could be assessed using an approach outlined by Ohgoshi et al, 1993. Zeolite A is prepared in the presence of a cationic platinum complex (Weisz et al, 1962), trapping the platinum within the cavities during the formation of the crystalline material (Pt-A). Butene and isobutane are too large to fit through the 5 Å port dimensions of A zeolite, shielding the Pt atoms from these reactants.

The Pt-A could be physically mixed with EMT to form a hybrid catalyst. The performance of the hybrid catalyst could be compared to EMT, where no spillover activator is provided. If the results of the two experiments are similar, this suggests that hydrogen spillover is not contributing an important effect to the reaction. Note that this criteria assumes that the distance of separation between the activator (Pt in A zeolite) and the acceptor (acid sites of EMT) phases is within the mobility range of spillover hydrogen. Evidence of hydrogen spillover participation is indicated by detectable differences in catalyst performance of the hybrid catalyst with EMT.

The method of bulk liquid collection could be improved, to enhance the accuracy of yield measurements and mass balance. The separator of the BTRS system could be explored for this application. A chilled fluid could flow through the copper coil surrounding the separator, to condense liquid product for the purpose of

bulk collection. Effluent gases from the separator could be measured and collected for bulk gas analysis.

Catalytic distillation may offer some promise for this reaction. The viability of this recommendation may be questioned, as this equipment is expensive to operate and requires stable catalyst activity.

A fixed bed reactor is poorly suited to butene/isobutane alkylation. It is worthwhile to consider a CSTR for this reaction, as higher local I/O ratios can be achieved using this reactor geometry. The BTRS supports the use of an external reactor permitting connection of a CSTR with minor equipment modifications. Cyclical feed flow could be explored to assess catalyst behaviour toward deactivation in a CSTR reactor environment.

REFERENCES

Aimoto, K., Fujimoto, K., Maeda, K., "Hydroisomerization of *n*-Pentane over Hybrid Catalysts Containing Supported Hydrogenation Catalyst", Studies in Surface Science and Catalysis 77, Inui, T., Fujimoto, K., Uchijima, T., Masai, M. (Eds.), 165-169 (1993)

Albright, L. F., Spalding, M. A., Kopser, C. G., Eckert, R. E., "Alkylation of Isobutane with C_4 Olefins. 2. Production and Characterization of Conjunct Polymers", Ind. Eng. Chem. Res. 27, 386-391 (1988)

Albright, L. F., Kranz, K. E., "Alkylation of Isobutane with Pentenes Using Sulfuric Acid as a Catalyst: Chemistry and Reaction Mechanisms", Ind. Eng. Chem. Res. 31, 475-481 (1992)

Albright, L. F., Kranz, K. E., Masters, K. R., "Alkylation of Isobutane with Light Olefins: Yields of Alkylates for Different Olefins", Ind. Eng. Chem. Res. 32, 2991-2996 (1993)

Annen, M. J., Young, D., Arhancet, J. P., Davis, M. E., Schramm, S., "Investigations into the Nature of the Hexagonal Polytype of Faujasite", Zeolites 11, 98-102 (1991)

Beck, J. S., Vartuli, J. C., Roth, W. J., Leonowics, M. E., Kresge, C. T., Schmitt, K. D., Chu, C. T-W., Olson, D. H., Sheppard, E. W., McCullen, S. B., Higgins, J. B., Schlenker, J. L., "A New Family of Mesoporous Molecular-Sieves Prepared with a Liquid Crystal Template" J. Am. Chem. Soc. 114, 10834-10843 (1992)

Bell, A. T., Manzer, L. E., Chen, N. Y, Weekman, V. W., Hegedus, L. L., Pereira, C. J., "Protecting the Environment through Catalysis", Chem. Eng. Prog., 26-34, Feb. (1995)

Benassi, E., Chapus, Th., Cheron, T., Cauffriez, H., Marcilly, C., Studies in Surface Science and Catalysis, Vol. 84, Weitkamp, J., Karge, H. G., Pfeifer, H., Holderich, W. (Eds.), 1663-1669 (1994)

Blasco, T., Corma, A., Martinez, A., Martinez-Escolano, P., "Supported Heteropolyacid (HPW) Catalysts for the Continuous Alkylation of Isobutane with 2-Butene: The Benefit of Using MCM-41 with Larger Pore Diameters", J. Catal 177, 306-313 (1998)

Bond, G. C., "A Short History of Hydrogen Spillover", Studies in Surface Science and Catalysis 17, 1-16 (1983)

Box, G. E. P., Hunter, W. G., Hunter, J. S., "Statistics for Experimenters", Wiley, N. Y. (1978)

Breck, "Zeolite Molecular Sieves: Structure, Chemistry and Use", Wiley, N. Y. (1974)

Burkett, S. L., Davis, M. E., "Structure-Directing Effects in the Crown Ether-Mediated Syntheses of FAU and EMT Zeolites", Microporous Materials 1, 265-282 (1993)

Cardona, F., Gnep, N. S., Guisnet, M., Szabo, G., Nascimento, P., "Reactions Involved in the Alkylation of Isobutane with 2-Butene and with Propene on a USHY Zeolite", Appl. Catal A: General 128, 243-257 (1995)

Chauvin, Y., Commereuc, D., Hugues, F., "Nickel-Based Heterogeneous Catalysts for Olefin Oligomerization I. Support and Anion Effects", Appl. Catal 42, 205-216 (1988)

Chauvin, Y., Olivier, H., Wyrvalski, C. N., Simon, L. C., de Souza, R. F., "Oligomerization of *n*-Butenes Catalyzed by Nickel Complexes Dissolved in Organochloroaluminate Ionic Liquids", J. Catal. 165, 275-278 (1997)

Chu, Y. F., Chester, W. A., "Reactions of Isobutane with Butene over Zeolite Catalysts", Zeolites 6, 195 (1986)

Conner Jr., W. C., Falconer, J. L., "Spillover in Heterogeneous Catalysis", Chem. Rev. 95, 759-788 (1995)

Conner, W., C., Teichner, S. J., Pajonk, G. M., "Spillover of Sorbed Species", Adv. in Catal. 34, 1-79 (1986)

Corma, A., Wojciechowski, B. W., "The Catalytic Cracking of Cumene", Catal. Rev. Sci. Eng. 24, 1 (1982)

Corma, A., "Application of Zeolites in Fluid Catalytic Cracking and Related Processes", Studies in Surface Science and Catalysis 49, 49-67 (1989)

Corma, A., Faraldos, M., Martinez, A., Mifsud, A., "Hydrogen Transfer on USY Zeolites during Gas Oil Cracking: Influence of the Adsorption Characteristics of the Zeolite Catalysts", J. Catal. 122, 230- 239 (1990)

Corma, A., Martinez, A., "Chemistry, Catalysts, and Processes for Isoparaffin-Olefin Alkylation: Actual Situation and Future Trends", Catal. Rev. - Sci. Eng. 35(4), 483-570 (1993)

Corma, A., Martinez, A., Martinez, C., "Isobutane/2-butene Alkylation on MCM-22 Catalyst. Influence of Zeolite Structure and Acidity on Activity and Selectivity", Catal. Letters 28, 187-201 (1994a)

Corma, A., Martinez, A., Martinez, C., "Isobutane/2-butene Alkylation on Ultrastable Y Zeolites: Influence of Zeolite Unit Cell Size", J. Catal. 146, 185-192 (1994b)

Corma, A., Gomez, V., Martinez, A., "Zeolite Beta as a Catalyst for Alkylation of Isobutane with 2-Butene. Influence of Synthesis Conditions and Process Variables", Appl. Catal. A 119, 83-96 (1994c)

Corma, A., Juan-Rajadell, M. I., Lopez-Nieto, J. M., Martinez, A., Martinez, C., "A Comparative Study of SO_4^{2-}/ZrO_2 and Zeolite Beta as Catalysts for the Isomerization of *n*-Butane and the Alkylation of Isobutane with 2-Butene", Appl. Catal. A: General 111, 175-189 (1994d)

Corma, A., Martinez, A., Martinez, C., "Influence of Process Variables on the Continuous Alkylation of Isobutane with 2-Butene on Superacid Sulfated Zirconia Catalysts", J. Catal. 149, 52-60 (1994e)

Corma, A., Martinez, A., Martinez, C., "The Role of Extraframework Aluminum Species in USY Catalysts during Isobutane/2-Butene Alkyaltion", Appl. Catal A 134, 169-182 (1996a)

Corma, A., Martinez, A., Arroyo, P. A., Monteiro, J. L. F., Sousa-Aguiar, E. F., "Isobutane/2-Butene Alkylation on Zeolite Beta: Influence of Post-Synthesis Treatments", Appl. Catal. A 142, 139-150 (1996b)

Corma, A., Martinez, A., Martinez, C., "The Effect of Sulfation Conditions and Activation Temperature of Sulfate-doped ZrO_2, TiO_2 and SnO_2 Catalysts during Isobutane/2-Butene Alkylation", Appl. Catal. A 144, 249-268 (1996c)

Corma, A., Martinez, A., Martinez, C., "Acidic Cs^+, NH_4^+ and K^+ Salts of 12-Tungstophosphoric Acid as Solid Catalysts for Isobutane/2-Butene Alkylation", J. Catal 164, 422-432 (1996d)

Crossland, C. S., "Advances in Solid Acid Alkylation", Worldwide Solid Acid Process Conference, Unpublished Notes, Nov. 14-16 (1993)

Delprato, F., Delmotte, L., Guth, J. L., Huve, L., "Synthesis of New Silica-Rich Cubic and Hexagonal Faujasites using Crown-Ether-Based Supramolecules as Templates", Zeolites 10, 546-552 (1990)

Denayer, J. F., Souverijns, W., Jacobs, P. A., Martens, J. A., Baron, G. V., "High-Temperature, Low-Pressure Adsorption of Branched C_5 - C_8 Alkanes on Zeolite Beta, ZSM-5, ZSM-22, Zeolite Y and Mordenite", J. Phys. Chem. B 102, 4588-4597 (1998)

Dmitriev, R., V., Defjuk, A. N., Minachev, C. M., Steinberg, K.-H., "Investigation of Hydrogen Spillover on Metal Containing Catalysts by Isotopic Exchange", Studies in Surface Science and Catalysis 17, 17-29 (1983)

Dougnier, F., Patarin, J., Guth, J. L., Anglerot, D., "Synthesis, Characterization, and Catalytic Properties of Silica-Rich Faujasite-Type Zeolite (FAU) and its Hexagonal Analog (EMT) Prepared by using Crown-Ethers as Templates", Zeolites 12, 160-166 (1992)

Feijen, E. J. P., Martens, J. A., Jacobs, P. A., "Zeolites and their Mechanism of Synthesis", Studies in Surface Science and Catalysis 84, 3-21 (1994a)

Feijen, E. J. P., De Vadder, K., Bosschaerts, M. H., Lievens, J. L., Martens, J. A., Grobet, P. J., Jacobs, P. A., "Role of 18-Crown-6 and 15-Crown-5 Ethers in the Crystallization of Polytype Faujasite Zeolites", J. Am. Chem. Soc. 116, 2950-2957 (1994b)

Feijen, E. J. P., Lievens, J. L., Martens, J. A., Grobet, P. J., Jacobs, P. A., "Silicon and Aluminum Ordering in Frameworks of FAU and EMT Aluminosilicate Zeolites Crystallized in the Presence of Crown Ethers", J. Phys. Chem. 100, 4970-4975 (1996)

Flego, C., Kiricsi, I., Parker Jr., W. O., Clerici, M. G., "Spectroscopic Studies of LaHY-FAU Catalyst Deactivation in the Alkylation of Isobutane with 1-Butene", Appl. Catal. A 124, 107-119 (1995)

Fujimoto, K., "Catalyst Design Based on Spillover Theory", Studies in Surface Science and Catalysis 77, Inui, T., Fujimoto, K., Uchijima, T., Masai, M. (Eds.), 9-16 (1993)

Garwood, W. E., Venuto, P. B., "Paraffin-Olefin Alkylation over Crystalline Aluminosilicate", J. Catal. 11, 175-177 (1968)

Gates, B. C., "Catalytic Chemistry", Wiley, pg. 272 (1992)

Gates, B. C., "Materials Chemistry: An Emerging Discipline", Am. Chem. Soc., 301-320 (1995)

Gonzalez, R., "Refineries need more Alkylation", Hydrocarbon Processing 71(7), 19, July (1992)

Gossens, A., e-mail 1998

Hutson Jr., T., Logan, R.S., "Estimate Alkyl Yield and Quality", Hydrocarbon Processing Sept., 107-110 (1975)

Jansen, J. C., "The Preparation of Molecular Sieves A. Synthesis of Zeolites", Studies in Surface Science and Catalysis 58, 77-136 (1991)

Kalliguine, S., personal communication (2000)

Kazansky, V. B., Senchenya, I. N., "Quantum Chemical Study of the Electronic Structure and Geometry of Surface Alkoxy Groups as Probable Active Intermediates of Heterogeneous Acidic Catalysts: What are the adsorbed Carbenium Ions?", J. Catal 119, 108-120 (1989)

Khan, M. R., Reynolds, J. G., "Formulating a Response to the Clean Air Act", Chemtech, 56-61, June (1996)

Kirsch, F. W., Potts, J. D., Barmby, D. S., "Isoparaffin-Olefin Alkylations with Crystalline Aluminosilicates I. Early studies - $C_4^=$ olefins", J. Catal. 27, 142-150 (1972)

Loenders, R., Jacobs, P. A., Martens, J. A., "Alkylation of Isobutane with 1-Butene on Zeolite Beta", J. Catal 176, 545-551 (1998)

Lohse, U., Pitsch, I., Schreier, E., Parlitz, B., Schnabel, K.-H., Appl. Catal. A 129, 189-202 (1995)

Martens, J. A., Jacobs, P. A., Cartlidge, S., "Investigation of the Pore Architecture of CSZ-1 Zeolites with the Decane Test Reaction", Zeolites 9, 423-427 (1989)

Martin, D., Duprez, D., "Surface Migration of Oxygen and Hydrogen in Supported Metal Catalysts", Studies in Surface Science and Catalysis 77, Inui, T., Fujimoto, K., Uchijima, T., Masai, M. (Eds.), 201-206 (1993)

Misono, M., Okuhara, T., "Solid Superacid Catalysts", Chemtech, 23-29, November (1993)

Mostad, H. B., Stocker, M., Karlsson, A., Rorvik, T., "Comparison of the Iso-Structural H-SAPO-37 and H-Faujasite as Catalysts for the Isobutane/2-Butene Alkylation", Appl. Catal. 144, 305-317 (1996)

Mostad, H. B., Stocker, M., Karlsson, A., Junggreen, H., Hustad, B., "La-EMT, a Promising Catalyst for Isobutane/2-butene Alkylation", Studies in Surface Science and Catalysis 105, 1413-1422 (1997)

Nivarthy, G. S., He, Y., Seshan, K., Lercher, J. A., "Elementary Mechanistic Steps and the Influence of Process Variables in Isobutane Alkylation over H-BEA", J. Catal 176, 192-203 (1998)

Ohgoshi, S., Nakamura, I., Wakushima, Y., "Hydrogenation of Isobutylene by Spiltover Hydrogen from Pt/KA-zeolite to NaY Zeolite", Studies in Surface Science and Catalysis 77, Inui, T., Fujimoto, K., Uchifima, T., Masai, M. (Eds.), 289-292 (1993)

Olah, G. A., Batamack, P., Deffieux, D., Torok, B., Wang, Q., Molnar, A., Prakash, G. K. S., "Acidity Dependence of the Trifluoromethanesulfonic Acid Catalyzed Isobutane-Isobutylene Alkylation Modified with Trifluoroacetic Acid or Water", Appl. Catal A: General 146, 107-117 (1996)

O'Young, C.-L., Xu, W.-W., Simon, M., Suib, S. L., "Skeletal Isomerization of *n*-Butenes on Zeolite Catalysts: Effects of Acidity", Studies in Surface Science and Catalysis 84, Eds. Weitkamp, J., Karge, H. G., Pfeifer, H., Holderich, W., 1671-1676 (1994)

Pine, L., Maher, P. J., Watcher, W. A., "Prediction of Cracking Catalyst Behavior by a Zeolite Unit Cell Size Model", J. Catal. 85, 466-476 (1984)

Querini, C. A., Roa, E., "Deactivation of Solid Acid Catalysts during Isobutane Alkylation with C_4 Olefins", Appl. Catal. A: General 163, 199-215 (1997)

Rao, P., Vatcha, S. R., "Solid-Acid Alkylation Process Development is at Crucial Stage", OGJ, 56-61, Sept. 9 (1996)

Reid, R. C., Prausnitz, J. M., Sherwood, T. K., "The Properties of Gases and Liquids", McGraw-Hill (1977)

Rhodes, A. K., "U.S. Refiners Must Increase Alkylation Capacity to Meet Demand", OGJ Special, 49-51, Aug. 22 (1994a)

Rhodes, A. K., "Searches for New Alkylation Catalysts, Processes Forge Ahead", OGJ Special, pg. 52-54, Aug. 22 (1994b)

Rhodes, A. K., "California refiners face hurdle in federal, state RFT rules", OGJ ,23-28, Oct. 10 (1994)

Rorvik, T., Dahl, E. M., Mostad, H. B., Ellestad, O. H., "Nafion-H as Catalyst for Isobutane/2-Butene Alkylation compared with a Cerium Exchanged Y Zeolite", Catal. Letters 33, 127-135 (1995)

Rorvik, T., Mostad, H., Ellestad, O. H., Stocker, M., "Isobutane/2-Butene Alkylation over Faujasite Type Zeolites in a Slurry Reactor. Effect of Operating Conditions and Catalyst Regeneration", Appl. Catal. A: General, 137, 235-253 (1996)

Rotman, D., "Biocatalysis and Solid-Acid Catalysts Remain Elusive but Lucrative Goals", Chemical Week, pg. 32, Feb. 14 (1996)

Santilli, D. S., Harris, T. V., Zones, S. I., "Inverse Shape Selectivity in Molecular Sieves - Observations, Modelling and Predictions", Microp. Mat'ls 1, 329-341 (1993)

Sheckler, J. C., Ross, L. J., Comey III, K. R., "New Process Additive Reduces HF Cloud-Forming Potential", OGJ Special, 60-63, Aug. 22 (1994)

Simpson, M. F., Wei, J., Sundaresan, S., "Kinetic Analysis of Isobutane/Butene Alkylation over Ultrastable H-Y Zeolite", Ind. Eng. Chem. Res. 35, 3861-3873 (1996)

Spencer, M. S., "Spillover on a Palladium Catalyst - an EPR Study", Appl. Catal. A 112, N23-N24 (1994)

Stach, H., Lohse, U., Thamm, H., Schirmer, W., "Adsorption Equilibria of Hydrocarbons on Highly Dealuminated Zeolites", Zeolites 6, 74-91 (1986)

Stocker, M., Mostad, H., Rorvik, T., "Isobutane/2-Butene Alkylation on Faujasite-Type Zeolites (H-EMT and H-FAU)", Catal. Letters 28, 203-209 (1994)

Stocker, M., Mostad, H., Karlsson, A., Junggreen, H., Hustad, B., "Isobutane/ 2-Butene Alkylation on Dealuminated H-EMT and H-FAU", Catal. Letters 40, 51-58 (1996)

Su, B. L., Barthomeuf, D., "Comparison of the Protonic Acidity of H-Y, LZY-82, H-SAPO-37, and H-EMT: Effect of the Structure and Nature of T Atoms", Zeolites 13, 626-633 (1993)

Taylor, R. J., Sherwood Jr., D. E., "Effects of Process Parameters on Isobutane/ 2-Butene Alkylation using a Solid Acid Catalyst", Appl. Catal. A: General 155, 195-215 (1997)

Teichner, S. J., "The History and Perspectives of Spillover", Studies in Surface Science and Catalysis 77, Inui, T., Fujimoto, K., Uchijima, T., Masai, M. (Eds.), 27-43 (1993)

Thomas, J. M., Ramdas, S., Millward, G. R., Klinowski, J., Audier, M., Gonzalez-Galbet, S., Fyfe, C. A., "Surprises in the Structural Chemistry of Zeolites", J. Solid State Chem. 45, 368-380 (1982)

Unverricht, S., Ernst, S., Weitkamp, J., Studies in Surface Science and Catalysis 84, (Eds.) Weitkamp, J., Karge, H. G., Pfeifer, H., Holderich, W., 1693-1700 (1994)

van Santen, R. A., "Theoretical Heterogeneous Catalysis", World Scientific, pgs. 316-331 (1991)

Ward, J., "The Nature of Active Sites on Zeolites I. The Decationated Y Zeolite", J. Catal. 9, 225-236 (1967)

Weisz, P. B., "Zeolites - New Horizons in Catalysis", Chemtech 3, 498-505, (1973)

Weisz, P. B., Prater, C. D., "Interpretation of Measurements in Experimental Catalysis", Advances in Catalysis 6, 143-196 (1954)

Weisz, P. B., Frilette, V. J., Maatman, R. W., Mower, E. B., "Catalysis by Crystalline Aluminosilicates II. Molecular-Shape Selective Reactions", J. Catal. 1, 307-312 (1962)

Weitkamp, J., Jacobs, P. A., "Isobutane/1-Butene Alkylation on Pentasil-Type Zeolite Catalysts", Proc. 10th Int'l Cong Catal, July 19-24, 1992, Budapest, Hungary, New Frontiers in Catalysis, Eds. Guczi, L., et. al., 1735-1738 (1993)

Weitkamp, J., Maixner, S., "Isobutane Butene Alkylation on LaNaY Zeolite - Characterization of Carbonaceous Deposits by CP/MAS C-13 NMR Spectroscopy", Zeolites 7, 6-8 (1987)

Xiao, X., Chen, J., Zhang, S., Tierney, J. W., Wender, I., "Alkylation of Isobutane and Butenes over Anion-Modified Zirconium Oxide Catalysts", Div. Fuel Chem, ACS 43(2), 215th ACS Nat'l Mtg, Dallas, Texas, Mar. 2 - Apr. 2 (1998)

Zholobenko, V., Garforth, A., Makarova, M., Zhao, J., Dwyer, J., "Pt/Zeolite Catalysts for Hydrocracking: A Comparative Study on FAU and EMT", Studies in Surface Science and Catalysis 94, Beyer, H. K., Karge, H. G., Kiricsi, I., Nagy, J. B., (Eds.), 560-567 (1995)

Appendix 1:

Catalyst Preparation and Characterization

A1.1 EMT SYNTHESIS

EMT is synthesized using the modified method of Feijen et al, 1994b, provided by Prof. Martens and Anne Gossens, Centre of Surface Science and Catalysis, KU Leuven. A description of the reagents employed in the synthesis is outlined in Table A1.1.

Table A1.1: Description of Reagents Employed for EMT Synthesis

Reagent	Chemical Formula	Supplier	Description
18-crown-6 ether	$C_{12}H_{24}O_6$	Acros Organics	99 % purity
double de-ionized water	H_2O	U of W	
sodium hydroxide pellets	NaOH	BDH	97.0 %
Gibbsite	$Al(OH)_3$	Fluka	64-66 %
Ludox HS-40	Colloidal SiO_2	Aldrich	40 % SiO_2 in H_2O

The Feijen method is written for a 40 mL teflon lined reactor and requires approximately 60 minute time interval to complete the gel preparation. NaOH (2.56 g) is mixed with 6.59 g of water under magnetic stirring. Gibbsite (2.08 g) is added to the mixture and heated to 80°C, with magnetic stirring, until all of the Gibbsite has dissolved (approximately 10 minutes).

Water (10.28 g) was added to 20.00 g Ludox HS-40 under mechanical stirring. The 18-crown-6 ether (3.41 g) was added to this sol and stirring was continued. When all of the Gibbsite was dissolved, the heat was turned off and the solution was allowed to cool. Some of the Al may precipitate while cooling but this does not affect the synthesis. When the aqueous solution of Gibbsite and sodium hydroxide had reached room temperature, the amount of water that had evaporated was determined and added back to the solution. This solution was immediately added to the silica sol followed by 3.52 g water and stirred for 15 minutes using a mechanical stirrer. The molar composition of the final hydrogel is as follows:

10.00 SiO_2 : 1.00 Al_2O_3 : 2.40 Na_2O : 140.25 H_2O : 0.97 18-crown-6 ether

The resulting gel was transferred into a 40 mL teflon lined reactor, sealed and then aged at room temperature for 3 days. The crystallization period was initiated by heating the hydrogel at 100°C for 9 days. After this time period had elapsed, the product was cooled to room temperature. The crystallized material was recovered by filtration, washed with double deionized water (four times the gel volume) and dried overnight at 80°C. The resulting product was calcined in flowing air at 425°C for 5 h. The average calcined product yield was approximately 10.50 g of Na-EMT per batch. Identification was confirmed using powder X-ray diffraction.

Since our laboratory does not possess a small teflon reactor, teflon bottles were evaluated as alternative vessels for catalyst synthesis. Two sizes are commercially available in the vicinity of 40 mL. The preparation method for a 40 mL reactor was successfully scaled up for use in a 60 mL teflon bottle as well as scaled down to perform the synthesis in a 35 mL teflon bottle (see Table A1.2).

Table A1.2: Reagents in EMT Synthesis (masses indicated in grams)

Reagent	Original Recipe* (40 Ml Telflon Lined Reactor)	Scale up to 60 mL Teflon Bottle	Scale down to 35 mL Teflon Bottle
Crown Ether	3.41	5.12	2.99
Water (total)	20.39	30.49	17.83
with NaOH	6.59	9.87	5.77
with Ludox HS-40	10.28	15.42	9.01
with final sol	3.52	5.20	3.05
NaOH Pellets	2.56	3.83	2.24
Gibbsite	2.08	3.12	1.72
Ludox HS-40	20.00	29.97	17.52

* Recipe provided by Prof. Marten's group, Centrum voor Oppervlaktechemie en Katalyse, KU Leuven, Belgium

The 60 mL teflon bottle method was primarily used as it produced the highest yield of product.

A1.2 PHASE IDENTIFICATION

A Siemens Diffractometer (laboratory of Prof. L. Nazar, Department of Chemistry, University of Waterloo) equipped with a CuKα source was used for powder XRD measurements to identify the phase of the zeolite. A current of 30 mA current and a voltage of 50 kV, were employed for the analysis. A step of 0.05 ° and a dwell time of 0.5 s were used for data collection.

The sample was bombarded with X-ray beams at an angle, θ. A portion of the X-rays were diffracted and measured by a radiation detector. The sample was rotated through a range of angles of $2° < 2\theta < 40°$ to obtain an entire spectrum. If a sample possessed a regular crystal structure, a distinctive pattern was observed.

The spectra can be compared to the literature pattern for EMT (Delprato et al, 1990) to confirm the phase identity of the sample.

A1.3 AMMONIUM ION EXCHANGE OF Na-EMT

The exchange process employed a 2 M solution of NH_4NO_3 with a concentration of 25 cm^3 of exchanging solution per gram of Na-EMT. Typically, the Na-EMT was exchange in batch sizes of approximately 15 g. The solid was added to the exchanging solution and heated at 70°C for 3 h. Once the exchange period had expired, the mixture was cooled to room temperature and filtered and washed thoroughly with double de-ionized water. The filter cake was heated at 80°C overnight to remove the loosely bound water. The dried material was calcined at 425°C in flowing air for 5 h. A total of three exchange cycles, followed by calcination, were employed to ensure high Na removal.

The batches of Na-EMT were combined to form two groups, G1 and G2.

G1: batches G5008 - G5013
G2: batches G5014 - G5019

Starting with G1, half of the mass from each batch (M1) were mixed together, forming set, S1 (see Figure A1.1). The first exchange process was applied to this material (G1-E1-S1). The solids were removed from the exchanging solution by filtration, heated overnight at 80°C and calcined in two separate batches (C1 and C2) at 425°C for 5 h in flowing air.

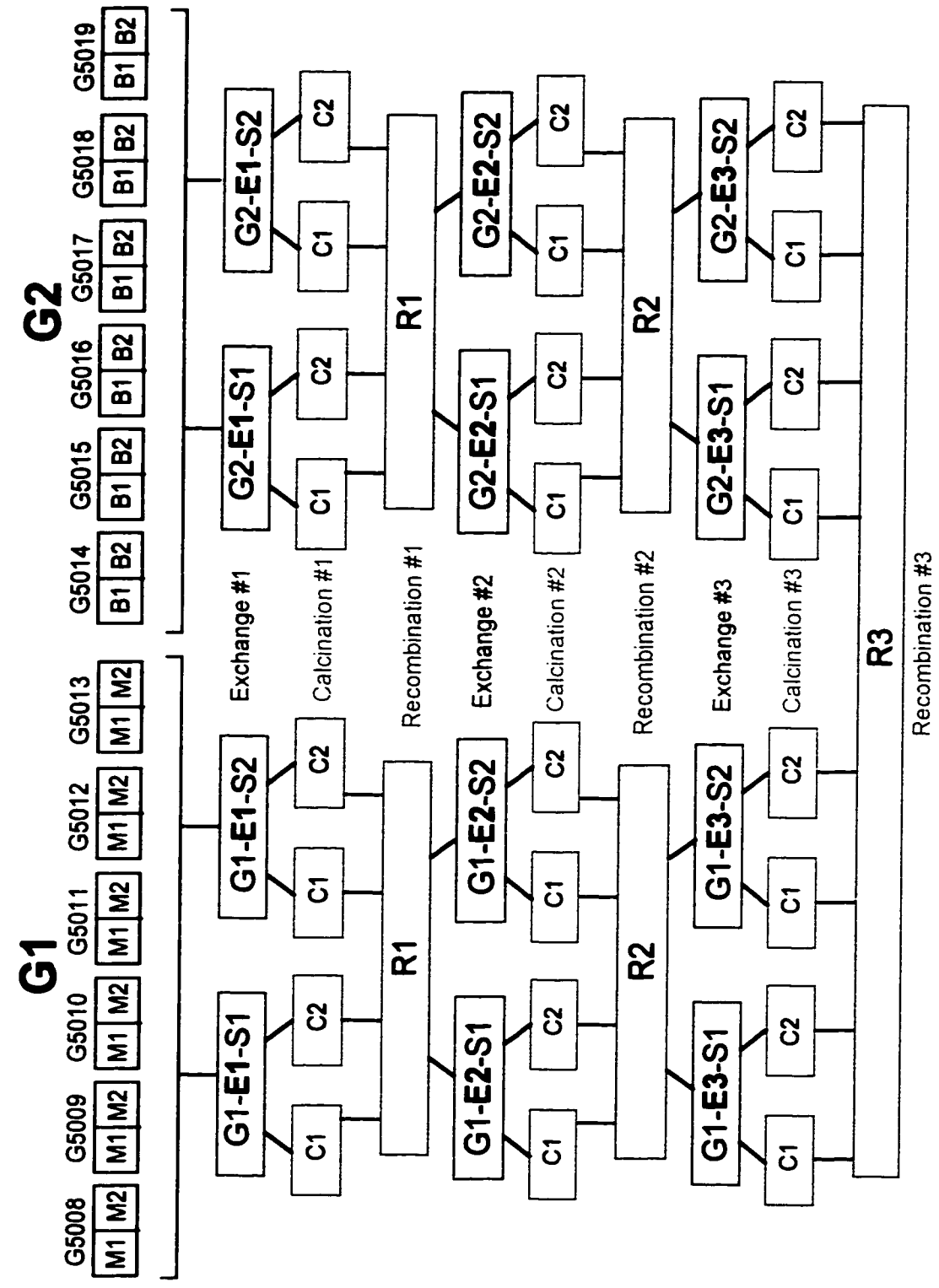

Figure A1.1: Methodology for Ammonium Ion Exchange of Na-EMT

The same treatment was applied to the other half of the six batches (M2) of G1. These were combined to form a second set (S2). All of the calcined material from the first exchange step was recombined and thoroughly mixed (R1). The resulting material was equally divided into two amounts, S1 and S2, for the second exchange step.

The same procedure was applied to the second and third exchange step of G1, as was adopted in the first exchange treatment. An identical approach was employed for G2. The final calcined, thrice exchanged product from G1 and G2, were recombined and mixed thoroughly for use in the catalytic study.

A1.4 Na CONTENT

A1.4.1 Experimental

Atomic absorption spectroscopy was used to evaluate the Na content as a measure of the ammonium ion exchange efficiency of Na-EMT. It was also used to compare the Na level of the commercial product, Y zeolite. The method of additions was employed for both materials, as this approach accounts for matrix effects in the sample analysis. The "sample mixture" was prepared by digesting 1 g zeolite in 10 mL concentrated HF and then diluting the mixture with double de-ionized water to a total of 100 g. A "standard solution" with a known amount of Na was also made.

The method of additions begins with the preparation of three separate solutions (see Figure A1-2). The Specimen solution consisted of equal volumes of diluent (double de-ionized water) and sample mixture. The A1 solution spiked the sample mixture with the standard solution and then diluted the total with diluent. The A1 solution was comprised of 50 % sample mixture, 25 % standard solution and 25 % diluent by volume. Finally, the A2 solution spiked the sample mixture more

extensively with the standard solution. It consisted of 50 % standard and 50 % sample mixture, by volume.

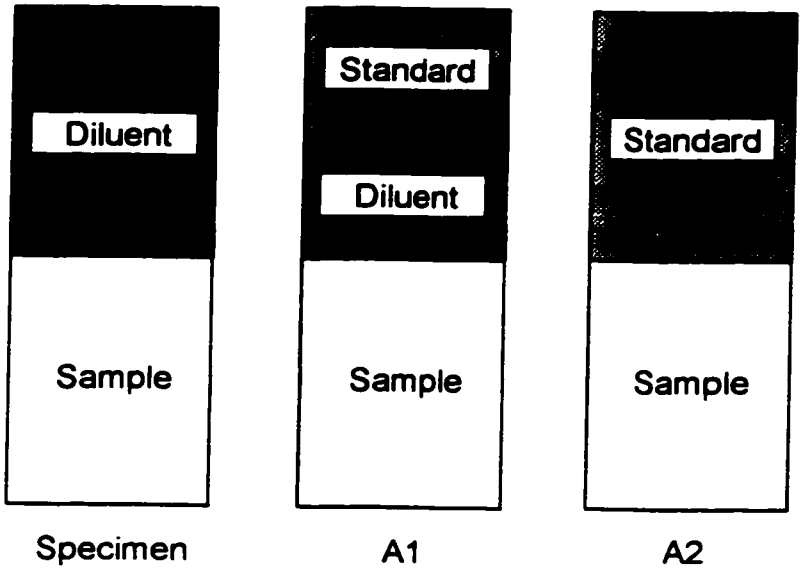

Figure A1.2: Solutions for Method of Additions

The sample absorbance was measured on a Perkin Elmer Atomic Absorbance Spectrometer 3100. The EMT sample mixture employed a wavelength of 589.0 nm, a slit width of 0.2 nm, a relative noise of 1.0. The Y sample mixture utilized a wavelength of 330 nm, a slit width of 0.7 nm and a relative noise of 0.63. All sample measurements utilized an ethylene flow rate of 2.0 L/min with air sustained at 9.0 L/min.

The three solutions were analysed and the absorbance plotted on an absorbance versus concentration graph. The "Specimen" absorbance was assigned a concentration of zero. The best-fit line was found through the three points, and the x-intercept determined. The concentration of the digested sample was taken as the negative value of the x-intercept for the best-fit line. The Na concentration was

calculated from the sample mixture Na level and corrected for the extent of dilution in the digestion process.

A1.4.2 Sample Calculation

1.04886 g EMT dissolved in 127.700 g sample (EMT, HF, H_2O)

From the absorbance spectra for the digested mixture of EMT, the x-intercept was calculated to be -2.09 ppm Na (see Figure A1.3)

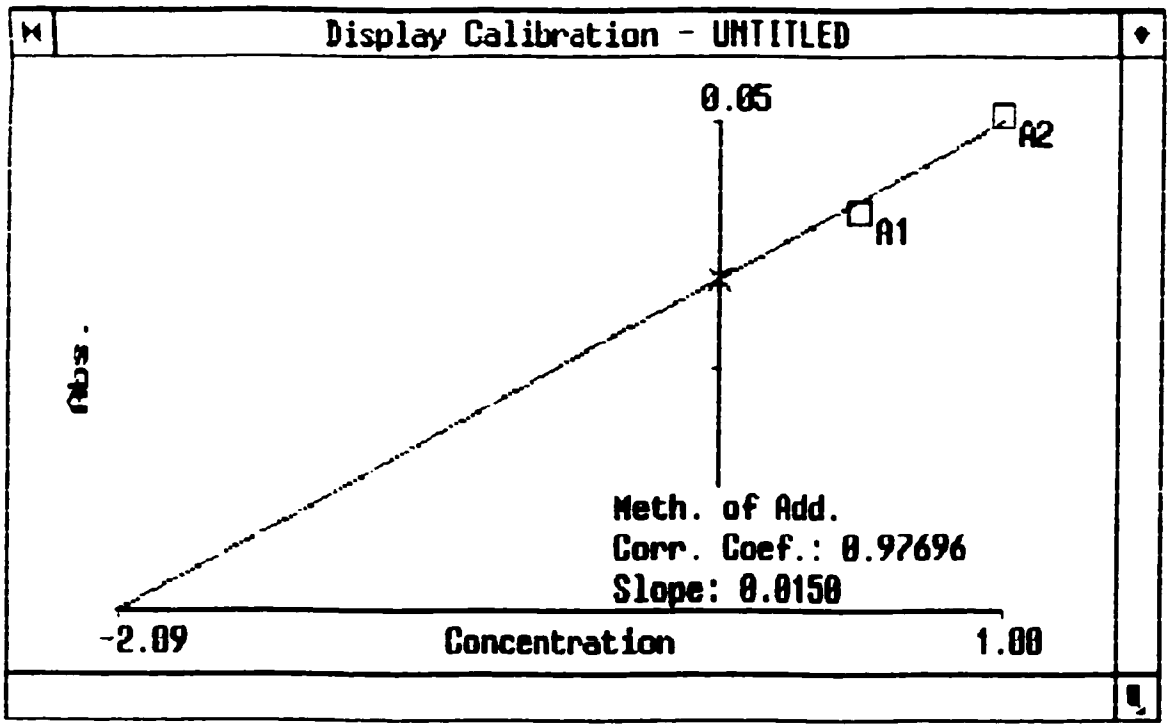

Figure A1.3: Absorbance Spectra for Digested EMT

The concentration of Na in the sample is calculated as follows:

$$\frac{2.09 \text{ g Na}}{10^6 \text{ g sample}} \left| \frac{127.700 \text{ g sample}}{1.04886 \text{ g EMT}} \right| \frac{10^6 \text{ g EMT}}{} = 254.5 \text{ ppm Na in EMT}$$

A1.5 ^{29}Si AND ^{27}Al MAS NMR

A1.5.1 Experimental

^{29}Si and ^{27}Al MAS NMR measurements were performed on a Bruker AMX 500 Spectrometer by Chris Kirby (PhD Candidate) in the laboratory of Prof. W. Powers, Department of Chemistry, University of Waterloo. Si spectra for EMT and Y (see Figures A1.4 and A1.5 respectively) were recorded at 99.36 MHz employing a pulse length of 1.5 μs, a recycle time of 15 s and a spinning rate of 20 kHz. A minimum of 1000 scans were performed for ^{29}Si MAS NMR data acquisition. The recording of Al spectra for EMT and Y (see Figures Al.6 and A1.7 respectively) were undertaken at 130.32 MHz using a pulse length of 1.5, a recycle time of 15 s and a spinning rate of 125 kHz. A total of 4096 scans were completed for ^{27}Al MAS NMR data analysis. All details for data acquisition are summarized on a side bar of the spectra.

The framework Si/Al molar ratio is given by the following equation:

$$\text{Si/Al} = \frac{\sum_{n=0}^{4} A\,\text{Si(nAl)}}{\sum_{n=0}^{4} (n/4)\,A\,\text{Si(nAl)}} \qquad \text{(A1-1)}$$

where A Si(nAl) is the area of the NMR signal attributed to the Si(nAl) units. The area of the intensity peak is found by multiplying the intensity by the peak width at half height.

Quantitative analysis is not readily available from ^{27}Al MAS NMR data due to broadening of the spectra by quadrupolar effects. The types of Al environments can be identified from the spectra but the relative amounts cannot be specified. A shift of 55 ppm is indicative of tetrahedral coordination of Al, -1.9 ppm identifies 6 coordinated Al environment and 15 ppm and 29.5 ppm representative of hybrid type of environments.

A1.5.2 Sample Calculation for Si/Al Ratio

The peak intensity and width from the spectra of EMT are recorded in Table A1.3. The product of these two measures determines the area of the peak. The Si/Al ratio for the sample can be calculated using equation A1-1.

Table A1.3: Sample Calculation of Si/Al Ratio for EMT using ^{29}Si NMR Data (see Figure A1.3)

Si(nAl)	n	Position [ppm]	Intensity [abs.]	Width [Hz]	Area	n/4 x Area
Si(0Al)	0	-108.0	897251	314.85	282499477.4	0
Si(1Al)	1	-102.6	607851	497.14	302187046.1	75546761.525
Si(2Al)	2	-96.9	61440	347.99	21380505.6	10690252.8
Si(3Al)	3	-92.2	14162	132.57	1877456.34	1408092.255

$$\text{Si/Al Ratio} = \frac{607944485.44}{87645106.58} = 6.94$$

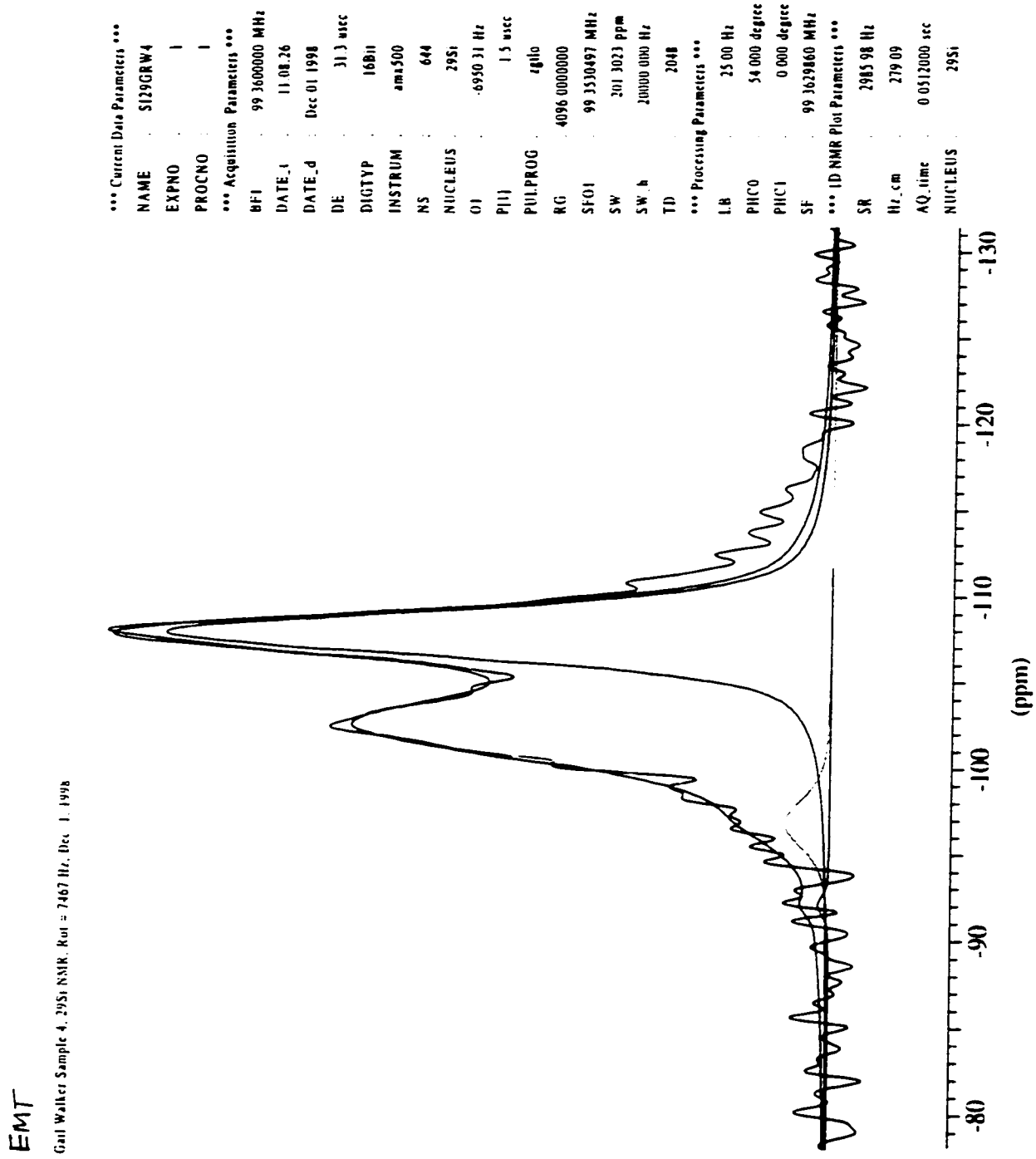

Figure AI.4: ^{29}Si MAS NMR for EMT Zeolite

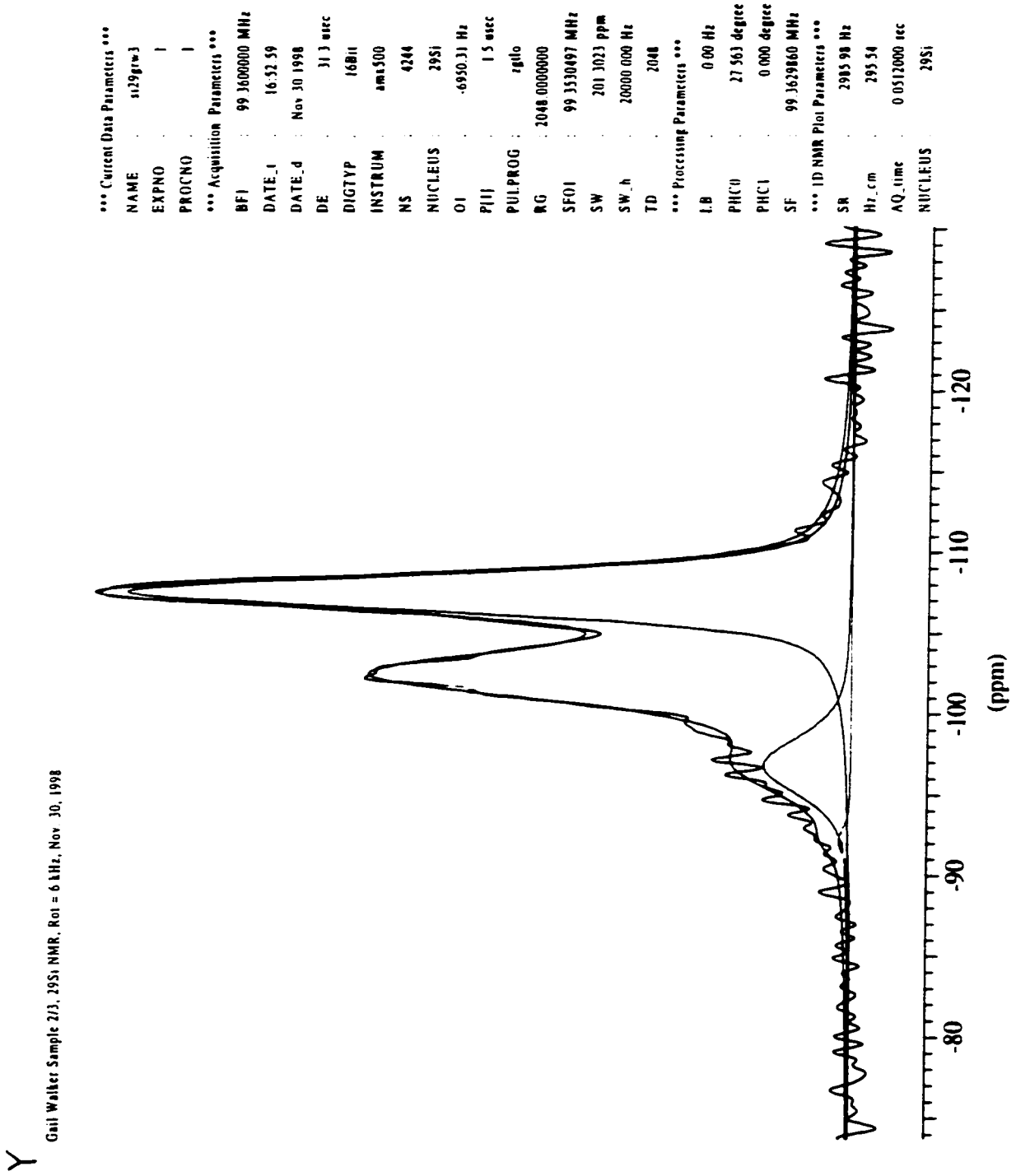

Figure AI.5: ^{29}Si MAS NMR for Y Zeolite

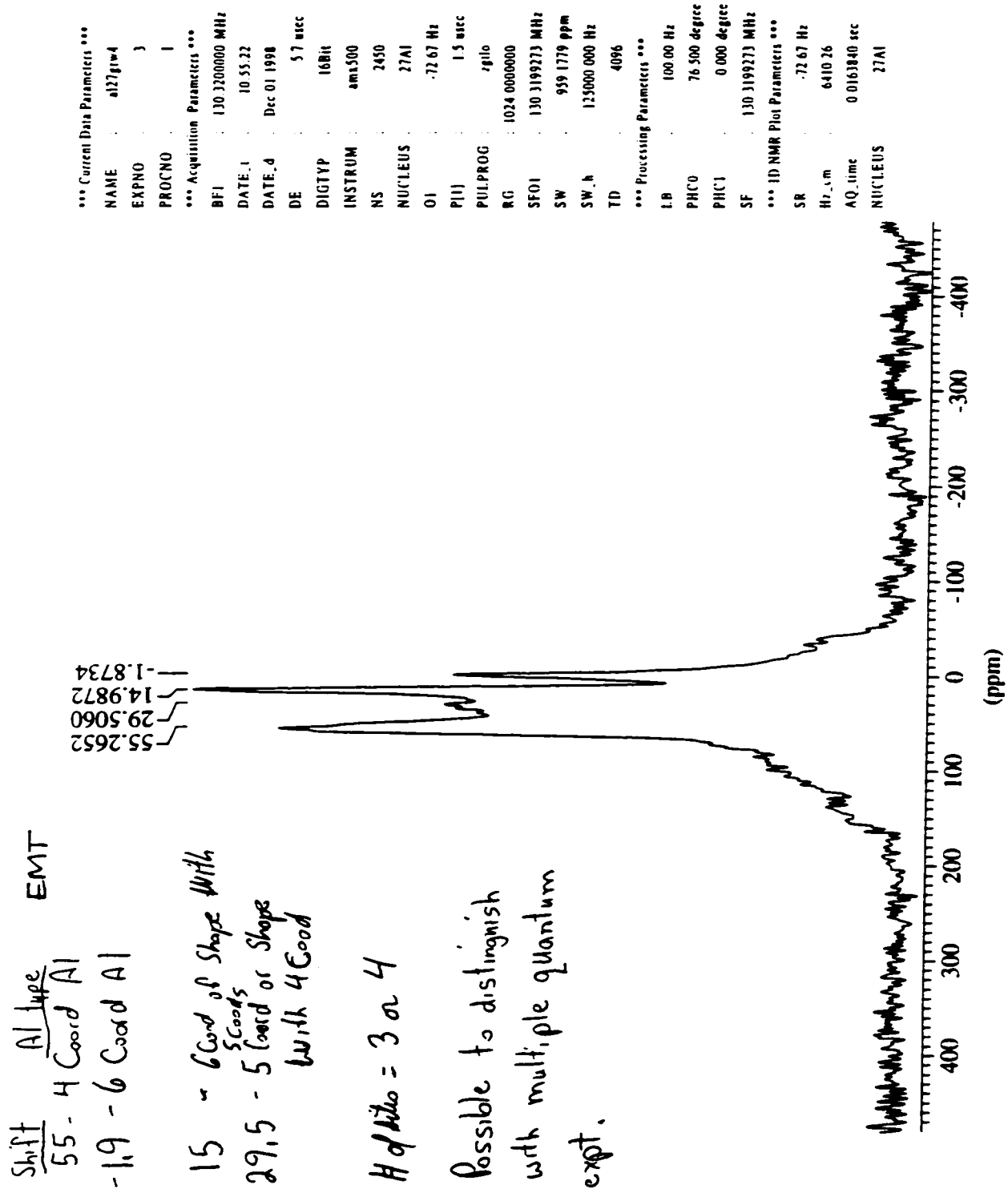

Figure AI.6: ^{27}Al MAS NMR for EMT Zeolite

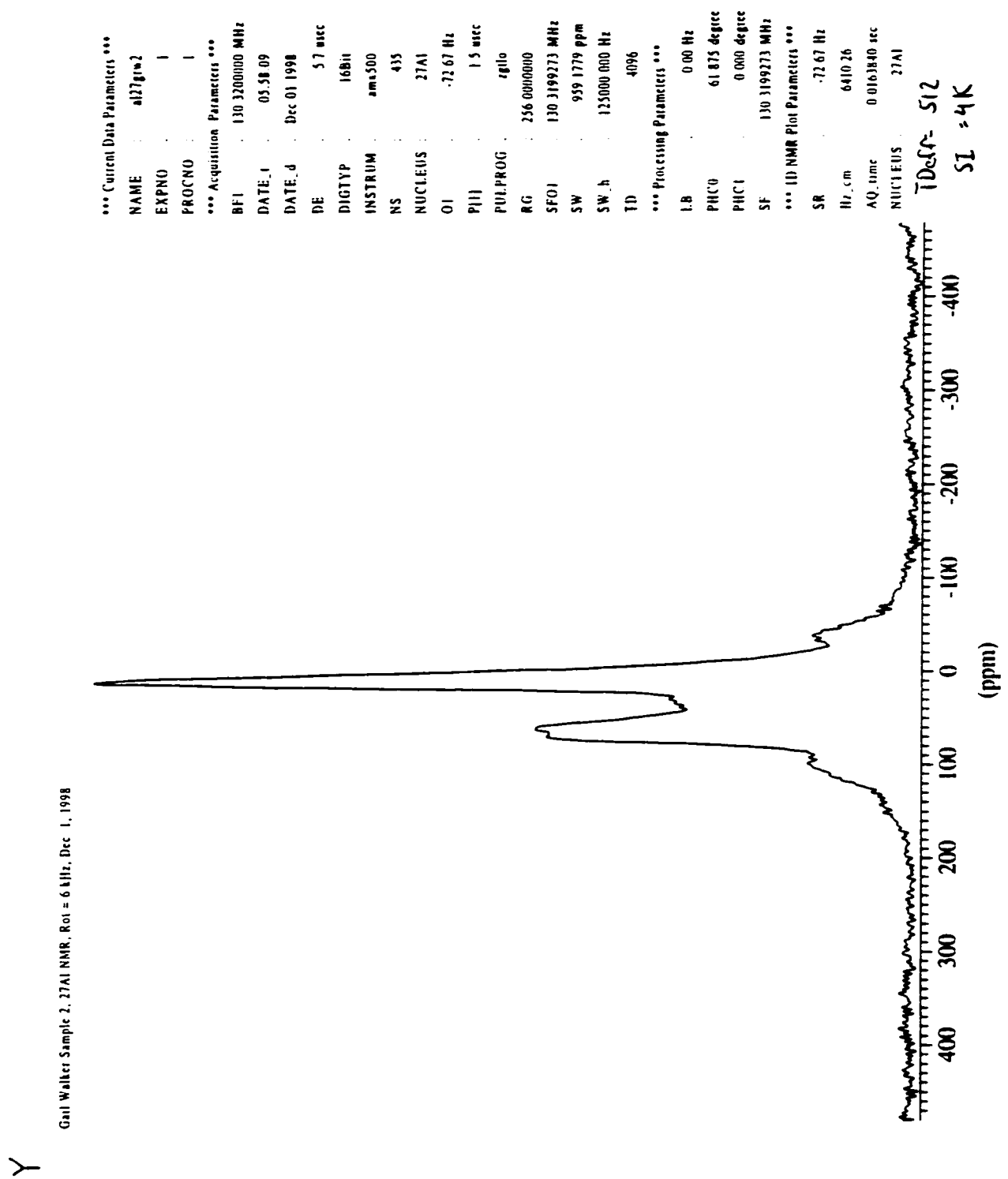

Figure AI.7: ^{27}Al MAS NMR for Y Zeolite

A1.6 TGA/DTA

A1.6.1 Experimental

Measurements were performed on a TA Instruments SDT 2960 system using fresh, calcined catalyst as the reference material. A 10 mg quantity was measured for both the sample and the reference material. A reactive gas (10 % O_2 in Ar) was used to combust and remove material trapped in the catalyst pores of the spent catalysts.

In freshly prepared catalysts, TGA/DTA measurements evaluated the temperature required to completely combust and remove the 18-crown-6 ether template. This provides insight into the selection of an appropriate calcination temperature for EMT.

TGA/DTA analysis on spent catalysts measured the amount of adsorbed species retained in the catalyst pores after deactivation. In general, it can be said that the temperature required for desorption is directly related to the molecular weight of the species retained in the pore network. That is, a high desorption temperature is required to remove a high molecular weight compound and a lower desorption temperature facilitates removal of low molecular weight species. In this manner, the desorption temperature provided insight into the relative size of the species, and the loss in mass was indicative of the amount of species.

The desorption temperature region ($25°C \geq T_d \geq 425°C$) was divided into three ranges: $T_d < 200°C$, $200°C \geq T_d \geq 300°C$ and $T_d > 300°C$. The % of material desorbed within each of these ranges provided an indication of low, medium and high molecular weight species retained on the catalyst surface. The sum of all of these ranges giave the total amount of material retained on the spent catalyst.

A1.6.2 Sample Calculation

The sample weight % was recorded for each temperature boundary range (see Table A1.4) for run F29Y (see Figure A1.8). The % material desorbed was given by the loss in mass % of the sample.

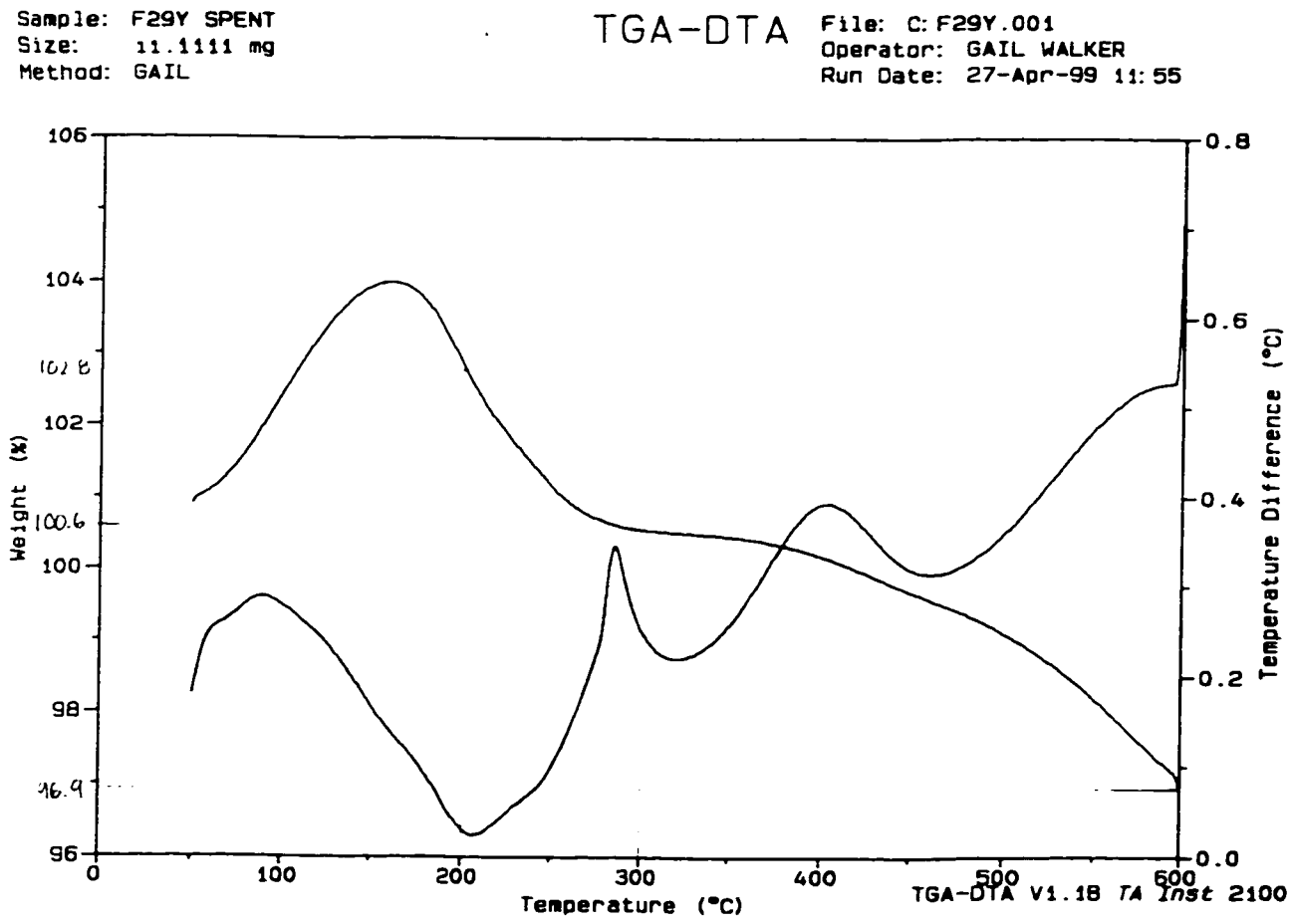

Figure A1.8: TGA/DTA Data for Run F29Y

Table A1.4: T_d vs. Weight % from TGA/DTA Data for F29Y (Figure Al.8)

T_d [°C]	Weight %
Initial	104.0
200	102.8
300	100.6
600	96.9

$$\% \text{ Loss in Mass } (T_d < 200°C) = \frac{104.0 - 102.8}{104.0} \times 100\ \%$$

$$= 1.2\ \%$$

A1.7 BET SURFACE AREA ANALYSIS

A1.7.1 Experimental

A Quantachrome Autosorb-1 system was employed for N_2 adsorption measurements to estimate catalyst surface area. The optimal sample size is one in which the total area measured is between 20 and 50 m^2. For fresh catalysts, a sample size of 0.1 g was employed. For spent catalyst measurements, the sample size was increased to 0.2 g.

The sample was outgassed at 100°C under vacuum for 3 h to remove physisorbed species. A known quantity of N_2 was admitted to the sample and the cell pressure was measured once equilibrium is established. This procedure was repeated until the maximum relative pressure (P/P° where P = cell pressure and P° = saturation pressure of N_2 at liquid nitrogen temperature) was reached. The linear region of this isotherm was used for data reduction to estimate the surface area. For microporous materials, this occurred at $P/P^\circ < 0.1$ range of the isotherm.

The multipoint BET (Brunauer-Emmett-Teller) method was employed to estimate the surface area:

$$\underbrace{\frac{1}{W\,[(P/P^\circ) - 1]}}_{y} = \underbrace{\frac{1}{W_m\,C}}_{\text{intercept}} + \underbrace{\frac{C - 1}{W_m\,C}}_{\text{slope}} \cdot \underbrace{\frac{P}{P^\circ}}_{x} \qquad \text{(A1-2)}$$

where

W = mass of N_2 adsorbed at a relative pressure, P/P° [g N_2]

P = pressure measured in sample cell [mm Hg]

P° = saturation pressure of the N_2 at the dewar (liquid N_2) bath temperature [mm Hg]

W_m = mass of N_2 required for monolayer surface coverage [g N_2/g sample]

C = constant related to the energy of adsorption of the first monolayer [dimensionless]

The best fit line through the linear portion (5 points) of the plot of $\{1/[W\,(P/P^\circ - 1)]\}$ versus $\{P/P^\circ\}$ was used to solve for W_m and C. The surface area was calculated as:

$$S = \frac{W_m\,N\,A}{M} \qquad \text{(A1-3)}$$

where

S = specific surface area [m^2/g sample]

N = Avogadro's number

= 6.022×10^{23} molecules/mole

A = X-sectional area of N_2 molecule

= 16.2×10^{-20} m^2/molecule N_2

m = mass of sample [g sample]

M = molar mass of nitrogen

= 28.0134 g N_2/mol N_2

AI.7.2 Sample Calculation

From the Multipoint BET plot, the y-intercept was found to be -3.291 x 10^{-4} and the slope was estimated to be 9.312 (see Figure A1.9).

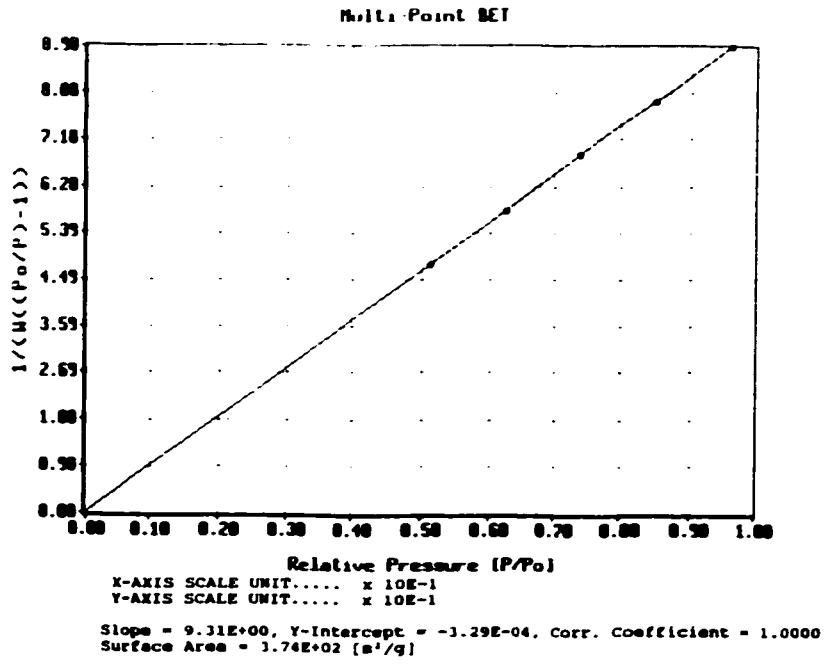

Figure A1.9: Multipoint BET plot for F29Y

Therefore,

$$\frac{1}{W_m C} = \frac{1}{-3.291 \times 10^{-4}} \qquad \text{(A1-4)}$$

and

$$\frac{C - 1}{W_m C} = 9.312 \qquad \text{(A1-5)}$$

There are two equations (equations (A1-4) and (1-5)) and two unknowns (W_m and C). Solve for W_m.

W_m = 0.10739 g N_2/g catalyst

Substitute the value for W_m into equation (A1-3) and solve for specific surface area.

$$S = \frac{0.10739 \text{ g } N_2}{\text{g catalyst}} \left| \frac{6.022 \times 10^{23} \text{ molec. } N_2}{\text{mol } N_2} \right| \frac{16.2 \times 10^{-20} \text{ m}^2}{\text{molec. } N_2} \left| \frac{\text{mol } N_2}{28.013 \text{ g } N_2} \right.$$

$$= 374 \text{ m}^2/\text{g}$$

A1.8 MEASUREMENT OF Pt DISPERSION

A1.8.1 Experimental

A Quantachrome Autosorb-1 system was used to perform H_2 chemisorption measurements. The isotherm generated from this data was used to evaluate the number of active sites of Pt per gram of sample. This method was used to estimate the percent Pt dispersion in the sample.

Approximately 1 g of solid was measured in the sample cell and inserted in the Analysis station. Prior to analysis, the sample must be treated to clean and stabilize the catalyst surface. This was accomplished by increasing the cell temperature at a rate of 5°C/min to 325°C in flowing helium (40 mL/min). The sample was outgassed at this temperature for 3 h. Upon completion of the calcination cycle, the sample was reduced at 425°C in a stream of 10 % H_2 in Ar flowing at 40 mL/min for 1 h. The gas flow was terminated and the cell was evacuated at 425°C for 2 h to remove all traces of hydrogen. The sample cell was cooled (under vacuum) to room temperature for adsorption measurements.

A total of 10 combined (physisorbed and chemisorbed gas measured together) points were collected in the pressure range of 80 and 800 mm Hg. A tolerance of 1 was employed for targeting the pressure set points, an equilibrium time of 3 min and a thermal equilibrium time of 10 min were specified as criteria for data acquisition.

Preselected amounts of hydrogen were sequentially added to the sample cell. An isotherm was generated, by plotting the adsorbed volume (V) vs. equilibrium pressure (P). Both physisorption and chemisorption contributed to this combined isotherm. A straight line was extrapolated from three or more data points in the "plateau" or low-slope region of the combined isotherm, to zero gas pressure (P=0). The y-intercept of this best fit line represented the monolayer chemisorbed volume, V_m. The monolayer uptake, N_m, can be calculated using:

$$N_m = 44.61\ V_m \qquad \text{(A1-4)}$$

where

N_m = monolayer uptake [μmol H_2/g sample]

V_m = molayer chemisorbed volume [mL H_2/g sample]

Pt atoms located inside Pt particles do not participate in reactions and similarly, do not contribute to H_2 chemisorption measurements. The % Pt dispersion, D, measures the fraction of the active Pt metal exposed on the surface which participates in reactions. A high Pt dispersion is desirable as this is it represents the most efficient use of the noble metal. The % Pt dispersion can be calculated from the following equation once N_m is known:

$$D = \frac{N_m S M}{100 L} \qquad \text{(A1-5)}$$

where

D = % Pt dispersion

S = adsorption stoichiometry

= 2 for H_2 chemisorption onto Pt

M = molar mass of Pt

L = % loading of Pt impregnated onto catalyst surface

A1.8.2 Sample Calculation

The data for fresh 0.5%Pt/EMT is shown in Figure A1.10. The monolayer uptake was calculated to be 9.753 μmol/g. Using equation (A1-5), the % Pt Dispersion, D, was estimated to be:

$$D = \frac{9.753\ \mu mol\ H_2}{g\ sample} \left| \frac{2\ mol\ Pt}{mol\ H_2} \right| \frac{195.09\ g\ Pt}{mol\ Pt} \left| \frac{mol\ H_2}{10^6\ \mu mol\ H_2} \right| \frac{100\ g\ sample}{0.5\ g\ Pt} \times 100\%$$

$$= 76.1\ \%$$

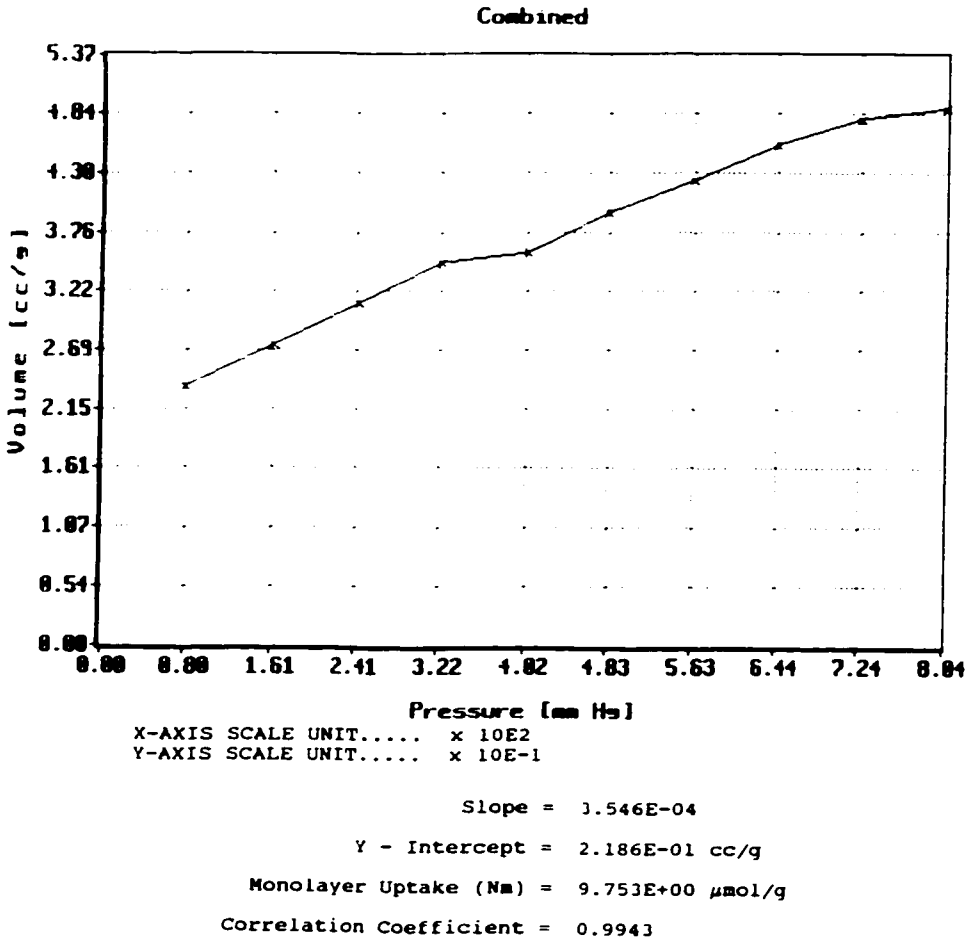

Figure A1.10: H_2 Chemisorption Data for 0.5%Pt/EMT

A1.9 MEASUREMENT OF PORE VOLUME

A1.9.1 Experimental

A Quantachrome Autosorb-1 system was utilized for nitrogen adsorption measurements to estimate pore volume. A 0.1 g sample was outgassed at 100°C under vacuum for 3 h to remove physisorbed species retained in the catalyst pores.

The adsorption isotherm using nitrogen as the adsorbate is determined. Particular attention is focussed in the region where the relative pressure, P/P_o (where P=cell pressure and P^o=saturation pressure of N_2 at liquid nitrogen temperature), approaches unity. The volume of nitrogen vapour, V_{ads}, which is adsorbed as P/P^o approaches unity is estimated. The volume of liquid nitrogen contained in the pores of the catalyst can be calculated using the following equation:

$$V_{liq} = \frac{P_a V_{ads} V_m}{R T} \qquad \text{(A1-6)}$$

Where

V_{liq} = pore volume [cm^3/g cat]

P_a = ambient pressure [atm]

V_{ads} = volume of nitrogen vapour adsorbed [cm^3/g cat]

V_m = molar volume of liquid nitrogen = 34.7 cm^3/mol

R = Universal Gas Constant

T = ambient temperature [K]

A1.9.2 Sample Calculation

The data for Y zeolite is shown in Figure A1.11. The value for V_{ads} is estimated to be 300 cm^3/g from the nitrogen isotherm. This value is substituted into equation (A1-6) to solve for V_{liq}.

$$V_{liq} = \frac{300\ cm^3}{g\ cat} \left| \frac{34.7\ cm^3}{mol\ N_2} \right| \frac{101.325\ kPa}{293\ K} \left| \frac{mol\ K}{8.314\ kPa\ L} \right| \frac{L}{1000\ cm^3}$$

$$= 0.43\ cm^3/g\ cat$$

The Autosorb-1 system software can provide an accurate estimate of the pore volume. The software estimates the pore volume to be 0.464 cm^3/g for Y zeolite.

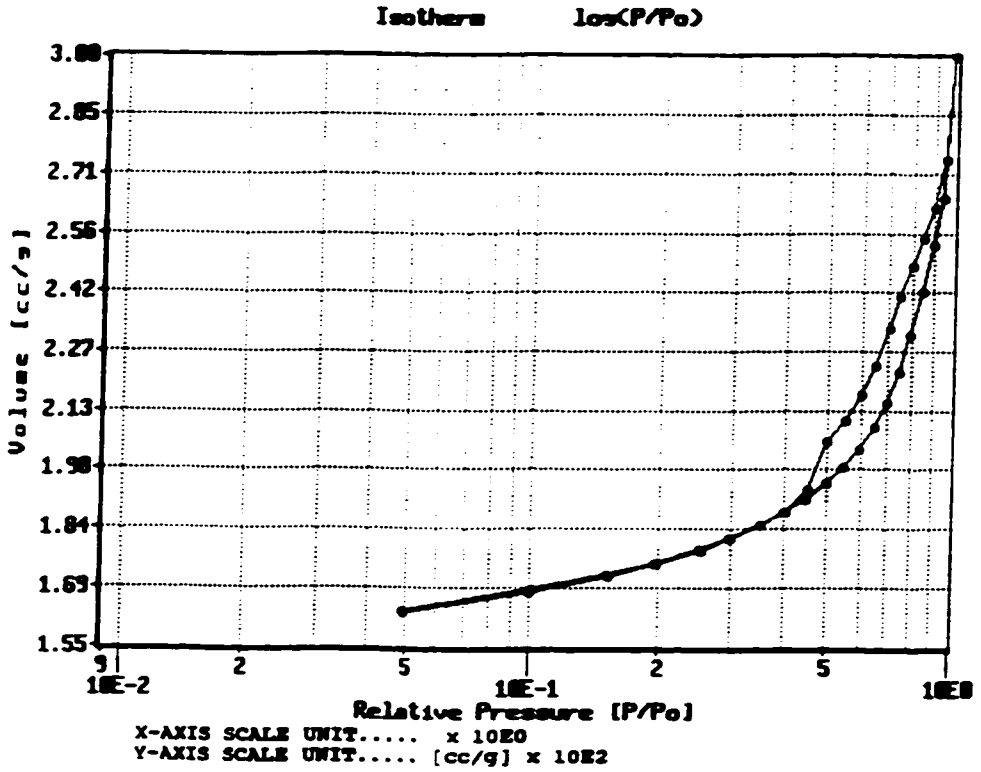

PORE VOLUME DATA

Total Pore Volume for pores with Radius less than 1357.1 Å at P/Po = 0.99289.....	4.639E-01	[cc/g
* t-Method Micro Pore Volume.....	2.206E-01	[cc/g
* MP-Method Micro Pore Volume.....	9.956E-02	[cc/g

PORE SIZE DATA

Average Pore Radius.....	1.431E+01	[Å]

* Note: MP and t-Method values based on data points with t-Tags.

Figure A1.11: N_2 Isotherm for Y Zeolite

Appendix 2:

BTRS System Diary

1995

June '95

- reviewed Altimira and Autoclave Engineer (AE) proposals for computer controlled flow reactor system
- finalized basic design of flow reactor system

Oct. '95

- AE awarded flow reactor contract

Nov. '95

- determined utility (electrical, compressed air, water) and space requirements for reactor system
- investigated pump and MFC flow ranges available from source contractors

Dec. '95

- reviewed BTRS system blueprints
- identified errors, omissions, and areas of ambiguity

1996

Jan. '96

- communicated list of errors, omissions and areas of ambiguity to AE
- faxed outline of software needs for sample collection and reactor control to AE

Feb. '96

- contacted Valco and investigated seat materials available for multiposition valves
- collaborated with PE to design on-line splitter for GC to be located in Heated Enclosure

Mar. '96

- finalized flow ranges for pumps and MFCs and seat material for multiposition valves

Apr. '96

- installed lab benches and desks for BTRS equipment, PC and GC in walk-in fume hood in E1-3523A
- arranged installation of cylinder bays for GC and reactor gas cylinders
- arranged installation of utility (electrical, compressed air and water) sources

May '96

- GC installed in walk-in fume hood
- attended 2-day training session in Erie, Pennsylvania at AE site

June '96

- communicated hardware and software concerns identified during training session at AE manufacturing facility
    - unit fails pressure test - leak in system
    - program ability to link 5 recipes (18 steps each) together in Sample Control Window
    - Sample Control Window won't progress past step 2 - bug in software
    - program ability to link 5 recipes (10 steps each) together in Automatic Control Window
    - Reactor Status Valve display is Offline when reactor actually On-line
    - reactor Furnace set point is retained rather than being set to "0" after failsafe shutdown activated

June '96 (Continued)

- add real-time plot pop-up screens for reactor pressure and temperature as well as MFC and liquid pump outputs
- MFCs and pumps activating alarm - reason unknown
- tune parameters for BTRS oven, HTL and Heated Enclosure as large temperature overshoots occur
- error in overview flow schematic for valving of Separator bypass
- incorrect flow range for MFC2

- mediated resolution to above issues with AE personnel

July '96

- BTRS equipment delivered to U of W but no Operating Manual provided
- equipment unpacked and arranged in walk-in fume hood
- tubing installed to bring gas supplies from external cylinders to equipment located in barricade
- pressure regulator installed on compressed air line
- equipment modules connected by AE personnel
- oven would not turn on
- two faulty S.S. relay fuse boxes replaced to rectify problem
- CSA certification completed on-site

Aug. '96

- SSI finalizes design of inlet check valve prototype capable of withstanding high upstream pressure for use in HPLC pumps
- modified GC and integrator wiring to facilitate communication with and PLC
- modified GC plumbing such that head pressure of carrier gas flowing through Heated Enclosure can be regulated by GC MFC
- installed split injector prototype in Heated Enclosure using needle valve with Vernier handle to regulate split flow rate
- BTRS manual arrives

Aug. '96

- pressure and temperature test reactor
- Reactor Status Valve in BTRS oven making squeaking noise
- identified major leak in Reactor Status Valve and smaller one in 16 loop Multiposition valve in Heated Enclosure
- numerous software bugs identified
    - DDE conversations not initiated upon start-up of software
    - furnace set point in active recipe and oven set point overridden and set to default values when Automatic Cycle program initiated
    - problem with Dwell Time and GC Enable in step 9 of Sample Control recipe
    - Sample Control won't progress past step 11 in recipe
    - duration of Sample Valve position coupled to Automatic Control recipe dwell times
    - Sample Valve only maintained in inject position for 1 min and then reverts to back to collect position. This injects contamination region after sample injection making analysis impossible
    - logic for sending Start signal to GC through Sample Control recipe needs redevelopment

Sept. '96

- replaced Valcon T seat in Reactor Status Valve
- aligned valve and leak tested
- split ratio of split injector prototype drifts significantly during sampling causing poor reproducibility in the analysis of standard mixture - consult with PE to identify potential causes
- tried to heat Heated Enclosure to high temperature to seal 16-loop valve - maximum temperature possible is ~ 250°C
- heater cartridge under designed for Heater Enclosure

Oct. '96

- new software bugs identified
    - Reactor Status valve switches to Offline position without instructions from Automatic Cycle recipe
- requested second inlet check valve matching prototype
- AE manual operating valves (6) leaking
- BPR leaking

Nov. '96

- installed higher wattage heater cartridge in heater block of Heated Enclosure
- tested operation of new cartridge
- AE personnel installed new AE manual operating valves with higher temperature seat rating
- AE personnel replaced Kalrez "O" ring, teflon back-up ring and seat in BPR
- AE personnel coded revision to software to correct identified bugs in system

Dec. '96

- re-designed split injector prototype in Heated Enclosure using piece of column to regulate flow rate of vented sample
- poor analysis of standard mixture still achieved using second split injector prototype

1997

Jan. '97

- independent thermocouple measurements indicate Heated Enclosure air temperature is 100°C less than block heater temperature

Feb. '97

- AE notified of Heated Enclosure temperature problem and authorization given to return unit

Mar. '97

- AE acknowledges inability of Heated Enclosure to reach blueprint temperature specifications
- AE attempts are unsuccessful to retrofit Heated Enclosure with a fan for the purpose of air circulation
- AE proposes new Heated Enclosure design similar to BTRS oven

June '97

- newly designed Heated Enclosure arrives at U of W

July '97

- Heated Enclosure tested
- new split injector prototype designed and installed in GC
- satisfactory reproducibility obtained

Aug. '97

- reactor skin temperature alarm sporadically activated triggering 100 % output from furnace - DANGEROUS!
- possible sources of problem identified as:
  - faulty thermocouple
  - software bug
  - faulty PLC module
- install new thermocouple for reactor skin temperature and alarm problem disappears

Nov. '97

- HTL temperature control problem sporadically activating alarm and initiating reactor shut-down
- broken ground solder on HTL pin connector isolated as source of problem
- HTL pin re-soldered and tested
- BPR found to be leaking again
- Teflon back-up ring and Kalrez "O" ring assembled in incorrect order!
- wrong BPR literature supplied in BTRS manual!!

Nov. '97 (Continued)

- outstanding software bugs identified
    - memory effect on Sample Control Window - GC Enable commands for first recipe retained for all subsequent recipes regardless of commands stored in recipe file
    - coupling between Automatic Cycle Recipe and Sample Control recipe preventing sample collection during transitional times
- Reactor Status valve squeaking and leaking again
- developed method to flush contamination region in Heated Enclosure to vent prior to sample injection
- alter plumbing of GC to permit venting of contamination region while still maintaining carrier flow to GC column
- tested system and verified operation

Dec. '97

- replaced Kalrez "O" ring, Teflon back-up ring and seat in BPR
- installed Valcon E seat in Reactor Status valve and align
- modified BTRS oven software to reflect reduced upper temperature limit for Valcon E seat
- second inlet check valve arrives
- new software bugs identified:
    - problem with Step 15 of Sample Control window - Step 16 initiated after 5 min. maximum if value greater than 5 min. entered for Dwell Time of step 15
- disk containing latest corrections to software bugs arrives
- installed software onto PC

1998

Jan. '98

- tested two pumps operating simultaneously for first time
- corrected software installed in Dec. '97 employed outdated version of software as a basis
    - GC indicated Ready by software even if it is not Ready
    - GC Start signal sent without command being issued
    - coupling of GC Delay and Dwell time in Sample Control window
    - Sample Valve won't switch from Collect to Inject despite instructions from Automatic Control recipe - no samples can be injected to GC
- some previously "cured" software bugs revisited!
- healthiest version of software sent to AE to have corrections re-coded
- revised software returned by AE

Feb. '98

- loaded corrected software onto PC and test
- first successful run with actual data achieved!

Mar. - Apr. '98

- seventeen successful runs performed on flow reactor

May '98

- colour problems on display of Overview screen
- 16-loop valve sticking making actuation impossible
- Valco recommends re-conditioning valve
- requested modification to software from AE to permit operation of Heated Enclosure at conditioning temperature conditions
- installed revised software onto PC
- flow restricted when reactor placed on-line
- in-line filters installed backwards!
- in-line filters replaced in upstream and downstream locations of reactor and filter holders oriented correctly

June '98

- reconditioned 16-loop valve
- actuation achieved but valve still squeaks
- inlet pump loses prime when flow rates greater than 40 % capacity attempted
- removed and cleaned pump head in ultrasonic bath
- re-installed pump head and confirmed operation
- reactor skin temperature problem resurfaces
- MFC malfunctioning and activating alarm
- replaced reactor skin temperature thermocouple
- alarm problems persist making operation of equipment impossible
- virus scanner installed onto PC and Word and Excel viruses detected
- re-loaded Wonderware software onto PC

July '98

- source of reactor skin temperature and MFC alarm problems identified as faulty PLC module
- replacement module sent by AE
- module installed and alarm problems corrected

Sept. '98

- needle, 3-way and check valves for manual control of liquid flow fail
- manual control system for liquid feed re-designed
- new valves and fresh in-line filters installed in all inlet gas and liquid feed lines

Oct. '98

- 16-loop valve sticks again
- re-condition valve successfully but valve squeaks during actuation

Nov. '98

- 16 loop valve sticks
- re-conditioning cannot correct problem
- 16-loop valve removed and shipped to Valco for servicing

Nov. '98 (Continued)

- Valcon E seat installed in 16-loop valve by Valco

Dec. 98

- repaired 16-loop valve arrives at U of W
- 16-loop valve installed and aligned
- Heated Enclosure software modified to reflect reduced upper temperature limit

1999

Mar. '99

- tube failure on inlet side of reactor due to metal fatigue (as a result of repeated reactor head assembly removal for the purpose of catalyst loading)
- reactor head tubing design improved to reduce likelihood of metal fatigue in the future
- new tubing installed and reactor pressure tested
- pump losing prime

Apr. '99

- unreliable pump operation

May '99

- pump operation continues to be unreliable
- last experiment completed

Appendix 3:

Flow Reactor Operation and Sample Calculations

A3.1 OPERATION OF FLOW REACTOR

A3.1.1 Overview of Wonderware Software

Computer control of the BTRS reactor and on-line sampling systems, are accessible through Wonderware software. Although reactor pressure regulation is manually controlled, pressure detection and data logging, are supported by the software. Programming of the GC is also manual. However, Wonderware software displays GC Ready signal, if both the integrator and GC are in the Ready status. In addition, the software provides means to communicate a Start signal the GC to activate GC analysis.

The System Overview window is a flow schematic of the entire reactor system, providing a real-time status of all measurable parameters. Manual control of all components of the BTRS system, excluding the Sample Valve position and Multiposition Trapping Valve position (see Sample Control window), are facilitated through the System Overview window. Set point temperatures for the BTRS oven, HTLs and Heated Enclosure are entered through this screen, as programmed changes of these elements, are not supported by the software. The Automatic Cycle,

Sample Control, Historical Data Display and PLC Alarm windows are linked to the System Overview screen.

The Automatic Control window allows for the creation, storage and activation of programmed events for elements in the BTRS reactor system. These include furnace control (ramp rate, set point, dwell time), Reactor Status Valve position (Online/Offline), MFC flow rates and pump flow rates. Specific settings for these inputs can be stored in a recipe. Five recipes, each containing 10 steps, can be linked together providing a total of 50 possible events for programmed control. Activation/termination of automatic control of the BTRS system is facilitated through the Automatic Cycle window. Entering a Start command initiates programmed control of the reactor according to the steps outlined in the active recipe. Automatic control can be interrupted or terminated at any time, through the Hold or Stop commands respectively.

The Sample Control window regulates sample collection and management in the Heated Enclosure. The loop position and direction of rotation of the Multiposition Trapping Valve, and the position of Sample Valve, are all controlled through this screen. In addition, a Start signal can be issued to the GC to activate GC analysis. A total of 18 steps are available in each recipe, with the ability to link 5 recipes together, for programmed control. Initiation of the recipe is automatically activated when a Start signal is toggled from the Automatic Cycle window.

The PLC Alarms window is a colour coded screen which displays the current status of all system alarms. If a dangerous operating condition is detected by the PLC, an alarm is immediately annunciated. The PLC Alarm icon flashes red on the System Overview screen and the specific alarm condition flashes red on the PLC Alarm window. A two-level protocol for alarms is employed: High alarm and High/High Alarm. The first level (High alarm) warns the operator, that a condition approaching dangerous levels is detected. This allows time for the operator to intervene and correct the problem. The second alarm level (High/High alarm) is activated when a dangerous operating condition is measured and automatically disables the system. Reactant flow to the system is immediately terminated and the

Reactor Status Valve is switched to the off-line position. All furnaces and heaters are shut off and computer control is disengaged. Once the alarm condition has cleared, the alarm can be Reset, the system Enabled and normal operation resumed.

A data log, recording the levels of all operating conditions, alarm activations and set-point changes of controllers, is automatically activated upon start-up of Wonderware software. A history of all measurable elements in the system, can be viewed through the Historical Data Display window.

A3.1.2 Catalyst Addition

The reactor was removed from the system by disconnecting V-R12 and V-R13 (see the AE BTRS Oven Flow Schematic blueprint). The gland at the reactor bottom was detached and glass wool was inserted around the thermowell base assembled to the gland. This serves to trap solids or glass beads that may become entrained in the flowing mixture. The gland was re-attached to the reactor base. This procedure was routinely performed every 20 experiments.

The top gland of the reactor was removed to permit catalyst addition. Silica beads (1 mm diameter) were poured into the reactor to a depth of 16.25 cm (see Figure A3.1). Three grams of uncalcined catalyst ($250\mu m \leq d_p \leq 500\mu m$) were physically combined with 3 g silica beads. This mixture was poured on top of the glass beads, achieving a bed height of approximately 9.0 cm. Silica beads were added to the top of the catalyst bed, to fill the remaining void space in the reactor (approximately 16.25 cm depth). Glass wool was placed on top of the glass beads, to contain them during the gland assembly, as well as in the gland opening to trap particulate matter that may become entrained. The gland was re-connected to the reactor and the entire assembly was re-attached to the BTRS system. Three thermocouples were inserted at varying depths to monitor the temperatures in the pre-reaction zone, the catalyst bed and the post-reaction zone (see Figure A3.1).

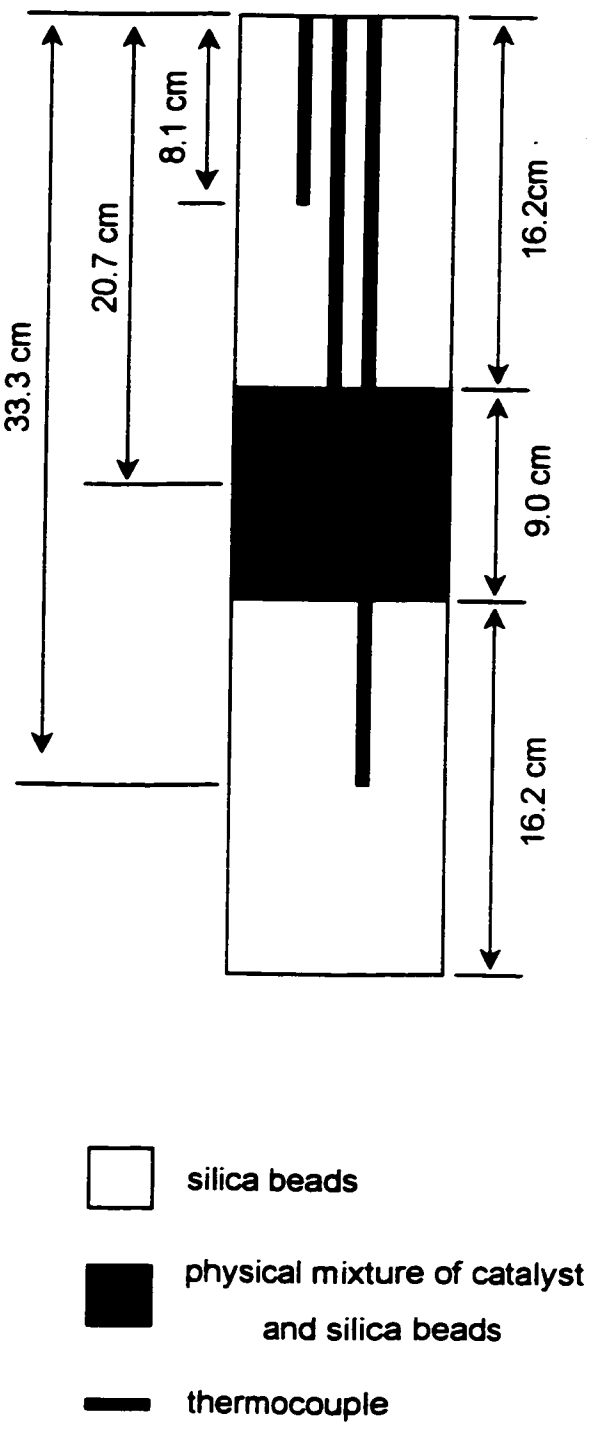

Figure A3.1: Catalyst Bed in Flow Reactor

A3.1.3 Calcination/Reduction Procedure

The Wonderware software was loaded and the system was Enabled from the System Overview screen. Valves V-R14, V-R12, V-R16, V-R13 and V-R15 were opened, putting the feed stream on-line to the reactor. The Reactor Status Valve was activated to the off-line position and nitrogen was flushed through the Reactor Purge Feed line for a few minutes by opening V-S11, V-S12 and V-S13. Upon completion of the flush step, these three valves were closed and Reactor Status Valve was returned to the on-line position.

The catalyst was calcined *in situ* prior to the experiment. The gas supply for the calcination cycle was determined by the position of two three-way valves on the input sides of both MFCs (see Figure A3.2). The three-way valves connect nitrogen, bench air and a gas mixture of 10 % hydrogen in argon to the MFC inlets such that pure nitrogen, air or nitrogen/hydrogen/argon mix can selected as the on-line supply for the system.

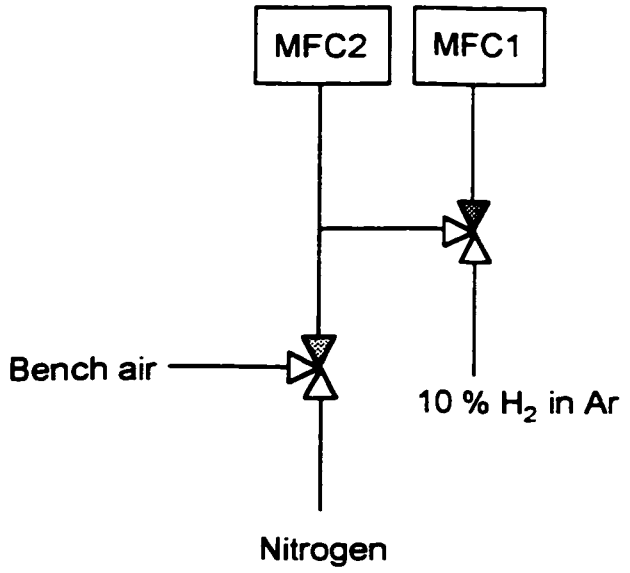

Figure A3.2: Gas supplies for MFC Inlets

The calcination program was entered through the Automatic Cycle window (see sample calcination program in Table A3.1). A N_2 flow rate of 50 sccm (sum of MF1 and MF2) was employed for the calcination cycle, with equal flow rates being supplied by each MFC (see Step 1 in Table A3.1). The reactor temperature was increased at a rate of 5°C/min to 425°C (Rxr Temp) and maintained at this temperature for 5 h or 300 minutes (Dwell). The Transition Time column of the recipe, was the period required for the reactor temperature to increase from the initial condition to the Rxr Temp level. Since the desired rate of temperature increase was 5°C/min, the time required to reach 425°C from room temperature (20°C), is 81 minutes. The Rxr Status was programmed to the on-line position to permit regulation of gas flow using the MFCs. The effluent from the reactor was vented through the drain tube of the Separator by closing valves V-P13 and V-P14 and opening V-P11 and V-P12. This is desirable to prevent deposition of contaminants, which may be removed by the calcination cycle, in the components of the Heated Enclosure.

Table A3.1: Automatic Cycle Recipe for Calcination Cycle

Step	MFC1 [sccm]	MFC2 [sccm]	Pump-1 [mL/min]	Pump-2 [mL/min]	Rxr Status	Rxr Temp [°C]	Transition [min]	Dwell [min]
1	25	25	0.00	0.00	Online	425	81	300
2	10	10	0.00	0.00	Offline	50	10	999

Once the calcination cycle (Step 1) was completed, the reactor was cooled to the reaction temperature level (in this example, the reaction temperature is 50°C) through Step 2 of the Calcination Program. If bench air was used during the calcination cycle, the gas flow was switched to nitrogen for the last 5 minutes of the calcination program.

No samples were collected during the calcination cycle. The Multiposition trapping valve was maintained in the same position throughout the calcination period. This was achieved by using the sample recipe provided in Table A3.2 for Sample Control.

Table A3.2: Sample Control Recipe for Calcination Cycle

Step	Loop No.	Direction (CW/CCW)	Sample (Collect/Inject)	GC Delay [sec]	Dwell Time [min]	GC Enable Enable/Disable
1	1	CW	Collect	0	999	Disable
2	1	CW	Collect	0	999	Disable

A3.1.4 Feed Sampling

The set point for the BTRS oven was calculated as being the reaction temperature minus a few degrees. This value was manually entered on the System Overview Screen. Temperatures of 200°C were entered for the set points of both HTLs, which provide connections to and from the Heated Enclosure. The Heated Enclosure was set at 200°C and the Reactor Status Valve directed to the off-line position, through manual entry on the System Overview screen. The feed analysis program was loaded onto the GC.

The flow rates for MFC1 and MFC2 were increased to 50 % of the maximum range and the BPR position was adjusted such that a system pressure of 450 psi is measured. The MFC rates were reduced to the levels which were to be employed in the experiment and the position of the BPR was fine tuned such that the pressure was maintained constant at 382 psi.

The liquid pumps were primed by isolating the pump through closure of valves V-F32 and V-F42. Starting with pump 1, a flow rate was entered on the System Overview screen, choosing a rate of approximately 10 % of the total pump range (1 mL/min). Once a increase in the pump head pressure was observed, the flow rate is gradually increased to approximately 50 % of the pump range. This pump rate was maintained until a pressure of approximately 1000 psi is measured. At this point, valve V-F32 was opened to permit liquid flow to the reactor system and the pump flow was adjusted to experiment level. An analogous approach was employed to prime pump 2.

Verification of liquid delivery was accomplished by manual flow measurement of the effluent exiting the Reactant Vent line. A dramatic increase in the flow rate occurred when the liquid front reaches the vent line. Once this event was detected, the feed sampling program was activated. The pump flow rates employed in the reaction program were applied in the feed sampling program (see Table A3.3).

Table A3.3: Automatic Cycle Recipe for Feed Sampling Program (T_{furn}=48°C; N_2 flow=35 sccm; Liquid Feed=2.76mL/min)

Step	MFC1 [sccm]	MFC2 [sccm]	Pump-1 [mL/min]	Pump-2 [mL/min]	Rxr Status	Rxr Temp [°C]	Transition [min]	Dwell [min]
1	21	14	0.00	2.76	Offline	48	1	999

Liquid flow was sustained for 30 min prior to collection of the first sample. This is important to provide uniform feed composition throughout the system as well as ensuring consistent sample injection into the GC. A total of 5 feed samples were collected and stored for analysis. At the conclusion of the sampling period, the loops were sequentially flushed and sent to the on-line GC system for detection. Note that the contamination region (orange lines in Figure 4.2) must be flushed prior to injection of the first sample to the GC (facilitated by Step 7 in Table A3.4).

Table A3.4: Sample Control Recipe for Feed Analysis

Step	Loop No	Direction (CW/CCW)	Sample (Collect/ Inject)	GC Delay [sec]	Dwell Time [min]	GC Enable (Enable/ Disable)	GC Valve[1] (Off/On)
1	1	CW	Collect	0	30	Disable	Off
2	2	CW	Collect	0	1	Disable	Off
3	3	CW	Collect	0	1	Disable	Off
4	4	CW	Collect	0	1	Disable	Off
5	5	CW	Collect	0	1	Disable	Off
6	6	CW	Collect	0	1	Disable	Off
7	6	CW	Inject	0	10	Disable	On
8	5	CCW	Inject	0	5	Enable	Off
9	4	CCW	Inject	0	5	Disable	Off
10	3	CCW	Inject	0	5	Disable	Off
11	2	CCW	Inject	0	5	Disable	Off
12	1	CCW	Inject	0	15	Disable	Off

1 GC Valve position manually controlled through touch pad of GC

The GC analysis of the five samples were compared. If consistent feed composition was measured, the feed analysis program was terminated and the reaction program was initiated. Feed flow was maintained off line between the feed analysis and reaction period.

A3.1.5 Reaction Sampling and Product Analysis

An acetone/ice water bath mixture was prepared in a 2 L beaker. The opening of a 250 mL Erlenmeyer flask was covered with parafilm and a small cut was made in the center of the parafilm cover. The alkylate analysis program was loaded onto the GC and the GC valve was set to the Off position.

The reaction recipes were loaded onto the Automatic Cycle (see Table A3.5). and Sample Control (see table A3.6) windows. Note that a delay of 5 min was provided for the reaction front to reach the Heated Enclosure (dwell time of 6 min in Step 1 includes delay of 5 min plus 1 min sample collection time period). The

program, with the exception of the active step of the recipe, can be edited during programmed operation, if the delay is observed to be longer than 5 min.

Programmed operation of the equipment was activated from the Automatic Cycle window. The flow rate of the effluent from the Reactant Vent was immediately measured with a bubble flow meter. When the reaction front was detected, the current sample loop of the Multiposition valve was noted. The sample contents of this loop are for 1 min TOS. The Reactant Vent line was immediately immersed in the acetone/ice water bath, with the end of the tubing placed through the parafilm hole and pointing into the Erlenmeyer flask. The Erlenmeyer flask was partially immersed in the acetone/ice water bath. This will serve to collect the liquid product over the course of the reaction.

Table A3.5: Automatic Cycle Recipe for Reaction
(T_{furn}=48°C; N_2 flow=35 sccm; Liquid Feed=2.76mL/min; t_{rxn}=1h)

Step	MFC1 [sccm]	MFC2 [sccm]	Pump-1 [mL/min]	Pump-2 [mL/min]	Rxr Status	Rxr Temp [°C]	Transition [min]	Dwell [min]
1	21	14	0.00	2.76	On-line	48	1	70
2	21	14	0.00	0.00	Off-line	25	1	10
3	5	5	0.00	0.00	Off-line	25	1	999
4	5	5	0.00	0.00	Off-line	25	1	999

Samples were collected every 1 min for the first 10 min of the reaction period (see Table A3.6). Thereafter, the samples were collected at different time frequencies to monitor the progression of catalyst activity over a total reaction period of 1 h. At the conclusion of the 1 h reaction period, the Erlenmeyer flask and the mass of the bulk liquid sample were measured. The GC valve was positioned in the On position to permit venting of the contamination region during Step 17 of Table A3.6.

Table A3.6: Sample Control Recipe for Reaction - Sample Collection (15 samples collected, t_{rxn}=1h)

Step	Loop No	Direction (CW/CCW)	Sample (Collect/ Inject)	GC Delay [sec]	Dwell Time [min]	GC Enable (Enable/ Disable)	GC Valve[1] (Off/On)
1	1	CW	Collect	0	6	Disable	Off
2	2	CW	Collect	0	1	Disable	Off
3	3	CW	Collect	0	1	Disable	Off
4	4	CW	Collect	0	1	Disable	Off
5	5	CW	Collect	0	1	Disable	Off
6	6	CW	Collect	0	1	Disable	Off
7	7	CW	Collect	0	1	Disable	Off
8	8	CW	Collect	0	1	Disable	Off
9	9	CW	Collect	0	1	Disable	Off
10	10	CW	Collect	0	1	Disable	Off
11	11	CW	Collect	0	2	Disable	Off
12	12	CW	Collect	0	3	Disable	Off
13	13	CW	Collect	0	5	Disable	Off
14	14	CW	Collect	0	10	Disable	Off
15	15	CW	Collect	0	30	Disable	Off
16	16	CW	Collect	0	1	Disable	Off
17	16	CW	Inject	0	10	Disable	On

1 GC Valve position manually controlled through touch pad of GC

Once the contamination region was flushed out, the samples were sequentially sent to the GC for analysis (see Table A3.7). Analysis time for each sample (including cool down time) was 105 min during summer months, but can be reduced to 95 min during winter months.

At the conclusion of the product analysis, the reaction program was stopped from the Automatic Cycle screen. The reactor was removed by disconnecting valves V-R12 and V-R13. The top gland of the reactor was removed and the entire contents were poured into a large beaker. The catalyst was separated from the glass beads by sieving, and retained for spent catalyst characterization. The glass beads were re-cycled by washing with double de-ionized water until all particulate matter was removed, and then dried overnight at 80°C. The reactor was cleaned to remove catalyst residue from the internal surfaces ,and prepare it for the next experiment.

Table A3.7: Sample Control Recipe for Reaction - Product Analysis
(15 samples analysed)

Step	Loop No	Direction (CW/CCW)	Sample (Collect/ Inject)	GC Delay [sec]	Dwell Time [min]	GC Enable (Enable/ Disable)	GC Valve[1] (Off/On)
1	1	CW	Inject	0	105	Enable	Off
2	2	CW	Inject	0	105	Enable	Off
6	3	CW	Inject	0	105	Enable	Off
4	4	CW	Inject	0	105	Enable	Off
5	5	CW	Inject	0	105	Enable	Off
6	6	CW	Inject	0	105	Enable	Off
7	7	CW	Inject	0	105	Enable	Off
8	8	CW	Inject	0	105	Enable	Off
9	9	CW	Inject	0	105	Enable	Off
10	10	CW	Inject	0	105	Enable	Off
11	11	CW	Inject	0	105	Enable	Off
12	12	CW	Inject	0	105	Enable	Off
13	13	CW	Inject	0	105	Enable	Off
14	14	CW	Inject	0	105	Enable	Off
15	15	CW	Inject	0	105	Enable	Off
16	16	CW	Collect	0	999	Disable	Off
17	16	CW	Collect	0	999	Disable	Off

1 GC Valve position manually controlled through touch pad of GC

A3.2 SAMPLE CALCULATIONS

A3.2.1 Butene WHSV

(Run F66EMT)

The butene mass flow rate was calculated using GC feed analysis and pump flow rate (see Table A3.7).

From Table A3.7, 1-$C_4^=$ mass flow rate = 0.09197 g/min.

Butene WHSV

$$= \frac{0.09197 \text{ g } 1\text{-}C_4^{=}}{\text{min}} \left| \frac{60 \text{ min}}{\text{h}} \right| \frac{}{2.78 \text{ g calcined catalyst}}$$

$$= 2.0 \text{ h}^{-1}$$

Table A3.7: Calculation of Butene Mass Flow Rate for Run F66EMT (Total liquid feed flow = 2.78 mL/min)

Component	GC Analysis [mass %]	Density[1] [g/mL]	Volume[2] [mL]	Volume[3] [%]	Volumetric Flow Rate[4] [mL/min]	Mass Flow Rate[5] [mL/min]
C_3	0.77	0.582	0.0132	0.74	0.02050	0.01193
i-C_4	91.08	0.557	1.6353	91.54	2.54475	1.41743
1-$C_4^{=}$	5.91	0.595	0.0993	5.56	0.15457	0.09197
n-C_4	2.24	0.579	0.0387	2.16	0.06017	0.03484
Total			1.78644		2.78	1.55617

1 data from Reid et al, 1977
2 basis of 100 g feed mixture: volume of component i [mL] = mass of component i [g] x density of component i [g/mL]
3 volume % of component i = volume component i [mL] ÷ total feed volume [mL] (basis 100 g feed)
4 volumetric flow rate of component i [mL/min] = volume % component ÷ 100 x Total Feed Volumetric Flow Rate [mL/min]
5 Mass flow rate of component i [g/min] = volumetric flow rate of component i [mL/min] x density of component i [g/mL]

A3.2.2 Butene Conversion

(Run F66EMT)

Mass Fraction of 1-$C_4^{=}$ Content in Feed = 0.0591 (see Table A3.7)

TOS = 1 min

1-$C_4^{=}$ Peak Area = 110200 (see Appendix A4.2)

Total Sample Peak Area = 61907245 (see Appendix A4.2)

Butene Conversion

$$= \frac{\left[0.0591 - \frac{110200}{61907245} \right]}{0.0591} \times 100\ \%$$

= 97 %

A3.2.3 Mass Balance in Flow Reactor

(Run F66EMT)

IN

2.87 Mass of $C_4^=$ converted during 1 h reaction period [g]

1.80 Mass of *i*-C_4 converted during Useful Catalyst Lifetime[1] [g]

4.67 Total Mass In [g]

OUT

1.43 Mass Liquid Collected over 1 h reaction period [g]

0.24 Mass Solid retained on Catalyst Surface (TGA/DTA)[2] [g]

1.67 Total Mass Out [g]

1 mass of *i*-C_4 converted ~ $C_4^=$ mass flow rate x Useful Catalyst Lifetime period

2 mass solid retained = total mass % (TGA/DTA) x 2.78 g catalyst

Mass Balance

$$= \frac{1.67}{4.67} \times 100\ \%$$

= 36 %

A3.2.4 Number of Successful Catalyst Cycles

(Run F21Y)

$C_4^=$ mass flow rate = 0.1167814 g/min

Useful Catalyst Lifetime period = 4.5 min

mass catalyst = 2.781 g (calcined)

Acid site density = 110 + 41 = 151 μmol Al/g catalyst (see Table 2.5)

Time Required to Saturate Catalyst Surface with Butene

$$= \frac{2.781\ \text{g calcined catalyst}}{} \left| \frac{(110+41)\ \mu\text{mol Al}}{\text{g cat}} \right| \frac{1\ \mu\text{mol } C_4^=}{1\ \mu\text{mol Al}} \left| \frac{\text{mol } C_4^=}{10^6\ \mu\text{mol } C_4^=} \right.$$

$$\times \frac{56.108\ \text{g } C_4^=}{\text{mol } C_4^=} \left| \frac{\text{min}}{0.1167814\ C_4^=} \right.$$

= 0.201757 min for saturation of all acid sites with $C_4^=$

Successful Catalyst Cycles

$$= \frac{4.5\ \text{min}}{0.201757\ \text{min}}$$

= 22 cycles

A3.2.5 Lennard Jones Diameter

The Lennard-Jones diameters were calculated for the TMP isomers using method outlined in Reid et al, 1977, pg 24

$$\sigma\left(\frac{P_c}{T_c}\right)^{1/3} = 2.3551 - 0.087\,\omega$$

Values for P_c, T_c and ω are taken from Reid et al, 1977.

Table A3.8: Calculation of Lennard-Jones Diameter for TMP Isomers

Component	P_c [atm]	T_c [K]	ω	Lennard-Jones Diameter [Å]
2,2,4-TMP	25.3	543.9	0.303	6.5
2,2,3-TMP	26.9	563.4	0.297	6.4
2,3,4-TMP	26.9	566.3	0.317	6.4
2,3,3-TMP	27.8	573.5	0.290	6.4

Appendix 4:

Raw Data

A4.1 EXPERIMENTAL SUMMARY FOR PROCESS AND CATALYST EFFECTS

Table A4.1: Experimental Summary for Effect of Calcination Temperature (t_{calc}=3h; P=382psig; I/O=11; t_{rxn}=1h)

Catalyst	T_{rxn} [°C]	T_{calc}=425°C	T_{calc}=540°C
EMT	55	F28EMT	F23EMT
	77	F31EMT	
	88		F22EMT
	100	F34EMT	
Y	70	F29Y	
	86		F21Y
	100	F33Y	

Table A4.2: Experimental Summary for Effect of Reaction Temperature (T_{calc}=425°C; t_{calc}=3h; P=382psig; I/O=11; t_{rxn}=1h)

Catalyst	T_{rxn} [°C]	Run Number
EMT	33	F25EMT
	55	F28EMT
	77	F31EMT
	100	F34EMT
Y	29	F27Y
	53	F24Y, F36Y
	70	F29Y
	100	F33Y

Table A4.3: Experimental Summary for Effect of Butene WHSV
(Y; T_{calc}=540°C; t_{calc}=3h ; T_{rxn}=80°C; P=382psig)

Butene WHSV [h^{-1}]	Duration [min]	I/O	Run Number
0.51	19	58	F11Y
	55	58	F13Y
2.57	19	12	F21Y

Table A4.4: Experimental Summary for Effect of Pt Supported on Acidic Carrier
(T_{calc}=325°C; t_{calc}=3h; T_{red}=425°C; t_{red}=3h; T_{rxn}=50°C; P=382psig; I/O=15)

Catalyst	Pt Loading [mass %]	Nomenclature	Fresh	Regenerated
EMT	0	EMT	F66EMT F68AEMT	F67EMTr
	0.1	0.1%Pt/EMT	F62Pt1EMT	F45Pt1EMTr F63Pt1EMTr
	0.5	0.5%Pt/EMT	F49Pt5EMT	F48Pt5EMTr F50Pt5EMTr F60Pt5EMTr
Y	0	Y	F54Y	F55Yr
	0.5	0.5%Pt/Y	F44Pt5Y F56Pt5Y	F58Pt5Yr

A4.2: RAW DATA

Table A4.5: Complete Experimental Summary

Run	Catalyst System	T_{calc} [°C]	T_{red} [°C]	T_{run} [°C]	Duration [min]	I/O (molar)	$C_4^=$ WHSV [h^{-1}]	S.A. Spent [m^2/g]	S.A. Fresh [m^2/g]	Yield [$gC_5^=/gcat/gC_4^=fed$]
F11Y	Y	540	n.a.	80	19	57.8	0.51	407	620	n.a.
F13Y	Y	540	n.a.	80	55	58.4	0.51	284	620	n.a.
F15Y Pulse	Y, Pulse feed	540	n.a.	80	40	59	0.49	396	620	n.a.
					30	3000	0.01			
					30	59	0.49			
					20	3000	0.01			
F21Y	Y	540	n.a.	86	19	12.0	2.57	205	620	n.a.
F22EMT	EMT	540	n.a.	88	15	11.6	2.62	121	755	n.a.
F23EMT	EMT	540	n.a.	56	13	11.7	2.55	148	755	n.a.
F24Y	Y	425	n.a.	56	60	11.1	2.70	372	620	n.a.
F25EMT	EMT	425	n.a.	33	60	11.1	2.71	470	755	n.a.
F27Y	Y	425	n.a.	29	60	11.2	2.72	386	620	n.a.
F28EMT	EMT	425	n.a.	55	60	11.3	2.68	377	755	0.101
F29Y	Y	425	n.a.	70	60	11.2	2.67	374	620	0.084
F31EMT	EMT	425	n.a.	77	60	11.4	2.65	348	755	0.104
F33Y	Y	425	n.a.	100	60	11.5	2.62	329	620	0.088
F34EMT	EMT	425	n.a.	100	60	11.5	2.61	309	755	0.113
F36Y	Y	425	n.a.	49	60	11.5	2.61	350	620	0.064
F44Pt5Y	0.5%Pt/Y	325	425	52	60	15.3	2.00	280	581	0.076
F45Pt1EMTr	recalc. 0.1%Pt/EMT	325	425	52	60	15.2	2.02	254	616	0.092
F48Pt5EMTr	recalc. 0.5%Pt/EMT	325	425	52	60	15.2	2.03	294	589	0.109
F49Pt5EMT	0.5%Pt/EMT	325	425	51	60	15.2	2.02	recalc	589	0.095
F50Pt5EMTr	recalc. 0.5%Pt/EMT	325	425	50	60	15.0	2.05	recalc	589	0.081
F54Y	Y	425	n.a.	50	60	15.2	2.03	372	620	0.068
F55Yr	recalc. Y	425	n.a.	50	60	14.4	2.13	281	620	0.049
F56Pt5Y	0.5%Pt/Y	325	425	53	60	14.5	2.12	recalc	581	0.050
F58Pt5Yr	recalc. 0.5%Pt/Y	325	425	52	60	14.5	2.11	260	581	0.050
F60Pt5EMTr	recalc. 0.5%Pt/EMT	325	425	52	60	14.5	2.11	198	589	0.073
F62Pt1EMT	0.1%Pt/EMT	325	425	50	60	14.6	2.10	recalc	616	0.078
F63Pt1EMTr	recalc. 0.1%Pt/EMT	325	425	50	60	14.8	2.07	231	616	0.064
F66EMT	EMT	425	n.a.	53	60	14.9	2.07	377	755	0.079
F67EMTr	recalc. EMT	425	n.a.	52	60	15.0	2.06	287	755	0.062
F68EMT	EMT	425	n.a.	53	60	14.9	2.06	124	385.5	0.085

F11Y

(Y; Tcalc=540degC; Trxn=80degC; P=382psig; I/O=57.8; butene WHSV=0 51h-1; t=19min; mcat=2.78g)

Samp t (min)	6	20	25	30	****	60		
T.O.S. (min.)	**1**	**15**	**20**	**25**	**51**	**55**		
1-C4= Disapp. [%]	100	100	100	100		100	****	data from pulse experiment (F15Y pulse)
t-2-C4= Prod. [%]	0	0	0	0		24		
c-2-C4= Prod. [%]	0	0	0	0		0		
Butene Disapp. [%]	**100**	**100**	**100**	**100**	**80**	**76**		
n-Butane Change [%]	3	1	1	5		3		
C5+ Product Analysis [mass %]								
C5-C7	21	32	32	32		15		
C8	**78**	**63**	**65**	**66**		**83**		
C9+	1	5	3	2		2		
C8 Distribution [mass %]								
TMP	**83**	**76**	**75**	**76**		**61**		
DMH	13	20	20	20		27		
C8=	3	4	5	5		12		
TMP Isomer Distribution [%]								
2,2,4-TMP	39	50	46	46		30		
2,2,3-TMP	7	9	8	8		5		
2,3,4-TMP	25	15	18	19		33		
2,3,3-TMP	30	26	28	28		32		
Indicators [mass fraction]								
TMP	**6.18**	**3.89**	**3.75**	**3.89**		**2.28**		
DMH								
TMP+DMH	20.0	7.8	9.6	12.3		6.3		
C8= + C9+								
(2,2,3-+2,2,4-TMP)	0.83	1.45	1.18	1.15		0.54		
(2,3,4-+2,3,3-TMP)								
DMH Isomer Distribution [%]								
2,5-DMH	19	19	16	16		0		
2,4-DMH	40	40	36	35		21		
2,3-DMH	41	35	37	37		36		
3,4-DMH	0	6	11	12		42		

F11Y

(Y, Tcalc=540degC, Trxn=80degC, P=382psig, I/O=57 8, butene WHSV=0 51h-1, t=19min, mcat=2 78g)

TOS [min]	1	15	20	25	51	55					
Propane	343700	375740	361180	452700		442320					
Isobutane	39386540	37916100	39916360	50170900		50037100					
1-butene											
n-butane	1071920	1022900	1070260	1412900		1352460					
t-2-butene						218100					
c-2-butene											
C5-C7	113390	280196	284538	372467		42337					
C5		108020	110020	141400							
2,3-DMB	39571	53547	55887	73472		14620					
2,2-DMP	9505	17744	17095	21643							
3-MP	9268	14752	14736	19566		5500					
2,4-DMP	36961	46244	47139	62896		12608					
2,2,3-TMB											
2-MHx		6032	5262	7350							
2,3-DMP	18085	27511	28264	38161		9609					
3-MHx		6346	6135	7979							
C8	413742	550303	584973	780762		226433					
2,2,4-TMP	132852	209038	202122	271955		41756					
2,5-DMHx	10307	20161	19051	24668							
2,2,3-TMP	22770	39700	35431	45379		6931					
2,4-DMHx	22389	43617	41889	53598		13063					
2,3,4-TMP	85449	63911	79493	110318		45652					
2,3,3-TMP	103011	107701	122434	165427		44621					
2,3-DMHx	23001	38110	43260	56436		21948					
1 DMHx=											
3,4-DMHx		6073	12974	17614		25846					
2 DMHx=						14384					
3 DMHx=						7193					
4 DMHx=											
5 DMHx=	13963	21992	22997	28429		5039					
6 DMHx=			5322	6938							
7 DMHx=											
8 DMHx=											
C9+	6032	46099	29478	25190		5322					
C5+	533164	876598	898989	1178419		274092					
Tot Peak Area	41335324	40191338	42246789	53214919		52324072					
Feed Analysis	Inj 1	Inj 2	Inj 3	Inj 4		Inj 5	Inj 6	Inj 7	Inj 8	Avg	Mass %
C3	21811	22132	23017	23695		20052	23270	20836	24148	22370	0 86
i-C4	2413079	2252501	2532986	2627719		2191759	2514630	2173455	2657030	2420395	94 85
1-C4=	36806	35099	47252	36807		47987	35109	45815	35111	39998	1 77
n-C4	62822	59993	67270	71747		56347	66435	57014	70493	64015	2 52
I/O Mass Ratio	65 56	64 18	53 61	71 39		45 67	71 62	47 44	75 68	**60.51**	

F13Y

(Y; Tcalc=540degC; Trxn=80degC; P=382psig; I/O=58.42; butene WHSV=0.51h-1; t=55min; mcat=2.78g)

Samp t [min]	6	7	8	9	10	11	12	13	14	15	17	20	25
T.O.S. [min.]	**1**	**2**	**3**	**4**	**5**	**6**	**7**	**8**	**9**	**10**	**12**	**15**	**20**
1-C4= Disapp. [%]	100	100	100	100	100	100	100	100	100	100	100	100	100
t-2-C4= Prod. [%]	0	0	0	0	0	0	0	0	0	0	0	0	0
c-2-C4= Prod. [%]	0	0	0	0	0	0	0	0	0	0	0	0	0
Butene Disapp. [%]	**100**	**100**	**100**	**100**	**100**	**100**	**100**	**100**	**100**	**100**	**100**	**100**	**100**
n-Butane Change [%]	6	7	5	5	6	-1	6	7	7	7	4	6	6
C5+ Product Analysis [mass %]													
C5-C7	18	16	36	35	35	27	34	22	22	23	23	32	30
C8	**67**	**56**	**57**	**64**	**61**	**73**	**58**	**69**	**78**	**76**	**75**	**65**	**63**
C9+	16	28	7	1	3	0	7	8	0	1	2	3	6
C8 Distribution [mass %]													
TMP	**81**	**80**	**78**	**77**	**77**	**78**	**76**	**77**	**78**	**77**	**78**	**76**	**75**
DMH	15	16	18	19	19	19	20	19	18	19	19	20	20
C8=	4	4	4	4	4	3	4	4	4	4	3	5	5
TMP Isomer Distribution [%]													
2,2,4-TMP	**48**	**49**	**52**	**51**	**53**	**54**	**53**	**51**	**49**	**50**	**51**	**48**	**47**
2,2,3-TMP	9	10	11	11	11	12	11	10	9	10	9	9	8
2,3,4-TMP	17	15	14	14	13	12	13	14	16	15	14	16	18
2,3,3-TMP	26	26	24	24	23	22	23	25	26	26	25	27	28
Indicators [mass fraction]													
TMP	**6.39**	**3.50**	**3.48**	**4.02**	**3.98**	**4.06**	**3.78**	**4.12**	**4.35**	**4.17**	**4.08**	**3.85**	**3.79**
DMH													
TMP+DMH	3.5	1.8	5.8	15.5	10.1	29.4	5.6	6.1	26.1	18.0	15.0	10.4	6.2
C8= + C9+													
(2,2,3-+2,2,4-TMP)	1.33	1.44	1.68	1.67	1.80	1.95	1.72	1.58	1.41	1.46	1.56	1.32	1.22
(2,3,4-+2,3,3-TMP)													
DMH Isomer Distribution [%]													
2,5-DMH	22	22	23	21	22	23	22	21	20	20	20	18	17
2,4-DMH	44	45	45	42	44	47	45	45	43	43	46	40	39
2,3-DMH	35	33	33	32	30	29	34	34	38	37	34	37	37
3,4-DMH	0	0	0	5	5	0	0	0	0	0	0	6	7

F13Y

(Y, Tcalc=540degC, Trxn=80degC, P=382psig, I/O=58 42, butene WHSV=0 51h-1, t=55min, mcat=2 78g)

TOS [min]	1	2	3	4	5	6	7	8	9	10	12	15	20
Propane	295980	103900	284600	333920	313200	271860	247800	280480	302100	273620		322820	321740
Isobutane	36150300	14091200	30434160	37866480	35353320	23818240	29806340	31409320	32863680	29198560	12106300	36079460	36385780
1-butene													
n-butane	943700	371140	787400	986060	931080	575980	784640	825580	861280	771040	308020	949900	952600
t-2-butene													
c-2-butene													
C5-C7	108674	68785	266162	354706	328330	81491	299562	139576	110014	124476	60761	266573	268358
C5			111380	135260	130840		118060					102140	101060
2,3-DMB	34187	22517	49730	67384	61199	27720	56149	42380	37259	41812	20055	51232	52290
2,2-DMP	10277	6700	16672	24063	21305	10307	20330	15061	11754	13690	6803	16404	16538
3-MP	9390	5989	13136	18718	16462	7896	15806	11953	9734	11222	5526	13836	14085
2,4-DMP	35617	21936	41805	57527	53237	22479	47001	36131	32360	36219	18000	44598	45077
2,2,3-TMB													
2-MHx			5631	8450	7728		7225	5382				5492	5696
2,3-DMP	19203	11643	22625	34807	30298	13089	27919	22857	18907	21533	10377	26762	27552
3-MHx			5183	8497	7261		7072	5812				6109	6060
C8	409673	234892	414051	650486	567028	220680	505648	434145	387425	417734	200328	549012	554710
2,2,4-TMP	**158516**	**92196**	**167640**	**257046**	**230593**	**93167**	**201061**	**171089**	**148720**	**161297**	**80021**	**199882**	**194355**
2,5-DMHx	13395	8191	16474	25775	23590	9842	21924	17378	13791	15782	7790	19607	18939
2,2,3-TMP	31402	18303	34964	55245	49142	20003	40340	34379	28565	31002	14703	36531	34346
2,4-DMHx	27102	17043	32669	52566	47495	19974	45089	36565	29651	33431	17401	42602	42479
2,3,4-TMP	55705	28951	44278	68650	55942	21032	51260	47786	47145	48456	22314	67472	73180
2,3,3-TMP	86626	47968	76670	118588	99330	37058	89269	82189	78978	82809	38385	111008	115031
2,3-DMHx	21560	12690	23909	39884	32886	12344	34157	27458	26285	28382	12865	39301	41178
1 DMHx=												5024	5667
3,4-DMHx				6135	5212							6119	7366
2 DMHx=													
3 DMHx=													
4 DMHx=													
5 DMHx=	15367	9550	17447	26597	22838	7260	22548	17301	14290	16575	6849	21466	22169
6 DMHx=													
C9+	96962	118918	50434	13738	31119	0	64181	51030	0	5761	6032	23587	56827
C5+	615309	422595	730647	1018930	926477	302171	869391	624751	497439	547971	267121	839172	879895
Tot Peak Area	38005289	14884935	32236807	40205390	37524077	24968251	31708171	33140131	34524499	30791191	12681441	38191352	38540015
Feed Analysis	Inj 1	Inj 2	Inj 3	Inj 4	Inj 5	Inj 6	Inj 7	Inj 8	Avg	Mass %			
C3	14971	11396	13370	13643	15565	14025	13852	14427	13906	0 92			
i-C4	1774607	1046230	1382735	1544128	1855039	1632041	1530496	1635923	1550150	95 14			
1-C4=	29137	18425	23354	24713	33291	25524	24331	28423	25900	1 61			
n-C4	44016	24789	33947	38993	45873	40636	37740	40317	38289	2 34			
I/O Mass Ratio	60 91	56 78	59 21	62 48	55 72	63 94	62 90	57 56	59 85				

F15Y Pulse

(Y pulse feed; Tcalc=540degC; Trxn=80degC; P=382psig; I/O=59(40min),I/O=3000(30min),I/O=59(30min),I/O=3000(20min); t=2h; mcat=2.78g)

Samp t [min]	6	20	35	40	45	55	60	70	85	90	100	105	125	125
T.O.S. [min.]	**1**	**15**	**30**	**35**	**40**	**50**	**55**	**65**	**80**	**85**	**95**	**100**	**120**	**120**
1-C4= Disapp. [%]	100	100	100	100	100	76	77	74	100	100	100	100	100	100
t-2-C4= Prod. [%]	0	0	0	0	0	0	0	0	0	0	0	0	5	0
c-2-C4= Prod. [%]	0	0	0	0	0	0	0	0	0	0	0	0	0	0
Butene Disapp. [%]	**100**	**100**	**100**	**100**	**100**	**76**	**77**	**74**	**100**	**100**	**100**	**100**	**95**	**100**
n-Butane Change [%]	-12	2	0	4	-2	3	4	6	3	1	3	2	45	-100
C5+ Product Analysis [mass %]														
C5-C7	0	32	18	15	6	6	11	0	18	17	14	9	7	100
C8	**6**	**62**	**70**	**69**	**48**	**54**	**77**	**49**	**69**	**67**	**75**	**61**	**45**	**0**
C9+	94	6	12	16	46	39	12	51	13	17	11	30	48	0
C8 Distribution [mass %]														
TMP	**100**	**76**	**74**	**82**	**90**	**90**	**91**	**100**	**76**	**76**	**84**	**92**	**85**	**0**
DMH	0	20	21	16	10	10	9	0	20	20	16	8	11	0
C8=	0	4	4	2	0	0	0	0	4	4	0	0	4	0
TMP Isomer Distribution [%]														
2,2,4-TMP	**100**	**52**	**44**	**42**	**41**	**38**	**37**	**49**	**40**	**37**	**32**	**33**	**32**	**0**
2,2,3-TMP	0	10	8	7	5	5	5	0	6	5	4	0	4	0
2,3,4-TMP	0	14	19	21	23	26	27	25	24	27	32	34	34	0
2,3,3-TMP	0	24	30	30	31	31	32	26	30	31	32	33	31	0
Indicators [mass fraction]														
TMP	**inf**	**3.77**	**3.47**	**5.30**	**8.82**	**8.53**	**10.39**	**#DIV/0!**	**3.83**	**3.80**	**5.10**	**11.93**	**7.63**	**0.00**
DMH														
TMP+DMH	0.07	7.25	4.57	3.94	1.04	1.38	6.46	0.95	4.36	3.32	6.56	2.02	0.86	0.00
C8= + C9+														
(2,2,3-+2,2,4-TMP)	**infinite**	**1.64**	**1.06**	**0.95**	**0.85**	**0.76**	**0.71**	**0.95**	**0.84**	**0.73**	**0.57**	**0.49**	**0.55**	**0.00**
(2,3,4-+2,3,3-TMP)														
DMH Isomer Distribution [%]														
2,5-DMH	**0**	**19**	**16**	**17**	**0**	**0**	**0**	**0**	**14**	**13**	**0**	**0**	**0**	**0**
2,4-DMH	**0**	**44**	**40**	**40**	**45**	**40**	**43**	**0**	**32**	**31**	**25**	**0**	**33**	**0**
2,3-DMH	**0**	**32**	**38**	**43**	**55**	**60**	**57**	**0**	**40**	**42**	**51**	**100**	**67**	**0**
3,4-DMH	**0**	**5**	**6**	**0**	**0**	**0**	**0**	**0**	**14**	**15**	**25**	**0**	**0**	**0**

F15Y Pulse

(Y pulse feed, Tcalc=540degC, Trxn=80degC, P=382psig, I/O=59(40min),I/O=3000(30min),I/O=59(30min),I/O=3000(20min), t=2h, mcat=2 78g)

TOS [min]	1	15	30	35	40	50	55	65	80	85	95	100	120	120
Propane	110600	306780	280040	336320	207520	297040	329760	287900	346300	388240	414520	346140	2873500	
Isobutane	10521360	33938820	27255120	37532120	20957260	31772420	37252840	33927080	39156760	39957180	45583580	36199720	206100760	
1-butene						101600	112560	117300						
n-butane	241800	914020	717720	1011900	532640	848140	1003040	925500	1057260	1056440	1209700	950820	7781720	
t-2-butene													147840	
c-2-butene														
C5-C7	0	295058	120260	76049	15065	16377	23155	0	152509	133482	41894	12165	35561	22323
Unknowns													7096	
C5		111620												
2,3-DMB		56904	32956	25262	7454	8025	8561		50163	44711	16634	6133	13996	
2,2-DMP		19460	10351	6556					13580	12197				
3-MP		15480	8023	6446					13156	12107				
2,4-DMP		49457	29790	23544	7611	8352	9371		43253	39489	15557	6032	13200	
2,2,3-TMB			19070											
2-MHx		6511												
2,3-DMP		28879	19070	14241			5223		26897	24978	9703		8365	
3-MHx		6747							5460					
C8	12667	568092	471016	354301	112191	139206	160008	26495	588083	538299	221501	80470	240690	
Unknowns														
2,2,4-TMP	**12667**	**226020**	**152182**	**122949**	**40822**	**47437**	**53426**	**12896**	**178692**	**151428**	**59921**	**24420**	**64407**	
2,5-DMHx		21732	15993	9104					16111	13728				
2,2,3-TMP		42562	27523	19660	5367	6346	7144		26716	21235	7270		7797	
2,4-DMHx		50261	40403	22237	5090	5865	6037		37409	33055	8936		8774	
2,3,4-TMP		59575	65778	62265	23052	31842	38773	6754	107618	111218	59569	25238	68596	
2,3,3-TMP		104388	104230	87194	31528	38977	46617	6845	136107	126720	58411	24590	63227	
1 DMHx=														
2,3-DMHx		37203	38211	23782	6332	8739	8011		46897	45128	18407	6222	17969	
2 DMHx=														
3,4-DMHx		5464	6206						16786	16094	8987			
3 DMHx=														
4 DMHx=														
5 DMHx=		20887	20490	7110					21747	19693			9920	
6 DMHx=														
C9+	193368	54618	78118	81097	107566	100625	24780	27767	108288	136684	33786	39922	258745	
C5+	206035	917768	669394	511447	234822	256208	207943	54262	848880	808465	297181	132557	534996	1295073
Tot Peak Area	11079795	36077388	28922274	39391787	21932242	33275408	38906143	35312042	41409200	42210325	47504981	37629237	217438816	22323
FEED ANAL.	Inj 1	Inj 2	Inj 3	Inj 4	Inj 5	Inj 6	Inj 7	Inj 8	Avg	Mass %				
C3	20292	21483	22487	19923	18960	22270	19309	19577	20538	0 92				
I-C4	2211568	2402444	2332710	2014358	2059596	2497250	1879306	2100364	2187200	95 34				
1-C4=	34848	41680	31082	37258	27617	45973	24739	43129	35791	1 27				
n-C4	56359	63921	60478	51606	51376	64387	46759	53769	56082	2 47				

Run F21Y

(Y; Tcalc=540degC; Trxn=86degC; P=382psig; I/O=12 0; butene WHSV=2.57h-1; t=19min, mcat=2 78g)

Samp t [min]	8	9	10	11	12	13	14	15	16	18	20	24	26
T.O.S. [min.]	**1**	**2**	**3**	**4**	**5**	**6**	**7**	**8**	**9**	**11**	**13**	**17**	**19**
1-C4= Disapp. [%]	100	100	100	100	100	100	100	100	97	100	100	85	27
t-2-C4= Prod. [%]	0	0	0	0	7	21	28	33	36	40	38	33	10
c-2-C4= Prod. [%]	0	0	0	0	3	10	14	17	19	23	23	21	7
Butene Disapp. [%]	**100**	**100**	**100**	**100**	**90**	**70**	**58**	**49**	**42**	**37**	**39**	**30**	**10**
n-Butane Change [%]	-2	12	11	8	6	4	3	2	3	10	6	2	-1
C5+ Product Analysis [mass %]													
C5-C7	18	42	32	32	26	12	0	0	0	0	0	0.0	0.0
C8	**45**	**45**	**34**	**43**	**42**	**41**	**13**	**21**	**35**	**27**	**44**	**43**	**65**
C9+	37	14	34	25	32	47	87	79	65	73	56	57	35
C8 Distribution [mass %]													
TMP	**63**	**68**	**76**	**64**	**58**	**48**	**23**	**0**	**0**	**2**	**0**	**0**	**0**
DMH	26	24	17	23	22	31	38	33	36	29	33	30	17
C8=	11	8	7	12	20	22	39	67	64	68	67	70	83
TMP Isomer Distribution [%]													
2,2,4-TMP	**41**	**52**	**48**	**45**	**39**	**33**	**50**	**0**	**0**	**0**	**0**	**0**	**0**
2,2,3-TMP	6	6	3	4	3	10	0	0	0	0	0	0	0
2,3,4-TMP	22	18	21	23	27	29	50	0	0	100	0	0	0
2,3,3-TMP	31	25	28	28	30	28	0	0	0	0	0	0	0
Indicators [mass fraction]													
TMP	**2.46**	**2.89**	**4.44**	**2.74**	**2.63**	**1.55**	**0.60**	**0.00**	**0.00**	**0.08**	**0.00**	**0.00**	**0.00**
DMH													
TMP+DMH	0.95	2.37	0.88	1.26	0.84	0.57	0.09	0.08	0.14	0.09	0.17	0.15	0.13
C8= + C9+													
(2,2,3-+2,2,4-TMP)	0.89	1.36	1.07	0.96	0.75	0.75	1.00	0.00	0.00	0.00	0.00	0.00	0.00
(2,3,4-+2,3,3-TMP)													
DMH Isomer Distribution [%]													
2,5-DMH	17	20	19	17	15	5	0	0	0	0	0	0	0
2,4-DMH	42	47	31	43	36	4	0	13	10	11	11	11	0
2,3-DMH	39	33	50	40	49	35	0	11	8	10	10	10	0
3,4-DMH	2	0	0	0	0	56	100	76	82	80	79	79	100

Run F21Y

(Y, Tcalc=540degC, Trxn=86degC, P=382psig, I/O=12 0, butene WHSV=2 57h-1, t=19min, mcat=2 78g)

TOS [min]	1	2	3	4	5	6	7	8	9	11	13	17	19
Propane	197360	266660	114040	300200	309100	314440		200840	294500	250000	221200	287860	321660
Isobutane	19094400	30900000	13999080	36630580	38480580	39680740	11480800	24952760	37637480	31340200	27405980	36570860	39773660
1-butene									102960			459660	2388560
n-butane	490740	839500	383740	965040	979480	985400	282600	603640	922100	834380	685660	887640	955320
t-2-butene					228300	664540	262780	676440	1085800	1028200	842120	989600	324740
c-2-butene					100600	311460	129900	346300	591860	604640	497580	617300	218340
C5-C7	567828	949572	402667	855476	557041	127628	0	0	0	5568	0	0	0
C5	200920	373020	159160	330140	211720								
2,3-DMB	96971	173942	73835	155887	100527	36235							
2,2-DMP	39514	72310	30126	61807	39212	13956							
3-MP	32959	58367	25579	56286	41085	19512							
2,4-DMP	90190	130924	55035	114872	73046	24801				5568			
2,2,3-TMB		7340		7569									
2-MHx	19232	24455	10236	20983	13691								
2,3-DMP	68111	84774	37764	84209	60927	25261							
3-MHx	19931	24440	10932	23723	16833	7863							
C8	1386395	1020392	432771	1153335	912362	431328	44439	145081	251237	327216	196454	228332	35002
2,2,4-TMP	**360879**	**363343**	**158709**	**333022**	**208795**	**69060**	**5048**						
2,5-DMHx	61949	48950	13882	46858	29537	7171							
2,2,3-TMP	53681	38661	10640	30713	17697	19889							
2,4-DMHx	149394	113366	22847	116075	72736	5573		6082	8634	10238	7306	7866	
2,3,4-TMP	190655	123066	67331	170298	142203	60105	5066			7653			
2,3,3-TMP	272877	173156	91246	207763	161648	57402							
2,3-DMHx	139421	79267	37082	107583	99445	45816		5571	7301	9351	6430	6953	
3,4-DMHx	5990					74103	16886	36927	73454	75976	51191	54705	6114
1 DMHx=	39207	23666	15830	71524	119519	70505	17439	81687	131373	169030	108824	122678	23641
2 DMHx=	8502	5645		9380	19484								
3 DMHx=													
4 DMHx=													
5 DMHx=	103840	51272	15204	60119	41298	7756							
6 DMHx=						14928		14814	30475	54968	22703	36130	5247
C9+	1144247	316172	426107	659877	690649	503640	299566	530183	458645	894334	250626	307794	19235
C6+	3098470	2286136	1261545	2668688	2160052	1062596	344005	675264	709882	1227118	447080	536126	54237.
Tot Peak Area	22880970	34292296	15758405	40564508	42258112	43019176	12500085	27108944	40752722	34679898	29602040	39731746	43818177
Feed Analysis	Inj 1	Inj 2	Inj 3	Inj 4	Inj 5	Avg	Mass %						
C3	14196	14797	13279	17012	11677	14192	0 80	Avg Mass I/O Ratio			11 98		
i-C4	1745833	1815391	1349449	2119341	897858	1585574	89 54	Avg Molar I/O Ratio			**11.562**		
1-C4=	145978	152839	115276	173169	74169	132286	7 47						
n-C4	43097	45605	33722	51401	20355	38836	2 19						
I/O Mass Ratio	11 960	11 878	11 706	12 239	12 106	**11.978**							

F22EMT

(EMT; Tcalc=540degC; Trxn=88degC; P=382psig; I/O=11.6; butene WHSV=2.62h-1; t=15min; mcat=2.78g)

Samp t [min]	9	10	11	13	14	15	16	18	19
T.O.S. [min.]	**1**	**2**	**3**	**5**	**6**	**7**	**8**	**10**	**11**
1-C4= Disapp. [%]	100	100	100	100	100	100	100	100	100
t-2-C4= Prod. [%]	0	0	0	0	0	6	16	27	30
c-2-C4= Prod. [%]	0	0	0	0	0	0	7	11	13
Butene Disapp. [%]	**100**	**100**	**100**	**100**	**100**	**94**	**78**	**61**	**57**
n-Butane Change [%]	7	7	11	9	7	6	4	2	4
C5+ Product Analysis [mass %]									
C5-C7	31	30	37	31	26	22	10	2	1
C8	**48**	**39**	**45**	**48**	**50**	**39**	**35**	**37**	**41**
C9+	21	31	18	21	24	40	55	61	58
C8 Distribution [mass %]									
TMP	**65**	**63**	**64**	**63**	**59**	**60**	**47**	**11**	**10**
DMH	27	28	29	28	28	25	26	17	20
C8=	9	9	8	9	14	15	27	71	70
TMP Isomer Distribution [%]									
2,2,4-TMP	**54**	**56**	**58**	**53**	**45**	**40**	**36**	**34**	**38**
2,2,3-TMP	14	14	13	10	8	5	4	0	0
2,3,4-TMP	12	10	10	14	20	26	29	37	35
2,3,3-TMP	20	20	18	24	28	29	31	30	26
Indicators [mass fraction]									
TMP	**2.39**	**2.23**	**2.24**	**2.30**	**2.13**	**2.40**	**1.78**	**0.64**	**0.48**
DMH									
TMP+DMH	1.72	1.03	1.92	1.76	1.41	0.73	0.40	0.12	0.14
C8= + C9+									
(2,2,3-+2,2,4-TMP)	2.12	2.31	2.50	1.69	1.11	0.82	0.66	0.51	0.62
(2,3,4-+2,3,3-TMP)									
DMH Isomer Distribution [%]									
2,5-DMH	21	21	21	19	15	13	7	19	21
2,4-DMH	48	50	51	45	38	32	24	17	17
2,3-DMH	28	27	25	37	45	55	62	30	35
3,4-DMH	2	2	2	0	2	0	7	34	28

F22EMT

(EMT, Tcalc=540degC, Trxn=88degC, P=382psig, I/O=11 6, butene WHSV=2 62h-1, t=15min, mcat=2 78g)

TOS [min]	1	2	3	5	6	7	8	10	11
Propane	244140	242540	240580	210680	308600	329320	245080	256580	244700
Isobutane	28503780	26976340	27992260	25605920	37726640	40848800	28958980	31264360	30759840
1-butene									
n-butane	758880	712380	763820	684980	983880	1037780	719340	755140	754620
t-2-butene						216380	372280	680920	746440
c-2-butene							153260	288240	315520
C5-C7	887698	752833	864223	670806	710072	503037	119231	13307	7047
C5	300820	286400	325320	232060	254080	174940			
2,3-DMB	142695	123098	143663	112155	116240	83783	27864		
2,2-DMP	68698	60129	70984	52219	51262	35748	12696		
3-MP	52073	43874	51413	43549	47749	39135	17021	7751	7047
2,4-DMP	147915	110715	126339	98033	96599	65852	22229		
2,2,3-TMB	11251	8183	8833	8307	9346	7353			
2-MHx	36097	26788	30753	24475	24264	15452	5923		
2,3-DMP	97323	70396	80435	76611	84908	62019	24718	5556	
3-MHx	30826	23250	26483	23397	25624	18755	8780		
C8	1366956	968889	1034054	1038669	1403040	900023	427672	221820	217739
2,2,4-TMP	**474061**	**341480**	**383391**	**349779**	**372096**	**217151**	**72639**	**8291**	**8042**
2,5-DMHx	78016	57480	62410	53038	58614	30432	7331	7448	9277
2,2,3-TMP	125456	85062	88558	63343	62069	27810	7329		
2,4-DMHx	177444	137439	151921	128521	148067	72098	27415	6619	7214
2,3,4-TMP	101815	62841	69343	89462	161238	141146	58156	9077	7394
2,3,3-TMP	180668	122031	119615	154983	229936	156896	62105	7339	5475
2,3-DMHx	104683	73592	74228	104811	173692	123823	69593	11505	15084
3,4-DMHx	8147	5975	6635		6649		7856	13026	12046
1 DMHx=	20443	15666	17233	30211	90922	64802	52973	43154	36686
2 DMHx=	8002	6444	6225	6710	9680	20354	42658	83511	82670
3 DMHx=									
4 DMHx=									
5 DMHx=	88201	60879	54495	57811	90078	45511	14337	6193	5851
6 DMHx=							5380	25657	28000
C9+	609781	778551	421309	441102	667325	925111	670326	366414	311629
C5+	2864435	2500273	2319586	2150577	2780437	2328171	1217229	601541	536415
Tot Peak Area	32371235	30431533	31316246	28652157	41799557	44760451	31512909	33558541	33042015
Feed Analysis		Inj 1	Inj 2	Inj 3	Inj 4	Inj 5	Avg	Mass %	
C3		12713	15149	15494	10412	16026	13959	0 78	
i-C4		1231112	1834205	1915520	1025992	1976396	1596645	89 54	
1-C4=		102431	153700	160960	85525	164380	133399	7 48	
n-C4		29681	45273	47670	24340	48972	39187	2 20	
I/O Mass Ratio		12 019	11 934	11 901	11 996	12 023	**11.975**		

F23EMT

(EMT; Tcalc=540degC; Trxn=56degC; P=382psig; I/O=11.7; butene WHSV=2.55h-1; t=13min; mcat=2.78g)

Samp t [min]	8	9	10	11	12	13	14	15	16	17	18	20	21
T.O.S. [min.]	1	2	3	4	5	6	7	8	9	10	11	13	14
1-C4= Disapp. [%]	91	100	100	100	100	100	100	100	100	100	100	100	100
t-2-C4= Prod. [%]	0	0	0	0	4	8	13	18	21	23	25	29	31
c-2-C4= Prod. [%]	0	0	0	0	0	3	0	8	10	11	12	15	17
Butene Disapp. [%]	91	100	100	100	96	89	87	74	69	66	63	56	52
n-Butane Change [%]	5	16	18	14	9	12	12	9	7	10	11	9	9
C5+ Product Analysis [mass %]													
C5-C7	20	24	29	25	19	18	10	7	9	8	7	5	4
C8	49	53	54	56	51	50	41	34	46	48	39	43	38
C9+	32	23	17	19	30	32	49	59	45	44	54	52	58
C8 Distribution [mass %]													
TMP	79	78	81	75	66	63	69	60	51	46	42	23	19
DMH	11	12	11	13	17	19	12	15	15	14	18	12	20
C8=	10	10	8	12	15	18	19	24	34	40	40	65	61
TMP Isomer Distribution [%]													
2,2,4-TMP	32	32	37	34	34	33	37	34	32	32	34	38	41
2,2,3-TMP	13	12	8	14	9	9	8	6	9	9	6	8	9
2,3,4-TMP	23	23	23	22	26	26	24	27	27	26	27	17	26
2,3,3-TMP	32	33	33	29	32	32	31	32	31	32	33	38	24
Indicators [mass fraction]													
TMP	7.14	6.29	7.31	5.76	4.01	3.41	5.63	3.89	3.49	3.30	2.32	1.97	0.92
DMH													
TMP+DMH	1.20	1.70	2.27	1.94	1.15	1.00	0.60	0.38	0.51	0.46	0.34	0.19	0.18
C8= + C9+													
(2,2,3-+2,2,4-TMP)	0.80	0.78	0.79	0.96	0.74	0.72	0.82	0.69	0.71	0.70	0.66	0.83	1.00
(2,3,4-+2,3,3-TMP)													
DMH Isomer Distribution [%]													
2,5-DMH	18	17	20	18	13	11	19	10	8	7	11	0	0
2,4-DMH	14	13	26	13	31	32	30	17	6	8	9	19	13
2,3-DMH	68	70	54	70	56	54	51	62	58	48	58	46	29
3,4-DMH	0	0	0	0	0	2	0	10	27	37	22	35	58

F23EMT

(EMT, Tcalc=540degC Tmn=56degC, P=382psig I/O=11 7 butene WHSV=2 55h-1 t=13min, mcat=2 78g)

TOS (min)	1	2	3	4	5	6	7	8	9	10	11	13	14
Propene	323520	349500	166800	415640	426980	406180	125460	279380	417460	430080	312580	348920	348400
Isobutene	35718640	40436920	20518000	46591340	46918000	46384100	15738840	32577260	46058500	50505200	36845700	41566360	41689040
1-butene	265000												
n-butene	933800	1127120	571600	1256260	1229520	1236480	419000	847060	1170600	1303960	969640	1068260	1073200
t-2-butene					135760	297040	161420	477700	772480	938840	738200	964740	1034620
c-2-butene						115580		214820	360820	435700	351520	502960	554180
C5-C7	702838	585641	284011	590256	548811	434097	70625	110645	145478	109870	72263	38617	32256
C5	196340	220620	113920	223120	189340	151520							
2,3-DMB	121943	91576	47084	92599	84389	65610	18022	25927	31871	25488	16761	9782	8250
2,2-DMP	41018	31213	16812	34315	32301	26224	7326	10589	13193	10631	6991		
3-MP	58050	42302	21980	45500	44719	38155	11092	17486	22487	19047	12970	10023	8978
2,4-DMP	133483	90403	44191	88747	81501	61092	17521	24470	30507	22345	13765	7976	6330
2,2,3-TMB	14069	9434		9472	9186	6918							
2-MHx	17989	13441	6911	14780	14764	11166			6238				
2,3-DMP	98229	70342	34654	72839	73686	57155	16664	24264	30964	24086	15981	10836	8698
3-MHx	21717	16310	8459	17884	18925	16257		7909	10196	8273	5795		
C8	1711600	1308858	554984	1344447	1458850	1205116	283101	508308	760977	616865	394763	305085	329831
2,2,4-TMP	429931	324184	163510	349231	338028	253487	73357	105087	126228	91299	56566	31935	24928
2,5-DMHx	34999	27418	12383	30830	32005	25266	6510	8163	9482	6462	8216		
2,2,3-TMP	174115	122408	34377	146317	84002	66192	14753	19635	36572	26840	9185	6674	5714
2,4-DMHx	26238	20958	15810	22682	76748	72491	10529	13294	7052	7040	6474	8283	8524
2,3,4-TMP	313102	238713	101226	222099	253655	198775	47583	82601	106288	74888	44998	14491	16091
2,3,3-TMP	438651	333741	148345	295609	314445	245965	60174	99232	122315	92848	55005	32057	14549
2,3-DMHx	128333	113658	33052	122490	137546	121231	17723	49099	65446	41348	41400	19871	19163
3,4-DMHx						5212		8201	30096	31859	15376	15133	38902
1 DMHx=	94192	61067	30655	94048	141853	148781	37573	60728	132703	110149	54980	62772	49501
2 DMHx=	6079	5095		5875	10228	17051	7230	44972	93297	100324	77662	133191	118042
3 DMHx=													
4 DMHx=										5167			
5 DMHx=	63771	54271	15636	55266	64874	50665	7669	13165	13486	10037	7428	5032	
6 DMHx=	5189	5163			5466			5121	18014	18634	17475	35626	33519
C9+	1112314	569593	177720	459166	851254	768439	334881	899195	738428	567043	547532	442407	494665
C5+	3526752	2461890	1026725	2402869	2856915	2407652	688607	1519148	1644883	1293778	1014558	846089	855852
Tot Peak Area	40767712	44375430	22283125	50666109	51567175	50847032	17133327	35700548	50063923	54471858	39880678	44794369	45001112
FEED ANAL	Inj 1	Inj 2	Inj 3	Inj 4	Inj 5	Avg	Mass %						
C3	17710	13541	13120	8895	16547	13963	0 78		Avg. Mass I/O Ratio		12.12		
i-C4	2165189	1642138	1539647	663485	2049673	1612026	89 64		Avg. Molar I/O Ratio		11 888		
1-C4=	176032	137267	129680	54009	168435	133085	7 40						
n-C4	52276	40534	38449	14623	50214	39219	2 18						
I/O Mass Ratio	12 300	11 963	11 873	12 285	12 169	12 118	g Mass I/O Ratio						

Run F24Y

(Y; Tcalc=425degC; Trxn=56degC; P=382psig, I/O=11.1; butene WHSV=2.70h-1; t=1h; mcat=2.78g)

Samp t [min]	9	10	11	12	13	14	15	16	17	18	20	23	28	38	68
T.O.S. [min.]	**1**	**2**	**3**	**4**	**5**	**6**	**7**	**8**	**9**	**10**	**12**	**15**	**20**	**30**	**60**
1-C4= Disapp. [%]	95	100	100	100	100	100	100	100	100	97	97	100	96	96	93
t-2-C4= Prod. [%]	0	0	0	0	0	0	0	8	22	32	34	43	39	41	43
c-2-C4= Prod. [%]	0	0	0	0	0	0	0	3	9	15	17	25	24	28	32
Butene Disapp. [%]	**95**	**100**	**100**	**100**	**100**	**100**	**100**	**89**	**68**	**50**	**46**	**32**	**34**	**27**	**19**
n-Butane Change [%]	8	-2	9	7	9	8	6	7	-6	3	2	12	1	2	3
C5+ Product Analysis [mass %]															
C5-C7	31	13	30	31	30	27	23	18	1	1	0	0	0	0	0
C8	**48**	**29**	**49**	**49**	**48**	**47**	**51**	**46**	**9**	**31**	**40**	**54**	**53**	**54**	**50**
C9+	21	59	21	20	21	27	26	36	90	67	60	46	47	46	50
C8 Distribution [mass %]															
TMP	**73**	**68**	**70**	**68**	**68**	**69**	**64**	**59**	**37**	**11**	**7**	**3**	**3**	**1**	**0**
DMH	22	26	24	27	27	26	31	37	44	43	33	25	26	23	20
C8=	5	6	6	5	5	5	5	4	19	46	60	72	71	75	80
TMP Distribution [%]															
2,2,4-TMP	**39**	**38**	**41**	**45**	**41**	**39**	**35**	**29**	**24**	**26**	**20**	**0**	**0**	**0**	**0**
2,2,3-TMP	5	6	6	6	5	5	4	3	5	14	0	0	0	0	0
2,3,4-TMP	24	23	22	19	22	25	29	33	36	38	62	100	100	100	0
2,3,3-TMP	31	33	31	30	31	32	32	35	35	22	19	0	0	0	0
Indicators [mass fraction]															
TMP	**3.27**	**2.66**	**2.95**	**2.53**	**2.49**	**2.67**	**2.02**	**1.62**	**0.85**	**0.25**	**0.21**	**0.11**	**0.11**	**0.06**	**0.00**
DMH															
TMP+DMH	1.94	0.45	1.89	1.99	1.92	1.53	1.70	1.18	0.07	0.21	0.19	0.18	0.18	0.15	0.11
C8= + C9+															
(2,2,3-+2,2,4-TMP)	0.80	0.78	0.87	1.02	0.87	0.76	0.64	0.47	0.41	0.65	0.24	0.00	0.00	0.00	0.00
(2,3,4-+2,3,3-TMP)															
DMH Distribution [%]															
2,5-DMH	13	12	13	12	11	11	8	4	4	0	0	0	0	0	0
2,4-DMH	33	28	30	31	29	26	23	15	2	5	7	9	9	10	11
2,3-DMH	31	35	39	37	38	41	31	28	20	8	6	7	6	7	17
3,4-DMH	23	24	17	19	22	22	38	54	74	86	88	84	85	84	72

Run F24Y

(Y, Tcalc=425degC, Trxn=56degC, P=382psig, I/O=11 1, butene WHSV=2 70h-1, t=1h, mcat=2 78g)

TOS [min]	1	2	3	4	5	6	7	8	9	10	12	15	20	30	60
Propane	478240	433580	375740	432380	458180	363160	394820	398200	468620	425300	341800	289520	425420	440060	423880
Isobutane	57981300	46762180	42169220	49763740	52446320	42046560	44714500	46053640	56357700	50122400	40235980	36437700	50164820	53706600	48621840
1-butene	227980									133220	118580		155020	159600	266620
n-butane	1560000	1223920	1153740	1344840	1427620	1145720	1188140	1224600	1451680	1286980	1025700	1024040	1257440	1366080	1239280
t-2-butene								322780	1177640	1341340	1150140	1311820	1641140	1866220	1741080
c-2-butene								120300	495620	640400	584120	780960	991640	1249080	1323620
C5-C7	**964087**	**806069**	**768008**	**1020967**	**968433**	**719647**	**596215**	**368418**	**90946**	**19595**	**0**	**0**	**0**	**0**	**0**
C5	390280	291900	314260	388400	375360	272120	210460	135140							
2,3-DMB	172916	133817	136795	179766	172450	124856	102491	61784	20387	5960					
2,2-DMP	57235	48312	50570	68592	62447	44150	34920	20705	7465						
3-MP	69322	57870	57778	77112	74433	55150	49905	34453	17628	7915					
2,4-DMP	136544	117477	100548	135007	123788	94453	79247	44382	15323						
2,2,3-TMB	10305	8410	6742	9273	8779	7112	5356								
2-MHx	21430	21150	17709	24167	20943	15959	13382	7411							
2,3-DMP	101003	100385	81451	108666	102865	84039	79034	50977	22775	5710					
3-MHx	25052	26748	22155	29984	27368	21808	20420	13566	7367						
C8	**1526309**	**1809119**	**1281970**	**1602610**	**1546279**	**1263305**	**1324238**	**966664**	**707819**	**444019**	**459696**	**435049**	**438337**	**428476**	**284987**
2,2,4-TMP	**437481**	**469659**	**367655**	**496374**	**431925**	**338038**	**293537**	**183946**	**61834**	**12232**	**6171**				
2,5-DMHx	43150	54286	41142	52574	47393	36758	33238	12457	13734						
2,2,3-TMP	56478	70401	50488	61244	54455	40173	34756	18333	14099	6513					
2,4-DMHx	112508	131436	92407	132907	122472	85969	96317	51861	6890	10214	10091	10492	10212	9918	6011
2,3,4-TMP	269094	289286	199143	211235	232218	218081	240082	188145	94061	18126	19549	12601	12545	6027	
2,3,3-TMP	346320	404046	282395	328057	325600	278267	272666	201897	92838	10641	5903				
2,3-DMHx	105271	164090	120473	160365	158902	133125	130564	97693	61262	16204	8617	7255	7067	6510	9850
3,4-DMHx	78325	113275	51084	83019	90104	71260	156176	190494	228690	165405	133475	93006	96211	83268	40859
1 DMHx=															
2 DMHx=	6586	7788	6281	6312	6707	5835	7036	10473	97195	165180	204970	227401	231487	236088	167595
3 DMHx=															
4 DMHx=									5313						
5 DMHx=	71096	99745	70902	80523	76503	55799	59866	30365	11605	5137					
6 DMHx=		5107							20298	34367	70820	84294	80815	86665	60672
C9+	670751	3691397	561401	675847	676912	724632	670948	745413	7524410	949420	701910	369044	392520	359462	286845
C5+	3181147	6306585	2631379	3299424	3191624	2707584	2590401	2079495	8323174	1413024	1161506	804093	830857	787938	571832
Tot Peak Area	63428667	54726265	46330079	54840384	57523744	46263024	48887861	50199015	67778814	54722264	44033706	39867173	54474697	58326498	52864532
FEED ANAL.		Inj 1	Inj 2	Inj 3	Inj 4	Inj 5	Avg	Mass %							
C3		24431	22311	22336	21579	22700	22671	0 75							
i-C4		2877294	2661261	2611696	2533882	2725376	2681902	89 23							
1-C4=		250745	233177	228710	215995	233654	232456	7 73							
n-C4		73578	68343	66882	65706	69206	68743	2 29							
I/O Mass Ratio		11 475	11 413	11 419	11 731	11 664	**11.641**								

Run F25EMT

(EMT; Tcalc=425degC; Trxn=33degC; P=382psig; I/O=11.1; butene WHSV=2.71h-1; t=1h; mcat=2.78g)

Samp t [min]	10	11	12	13	14	15	16	17	18	19	21	24	29	69
T.O.S. [min.]	**1**	**2**	**3**	**4**	**5**	**6**	**7**	**8**	**9**	**10**	**12**	**15**	**20**	**60**
1-C4= Disapp. [%]	100	100	100	100	100	100	100	100	100	100	100	100	100	96
t-2-C4= Prod. [%]	0	0	0	0	6	10	13	20	21	24	30	32	35	40
c-2-C4= Prod. [%]	0	0	0	0	0	0	4	6	6	8	11	13	17	29
Butene Disapp. [%]	**100**	**100**	**100**	**100**	**94**	**90**	**83**	**74**	**73**	**67**	**58**	**55**	**49**	**27**
n-Butane Change [%]	7	8	9	5	3	2	4	24	5	0	7	2	1	0
C5+ Product Analysis [mass %]														
C5-C7	27	26	19	7	5	4	4	4	3	1	1	1	0	0
C8	**37**	**51**	**47**	**43**	**29**	**23**	**46**	**32**	**37**	**27**	**32**	**40**	**36**	**54**
C9+	36	23	34	49	67	74	50	64	60	72	68	59	64	46
C8 Distribution [mass %]														
TMP	**82**	**75**	**70**	**60**	**56**	**50**	**34**	**20**	**11**	**6**	**0**	**0**	**0**	**0**
DMH	17	23	28	35	39	46	56	74	67	61	45	34	30	23
C8=	1	2	2	5	5	4	10	6	22	34	55	66	70	77
TMP Isomer Distribution [%]														
2,2,4-TMP	**33**	**33**	**30**	**26**	**22**	**19**	**12**	**13**	**0**	**0**	**0**	**0**	**0**	**0**
2,2,3-TMP	10	5	4	4	4	3	3	0	0	0	0	0	0	0
2,3,4-TMP	24	27	30	32	37	39	43	33	32	51	0	0	0	0
2,3,3-TMP	33	36	36	38	38	39	42	54	68	49	0	0	0	0
Indicators [mass fraction]														
TMP	**4.91**	**3.27**	**2.53**	**1.70**	**1.42**	**1.11**	**0.60**	**0.27**	**0.16**	**0.09**	**0.00**	**0.00**	**0.00**	**0.00**
DMH														
TMP+DMH	0.98	2.11	1.30	0.79	0.40	0.29	0.75	0.46	0.41	0.22	0.17	0.16	0.12	0.15
C8= + C9+														
(2,2,3-+2,2,4-TMP)	0.73	0.61	0.52	0.43	0.34	0.28	0.18	0.15	0.00	0.00	0.00	0.00	0.00	0.00
(2,3,4-+2,3,3-TMP)														
DMH Isomer Distribution [%]														
2,5-DMH	12	7	5	3	3	0	1	0	3	2	0	0	0	0
2,4-DMH	9	9	7	7	7	4	4	3	2	3	6	9	9	10
2,3-DMH	26	24	22	25	19	16	14	9	6	4	4	0	4	11
3,4-DMH	53	60	65	65	71	80	81	88	89	91	89	91	87	79

Run F25EM1
(EMT, Tcalc=425degC, Trxn=33degC, P=382psig, I/O=11 1, butene WHSV=2 71h-1, t=1h, mcat=2 78g)

TOS [min]	1	2	3	4	5	6	7	8	9	10	12	15	20	60
Propane	618940	443020	422900	432000	466320	384800	444140	205100	420620	454000	346260	430200	357000	460840
Isobutane	68025220	48715880	48326620	50439080	53097260	42625020	49274480	35556660	50571960	49198720	38110860	49813240	44845600	52891420
1-butene														190760
n-butane	1762400	1274440	1282920	1310060	1367820	1095600	1272820	1091120	1294800	1224760	1013940	1255760	1123520	1315220
t-2-butene					273720	368840	546440	589920	870540	999080	959340	1313760	1309420	1770980
c-2-butene							149320	172720	268860	348400	367160	537320	623680	1264420
C5-C7	**442880**	**345674**	**306315**	**169191**	**123596**	**81970**	**74828**	**31316**	**27379**	**17704**	**7463**	**6129**	**0**	**0**
C5	171080	122460	109580											
2,3-DMB	67877	49249	41217	34439	24264	13627	9314							
2,2-DMP	23022	17420	14910	13113	9719	6045	5359							
3-MP	44738	34687	30854	28795	25163	19178	19839	14703	12840	11097	7463	6129		
2,4-DMP	56531	46800	38533	31244	20943	11459	7281							
2,2,3-TMB	7917	6865	5560											
2-MHx	8175	7768	7314	6387										
2,3-DMP	50978	48119	45336	42781	33177	23082	22706	10617	8594	6607				
3-MHx	12562	12306	12011	12432	10330	8579	10329	5996	5945					
C8	**605274**	**578043**	**753667**	**971570**	**746299**	**510688**	**867969**	**259788**	**350657**	**432112**	**292728**	**297816**	**408349**	**396667**
2,2,4-TMP	**161449**	**165476**	**158756**	**150029**	**90163**	**48263**	**34625**	**6899**						
2,5-DMHx	11703	10512	10921	11910	8736		5617		7535	5941				
2,2,3-TMP	47217	27044	23055	23806	15149	7791	9526							
2,4-DMHx	9555	14590	15036	24459	21026	10229	19198	5524	5345	7914	8484	9099	10662	9343
2,3,4-TMP	121143	135128	156385	186688	152768	100026	124587	17029	11891	12152				
2,3,3-TMP	166019	180825	190993	220769	159273	101575	123795	28308	25316	11748				
2,3-DMHx	25736	36712	46591	84431	54775	36696	68788	17581	12977	10961	5734		5352	10251
3,4-DMHx	53903	93913	136309	220518	208442	185911	394498	169603	208955	237928	116417	92661	108267	73390
1 DMHx=														
2 DMHx=					7978	8978	56825	14844	62304	121944	128414	155536	224873	221484
3 DMHx=														
4 DMHx=							5076							
5 DMHx=	8549	13843	15621	43745	27989	11229	11936							
6 DMHx=				5215			13488		16334	23524	33679	40520	59195	82099
C9+	601373	301564	552767	1117285	1741862	1674213	952231	517635	577359	1135386	624073	438267	735968	337468
C8+	1649527	1325281	1611749	2258046	2611757	2266871	1895018	808739	955395	1585202	924264	742212	1144317	734035
Tot Peak Area	72056087	51758621	51644189	54439186	57816877	46741131	53582218	38424259	54113315	53461762	41354664	53555172	48779857	57363255
Feed Analysis		Inj 1	Inj 2	Inj 3	Inj 4	Inj 5	Avg	Mass %						
C3		22467	19825	21286	22183		21440	0 76		Avg Mass I/O Ratio		11 54		
i-C4		2614861	2323278	2491499	2648377		2519504	89 22		Avg Molar I/O Ratio		**11.142**		
1-C4=		227202	203480	215985	226225		218223	7 73						
n-C4		66698	60362	64289	67139		64622	2 29						
I/O Mass Ratio		11 509	11 418	11 536	11 707		**11.642**							

Run F27Y
(Y; Tcalc=425degC; Trxn=29degC; P=382psig; I/O=11.2; butene WHSV=2.72h-1; t=1h; mcat=2.78g)

Samp t [min]	9	10	11	12	13	14	15	16	17	18	20	23	28	38	68
T.O.S. [min.]	1	2	3	4	5	6	7	8	9	10	12	15	20	30	60
1-C4= Disapp. [%]	91	100	100	100	100	100	100	100	100	100	96	96	96	94	86
t-2-C4= Prod. [%]	0	0	0	0	0	4	13	20	30	29	37	31	32	31	28
c-2-C4= Prod. [%]	0	0	0	0	0	0	5	8	18	21	35	29	32	38	41
Butene Disapp. [%]	91	100	100	100	100	96	82	72	51	50	24	37	33	25	17
n-Butane Change [%]	5	8	25	9	-6	4	4	3	22	7	25	3	3	2	-2
C5+ Product Analysis [mass %]															
C5-C7	34	31	32	26	5	13	8	3	1	1	0	0	0	0	0
C8	16	37	59	51	20	35	50	37	43	46	34	34	45	49	37
C9+	50	33	8	23	75	53	42	60	56	53	66	66	55	51	63
C8 Distribution [mass %]															
TMP	87	83	74	71	62	64	57	42	21	8	3	2	2	2	0
DMH	13	15	25	27	33	34	40	50	56	50	28	24	25	20	14
C8=	0	1	1	2	5	3	3	8	23	41	69	74	73	78	86
TMP Distribution [%]															
2,2,4-TMP	0	31	30	29	22	23	18	12	7	0	0	0	0	0	0
2,2,3-TMP	6	4	4	4	5	3	4	4	0	0	0	0	0	0	0
2,3,4-TMP	45	29	29	29	32	33	39	42	50	70	100	100	100	100	0
2,3,3-TMP	50	37	37	38	40	40	40	42	44	30	0	0	0	0	0
Indicators [mass fraction]															
TMP	6.58	5.46	2.99	2.64	1.86	1.89	1.44	0.84	0.38	0.16	0.11	0.10	0.06	0.09	0.00
DMH															
TMP+DMH	0.33	1.10	6.51	2.16	0.25	0.63	1.12	0.54	0.49	0.37	0.12	0.10	0.14	0.12	0.05
C8= + C9+															
(2,2,3-+2,2,4-TMP)	0.06	0.53	0.51	0.51	0.37	0.37	0.27	0.19	0.07	0.00	0.00	0.00	0.00	0.00	#DIV/0!
(2,3,4-+2,3,3-TMP)															
DMH Distribution [%]															
2,5-DMH	0	10	6	6	6	4	3	0	2	0	0	0	0	0	0
2,4-DMH	37	20	19	18	14	6	6	4	2	3	6	11	8	10	0
2,3-DMH	32	18	24	25	27	26	17	11	4	3	8	0	10	0	0
3,4-DMH	31	52	51	50	53	65	74	86	92	94	85	89	81	90	100

Run F27Y

(Y, Tcalc=425degC, Trxn=29degC, P=382psig, I/O=11 2, butene WHSV=2 72h-1, t=1h, mcat=2 78g)

TOS (min)															
Propane	581100	409000	238960	395820	422880	456400	341500	409420	206480	408480	169000	323400	401840	399000	447780
Isobutane	69689120	46447120	34153980	45519900	48629960	49642180	40587180	48424980	30909240	47903280	31183080	39040280	48073200	48122680	49940220
1-butene	512800										121260	116000	143820	232380	567440
n-butane	1757620	1220040	1051820	1205620	1247360	1280000	1037440	1226240	941180	1258380	997360	991220	1214640	1198700	1197340
t-2-butene						178240	430500	795060	798540	1163920	993840	996580	1265100	1255860	1180060
c-2-butene							172860	333580	473780	820860	946320	946720	1290760	1501340	1687960
C5-C7	**372971**	**505151**	**483867**	**413373**	**424363**	**319104**	**95804**	**45167**	**18111**	**5130**	**0**	**0**	**0**	**0**	**0**
C5	189100	170260	172280	154080	135980	101960									
2,3-DMB	68011	98800	83049	68233	70898	56090	18145	6303							
2,2-DMP	15477	27902	25916	22394	22665	15578	5687								
3-MP	29162	51807	46007	39054	42333	36241	17887	12242	7754	5130					
2,4-DMP	36682	63857	59064	46644	50413	35855	14675	5014							
2,2,3-TMB		6451													
2-MHx		9265	10319	9111	10871	6649									
2,3-DMP	29323	62713	69879	58733	71938	53471	31498	16192	8357						
3-MHx	5216	14096	17353	15124	19265	13260	7912	5406							
C8	**180607**	**608910**	**690735**	**799159**	**1619036**	**875743**	**626484**	**509173**	**493887**	**421862**	**537680**	**257007**	**400269**	**303306**	**202278**
2,2,4-TMP		**155427**	**195449**	**187585**	**222054**	**130874**	**63652**	**26334**	**6971**						
2,5-DMHx		9534	13403	12744	30815	10659	7201		5917						
2,2,3-TMP	8827	21434	27928	23926	49010	18855	12835	8080							
2,4-DMHx	8753	18821	42472	39842	74312	16954	14177	9121	6325	7158	9727	6435	8185	5883	
2,3,4-TMP	69931	145346	193058	164360	323347	186312	140091	90245	51883	24418	16445	6111	6429	5203	
2,3,3-TMP	78024	185615	242825	214687	404567	222548	142916	89342	45413	10550					
2,3-DMHx	7716	16340	52722	54782	145544	76210	42510	26873	10797	6014	12907		10456		
3,4-DMHx	7356	48268	111768	108956	286100	191326	185414	218536	251236	199300	129359	54441	81284	54157	28101
1 DMHx=															
2 DMHx=					7760	6045	7842	26348	95905	132880	268578	153204	229669	185767	139689
3 DMHx=											5878				
4 DMHx=															
5 DMHx=		8125	11110	12277	70259	15960	9846	7614							
6 DMHx=					5268			6680	19440	41542	94786	36816	64246	52295	34486
C9+	543719	539035	124000	352521	6125732	1336533	527152	823511	651282	485481	1046872	501726	479688	319772	341190
C5+	1097297	1653096	1498602	1565053	8169131	2531380	1249440	1377841	1161280	912473	1584552	758733	879957	623077	543466
Tot Peak Area	73637937	49729256	36943362	48686393	58469331	54088200	43818920	52567121	34016720	51646533	35049092	42226213	51978557	51831697	53876306

FEED ANAL.	Inj 1	Inj 2	Inj 3	Inj 4	Inj 5	Avg	Mass %
C3	22710					22710	0 76
I-C4	2672465					2672465	89 27
1-C4=	230606					230606	7 70
n-C4	67935					67935	2 27
I/O Mass Ratio	11 589					**11.589**	

F28EMT

(EMT; Tcalc=425degC; Trxn=55degC, P=382psig; I/O=11.25; butene WHSV=2.7h-1; mcat=2.78g)

Samp t [min]	9	10	11	12	13	14	15	16	17	18	20	23	28	38	68
T.O.S. [min.]	**1**	**2**	**3**	**4**	**5**	**6**	**7**	**8**	**9**	**10**	**12**	**15**	**20**	**30**	**60**
1-C4= Disapp. [%]	91	96	100	100	100	100	100	100	100	100	100	100	100	100	97
t-2-C4= Prod. [%]	0	0	0	0	0	0	0	0	4	7	16	29	38	43	46
c-2-C4= Prod. [%]	0	0	0	0	0	0	0	0	0	4	6	11	15	19	24
Butene Disapp. [%]	**91**	**96**	**100**	**100**	**100**	**100**	**100**	**100**	**96**	**89**	**78**	**60**	**47**	**38**	**27**
n-Butane Change [%	7	9	11	17	8	6	6	4	12	21	6	3	2	1	-1
C5+ Product Distribution [%]															
C5-C7	42	28	37	35	24	29	26	18	13	13	12	4	1	0	0
C8	51	50	56	50	45	53	58	47	52	51	48	56	47	58	45
C9+	7	21	7	15	30	19	16	35	35	36	40	40	53	42	55
C8 Distribution [%]															
TMP	**82**	**78**	**77**	**77**	**70**	**72**	**69**	**61**	**61**	**59**	**55**	**16**	**0**	**0**	**0**
DMH	15	17	18	23	24	23	26	32	33	34	40	47	33	26	23
C8=	3	5	5	0	6	5	6	8	6	7	5	37	67	74	77
TMP Isomer Distribution [%]															
2,2,4-TMP	**47**	**43**	**45**	**43**	**44**	**45**	**42**	**38**	**41**	**38**	**33**	**31**	**0**	**0**	**0**
2,2,3-TMP	16	18	16	16	10	7	6	8	7	5	4	0	0	0	0
2,3,4-TMP	12	14	14	15	18	19	22	23	23	26	30	35	0	0	0
2,3,3-TMP	24	26	26	25	28	29	30	31	30	32	34	34	0	0	0
Indicators [mass fraction]															
TMP	5.42	4.58	4.38	3.27	2.98	3.19	2.67	1.91	1.88	1.73	1.37	0.33	0.00	0.00	0.00
DMH															
TMP+DMH	5.72	1.99	5.57	3.26	1.29	2.32	2.87	1.12	1.27	1.21	1.06	0.58	0.19	0.18	0.11
C8= + C9+															
(2,2,3-+2,2,4-TMP)	1.75	1.54	1.55	1.46	1.18	1.08	0.94	0.83	0.90	0.70	0.58	0.44	#DIV/0!	#DIV/0!	#DIV/0!
(2,3,4-+2,3,3-TMP)															
DMH Isomer Distribution [%]															
2,5-DMH	19	18	17	13	13	10	8	9	8	5	4	6	0	0	0
2,4-DMH	13	10	11	8	27	24	23	22	17	17	11	5	9	11	13
2,3-DMH	48	53	52	41	40	44	45	38	37	33	28	15	6	6	0
3,4-DMH	21	19	20	38	20	23	24	31	39	46	58	74	86	84	87

F28EMT

(EMT, Tcalc=425degC, Trxn=55degC, P=382psig, I/O=11 25, butene WHSV=2 7h-1, mcat=2 78g)

TOS (min)															
Propane	398000	324900	381680	317800	418300	413360	384920	422620	266060	228720	380520	330900	411420	396080	410000
Isobutane	51347680	40299320	44538880	41833780	49110120	45517780	35770180	46642060	28604260	33827600	46008580	39054340	48540860	46325000	46495780
1-butene	363040	137940													117740
n-butane	1323440	1078400	1194980	1194980	1301380	1176260	934540	1203140	802460	1005420	1182560	967700	1211500	1149780	1125120
t-2-butene									108000	203960	597260	921020	1506640	1643240	1768260
c-2-butene										118700	220460	355140	617020	747740	926300
C5-C7	**646935**	**591666**	**596478**	**588381**	**641600**	**524368**	**463457**	**489285**	**262211**	**203524**	**126816**	**17636**	**5374**	**0**	**0**
C5	250900	221720	243920	251120	236900	184680	162460	169740							
2,3-DMB	106766	92194	94252	93740	101328	80173	69878	74529	51597	49232	24957				
2,2-DMP	38509	34611	36188	35896	39697	31195	27486	30368	21731	19823	10870				
3-MP	49297	43506	44581	44061	51470	42424	37549	43644	34206	31059	22131	9373	5374		
2,4-DMP	96264	90120	81759	73730	91074	76741	65423	64261	54930	38295	22234				
2,2,3-TMB	9693	8924	8792	7416	9826	8312	7480	8147	7283						
2-MHx	14179	15220	13198	12498	16399	14432	13035	13749	12646	8496	5428				
2,3-DMP	65474	68329	60110	55612	74903	68503	63239	66301	61426	43611	30252	8263			
3-MHx	15853	17042	15678	14308	20003	17908	16907	18546	18392	13008	10644				
C8	**781791**	**1065936**	**896008**	**847489**	**1191565**	**968100**	**1036656**	**1302991**	**1065648**	**810645**	**618672**	**260923**	**350187**	**392452**	**274575**
2,2,4-TMP	**302614**	**352473**	**309939**	**278135**	**368506**	**310687**	**299302**	**298309**	**264729**	**173212**	**93839**	**12532**			
2,5-DMHx	21861	31672	26794	25370	35325	20781	21816	35728	28384	13037	7840	7941			
2,2,3-TMP	103052	146589	109546	106784	84142	47573	46314	61145	43977	23037	9914				
2,4-DMHx	15135	18221	17808	16630	76003	51032	60925	90413	57337	46581	22156	6164	10016	10948	8072
2,3,4-TMP	79043	112601	93694	100374	147639	133228	155261	185677	148292	125167	83864	14371			
2,3,3-TMP	153253	211105	177358	163720	237336	199351	211725	245639	194828	153861	95557	13804			
2,3-DMHx	56022	95863	82271	80705	113009	95846	120453	157031	126818	89734	57468	18132	6587	5676	
3,4-DMHx	24633	33953	30850	75771	56321	49225	63582	130215	134295	125623	119714	90812	99611	85389	53854
1 DMHx=															
2 DMHx=							5006	6603	6601	12202	14628	78660	173673	218837	176202
3 DMHx=															
4 DMHx=															
5 DMHx=	26178	53459	46748		68129	50177	52171	87225	60387	48391	13692		5715		
6 DMHx=					5155			5006				18507	54585	71602	36447
C9+	105832	451118	105542	259690	795724	340493	284359	971543	716532	560354	432381	187002	393763	289825	335114
C5+	1534558	2098720	1599028	1695560	2628889	1822961	1784371	2763819	2044391	1574723	1077569	465561	749324	682277	609689
Tot Peak Area	54966718	43939280	47714568	45042120	53458689	48930361	38874011	51031639	31825171	36840423	49246489	41739521	52419744	50196377	50526589
Feed Analysis		Inj 1	Inj 2	Inj 3	Inj 4	Inj 5	Avg	Mass %							
C3		22508	20201	19686	21330	20582	20861	0 75		Avg Mass I/O Ratio		11 65			
i-C4		2693271	2404112	2337586	2529444	2506328	2494148	89 33		Avg Molar I/O Ratio		**11.250**			
1-C4=		230820	207558	201995	217192	212358	213985	7 66							
n-C4		67669	60868	59583	64504	62763	63077	2 26							
I/O Mass Ratio		11 668	11 583	11 572	11 646	11 802	11 654								

Run F29Y

(Y; Tcalc=425degC; Trxn=70degC; P=382psig, I/O=11.2; butene WHSV=2.67h-1; t=1h; mcat=2.78g)

Samp t [min]	13	14	15	16	17	18	19	20	23	26	31	41	71
T.O.S. [min.]	**1**	**2**	**3**	**4**	**5**	**6**	**7**	**8**	**10**	**15**	**20**	**30**	**60**
1-C4= Disapp. [%]	100	100	100	100	100	100	100	100	100	100	96	96	97
t-2-C4= Prod. [%]	0	0	0	0	0	0	0	0	25	43	49	47	47
c-2-C4= Prod. [%]	0	0	0	0	0	0	0	0	11	22	26	26	22
Butene Disapp. [%]	**100**	**100**	**100**	**100**	**100**	**100**	**100**	**100**	**64**	**36**	**20**	**24**	**28**
n-Butane Change [%]	7	10	13	8	-3	2	13	4	9	1	10	3	2
C5+ Product Analysis [mass %]													
C5-C7	44	35	52	36	30	30	30	30	11	1	0	0	0
C8	**45**	**50**	**43**	**54**	**53**	**48**	**54**	**50**	**56**	**58**	**73**	**67**	**67**
C9+	11	14	4	10	17	21	16	20	33	41	27	33	33
C8 Distribution [mass %]													
TMP	**68**	**63**	**71**	**63**	**65**	**62**	**63**	**60**	**43**	**8**	**3**	**3**	**0**
DMH	26	29	25	30	28	30	31	32	39	25	23	21	24
C8=	6	8	4	7	7	8	7	8	17	67	74	76	76
TMP Isomer Distribution [%]													
2,2,4-TMP	**59**	**55**	**66**	**56**	**56**	**50**	**51**	**44**	**31**	**35**	**0**	**0**	**0**
2,2,3-TMP	9	9	9	9	7	7	6	5	3	0	0	0	0
2,3,4-TMP	12	13	9	13	14	16	17	21	33	48	100	100	0
2,3,3-TMP	21	23	17	22	23	27	25	29	33	17	0	0	0
Indicators [mass fraction]													
TMP	**2.64**	**2.20**	**2.80**	**2.12**	**2.35**	**2.06**	**2.04**	**1.86**	**1.10**	**0.32**	**0.13**	**0.15**	**0.00**
DMH													
TMP+DMH	2.98	2.49	6.89	3.46	2.35	1.77	2.52	1.94	1.10	0.24	0.23	0.19	0.19
C8= + C9+													
(2,2,3-+2,2,4-TMP)	2.06	1.76	2.89	1.85	1.71	1.37	1.36	0.99	0.51	0.53	0.00	0.00	0.00
(2,3,4-+2,3,3-TMP)													
DMH Isomer Distribution [%]													
2,5-DMH	23	21	24	21	19	18	17	14	5	5	0	0	0
2,4-DMH	48	46	53	47	45	44	40	35	14	8	11	19	11
2,3-DMH	23	25	19	26	28	30	33	34	26	10	9	0	7
3,4-DMH	6	8	4	7	8	7	10	17	55	77	80	81	82

Run F29Y
(Y, Tcalc=425degC, Trxn=70degC, P=382psig, I/O=11 2, butene WHSV=2 67h-1, t=1h, mcat=2 78g)

TOS [min]	1	2	3	4	5	6	7	8	10	15	20	30	60
Propane	325800	298800	230260	216400	248700	432780	234900	341040	258100	264420	275100	342560	359780
Isobutane	39820100	35965620	23818600	21026560	21452320	47146220	27668980	39469740	29675540	28133860	34335920	42767160	42994960
1-butene											128500	128360	124220
n-butane	1087180	1015520	706160	644360	570520	1209820	814600	1030200	819040	710500	934160	1085980	1078560
t-2-butene									639320	1010340	1424400	1667320	1671360
c-2-butene									272460	512560	758540	926600	795240
C5-C7	**1561423**	**1302602**	**1603007**	**1630692**	**1079464**	**1091064**	**979095**	**845081**	**196266**	**10919**	**0**	**0**	**0**
C5	588880	533080	512860	517240	272080	463100	323220	334420					
2,3-DMB	280879	212075	287886	303479	185593	168112	161306	146519	52294				
2,2-DMP	131483	99980	143746	148931	89166	76922	73722	62901	20897	5399			
3-MP	94695	71066	99915	107827	73743	59695	64546	54566	26314				
2,4-DMP	234222	184212	234735	260301	208207	141930	154022	110455	39767	5520			
2,2,3-TMB	12263	8973	11665	13519	11668	8149	8989	5604					
2-MHx	48009	42893	47496	59625	46595	33801	35444	22444	7433				
2,3-DMP	129356	112199	123535	164214	146160	105083	120037	83246	37984				
3-MHx	41636	38124	41169	55756	46242	34272	37809	24926	11566				
C8	**1611780**	**1851957**	**1243034**	**2439613**	**1911648**	**1756471**	**1749610**	**1384840**	**1002172**	**518872**	**459102**	**358225**	**366294**
2,2,4-TMP	**643772**	**637918**	**576763**	**863977**	**700438**	**660378**	**663639**	**368148**	**133167**	**14411**			
2,5-DMHx	93975	112438	76707	148732	103142	96192	90886	60979	19886	6061			
2,2,3-TMP	93348	106696	74568	132925	88168	79647	67346	44650	13262				
2,4-DMHx	201037	246002	166000	337880	240504	232565	214696	156421	55156	10850	11292	14202	9459
2,3,4-TMP	130898	154057	78328	193474	177280	170200	189045	178755	143591	20073	13805	11133	
2,3,3-TMP	226272	270082	147284	345093	284288	290205	275290	240247	145093	7200			
2,3-DMHx	94828	132906	59588	184603	148500	160840	177456	150849	102857	12580	9188		6407
3,4-DMHx	25059	40209	11373	52632	40609	39389	52632	77924	216613	100426	83922	62285	71338
1 DMHx=													
2 DMHx=	6873	9740	5642	11136	9034	9200	8424	7635	101112	245801	248776	197025	200878
3 DMHx=													
4 DMHx=													
5 DMHx=	95718	141909	46791	164146	119685	126855	110096	99232	49935	5765			
6 DMHx=				5015					21510	95705	92119	73580	78212
C9+	403759	530939	120363	473318	630933	777290	529102	552930	583902	362034	173193	179232	179567
C5+	3576962	3685498	2866404	4543823	3622035	3623825	3257807	2782851	1782329	891825	632295	537457	545861
Tot Peak Area	44810042	40965438	27621424	26431143	25893575	52412645	31976287	43623831	33174329	31010945	37730375	46528837	46774741
Feed Analysis		Inj 1	Inj 2	Inj 3	Inj 4	Inj 5	Avg	Mass %					
C3		15360	16384	16393	16003	21731	17174	0 75					
i-C4		1601462	1965158	1969365	1928514	2717689	2036438	89 33	Avg Mass I/O Ratio			11 64	
1-C4=		138689	170060	170342	166441	227416	174590	7 66	Avg Molar I/O Ratio			**11.236**	
n-C4		40302	50295	50266	49358	67435	51531	2 26					
I/O Mass Ratio		11 547	11 556	11 561	11 587	11 950	**11.640**						

F31EMT

(EMT; Tcalc=425degC; Trxn=77degC; P=382psig; I/O=11.4; butene WHSV=2.65h-1; t=1h; mcat=2.78g)

Samp t (min)	9	10	11	12	13	14	15	16	17	19	22	27	37	67
T.O.S. (min.)	2	3	4	5	6	7	8	9	10	12	15	20	30	60
1-C4= Disapp. [%]	100	100	100	100	100	100	100	100	100	100	100	100	100	100
t-2-C4= Prod. [%]	0	0	0	0	0	0	9	17	23	33	34	34	39	39
c-2-C4= Prod. [%]	0	0	0	0	0	0	4	7	9	14	14	14	16	17
Butene Disapp. [%]	100	100	100	100	100	100	87	76	67	53	52	52	45	44
n-Butane Change [%]	5	9	7	5	6	7	8	4	5	3	-1	4	3	-5
C5+ Product Analysis [mass %]														
C5-C7	23	29	25	23	23	20	13	8	4	2	0	1	0	0
C8	53	55	54	57	49	48	48	51	51	57	59	63	58	61
C9+	24	16	21	19	28	31	39	41	45	42	41	36	42	39
C8 Distribution [mass %]														
TMP	61	61	60	57	57	52	47	17	6	0	0	0	0	0
DMH	24	26	26	30	28	33	36	50	44	36	30	31	26	24
C8=	15	13	14	13	15	16	16	33	49	64	70	69	74	76
TMP Distribution [%]														
2,2,4-TMP	50	47	45	43	40	35	31	32	25	0	0	0	0	0
2,2,3-TMP	13	9	8	7	5	3	2	0	0	0	0	0	0	0
2,3,4-TMP	13	17	18	20	24	30	36	38	38	0	0	0	0	0
2,3,3-TMP	24	27	28	29	30	32	31	30	37	0	0	0	0	0
Indicators [mass fraction]														
TMP	2.51	2.40	2.33	1.94	2.06	1.59	1.30	0.34	0.14	0.00	0.00	0.00	0.00	0.00
DMH														
TMP+DMH	1.41	2.04	1.65	1.85	1.17	1.05	0.86	0.60	0.36	0.26	0.21	0.25	0.18	0.17
C8= + C9+														
(2,2,3-+2,2,4-TMP)	1.75	1.27	1.14	1.02	0.84	0.62	0.50	0.47	0.33	0.00	0.00	0.00	0.00	0.00
(2,3,4-+2,3,3-TMP)														
DMH Isomer Distribution [%]														
2,5-DMH	15	13	13	11	11	6	4	7	8	3	0	0	0	0
2,4-DMH	39	34	31	27	24	18	13	2	3	6	12	9	9	11
2,3-DMH	36	41	41	38	44	37	41	20	25	13	11	12	11	6
3,4-DMH	10	12	15	23	21	40	42	70	64	78	77	79	80	83

F31EMT

(EMT, Tcalc=425degC, Trxn=77degC, P=382psig, I/O=11 4, butene WHSV=2 65h-1, t=1h, mcat=2 78g)

TOS [min]	2	3	4	5	6	7	8	9	10	12	15	20	30	60
Propane	358200	372360	357200	325420	355420	377460	284420	356180	313120	358320	297080	274600	279280	324320
Isobutane	39991780	42439780	40302000	36822840	42777880	46696960	36069200	42727240	33642340	44536160	29582320	35544940	27033580	29508300
1-butene														
n-butane	1075000	1140100	1081140	966400	1117860	1226700	941980	1071960	860020	1111120	713560	893240	683180	684440
t-2-butene							268280	603860	640740	1209160	836060	995660	867220	951060
c-2-butene							106400	242740	260140	497180	341040	415600	369260	414660
C5-C7	**913154**	**807220**	**779742**	**645845**	**635510**	**525678**	**159891**	**80640**	**34501**	**12927**	**0**	**5630**	**0**	**0**
C5	323480	296820	276460	215060	229740	185960								
2,3-DMB	141619	134944	129434	104620	104331	84738	36659	14121	5232					
2,2-DMP	60703	55643	52329	43199	43288	34831	16265	8602						
3-MP	55803	55566	53870	46782	48756	45208	25836	18460	12650	7627		5630		
2,4-DMP	145507	114516	112842	95062	81864	64294	27817	10835		5300				
2,2,3-TMB	12340	10724	11199	9840	9167	8060								
2-MHx	32095	23173	23233	20885	17909	14365	6716							
2,3-DMP	109892	90805	94623	86474	78220	68618	34322	18857	9710					
3-MHx	31715	25029	25752	23923	22235	19604	12276	9765	6909					
C8	**2115219**	**1504014**	**1654590**	**1588327**	**1356299**	**1240630**	**572582**	**542311**	**470014**	**479709**	**413194**	**368367**	**423636**	**361131**
2,2,4-TMP	**648084**	**434704**	**448560**	**394911**	**313619**	**224262**	**83898**	**29767**	**7274**					
2,5-DMHx	79148	50329	54522	51730	40212	22863	8248	20135	17169	5136				
2,2,3-TMP	172398	81168	83595	66419	40599	20912	6513							
2,4-DMHx	200173	129454	133082	128583	91841	72780	26602	5303	7220	10688	14621	9991	10308	9196
2,3,4-TMP	165315	160990	163428	162269	187494	192721	97401	35154	11246					
2,3,3-TMP	304510	245324	281992	267880	232841	205339	83385	28272	10704					
2,3-DMHx	185094	155962	176201	180231	164521	149096	85990	55321	51181	22120	13880	14322	12027	5366
3,4-DMHx	50664	47792	64986	109735	78658	159813	87994	191958	132686	133524	94641	91645	89602	71679
1 DMHx=														
2 DMHx=	10020	7144	6968	6648	7028	8854	11572	55069	116257	173374	182041	164426	187753	165135
3 DMHx=														
4 DMHx=								10434	9150	9054	7838			
5 DMHx=	136292	82411	93563	90125	76475	54859	10110	5154				7576	7546	6411
6 DMHx=	5864		5682					23107	32445	77854	67045	52654	86643	81729
7 DMHx=	34702	28217	41802	29622	40325	36906	8528	6112						
8 DMHx=	122955	80519	80209	80174	82686	92225	62341	76525	74682	47959	33128	27753	29757	21615
C9+	971842	441580	638711	540259	778878	809695	468654	431142	418975	354137	289998	212345	306983	226087
C5+	4000215	2752814	3073043	2774431	2770687	2576003	1201127	1054093	923490	846773	703192	586342	730619	587218
Tot Peak Area	45425195	46705054	44813383	40889091	47021847	50877123	38871407	46056073	36379710	48061533	32132212	38294782	29593879	32055338
FEED ANAL.		Inj 1	Inj 2	Inj 3	Inj 4	Inj 5	Avg	Mass %						
C3		19221	18345	18081	18050	14811	17702	0 75						
i-C4		2300990	2250098	2211863	2202486	1645529	2122193	89 41	Average Mass I/O Ratio				11 77	
1-C4=		195299	191639	188427	187171	139374	180382	7 60	Average Molar I/O Ratio				**11.359**	
n-C4		57688	56834	55575	55628	40695	53284	2 24						
I/O Mass Ratio		11 782	11 741	11 739	11 767	11 807	**11.767**							

Run F33Y
(Y; Tcalc=425degC; Trxn=100degC; P=382psig; I/O=11.5; butene WHVS=2.62h-1; t=1h; mcat=2.78g)

T.O.S. [min.]	1	2	3	4	5	6	7	8	9	10	12	15	20	30	60
1-C4= Disapp. [%]	95	100	100	100	100	100	97	96	96	95	96	96	95	95	96
t-2-C4= Prod. [%]	0	0	0	0	5	25	31	34	37	37	40	42	41	44	46
c-2-C4= Prod. [%]	0	0	0	0	0	11	14	15	17	17	18	19	19	20	21
Butene Disapp. [%]	**95**	**100**	**100**	**100**	**95**	**65**	**52**	**47**	**42**	**42**	**38**	**34**	**35**	**31**	**28**
n-Butane Change [%]	7	11	9	8	8	6	2	2	5	3	4	3	3	4	3
C5+ Product Analysis [mass %]															
C5-C7	50	54	54	50	34	18	10	7	4	3	1	1	1	0	1
C8	**41**	**40**	**40**	**36**	**43**	**55**	**54**	**57**	**57**	**69**	**60**	**67**	**52**	**65**	**77**
C9+	9	6	6	14	23	28	37	36	39	28	38	32	47	35	22
C8 Distribution [mass %]															
TMP	**61**	**60**	**60**	**59**	**62**	**38**	**7**	**6**	**2**	**0**	**0**	**0**	**0**	**0**	**0**
DMH	32	34	34	37	30	42	39	44	35	38	32	31	24	26	25
C8=	6	6	6	4	8	20	54	51	63	62	68	69	76	74	75
TMP Isomer Distribution [%]															
2,2,4-TMP	**56**	**58**	**57**	**54**	**34**	**33**	**48**	**56**	**100**	**0**	**0**	**0**	**0**	**0**	**0**
2,2,3-TMP	9	8	7	6	23	21	0	0	0	0	0	0	0	0	0
2,3,4-TMP	13	12	15	17	22	26	52	23	0	0	0	0	0	0	0
2,3,3-TMP	22	21	21	24	21	20	0	21	0	0	0	0	0	0	0
Indicators [mass fraction]															
TMP	**1.91**	**1.77**	**1.78**	**1.62**	**2.04**	**0.89**	**0.19**	**0.13**	**0.06**	**0.00**	**0.00**	**0.00**	**0.00**	**0.00**	**0.00**
DMH															
TMP+DMH	3.36	4.39	4.44	2.34	1.46	1.14	0.38	0.43	0.28	0.37	0.24	0.27	0.14	0.20	0.24
C8= + C9+															
(2,2,3-+2,2,4-TMP)	1.86	1.96	1.78	1.46	1.33	1.19	0.92	1.28	0.00	0.00	0.00	0.00	0.00	0.00	0.00
(2,3,4-+2,3,3-TMP)															
DMH Isomer Distribution [%]															
2,5-DMH	25	25	25	21	18	5	0	8	11	4	0	6	0	0	0
2,4-DMH	47	48	49	45	0	2	9	5	9	8	9	9	16	16	11
2,3-DMH	20	20	20	26	40	29	14	11	15	10	11	6	0	10	6
3,4-DMH	8	7	6	8	42	64	78	76	65	78	80	79	84	74	82

Run F33Y

(Y, Tcalc=425degC, Trxn=100degC, P=382psig, I/O=11 5, butene WHVS=2 62h-1, t=1h, mcat=2 78g)

TOS [min]	1	2	3	4	5	6	7	8	9	10	12	15	20	30	60
Propane	540320	356580	337700	355240	337960	313960	330160	389260	258480	348300	318400	352740	306500	254680	348660
Isobutane	64065980	39902300	36616200	38121380	42295860	39815360	39660760	50658180	32694140	41528120	40578000	44935720	36484080	31389280	43431880
1-butene	259340						101980	147260	118480	153620	131060	158880	141440	116240	157400
n-butane	1716040	1090460	973040	997840	1120020	1021080	962980	1250020	822700	1015640	1007480	1106700	895800	777740	1069180
t-2-butene					168400	801680	988920	1429060	971100	1240660	1307220	1528240	1225240	1117980	1636740
c-2-butene						347160	434620	639420	437660	558100	594660	703140	555560	513560	758420
C6-C7	**2900631**	**1713984**	**1285352**	**1188307**	**1016128**	**201830**	**26434**	**62613**	**17617**	**12626**	**7240**	**7543**	**5403**	**0**	**6415**
C5	1200340	731620	532500	501300	363920										
2,3-DMB	510120	299805	226327	210816	179686	50227	7024	11752	5590						
2,2-DMP	248045	147649	112608	100742	84815	24746		7066							
3-MP	144163	85721	67982	64337	68419	26385	8293	11680	6363	5740					
2,4-DMP	385863	215772	163709	145776	132133	38964	5875	8259	5664	6785	7240	7543	5403		6415
2,2,3-TMB	21917	11921	8736	8288	8512			10501							
2-MHx	90672	51290	39714	34130	33407	10462									
2,3-DMP	226107	128087	100240	92986	110083	37747	5242	7668							
3-MHx	73404	42119	33536	29932	35153	13299		5587							
C8	**2379446**	**1259060**	**936909**	**863552**	**1272111**	**613280**	**147901**	**506397**	**262615**	**306397**	**348041**	**382277**	**198933**	**202600**	**410378**
2,2,4-TMP	**815319**	**438153**	**323399**	**274897**	**266776**	**77169**	**6143**	**16880**	**5321**						
2,5-DMHx	187648	105582	80083	68147	67371	12384		18105	9981	5061		7058			
2,2,3-TMP	134453	60647	38732	30092	180755	48615									
2,4-DMHx	361597	204200	156246	141599		5461	5000	10525	8459	9216	9804	10686	7316	8274	11409
2,3,4-TMP	187033	93097	82471	86948	169368	59233	5562	6439							
2,3,3-TMP	323715	161866	120535	121502	168019	46540		5942							
2,3-DMHx	154247	86558	63417	81535	154987	74960	7912	24476	13772	11939	12123	7193		5405	6502
3,4-DMHx	61401	30434	17554	25733	162479	166874	44818	169866	60047	90413	87877	94186	39854	39174	83268
1,DMHx=															
2 DMHx=	13645	8717	6436	7013	21845	72257	52598	180499	120972	142590	165243	186882	113837	114604	207043
3 DMHx=															
4 DMHx=															
5 DMHx=	140388	69806	48036	26086	80511	26299	5208	10972	7938	7741	7948	7600	5198		5789
6 DMHx=						23488	21660	65693	36125	38437	65046	68672	32728	35143	96367
C9+	508103	190414	144192	322037	696234	309852	101364	321545	178187	122584	222056	182179	180063	110761	114701
C5+	5788180	3163458	2366453	2373896	2984473	1124962	275699	892455	458419	440506	577337	571999	384399	313361	531494
Tot Peak Area	72369860	44512798	40293393	41848356	46906713	43424202	42755119	55405655	35323319	44726846	43919497	48654279	39437459	33969281	47175354
FEED ANAL.		Inj 1	Inj 2	Inj 3	Inj 4	Inj 5	Avg	Mass %							
C3		17255	15767	15794	18541	20624	17596	0 73							
i-C4		2021376	1915354	2006636	2316989	2527123	2157496	89 56		Avg Mass I/O Ratio		11 93			
1-C4=		170077	162649	170031	193589	206897	180649	7 50		Avg Molar I/O Ratio		**11.515**			
n-C4		49671	48009	50371	57473	60507	53206	2 21							
I/O Mass Ratio		11 885	11 776	11 802	11 969	12 214	**11.929**								

Run F34EMT

(EMT; Tcalc=425degC; Trxn=100degC; P=382psig; I/O=11 5; butene WHSV=2 72h-1; t=1h; mcat=2.78g)

Samp t [min]	8	9	10	11	12	13	14	15	16	18	21	26	36	66
T.O.S. [min.]	**2**	**3**	**4**	**5**	**6**	**7**	**8**	**9**	**10**	**12**	**15**	**20**	**30**	**60**
1-C4= Disapp. [%]	100	100	100	100	100	100	100	100	100	97	97	96	96	96
t-2-C4= Prod. [%]	0	0	0	0	0	8	15	22	22	30	33	42	39	34
c-2-C4= Prod. [%]	0	0	0	0	0	4	7	10	10	14	15	19	18	16
Butene Disapp. [%]	**100**	**100**	**100**	**100**	**100**	**88**	**78**	**68**	**68**	**53**	**49**	**35**	**38**	**46**
n-Butane Change [%]	12	10	12	11	10	8	6	6	7	4	4	4	4	4
C5+ Product Analysis (mass %)														
C5-C7	40	46	41	35	34	30	25	18	18	11	2	1	1	3
C8	44	43	46	47	45	42	43	48	48	57	57	70	65	67
C9+	16	11	13	18	21	28	32	34	34	32	41	29	34	30
C8 Distribution [mass %]														
TMP	**60**	**59**	**62**	**60**	**59**	**57**	**50**	**38**	**38**	**16**	**4**	**2**	**0**	**0**
DMH	33	34	32	34	35	36	41	46	46	37	36	30	30	39
C8=	6	7	5	6	6	7	10	16	16	48	60	68	70	61
TMP Isomer Distribution [%]														
2,2,4-TMP	**56**	**56**	**50**	**46**	**43**	**42**	**41**	**48**	**48**	**21**	**0**	**0**	**0**	**0**
2,2,3-TMP	14	13	11	9	8	6	4	0	0	31	0	0	0	0
2,3,4-TMP	10	11	15	19	22	24	26	29	29	27	61	100	0	0
2,3,3-TMP	20	20	24	26	27	27	28	23	23	20	39	0	0	0
Indicators (mass fraction)														
TMP	**1.81**	**1.74**	**1.93**	**1.77**	**1.72**	**1.59**	**1.22**	**0.83**	**0.83**	**0.42**	**0.12**	**0.08**	**0.00**	**0.00**
DMH														
TMP+DMH	2.22	2.92	2.72	2.11	1.78	1.25	1.09	0.98	0.98	0.50	0.30	0.29	0.25	0.36
C8= + C9+														
(2,2,3-+2,2,4-TMP)	2.30	2.21	1.55	1.22	1.06	0.94	0.83	0.91	0.91	1.09	0.00	0.00	0.00	0.00
(2,3,4-+2,3,3-TMP)														
DMH Isomer Distribution [%]														
2,5-DMH	23	22	20	18	16	13	10	5	5	0	9	6	10	5
2,4-DMH	47	46	44	41	38	31	25	19	19	7	7	9	11	7
2,3-DMH	21	23	27	29	33	38	39	37	37	17	16	11	16	14
3,4-DMH	8	9	9	12	13	19	27	39	39	76	68	74	63	74

Run F34EMT

(EMT, Tcalc=425degC, Trxn=100degC, P=382psig, I/O=11 5, butene WHSV=2 72h-1, t=1h, mcat=2 78g)

TOS [min]	2	3	4	5	6	7	8	9	10	12	15	20	30	60
Propane	327220	344300	314280	291240	308260	322940	355240	273000	273000	335740	323900	330120	254920	303840
Isobutane	36467720	35571120	35950880	34354080	36487960	38593860	43249960	32720900	32720900	40404060	39851720	42788060	32031560	36717620
1-butene										101720	108660	140760	103260	104420
n-butane	1008740	957420	994200	967940	992400	1010220	1108160	829720	829720	993420	983040	1064820	797380	906320
t-2-butene						260540	538180	582100	582100	974800	1047980	1457200	1024100	1020380
c-2-butene						119120	246320	267160	267160	446780	484480	677120	476300	469680
C5-C7	**1259623**	**1175169**	**1277735**	**1320623**	**984452**	**665422**	**449730**	**132916**	**132916**	**48106**	**14067**	**6911**	**5238**	**11545**
C5	566400	466580	475660	461020	358720	243460	157360							
2,3-DMB	246122	198832	221387	227134	167840	113120	75033	32339	32339	8359				
2,2-DMP	120897	97648	103780	107604	79628	53843	36533	16376	16376	5983				
3-MP	74026	61104	69263	74529	58736	43259	33600	17242	17242	9935	8007			5789
2,4-DMP	20639	164329	186580	199236	137619	87563	58035	25544	25544	5039	6050	6911	5238	5756
2,2,3-TMB	15043	12341	14263	17129	12269	7726				6878				
2-MHx	50792	40663	45082	49908	35181	22843	16619	7515	7515					
2,3-DMP	125319	100510	122964	139521	101812	70471	53481	24329	24329	6778				
3-MHx	40385	33162	38756	44542	32647	23137	19069	9570	9570	5133				
C8	**1361705**	**1096337**	**1420202**	**1786327**	**1322250**	**923092**	**778369**	**356906**	**356906**	**244087**	**366942**	**434488**	**266856**	**307079**
2,2,4-TMP	**461385**	**361583**	**442909**	**490119**	**341446**	**222506**	**169224**	**64498**	**64498**	**7998**				
2,5-DMHx	105904	82928	93209	106855	73163	44448	30758	8857	8857		12057	8236	7576	5920
2,2,3-TMP	111551	85613	95240	99944	63044	32387	15779			11800				
2,4-DMHx	215558	172770	201546	250273	171652	101169	78227	31162	31162	6239	8798	11235	8593	8700
2,3,4-TMP	83146	74124	135912	204606	170054	128806	101700	39110	39110	10363	9260	9806		
2,3,3-TMP	166205	127990	211916	278265	210635	143065	108837	31476	31476	7756	5826			
2,3-DMHx	94256	85781	121724	177295	150799	124699	122786	59698	59698	15416	20524	13751	12682	16218
3,4-DMHx	38526	32492	42796	71353	60776	61363	84073	63718	63718	67678	89295	96390	49058	87855
1 DMHx=														
2 DMHx=	10172	13984	8982	12192	13091	20554	18906	22234	22234	78738	130268	193907	118002	116208
3 DMHx=														
4 DMHx=							7211	6739	6739					
5 DMHx=	75002	58092	65968	95425	67590	44095	32828	8481	8481	8349	20897	8823	7467	9282
6 DMHx=							18040	19932	19932	29750	70017	92340	53478	62896
C9+	489096	278818	419464	688627	617472	621498	569031	247774	247774	137343	260940	178458	135617	136860
C5+	3110424	2549324	3117401	3795577	2924174	2210012	1797130	736594	736594	429535	641939	619857	397711	455484
Tot Peak Area	40914104	39422164	40376761	39408837	40712794	42516692	47294990	35409474	35142314	43239275	42957239	46400817	34608931	39508064
FEED ANAL.		Inj 1	Inj 2	Inj 3	Inj 4	Inj 5	Avg	Mass %						
C3		17905	17804	16496	15396	17313	16900	0 73						
i-C4		2181826	2261972	2114054	1600860	2217005	2075143	89 56	Average Mass I/O Ratio				11 94	
1-C4=		183171	189430	178225	134523	183445	173759	7 50	Average Molar I/O Ratio				**11.526**	
n-C4		54240	55599	52928	38546	54316	51126	2 21						
I/O Mass Ratio		11 911	11 941	11 862	11 900	12 085	**11.940**							

Run F36Y

(Y; Tcalc=425degC; Trxn=49degC; P=382psig; I/O=11.5; butene WHSV=2.61h-1; t=1h; mcat=2.78g)

Samp t [min]	8	9	10	11	12	13	14	15	16	17	19	22	27	37	67
T.O.S. [min.]	**1**	**2**	**3**	**4**	**5**	**6**	**7**	**8**	**9**	**10**	**12**	**15**	**20**	**30**	**60**
1-C4= Disapp. [%]	96	100	100	100	100	100	100	100	100	100	100	100	100	95	91
t-2-C4= Prod. [%]	0	0	0	0	4	11	19	26	31	32	34	35	38	36	35
c-2-C4= Prod. [%]	0	0	0	0	0	5	8	12	18	21	26	27	33	35	40
Butene Disapp. [%]	**96**	**100**	**100**	**100**	**96**	**85**	**74**	**62**	**52**	**46**	**40**	**39**	**28**	**24**	**16**
n-Butane Change [%]	6	8	8	9	3	0	1	1	5	3	4	2	8	0	1
C5+ Product Analysis [mass %]															
C5-C7	43	32	27	25	19	10	6	3	1	0	0	0	0	0	0
C8	**54**	**62**	**60**	**60**	**48**	**51**	**50**	**45**	**32**	**44**	**52**	**59**	**64**	**49**	**100**
C9+	3	5	13	15	33	39	44	53	67	56	48	41	36	51	0
C8 Product Distribution [mass %]															
TMP	**77**	**69**	**64**	**61**	**62**	**56**	**44**	**16**	**6**	**2**	**2**	**3**	**2**	**2**	**0**
DMH	19	24	26	28	28	30	34	42	37	31	26	18	22	17	12
C8=	5	7	10	12	11	13	21	42	57	67	72	80	77	81	88
TMP Distribution [%]															
2,2,4-TMP	**32**	**33**	**33**	**33**	**30**	**25**	**21**	**17**	**0**	**0**	**0**	**0**	**0**	**0**	**0**
2,2,3-TMP	5	4	5	5	3	3	3	0	0	0	0	0	0	0	0
2,3,4-TMP	29	29	27	28	31	35	37	35	63	100	100	100	100	100	0
2,3,3-TMP	34	34	34	34	36	37	38	48	37	0	0	0	0	0	0
Indicators [mass fraction]															
TMP	**4.06**	**2.83**	**2.42**	**2.18**	**2.23**	**1.85**	**1.30**	**0.37**	**0.16**	**0.07**	**0.07**	**0.14**	**0.07**	**0.12**	**0.00**
DMH															
TMP+DMH	9.28	6.10	2.80	2.46	1.12	0.96	0.71	0.36	0.16	0.17	0.17	0.13	0.18	0.10	0.14
C8= + C9+															
(2,2,3-+2,2,4-TMP)	0.58	0.59	0.63	0.61	0.50	0.39	0.33	0.21	0.00	0.00	0.00	0.00	0.00	0.00	0.00
(2,3,4-+2,3,3-TMP)															
DMH Distribution [%]															
2,5-DMH	12	6	9	8	5	3	0	4	0	0	0	0	0	0	0
2,4-DMH	27	21	25	22	13	9	6	4	5	9	10	17	10	12	28
2,3-DMH	31	33	30	32	29	23	9	7	5	0	0	13	0	0	0
3,4-DMH	30	41	36	38	53	64	84	86	90	91	90	70	90	88	72

Run F36Y
(Y, Tcalc=425degC, Trxn=49degC, P=382psig, I/O=11 5, butene WHSV=2 61h-1, t=1h, mcat=2 78g)

TOS (min)	1	2	3	4	5	6	7	8	9	10	12	15	20	30	60
Propane	420180	326920	313920	295420	303980	352900	273960	309020	283560	310260	293200	257920	229480	327940	329440
Isobutane	55056580	39782080	38074460	36358860	35965880	40138180	32253900	38084240	36253780	39141200	36626560	31966380	25492060	41017160	41431860
1-butene	171040													170920	293880
n-butane	1357080	1019980	975460	943600	879440	954740	771100	919240	906680	951920	896200	770400	657340	975880	989040
t-2-butene					110220	354520	483880	792820	910280	1018320	1013060	891680	797460	1177980	1175640
c-2-butene						150400	205740	383580	518940	666120	759540	683240	691160	1172280	1321720
C5-C7	**617416**	**585337**	**517313**	**480895**	**334056**	**164574**	**55130**	**21190**	**5124**	**0**	**0**	**0**	**0**	**0**	**0**
C5	250160	204580	194260	174600	112260										
2,3-DMB	115251	104675	87567	82312	58676	39571	14010	5150							
2,2-DMP	32286	34308	29870	27868	19008	12735									
3-MP	50713	50682	42869	41580	31585	25424	13217	8031	5124						
2,4-DMP	75536	78190	65933	60448	43776	30738	10659								
2,2,3-TMB	6586	5647		5038											
2-MHx	10440	12783	11971	10720	7488	5560									
2,3-DMP	62675	75600	67326	62182	48688	40070	17244	8009							
3-MHx	13769	18872	17517	16147	12575	10476									
C8	**783236**	**1130748**	**1169139**	**1134000**	**866347**	**844301**	**438737**	**349021**	**320418**	**263991**	**305650**	**227407**	**366652**	**269682**	**159289**
2,2,4-TMP	**192372**	**256767**	**246773**	**224100**	**158949**	**117778**	**41926**	**9321**							
2,5-DMHx	17115	15682	28233	25622	11391	8858		5573							
2,2,3-TMP	28257	32200	40153	35361	18275	16472	6171								
2,4-DMHx	40063	57847	76848	68202	31571	23777	9198	5539	6529	7349	7710	6820	8366	5714	5530
2,3,4-TMP	173255	223632	202564	192966	164573	164940	72926	19051	12382	5499	5450	5775	5590	5571	
2,3,3-TMP	205356	264710	253607	235717	192522	175965	74180	25916	7264						
2,3-DMHx	45532	89928	92204	101303	69296	59353	14134	9649	5411			5206			
3,4-DMHx	44844	111578	109652	120293	127041	164276	126895	127436	107146	73898	71285	27803	71647	40740	13882
1 DMHx=															
2 DMHx=			5586	5170		10269	31197	75219	107195	123747	151923	140257	198033	163913	108355
3 DMHx=															
4 DMHx=															
5 DMHx=	13425	32738	42942	42567	16796	20640	6408								
6 DMHx=								17059	27193	30058	45064	28197	68585	48475	
7 DMHx=	6953	11021	15771	18746	15765	14188	7535	5031							31522
8 DMHx=	16064	34645	54806	63953	60168	67785	48167	49227	47298	23440	24218	13349	14431	5269	
C9+	44008	94188	255282	276833	599401	649038	391017	410761	666017	338151	278148	160135	205347	284145	0
C5+	1444660	1810273	1941734	1891728	1799804	1657913	884884	780972	991559	602142	583798	387542	571999	553827	159289
Tot Peak Area	58449540	42939253	41305574	39489608	39059324	43608653	34873464	41269872	39345859	42023842	39412818	34273922	27748339	44223707	44379149
FEED ANAL.		Inj 1	Inj 2	Inj 3	Inj 4	Inj 5	Avg	Mass %							
C3		18825	15463	16619	15438		16586	0 72							
i-C4		2351338	1945098	2049751	1942401		2072147	89 60							
1-C4=		194645	163620	171701	163011		173244	7 49							
n-C4		56886	48049	50396	47864		50799	2 20							
I/O Mass Ratio		12 080	11 888	11 938	11 916		**11.955**								

Run F44PTY

(0.5%Pt/Y; Tcalc=325degC; Tred=425degC; Trxn=52degC; P=382psig; I/O=15.3; butene WHSV=2.0h-1; t=1h; mcat=2.78g)

Samp t [min]	8	9	10	11	12	13	14	15	16	17	19	22	27	37	67
T.O.S. [min.]	**1**	**2**	**3**	**4**	**5**	**6**	**7**	**8**	**9**	**10**	**12**	**15**	**20**	**30**	**60**
1-C4= Disapp. [%]	90	100	100	100	100	100	100	100	100	100	100	100	100	100	100
t-2-C4= Prod. [%]	0	0	0	0	0	0	0	9	16	25	35	37	39	40	43
c-2-C4= Prod. [%]	0	0	0	0	0	0	0	0	6	12	21	22	28	30	31
Butene Disapp. [%]	**90**	**100**	**100**	**100**	**100**	**100**	**100**	**91**	**78**	**62**	**43**	**41**	**33**	**30**	**27**
n-Butane Change [%]	11	9	9	9	8	7	9	6	6	5	4	4	4	2	3
C5+ Product Analysis [mass %]															
C5-C7	25	30	27	27	26	27	16	14	11	6	0	0	0	0	0
C8	**68**	**57**	**54**	**56**	**54**	**51**	**62**	**58**	**46**	**46**	**52**	**62**	**74**	**63**	**69**
C9+	7	13	19	18	20	22	22	28	43	48	48	38	26	37	31
C8 Distribution [mass %]															
TMP	**80**	**76**	**76**	**76**	**75**	**73**	**66**	**59**	**56**	**22**	**0**	**0**	**0**	**0**	**0**
DMH	18	20	21	22	20	23	31	37	36	46	28	29	23	21	15
C8=	3	4	3	2	5	4	3	4	8	31	72	71	77	79	85
TMP Distribution [%]															
2,2,4-TMP	**33**	**32**	**32**	**31**	**31**	**32**	**33**	**33**	**30**	**35**	**0**	**0**	**0**	**0**	**0**
2,2,3-TMP	3	3	4	3	3	4	3	3	0	0	0	0	0	0	0
2,3,4-TMP	29	32	30	32	32	31	30	32	35	39	0	0	0	0	0
2,3,3-TMP	35	33	34	34	34	33	34	32	35	26	0	0	0	0	0
Indicators [mass fraction]															
TMP	**4.47**	**3.88**	**3.59**	**3.42**	**3.73**	**3.23**	**2.14**	**1.62**	**1.58**	**0.48**	**0.00**	**0.00**	**0.00**	**0.00**	**0.00**
DMH															
TMP+DMH	7.36	3.73	2.50	2.86	2.28	2.05	2.53	1.86	0.93	0.51	0.17	0.21	0.20	0.15	0.11
C8= + C9+															
(2,2,3-+2,2,4-TMP)	0.56	0.54	0.56	0.52	0.52	0.56	0.56	0.56	0.44	0.54	0.00	0.00	0.00	0.00	0.00
(2,3,4-+2,3,3-TMP)															
DMH Distribution [%]	1	2	3	4	5	6	7	8	9	10	12	15	20	30	60
2,5-DMH	11	9	8	7	8	7	5	4	0	0	0	0	0	0	0
2,4-DMH	19	14	20	12	13	19	9	11	9	7	12	14	13	16	21
2,3-DMH	36	44	39	36	38	35	30	29	14	8	0	0	0	0	0
3,4-DMH	34	34	34	45	42	38	57	56	76	85	88	86	87	84	79

Run F44PTY
(0 5%Pt/Y, Tcalc=325degC, Tred=425degC, Trxn=52degC, P=382psig, I/O=15 3, butene WHSV=2 0h-1, t=1h, mcat=2 78g)

TOS [min]	1	2	3	4	5	6	7	8	9	10	12	15	20	30	60
Propane	161760	230040	233580	238720	256900	308420	233500	280500	254480	260220	254400	218900	266880	290480	269380
Isobutane	21947360	29346600	29005500	29052280	30746440	36755640	28294180	33262060	30648940	31344200	30721500	26324020	31814400	35371140	32876880
1-butene	137580														
n-butane	553140	732660	728980	731600	762620	902720	706460	808980	742220	749460	731840	627080	753920	822820	774300
t-2-butene								173840	299380	488540	665280	595600	761680	854760	862540
c-2-butene									117180	232420	398940	351900	540060	652880	615360
C5-C7	**115561**	**291602**	**304935**	**306193**	**320813**	**328341**	**144370**	**125173**	**62824**	**26491**	**0**	**0**	**0**	**0**	**0**
C5		112420	114100	112720	117700	126940									
2,3-DMB	35745	52733	55659	55181	57418	59184	40395	33489	17086	7536					
2,2-DMP	9609	14647	15671	16236	17674	18053	13025	11398	5599						
3-MP	14957	22882	24209	25142	26416	27799	21260	19092	12219	6704					
2,4-DMP	27809	40835	42951	42617	44265	42882	30614	25252	12230	5430					
2,2,3-TMB															
2-MHx		5432	5679	6267	6264	5960									
2,3-DMP	22391	34894	37869	39212	41387	38390	31323	28166	15690	6821					
3-MHx	5050	7759	8797	8818	9689	9133	7753	7776							
C8	**321947**	**556060**	**615653**	**638657**	**674933**	**615541**	**542036**	**510619**	**264727**	**222681**	**149439**	**128180**	**179349**	**172494**	**183089**
2,2,4-TMP	**84161**	**135210**	**149359**	**149906**	**158345**	**144775**	**117640**	**98896**	**45288**	**17436**					
2,5-DMHx	6332	9481	10166	10488	10633	9774	7727	7256							
2,2,3-TMP	8076	13988	16985	15350	16082	16812	11016	9942							
2,4-DMHx	10651	14987	25334	16674	17391	26891	14387	21001	8687	7289	5118	5166	5565	5730	5769
2,3,4-TMP	74283	135406	141422	155723	160319	139897	109114	96036	52456	19566					
2,3,3-TMP	89564	140401	158229	162696	172620	148748	120325	98500	51520	12981					
2,3-DMHx	20878	47842	50599	50823	51607	49405	50262	53695	13544	8567					
3,4-DMHx	19490	37128	43681	63614	56545	53424	94906	105360	72116	87466	36577	31537	35696	31007	21185
1 DMHx=															
2 DMHx=					5573		5629	8556	15075	54038	83555	72583	104375	110493	121701
3 DMHx=															
4 DMHx=															
5 DMHx=	8512	21617	19878	13383	25818	25815	11030	11377	6041	15338					
6 DMHx=											24189	18894	33713	25264	34434
C9+	34050	121713	218120	205605	251022	262039	190688	243649	242115	230359	135226	79569	63280	101521	82116
C5+	471558	969375	1138708	1150455	1246768	1205921	877094	879441	569666	479531	284665	207749	242629	274015	265205
Tot Peak Area	23271398	31278675	31106768	31173055	33012728	39172701	30111234	35404821	32514686	33321951	32657685	27973349	33839509	37613215	35048305

Feed Analysis	Inj 1	Inj 2	Inj 3				Avg	Mass %
C3	15664	14410	14483				14852	0 75
i-C4	1883271	1734893	1782403				1800189	91 35
1-C4=	118726	110123	111245				113365	5 75
n-C4	44300	41321	41265				42295	2 15
I/O Mass Ratio	15 862	15 754	16 022				15 880	
Average I/O Molar Ratio		**15.329**						

Run F45Pt1EMTr
(recalcined 0.1%Pt/EMT; Tcalc=325degC; Tred=425degC; Trxn=52degC; P=382psig; I/O=15.2; butene WHSV=2.02h-1; t=1h; mcat=2.78g)

Samp t [min]	11	12	13	14	15	16	17	18	19	20	22	25	30	40	70
T.O.S. [min.]	**1**	**2**	**3**	**4**	**5**	**6**	**7**	**8**	**9**	**10**	**12**	**15**	**20**	**30**	**60**
1-C4= Disapp. [%]	57	93	100	100	100	100	100	100	100	100	100	100	100	100	100
t-2-C4= Prod. [%]	0	0	0	0	0	0	0	0	0	0	11	22	31	40	47
c-2-C4= Prod. [%]	0	0	0	0	0	0	0	0	0	0	0	9	12	17	23
Butene Disapp. [%]	**57**	**93**	**100**	**100**	**100**	**100**	**100**	**100**	**100**	**100**	**89**	**69**	**57**	**43**	**30**
n-Butane Change [%]	7	6	9	10	9	9	9	9	9	7	6	5	3	3	3
C5+ Product Analysis [mass %]															
C5-C7	39	26	27	26	26	26	26	27	17	21	14	11	2	0	0
C8	**60**	**57**	**62**	**63**	**62**	**62**	**62**	**58**	**68**	**58**	**65**	**63**	**50**	**54**	**82**
C9+	2	17	10	11	13	12	12	15	15	21	21	26	48	46	18
C8 Product Distribution [mass %]															
TMP	**84**	**80**	**79**	**78**	**77**	**76**	**76**	**76**	**69**	**67**	**70**	**61**	**16**	**0**	**0**
DMH	12	14	15	17	18	19	18	18	26	27	25	24	36	29	17
C8=	3	6	5	6	5	6	6	6	5	6	5	15	48	71	83
TMP Isomer Distribution [%]															
2,2,4-TMP	**49**	**43**	**42**	**41**	**40**	**41**	**40**	**39**	**40**	**37**	**34**	**30**	**28**	**0**	**0**
2,2,3-TMP	19	24	22	21	18	18	18	16	10	9	7	5	0	0	0
2,3,4-TMP	11	12	13	14	16	16	16	17	21	23	26	30	34	0	0
2,3,3-TMP	21	22	23	24	26	26	26	27	28	31	33	35	38	0	0
Indicators [mass fraction]															
TMP	**6.79**	**5.63**	**5.19**	**4.66**	**4.24**	**4.09**	**4.11**	**4.17**	**2.64**	**2.50**	**2.79**	**2.57**	**0.44**	**0.00**	**0.00**
DMH															
TMP+DMH	16.51	2.61	4.35	4.11	3.67	3.78	3.71	2.92	3.55	2.27	2.62	1.51	0.36	0.19	0.17
C8= + C9+															
(2,2,3-+2,2,4-TMP)	2.12	1.99	1.82	1.65	1.39	1.43	1.37	1.23	1.01	0.86	0.70	0.54	0.39	0.00	0.00
(2,3,4-+2,3,3-TMP)															
DMH Isomer Distribution [%]															
2,5-DMH	19	21	19	17	15	15	15	15	10	9	9	6	0	0	0
2,4-DMH	12	11	11	10	10	10	10	11	23	22	17	10	8	13	21
2,3-DMH	52	54	55	55	48	46	49	48	35	36	37	29	12	0	0
3,4-DMH	17	14	15	18	27	29	25	26	32	33	37	55	80	87	79

Run F45Pt1EM1r
(recalcined 0 1%Pt/EM1, Tcalc=325degC, Tred=425degC, Trxn=52degC, P=382psig, I/O=15 2, butene WHSV=2 02h-1, t=1h, mcat=2 78g)

TOS (min)	1	2	3	4	5	6	7	8	9	10	12	15	20	30	60
Propane	205040	222220	247820	229320	255620	251280	258080	264620	234160	268580	263520	269720	268560	254240	260780
Isobutane	32681960	29698100	30616180	27626420	30141100	29451640	30130680	31000340	27534860	31379080	31326440	32078780	32129000	30872580	31779840
1-butene	883920	131980													
n-butane	821920	745620	787880	713740	771620	754140	770560	784360	696580	785920	768340	781000	764740	738500	757380
t-2-butene											213480	441840	611180	766140	918860
c-2-butene												180180	239900	321520	458440
C6-C7	**272837**	**396821**	**423872**	**379626**	**387250**	**372893**	**363661**	**334210**	**181146**	**284497**	**126111**	**69221**	**5828**	**0**	**0**
C5	107300	146820	154440	138180	141020	135100	131560	126520		103740					
2,3-DMB	44523	61491	65360	58302	59110	57125	56179	52751	44292	43622	30600	17615			
2,2-DMP	15990	23087	24795	22339	22413	21922	21664	20036	16545	16237	11224	6230			
3-MP	18586	26711	29357	27071	27856	27525	27670	25800	22798	23218	17387	11540	5828		
2,4-DMP	46453	67825	70530	61950	61641	57910	56180	48374	43873	42468	29917	16743			
2,2,3-TMB		5930	6210	5711	5883	6026	5422	5027							
2-MHx	6367	10220	11409	9922	10245	9940	8949	7806	7336	7120					
2,3-DMP	27351	44056	49220	44943	46825	45902	44631	37995	36838	38222	28290	17093			
3-MHx	6267	10681	12551	11408	12257	11443	11406	9901	9464	9870	7693				
C8	**423906**	**862460**	**962783**	**903229**	**931214**	**896151**	**890726**	**718407**	**738828**	**810604**	**583436**	**385500**	**191436**	**183080**	**187185**
2,2,4-TMP	**174487**	**296523**	**324115**	**290693**	**288728**	**276371**	**268572**	**213382**	**206074**	**204787**	**139860**	**71552**	**8626**		
2,5-DMHx	10167	25291	28217	25842	25572	25371	25099	19648	19187	19273	12607	5325			
2,2,3-TMP	68858	164487	168943	145240	126068	123680	116996	86382	51371	48562	28514	11446			
2,4-DMHx	6578	14114	15600	14480	16039	15959	16262	13792	44643	47543	25116	9159	5244	6807	6655
2,3,4-TMP	38684	80653	96277	95787	112507	105689	109192	95023	109095	123292	105334	70197	10361		
2,3,3-TMP	76142	150828	174585	169159	186117	173764	172781	149396	144738	170087	135957	82597	11489		
2,3-DMHx	27291	66274	80718	83323	80963	75726	80194	62920	67218	79796	54111	26822	8627		
3,4-DMHx	8708	17113	22753	26778	45655	48824	40719	34028	62939	72008	54944	50600	55852	46798	25643
1 DMHx=															
2 DMHx=											10118	35719	73246	102613	115155
3 DMHx=															
4 DMHx=															
5 DMHx=	12990	48177	51575	51927	49565	50767	50910	43836	33563	38701	16885	9503			
6 DMHx=										6455		12580	17991	26862	39732
C9+	11892	263684	157784	155428	190686	172807	172713	187344	165106	292332	185175	159742	184962	157003	40747
C6+	708634	1522965	1544439	1438483	1509150	1440851	1417099	1239961	1085080	1387333	893722	614463	382226	340083	227932
Tot Peak Area	35301474	32320885	33196319	30007963	32677490	31897911	32576419	33289281	29550680	33820913	33465502	34185803	34155706	32971543	33944792
FEED ANAL.		Inj 1	Inj 2	Inj 3	Inj 4	Inj 5	Avg	Mass %							
C3		13716	12728	12663	13895	14434	13487	0 75							
i-C4		1645782	1551900	1552553	1716830	1790705	1651554	91 28							
1-C4=		104396	99235	99322	108681	113424	105012	5 80							
n-C4		39107	37152	37183	40487	42433	39272	2 17							
I/O Mass Ratio		15 765	15 639	15 632	15 797	15 788	15 724								

Run F48PI5EMTr
(recalcined 0.5%Pt/EMT; tcalc=325degC; Tred=425degC; Trxn=52degC; P=382psig; I/O=15.2; butene WHVS=2.03h-1; t=1; mcat=2.78g)

Samp t [min]	9	10	11	12	13	14	15	16	17	18	20	23	28	38	68
T.O.S. [min.]	1	2	3	4	5	6	7	8	9	10	12	15	20	30	60
1-C4= Disapp. [%]	54	88	100	100	100	100	100	100	100	100	100	100	100	100	100
t-2-C4= Prod. [%]	0	0	0	0	0	0	0	0	0	9	20	33	38	43	46
c-2-C4= Prod. [%]	0	0	0	0	0	0	0	0	0	0	7	14	15	19	24
Butene Disapp. [%]	54	88	100	100	100	100	100	100	100	91	73	53	47	38	30
n-Butane Change [%]	6	6	9	7	7	8	8	8	10	9	9	7	1	1	3
C5+ Product Analysis															
C5-C7	42	29	28	27	28	16	20	13	11	11	4	0	0	0	0
C8	58	63	63	63	58	66	56	57	57	56	44	55	55	58	69
C9+	0	8	9	10	14	18	24	30	32	33	52	45	45	42	31
C8 Product Distribution															
TMP	91	81	79	79	76	71	70	70	66	61	29	3	0	0	0
DMH	7	14	15	16	18	24	25	26	30	34	55	35	26	29	18
C8=	3	5	6	5	6	5	5	4	4	4	16	62	74	71	82
TMP Isomer Distribution															
2,2,4-TMP	46	40	41	39	39	39	35	32	27	25	31	0	0	0	0
2,2,3-TMP	19	22	14	18	16	9	8	5	5	4	0	0	0	0	0
2,3,4-TMP	10	13	16	16	17	22	25	30	33	34	35	0	0	0	0
2,3,3-TMP	25	25	29	27	29	31	33	34	35	37	34	100	0	0	0
Indicators [mass fraction]															
TMP	13.69	5.92	5.28	4.96	4.12	2.99	2.86	2.73	2.24	1.80	0.62	0.09	0.00	0.00	0.00
DMH															
TMP+DMH	36.44	5.35	4.48	4.32	3.19	2.84	2.00	1.65	1.58	1.51	0.62	0.26	0.17	0.20	0.14
C8= + C9+															
(2,2,3-+2,2,4-TMP)	1.86	1.64	1.22	1.33	1.20	0.90	0.74	0.57	0.48	0.40	0.45	0.00	0.00	0.00	0.00
(2,3,4-+2,3,3-TMP)															
DMH Isomer Distribution															
2,5-DMH	39	19	16	17	15	10	10	5	6	4	0	0	0	0	0
2,4-DMH	0	11	8	10	10	20	23	16	11	6	0	10	13	11	20
2,3-DMH	61	52	56	51	49	47	38	40	32	27	14	10	0	9	0
3,4-DMH	0	19	21	22	27	23	29	39	52	62	86	80	87	80	80

Run F48P15EMTr
(recalcined 0 5%Pt/EMT, tcalc=325degC, Tred=425degC, Trxn=52degC, P=382psig, I/O=15 2, butene WHVS=2 03h-1, t=1, mcat=2 78g)

TOS [min]	1	2	3	4	5	6	7	8	9	10	12	15	20	30	60
Propane	233640	257900	262280	279480	286440	236100	276700	280980	278700	279380	238340	260820	279980	292340	274340
Isobutane	35347900	33655200	31863940	33327000	33959980	27167860	32286960	33219700	33386400	33729640	28741480	31417920	33969020	35969980	34592420
1-butene	1027760	263000													
n-butane	879840	842180	817200	839940	862180	689940	823560	843900	854280	856340	724260	784140	800180	854420	835560
t-2-butene										182380	346060	647060	793020	951540	989760
c-2-butene											123220	262660	316440	427900	508420
C6-C7	**249912**	**383169**	**387176**	**392888**	**442940**	**183986**	**288851**	**165973**	**120268**	**83356**	**13644**	**0**	**0**	**0**	**0**
C5	100920	138320	135720	142580	129700		103360								
2,3-DMB	40058	60843	61461	61015	55675	43085	44792	38618	28030	18393					
2,2-DMP	13196	20711	21750	21994	20448	15969	15974	13397	10340	7387					
3-MP	17549	27165	28484	29538	28276	22553	23741	22155	18436	15074	7527				
2,4-DMP	42484	67047	65628	62030	55679	44600	42681	35976	25585	15155					
2,2,3-TMB		5954	6140	6449	6357			5044							
2-MHx	5057	8871	9455	9430	88678	7512	7277	5983							
2,3-DMP	25277	44178	47462	48537	46360	40210	41523	36177	29888	20996	6117				
3-MHx	5371	10070	11076	11315	11767	10057	9503	8623	7989	6351					
C8	**344342**	**827014**	**874264**	**919014**	**912160**	**769439**	**796462**	**721493**	**634721**	**440900**	**164392**	**161023**	**219230**	**246126**	**182133**
2,2,4-TMP	**142919**	**267550**	**281609**	**282208**	**266091**	**211781**	**194096**	**169399**	**116060**	**68111**	**14016**				
2,5-DMHx	8988	21521	20465	24521	24430	18933	18684	8827	10699	5487					
2,2,3-TMP	60127	149005	97569	130505	109593	47030	42922	24727	21166	9768					
2,4-DMHx		12316	10346	15186	16433	36437	45567	29368	20302	9689		5753	7422	7957	6249
2,3,4-TMP	31817	84964	109477	113384	115240	119358	138453	149942	138519	92793	15537				
2,3,3-TMP	77310	169678	201625	197840	197817	166781	183344	171342	146258	100171	15286	5026			
2,3-DMHx	13985	58583	72859	74196	81992	85604	74350	74114	59557	41236	11812	5437		6376	
3,4-DMHx		21041	27114	32323	44496	41313	57274	72907	97065	93883	73721	45095	49575	57745	25795
1 DMHx=															
2 DMHx=										9250	24021	80596	123359	137017	122792
3 DMHx=															
4 DMHx=															
5 DMHx=	9196	42356	53200	48851	49295	42202	41772	30867	26105	10412					
6 DMHx=					6773							19116	38874	37031	27297
C9+	0	104410	130114	152380	211942	213975	336438	388738	358589	260067	185331	133370	179014	180029	81097
C6+	594254	1314583	1391554	1464282	1567042	1167400	1421751	1276204	1113578	784223	353367	294393	398244	426155	263230
Tot Peak Area	38083394	36332863	34334974	35910702	36675642	29261300	34808971	35620784	35632958	35831963	30403507	33404333	36240444	38494435	36955310
FEED ANAL.	Inj 1,2	Inj 3,4	Inj 5,6	Inj 7,8	Inj 9,10	Inj 11,12	Avg	Mass %							
C3	13246	13275	14345	13714	12612	12581	13295	0 75							
i-C4	1604909	1635118	1763578	1668810	1519776	1531788	1620663	91 26							
1-C4=	102450	103575	111656	106264	97260	97740	103157	5 81							
n-C4	38628	38802	42080	40136	36619	36774	38840	2 19							
I/O Mass Ratio	15 665	15 787	15 795	15 704	15 626	15 672	15 708								

Run F49Pt5EMT

(0.5%Pt/EMT; Tcalc=325degC; Tred=425degC; Trxn=51degC; P=382psig; I/O=15.2; butene WHSV=2.02h-1; t=1h; mcat=2.78g)

Samp t [min]	10	11	12	13	14	15	16	17	18	19	21	24	29	39	69
T.O.S. [min.]	**1**	**2**	**3**	**4**	**5**	**6**	**7**	**8**	**9**	**10**	**12**	**15**	**20**	**30**	**60**
1-C4= Disapp. [%]	82	94	100	100	100	100	100	100	100	100	100	100	100	100	100
t-2-C4= Prod. [%]	0	0	0	0	0	0	0	0	0	0	15	24	30	37	42
c-2-C4= Prod. [%]	0	0	0	0	0	0	0	0	0	0	0	10	13	18	26
Butene Disapp. [%]	**82**	**94**	**100**	**100**	**100**	**100**	**100**	**100**	**100**	**100**	**85**	**67**	**56**	**45**	**32**
n-Butane Change [%]	9	9	7	6	9	9	9	9	9	8	6	7	5	4	6
C5+ Product Analysis [mass %]															
C5-C7	43	27	26	18	28	25	23	20	13	11	7	5	2	0	0
C8	**57**	**64**	**61**	**61**	**58**	**61**	**62**	**61**	**58**	**53**	**44**	**37**	**53**	**57**	**62**
C9+	0	9	13	20	14	14	15	19	30	36	49	57	45	43	38
C8 Distribution [mass %]															
TMP	**94**	**80**	**77**	**75**	**79**	**76**	**74**	**70**	**72**	**68**	**62**	**50**	**20**	**4**	**0**
DMH	6	16	19	18	19	19	21	25	24	28	28	28	35	27	20
C8=	0	5	5	6	2	5	5	4	5	4	10	22	45	69	80
TMP Isomer Distribution [%]															
2,2,4-TMP	**27**	**32**	**37**	**30**	**38**	**35**	**34**	**32**	**31**	**28**	**29**	**29**	**39**	**0**	**0**
2,2,3-TMP	8	16	12	17	17	16	8	8	6	6	5	5	0	0	0
2,3,4-TMP	24	21	20	20	18	21	26	28	29	31	30	31	28	0	0
2,3,3-TMP	41	32	32	33	27	29	32	32	34	34	36	35	33	100	0
Indicators [mass fraction]															
TMP	**15.59**	**5.09**	**4.14**	**4.11**	**4.24**	**3.99**	**3.49**	**2.77**	**3.00**	**2.41**	**2.21**	**1.76**	**0.57**	**0.15**	**0.00**
DMH															
TMP+DMH	n.a.	5.23	3.61	2.37	3.69	3.39	3.29	2.71	1.71	1.33	0.75	0.45	0.42	0.21	0.15
C8= + C9+															
(2,2,3-+2,2,4-TMP)	0.55	0.90	0.93	0.91	1.21	1.02	0.72	0.66	0.58	0.52	0.52	0.50	0.64	0.00	0.00
(2,3,4-+2,3,3-TMP)															
DMH Isomer Distribution [%]															
2,5-DMH	0	14	11	13	15	13	10	8	7	5	6	10	0	0	0
2,4-DMH	0	9	7	8	9	8	21	21	9	8	4	0	7	12	18
2,3-DMH	100	47	62	55	47	53	41	35	37	30	25	17	17	0	0
3,4-DMH	0	31	20	24	29	25	28	36	47	57	65	73	75	88	82

Run F49f15EMT
(0 5%Pt/EMT, Tcalc=325degC, Tred=425degC, Trxn=51degC, P=382psig, I/O=15 2, butene WHSV=2 02h-1, t=1h, mcat=2 78g)

TOS (min)	1	2	3	4	5	6	7	8	9	10	12	15	20	30	60
Propane	273780	237320	245840	248980	236540	271240	264000	268980	270700	237040	240280	268380	282500	276680	253240
Isobutane	46688840	31206720	30605060	29856800	28496380	32436580	31486840	32055300	32200720	28486780	29135780	32558440	34143860	33462540	31220120
1-butene	500150	125280													
n-butane	1157040	791800	766480	745960	724180	822540	803760	819560	816680	718600	721620	808860	828060	807120	765420
t-2-butene											273740	480460	638160	762220	814200
c-2-butene												193540	278680	376980	493900
C6-C7	**92485**	**338637**	**343037**	**272129**	**307669**	**338941**	**315956**	**308586**	**171858**	**119706**	**82053**	**40668**	**6122**	**0**	**0**
C5		125520	125500	109040	115740	123120	115960	104260							
2,3-DMB	30859	53148	54665	38554	49760	52445	49776	48248	41135	28637	26400	10498			
2,2-DMP	9431	17550	18546	13079	18163	18808	17019	16859	14886	10148	5045				
3-MP	12665	24426	25383	17971	23880	25833	24647	25202	22590	17864	11369	8931	6122		
2,4-DMP	24462	55401	56043	41907	47811	52256	49553	48164	39855	28118	15874	9840			
2,2,3-TMB		5511	5892			5572		5826							
2-MHx		7341	4818	7027	7324	8039	7408	7386	6426						
2,3-DMP	15068	40650	42319	36142	36262	42059	41569	42349	37555	27251	18364	11399			
3-MHx		9090	9871	8409	8729	10809	10023	10292	9411	7687	5001				
C8	**121345**	**812877**	**802328**	**917315**	**647490**	**833053**	**843268**	**822367**	**778282**	**600816**	**516688**	**278120**	**206964**	**182699**	**162366**
2,2,4-TMP	**30859**	**205784**	**226916**	**209784**	**196348**	**219506**	**210436**	**206209**	**170686**	**116926**	**93075**	**39747**	**16116**		
2,5-DMHx		17362	16749	21895	17628	20829	18787	19020	12080	8543	8499	7642			
2,2,3-TMP	9553	100442	71026	118585	85565	98682	50410	51837	33177	23436	16045	6597			
2,4-DMHx		11114	9952	13801	11248	13276	38081	48512	17502	13395	5797		5174	6088	5952
2,3,4-TMP	27022	134523	123103	134618	91229	131756	162167	181756	161628	128168	96290	43505	11594		
2,3,3-TMP	46598	206290	195541	227122	141360	180669	201093	209077	191887	140059	115540	48863	13611	7349	
2,3-DMHx	7313	59654	92422	92284	56857	83841	72669	82829	68788	50065	36229	13325	12586		
3,4-DMHx		38864	29545	39926	35718	40083	49398	83633	87462	97128	94403	57765	54313	42642	27268
1,DMHx=															
2 DMHx=											29741	42405	69466	99418	106130
3 DMHx=															
4 DMHx=															
5 DMHx=		38864	38074	54023	11537	44411	40228	40494	35072	24095	20069	5108			
6 DMHx=				5297								13163	24104	27102	23006
C9+		109145	173517	303007	160597	188479	203613	284741	398640	409512	574289	424391	174847	137775	98347
C6+	213830	1260659	1318882	1492451	1115756	1360473	1362836	1515694	1348780	1130032	1172030	743179	387933	320374	260703
Tot Peak Area	48833640	33621779	32936262	32344191	30572856	34890833	33917436	34659534	34636880	30572452	31543450	34859319	36280513	35628934	33313683
Feed Analysis		Inj 1	Inj 2	Inj 3	Inj 4	Inj 5	Avg	Mass %							
C3		14792	12812	12812	13590		13502	0 76		Avg Mass I/O Ratio		15 78			
i-C4		1817472	1538912	1533629	1626039		1629013	91 29		Avg Molar I/O Ratio		**15.234**			
1-C4=		114233	97992	97647	102892		103191	5 78							
n-C4		42715	36818	36575	38643		38688	2 17							
I/O Mass Ratio		15 910	15 704	15 706	15 803		15 781								

Run F50Pt5EMTr
(recalcined 0 5 % Pt/EMT; Tcalc=325degC; Tred=425degC; Trxn=50degC; P=382psig; I/O=15 0; butene WHSV=2 05h-1; t=1h; mcat=2 78g)

Samp t [min]	12	13	14	15	16	17	18	19	20	22	25	30	40	70
T.O.S. [min.]	1	2	3	4	5	6	7	8	9	11	14	19	29	59
1-C4= Disapp. [%]	82	94	100	100	100	100	100	100	100	100	100	100	100	100
t-2-C4= Prod. [%]	0	0	0	0	0	0	0	0	0	8	8	31	33	44
c-2-C4= Prod. [%]	0	0	0	0	0	0	0	0	0	0	0	13	13	21
Butene Disapp. [%]	82	94	100	100	100	100	100	100	100	92	92	66	63	35
n-Butane Change [%]	7	5	7	8	8	8	9	8	10	7	8	9	6	8
C5+ Product Analysis [%]														
C5-C7	29	27	24	25	26	25	29	25	16	10	7	2	0	0
C8	57	57	55	57	59	60	58	62	67	55	51	62	50	62
C9+	14	16	21	18	15	15	13	13	17	34	42	36	50	38
C8 Distribution [mass %]														
TMP	86	80	77	77	77	78	78	74	72	66	50	24	3	0
DMH	10	14	17	17	17	17	17	22	22	28	33	29	37	24
C8=	3	6	6	6	6	5	4	4	5	6	17	47	60	76
TMP Isomer Distribution [%]														
2,2,4-TMP	54	43	42	41	40	38	38	38	36	29	30	43	0	0
2,2,3-TMP	20	23	22	19	18	16	13	9	8	7	6	0	0	0
2,3,4-TMP	6	12	12	14	15	18	20	23	25	31	31	27	0	0
2,3,3-TMP	21	22	24	26	26	28	29	30	31	34	34	30	100	0
Indicators [mass fraction]														
TMP	8.51	5.74	4.59	4.39	4.49	4.48	4.56	3.30	3.28	2.34	1.52	0.84	0.09	0.00
DMH														
TMP+DMH	3.44	2.74	2.17	2.57	3.00	3.14	3.52	3.81	3.12	1.39	0.82	0.51	0.25	0.18
C8= + C9+														
(2,2,3-+2,2,4-TMP)	2.83	1.93	1.77	1.53	1.41	1.18	1.05	0.90	0.81	0.55	0.55	0.77	0.00	0.00
(2,3,4-+2,3,3-TMP)														
DMH Isomer Distribution [%]														
2,5-DMH	32	2	18	17	17	16	15	11	11	6	0	0	0	0
2,4-DMH	0	13	10	11	10	11	10	28	22	13	6	0	9	15
2,3-DMH	45	63	55	52	53	48	50	38	42	32	21	15	9	0
3,4-DMH	23	21	17	20	20	25	25	24	26	49	73	85	82	85

F50Pt5EMTr

(recalcined 0 5%Pt/EMT, Tcalc=325degC, Tred=425degC, Trxn=50degC, P=382psig, I/O=15 0, butene WHSV=2 05h-1, t=1h, mcat=2 78g)

TOS (min)	1	2	3	4	5	6	7	8	9	11	14	19	29	59
Propane	161720	220480	238620	211080	245660	246320	255140	262420	228100	257780	261800	241600	261040	235580
Isobutane	20991300	29803780	30242220	26166440	29633460	29206760	30033160	30895760	26847720	30959800	32054440	28907460	31596960	28667920
1-butene	232360	112880												
n-butane	525940	745560	769720	676680	760500	746400	772040	790580	693940	785900	805320	738340	786860	728840
t-2-butene										164340	156760	555300	653960	793740
c-2-butene												238420	265140	379860
C6-C7	**138248**	**390610**	**387622**	**341706**	**363223**	**332852**	**358422**	**321256**	**164663**	**113123**	**47609**	**5618**	**0**	**0**
C5		143560	143220	123560	131860	123440	120980	119480						
2,3-DMB	46091	59767	59995	52488	56081	51815	51405	50484	40072	27041	12448			
2,2-DMP	13612	23217	23042	19719	21072	19141	18943	18627	14518	10326				
3-MP	15488	28223	29095	25279	27376	25602	25343	25086	20849	16404	10400	5618		
2,4-DMP	34964	63381	63069	54563	57153	52375	79798	48843	39400	25869	11592			
2,2,3-TMB		5349		5421	5635		5276							
2-MHx	5394	10377	10725	8954	9232	8453	7632	7826	6474					
2,3-DMP	22699	45262	47264	41351	43742	42012	39295	40976	34494	26517	13069			
3-MHx		11374	11112	10371	11072	10014	9750	9934	8846	6966				
C8	**274488**	**834233**	**878860**	**779160**	**821029**	**786646**	**717647**	**782320**	**686580**	**607672**	**345164**	**170769**	**177870**	**173699**
2,2,4-TMP	**127860**	**284029**	**286917**	**245232**	**263796**	**232473**	**213466**	**219443**	**181618**	**116406**	**50884**	**18111**		
2,5-DMHx	9042	2641	26889	22780	23582	21338	18228	19467	16274	10428				
2,2,3-TMP	47426	154138	146259	115718	116589	99300	73979	52758	41190	26751	9988			
2,4-DMHx		15218	14862	14683	14484	14981	12798	48385	32882	23118	6846		5952	6492
2,3,4-TMP	13227	78076	82614	82887	95089	108079	109961	132832	122499	124216	52655	11102		
2,3,3-TMP	48714	148747	162511	152706	167679	172930	165074	170423	152427	135136	58351	12555	5687	
2,3-DMHx	12533	73214	81403	70694	75276	66191	61977	65499	63335	54556	23301	7349	5692	
3,4-DMHx	6311	24827	24771	27852	27605	34206	30306	41045	39335	83637	83089	42153	53910	36056
1 DMHx=														
2 DMHx=										11561	41347	62651	77213	105786
3 DMHx=														
4 DMHx=														
5 DMHx=	9375	53343	52634	46598	46927	37148	31858	32468	37020	22764	6822			
6 DMHx=											11881	16848	29416	25365
C9+	67776	231554	328904	238869	211067	201182	163050	164280	171494	377789	289651	100395	175782	107346
C5+	480512	1456297	1595286	1359725	1395319	1320680	1239119	1267856	1022727	1098484	682324	276782	353652	281045
Tot Peak Area	22391832	32338997	32845846	28413925	32034939	31520160	32299459	33216616	28792487	33266304	33960644	30719482	33652472	30707125
FEED ANAL.		Inj 1	Inj 2	Inj 3	Inj 4	Inj 5	Avg	Mass %						
C3		13260	11768	12041	12105	11226	12080	0 75						
i-C4		1612474	1430884	1464755	1463586	1355949	1465530	91 19						
1-C4=		102785	92194	94199	94030	87728	94187	5 86						
n-C4		38501	34610	35385	35362	32879	35347	2 20						
I/O Mass Ratio		15 688	15 520	15 550	15 565	15 456	15 556							

Run F54Y
(Y; Tcalc=425degC; Trxn=50degC; P=382psig; I/O=15.2; butene WHSV=2.03h-1; t=1h; mcat=2.78g)

Samp t [min]	11	12	13	14	15	16	17	18	19	20	22	25	30	40	70
T.O.S. [min.]	**1**	**2**	**3**	**4**	**5**	**6**	**7**	**8**	**9**	**10**	**12**	**15**	**20**	**30**	**60**
1-C4= Disapp. [%]	88	95	100	100	100	100	100	100	100	100	100	100	100	97	95
t-2-C4= Prod. [%]	0	0	0	0	0	0	0	5	16	35	35	37	40	42	44
c-2-C4= Prod. [%]	0	0	0	0	0	0	0	0	7	14	17	19	28	23	35
Butene Disapp. [%]	**88**	**95**	**100**	**100**	**100**	**100**	**100**	**95**	**77**	**51**	**48**	**44**	**32**	**32**	**16**
n-Butane Change [%]	13	15	13	14	14	14	17	17	16	11	10	10	8	9	9
C5+ Product Analysis [mass %]															
C5-C7	34	31	31	30	29	24	12	8	4	2	0	0	0	0	0
C8	**55**	**53**	**55**	**54**	**55**	**53**	**54**	**47**	**45**	**42**	**41**	**44**	**54**	**60**	**71**
C9+	11	16	14	16	16	23	34	45	51	56	59	56	46	40	29
C8 Distribution [mass %]															
TMP	**75**	**74**	**72**	**71**	**69**	**68**	**65**	**63**	**47**	**42**	**15**	**7**	**2**	**2**	**2**
DMH	20	21	22	23	25	27	30	32	42	37	36	26	25	26	21
C8=	5	5	5	6	6	5	5	5	11	21	49	67	73	72	77
TMP Isomer Distribution [%]															
2,2,4-TMP	**39**	**40**	**41**	**41**	**43**	**42**	**37**	**33**	**28**	**25**	**23**	**20**	**0**	**0**	**0**
2,2,3-TMP	6	7	7	7	6	6	5	5	5	5	0	0	0	0	0
2,3,4-TMP	23	21	21	20	20	21	25	29	34	34	51	51	100	100	100
2,3,3-TMP	31	32	31	31	31	31	32	33	33	36	26	30	0	0	0
Indicators [mass fraction]															
TMP	**3.69**	**3.53**	**3.25**	**3.05**	**2.81**	**2.51**	**2.14**	**1.97**	**1.12**	**1.14**	**0.42**	**0.27**	**0.08**	**0.07**	**0.08**
DMH															
TMP+DMH	3.95	2.69	3.14	2.68	2.71	1.97	1.39	0.94	0.72	0.51	0.26	0.17	0.17	0.20	0.19
C8= + C9+															
(2,2,3-+2,2,4-TMP)	0.83	0.89	0.94	0.93	0.96	0.92	0.74	0.61	0.49	0.43	0.30	0.25	0.00	0.00	0.00
(2,3,4-+2,3,3-TMP)															
DMH Isomer Distribution [%]															
2,5-DMH	14	14	13	13	13	11	11	8	5	4	0	0	0	0	0
2,4-DMH	35	35	32	33	31	26	28	21	12	0	4	7	10	10	11
2,3-DMH	32	39	38	40	41	37	37	31	25	20	12	5	5	5	7
3,4-DMH	19	13	16	14	15	26	24	40	58	76	84	88	85	84	81

Run F54Y
(Y, Tcalc=425degC, Trxn=50degC, P=382psig, I/O=15 2, butene WHSV=2 03h-1, t=1h, mcat=2 78g)

TOS (min)	1	2	3	4	5	6	7	8	9	10	12	15	20	30	60
Propane	327840	375180	422900	453160	394040	463580	428320	434040	434820	390100	390100	449020	400220	464400	467620
Isobutane	43783560	45678920	49516540	51564260	44943920	52177140	47976060	48681540	48820360	45503980	45503980	51313800	46583280	53668880	54140940
1-butene	318460	134720												102640	159280
n-butane	1165800	1245760	1328740	1399860	1219600	1403580	1293760	1307580	1310200	1174800	1174800	1313580	1179980	1370600	1376840
t-2-butene								139040	469020	986840	990820	1175560	1168700	1400920	1464220
c-2-butene									209440	394740	482220	606180	802420	784100	1193340
C5-C7	**563236**	**703775**	**826339**	**863777**	**748672**	**843918**	**137302**	**84117**	**30012**	**15488**	**0**	**0**	**0**	**0**	**0**
C5	219500	267800	305100	322760	273300	220580									
2,3-DMB	102590	126179	147727	153225	131649	116283	36897	17210	9814	7755					
2,2-DMP	31152	41788	51776	54702	48221	39631	5147	5106							
3-MP	39183	50946	61362	64567	57143	52532	21510	11640	5033						
2,4-DMP	84517	101021	118432	120042	104634	88899	43807	10954	5147						
2,2,3-TMB	5986	7153	7720	8311	7004	7020									
2-MHx	11518	15239	18749	19822	18070	14726									
2,3-DMP	56279	75096	90992	95332	85675	83246	29941	19207	10018	7733					
3-MHx	12511	18553	23481	25016	22976	21001									
C8	**905823**	**1228420**	**1486447**	**1560884**	**1412202**	**1399628**	**614218**	**376681**	**337650**	**326244**	**338144**	**358213**	**347816**	**446817**	**347902**
2,2,4-TMP	**265247**	**362940**	**444035**	**458751**	**417343**	**399290**	**148590**	**78314**	**44433**	**34151**	**11658**	**5010**			
2,5-DMHx	26047	35862	43189	46689	44009	41693	20390	9643	7090	5030					
2,2,3-TMP	41458	62387	76646	76791	63635	57041	20077	11870	7940	6830					
2,4-DMHx	64374	88690	107435	118964	109436	98550	51900	25307	17015		5100	6513	8694	11830	8239
2,3,4-TMP	157617	193674	220865	226806	197094	199650	100400	68820	53945	46445	25855	12776	6955	7563	6073
2,3,3-TMP	213036	286404	334457	346307	302317	294714	128511	78311	52370	49177	13180	7510			
2,3-DMHx	58929	99638	127521	146507	141491	140242	68585	37362	35460	24068	14597	5060	4347	6199	5267
3,4-DMHx	34118	32365	53397	51887	53797	98545	44484	48220	82257	91242	102182	81570	73992	98270	59066
1 DMHx=															
2 DMHx=		5596	6401	6720	6544	6316	6609	11386	27626	51776	142015	164325	180153	224540	195758
3 DMHx=															
4 DMHx=															
5 DMHx=	44997	60864	72501	81462	76536	63587	24672	7448	9514	11211	9778	9107		5212	
6 DMHx=										5314	13779	66342	73675	93203	73499
C9+	173110	365964	369087	460696	406742	606711	389010	360660	382659	433658	486249	455454	296223	297878	140965
C5+	1642169	2298159	2680873	2885357	2567616	2650257	1140530	801458	750321	774390	824393	813667	644039	744695	488867
Tot Peak Area	47237829	49732739	53949053	56302637	49125176	56694557	50838670	51363658	51784721	48830110	48884093	55065627	49976219	57752135	58097767
Feed Analysis	Inj 1	Inj 2	Inj 3	Inj 4	Inj 5	Avg	Mass %								
C3	13410	11768	11827	12319	12778	12420	0 74								
i-C4	1654456	1448580	1435022	1519065	1586500	1528725	91 29		Avg Mass I/O ratio		15 76				
1-C4=	104348	92411	91529	96376	100114	96956	5 79		Avg Molar I/O ratio		**15.217**				
n-C4	39121	34822	34529	36118	37695	36457	2 18								
I/O Mass Ratio	15 855	15 675	15 678	15 762	15 847	15 764									

Run F55Yr

(recalcined Y; Tcalc=425degC; Trxn=50degC; P=382psig; I/O=14.4; butene WHSV=2.13h-1; t=1h; mcat=2.78g)

Samp t [min]	10	11	12	13	14	15	16	17	18	19	21	24	29	39	69
T.O.S. [min.]	**1**	**2**	**3**	**4**	**5**	**6**	**7**	**8**	**9**	**10**	**12**	**15**	**20**	**30**	**60**
1-C4= Disapp. [%]	67	95	100	100	100	100	100	100	100	100	100	100	96	97	95
t-2-C4= Prod. [%]	0	0	0	0	0	4	16	25	30	33	35	37	38	40	40
c-2-C4= Prod. [%]	0	0	0	0	0	0	6	11	14	16	17	22	25	28	36
Butene Disapp. [%]	**67**	**95**	**100**	**100**	**100**	**96**	**78**	**64**	**56**	**52**	**48**	**41**	**33**	**29**	**19**
n-Butane Change [%]	-1	6	6	6	6	5	4	2	3	2	3	1	1	2	0
C5+ Product Analysis [mass %]															
C5-C7	33	31	28	26	23	13	8	3	1	0	0	0	0	0	0
C8	**33**	**56**	**57**	**56**	**55**	**57**	**51**	**40**	**52**	**58**	**61**	**61**	**63**	**69**	**74**
C9+	33	14	15	18	23	30	41	57	48	42	39	39	37	31	26
C8 Distribution [mass %]															
TMP	**78**	**73**	**68**	**63**	**59**	**53**	**37**	**9**	**5**	**0**	**1**	**1**	**5**	**2**	**0**
DMH	18	22	28	32	37	42	50	54	43	40	32	26	24	22	18
C8=	4	5	4	4	4	5	13	37	53	60	67	73	71	76	82
TMP Isomer Distribution [%]															
2,2,4-TMP	**46**	**36**	**35**	**35**	**33**	**26**	**20**	**24**	**0**	**0**	**0**	**0**	**70**	**0**	**0**
2,2,3-TMP	5	4	5	5	4	3	6	0	0	0	0	0	0	0	0
2,3,4-TMP	15	25	27	28	31	37	40	38	67	0	100	100	30	100	0
2,3,3-TMP	34	34	33	33	32	34	35	37	33	0	0	0	0	0	0
Indicators [mass fraction]															
TMP	**4.35**	**3.34**	**2.43**	**1.95**	**1.58**	**1.28**	**0.74**	**0.17**	**0.11**	**0.00**	**0.04**	**0.06**	**0.20**	**0.07**	**0.00**
DMH															
TMP+DMH	0.92	3.26	3.19	2.68	2.10	1.66	0.92	0.35	0.33	0.30	0.25	0.20	0.22	0.20	0.15
C8= + C9+															
(2,2,3-+2,2,4-TMP)	1.04	0.69	0.67	0.66	0.58	0.41	0.34	0.32	0.00	0.00	0.00	0.00	2.37	0.00	0.00
(2,3,4-+2,3,3-TMP)															
DMH Isomer Distribution [%]															
2,5-DMH	15	7	9	8	6	3	2	4	0	0	0	0	0	0	0
2,4-DMH	25	26	23	21	17	11	0	4	6	11	14	10	15	11	18
2,3-DMH	31	44	34	32	29	25	19	6	5	5	0	5	6	6	0
3,4-DMH	29	23	34	40	48	62	79	86	89	84	86	85	79	82	82

Run F55Yr
(recalcined Y, Tcalc=425degC, Trxn=50degC, P=382psig, I/O=14 4, butene WHSV=2 13h-1, t=1h, mcat=2 78g)

TOS (min)	1	2	3	4	5	6	7	8	9	10	12	15	20	30	60
Propane	320720	368780	425440	465520	408040	445700	414700	418220	417840	369700	419740	433340	418420	433980	439060
Isobutane	42651600	46679680	50878960	53981680	47231620	51340520	47796660	48756760	48681260	43773320	48786720	50847660	49027220	50808180	51050560
1-butene	900280	163760											112340	115040	163740
n-butane	1043820	1236540	1340720	1433240	1249540	1339020	1231640	1243420	1241200	1111460	1246500	1276540	1241020	1292040	1275820
t-2-butene						131360	487140	800300	955220	925400	1105420	1235700	1224040	1324120	1330980
c-2-butene							183620	340640	439880	440960	533500	727100	797140	918600	1212780
C5-C7	**212566**	**526444**	**565215**	**565468**	**389538**	**184131**	**76434**	**23564**	**6089**	**0**	**0**	**0**	**0**	**0**	**0**
C5	102220	197800	205720	203640	138580										
2,3-DMB	39667	94371	100686	98763	68484	46724	16310	5516							
2,2-DMP	10320	29103	32415	33065	22644	15041	5924								
3-MP	14907	41599	47097	49088	37057	29948	16174	9173	6089						
2,4-DMP	26199	70720	72237	69200	46170	30019	10182								
2,2,3-TMB		5883	6572	6483											
2-MHx		10217	11340	11867	5291	5284									
2,3-DMP	19253	62722	72189	74984	57482	45570	21310	8875							
3-MHx		14029	16959	18378	13830	11545	6534								
C8	**214103**	**952429**	**1151732**	**1197986**	**937700**	**819825**	**519976**	**375289**	**357990**	**319045**	**426691**	**430342**	**418107**	**401083**	**312857**
2,2,4-TMP	**77159**	**254509**	**269253**	**266064**	**179660**	**113452**	**37672**	**8225**					**14097**		
2,5-DMHx	5806	15634	27671	29578	20972	10233	5507	7763							
2,2,3-TMP	7926	31228	42296	35118	23320	14646	10979								
2,4-DMHx	9667	53203	75342	80321	57870	36737		7148	8904	13846	18617	11450	15342	9948	10250
2,3,4-TMP	24508	177150	209746	209442	170671	161767	76075	12936	11132		5827	6074	5936	6174	
2,3,3-TMP	57122	234573	258204	247017	177298	148183	67511	12649	5586						
2,3-DMHx	11904	91035	110277	123932	101165	84645	48033	12798	7479	6421		5393	5654	5656	
3,4-DMHx	10925	48670	107660	154166	169491	210857	204858	176324	136217	107768	117711	93179	80216	72922	46372
1 DMHx=															
2 DMHx=			5534	5856		5849	44279	102294	138148	145000	196195	221412	213122	214806	183460
3 DMHx=						5303									
4 DMHx=							5005								
5 DMHx=	9086	46427	45749	46492	37253	28153	7957	6199	6063	5157	5900				
6 DMHx=							12100	28953	44461	40853	82441	92834	83740	91577	72775
C9+	213797	231355	293560	374453	391211	430112	421097	536184	329691	231822	275222	275888	249175	177426	109216
C5+	640466	1710228	2010507	2137907	1718449	1434068	1017507	935037	693770	550867	701913	706230	667282	578509	422073
Tot Peak Area	45556886	50158988	54655627	58018347	50607649	54690668	51131267	52494377	51989290	46730747	52260293	54499470	52690322	54551869	54682233
Feed Analysis		Inj 1	Inj 2	Inj 3	Inj 4	Inj 5	Avg	Mass %							
C3		23244	20507	20590	23135	19165	21328	0 78							
i-C4		2702502	2368125	2377076	2716082	2195844	2471926	90 81		Avg Mass I/O Ratio		14 93			
1-C4=		180012	159003	159551	180978	147917	165492	6 08		Avg Molar I/O Ratio		**14.414**			
n-C4		68691	60613	60879	69202	57071	63291	2 33							
I/O Mass Ratio		15 013	14 894	14 899	15 008	14 845	14 932								

Run F56Pt5Y

(0.5%Pt/Y; Tcalc=325degC; Tred=425degC, Trxn=53degC; P=382psig; I/O=14.5; butene WHSV=2.12h-1; t=1h; mcat=2.78g)

Samp t [min	11	12	13	14	15	16	17	18	19	20	22	25	30	40	70
T.O.S. [min	1	2	3	4	5	6	7	8	9	10	12	15	20	30	60
1-C4= Disap	89	96	100	100	100	100	100	100	100	100	100	100	100	100	96
t-2-C4= Pro	0	0	0	0	0	0	0	5	12	23	32	36	39	37	42
c-2-C4= Pro	0	0	0	0	0	0	0	0	4	9	15	19	24	17	33
Butene Dis	89	96	100	100	100	100	100	95	84	68	54	44	38	45	21
n-Butane Ch	6	7	8	8	8	6	8	8	7	5	3	5	5	6	3
C5+ Product Analysis [mass %]															
C5-C7	33	27	27	27	26	18	23	22	12	6	1	2	0	0	0
C8	60	56	56	56	56	58	55	55	57	53	49	56	58	62	71
C9+	8	17	16	17	18	25	22	23	31	42	50	42	42	38	29
C8 Distribution [mass %]															
TMP	71	69	68	66	64	61	62	61	53	31	7	0	0	0	0
DMH	24	26	27	29	30	33	33	34	42	48	39	32	27	24	21
C8=	4	5	5	5	5	6	5	5	5	21	54	68	73	76	79
TMP Isomer Distribution [%]															
2,2,4-TMP	33	33	36	40	39	32	33	32	28	26	33	0	0	0	0
2,2,3-TMP	5	5	5	5	5	5	4	3	3	7	0	0	0	0	0
2,3,4-TMP	30	30	27	24	25	29	30	32	37	38	33	0	0	0	0
2,3,3-TMP	33	32	32	32	31	34	33	33	32	30	34	0	0	0	0
Indicators [mass fraction]															
TMP	2.91	2.68	2.55	2.32	2.12	1.83	1.87	1.79	1.26	0.64	0.19	0.00	0.00	0.00	0.00
DMH															
TMP+DMH	5.57	2.71	2.73	2.70	2.58	1.95	2.18	1.99	1.63	0.78	0.29	0.22	0.19	0.18	0.17
C8= + C9+															
(2,2,3-+2,2,4	0.61	0.62	0.69	0.80	0.78	0.57	0.59	0.54	0.45	0.46	0.50	0.00	0.00	0.00	0.00
(2,3,4-+2,3,3-TMP)															
DMH Isomer Distribution [%]															
2,5-DMH	9	9	9	10	9	7	7	4	3	0	0	0	0	0	0
2,4-DMH	25	24	23	23	24	20	20	14	7	3	7	9	12	14	13
2,3-DMH	31	34	36	38	35	34	30	30	25	17	6	0	0	0	0
3,4-DMH	35	34	32	29	32	39	44	52	66	81	87	91	88	86	87

Run F56Pt5Y

(0.5%Pt/Y; Tcalc=325degC; Tred=425degC; Trxn=53degC; P=382psig; I/O=14.5; butene WHSV=2.12h-1; t=1h; mcat=2.78g)

TOS [min]	1	2	3	4	5	6	7	8	9	10	12	15	20	30	60
Propane	404400	366520	394520	369160	410160	390060	400420	395400	357420	406480	412360	394220	363820	378240	366540
Isobutane	57199780	45357980	46707220	43325420	47532040	43567720	45842180	45688180	41796620	47482740	48680820	46112780	42375460	44040500	42635440
1-butene	413880	132580													113340
n-butane	1498280	1207680	1259340	1170240	1278900	1150340	1224300	1219000	1094600	1228960	1239040	1195020	1101540	1149780	1090140
t-2-butene								140560	323080	712860	1003020	1084060	1056700	1059240	1161520
c-2-butene									118320	277420	457640	573780	653680	494080	912540
C6-C7	566515	539028	599602	543093	584883	390477	439326	353183	116644	45627	6683	14479	0	0	0
C5	218000	199860	220780	209000	212620	161440	159620	126840							
2,3-DMB	101486	96387	105382	99216	100333	60047	76994	60923	29771	11394					
2,2-DMP	27008	29845	35420	35682	36191	20236	25049	19717	9971						
3-MP	41644	42080	47575	16203	47571	27430	38164	32826	20156	12048	6683				
2,4-DMP	78026	74338	80868	76124	76708	46308	56597	44401	20667	8219					
2,2,3-TMB	6603	6136	6442	5755	6195										
2-MHx	10030	10613	12911	13255	13528	8944	8765	6739				14479			
2,3-DMP	60490	64710	72410	69576	72468	52057	59356	49138	28156	13866					
3-MHx	13228	15059	17814	18282	19269	14015	14781	12599	7823						
C8	1009727	1107310	1233127	1140691	1244649	1270824	1072006	874114	539813	414015	335162	323373	265669	286856	267726
2,2,4-TMP	237474	256122	302241	299778	311550	244068	218670	167805	80968	31300	8106				
2,5-DMHx	22964	24990	31134	32337	34610	31730	23925	12696	6812						
2,2,3-TMP	33576	37900	40303	35972	39431	37506	29245	18398	8208	8728					
2,4-DMHx	62000	68816	74858	76371	89857	84846	69589	41866	14818	5359	8705	9650	8458	9498	7033
2,3,4-TMP	212934	226574	226255	179916	200298	226230	201727	171445	104558	48171	7894				
2,3,3-TMP	234825	247414	268836	238121	248389	266306	217035	175002	92665	38452	8242				
2,3-DMHx	76469	95871	118544	123163	133003	142810	106315	88301	55976	32895	8069				
3,4-DMHx	85899	96391	104562	93660	119829	164507	156658	155176	149280	160419	113084	93811	63764	58996	47908
1:DMHx=															
2:DMHx=		5234	5407	5460	6012	6424	5535	13939	12754	67107	131652	160016	150619	155719	150766
3:DMHx=															
4:DMHx=															
5:DMHx=	43586	47998	60987	55813	61670	66397	43306	29486	13574	5705	5510				
6:DMHx=										15879	43901	59896	42728	62642	62019
C9+	129851	335036	361507	339175	388638	541250	421066	373402	288498	326523	343213	241857	194327	172903	110742
Tot. Peak Area	61212433	49046134	50555316	46887679	51439270	47310671	49399297	49043839	44516375	50617105	52020298	49365789	45357416	47087518	45745448
Feed Analysis		Inj.1	Inj.2	Inj. 3	Inj. 4	Inj. 5	Avg.	Mass %							
C3		23750	21795	20975	22051	22712	22257	0.78							
i-C4		2785000	2536799	2428342	2566129	2663070	2595868	90.87							
1-C4=		184293	169142	162319	170686	176690	172626	6.04							
n-C4		70126	64442	61846	65064	67457	65787	2.30							
I/O Mass Ratio		15.112	14.998	14.960	15.034	15.072	15.035								

Run F58Pt5Yr

(recalcined 0.5%Pt/Y; Tcalc=325degC; Tred=425degC; Trxn=52degC; P=382psig; I/O=14.5; butene WHSV=2.11h-1; t=1h; mcat=2.78g)

Samp t [min]	11	12	13	14	15	16	17	18	19	21	30	40	70
T.O.S. [min.]	**1**	**2**	**3**	**4**	**5**	**6**	**7**	**8**	**9**	**11**	**20**	**30**	**60**
1-C4= Disapp. [%]	80	91	100	100	100	100	100	100	100	100	96	95	94
t-2-C4= Prod. [%]	0	0	0	0	0	0	11	25	31	34	36	37	37
c-2-C4= Prod. [%]	0	0	0	0	0	0	5	13	19	20	30	33	38
Butene Disapp. [%]	**80**	**91**	**100**	**100**	**100**	**100**	**84**	**61**	**50**	**46**	**30**	**26**	**19**
n-Butane Change [%]	2	4	8	8	7	7	6	4	4	5	5	4	4
C5+ Product Analysis [mass %]													
C5-C7	17	32	33	27	23	21	10	4	0	0	0	0	0
C8	27	53	54	56	54	54	48	49	54	54	65	66	68
C9+	57	15	13	17	23	25	41	47	46	46	35	34	32
C8 Distribution													
TMP	75	74	73	67	62	56	35	16	4	0	2	2	0
DMH	20	22	23	28	33	40	59	51	41	31	23	21	18
C8=	5	5	4	5	5	4	6	33	55	69	75	77	82
TMP Isomer Distribution [%]													
2,2,4-TMP	**39**	**39**	**39**	**36**	**36**	**34**	**38**	**29**	**0**	**#DIV/0!**	**0**	**0**	**#DIV/0!**
2,2,3-TMP	5	5	5	5	4	4	4	0	0	#DIV/0!	0	0	#DIV/0!
2,3,4-TMP	25	24	24	26	28	31	6	48	50	#DIV/0!	100	100	#DIV/0!
2,3,3-TMP	31	32	32	32	32	31	52	23	50	#DIV/0!	0	0	#DIV/0!
Indicators [mass fraction]													
TMP	**3.74**	**3.41**	**3.19**	**2.38**	**1.85**	**1.39**	**0.59**	**0.32**	**0.10**	**0.00**	**0.07**	**0.07**	**0.00**
DMH													
TMP+DMH	0.43	2.86	3.48	2.70	1.99	1.89	1.03	0.52	0.32	0.20	0.19	0.18	0.14
C8= + C9+													
(2,2,3-+2,2,4-TMP)	0.78	0.79	0.79	0.71	0.68	0.61	0.74	0.41	0.00	#DIV/0!	0.00	0.00	#DIV/0!
(2,3,4-+2,3,3-TMP)													
DMH Isomer Distribution [%]													
2,5-DMH	13	12	11	9	7	5	2	5	0	0	0	0	0
2,4-DMH	28	28	29	24	17	15	5	4	7	9	12	12	14
2,3-DMH	38	43	40	34	34	28	21	8	11	0	0	0	0
3,4-DMH	21	17	20	32	42	51	72	83	81	91	88	88	86

Run F58P15Yr
(recalcined 0 5%Pt/Y, Tcalc=325degC, Tred=425degC, Trxn=52degC, P=382psig, I/O=14 5, butene WHSV=2 11h-1, t=1h, mcat=2 78g)

TOS [min]	1	2	3	4	5	6	7	8	9	11	20	30	60
Propane	263380	353280	432120	386840	418260	412640	401700	393680	349920	407100	401600	421760	421320
Isobutane	40702260	48204500	53386480	46654840	49222980	48206280	47267860	46180760	41947820	48611380	47621320	49842240	50211860
1-butene	542420	271820									122860	145760	190640
n-butane	1053900	1246800	1420460	1249660	1309020	1271340	1231460	1194020	1074880	1259600	1237700	1280280	1286480
t-2-butene							339580	757360	842380	1063420	1107280	1180560	1198560
c-2-butene							142640	400660	500000	630220	920560	1053900	1229900
C6-C7	**360061**	**529180**	**629922**	**551399**	**487649**	**336926**	**101060**	**24237**	**0**	**0**	**0**	**0**	**0**
C5	145040	209520	243680	200820	175040	113180							
2,3-DMB	64191	93187	112268	96064	82373	57923	23753						
2,2-DMP	19186	29681	36511	32880	29574	20382	8542	6623					
3-MP	26324	39234	49704	45682	43489	34088	19259	8544					
2,4-DMP	51786	71626	82475	72213	59575	39648	15340						
2,2,3-TMB		5866	6602	5980	5155								
2-MHx	7358	10598	12296	12001	11039	7558							
2,3-DMP	37623	56352	69542	68783	64161	50637	26518	9070					
3-MHx	8553	13116	16844	16976	17243	13510	7638						
C8	**579317**	**880620**	**1026566**	**1167690**	**1114756**	**877739**	**469497**	**336990**	**251953**	**339461**	**328896**	**320461**	**276218**
2,2,4-TMP	**168294**	**261456**	**288735**	**284233**	**247696**	**184034**	**82958**	**16789**					
2,5-DMHx	15565	23596	26234	29103	27222	18659	6384	8583					
2,2,3-TMP	20784	34145	41004	39271	29071	20252	7125						
2,4-DMHx	32025	52961	68503	79390	64838	54362	13805	6714	7494	9823	9039	8431	6894
2,3,4-TMP	107301	156264	181381	205894	192432	150384	9188	26141	5339		5006	5059	
2,3,3-TMP	136235	206997	236813	251615	216434	152788	85287	12703	5438				
2,3-DMHx	43879	81720	93028	113116	124861	98378	58891	13272	11633				
3,4-DMHx	24057	31948	46783	106469	154406	179890	198654	143069	83656	96613	66700	59172	42206
1 DMHx=													
2 DMHx=				5315	5997	6247	15531	85358	112797	172359	174527	178653	167007
3 DMHx=													
4 DMHx=													
5 DMHx=	31177	41533	43085	53284	51800	32745	11774			5084			
6 DMHx=								25361	25596	55582	73623	69136	60111
C9+	1233587	251580	239078	352438	473420	405745	399991	320643	212506	288523	174719	166119	127881
C6+	2172965	1661380	1894566	2071527	2075825	1620410	970538	681870	464459	627984	503614	486570	404099
Tot Peak Area	44734925	51737780	57133626	50362867	53026085	51510670	50353778	49608350	44679459	51969484	50994374	53357170	53712959
FEED ANAL.		Inj 1	Inj 2	Inj 3	Inj 4	Inj 5	Avg	Mass %					
C3		19802	17684	17521	17871	21791	18934	0 77					
i-C4		2335882	2078799	2057617	2085319	2587354	2228994	90 88					
1-C4=		154819	139163	137731	139332	170376	148284	6 05					
n-C4		58952	53118	52472	53123	65221	56577	2 31					
I/O Mass Ratio		15 088	14 938	14 939	14 967	15 186	15 024						

Run F60Pt5EMTr
(recalcined 0.5%Pt/EMT, Tcalc=325degC, Tred=425degC, P=382psig, I/O=14.5, butene WHSV=2.1h-1, t=1h, mcat=1h)

Samp.t (min)	10	11	12	13	14	15	16	17	18	19	21	24	29	39	69
T.O.S. (min.)	**1**	**2**	**3**	**4**	**5**	**6**	**7**	**8**	**9**	**10**	**12**	**15**	**20**	**30**	**60**
1-C4= Disapp. (%)	86	98	100	100	100	100	100	100	100	100	100	100	100	100	100
t-2-C4= Prod. (%)	0	0	0	0	0	0	0	0	0	4	17	33	38	42	47
c-2-C4= Prod. (%)	0	0	0	0	0	0	0	0	0	0	6	14	15	19	25
Butene Disapp. (%)	**86**	**98**	**100**	**100**	**100**	**100**	**100**	**100**	**100**	**96**	**77**	**52**	**47**	**39**	**28**
n-Butane Change (%)	0	6	4	6	7	7	7	6	6	6	5	2	1	1	3
C5+ Product Analysis (mass %)	86	98	100	100	100	100	100	100	100	96	77	52	47	39	28
C5-C7	24	21	20	23	22	22	21	21	18	10	8	2	0	0	0
C8	**57**	**53**	**44**	**55**	**53**	**55**	**56**	**58**	**52**	**49**	**59**	**55**	**38**	**46**	**60**
C9+	19	25	36	22	25	23	23	21	31	41	33	43	62	54	40
C8 Distribution (mass %)															
TMP	**71**	**77**	**77**	**74**	**74**	**67**	**66**	**66**	**65**	**62**	**44**	**7**	**0**	**0**	**0**
DMH	19	16	16	19	19	26	27	28	29	33	42	41	33	25	22
C8=	11	7	7	7	7	7	7	6	6	5	15	53	67	75	78
TMP Distribution (%)															
2,2,4-TMP	**31**	**41**	**41**	**42**	**42**	**43**	**40**	**38**	**34**	**30**	**23**	**24**	**0**	**0**	**0**
2,2,3-TMP	26	23	21	20	19	11	9	8	7	5	4	0	0	0	0
2,3,4-TMP	15	12	13	14	14	18	21	23	27	31	37	35	0	0	0
2,3,3-TMP	28	23	24	25	25	28	30	31	33	34	36	40	0	0	0
Indicators (mass fraction)															
TMP/DMH	**3.80**	**4.89**	**4.88**	**3.97**	**3.84**	**2.58**	**2.45**	**2.36**	**2.19**	**1.86**	**1.04**	**0.16**	**0.00**	**0.00**	**0.00**
TMP+DMH/C8= + C9+	2.00	1.68	1.06	1.93	1.71	1.86	1.96	2.21	1.44	1.07	1.20	0.36	0.14	0.13	0.15
(2,2,3-+2,2,4-TMP)/(2,3,4-+2,3,3-TMP)	1.34	1.82	1.69	1.60	1.53	1.17	0.96	0.84	0.68	0.54	0.36	0.32	0.00	0.00	0.00
DMH Isomer Distribution															
2,5-DMH	16	18	18	15	15	11	10	9	8	4	0	4	0	0	0
2,4-DMH	10	11	10	10	10	27	23	20	20	15	5	6	9	12	21
2,3-DMH	52	50	57	51	54	40	37	36	34	32	26	10	9	5	0
3,4-DMH	22	21	14	24	21	22	30	35	39	50	69	80	82	82	79

Run F60P15EM1r
(recalcined 0 5%Pt/EMT, Tcalc=325degC, Tred=425degC, P=382psig, I/O=14 5, butene WHSV=2 1h-1, t=1h, rncat=1h)

TOS [min]	1	2	3	4	5	6	7	8	9	10	12	15	20	30	60
Propane	374640	341060	387240	420040	363440	401660	393900	412620	402600	347500	391200	389220	391240	404200	385880
Isobutane	40068500	42955320	46407180	49057180	42296300	46365640	45548080	47565680	46992460	41313180	46276340	46743240	46483440	48616260	46761380
1-butene	369740	61360													
n-butane	999560	1146940	1228300	1309320	1134560	1236360	1211140	1253640	1241600	1082560	1190780	1169800	1165420	1215940	1191020
t-2-butene										114540	512640	1006200	1145200	1343880	1427560
c-2-butene											181080	430580	451820	593260	767160
C5-C7	**434339**	**566034**	**660066**	**674471**	**560254**	**561848**	**506766**	**494028**	**410854**	**184203**	**77406**	**11772**	**0**	**0**	**0**
C5	309140	231060	241700	244080	200140	199460	181480	171360	143740						
2,3-DMB	25031	97771	103375	105126	86968	86991	77903	75163	62356	41156	15091				
2,2-DMP	8820	35723	38661	39849	33807	33334	29118	27636	22724	15538	6900				
3-MP	11509	42939	46918	49344	42452	43236	39852	39026	34954	26175	16103	6692			
2,4-DMP	36567	104937	107890	106095	84888	83881	74127	69883	57420	36348	12204				
2,2,3-TMB			10095	10166	8676	9106	8428	8480	7501	5402					
2-MHx	6572	8198	16470	17386	15280	15244	12997	12063	9953	6904					
2,3-DMP	29258	27563	76886	82014	69944	72015	66245	64383	57625	41801	19926	5080			
3-MHx	7442	17843	18071	20411	18099	18581	16616	16034	14581	10879	7182				
C8	**1052983**	**1408495**	**1488277**	**1602601**	**1338078**	**1417666**	**1327023**	**1300702**	**1212966**	**915988**	**545047**	**394845**	**394768**	**390378**	**332917**
2,2,4-TMP	**229417**	**448921**	**477354**	**494067**	**412699**	**409261**	**352097**	**324976**	**264309**	**170883**	**54620**	**6320**			
2,5-DMHx	31151	40020	42640	45626	39558	40582	34428	31644	27001	12095		6585			
2,2,3-TMP	196611	250806	246800	237610	183774	101408	78708	66517	51590	27447	8428				
2,4-DMHx	19453	23301	24411	29186	26617	99282	82332	72860	70156	44117	11373	9096	11579	12088	15696
2,3,4-TMP	109181	133822	150052	162664	140403	165865	183412	197466	209494	173741	88383	9137			
2,3,3-TMP	208542	249947	278057	295689	248927	268798	264012	267151	257651	191350	86009	10518			
2,3-DMHx	102121	111813	135444	152740	137559	145133	133534	130391	121817	96382	58635	16571	11704	5111	
3,4-DMHx	43017	46633	33747	72125	52913	81801	107889	128319	138371	150150	158308	128470	105221	79824	57866
1,DMHx=															
2 DMHx=	6741	5067	5854	6176	5919	6333	5315	5448		5216	49264	140513	174201	201034	183271
3 DMHx=															
4 DMHx=											5977				
5 DMHx=	98249	86456	87131	98812	83394	92927	78839	69915	66195	44627	11403	7750	7778	6227	
6 DMHx=	8500	11709	6787	7906	6315	6276	6457	6015	6382		12647	59885	84285	86094	76084
C9+	355352	674717	1208445	658425	630434	599856	541817	471184	716930	760203	307865	312799	631695	464593	225822
C5+	1842674	2649246	3356788	2935497	2528766	2579370	2375606	2255914	2340750	1860394	930318	719416	1026463	854971	558739
Tot Peak Area	43655114	47153926	51379508	53722037	46323066	50583030	49528726	51487854	50977410	44718174	49301278	50027876	50211763	52435251	50324579
FEED ANAL.		Inj 1	Inj 2	Inj 3	Inj 4	Inj 5	Avg	Mass %							
C3		19739	17977	18117	19444	18544	18764	0 76							
i-C4		2358899	2158938	2184557	2315452	2199961	2243561	90 91							
1-C4=		156271	143946	145473	153193	146296	149036	6 04							
n-C4		59308	54680	55408	58135	55576	56621	2 29							
I/O Mass Ratio		15 095	14 998	15 017	15 115	15 038	15 052								

Run F62Pt1EMT

(0.1%Pt/EMT; Tcalc=325degC; Tred=425degC; Trxn=50degC; P=382psig; I/O=14.6; butene WHSV=2.10h-1; t=1h; mcat=2.78g)

T.O.S. [min.]	1	2	3	4	5	6	7	8	9	10	12	15	20	30	60
1-C4= Disapp. [%]	88	96	100	100	100	100	100	100	100	100	100	100	100	100	97
t-2-C4= Prod. [%]	0	0	0	0	0	0	0	0	8	13	20	27	33	39	43
c-2-C4= Prod. [%]	0	0	0	0	0	0	0	0	0	5	7	11	14	20	28
Butene Disapp. [%]	88	96	100	100	100	100	100	100	92	82	73	61	54	41	26
n-Butane Change [%]	7	8	7	9	9	8	5	8	8	8	9	7	5	3	5
C5+ Product Analysis [mass %]															
C5-C7	26	24	24	24	24	22	19	19	16	10	7	5	4	0	0
C8	64	60	63	62	62	61	60	56	53	54	48	41	53	66	66
C9+	10	16	13	14	14	17	22	24	31	36	46	53	43	34	34
C8 Distribution [mass %]															
TMP	80	78	78	77	75	73	68	67	65	65	52	39	20	6	0
DMH	15	16	16	17	19	21	26	28	29	29	33	33	37	26	22
C8=	6	6	6	6	6	6	6	5	6	6	15	28	43	68	78
TMP Isomer Distribution [%]															
2,2,4-TMP	36	36	36	35	36	34	35	34	31	29	28	29	36	34	0
2,2,3-TMP	20	19	18	17	16	14	9	8	8	6	5	5	8	0	0
2,3,4-TMP	15	17	18	19	20	22	25	27	29	31	32	30	18	32	0
2,3,3-TMP	28	28	29	29	29	29	31	32	33	34	34	36	38	34	0
Indicators [mass fraction]															
TMP	5.47	4.95	4.75	4.44	3.89	3.57	2.58	2.41	2.23	2.22	1.58	1.17	0.56	0.22	0.00
DMH															
TMP+DMH	4.27	2.94	3.55	3.32	3.25	2.77	2.22	1.95	1.45	1.30	0.75	0.46	0.46	0.27	0.17
C8= + C9+															
(2,2,3-+2,2,4-TMP)	1.32	1.22	1.15	1.09	1.06	0.95	0.78	0.72	0.62	0.53	0.51	0.52	0.79	0.51	0.00
(2,3,4-+2,3,3-TMP)															
DMH Isomer Distribution [%]															
2,5-DMH	17	15	14	14	12	11	9	8	7	5	3	7	4	0	0
2,4-DMH	10	9	9	8	9	8	22	18	19	8	6	4	6	11	14
2,3-DMH	55	52	50	48	44	43	35	33	32	34	28	12	16	12	0
3,4-DMH	18	24	27	30	35	38	35	40	43	54	63	77	74	77	86

Run F62P11EMT

(0 1%Pt/EMT, Tcalc=325degC, Tred=425degC, Trxn=50degC, P=382psig, I/O=14 6, butene WHSV=2 10h-1, t=1h, mcat=2 78g)

TOS (min)	1	2	3	4	5	6	7	8	9	10	12	15	20	30	60
Propane	336640	324240	355740	402220	369620	406220	396560	398000	390420	341760	377020	392120	393620	410120	385940
Isobutane	46751160	41206520	43426980	48349480	43888940	47775760	42920260	46595600	46149260	40931440	44892640	47087760	46999960	49623300	46985040
1-butene	373280	115300													104400
n-butane	1248100	1111840	1156020	1303580	1184560	1283620	1128080	1244400	1235120	1091900	1203640	1233540	1205320	1246480	1202520
t-2-butene									240380	349660	578260	830000	987500	1235580	1302200
c-2-butene										123760	213080	348280	415960	628260	832540
C5-C7	**604160**	**548605**	**566519**	**614296**	**537475**	**539325**	**471356**	**426002**	**338135**	**151248**	**105227**	**62798**	**31744**	**0**	**0**
C5	221960	196980	204340	225940	189100	188700	157280	150980	117580						
2,3-DMB	95071	87195	89585	96690	84836	84676	72387	65206	50236	34644	23970	13418	7793		
2,2-DMP	31921	29635	30750	33328	30072	30485	26516	24124	18409	12861	9298	5622			
3-MP	40594	37894	39496	43341	39684	40892	36363	33908	28318	20870	17005	11095	8321		
2,4-DMP	103948	94202	95465	99814	86766	84708	74752	63150	49824	34190	22940	12957	7399		
2,2,3-TMB	10074	9094	9300	9970	9203	9175	8750	7474	6266						
2-MHx	13927	12900	13316	14076	13219	13471	12682	10517	8538	5823					
2,3-DMP	70986	66095	68873	74133	68418	70320	66311	56163	47385	33574	24822	14504	8231		
3-MHx	15679	14610	15394	17004	16177	16898	16315	14480	11579	9286	7192	5202			
C8	**1472946**	**1380453**	**1460729**	**1556248**	**1421220**	**1526402**	**1491462**	**1260374**	**1116148**	**803933**	**686689**	**486382**	**407407**	**376220**	**310696**
2,2,4-TMP	**428535**	**392968**	**404381**	**424400**	**381322**	**383486**	**356949**	**281558**	**221344**	**150986**	**101367**	**66657**	**29973**	**7334**	
2,5-DMHx	36215	32907	34211	36525	33202	35331	34196	27142	22029	11328	6315	11424	5399		
2,2,3-TMP	239338	201855	204144	200154	165554	160883	86866	68547	55873	29180	19690	9159	6733		
2,4-DMHx	20566	19873	21078	22706	23669	25088	86419	64127	60879	18123	14208	6604	9287	10475	9433
2,3,4-TMP	181798	182624	201598	224561	209460	246062	252215	223499	209466	162072	113891	57253	15154	6998	
2,3,3-TMP	325301	303800	327661	348927	307278	329536	315551	263896	236393	179636	123670	67786	31338	7495	
2,3-DMHx	118733	113643	120664	129663	121373	135294	135393	115911	102992	79811	62541	19744	23599	11952	
3,4-DMHx	39227	51916	63633	80976	95051	117806	135900	139905	138140	125907	143896	124131	111145	77072	59477
1 DMHx=											5410				
2 DMHx=	5454	5174	5314	5703	5245	6080	6089		14606	13617	60006	91957	132253	172658	172471
3 DMHx=															
4 DMHx=											5929	6489	6882		
5 DMHx=	71934	69698	71685	77719	72631	80108	76554	60444	49131	33274	13866	8259		6710	
6 DMHx=	5845	5995	6360	6914	6435	6728	6330	5345	5295		14900	26919	35644	75526	69215
C9+	241869	360748	304703	351866	326427	424856	542585	542677	653973	533962	684303	624755	329009	197249	162089
C5+	2318975	2289806	2331951	2524410	2285122	2490583	2505403	2219053	2108256	1489143	1475219	1172935	768160	573469	472685
Tot Peak Area	51028155	45047706	47270691	52579690	47728242	51956183	46950303	50457053	50123436	44203903	48526779	50716355	50354560	53088949	50452785
Feed Analysis		Inj 1	Inj 2	Inj 3	Inj 4	Inj 5	Avg	Mass %							
C3		18701	19299	18708	19540	19552	19160	0 76							
i-C4		2265871	2319728	2239606	2341678	2356598	2304696	90 96		Avg Mass I/O Ratio		15 16			
1-C4=		149502	153130	147983	153898	155376	151978	6 00		Avg Molar I/O Ratio		**14.638**			
n-C4		56982	58357	56340	58049	59201	57786	2 28							
I/O Mass Ratio		15 156	15 149	15 134	15 216	15 167	15 164								

Run F63Pt1EMTr

(recalcined 0.1%Pt/EMT; Tcalc=325degC; Tred=425degC; Trxn=50degC; P=382psig; I/O=14.8; butene WHSV=2.10h-1; t=1h; mcat=2.78g)

Samp t [min]	10	11	12	13	14	15	16	17	18	19	21	24	29	39
T.O.S. [min.]	1	2	3	4	5	6	7	8	9	10	12	15	20	30
1-C4= Disapp. [%]	82	95	100	100	100	100	100	100	100	100	100	100	100	100
t-2-C4= Prod. [%]	0	0	0	0	0	0	0	6	12	17	24	36	36	41
c-2-C4= Prod. [%]	0	0	0	0	0	0	0	0	4	6	9	15	15	18
Butene Disapp. [%]	**82**	**95**	**100**	**100**	**100**	**100**	**100**	**94**	**84**	**77**	**67**	**49**	**49**	**42**
n-Butane Change [%]	7	8	8	8	8	8	7	6	5	5	4	2	3	2
C5+ Product Analysis [mass %]														
C5-C7	29	26	25	24	22	21	19	16	10	7	6	19	1	0
C8	**64**	**59**	**62**	**63**	**63**	**63**	**61**	**55**	**52**	**47**	**48**	**39**	**56**	**62**
C9+	7	15	13	13	14	17	20	29	39	45	46	42	43	38
C8 Product Distribution [mass %]														
TMP	**82**	**80**	**80**	**77**	**75**	**69**	**68**	**64**	**62**	**52**	**37**	**19**	**8**	**5**
DMH	14	15	15	18	20	25	27	31	33	35	38	39	29	26
C8=	4	5	5	6	6	6	5	6	5	13	25	42	63	70
TMP Isomer Distribution [%]														
2,2,4-TMP	**38**	**36**	**35**	**35**	**34**	**34**	**32**	**29**	**28**	**28**	**27**	**52**	**29**	**36**
2,2,3-TMP	20	19	17	15	14	8	7	7	6	5	5	6	0	0
2,3,4-TMP	15	16	18	20	22	25	28	31	33	33	33	16	34	30
2,3,3-TMP	26	28	29	30	30	32	33	33	34	34	35	26	37	34
Indicators [mass fraction]														
TMP	**5.88**	**5.52**	**5.43**	**4.30**	**3.82**	**2.72**	**2.46**	**2.08**	**1.85**	**1.49**	**0.95**	**0.48**	**0.26**	**0.18**
DMH														
TMP+DMH	6.17	3.00	3.63	3.73	3.33	2.92	2.50	1.62	1.19	0.80	0.62	0.39	0.26	0.23
C8= + C9+														
(2,2,3-+2,2,4-TMP)	1.41	1.24	1.12	1.01	0.94	0.75	0.65	0.56	0.50	0.48	0.47	1.38	0.42	0.57
(2,3,4-+2,3,3-TMP)														
DMH Distribution [%]														
2,5-DMH	17	16	15	12	11	8	7	6	4	3	4	12	0	0
2,4-DMH	11	10	10	8	8	22	21	17	12	6	3	5	10	11
2,3-DMH	55	55	56	47	44	35	34	32	32	30	23	22	9	11
3,4-DMH	18	19	19	33	36	35	38	45	52	61	69	61	81	78

Run F63Pt1EMTr
(recalcined 0 1%Pt/EMT, Tcalc=325degC, Tred=425degC, Trxn=50degC, P=382psig, I/O=14 8, butene WHSV=2 10h-1, t=1h, mcat=2 78g)

TOS [min]	1	2	3	4	5	6	7	8	9	10	12	15	20	30
Propane	329280	326580	326560	399480	349580	387940	374400	386260	383140	332560	369240	371320	377640	389840
Isobutane	47388180	41947620	40154900	47969000	41627960	45798360	44060660	46206300	45824720	40176160	44563920	44911800	45657980	47656520
1-butene	536820	138040												
n-butane	1249380	1121380	1066100	1273240	1109360	1210920	1155800	1194520	1174360	1022260	1125200	1125080	1139000	1180120
t-2-butene								169660	345360	426460	690080	1047220	1055340	1233100
c-2-butene									123900	156480	261260	429860	438940	542420
C5-C7	**570621**	**590684**	**512171**	**580806**	**477834**	**465833**	**385793**	**299458**	**138622**	**86814**	**59690**	**221862**	**5426**	**0**
C5	212080	241740	189660	213340	171800	166280	136220	103880						
2,3-DMB	90408	87346	80908	90964	74073	71551	58528	43972	30756	18929	11947	53534		
2,2-DMP	29848	29103	27483	31305	26235	25396	20954	16244	11988	7935	5419	5791		
3-MP	38260	37695	35669	41744	35849	36226	31703	27193	21569	15516	11944	53376	5426	
2,4-DMP	99094	94474	85012	93620	74367	69692	55247	40549	27601	16624	10368	38087		
2,2,3-TMB	9382	8805	8416	9584	8275	8377	7102	5089				5709		
2-MHx	12337	12187	11374	12791	11351	11027	9224	7209	5228					
2,3-DMP	65130	65040	61161	71479	61522	62422	53792	43775	32190	20941	14413	38510		
3-MHx	14082	14294	12488	15979	14362	14862	13023	11547	9190	6869	5599	26855		
C8	**1277890**	**1351389**	**1276878**	**1630313**	**1360244**	**1394883**	**1219201**	**1047668**	**761013**	**558380**	**500007**	**480224**	**359845**	**373172**
2,2,4-TMP	**399986**	**394968**	**362396**	**408780**	**346242**	**330127**	**262293**	**192965**	**128926**	**80431**	**49320**	**45091**	**8043**	**6451**
2,5-DMHx	29681	30813	28534	33081	29291	29265	24117	18554	10474	5154	8546	21127		
2,2,3-TMP	211654	205496	178800	179935	145756	80357	60997	45096	25780	13316	9106	5375		
2,4-DMHx	19057	20085	18927	22949	22511	76841	68727	55596	28898	12687	6296	8630	10042	10593
2,3,4-TMP	157296	178037	187235	231568	221183	243003	231807	206009	150608	96940	60796	13643	9239	5267
2,3,3-TMP	275891	305597	294915	352365	303681	307264	268045	222470	157091	99928	63609	22811	10130	5988
2,3-DMHx	97611	108886	105785	126766	117506	124265	114273	102357	80679	58675	44718	39883	9578	10765
3,4-DMHx	31200	36564	35166	89764	97045	122991	127844	144129	129280	118865	132354	110353	84819	74690
1 DMHx=														
2 DMHx=				5280	5030	5182	5071	12485	14743	43862	83052	132072	153332	175726
3 DMHx=														
4 DMHx=														
5 DMHx=	55514	65098	59718	73026	66187	69144	56027	47987	24534	5380	14819	6428	6825	6309
6 DMHx=		5845	5400	6799	5812	6444				23142	27391	54811	67837	77383
C9+	142548	355451	268587	302205	308169	369231	402703	547543	559857	532538	476389	491936	274240	228748
C5+	1991059	2297524	2057636	2413324	2146247	2229947	2007697	1894669	1449392	1177732	1036086	1174022	639511	601920
Tot Peak Area	51494719	45831144	43605196	52055044	45233147	49627167	47598557	49851409	49176972	43135172	47784526	48629442	48869471	51061500
FEED ANAL.		Inj 1	Inj 2	Inj 3	Inj 4	Inj 5	Avg	Mass %						
C3		21125	18919	18506	19673	20417	19728	0.74						
i-C4		2583099	2311216	2260896	2404147	2507648	2413401	91.05						
1-C4=		167684	151505	148436	156904	163469	157600	5.95						
n-C4		63699	57654	56566	59881	62204	60001	2.26						
I/O Mass Ratio		15.405	15.255	15.231	15.322	15.340	15.311							

Run F66EMT

(EMT; Tcalc=425degC; Trxn=53degC; P=382psig; I/O=14.9; butene WHSV=2.07h-1; t=1h; mcat=2.78g)

Samp t [min]	10	11	12	13	14	15	16	17	18	19	21	24	29	39	69
T.O.S. [min.]	**1**	**2**	**3**	**4**	**5**	**6**	**7**	**8**	**9**	**10**	**12**	**15**	**20**	**30**	**60**
1-C4= Disapp. [%]	97	100	100	100	100	100	100	100	100	100	100	100	100	100	96
t-2-C4= Prod. [%]	0	0	0	0	0	0	0	0	0	7	14	22	33	38	42
c-2-C4= Prod. [%]	0	0	0	0	0	0	0	0	0	0	5	9	17	21	29
Butene Disapp. [%]	**97**	**100**	**100**	**100**	**100**	**100**	**100**	**100**	**100**	**93**	**80**	**69**	**50**	**41**	**25**
n-Butane Change [%]	6	5	7	7	8	22	8	8	3	6	3	3	3	2	2
C5+ Product Analysis [mass %]															
C5-C7	34	22	21	21	22	21	20	20	16	16	8	6	4	0	0
C8	**53**	**57**	**57**	**56**	**60**	**63**	**57**	**61**	**57**	**55**	**48**	**46**	**52**	**60**	**62**
C9+	13	21	22	23	18	17	23	19	28	29	45	47	44	40	38
C8 Distribution [mass %]															
TMP	**79**	**73**	**72**	**72**	**73**	**70**	**70**	**70**	**68**	**66**	**59**	**50**	**29**	**7**	**0**
DMH	16	20	21	21	20	25	24	25	27	29	32	33	30	28	23
C8=	5	7	7	7	6	6	5	5	5	5	8	17	41	65	77
TMP Isomer Distribution [%]															
2,2,4-TMP	**46**	**40**	**37**	**37**	**36**	**34**	**30**	**28**	**27**	**28**	**27**	**24**	**22**	**26**	**0**
2,2,3-TMP	21	19	17	16	15	8	8	7	7	7	7	5	6	0	0
2,3,4-TMP	12	16	18	19	21	26	29	31	31	30	31	35	36	35	0
2,3,3-TMP	21	26	27	27	28	32	33	34	34	35	35	36	36	40	0
Indicators [mass fraction]															
TMP	**4.98**	**3.61**	**3.44**	**3.46**	**3.58**	**2.83**	**2.87**	**2.81**	**2.51**	**2.26**	**1.86**	**1.52**	**0.96**	**0.25**	**0.00**
DMH															
TMP+DMH	3.27	2.14	2.01	1.91	2.63	2.92	2.09	2.62	1.76	1.64	0.90	0.70	0.46	0.26	0.16
C8= + C9+															
(2,2,3-+2,2,4-TMP)	2.03	1.41	1.20	1.15	1.03	0.73	0.60	0.54	0.53	0.55	0.51	0.41	0.40	0.35	0.00
(2,3,4-+2,3,3-TMP)															
DMH Isomer Distribution [%]															
2,5-DMH	19	14	13	13	12	9	8	7	7	6	5	2	0	0	0
2,4-DMH	12	9	9	8	9	24	21	20	19	18	15	9	7	11	13
2,3-DMH	54	46	46	44	44	35	34	34	32	32	29	26	12	8	0
3,4-DMH	15	30	32	35	36	32	36	39	42	44	51	64	81	82	87

Run F66EMT
(EMT, Tcalc=425degC, Trxn=53degC, P=382psig, I/O=14 9, butene WHSV=2 07h-1, t=1h, mcat=2 78g)

TOS [min]	1	2	3	4	5	6	7	8	9	10	12	15	20	30	60
Propane	422260	353300	343280	315680	351840	196080	353320	355480	325860	358540	382900	374180	345000	361980	366660
Isobutane	57911020	43700060	40449000	36627040	40661900	23274940	40947140	41671740	35635700	41426480	44968080	44250240	40811880	43180480	44131760
1-butene	110200														108640
n-butane	1465280	1123080	1059740	964580	1070200	719280	1070220	1087340	893540	1063460	1124320	1101000	1006420	1059280	1077920
t-2-butene										179960	414740	620600	841720	1037440	1176200
c-2-butene											152740	248080	446340	567120	821500
C5-C7	**676541**	**559859**	**513990**	**459696**	**475008**	**444312**	**498251**	**385636**	**324963**	**310582**	**148107**	**87305**	**26560**	**0**	**0**
C5	268500	199840	185180	164260	167900	147940	148140	137460	107520	106700					
2,3-DMB	107430	86634	79603	71694	75216	71600	63692	59953	50470	47194	33780	19769	6548		
2,2-DMP	40363	33389	29931	26746	27438	25002	21407	20057	17447	16692	12440	7463			
3-MP	48581	40525	37451	33726	35254	34027	30760	29418	26564	26289	21205	14519	6462		
2,4-DMP	99720	88589	80075	72013	75016	73014	62760	58879	50437	45905	32504	18697	6041		
2,2,3-TMB	9735	8759	8204	7396	7999	8097	7543	7330	6433	5847					
2-MHx	15752	15182	13572	12006	11946	11030	9090	8607	7899	7177	5461				
2,3-DMP	69275	69486	63809	57454	59614	59466	52795	51947	47131	43699	33510	20566	7509		
3-MHx	17185	17455	16165	14401	14625	14136	12064	11985	11062	11079	9207	6291			
C8	**1066300**	**1474239**	**1421028**	**1233956**	**1288360**	**1326459**	**1186307**	**1199622**	**1174172**	**1071037**	**889019**	**643526**	**366332**	**314546**	**283714**
2,2,4-TMP	**390953**	**423609**	**378713**	**333106**	**335735**	**312382**	**248524**	**234138**	**217029**	**197030**	**140648**	**78297**	**22920**	**5686**	
2,5-DMHx	32963	42898	39178	32709	32248	29592	23608	22059	21450	19317	14003	5037			
2,2,3-TMP	173616	202544	178352	144101	143208	76923	64152	61736	58534	51929	37309	16070	6197		
2,4-DMHx	19479	27488	25821	21809	22431	77065	61229	59950	60592	55893	42417	18083	7780	9203	8554
2,3,4-TMP	99422	170183	184008	170221	197632	242180	243458	257680	246596	210173	165718	112713	36423	7627	
2,3,3-TMP	178784	274821	278540	244174	266693	291399	276897	285841	274783	242531	185371	116444	36454	8702	
2,3-DMHx	91672	137869	134895	113437	115023	113798	99830	100627	102483	97812	83690	54271	12823	6916	
3,4-DMHx	25252	88542	96117	89501	94060	106039	105447	116448	132834	137468	144634	135000	85978	71084	56101
1 DMHx=															
2 DMHx=		6580	6305	5363	5262	5272	5130	6932	5353	11882	35849	69619	100934	138478	153453
3 DMHx=															
4 DMHx=															
5 DMHx=	54159	92923	91351	73364	70367	65523	52428	48614	49052	47002	39480	18326	5951	5803	
6 DMHx=		6782	7748	6171	5701	6286	5604	5497	5466			19666	39872	61046	65606
C9+	255644	533111	548120	515239	377648	351042	473834	373248	573264	560074	832237	654299	304497	210930	177409
C5+	1998485	2567209	2483138	2208891	2141016	2121813	2068392	1958406	2072399	1941693	1869363	1385130	686389	525475	461123
Tot Peak Area	61907245	47743649	44335158	40116191	44224956	26312113	44439072	45072966	38927499	44970133	48759403	47731150	43691409	46164655	47322303
Feed Analysis		Inj 1	Inj 2	Inj 3	Inj 4	Inj 5	Avg	Mass %							
C3		20175	18137	17972	16732	16589	17921	0 77							
i-C4		2406365	2150897	2131021	1979826	1976780	2128978	91 08		Avg Mass I/O Ratio		15 41			
1-C4=		154955	139665	138471	129070	128531	138138	5 91		Avg Molar I/O Ratio		**14.873**			
n-C4		58569	52885	52431	48919	48852	52331	2 24							
I/O Mass Ratio		15 529	15 400	15 390	15 339	15 380	15 408								

Run F67EMTr
(recalcined EMT; Tcalc=425degC; Trxn=52degC; P=382psig; I/O=15.0; butene WHSV=2.06h-1; t=1h, mcat=2.78g)

Samp t [min]	11	12	13	14	15	16	17	18	19	21	24	29	39	69	70
T.O.S. [min.]	**2**	**3**	**4**	**5**	**6**	**7**	**8**	**9**	**10**	**12**	**15**	**20**	**30**	**60**	**61**
1-C4= Disapp. [%]	95	100	100	100	100	100	100	100	100	100	100	100	100	100	100
t-2-C4= Prod. [%]	0	0	0	0	6	10	16	20	20	23	33	37	42	47	48
c-2-C4= Prod. [%]	0	0	0	0	0	0	7	8	8	9	16	17	20	28	29
T.O.S. [min.]	**2**	**3**	**4**	**5**	**6**	**7**	**8**	**9**	**10**	**12**	**15**	**20**	**30**	**60**	**61**
Butene Disapp. [%]	**95**	**100**	**100**	**100**	**94**	**90**	**77**	**73**	**72**	**67**	**51**	**46**	**38**	**25**	**23**
n-Butane Change [%]	8	7	8	8	7	6	4	5	5	5	3	4	3	4	7
C5+ Product Analysis [mass %]															
C5-C7	23	22	20	19	12	10	7	9	9	6	2	0	0	0	0
C8	**62**	**58**	**61**	**61**	**64**	**55**	**48**	**57**	**59**	**49**	**45**	**51**	**63**	**72**	**70**
C9+	15	20	19	20	24	34	45	34	32	45	53	49	37	28	30
C8 Distribution [mass %]															
TMP	**76**	**75**	**67**	**65**	**62**	**62**	**56**	**53**	**49**	**40**	**22**	**8**	**0**	**0**	**0**
DMH	19	20	27	30	32	32	31	33	34	36	33	29	25	19	19
C8=	5	5	5	5	6	6	13	14	17	23	45	63	75	81	81
TMP Isomer Distribution [%]															
2,2,4-TMP	**31**	**31**	**31**	**31**	**30**	**29**	**28**	**27**	**26**	**24**	**22**	**32**	**0**	**0**	**0**
2,2,3-TMP	13	13	8	7	7	6	5	5	4	5	0	0	0	0	0
2,3,4-TMP	24	26	29	30	30	32	33	34	35	36	42	32	0	0	0
2,3,3-TMP	31	31	33	32	33	33	34	35	35	36	36	36	0	0	0
Indicators [mass fraction]															
TMP	**4.01**	**3.67**	**2.45**	**2.18**	**1.94**	**1.97**	**1.79**	**1.61**	**1.47**	**1.11**	**0.65**	**0.29**	**0.00**	**0.00**	**0.00**
DMH															
TMP+DMH	3.23	2.40	2.61	2.50	2.16	1.39	0.82	1.17	1.15	0.66	0.34	0.23	0.18	0.16	0.15
C8= + C9+															
(2,2,3-+2,2,4-TMP)	0.81	0.76	0.63	0.61	0.58	0.54	0.49	0.46	0.44	0.40	0.28	0.47	0.00	0.00	0.00
(2,3,4-+2,3,3-TMP)															
DMH Isomer Distribution [%]															
2,5-DMH	11	10	7	6	6	4	3	3	6	5	5	6	0	0	0
2,4-DMH	7	7	19	18	16	12	9	7	0	3	6	10	13	16	16
2,3-DMH	44	42	33	33	31	34	32	29	28	24	15	9	0	0	0
3,4-DMH	38	41	41	44	47	50	56	61	66	68	74	75	87	84	84

Run F67EMTr
(recalcined EMT, Tcalc=425degC, Trxn=52degC, P=382psig, I/O=15 0, butene WHSV=2 06h-1, t=1h, mcat=2 78g)

TOS (min)	2	3	4	5	6	7	8	9	10	12	15	20	30	60	61
Propane	317540	379680	402980	328360	358860	352220	370760	356160	313360	356060	356080	372140	371780	345620	277560
Isobutane	40357080	45802120	47464180	38590600	41720960	41039540	43328960	42170040	37633180	42060020	42679920	44497200	44668100	41122540	32819540
1-butene	115340														
n-butane	1050160	1170680	1219740	995160	1068100	1043320	1088400	1060060	942520	1053080	1050560	1098020	1097400	1022660	840920
t-2-butene					155980	253440	445880	523420	475480	620980	901380	1033900	1174520	1211540	1004140
c-2-butene							179540	208300	185920	245280	428740	471440	576260	726480	594220
C6-C7	**390671**	**410167**	**394977**	**291391**	**175246**	**144364**	**110191**	**89042**	**73129**	**61354**	**18177**	**0**	**0**	**0**	**0**
C5	135640	152940	141280	101320											
2,3-DMB	62578	63549	60011	43920	39931	33232	25872	20566	16668	13091	5239				
2,2-DMP	20619	21660	21369	16142	14997	12862	9802	7997	6609	5531	6281				
3-MP	29993	31287	32332	24477	24186	20874	17249	14829	12749	11544					
2,4-DMP	62702	59749	56053	40829	36320	30139	23644	18212	14231	11360					
2,2,3-TMB	7515	7569	7601	5584	5080										
2-MHx	8854	8883	9190	7194	6493	5626									
2,3-DMP	51430	52589	54004	41478	37991	32552	26281	21105	17357	14746	6657				
3-MHx	11340	11931	13137	10447	10248	9079	7343	6333	5515	5082					
C8	**1075152**	**1107681**	**1210075**	**959022**	**935768**	**786096**	**714139**	**584269**	**496823**	**520752**	**393576**	**364741**	**324232**	**268778**	**263131**
2,2,4-TMP	**256086**	**264581**	**282824**	**191617**	**173388**	**143790**	**111028**	**82628**	**64329**	**60721**	**18774**	**9734**			
2,5-DMHx	21828	22201	23317	17923	16766	10719	7372	6321	10648	8541	5916	6009			
2,2,3-TMP	110305	103513	61392	44890	40051	29055	20325	14082	10989	9579					
2,4-DMHx	15206	16820	62294	50833	48573	30761	19566	12955		6447	8465	10246	10106	7821	7766
2,3,4-TMP	195378	211384	233869	185858	175331	156148	131688	105234	84765	74671	35893	9801			
2,3,3-TMP	256975	258366	265177	201938	190670	162007	137264	106623	84907	74409	30739	10839			
2,3-DMHx	89164	94776	109726	93281	93251	83528	71178	55180	46281	45272	19719	9721			
3,4-DMHx	78043	91959	136099	124899	139714	124079	125726	117642	109590	129175	96425	78339	69474	41458	41254
1 DMHx=															
2 DMHx=			5558	5023	15102	11696	45408	50933	54400	78320	124195	152253	165890	149889	148134
3 DMHx=															
4 DMHx=															
5 DMHx=	47001	48867	54006	42860	42922	34313	32973	17553	15299	13997	6188	6760	5414		
6 DMHx=	5166	5214	5813				11611	15108	15415	29620	47261	71039	73348	59610	65977
C9+	264972	385665	372856	316442	347931	487177	671341	344535	273810	484829	464491	347066	189377	100001	114849
C6+	1730795	1903503	1977908	1566855	1458945	1417637	1495671	1017836	843562	1066935	876243	711807	513609	358779	377980
Tot Peak Area	43570915	49255983	51064808	41480975	44762845	44106157	46909211	45335816	40208102	45157075	45864183	47713067	47825409	44061139	35320140
Feed Analysis		Inj 1	Inj 2	Inj 3	Inj 4	Inj 5	Avg	Mass %							
C3		20515	18587	17803	18088	18124	18623	0 76							
i-C4		2487226	2217021	2107785	2141222	2166248	2223900	91 13	Avg	Mass I/O Ratio		15 49			
1-C4=		159254	143282	136690	138674	139738	143528	5 88	Avg	Molar I/O Ratio		**14.954**			
n-C4		60149	54007	51501	52540	52910	54221	2 22							
I/O Mass Ratio		15 618	15 473	15 420	15 441	15 502	15 491								

Run F68EMT
(EMT, Tcalc=425degC, Trxn=53degC, P=382psig, I/O=14 9, butene WHSV=2 06h-1, mcat=2 78g)

Samp t [min]	10	11	12	13	14	15	16	17	18	19	21	24	29	39	69
T.O.S. [min.]	**1**	**2**	**3**	**4**	**5**	**6**	**7**	**8**	**9**	**10**	**12**	**15**	**20**	**30**	**60**
1-C4= Disapp [%]	86	100	100	100	100	100	100	100	100	100	100	100	100	100	100
t-2-C4= Prod [%]	0	0	0	0	0	0	0	0	0	10	20	28	33	37	42
c-2-C4= Prod [%]	0	0	0	0	0	0	0	0	0	0	7	12	14	18	24
Butene Disapp. [%]	**86**	**100**	**100**	**100**	**100**	**100**	**100**	**100**	**100**	**90**	**73**	**60**	**53**	**45**	**34**
n-Butane Change [%]	7	7	27	6	8	7	7	6	5	4	4	2	2	2	4
C5+ Product Analysis [mass %]															
C5-C7	36	24	22	23	23	20	21	18	12	8	6	3	1	0	0
C8	**53**	**58**	**62**	**60**	**61**	**65**	**59**	**56**	**53**	**47**	**44**	**39**	**43**	**51**	**62**
C9+	11	17	15	16	16	25	21	26	35	45	50	58	56	49	38
C8 Distribution [mass %]															
TMP	**84**	**79**	**75**	**74**	**72**	**68**	**69**	**68**	**64**	**59**	**42**	**27**	**10**	**7**	**0**
DMH	13	15	18	20	21	26	25	27	31	36	41	40	38	28	24
C8=	2	5	6	6	6	6	6	5	5	5	17	33	52	65	76
TMP Isomer Distribution															
2,2,4-TMP	**40**	**36**	**36**	**37**	**36**	**35**	**32**	**28**	**25**	**23**	**25**	**28**	**30**	**30**	**0**
2,2,3-TMP	18	18	17	16	15	8	6	6	6	4	5	6	0	0	0
2,3,4-TMP	15	17	18	18	20	25	29	31	34	36	34	35	31	31	0
2,3,3-TMP	26	29	29	29	29	32	34	35	36	36	36	31	38	38	0
Indicators [mass fraction]															
TMP	**6.29**	**5.15**	**4.08**	**3.76**	**3.37**	**2.61**	**2.78**	**2.61**	**2.06**	**1.64**	**1.01**	**0.68**	**0.26**	**0.26**	**0.00**
DMH															
TMP+DMH	4 42	2 66	3 07	2 84	2 86	1 86	2 30	1 85	1 33	0 96	0 64	0 37	0 26	0 22	0 17
C8= + C9+															
(2,2,3-+2,2,4-TMP)	1 42	1 19	1 14	1 13	1 04	0 76	0 60	0 52	0 44	0 39	0 43	0 52	0 44	0 44	0 00
(2,3,4-+2,3,3-TMP)															
DMH Isomer Distribution															
2,5-DMH	18	16	13	13	12	9	6	7	5	3	0	4	4	0	0
2,4-DMH	12	10	8	9	8	22	18	19	14	6	5	5	7	11	14
2,3-DMH	50	55	46	46	43	35	36	32	30	29	24	10	16	7	0
3,4-DMH	21	19	33	33	38	34	39	41	51	62	71	81	72	82	86

Run F68EMT
(EMT, Tcalc=425degC, Trxn=53degC, P=382psig, I/O=14 9, butene WHSV=2 06h-1, mcat=2 78g)

TOS [min]	1	2	3	4	5	6	7	8	9	10	12	15	20	30	60
Propane	332500	334940	156820	373980	333380	374100	364860	379940	378060	330260	371140	372680	383380	383620	366040
Isobutane	47510600	42407280	18748020	43932620	39162840	43458580	42227480	44392280	44607320	39407460	44220980	44836920	46209620	46297440	44225800
1-butene	406440														
n-butane	1214880	1104120	627260	1137520	1022260	1128580	1090580	1135360	1130840	990380	1097580	1094940	1127480	1137480	1097860
t-2-butene										246260	557220	803700	948660	1084420	1179140
c-2-butene											192940	339480	410080	517900	659100
C5-C7	**466914**	**512891**	**570664**	**530993**	**437805**	**439297**	**399626**	**364242**	**222495**	**110668**	**69884**	**33752**	**6511**	**0**	**0**
C5	190580	189440	178340	190280	157480	153680	140020	124020	35692						
2,3-DMB	76875	81903	96315	83210	68226	68974	62670	57009	41764	24941	14076	7992			
2,2-DMP	25247	23883	33780	29608	24487	24018	21571	19369	14814	9493	6199				
3-MP	32556	36541	43794	39330	33187	33998	31563	30545	25978	18959	14042	9213	6511		
2,4-DMP	71614	85797	101362	84113	67336	67886	60226	53762	38679	21828	12245	6907			
2,2,3-TMB	6880	7860	9961	9060	7323	7891	7429	7121	5651						
2-MHx	8722	12131	14813	13277	10916	10690	9267	8502	6680						
2,3-DMP	44704	61429	74923	66615	55229	58478	54221	51667	42626	27226	17036	9640			
3-MHx	9736	13907	17366	15500	13621	13682	12858	12247	10611	8221	6286				
C8	**686281**	**1215069**	**1584391**	**1362546**	**1143647**	**1230323**	**1136349**	**1127112**	**970292**	**641666**	**474494**	**377666**	**313411**	**347869**	**298696**
2,2,4-TMP	**233276**	**349078**	**432767**	**370836**	**296917**	**293323**	**248808**	**214141**	**164368**	**89064**	**60026**	**28639**	**9444**	**7291**	
2,5-DMHx	16511	29638	38801	34449	28537	28866	17882	21593	16138	7735		5415	5169		
2,2,3-TMP	106355	174770	203465	165670	125644	69272	46352	48232	36044	16893	9402	6269			
2,4-DMHx	10777	19467	24463	22941	19271	70428	52010	58738	40831	14199	9851	7290	8543	10237	10205
2,3,4-TMP	86764	161416	214309	181654	164540	206399	225707	239723	208432	136688	67411	35771	9718	7524	
2,3,3-TMP	151914	277452	344892	293573	240677	269475	268540	264731	222986	137109	71725	31642	11875	9110	
2,3-DMHx	45737	102823	134112	122521	105509	111956	102206	99155	90184	66616	47556	15257	19530	6860	
3,4-DMHx	18957	35098	95420	89040	92329	110461	111782	126610	155198	143250	139381	122606	86852	79227	61610
1 DMHx=															
2 DMHx=			6024	5372					5197	7737	51393	96910	122516	153976	171661
3 DMHx=															
4 DMHx=											6484				
5 DMHx=	14990	59570	83549	70225	64172	64246	57308	48881	40914	22385	8052	6369	6513	6160	
6 DMHx=		5757	6599	6265	6051	5897	5754	5308			13214	21598	33251	67604	55119
C9+	136530	366281	387939	369363	305540	554670	404595	525203	646412	607306	534543	561003	413057	329339	183929
C5+	1288725	2094241	2542984	2262902	1886992	2224290	1940769	2016557	1839199	1359640	1078921	972421	732979	677328	482524
Tot Peak Area	50753145	45940581	22075084	47707022	42405472	47185550	45623689	47924137	47955419	42334000	47325841	48080661	49402119	49580288	47351364
Feed Analysis		Inj 1	Inj 2	Inj 3	Inj 4	Inj 5	Avg	Mass %							
C3		19091	17175	16540	16825	17392	17405	0 77							
i-C4		2267269	2035835	1959414	1999852	2084019	2069278	91 11		Avg Mass I/O Ratio		15 48			
1-C4=		145659	131935	127163	129456	134067	133656	5 88		Avg Molar I/O Ratio		14 94			
n-C4		55368	50187	48339	49319	51165	50876	2 24							
I/O Mass Ratio		15 566	15 431	15 409	15 448	15 545	15 480								

A4.3 SENSITIVITY ANALYSIS

Table A4.6: Experimental Summary for Replicated Experiments

Catalyst	Replicated Runs
Recalcined 0.5%Pt/EMT	F48Pt5EMTr F50Pt5EMTr F60Pt5EMTr
Recalcined 0.1%Pt/EMT	F63Pt1EMTr F45Pt1EMTr
Fresh 0.5%Pt/Y	F44Pt5Y F56Pt5Y
Fresh EMT	F66EMT F68EMT

Sensitivity Analysis - Useful Catalyst Lifetime, Yield*, Mass Liquid*, SA Spent Catalyst*
(where * denotes from 2 to 7 min TOS)

		SD				
Useful Catalyst Lifetime [min]	11.8	0.9	12.8	11.5	11	F48Pt5EMTr, F50Pt5EMTr, F60Pt5EMTr
	11.7	0.8	11.1	12.2		F63Pt1EMTr, F45Pt1EMTr
	8.0	0.5	7.9	8.3		F44Pt5Y, F56Pt5Y
	10.6	0.6	11.1	10.2		F66EMT, F68Pt5AEMT
		0.7				
Yield [gC5+/gcat/gC4=fed]	0.095128	0.01936	0.109488	0.080768	0.0726484	F48Pt5EMTr, F50Pt5EMTr, F60Pt5EMTr
	0.064615	0.0193	0.064615	0.09197		F63Pt1EMTr, F45Pt1EMTr
	0.062930	0.0179	0.0503001	0.0755603		F44Pt5Y, F56Pt5Y
	0.082852	0.0057	0.0788383	0.086866		F66EMT, F68EMT
		0.01556				
Mass Liquid [g]	1.975000	0.39145	2.34	1.61	1.73	F48Pt5EMTr, F50Pt5EMTr, F60Pt5EMTr
	1.710000	0.1838	1.58	1.84		F63Pt1EMTr, F45Pt1EMTr
	1.375000	0.5020	1.02	1.73		F44Pt5Y, F56Pt5Y
	1.725000	0.0919	1.79	1.66		F66EMT, F68Pt5AEMT
		0.29232				
SA Spent Catalyst [m2/g]	246.0	67.9	294	198		F48Pt5EMTr, F60Pt5EMTr
	242.5	16.3	231	254		F63Pt1EMTr, F45Pt1EMTr
	279.5	0.7	280	279		F44Pt5Y, F58Pt5Y** samples lost due to malfunctioning multiposition valve
		28.3				

Sensitivity Analysis - (C5-C7) in C5+ [%]
(2 to 7 min TOS)

TOS [min]	SD	F50Pt5EMTr	F60Pt5EMTr	F48Pt5EMTr	SD	F63Pt1EMTr	F45Pt1EMTr	SD	F44Pt5Y	F56Pt5Y	SD	F66EMT	F68EMT
1	9.3	29	24	42	7.1	29	39	5.7	25	33	1.4	34	36
2	4.2	27	21	29	0.0	26	26	2.1	30	27	1.4	22	24
3	4.0	24	20	28	1.4	25	27	0.0	27	27	0.7	21	22
4	2.0	25	23	27	1.4	24	26	0.0	27	27	1.4	21	23
5	3.1	26	22	28	2.8	22	26	0.0	26	26	0.7	22	23
6	4.6	25	22	16	3.5	21	26	6.4	27	18	0.7	21	20
7	4.9	29	21	20	4.9	19	26	4.9	16	23	0.7	20	21
8	6.1	25	21	13	7.8	16	27	5.7	14	22	1.4	20	18
9	3.6	16	18	11	4.9	10	17	0.7	11	12	2.8	16	12
10	1.0	12	10	11	9.9	7	21	0.0	6	6	5.7	16	8
12	3.1	10	8	4	5.7	6	14	0.7	0	1	1.4	8	6
15	3.6	7	2	0	5.7	19	11	1.4	0	2	2.1	6	3
20	1.2	2	0	0	0.7	1	2	0.0	0	0	2.1	4	1
30	0.0	0	0	0	0.0	0	0	0.0	0	0	0.0	0	0
60	0.0	0	0	0	0.0	0	0	0.0	0	0	0.0	0	0
SD	3.8				2.4				2.2			0.9	
Average SD		2.3											

Sensitivity Analysis - C8 in C5+ [%]
(2 to 7 min TOS)

TOS [min]	SD	F50Pt5EMTr	F60Pt5EMTr	F48Pt5EMTr	SD	F63Pt1EMTr	F45Pt1EMTr	SD	F44Pt5Y	F56Pt5Y	SD	F66EMT	F68EMT
1	0.6	57	57	58	2.8	64	60	5.7	68	60	0.0	53	53
2	4.6	57	54	63	1.4	59	57	0.7	57	56	0.7	57	58
3	9.5	55	44	63	0.0	62	62	1.4	54	56	3.5	57	62
4	4.2	57	55	63	0.0	63	63	0.0	56	56	2.8	56	60
5	3.2	59	53	58	0.7	63	62	1.4	54	56	0.7	60	61
6	5.5	60	55	66	0.7	63	62	4.9	51	58	5.7	63	55
7	1.2	58	56	56	0.7	61	62	4.9	62	55	1.4	57	59
8	3.2	62	56	57	2.1	55	58	2.1	58	55	3.5	61	56
9	7.6	67	52	57	11.3	52	68	7.8	46	57	2.8	57	53
10	3.8	55	49	56	7.8	47	58	4.9	46	53	5.7	55	47
12	7.5	53	59	44	12.0	48	65	2.1	52	49	2.8	48	44
15	2.3	51	55	55	17.0	39	63	4.2	62	56	4.9	46	39
20	12.3	62	38	55	4.2	56	50	11.3	74	58	6.4	52	43
30	6.1	50	46	58	5.7	62	54	0.7	63	62	6.4	60	51
60	4.7	62	60	69	1.4	80	82	1.4	69	71	0.0	62	62
SD	4.7				0.6			2.2			2.5		
Average SD		2.5											

Sensitivity Analysis - C9+ in C5+ [%]
(2 to 7 min TOS)

TOS [min]	SD	F50Pt5EMTr	F60Pt5EMTr	F48Pt5EMTr	SD	F63Pt1EMTr	F45Pt1EMTr	SD	F44Pt5Y	F56Pt5Y	SD	F66EMT	F68EMT
1	9.8	14	19	0	3.5	7	2	0.7	7	8	1.4	13	11
2	8.5	16	25	8	1.4	15	17	2.8	13	17	2.8	21	17
3	13.5	21	36	9	2.1	13	10	2.1	19	16	4.9	22	15
4	6.1	18	22	10	1.4	13	11	0.7	18	17	4.9	23	16
5	6.1	15	25	14	0.7	14	13	1.4	20	18	1.4	18	16
6	4.0	15	23	18	3.5	17	12	2.1	22	25	5.7	17	25
7	6.1	13	23	24	5.7	20	12	0.0	22	22	1.4	23	21
8	8.5	13	21	30	9.9	29	15	3.5	28	23	4.9	19	26
9	8.4	17	31	32	17.0	39	15	8.5	43	31	4.9	28	35
10	4.6	33	41	33	17.0	45	21	4.2	48	42	11.3	29	45
12	10.7	34	33	52	17.7	46	21	1.4	48	50	3.5	45	50
15	1.5	42	43	45	11.3	42	26	2.8	38	42	7.8	47	58
20	13.2	36	62	45	3.5	43	48	11.3	26	42	8.5	44	56
30	6.1	50	54	42	5.7	38	46	0.7	37	38	6.4	40	49
60	4.7	38	40	31			18	1.4	31	29	0.0	38	38
SD	7.4				2.5			1.5			3.5		
Average SD		3.7											

Sensitivity Analyisis - TMP in C8 [%]
(2 to 7 min TOS)

TOS [min]	SD	F50Pt5EMTr	F60Pt5EMTr	F48Pt5EMTr	SD	F63Pt1EMTr	F45Pt1EMTr	SD	F44Pt5Y	F56Pt5Y	SD	F66EMT	F68EMT
1	10.4	86	71	91	1.4	82	84	6.4	80	71	3.5	79	84
2	2.1	80	77	81	0.0	80	80	4.9	76	69	4.2	73	79
3	1.2	77	77	79	0.7	80	79	5.7	76	68	2.1	72	75
4	2.5	77	74	79	0.7	77	78	7.1	76	66	1.4	72	74
5	1.5	77	74	76	1.4	75	77	7.8	75	64	0.7	73	72
6	5.6	78	67	71	4.9	69	76	8.5	73	61	1.4	70	68
7	6.1	78	66	70	5.7	68	76	2.8	66	62	0.7	70	69
8	4.0	74	66	70	8.5	64	76	1.4	59	61	1.4	70	68
9	3.8	72	65	66	4.9	62	69	2.1	56	53	2.8	68	64
10	4.9	70	62	61	10.6	52	67	6.4	22	31	4.9	66	59
12	18.1	65	44	29	23.3	37	70	4.9	0	7	12.0	59	42
15	26.1	50	7	3	29.7	19	61	0.0	0	0	16.3	50	27
20	13.9	24	0	0	5.7	8	16	0.0	0	0	13.4	29	10
30	1.7	3	0	0	3.5	5	0	0.0	0	0	0.0	7	7
60	0.0	0	0	0		0	0	0.0	0	0	0.0	0	0
SD	3.2				2.2			6.1			1.8		

Sensitivity Analysis - DMH in C8 [%]
(2 to 7 min TOS)

TOS [min]	SD	F50Pt5EMTr	F60Pt5EMTr	F48Pt5EMTr	SD	F63Pt1EMTr	F45Pt1EMTr	SD	F44Pt5Y	F56Pt5Y	SD	F66EMT	F68EMT
1	6.2	10	19	7	1.4	14	12	4.2	18	24	2.1	16	13
2	1.2	14	16	14	0.7	15	14	4.2	20	26	3.5	20	15
3	1.0	17	16	15	0.0	15	15	4.2	21	27	2.1	21	18
4	1.5	17	19	16	0.7	18	17	4.9	22	29	0.7	21	20
5	1.0	17	19	18	1.4	20	18	7.1	20	30	0.7	20	21
6	4.7	17	26	24	4.2	25	19	7.1	23	33	0.7	25	26
7	5.3	17	27	25	6.4	27	18	1.4	31	33	0.7	24	25
8	3.1	22	28	26	9.2	31	18	2.1	37	34	1.4	25	27
9	4.4	22	29	30	4.9	33	26	4.2	36	42	2.8	27	31
10	5.5	24	33	34	5.7	35	27	1.4	46	48	4.9	29	36
12	13.0	29	42	55	9.2	38	25	7.8	28	39	6.4	32	41
15	4.2	33	41	35	10.6	39	24	2.1	29	32	4.9	33	40
20	3.5	29	33	26	4.9	29	36	2.8	23	27	5.7	30	38
30	6.1	37	25	29	2.1	26	29	2.1	21	24	0.0	28	28
60	3.1	24	22	18		0	17	4.2	15	21	0.7	23	24
SD	2.4				2.2			4.8			1.4		

Sensitivity Analysis - C8= in C8 [%]
(2 to 7 min TOS)

TOS [min]	SD	F50Pt5EMTr	F60Pt5EMTr	F48Pt5EMTr	SD	F63Pt11EMTr	F45Pt11EMTr	SD	F44Pt5Y	F56Pt5Y	SD	F66EMT	F68EMT
1	4.6	3	11	3	0.7	4	3	0.7	3	4	2.1	5	2
2	1.0	6	7	5	0.7	5	6	0.7	4	5	1.4	7	5
3	0.6	6	7	6	0.0	5	5	1.4	3	5	0.7	7	6
4	1.0	6	7	5	0.0	6	6	2.1	2	5	0.7	7	6
5	0.6	6	7	6	0.7	6	5	0.0	5	5	0.0	6	6
6	1.2	5	7	5	0.0	6	6	1.4	4	6	0.0	6	6
7	1.5	4	7	5	0.7	5	6	1.4	3	5	0.7	5	6
8	1.2	4	6	4	0.0	6	6	0.7	4	5	0.0	5	5
9	1.0	5	6	4	0.0	5	5	2.1	8	5	0.0	5	5
10	1.0	6	5	4	4.9	13	6	7.1	31	21	0.0	5	5
12	5.5	6	15	16	14.1	25	5	12.7	72	54	6.4	8	17
15	23.8	17	53	62	19.1	42	15	2.1	71	68	11.3	17	33
20	14.0	47	67	74	10.6	63	48	2.8	77	73	7.8	41	52
30	7.8	60	75	71	0.7	70	71	2.1	79	76	0.0	65	65
60	3.1	76	78	82	0.0	0	83	4.2	85	79	0.7	77	76
SD	1.0				0.4			1.2			0.6		
Average SD		0.8											

Sensitivity Analysis - 2,2,4-TMP in TMP [%]

TOS [min]	SD	F50Pt5EMTr	F60Pt5EMTr	F48Pt5EMTr	SD	F63Pt1EMTr	F45Pt1EMTr	SD	F44Pt5Y	F56Pt5Y	SD	F66EMT	F68EMT
1	11.7	54	31	46	7.8	38	49	0.0	33	33	4.2	46	40
2	1.5	43	41	40	4.9	36	43	0.7	32	33	2.8	40	36
3	0.6	42	41	41	4.9	35	42	2.8	32	36	0.7	37	36
4	1.5	41	42	39	4.2	35	41	6.4	31	40	0.0	37	37
5	1.5	40	42	39	4.2	34	40	5.7	31	39	0.0	36	36
6	2.6	38	43	39	4.9	34	41	0.0	32	32	0.7	34	35
7	2.5	38	40	35	5.7	32	40	0.0	33	33	1.4	30	32
8	3.5	38	38	32	7.1	29	39	0.7	33	32	0.0	28	28
9	4.7	36	34	27	8.5	28	40	1.4	30	28	1.4	27	25
10	4.5	34	30	25	6.4	28	37	7.1	35	25	3.5	28	23
12	4.2	29	23	31	4.9	27	34	23.3	0	33	1.4	27	25
15	15.9	30	24	0	15.6	52	30	0.0	0	0	2.8	24	28
20	24.8	43	0	0	0.7	29	28	0.0	0	0	5.7	22	30
30	0.0	0	0	0	25.5	36	0	0.0	0	0	2.8	26	30
60	0.0	0	0	0	0.0	0	0	0.0	0	0	0.0	0	0
SD	1.7				4.8			2.6			0.9		
Average SD		2.5											

Sensitivity Analysis - 2,2,3-TMP in TMP [%]

TOS [min]	SD	F50Pt5EMTr	F60Pt5EMTr	F48Pt5EMTr	SD	F63Pt1EMTr	F45Pt1EMTr	SD	F44Pt5Y	F56Pt5Y	SD	F66EMT	F68EMT
1	3.8	20	26	19	0.7	20	19	1.4	3	5	2.1	21	18
2	0.6	23	23	22	3.5	19	24	1.4	3	5	0.7	19	18
3	4.4	22	21	14	3.5	17	22	0.7	4	5	0.0	17	17
4	1.0	19	20	18	4.2	15	21	1.4	3	5	0.0	16	16
5	1.5	18	19	16	2.8	14	18	1.4	3	5	0.0	15	15
6	3.6	16	11	9	7.1	8	18	0.7	4	5	0.0	8	8
7	2.6	13	9	8	7.8	7	18	0.7	3	4	1.4	8	6
8	2.1	9	8	5	6.4	7	16	0.0	3	3	0.7	7	6
9	1.5	8	7	5	2.8	6	10	2.1	0	3	0.7	7	6
10	1.5	7	5	4	2.8	5	9	4.9	0	7	2.1	7	4
12	3.5	7	4	0	1.4	5	7	0.0	0	0	1.4	7	5
15	3.5	6	0	0	0.7	6	5	0.0	0	0	0.7	5	6
20	0.0	0	0	0	0.0	0	0	0.0	0	0	4.2	6	0
30	0.0	0	0	0	0.0	0	0	0.0	0	0	0.0	0	0
60	0.0	0	0	0	0.0	0	0	0.0	0	0	0.0	0	0
SD	2.3				4.8			1.1			0.4		
Average SD		2.1											

Sensitivity Analysis - 2,3,4-TMP in TMP [%]
(2 to 7 min TOS)

TOS [min]	SD	F50Pt5EMTr	F60Pt5EMTr	F48Pt5EMTr	SD	F63Pt1EMTr	F45Pt1EMTr	SD	F44Pt5Y	F56Pt5Y	SD	F66EMT	F68EMT
1	4.5	6	15	10	2.8	15	11	0.7	29	30	2.1	12	15
2	0.6	12	12	13	2.8	16	12	1.4	32	30	0.7	16	17
3	2.1	12	13	16	3.5	18	13	2.1	30	27	0.0	18	18
4	1.2	14	14	16	4.2	20	14	5.7	32	24	0.7	19	18
5	1.5	15	14	17	4.2	22	16	4.9	32	25	0.7	21	20
6	2.3	18	18	22	6.4	25	16	1.4	31	29	0.7	26	25
7	2.6	20	21	25	8.5	28	16	0.0	30	30	0.0	29	29
8	4.0	23	23	30	9.9	31	17	0.0	32	32	0.0	31	31
9	4.2	25	27	33	8.5	33	21	1.4	35	37	2.1	31	34
10	3.5	27	31	34	7.1	33	23	0.7	39	38	4.2	30	36
12	3.1	31	37	35	4.9	33	26	23.3	0	33	2.1	31	34
15	19.2	31	35	0	9.9	16	30	0.0	0	0	0.0	35	35
20	15.6	27	0	0	0.0	34	34	0.0	0	0	3.5	36	31
30	0.0	0	0	0	21.2	30	0	0.0	0	0	2.8	35	31
60	0.0	0	0	0	0.0	0	0	0.0	0	0	0.0	0	0
SD	1.7				4.9			2.6			0.5		
Average SD		2.4											

Sensitivity Analysis - 2,3,3-TMP in TMP [%]
(2 to 7 min)

TOS [min]	SD	F50Pt5EMTr	F60Pt5EMTr	F48Pt5EMTr	SD	F63Pt1EMTr	F45Pt1EMTr	SD	F44Pt5Y	F56Pt5Y	SD	F66EMT	F68EMT
1	3.5	21	28	25	3.5	26	21	2.1	35	32	3.5	21	26
2	1.5	22	23	25	4.2	28	22	0.7	33	32	2.1	26	29
3	2.9	24	24	29	4.2	29	23	1.4	34	32	1.4	27	29
4	1.0	26	25	27	4.2	30	24	1.4	34	32	1.4	27	29
5	2.1	26	25	29	2.8	30	26	2.1	34	31	0.7	28	29
6	1.7	28	28	31	4.2	32	26	0.7	33	34	0.0	32	32
7	2.1	29	30	33	4.9	33	26	0.7	34	33	0.7	33	34
8	2.1	30	31	34	4.2	33	27	0.7	32	33	0.7	34	35
9	2.0	31	33	35	4.2	34	28	2.1	35	32	1.4	34	36
10	2.5	32	34	37	2.1	34	31	2.8	26	30	0.7	35	36
12	1.2	34	36	34	1.4	35	33	24.0	0	34	0.7	35	36
15	36.5	34	40	100	6.4	26	35	0.0	0	0	3.5	35	31
20	17.3	30	0	0	0.7	37	38	0.0	0	0	1.4	36	38
30	57.7	100	0	0	24.0	34	0	0.0	0	0	1.4	40	38
60	0.0	0	0	0	0.0	0	0	0.0	0	0	0.0	0	0
SD	1.9				4.1			1.2			1.1		
Average SD		2.1											

Sensitivity Analysis - TMP/DMH (mass fraction)
(2 to 7 min)

TOS (min)	SD	F50Pt5EMTr	F60Pt5EMTr	F48Pt5EMTr	SD	F63Pt1EMTr	F45Pt1EMTr	SD	F44Pt5Y	F56Pt5Y	SD	F66EMT	F68EMT
1	4.90	8.51	2.83	13.59	0.64	5.88	6.79	1.10	4.47	2.91	0.93	4.98	6.29
2	0.55	5.74	4.89	5.92	0.08	5.52	5.63	0.85	3.88	2.68	1.09	3.61	5.15
3	0.35	4.59	4.88	5.28	0.17	5.43	5.19	0.74	3.59	2.55	0.45	3.44	4.08
4	0.49	4.39	3.97	4.95	0.25	4.30	4.66	0.78	3.42	2.32	0.21	3.46	3.76
5	0.33	4.49	3.84	4.12	0.30	3.82	4.24	1.14	3.73	2.12	0.15	3.58	3.37
6	1.00	4.48	2.58	2.99	0.97	2.72	4.09	0.99	3.23	1.83	0.16	2.83	2.61
7	1.12	4.56	2.45	2.85	1.17	2.46	4.11	0.19	2.14	1.87	0.06	2.87	2.78
8	0.47	3.30	2.36	2.73	1.48	2.08	4.17	0.12	1.62	1.79	0.21	2.81	2.51
9	0.62	3.28	2.19	2.24	0.56	1.85	2.64	0.23	1.58	1.26	0.32	2.51	2.06
10	0.62	2.90	1.86	1.80	0.71	1.49	2.50	0.11	0.48	0.64	0.44	2.26	1.64
12	0.94	2.34	1.04	0.52	1.30	0.95	2.79	0.13	0.00	0.19	0.60	1.86	1.01
15	0.81	1.52	0.16	0.09	1.48	0.48	2.57	0.00	0.00	0.00	0.83	1.52	0.35
20	0.48	0.84	0.00	0.00	0.13	0.26	0.44	0.00	0.00	0.00	0.49	0.96	0.26
30	0.05	0.09	0.00	0.00	0.13	0.18	0.00	0.00	0.00	0.00	0.00	0.25	0.25
60	0.00	0.00	0.00	0.00	0.00	0.00	0.00	0.00	0.00	0.00	0.00	0.00	0.00
SD	0.64				0.49			0.78			0.35		
Average SD		0.57											

Sensitivity Analysis - (TMP + DMH)/(C8= + C9+)
(2 to 7 min TOS)

TOS [min]	SD	F50Pt5EM	F60Pt5EM	F48Pt5EMTr	SD	F63Pt1EM	F45Pt1EMTr	SD	F44Pt5Y	F56Pt5Y	SD	F66EMT	F68EMT
1	20.89	0.46	0.07	36.44	7.31	6.17	16.51	1.27	7.36	5.57	0.81	3.27	4.42
2	2.67	2.74	0.02	5.35	0.28	3.00	2.61	0.72	3.73	2.71	0.34	2.17	2.66
3	1.74	2.17	1.06	4.48	0.51	3.63	4.35	0.16	2.50	2.73	0.75	2.01	3.07
4	1.24	2.57	1.93	4.32	0.27	3.73	4.11	0.11	2.86	2.70	0.66	1.91	2.84
5	0.81	3.00	1.71	3.19	0.24	3.33	3.67	0.21	2.28	2.58	0.16	2.63	2.86
6	0.67	3.14	1.86	2.84	0.61	2.92	3.78	0.07	2.05	1.95	0.75	2.92	1.86
7	0.89	3.52	1.96	2.00	0.86	2.50	3.71	0.25	2.53	2.18	0.15	2.09	2.30
8	1.12	3.81	2.21	1.65	0.92	1.62	2.92	0.11	1.83	1.99	0.54	2.62	1.85
9	0.93	3.12	1.44	1.58	1.67	1.19	3.55	0.49	0.93	1.63	0.30	1.76	1.33
10	0.23	1.42	1.07	1.51	1.04	0.80	2.27	0.19	0.51	0.78	0.48	1.64	0.96
12	0.40	1.39	1.20	0.62	1.41	0.62	2.62	0.08	0.17	0.29	0.18	0.90	0.64
15	0.30	0.82	0.36	0.26	0.79	0.39	1.51	0.01	0.21	0.22	0.23	0.70	0.37
20	0.21	0.51	0.14	0.17	0.07	0.26	0.36	0.01	0.20	0.19	0.14	0.46	0.26
30	0.06	0.25	0.13	0.20	0.03	0.23	0.19	0.02	0.15	0.18	0.03	0.26	0.22
60	0.02	0.18	0.15	0.14	0.00	0.00	0.17	0.04	0.11	0.17	0.01	0.16	0.17
SD	1.34				0.46			0.25			0.01		
Average SD		0.63											

Sensitivity Analysis - (2,2,3-TMP + 2,2,4-TMP)/(2,3,3-TMP + 2,3,4-TMP) [mass fraction]
(2 to 7 min)

TOS [min]	SD	F50Pt5EMTr	F60Pt5EMTr	F48Pt5EMTr	SD	F63Pt1EMTr	F45Pt1EMTr	SD	F44Pt5Y	F56Pt5Y	SD	F66EMT	F68EMT
1	0.76	2.83	1.34	1.86	0.50	1.41	2.12	0.04	0.56	0.61	0.43	2.03	1.42
2	0.15	1.93	1.82	1.64	0.53	1.24	1.99	0.06	0.54	0.62	0.16	1.41	1.19
3	0.30	1.77	1.69	1.22	0.49	1.12	1.82	0.09	0.56	0.69	0.04	1.20	1.14
4	0.14	1.53	1.60	1.33	0.45	1.01	1.65	0.20	0.52	0.80	0.01	1.15	1.13
5	0.17	1.41	1.53	1.20	0.32	0.94	1.39	0.18	0.52	0.78	0.01	1.03	1.04
6	0.16	1.18	1.17	0.90	0.48	0.75	1.43	0.01	0.56	0.57	0.02	0.73	0.76
7	0.16	1.05	0.96	0.74	0.51	0.65	1.37	0.02	0.56	0.59	0.22	0.30	0.61
8	0.18	0.90	0.84	0.57	0.47	0.56	1.23	0.01	0.56	0.54	0.01	0.54	0.52
9	0.17	0.81	0.68	0.48	0.36	0.50	1.01	0.01	0.44	0.45	0.06	0.53	0.44
10	0.14	0.68	0.54	0.40	0.27	0.48	0.86	0.06	0.54	0.46	0.11	0.55	0.39
12	0.10	0.55	0.36	0.45	0.16	0.47	0.70	0.35	0.00	0.50	0.06	0.51	0.43
15	0.28	0.55	0.32	0.00	0.59	1.38	0.54	0.00	0.00	0.00	0.08	0.41	0.52
20	0.44	0.77	0.00	0.00	0.02	0.42	0.39	0.00	0.00	0.00	0.03	0.40	0.44
30	0.00	0.00	0.00	0.00	0.40	0.57	0.00	0.00	0.00	0.00	0.06	0.35	0.44
60	0.00	0.00	0.00	0.00	0.00	0.00	0.00	0.00	0.00	0.00	0.00	0.00	0.00
SD	0.18				0.46			0.09			0.08		